

Dipartimento di / Department of

SCIENZE DELL'AMBIENTE E DELLA TERRA / EARTH AND ENVIRONMENTAL SCIENCES

Dottorato di Ricerca Executive in / Executive PhD program  
SCIENZE CHIMICHE, GEOLOGICHE E AMBIENTALI  
CHEMICAL, GEOLOGICAL AND ENVIRONMENTAL SCIENCES  
Ciclo / Cycle 33°

Curriculum  
SCIENZE GEOLOGICHE / GEOLOGICAL SCIENCES

# **TREE STABILITY ANALYSIS: EXPERIMENTAL PULLING TESTS AND ANALYTICAL INTERPRETATION**

Cognome / Surname: SALA

Nome / Name: CRISTIAN

Matricola / Registration number: 835499

Tutore / Tutor: CROSTA GIOVANNI

Cotutore / Co-tutor: CANEPA DAVIDE

Supervisor: CASTELLANZA RICCARDO

Co-supervisor: GALLI ANDREA, CIANTIA MATTEO

Coordinatore / Coordinator: MALUSA' MARCO G.



## Index

Preface .....	1
Chapter 1	
Tree stability: a review .....	3
1.1 Introduction.....	3
1.2 Tree stability: methods .....	5
1.2.1 Overview of main presents methods.....	5
1.2.2 VTA – Visual Tree Assessment .....	7
1.2.3 SIM – Static Integrated Method (Pulling Test) .....	9
1.2.4 SIA – Static Integrating Assessment .....	17
1.2.5 DRE – Dynamic Root Evaluation.....	21
1.3 The methods: conclusions.....	25
References.....	26
Chapter 2	
Pulling tests results: some considerations.....	29
2.1 Introduction.....	29
2.2 Performed pulling tests .....	30
2.2.1 Applied method and instruments .....	30
2.2.2 Results report .....	31

## Index

---

2.3 The results.....	33
2.3.1 Moment-inclination curve .....	33
2.3.2 Safety factor.....	39
2.3.3 Load rate and inclination rate .....	44
2.3.4 Stiffness and maximum bending moment .....	52
2.4 Conclusions.....	57
Chapter 3	
Geotechnical soil characterization .....	59
3.1 Introduction.....	59
3.2 Geographical location .....	59
3.3 Soil granulometries .....	61
3.3.1 Materials and methods .....	61
3.3.2 Results of granulometric tests performed .....	65
3.3.3 Possible correlation between granulometry data and "pulling test".....	79
3.4 Direct shear test on urban soil samples.....	82
3.4.1 Materials and methods .....	82
3.4.2 Results direct shear tests performed .....	85
3.5 Conclusions.....	90
Chapter 4	
Proposal of a new fitting curve .....	93
4.1 Introduction.....	93
4.2 Limits of root stability evaluation method.....	93
4.3 Why is a new curve necessary? .....	96
4.4 Proposition a new interpolating equation .....	97
4.5 Proposition a remark on parameter $\phi_{70}$ .....	100
4.6 Conclusions.....	102
References.....	103

Chapter 5

Experimental pulling tests till overturning .....	105
5.1 Introduction.....	105
5.2 Description of the experimental work .....	105
5.3 Test 1 .....	107
5.3.1 3D modeling of the root system in Test 1.....	112
5.4 Test 2 .....	114
5.5 Conclusions.....	119
References.....	120

Chapter 6

Validation on experimental tests .....	121
6.1 Introduction.....	121
6.2 Standard analysis .....	121
6.3 Extended prediction on Test 1 and Test 2 .....	124
6.4 Small scale pulling tests.....	131
6.5 Conclusions.....	135
References.....	136

Chapter 7

Advanced approach in particular cases.....	137
7.1 The tree stability in not ordinary cases .....	137
7.2 Villa Litta study .....	137
7.2.1 Phase 1: Relief with Georadar to estimate the development of the root system in 3D.....	139
7.2.2 Phase 2: 3D geometry reconstruction of the stem and plant (3D terrestrial laser scanner survey) .....	140
7.2.3 Phase 3: Evaluation of soil resistance parameters (laboratory tests) .....	142

## Index

---

7.2.4 Phase 4: Estimation of wind action and predominant direction considering local variables .....	145
7.2.5 Phase 5: Verification of the stability of the plant with and without reinforcements and estimate of the increase in stability adopting FEM 3D .....	146
7.2.6 Phase 6: Installation of anchors (type Flying Fox - FastSystem) to increase the stability of the tree .....	150
7.2.7 Villa Litta study: conclusions .....	154
Chapter 8	
Conclusions.....	155
Appendix 1	
Pulling tests.....	159
Appendix 2	
Geographical location .....	375

## Preface

In recent years, society has increased the consideration of the importance of green areas for the protection of the planet and the health of people. In urban areas, in particular, the presence of trees significantly increases the quality of life of citizens under various aspects, i.e. greater shading and reduction of summer temperatures, reduction of pollutants in the air, reduction of stress and improvement of people's mood, etc.

However, trees can suffer biomechanical breakages for meteorological, phytopathological and anthropic reasons, causing considerable damage to things and people. There are, therefore, different methods for evaluating the stability of trees that can make it possible to predict their fall and avoid damage, but the matter is very complex and, in the current state of knowledge, these evaluations have some limitations.

In the last years the main method used to value the root stability of a tree is the SIM – Static Integrated Method (*pulling test*), because it is often the only one known and currently there are not other alternative methods with the same reliability and repeatability, although it has some limitations as other methods.

The purpose of this work was, therefore, to try to improve the method of evaluating the root stability of trees, taking advantage of the work experience of the Agro Service society, specialized in tree stability evaluation for public and private customers.

First of all, to improve root stability evaluation is necessary to observe several pulling tests and analyse their results. So, with the cooperation of Agro Service society, almost one hundred pulling tests are carried out since year 2017 to 2020 to be used for this research. More other pulling tests are

carried out in this time frame, but relative results are not considered for this study because the data quality is not enough high.

All the pulling tests are performed with FAKOPP instruments, that allowed to collect several points of the fitting overturning curve between root plate rotation and applied force. After the ordinary pulling phase until the rotation of  $0,2^\circ$ , as expected by the SIM, some of them are also recorded during the following unload phase, to analyse the behavior of tree-roots-soil system.

In the 11 different places where tests are carried out around Lombardy and Liguria regions, 18 soil samples are picked up to know the granulometry of these sites and its possible influence in pulling test results.

By the observation of the pulling tests data features and the mathematical anomalies of the ordinary method, a more general interpretative equation has been proposed critically compared to the classical Wessolly approach, in order to improve the evaluation of the root stability of the trees, increasing the public safety and the possibility to preserve monumental trees.

So this new proposed equation has been validated by some experimental pulling tests, consisting in real scale tests, traditional ones and until failure of the tree, and scale tests.

Finally, a work on increasing the safety of a tree with an advanced approach is reported, which was carried out by the same working group of this study. In spite of this approach can only be re-proposed for trees of particular value, i.e. monumental trees, due to its complexity and its excessive costs, this work was important to begin to deepen the topic of tree stability and from it we started to develop the following studies exposed in this thesis.



## Chapter 1

### Tree stability: a review

#### 1.1 Introduction

Stability assessment of trees is an important issue in management of urban areas, where accurate analysis techniques can substantially help in protecting both natural heritage (e.g. monumental and historic trees) and human activities. Sudden tree crashes may in fact induce severe damage to existing structures or goods (e.g. cars), imply the temporarily lack of serviceability of infrastructures (e.g. streets, railways, electric power plants...), and even cause the loss of human lives. Possible (and unfortunately diffused) lack of maintenance interventions and, in recent years, the effects of climate change with more and more intense wind gusts (on October 28th 2018, only in Italy the storm “Vaia” has caused the loss 6 to 8 million of cubic meters of standing trees, and 14 people died, as reported by Motta et al. 2018), also contribute to increase the emergency about the stability of trees. Nowadays tree risk assessment is in fact part of general risk management analyses (AIDTPG, 2015), and it requires specific risk mitigation strategies. In the last twenty years, the approaches usually adopted in practice have evolved from traditional Visual Tree Assessment (VTA; Mattheck and Breloer, 1998; requiring high agronomic expertise for tree inspection and symptoms recognition), towards the use of quantitative geometry-based indexes (like the ratio  $t/R$  of the thickness  $t$  of the wood to the radius  $R$  of the trunk; or the slenderness coefficient, i.e. the ratio of the height of the tree to the diameter of the trunk). The idea is to include traditional concepts from geotechnical and structural engineering (like e.g. equilibrium and compatibility equations, together with proper failure criteria) to the stability of a tree, thought as a “natural” and living structure (further details can be found in the comprehensive book published by Sani, 2017). Given the complexity of the problem,

related to high uncertainties in the definition of (i) the properties of the tree (i.e. the geometry and the strength of the trunk and of the roots), (ii) the soil mechanical properties and (iii) the actions (e.g. the wind loads), high multidisciplinary competences are required. The contribution of agronomists, biologists, engineers, physicists, is in fact fundamental in order to derive advanced interpretative models. In this perspective, in the paper, professional agronomist expertise has been combined with geotechnical engineering competences, in order to derive more accurate mechanical interpretations of the toppling mechanism of trees, involving the complete uprooting, as possibly induced by intense wind actions. Other possible failure mechanisms, such as trunk or branch breakages, for the sake of simplicity, will not be considered hereafter. The moment-rotation curve with respect to the base of the tree will be investigated both with reference to real scale and small scale experimental tests, and a new interpretative equation will be proposed.

In the last decades, important scientific researches have been conducted on this topic with the aim of defining valuable predictive models, either based on simplified descriptions of the root architecture and biomechanical properties (Blackwell et al. 1990; Pollen and Simon 2005; Schwarz et al. 2010), or on advanced Finite Element numerical model (Dupuy et al. 2005; Yang et al. 2014, 2017, 2018). An innovative interpretative framework was also recently discussed by Dattola et al. (2019), based on the concept of “macroelement”, by assimilating the entire root system to an isolated embedded foundation of a traditional civil structure. Large amount of experimental works have also been done, from early studies trying to empirically relating the stability of the tree to the properties and dimension of the crown (Guitard and Castera 1995; Ruel 2000; Sellier and Fourcaud 2009), Sani 2012, to advanced wind tunnel modelling or centrifuge tests on small scale tree models (Gromke and Ruck 2008; Cao et al. 2012, Zhang et al., 2020).

Despite such a relevant development at the scientific level, in standard agronomic practice the toppling resistance of trees is commonly estimated on the basis of on-site non-destructive pulling tests, thus bypassing the problem of a detailed characterization of the root geometry and of the soil. Predictions are obtained via a phenomenological interpretation of the test, based on the procedure proposed by Wessolly and Erb (1998). Such procedure (that will be illustrated later) was calibrated on a rich database of experimental pulling tests, run on trees with a diameter between 15 and

35 cm until the complete toppling, and identified a common interpolating equation.

Albeit the Wessolly equation is largely adopted in practice, some intrinsic as well as conceptual limitations will be pointed out in the present study, and a more general interpretative equation will be proposed and critically compared to the classical Wessolly approach. The aim is to provide practitioners of an enriched and physically based interpretative tool, without any additional computational costs. This will potentially induce positive outcomes not only in terms of increased accuracy in tree stability assessment, but more in general in the protection and maintenance of the arboreal heritage, with particular reference to historical and monumental trees.

## **1.2 Tree stability: methods**

### **1.2.1 Overview of main presents methods**

Up to now the subject of tree stability is developed thanks to the great job made by agronomists. The professional skills of agronomists and forestry doctors are regulated by law (law 7 January 1976, n. 3, mod. by law 10 February 1992, n. 152) according to which agronomists and forestry doctors carry out activities aimed at enhancing and managing agricultural, livestock and forestry production processes, protecting the environment and, in general, activities concerning the rural world (art. 2, 1° comma). So, an agronomist is a professional worker that is involved in every field of agriculture and zootechnics. Not only, their field of research is also everything that is related to trees, therefore their growth, their nutrition, their life and, in the end, their stability. Then, the agronomist decides if a tree is dangerous or not and consequently decides if it is necessary to cut it.

Principally, agronomists use only deterministic methods based on their own experience and attitude. In last years they understood the necessity to have a universal method that can be used in every situation. Therefore, agronomists develop an experimental method that consists in a traction test on the trunk of the tree and simulates the load caused by the wind.

All of these methods are not dangerous for the tree, in fact, they are methods that are not invasive for plants. They provide a sort of scale of the

hazard of the trees and a measure of a safety factor, as it will be shown in the following paragraphs.

These methods are provided in order to predict the level of hazard of a determined tree, and they could provide a risk mitigation strategy. Risk mitigation means to find a solution in order to decrease the damages caused by the wind speed, because the wind is the main cause of damages of trees in forests and in city areas. Understanding the phenomena of wind permits to plan damages mitigation strategies.

For this reason, it is also important to know the behaviour of the wind, a correct measure of it is necessary. Anyway, in some situation is not possible to install some device as anemometers. Where it is not possible to install them, agronomists prefer to stay in safety, so a high wind velocity is considered, about  $v = 33$  km/h, corresponding to  $v = 118$  km/h that is a huge velocity.

Let's see which methods are used in present days by agronomists (P.Sterken, 2006):

1. VTA-Visual Tree Assessment. This is a qualitative method that consists in the observation of the plant. This method is subjective and is more precise more the operator is able.
2. SIM-Static Integrated Method. This method is more objective and favourable with respect to the VTA method. In this case, trees are pulled in order to simulate wind loading.
3. SIA-Static Integrated Assessment. This method was developed by Wessolly after different experiences with SIM method. It is based on some tables developed considering the height and the diameter of a tree trunk and considering its exposure.
4. IBA-Integrierte Baum Analyse. Method developed in Germany and it is not used frequently for its theoretical to understand the reason why it is not used, because it is difficult, if not impossible, to know the history of a tree.
5. Dynamic Root Evaluation. It is a modern method that simulates the real dynamic behaviour of wind load. Thanks to the better technologies of our days, it is possible to measure, in a determined time interval, the velocity of the wind, by the installation of anemometers and the corresponding inclination.

In the following chapters, these methods will be presented in detail, except or IBA method, because of its low frequency of application.

### 1.2.2 VTA – Visual Tree Assessment

VTA is the oldest method developed and it is a subjective method based on the ability of the operator. A tree is a self-optimising mechanical structure (Mattheck and Breloer, 1994). A generating system which reacts to mechanical and physiological stresses by growing more vigorously to re-enforce weak areas, while depriving less stressed parts. This precept is described by Mattheck as the axiom of uniform stress. An understanding of the axiom of uniform stress allows an Arborist to make informed judgements about the condition of a tree. Mattheck introduced a biomechanically based system of visual tree assessment (VTA), which uses the reactive nature of tree growth. The basis behind VTA is the identification of symptoms, which the tree produces in reaction to a weak spot, or area of mechanical stress.

Although, Claus Mattheck stresses the limitations of this system by saying; "We can use VTA to state to what extent a defective tree is at greater risk of breaking, compared with a completely sound one. However, since nature's principle of lightweight structures allows a natural failure rate to occur even without defects, there can be no absolute guarantee of safety." It is essential that any arborist using VTA has a broad range of experience of different tree species, as individuals and in groups, to enable them to make informed and reasoned decisions about 'tree safety'.

The VTA method is an internationally spread and acknowledged method for trees inspection. This method consists in the individuation of the possible hazards and dangerousness of a tree.

The method consists on the measurement of the failure criteria and arrangement of the same. VTA helps to distinguish apparent hazardous trees from those that are hazardous. In this way safe trees are protected.

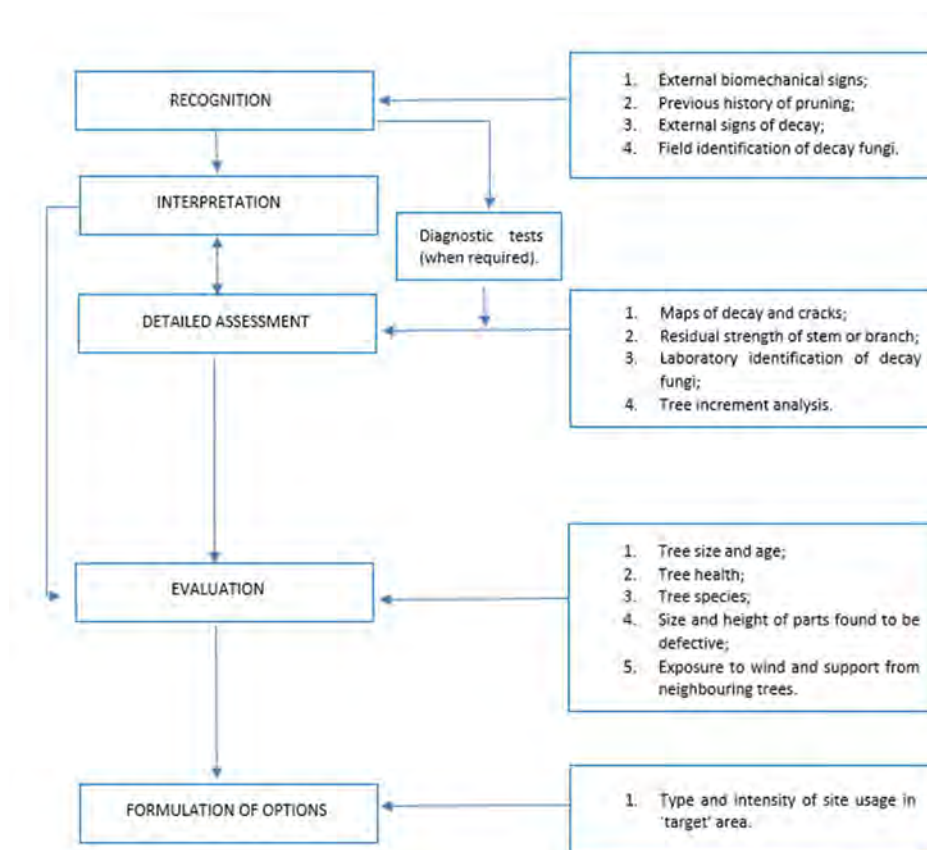
The final aim of this method is to give information about the body language and the mechanics of trees. It is a good method if matched to a deeper analysis (Smiley et al., 2011).

The passages of the method are the following:

1. **Inspection for detect symptoms:** it is the first look to the tree, and it is the first investigation of it.

2. **Confirmation of defects and measurement:** It is a deeper investigation and consists in the use of some instrument in order to clarify the drilling resistance, sound velocity in the trunk (it sets if the trunk is hollow or not), measurement of the wood strength and determination of the age of the tree.
3. **Assessment of the defects:** it is the establishment of the criteria for determining the safety of different typologies of trees: hollow trees, trees with root damages and health but high trees.
4. **Determination of further actions:** determinations of the post-analyse interventions.

Let's see a provisional scheme (Tab. 1.1) that gives an idea of the procedure of this method:



Tab. 1.1 Scheme of the procedure for VTA method (D. Lonsdale, 2007).

VTA method is one of the first methods used in order to determine the so-called tree risk assessment, that is the evaluation of the stability of a tree.

Tree risk assessment consists in the determination of the stability of a tree based on its exposure to wind and its actual health state (P.van Wassenauer et al., 2009). With this consideration is possible to determine the hazard of the tree. Together with hazard, as said, it is possible to evaluate also the exposure of the plant, related to the zone where it is located, and its resilience, that can be considered as the age of the plant. With these three parameters an easy estimation of risk of the tree can be done. As a matter of fact, risk is a function of the hazard, vulnerability, exposure and resilience, as the scientific community defines it.

### **1.2.3 SIM – Static Integrated Method (Pulling Test)**

The Static Integrating Method, called also “*pulling test*”, is an experimental method that consists in measuring the inclination of a tree subjected to a determined force (Wessolly and Erb, 1998). These typologies of tests are also called pulling tests because they consist in the simulation of a wind horizontal load on a tree and what is studied is the response of the tree to the applied wind. The aim, also in this case, is to estimate a safety factor and, consequently, tree risk assessment. The maximum load apply is compared with a statistical high wind force to provide the safety factor of the tree.

Pulling test consists in the application of an external load thanks to the installation of a rope that undergoes in traction. The role of the rope is to apply a horizontal load, that simulates a wind load. The difference with the real wind load is that with this method is possible to apply only a static force, while wind is a dynamic load. The rope is also anchored to the ground with the other head. Traction force can be applied thanks to a winch installed to the same rope.

Pulling test is the most used method in agronomic field. The reasons of its popularity are different:

- Precise estimation of safety factor;
- Easy application of the load;

## Chapter 1 - Tree stability: a review

---

- Easy repeatability of the experiment and, consequently, of the results;
- Possibility of applying loads in two or more directions (in different tests) and so obtain different results of safety factor;
- Relative low cost of the test;
- Obtain results in a short time after some cheap calculation made by a software.

The aim of the test is to simulate a horizontal wind load and to measure the inclination that corresponds to this load. All the measurements are possible through the use of some simple instruments:

- Dynamometer (Fig. 1.2): measures the load applied (in [kg]);
- Inclinator (Fig. 1.3): measures the inclination of the root plate (in [°]);
- Elastomer (Fig. 1.4): measures the variation of fibre length.

It provides a safety factor simply making the ratio between the maximum bending moment provided by the test and the bending moment caused by the wind.



**Fig. 1.2 Dynamometer mod. Fakopp.**





**Fig. 1.3 Inclinometer mod. Fakopp**



**Fig. 1.4 Elastometer mod. Fakopp.**

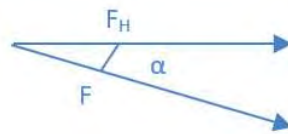
The inclinometer is installed just above the root plate, in order not to be influenced by some further inclination due to trunk deformation but only by the inclination of the base. The maximum inclination that a tree can tolerate without having damages is  $\theta=0.25^\circ$ , as will be explain better in the

following. This value is carried out by Wessolly after a lot of tests performed.

Elastometers are installed in a certain position of the trunk that will undergoes in tension or in compression in a certain height not important, but generally up to 1÷1.5m. The aim is to register the variation in length of the fibre of the timber.

Finally, the dynamometer is installed on the rope and its aim is to register the tension force applied. Important to say that the cable is installed in a convenient height near to the barycentre point of the tree. The external load is applied by a winch. The load measured is inclined of the same angle of the inclination of the rope, in order to obtain the horizontal load is necessary to make a correction, given by:

$$F_H = F \cdot \cos(\alpha)$$



Where:

- F is the applied inclined load in [N];
- $\alpha$  is the angle of inclination in [°].

This formula is simply given by the rectangular triangle theorem, as shown.

The bending moment of the test is computed as follow:

$$M = H \cdot F \cdot \cos(\alpha)$$

Where:

1. F is the force applied by the winch on the rope;
2. H is the height where the rope is installed;
3.  $\alpha$  is the angle of inclination of the cable;
4. D is the distance between the analysed tree and fixed point.

Here a simplification scheme of the procedure is reported (Fig. 1.5). To be noticed the fact that the rope is connected to a fixed point that can be another tree, as in the picture, or anything else.

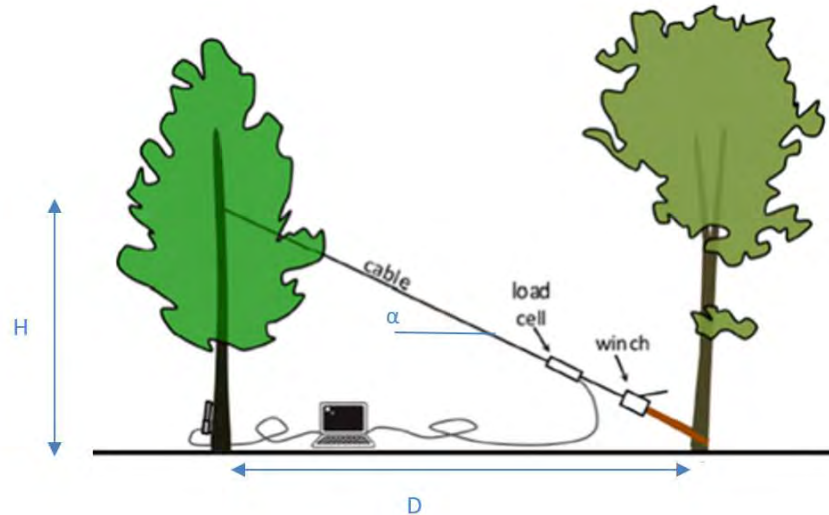


Fig. 1.5 Scheme of the procedure used (Fakopp instruction manual).

### 1.2.3.1 Wessolly's formulation

The professor of the University of Stuttgart Lothar Wessolly, thanks to a lot of pulling tests done, has obtained the following function that describes, for his aim, the moment-inclination curve that a tree follows when a traction is applied on it (Wessolly and Erb, 1998; Fig. 1.6):

$$\varphi = \frac{1}{3} \tan\left(\frac{100}{73.85} \frac{F}{F_{max}}\right) + \frac{1}{3} \left(\frac{F}{F_{max}}\right)^2 - \frac{1}{10} \left(\frac{F}{F_{max}}\right)$$

Where:

1.  $\varphi$  is the computed value of inclination, expressed in [°];
2.  $F$  is the instantaneous value of the force, in [N];
3.  $F_{max}$  is the maximum value that a tree can supports, again in [N].

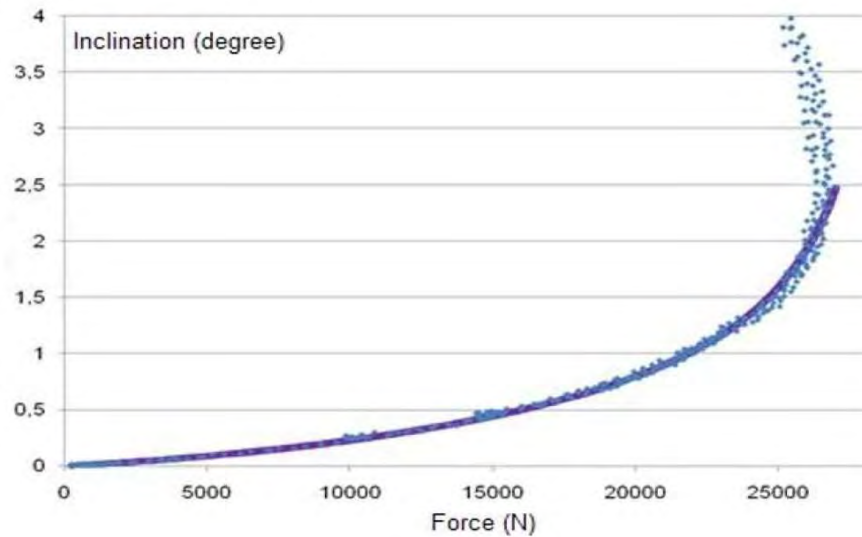


**Fig. 1.6 A typical tipping of uprooting curve which was recorded during an uprooting (Fakopp instruction manual).**

The maximum value of inclination that a tree can support without having any damage is  $\theta = 0.25^\circ$ , much less than the inclination in which the overturning of the trees occurs (usually at  $\theta = 2.5^\circ$ ). So pulling tests stop before  $\theta = 0.25^\circ$  and this is the reason SIM method is considered “non-destructive”. Fitting the equation to the measured load and inclination data, it is possible to estimate  $F_{max}$ , the horizontal load required to uproot the tree.

The Wessolly’s function is used in order to compute a value of  $\varphi$  (inclination) that is compared with the inclination assumed in the test with Least Square method:

$$(\theta_{calc} - \theta_{test})^2$$

Once computed the difference of each  $i$  value, it is calculated the sum:

$$\sum (\theta_{calc,i} - \theta_{test,i})^2$$

Finally, the minimum value is taken:

$$\min \left( \sum (\theta_{calc,i} - \theta_{test,i})^2 \right)$$

From the minimum value is possible to compute the  $F_{max}$  of the Wessolly's function simply using the Excel command "solver".

Successively the  $F_{max}$  is related with an estimated wind force, that depends from the type of the plant and the zone where the plant is located. Wind force can be computed as follows:

$$F = \frac{1}{2} \cdot c \cdot \rho \cdot A \cdot v^2$$

In this:

1.  $c$  is drag factor that depends on the species of the studied tree. Usual is taken a trivial value in the range of 0.25 – 0.30
2.  $\rho$  is air density. It is assumed equal to  $1.225 \frac{kg}{m^3}$ ;
3.  $A$  is an estimated value of the surface (area) of the foliage of the tree, measured in  $[m^2]$ ;
4.  $v$  is wind velocity. In order to stay in safety is taken equal to  $33 \frac{m}{s}$  that corresponds to  $118 \frac{km}{h}$ , huge value.

The commonest objection to winching is that a static force is applied, whereas gusts of wind sway the tree and the root system. However, observation on damages to roots and soil does not distinguish between trees uprooted by wind or by winches (Coutts, M.P., 1983).

The safety factor (SF) is the ratio between two loads, one is the applied load and the other is the reactive load (Fig. 1.7). In a mathematical point of view, it represents the ratio between the structure absolute strength and the applied load.

In engineering systems, it is considered as the ratio between the failure load of the system, called reaction loads, and the allowable load, or active loads. Consequently, the regime of safety side is present when the safety factor is bigger than 1, usually is taken a value of 1.5:  $SF = \frac{R}{S} \cong 1.5$ .

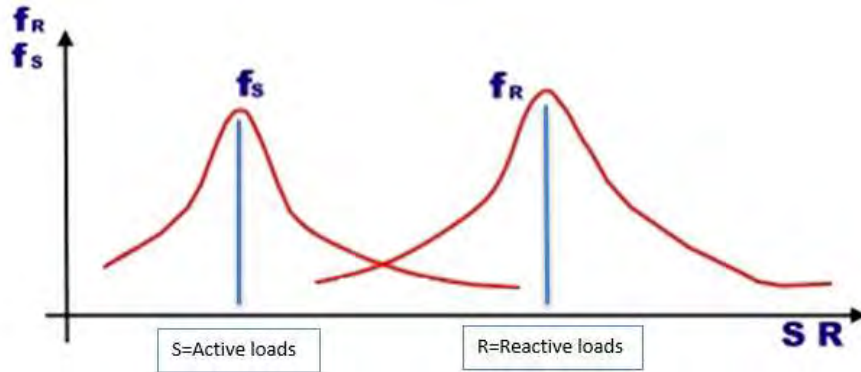


Fig. 1.7 Scheme of safety factor (Geronimi master thesis).

When a problem is not well known or it is characterised by uncertain variables, as the case of tree stability, is preferable to use a big safety factor, in order to stay in safety side. The safety factor for SIM, or pulling tests, is computed using Wessolly's maximum bending moment over moment caused by wind load on a tree, considering the maximum wind speed registered, in order to stay on the safety side.

Starting from the  $F_{max}$ , computed using the already provided Wessolly's formulation, it is possible to calculate the  $M_{max}$ , simply by:

$$M_{max} = F_{max} \cdot H_r$$

In which  $H_r$  is the height where the rope is installed, in [m].

Otherwise from the  $F_{wind} = \frac{1}{2} \cdot c \cdot \rho \cdot A \cdot v^2$  it is possible to find the bending moment caused by a wind of  $33 \frac{m}{s}$ :

$$M_{wind} = F_{wind} \cdot H_b = \frac{1}{2} \cdot c \cdot \rho \cdot A \cdot v^2 \cdot H_b$$

Where  $H_b$  is the barycentre of the tree, in [m].

Therefore, the safety factor for pulling tests can be provided simply by making the ratio between the two bending moments:

$$SF = \frac{M_{max}}{M_{wind}} = 2 \cdot \frac{F_{max} \cdot H_r}{c \cdot \rho \cdot A \cdot v^2 \cdot H_b}$$

### 1.2.4 SIA – Static Integrating Assessment

The Static Integrating Assessment method is a result of the SIM method. This method was developed by Wessolly after different experience with SIM (P.van Wassenauer and M.Richardson, 2009).

The SIA is based on the so-called Static Triangle. The static triangle takes into account the geometry of the structure, in agronomy field is the tree, and the material, in this case timber (Fig. 1.8). These two elements have to tolerate a specific load, therefore wind and weight of the trees, in order to maintain the equilibrium of the body. It is possible to apply these rules because the structure of a tree is assimilated to a structure of a building.

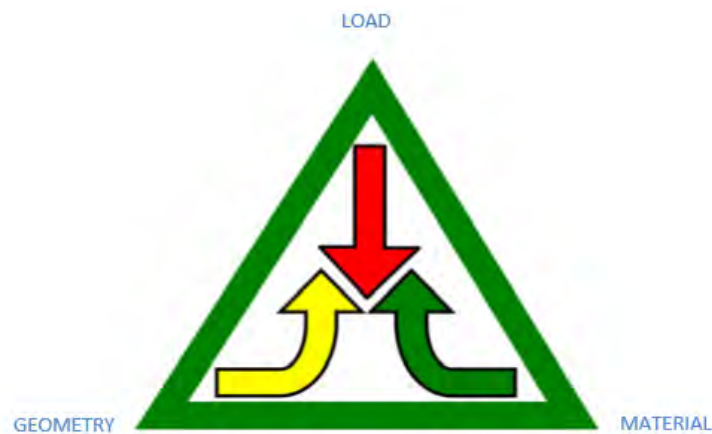


Fig. 1.8 Static triangle (Geronimi master thesis).

Wessolly starts from different pulling test results and it is possible to determine the stability of the tree by measuring the height and the diameter of a tree (P.van Wassenauer, and M.Richardson, 2009). By measuring the height and diameter of a tree along its exposure, an assessor can enter the data into a calculator to determine the value for the stability. Obviously for exposure is meant the exposure of a plant to the wind. Therefore, the zone where the tree is located is very important, because trees in country zones need stem bigger than trees in the city, where there is a smaller exposure.

Let's see a scheme:

1. Wessolly provides a diagram necessary to find the needed diameter of a specific tree starting from the height and the crown dimension (Fig. 1.9):

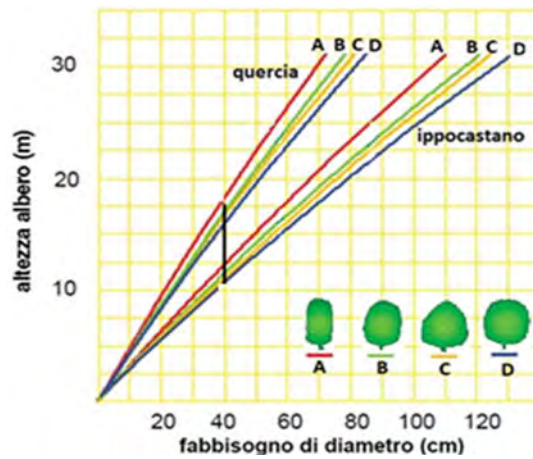


Fig. 1.9 Diagram A: estimation of the needed diameter (Geronimi master thesis).

This diagram is the natural consequence of more than 400 pulling tests provided by Wessolly. In fact, with his experience, he was able to relate the diameter of a tree with the bending moment caused by wind load (Fig. 1.10).

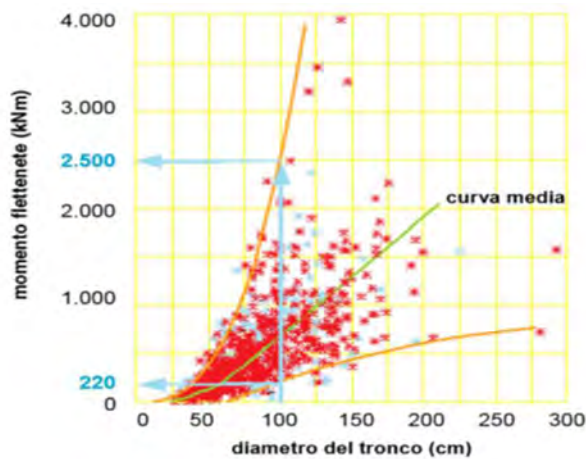


Fig. 1.10 Relation between bending moment and diameter of the stem (Geronimi master thesis).



2. By making the ratio between the measured diameter and the necessary diameter found using diagram A, it is possible to understand the static safety, as shown in diagram B (Fig. 1.11) by using the following expression:

$$F_s = 100 \cdot \left(\frac{d_m}{d_A}\right)^3$$

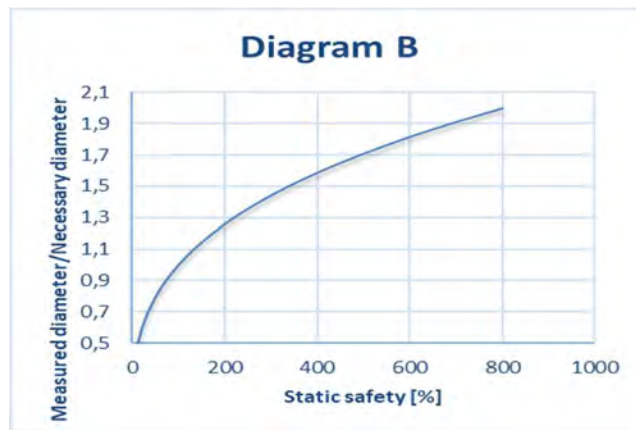


Fig. 1.11 Diagram B: Computation of static safety (Geronimi master thesis).

3. At this point it is possible to evaluate the minimum thickness of the side of hollow trees, as shown in diagram C (Fig. 1.12) following the expression:

$$\frac{tm_{side}}{d_m} = 0.223 \cdot \left(\frac{100}{F_s}\right)^{1.15}$$

Where:

- i.  $tm_{side}$  is the thickness of the hollow trunk, expressed in [m].

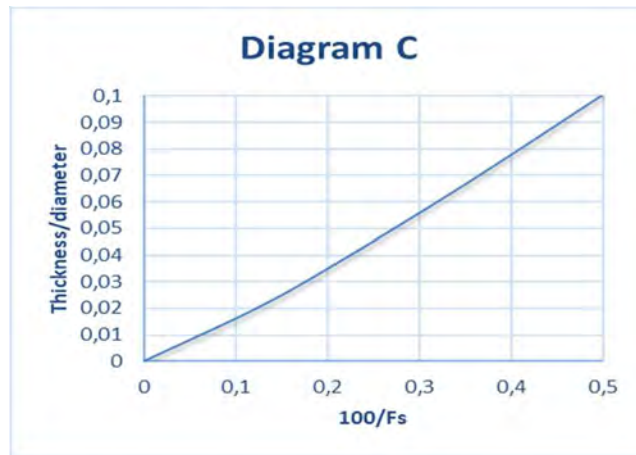


Fig. 1.12 Diagram C: Computation of minimum thickness of the aside (Geronimi master thesis).

4. In the end it is possible to evaluate the increase of security if the tree is pruned. This effect can be seen following the diagram D (Fig. 1.13). To is worth noting what represent the values of the graph:
  - ii. 1,2,3,4 represents the typology of the tree in base of the crown;
  - iii. A, B, C, D represent an interval of 2m in the height of the tree.

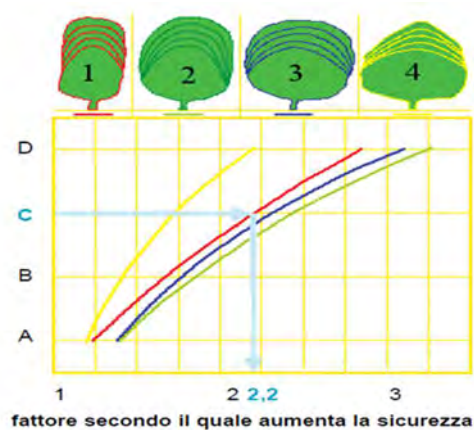


Fig. 1.13 Diagram D: Increasing of the safety factor (Geronimi master thesis).

### 1.2.5 DRE – Dynamic Root Evaluation

Dynamic Root Evaluation is a new method developed in last years and currently the most advanced commercial system is Dynaroot by Fakopp (Bejo et al, 2017). It permits to obtain a dynamic model of the safety in the real condition of the field because permits to register the real wind conditions, thanks to the installation of anemometers (Fig. 1.14).

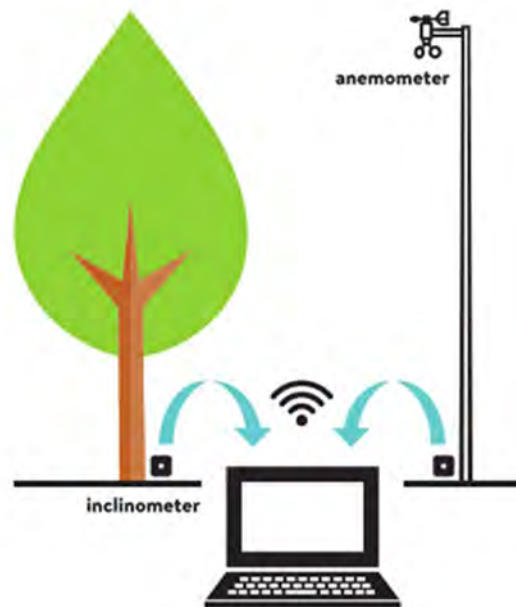


Fig. 1.14 Components of the Dynaroot system (Fakopp instructions manual).

When wind blows up to 25÷30km/h the system is activated and starts to register data of inclination of the root plate. Data are recorded for at least 3 hours. Then they are transferred into Dynaroot software that can calculate the safety factor.

The wind velocity is converted into wind pressure trough the expression:

$$p_w = \frac{\rho_{air}}{2} \cdot v_{wind}^2$$

Wind pressure is related with the inclination (Fig. 1.15):

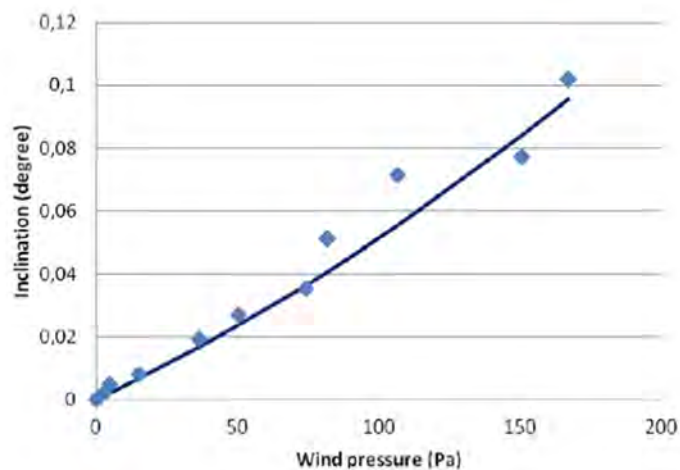


**Fig. 1.15 Graph Inclination – Wind pressure (Fakopp instructions manual).**

Safety factor is computed starting from this relationship. In this case is not used a force (wind force) in order to compute the safety factor but a pressure. The consequence is that the obtained factor cannot be compared to the one found using the classic static pulling test.

The problem of this method is that there is not a direct correlation between the wind intensity and the immediate, moment by moment, response of the tree, as shown in Fig. 1.16. Even if it were possible to find a correlation between wind pressure and inclination, as the graph in Fig. 1.16 shows, there is not a simple direct relation between wind pressure and inclination of the tree. So, to use the DRE method, a further step is necessary, as it will be shown in the following parts.

The behaviour of a tree in the wind is sensitive to the real conditions in nature. Small differences in initial conditions yield change largely the results for dynamic system. Trees are complex structures of a trunk and network of branches, twigs and leaf that change conditions during time. This situation reacts in an unpredictable manner to loading. Even wind changes over time, because can change direction and intensity. Sometimes there are more gusts than another time. It is easy to understand that the variation of initial conditions changes results. It is impossible to predict the behaviour of such system on the long run.

A definite relation between wind load and inclination exists, but it is a complex relation, it is not of immediate cause and effect.

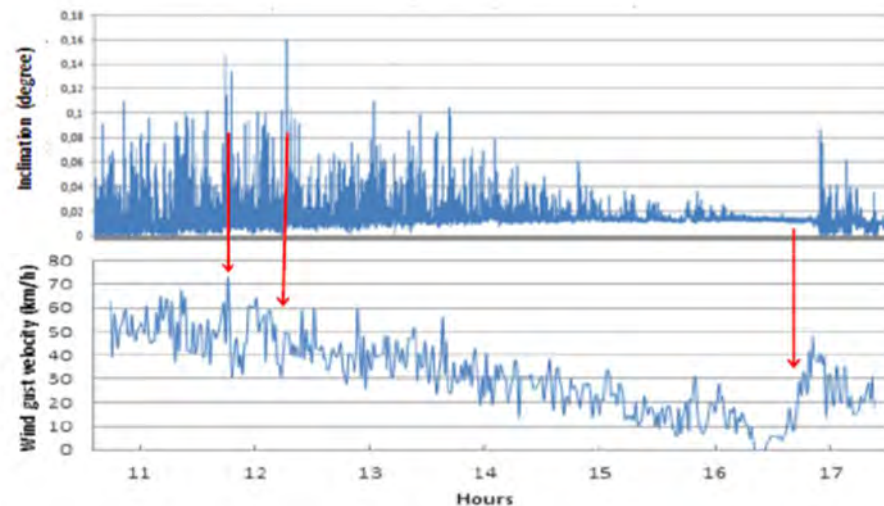


**Fig. 1.16 Two time series plot of inclination and wind velocity (Fakopp instructions manual).**

As it is possible to understand, the indirect correlation is given by the fact that for a pick of inclination corresponds a pick also in wind gust velocity, while for a successive pick in inclination does not correspond a pick in wind velocity. As consequence all the data has to be analysed more precisely.

The way to evaluate a system like this is the use of statistical parameters of the data taken over longer intervals. It means that there is no relationship at a given fixed moment, but there is relationship between the averages of wind intensity and inclination over a longer interval. Dynaroot works with these statistical parameters.

The advantage of using this method is that it offers inclination measurements under real life wind load conditions, which is a better approximation of the actual situation that eventually leads to the uprooting of a tree.

In the case of Dynaroot method the computation of safety factor is similar to the SIM, the difference is that are considered pressures instead the forces. The reason of this choice is to be reached in the nature of the

## Chapter 1 - Tree stability: a review

---

method, because in this case are not applied loads to the tree, but only wind pressure.

The comparison, as consequence, must be done between the maximum wind load registered in site and the wind load associated in a certain time interval.

Let's see the computation:

$$SF = \frac{M_{max}}{M_{wind}} = \frac{F_{max} \cdot H_b}{F_{wind} \cdot H_b}$$

But in Dynaroot case:

$$F_{max} = A \cdot p_{max} \cdot c_w$$

Remembering that:

1.  $c_v$  is a dimensionless gust factor, dimensionless value;
2.  $p_{max} = \frac{\rho_{air}}{2} \cdot v_{wind,max}^2$  is the pressure of the maximum wind speed registered in the site in  $[N/m^2]$ ;
3.  $A$  is the crown of the tree, in  $[m^2]$ .

Particular wind force is computed by:

$$F_{wind} = A \cdot p_{wind} \cdot c_w$$

Remembering again that  $p_{wind} = \frac{\rho_{air}}{2} \cdot v_{wind}^2$ .

Now the safety factor is computed:

$$SF = \frac{M_{max}}{M_{wind}} = \frac{F_{max} \cdot H_b}{F_{wind} \cdot H_b} = \frac{A \cdot p_{max} \cdot c_w \cdot H_b}{A \cdot p_{wind} \cdot c_w \cdot H_b}$$

Where  $H_b$  is again the barycentre of the plant.

Finally, it is easy to understand the reason why in the case of Dynaroot method is preferred to use the wind pressure:

$$SF = \frac{p_{max}}{p_{wind}}$$

As seen in Sani 2017, despite the fact that the first works date back to several decades ago, the Dynamic Root Evaluation are still in the embryonic phase of study and are therefore very different from each other according to the evaluation criterion adopted.

### **1.3 The methods: conclusions**

In the last years different methods of tree stability evaluation are developed to improve the knowledge of the matter and the accuracy of the results. The tree stability is, in fact, a complex topic and only in the last decades its study has started and developed, so several studies and proposals are currently underway to apply new evaluation methods or to improve existing ones. The applications of the different methods depends, also, on the particular tree problem and it is not always possible to apply the same method for all trees, for reasons of time and costs too.

Objectively, one of the most difficult aspects to evaluate is the anchoring capacity of trees to the ground because the root systems are underground and, therefore, difficult to analyse directly. The main method used to value the root stability of a tree is the SIM – Static Integrated Method (*pulling test*), because it is often the only one known and currently there are not other alternative methods with the same reliability and repeatability.

As shown in the following chapters, this is why this study focused on pulling test, because a possible improvement in this method could be of great help to better understand the stability of trees.

## References

- AIDTPG (2015). Linee guida per la gestione dei patrimoni arborei pubblici (nell'ottica del Risk Management). Associazione Italiana Direttori e Tecnici Pubblici Giardini, Editoriale Sometti (Mantova), 66p.
- Blackwell PG, Rennolls K, Coutts MP (1990) A root anchorage model for shallowly rooted Sitka spruce. *Forestry* 63:73–91. <https://doi.org/10.1093/forestry/63.1.73>
- Bejo, L., Divos, F., & Fathi, S. (2017). Dynamic root stability assessment-basics and practical examples. General Technical Report-Forest Products Laboratory, USDA Forest Service, (FPL-GTR-249), 270-277.
- Cao J, Tamura Y, Yoshida A (2012) Wind tunnel study on aerodynamic characteristics of shrubby specimens of three tree species. *Urban For Urban Green* 11:465–476. <https://doi.org/10.1016/j.ufug.2012.05.003>
- Coutts, M. P. (1983). Development of the structural root system of Sitka spruce. *Forestry: An International Journal of Forest Research*, 56(1), 1-16.
- Dattola G., Ciantia M. O., Galli A., Blyth L., Zhang X., Knappet J. A., Castellanza R., Sala C., Leung A.K., (2019) – A macroelement approach for the stability assessment of trees. *Lecture Notes in Civil Engineering*, 40, pp. 417-426.
- Dupuy L, Fourcaud T, Stokes A (2005) A numerical investigation into the influence of soil type and root architecture on tree anchorage. *Plant Soil* 278:119–134. <https://doi.org/10.1007/s11104-005-7577-2>
- Gromke C, Ruck B (2008) Aerodynamic modelling of trees for small-scale wind tunnel studies. *Forestry* 81:243–258. <https://doi.org/10.1093/forestry/cpn027>
- Guitard DGE, Castera P (1995) Experimental analysis and mechanical modelling of windinduced tree sways. In: Coutts MP, Grace J (eds) *Wind and trees*: 182–194. <https://doi.org/10.1017/cbo9780511600425.010>
- Lonsdale, D. (2007). Current issues in arboricultural risk assesment and management. *Arboricultural Journal: The International Journal of Urban Forestry* 30: 163-174.
- Mattheck, C., and Breloer, H. (1994). *The body language of trees: a handbook for failure analysis*. HMSO Publications Centre.



- Mattheck, C., and Breloer, H. (1998). La stabilità degli alberi. Fenomeni meccanici e implicazioni legali dei cedimenti degli alberi. Il Verde Editoriale, 281 p.
- Motta R., Ascoli D., Corona P., Marchetti M., Vacchiano G. (2018). Selvicoltura e schianti da vento. Il caso della “tempesta Vaia”. *Forest@ - Rivista di Selvicoltura ed Ecologia Forestale*, 15, 94-98. doi: <https://doi.org/10.3832/efor2990-015>
- Pollen N, Simon A (2005). Estimating the mechanical effects of riparian vegetation on stream bank stability using a fiber bundle model. *Water Resour Res* 41:1–11. <https://doi.org/10.1029/2004WR003801>
- Ruel J (2000) Factors influencing windthrow in balsam fir forests: from landscape studies to individual tree studies. *For Ecol Manag* 135:169–178
- Sani, L. (2017). *Statica delle strutture arboree*. Gifor, ISBN-13: 979-1220016698, 945 p.
- Sellier D, Fourcaud T (2009) Crown structure and wood properties: influence on tree sway and response to high winds. *Am J Bot* 96:885–896. <https://doi.org/10.3732/ajb.0800226>
- Schwarz M, Cohen D, Or D (2010) Root-soil mechanical interactions during pullout and failure of root bundles. *J Geophys Res Earth Surf* 115:1–19. <https://doi.org/10.1029/2009JF001603>
- Siegert, B. (2013). Comparative analysis of tools and methods for the evaluation of tree stability: results of a field test in Germany. *Arborist News* 2013 Vol.22 No.2 pp.26-31 ref.1. ISSN: 1542-2399, International Society of Arboriculture.
- Sterken, P. (2006). Prognosis of the development of decay and the fracture-safety of hollow trees. *Arboricultural Journal*, 29(4), 245-267.
- Van Wassenae, P., & Richardson, M. (2009). A review of tree risk assessment using minimally invasive technologies and two case studies. *Arboricultural Journal*, 32(4), 275-292.
- Yang M, Défossez P, Danjon F, Dupont S, Fourcaud T (2017) Which root architectural elements contribute the best to anchorage of Pinus species? Insights from in silico experiments. *Plant Soil*, 411:275–291. <https://doi.org/10.1007/s11104-016-2992-0>
- Yang M, Défossez P, Danjon F, Fourcaud T (2014) Tree stability under wind: simulating uprooting with root breakage using a finite element method. *Ann Bot* 114:695–709. <https://doi.org/10.1093/aob/mcu122>

## Chapter 1 - Tree stability: a review

---

- Yang M, Défossez P, Danjon F, Fourcaud T (2018) Analyzing key factors of roots and soil contributing to tree anchorage of Pinus species. *Trees - Struct Funct* 32:703–712. <https://doi.org/10.1007/s00468-018-1665-4>
- Zhang, X., Knappett, J.A., Leung, A.K. et al. Small-scale modelling of root-soil interaction of trees under lateral loads. *Plant Soil* (2020). <https://doi.org/10.1007/s11104-020-04636-8>
- Wessolly, L, and M. Erb. (1998). *Handbuch der Baumstatik und Baumkontrolle*. Patzer, Berlin.

## Chapter 2

### Pulling tests results: some considerations

#### 2.1 Introduction

Pulling tests are the most used by agronomists in order to determine the root stability of the trees, because can provide easily and directly if a tree is safe or if it is dangerous. This is possible thanks to the nature of the test, because it provides a direct safety factor with some cheap computation.

A thorough analysis can be performed in every situation that a tree is pulled out: lots of example can be provided. In this way a database of 108 tests is analysed. In the following some results of that, which data given by Agro Service.

In order to have a certain number of tests and therefore good statistical results, different elaborations are done to all the data. First of all, the SIM was applied, so, starting from the registered forces, the bending moment is computed for each inclination step. From this, it is possible to carry out bending moment-rotation curve for every test. Then the maximum wind moment is computed and, using the safety factor provided by the data, it is possible to find also the maximum bending moment that the tree can support. Since safety factor is already computed by agronomists, it is not necessary to apply Wessolly's equation for every single test, even if, in seek of clarity, sometimes it is computed in order to have a comparison between data and own results. Once all principal results are carried out, it is possible to make some consideration about that. In this way time step for each test is computed using the same procedure and consequently load rate and inclination rate are soon found.

In the next chapter some example of tests will be presented. Because of the huge number of graphs, it is impossible to insert every single result, therefore a selection is necessary. All pulling tests results are available in the attachments.

## 2.2 Performed pulling tests

### 2.2.1 Applied method and instruments

During this study, several pulling tests were run on real scale trees, following the loading scheme shown in previous chapter. They were conducted according with a “standard” non-destructive approach, consisting in a single loading phase on relatively large diameter trees, not exceeding a rotation of about  $0.2^\circ$ . The tests were controlled by professional agronomists of Agro Service S.r.l. and they were stopped before inducing irreversible damages to the trees. For the sake of clarity, a picture of the experimental set up of Test A in via Pellettier in Monza is shown below (Fig. 2.1), summarizes the tree typologies and the main geometrical characteristics for all the tests.



Fig. 2.1 Experimental set up of Test A in via Pellettier, Monza.

The load was applied for all test by means of a manual winch and measured by a commercial load cell (maximum capacity 5 tons; Fig. 2.2), whilst rotations of the trees where measured by means of a commercial small scale inclinometer (measurement range  $\pm 2^\circ$ ; resolution  $0.001^\circ$ ; Fig. 2.3).

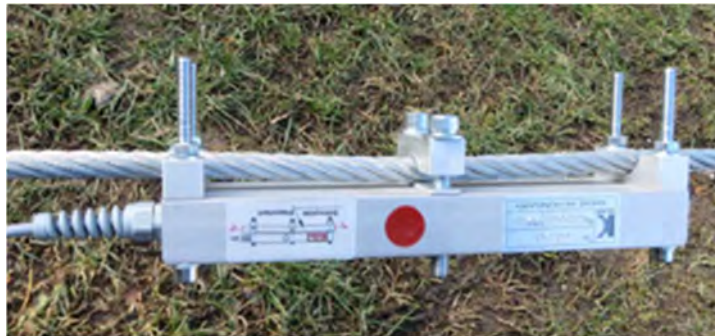


**Fig. 2.2 Adopted instrumental equipment for pulling test: load cell.**



**Fig. 2.3 Adopted instrumental equipment for pulling test: small scale inclinometer (Fakopp, 2020).**

## 2.2.2 Results report

After that each pulling test has carried out and relative data are elaborated, the results are shown in a report as shown in following figures. In particular below (Fig. 2.4) there is a photo of the tree analysed and a

## Chapter 2 - Pulling tests results: some considerations

graph with the data recorded by the individual sensors (dynamometer, inclinometers and elastometers, if used).

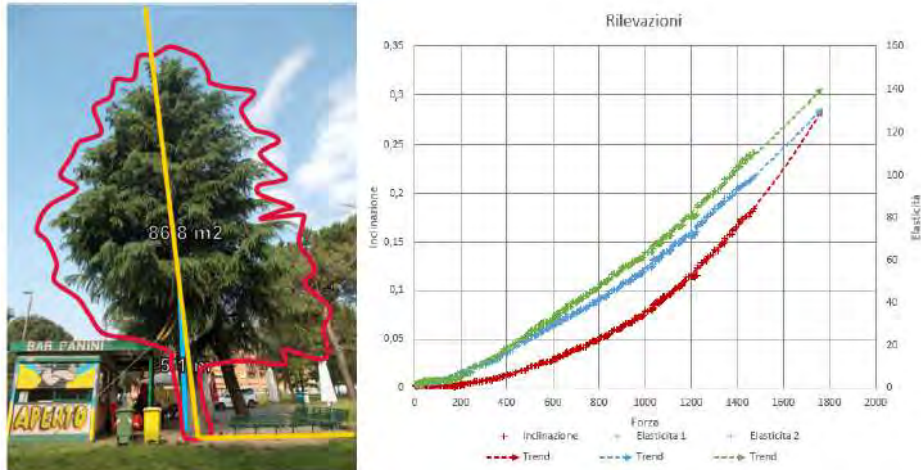


**Fig. 2.4 Image and graph of one of the pulling tests carried out in Parco via Togliatti, Rho.**

After that, the specific curve of the inclination reached by the plant in relation to the applied force is shown, as well as the safety factor (SF) and the data used to calculate it (Fig. 2.5).

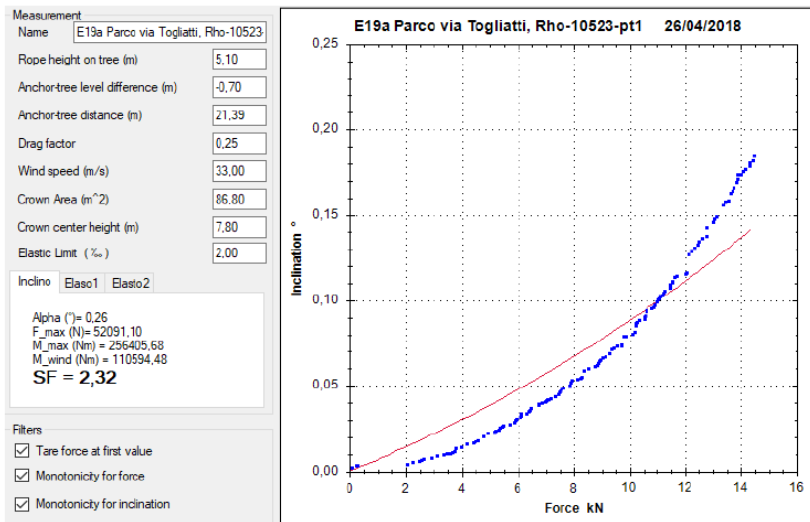


**Fig. 2.5 Data, SF and graph about inclinometer of one of the pulling tests carried out in Parco via Togliatti, Rho.**

Finally, the last graph shows the same results relating to the elongation of the fibers recorded by one of the elastometers applied, if used (Fig. 2.6).

The number of graphs shown in the report depends on the number and type of sensors used during the pulling test (1 or 2 inclinometers and possibly 2 elastometers).

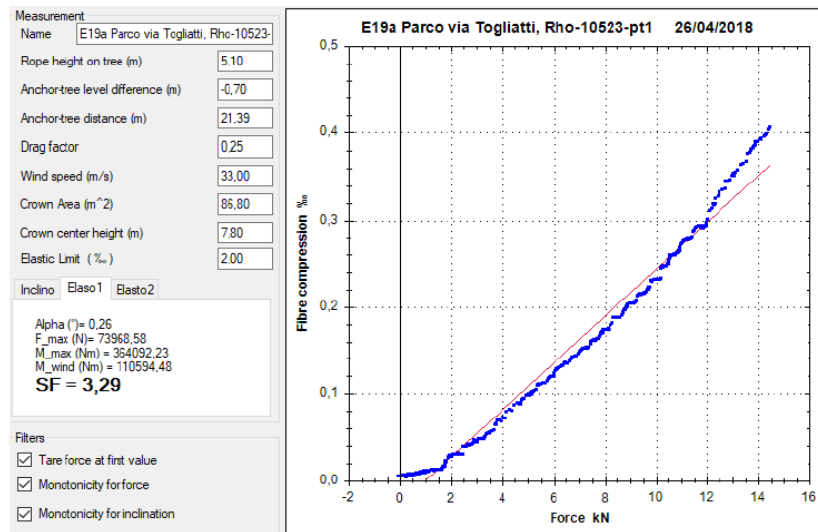


Fig. 2.6 Data, SF and graph about elastometer of one of the pulling tests carried out in Parco via Togliatti, Rho.

## 2.3 The results

### 2.3.1 Moment-inclination curve

In this first section moment-inclination curves will be presented. It is important to say how the work is organised. All the tests are divided into the place where trees are located, in this way is possible to compare the terrain properties, where known, that are similar each other, as shown further. Then a final moment-inclination curve is carried out with all the plants that are placed in that area. The starting point is the formula:

$$M = H \cdot F \cdot \cos(\alpha)$$

## Chapter 2 - Pulling tests results: some considerations

Where:

1.  $F$  is the force applied by the winch on the rope, transformed in  $[N]$  from  $[kg, force]$ :  $N = 9.81 \cdot Kg, force$ ;
2.  $H$  is the height where the rope is installed, expressed in  $[m]$ ;
3.  $\alpha$  is the angle of inclination of the cable, computed by the formula:  
 $\alpha = \tan^{-1}\left(\frac{H}{L}\right)$ , where  $L$  is the distance between tree and the fixed point where the rope is installed, it is in  $[m]$ ;
4.  $D$  is the distance between the analysed tree and fixed point in  $[m]$ .

First of all, the table with tree characteristics is shown, in order to have a good view of the properties of the tests (Tab. 2.7).

Tree Data	Novate 1	Novate 2 pt.1	Novate 2 pt.2	Novate 3 pt.1	Novate 3 pt.2	Novate 4	[u.o.m]
H_rope	7,00	6,50	6,50	5,50	5,50	2,70	m
$\Delta$ _h	0,90	1,10	0,10	0,00	0,60	0,20	m
D	19,92	14,23	9,48	9,48	19,07	16,67	m
Cw	0,25	0,25	0,25	0,25	0,25	0,25	
v	33,00	33,00	33,00	33,00	33,00	33,00	m/s
A	57,60	68,00	95,90	95,60	148,70	13,80	m <sup>2</sup>
H_bar	9,00	9,50	10,10	10,10	10,80	4,10	m
H_rope- $\Delta$ _h	6,10	5,40	6,40	5,50	4,90	2,50	m
Hypotenuse	20,83	15,22	11,44	10,96	19,69	16,86	m
$\alpha$	0,30	0,36	0,59	0,53	0,25	0,15	rad
$\rho$	1,23	1,23	1,23	1,23	1,23	1,23	kg/m <sup>3</sup>
F_wind	9604,98	11339,21	15991,62	15941,60	24796,19	2301,19	N
M_wind	86444,82	107722,52	161515,41	161010,15	267798,85	9434,89	Nm

**Tab. 2.7 Properties of the tests.**

All the voices are the same as the previous case, consequently the legend is not present in this section.

Then the graphs are shown.



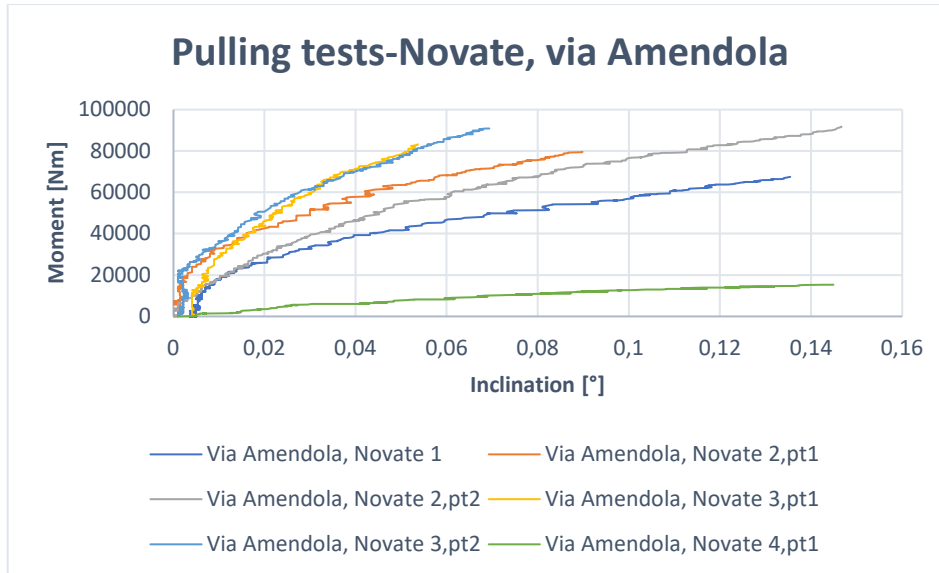


**Fig. 2.8 Pulling tests for plants sited in Novate Milanese.**

In this picture tests from Novate Milanese are present (Fig. 2.8). As it is possible to understand, moment and inclination for the first five tests are similar in the very beginning, where the slope of the curves are equal. This is possible if the stiffness of the plants is similar between them, as it will be shown later.

Another important consideration that can be made from the graph is the fact that the direction of the test is important. Even if two different tests are made on the same plant, as the case of tests number 2, divided into part one and part two, made on the same tree, the results in terms of maximum bending moment are different and, as consequence, also in terms of safety factor. Therefore, it is easy to understand that a tree is more hazardous in a direction than in another one. Moreover, the danger also depends on where the wind blows and it would be interesting to correlate it with the direction of pull. However the directions have not been considered in this work because, although there are always prevailing winds, in a given site it is difficult to estimate where the wind blows from because it can arrive from different directions and in an irregular way, for meteorological reasons, terrain conformation and presence of obstacles (i.e. mountains, buildings, other trees, etc.). Therefore it is considered more significant in terms of the danger of one direction than another where structural defects

## Chapter 2 - Pulling tests results: some considerations

are located on the tree (i.e. inclination of the stem, raised or damaged roots, wood degradation, etc.). In fact, the direction in which the pulling tests are carried out is chosen mainly on the basis of the defects detected by the visual analysis and the relative direction of the most probable fall, unless there are obstacles that prevent their execution.

Considerations about tree typology cannot be done with a few numbers of tests, even if there is test number 4, presented above, is very different from the other. This is a cypress, as the first one, the other two are cedars. Looking only the shape of the curve, one can take the conclusion that it is a dangerous tree because reaches high inclinations with a low bending moment, but, compared with wind velocity, this conclusion is false. In fact, the safety factor of this tree is about 6.42.

Pulling tests does not consider the terrain properties and only partially the typology of the tree. As seen, it is a deterministic model that acts with an external load, as wind. An analysis like this one explains this fact, because the curve shows the difference between different plants in a similar terrain. As consequence the differences between shapes and a final maximum bending moment depend only on the state of the plant, meant as response to wind load, and the direction of the load.

Lots of example can be done considering the tests done. In the following some tests coming from San Donato Milanese are taken. In the specific this is a rich set of data, with 12 different tests on different typologies of tree.

Again, as first part all the characteristics of the tree are taken into account (Tab. 2.9).

Tree Data	D11-55 pt.1	D11-55 pt.2	D11-56	D11-57	D11-58	D11-59	D11-63	D11-64	D11-65	D11-66	D11-83	D11-84	[u.o.m]
H_ropce	4,00	4,00	4,00	4,00	2,20	4,70	4,50	4,40	5,00	4,60	4,00	3,90	m
$\Delta$ _h	0,00	0,00	0,00	0,00	0,00	0,00	0,00	0,00	0,00	0,00	0,00	0,00	m
D	13,65	17,36	21,56	21,77	20,50	21,60	18,50	18,03	15,88	18,82	18,97	18,25	m
Cw	0,20	0,20	0,30	0,30	0,30	0,30	0,25	0,25	0,25	0,25	0,25	0,25	
v	33,00	33,00	33,00	33,00	33,00	33,00	33,00	33,00	33,00	33,00	33,00	33,00	m/s
A	73,00	77,00	69,00	66,00	83,00	98,00	100,00	110,00	140,00	136,00	89,00	97,00	m <sup>2</sup>
H_bar	5,40	5,40	6,60	7,30	9,00	8,30	7,00	8,50	9,30	7,80	8,00	7,90	m
H_ropce- $\Delta$ _h	4,00	4,00	4,00	4,00	2,20	4,70	4,50	4,40	5,00	4,60	4,00	3,90	m
Hypotenuse	14,22	17,81	21,93	22,13	20,62	22,11	19,04	18,56	16,65	19,37	19,39	18,66	m
$\alpha$	0,29	0,23	0,18	0,18	0,11	0,21	0,24	0,24	0,31	0,24	0,21	0,21	rad
$\rho$	1,23	1,23	1,23	1,23	1,23	1,23	1,23	1,23	1,23	1,23	1,23	1,23	kg/m <sup>3</sup>
F_wind	9738,38	10271,99	13807,16	13206,85	16608,61	19610,17	16675,31	18342,84	23345,44	22678,43	14841,03	16175,05	N
M_wind	52587,27	55468,76	91127,25	96409,99	149477,50	162764,39	116727,19	155914,17	217112,57	176891,72	118728,23	127782,92	Nm

**Tab. 2.9 Properties of the tree under tests-San Donato Milanese, Tevere square.**

This table shows the characteristics of the plants that are tested. In the following graph the corresponding bending moment correlated with the inclination is presented (Fig. 2.10).

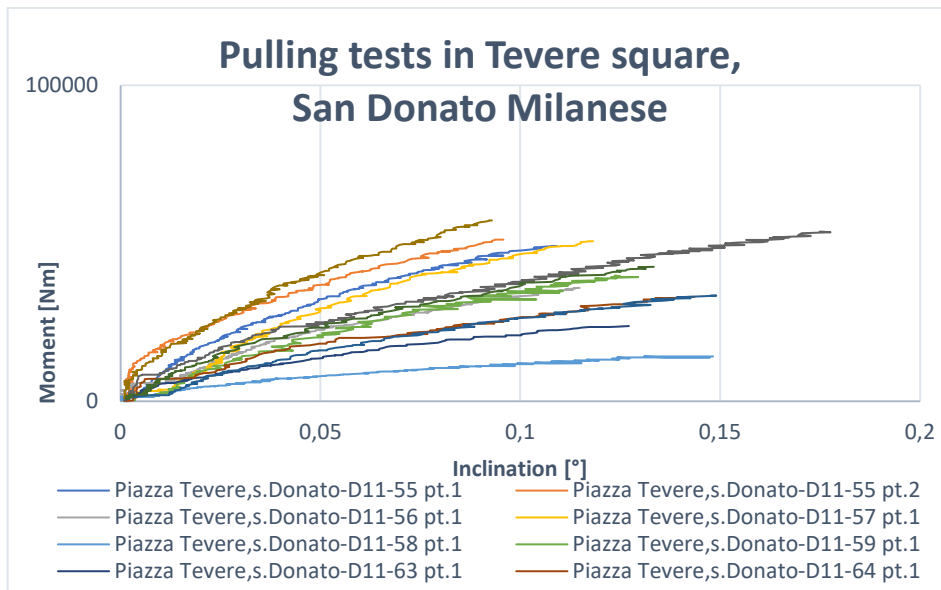


**Fig. 2.10 Pulling tests for plants sited in San Donato Milanese**

The shapes of the curves are always similar. Moreover, the values of inclination are equal to the previous example, even if the values of bending moments are a little bit lower than the previous. This can be explained as a difference in the external conditions in the tests and in the terrain.

There are not remarkable differences between the two set of tests, therefor the precedents considerations can be done also in this case. As it can be seen, also in this case the slope of the curves in the first part of the tests are very similar between them. Consequently, it is possible to affirm that the stiffness of the trees is related to the terrain. This can be a conclusion that comes from the fact that are tested different trees of different typologies in the same area, with the same terrain characteristics. The similar stiffness of trees of the same set, different from the stiffnesses of the first set, can depends from the terrain.

## Chapter 2 - Pulling tests results: some considerations

In order to have an overview of all the tests, in the following the final graph with every bending moment-inclination curve is presented (Fig. 2.11). It is difficult to read this type of graph, but it is presented only in seek of completeness and to have a general view of the results.

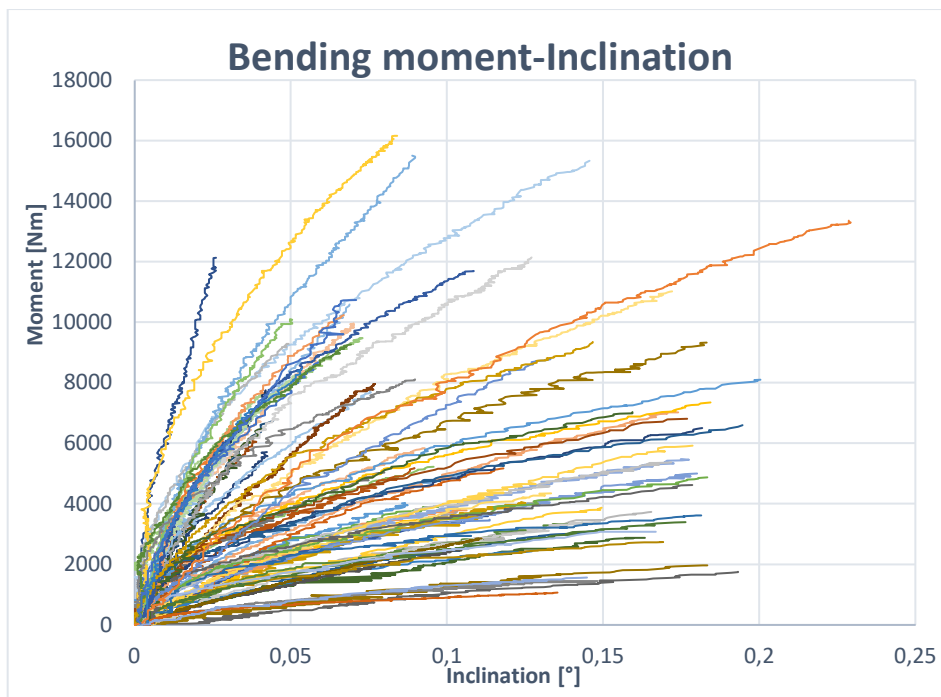


**Fig. 2.11 Bending moments-inclination curve for all the tests performed.**

This graph represents a general view of the shape of all the curves that are founded performing pulling-out tests. This is not a good solution to understand the problem, but it is important make some consideration.

First of all, every test presents a different shape from the other, therefor, each plant has an own behaviour with different properties, maximum bending moment and stiffness. It is not possible to make a general conclusion about safety; every plant has to be studied individually.

A second consideration is about bending moments values. Each test performed reaches different values of bending moments and consequently inclination. This is normal because of the different characteristics of the plants; every plant has a specific geometry and they are all different.

Moreover, as seen, moment changes also between directions of traction, therefor a unique shape will not reach.

However, a function that interpolates all the curves can be founded, as shown in the next chapter. It is different from Wessolly's one, because this one is an experimental curve that has not a mathematical origin that can works for found maximum bending moment and, consequently, safety factor, but cannot works in an engineering point of view.

### 2.3.2 Safety factor

The available data are completed with bending moment, inclination and safety factor. Safety factor comes from the ratio between maximum bending moment, computed by the operators using Wessolly's formula, and the wind moment, computed using some parameter already seen. Wind moment comes from wind load multiplied by an arm defined by the distance between barycentre of the plant and the terrain. In the case of the software used, safety factor is computed using the forces and not moments. Therefore, the formula used is the following:

$$SF = \frac{F_{max}}{F_{wind}} = 2 \cdot \frac{F_{max}}{c \cdot \rho \cdot A \cdot v^2}$$

In this first part no more computations are done. Every result obtained is in default. This choice comes from the will of having a good representation and a linear work.

## Chapter 2 - Pulling tests results: some considerations

Test location	# test	FS	Test location	# test	FS	Test location	# test	FS
Via Amendola, Novate 2,pt2	1	2.27	Parco via Togliatti-E19a-10531	26	2.35	Piazza Tevere,s.Donato-D11-55 pt.1	52	4.94
Via Amendola, Novate 1	2	3.17	Parco via Togliatti-E19a-10532	27	1.22	Piazza Tevere,s.Donato-D11-55 pt.2	53	5.40
Via Amendola, Novate 3,pt2	3	2.60	Parco via Togliatti-E19a-10536	28	1.86	Piazza Tevere,s.Donato-D11-56 pt.1	54	1.88
Via Amendola, Novate 2,pt1	4	4.49	Parco via Togliatti-E19a-10537	29	1.17	Piazza Tevere,s.Donato-D11-57 pt.1	55	2.38
Via Amendola, Novate 3,pt1	5	4.69	Parco via Togliatti-E19a-10574	30	3.07	Piazza Tevere,s.Donato-D11-58 pt.1	56	0.40
Via Amendola, Novate 4,pt1	6	6.42	Boschetti Monza-339-9351-pt.1	31	4.63	Piazza Tevere,s.Donato-D11-59 pt.1	57	1.19
Bollate, via Mozart -1,parte 1	7	4.03	Boschetti Monza-339-9351-pt.2	32	5.20	Piazza Tevere,s.Donato-D11-63 pt.1	58	0.88
Bollate, via Mozart- 1,parte 2	8	5.16	Boschetti Monza-339-9368-pt.1	33	5.30	Piazza Tevere,s.Donato-D11-64 pt.1	59	0.81
Bollate, via Mozart-2,parte 2	9	3.61	Boschetti Monza-339-9368-pt.2	34	7.42	Piazza Tevere,s.Donato-D11-65 pt.1	60	0.83
Bollate, via Mozart-2,parte 2	10	3.00	Boschetti Monza-339-9400-pt.1	35	2.12	Piazza Tevere,s.Donato-D11-66 pt.1	61	1.76
Bollate, via Mozart-3,parte 1	11	4.18	Boschetti Monza-339-9400-pt.2	36	1.92	Piazza Tevere,s.Donato-D11-83 pt.1	62	1.12
Bollate, via Mozart-3,parte 2	12	2.84	Boschetti Monza-393-11150-pt.1	37	3.21	Piazza Tevere,s.Donato-D11-84 pt.1	63	1.36
sacra Famiglia-Cesano Boscone	13	1.39	Boschetti Monza-393-11151-pt.1	38	3.26	Rimini Anthea-165-31755 pt.1	64	3.42
Scavi via Reiss-295	14	2.14	Boschetti Monza-393-11152-pt.1	39	1.99	Rimini Anthea-165-31755 pt.2	65	4.08
Scavi via Reiss-297	15	1.69	Boschetti Monza-400-11869-pt.1	40	1.80	Rimini Anthea-165-31756 pt.1	66	4.57
Uni. Federico II,NA-1	16	1.04	Boschetti Monza-400-11874-pt.1	41	1.11	Rimini Anthea-165-31756 pt.2	67	5.00
Uni. Federico II,NA-2-pt1	17	1.45	Boschetti Monza-400-11874-pt.2	42	0.85	Rimini Anthea-17223-38790 pt.1	68	3.88
Uni. Federico II,NA-2-pt2	18	1.51	Boschetti Monza-400-11878-pt.1	43	2.34	Rimini Anthea-17223-38790 pt.2	69	4.54
Via della Fara,BG- 331-1386-pt1	19	2.63	Boschetti Monza-400-11878-pt.2	44	0.82	Rimini Anthea-17223-38792 pt.1	70	0.90
Via della Fara,BG-331-1386-pt2	20	2.54	Piazza Moneta,Cesano Boscone-2	45	0.98	Rimini Anthea-17223-38792 pt.2	71	1.21
Via Savona,Mi-1	21	2.17	Piazza Moneta,Cesano Boscone-3	46	0.78	Rimini Anthea-17223-38793 pt.1	72	2.15
Parco via Togliatti-E19a-10523	22	2.32	Piazza Moneta,Cesano Boscone-4	47	0.90	Rimini Anthea-17223-38793 pt.2	73	1.64
Parco via Togliatti-E19a-10524	23	1.63	Piazza Moneta,Cesano Boscone-5	48	1.06	Rimini Anthea-17223-38797 pt.1	74	1.90
Parco via Togliatti-E19a-10529	24	1.83	Piazza Moneta,Cesano Boscone-16	49	2.45	Rimini Anthea-17223-38797 pt.2	75	1.60
Parco via Togliatti-E19a-10530	25	2.60	Piazza Moneta,Cesano Boscone-17	50	3.03	Rimini Anthea-17223-38798 pt.1	76	1.03
			Piazza Moneta,Cesano Boscone-18	51	3.64	Rimini Anthea-17223-38798 pt.2	77	1.16

**Tab. 2.12 Safety factors for the performed tests.**

In the table above the safety factor of the tests are grouped (Tab. 2.12). This is a purely expositive choice made in seek of simplicity. In the following a trend of safety factor is presented in relation with the number of the test corresponding; moreover, an optimal safety factor is inserted in order to understand immediately if a plant is safety or not, because it is difficult to understand only looking at the table.

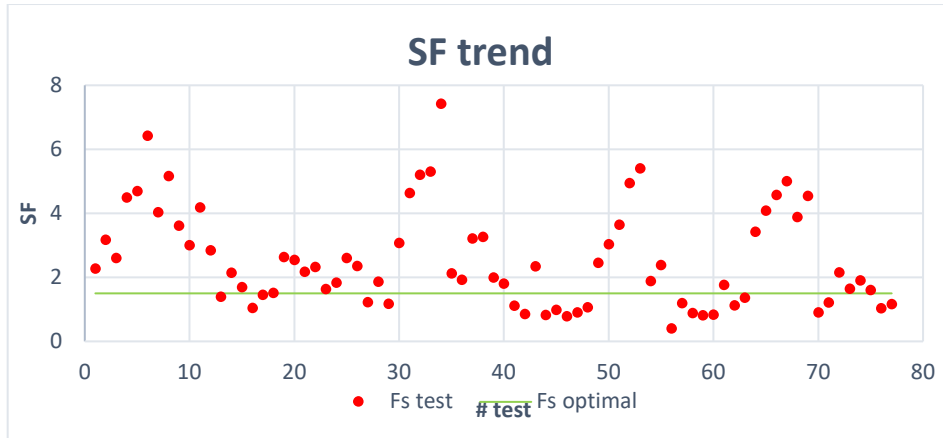


**Fig. 2.13 SF trend with test number and optimal safety factor.**

The graph above explains in a very visual analysis if a tree is safety or not (Fig. 2.13). The green line has the values of 1.5 and a tree with a lower safety factor is dangerous, while a higher value means that it is safe:

$$SF < 1.5 \rightarrow \text{dangerous tree}$$

$$SF > 1.5 \rightarrow \text{safe tree}$$

The theoretical Fs would be 1, but the value of 1.5 is a standard value fixed by experience and safety, considering some uncertainties in data recording and assignment of parameters in the calculations.

However, it is not secure that it is the right value and a tree that, for instance, has a SF=1.7 will not overturn, every case must be studied in deep.

In this case some tree is not in safe zone, the idea is that these trees must be cut, especially if they are located in public park, and can represent a hazard for the security of the people.

Other analysis with safety factor can be performed. One of them considering the distribution of them in relation with the species of trees. This operation is the following: the safety factors are been divided in ranges and grouped for the different species of trees, in order to try to find some statistical conclusion. The starting point is that some of the tests analysed reports also the typology of that particular tree and some

## Chapter 2 - Pulling tests results: some considerations

consideration about that can be done considering the safety factor. In this case the analysis is done excluding the place where the tree is located.

For the analysis are considered some species of trees, obviously those that are known from given data, and all trees of that species are grouped. Successively, safety factors are divided into six ranges:

1. Group of  $0 < SF < 1$ ;
2. Group of  $1 < SF < 2$ ;
3. Group of  $2 < SF < 3$ ;
4. Group of  $3 < SF < 4$ ;
5. Group of  $4 < SF < 5$ ;
6. Group of  $SF > 5$ .

Once the safety factors are divided, the plants for each species are counted in order to find the real number of plants for each range. The final trends are the following (Fig. 2.14; Fig. 2.15):

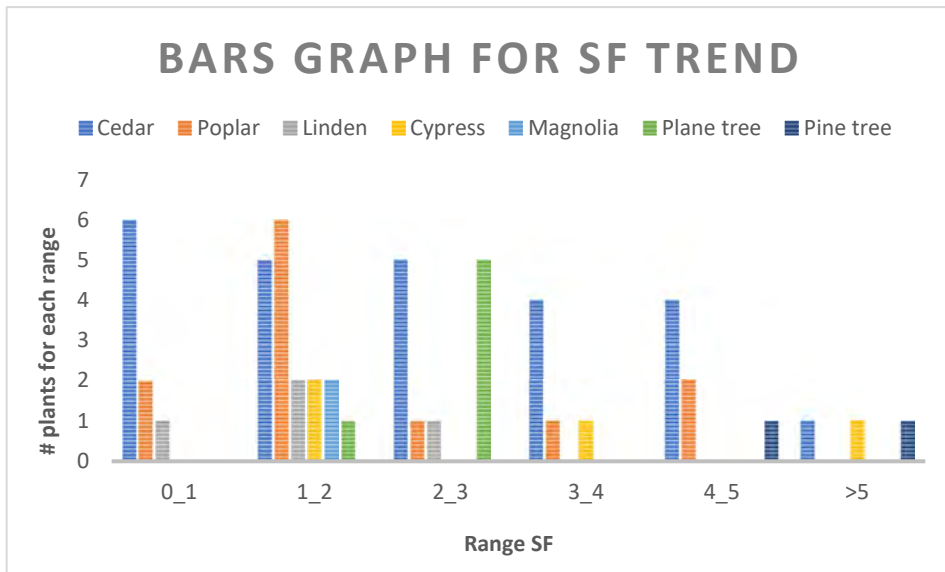


**Fig. 2.14** Bars graph that represents the trend of safety factor considering the species of trees.



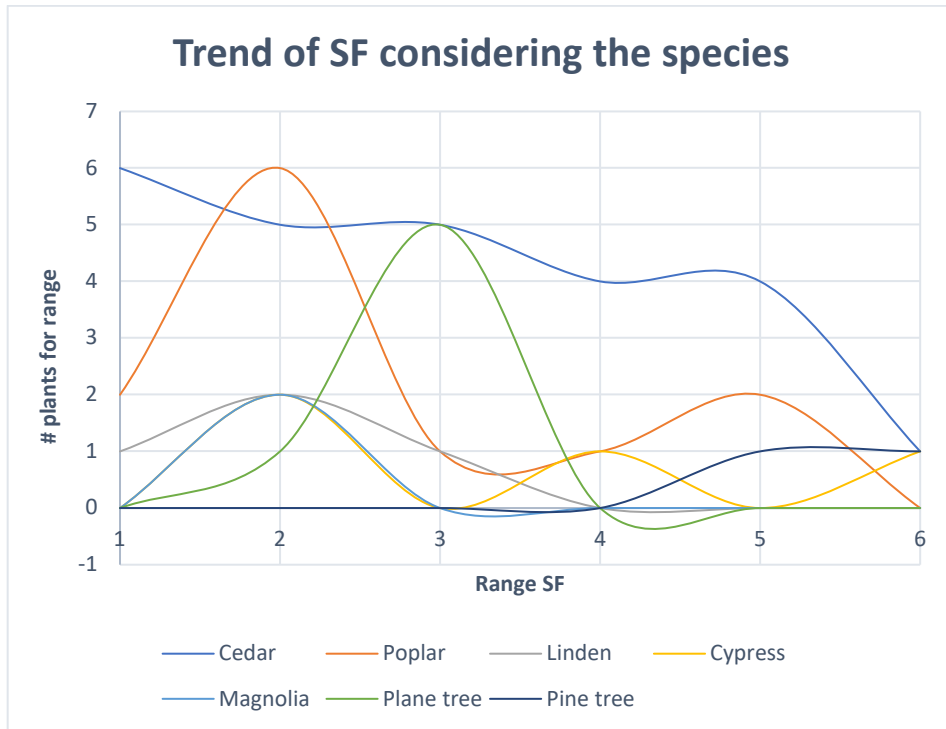


**Fig. 2.15 Distribution of Fs for each species.**

The two graphs want to represent the same thing in two different modes. The first one (Fig. 2.14) is better for the purpose of this work, because it groups the number of trees for each species, but the second one (Fig. 2.15) permits to observe an eventual shape of the curve. Observing the figures, from a statistical point of view not many considerations can be done. Only plane tree, orange curve, and lindens, green curve, assume shapes that can be considered as Gaussian's curves. Also red curve can be related to Gaussian curve, but in the last range it increases again. The other three are regular. Cedars decreases with higher safety factors. This fact can represent the fact that this specie is dangerous to be plant in public areas, because in the first range,  $0 < F_s < 1$ , there is a huge number of trees. The safest specie in these tests is pine tree, that sees an increasement with higher safety factor.

The same thing can be performed also dividing trees for zone where they are located, maintaining the same ranges already explained. In this

## Chapter 2 - Pulling tests results: some considerations

case only the two zones used in the previous chapter and another set of tests are taken:

- Novate Milanese, Amendola way;
- San Donato Milanese, Tevere square;
- Bollate, Mozart way.

The results are the following (Fig. 2.16):

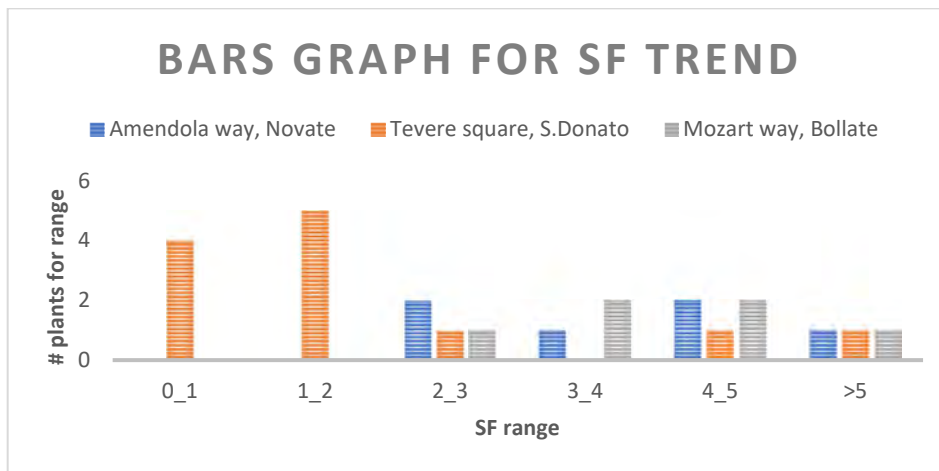


**Fig. 2.16** Bars graph that represents the trend of safety factor considering the zone of location.

Trees located in Tevere square, red bars, are dangerous. In fact, they have a low safety factor. Trees in Amendola way are safer than the other. Green bars, Mozart way's set of tests, have a Gauss shape, and they are safer than the other two sets. This consideration can make think that safety factor is conditioned also by the terrain; this fact must be considered in the next parts.

### 2.3.3 Load rate and inclination rate

Up to now the results were found directly from data with some further computation and consideration. In this section are presented useful information about load rate and inclination rate. Time is the fundamental

part of this computation, therefore it is used as the previous chapter. Time is divided into steps; one step is the length of time between the application of two successive loads. This operation permits to find the real duration of the test in seconds and it is easier to make the computations.

Bending moments, now, are related with time of application and the result is a graph with a linear curve. The load rate is the angular coefficient, slope, of the line that interpolates the curve:  $m = \frac{M}{t}$ , where:

1.  $M$  is the bending moment expressed in  $[kNm]$ ;
2.  $m$  is the angular coefficient, so the load rate, expressed in  $[kNm/s]$ ;
3.  $t$  is the time, expressed in  $[s]$ .

The same thing can be done also for inclination. The procedure is equal to which is used with moment, but in this case are considered inclinations and not bending moments. Therefore,  $i = \frac{\theta}{t}$ , where:

1.  $\theta$  is the inclination of the tree, expressed in  $[^\circ]$ ;
2.  $m$  is the angular coefficient, so the inclination rate, expressed in  $[^\circ/s]$ ;
3.  $t$  is the time, expressed in  $[s]$ .

In search of simplicity are reported here the results for the previous example, so Amendola way in Novate M.se and Tevere square in S. Donato M.se (Fig. 2.17).

Starting from the first reported example, let's see the results: in the first part only load rate is considered with some considerations, then also inclination rate will be presented only by a graphical point of view, because conclusions are similar.

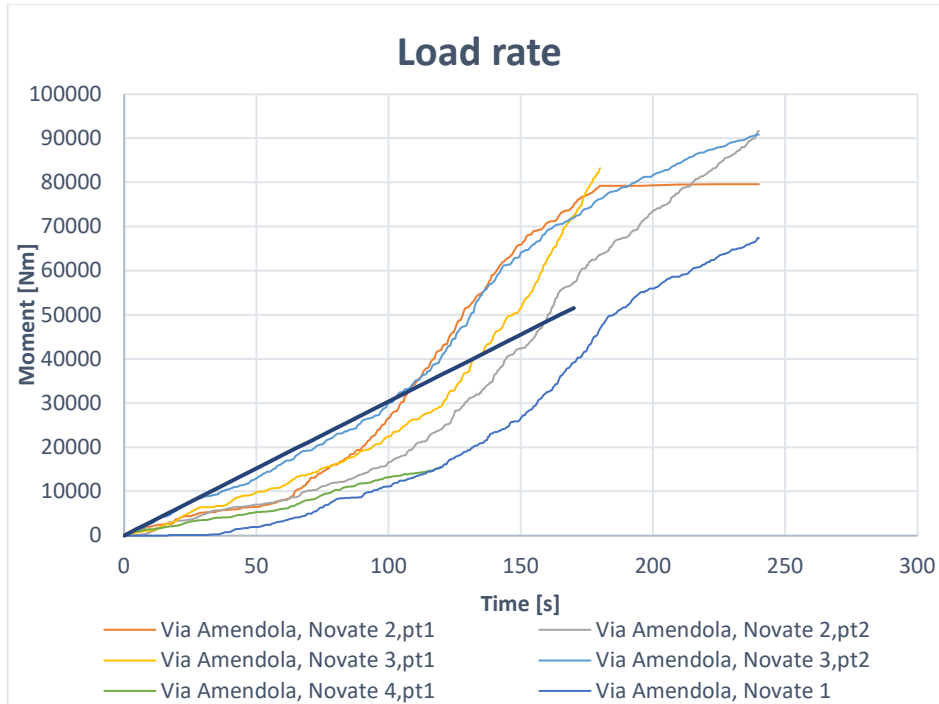


**Fig. 2.17** Load rate graph for example of via Amendola, Novate M.se.

The first graph represents the load rate for the first example given. As the graph shows, the curves can be interpolated with a linear function and the angular coefficient is the approximation of the load rate. In this case the value is similar for each test.

Considering the values, here the table is reported (Tab. 2.18)

Test	Load speed [u.o.m]
Via Amendola, Novate 1	229.63 Nm/s
Via Amendola, Novate 2,pt1	390.76 Nm/s
Via Amendola, Novate 2,pt2	333.31 Nm/s
Via Amendola, Novate 3,pt1	351.87 Nm/s
Via Amendola, Novate 3,pt2	388.97 Nm/s
Via Amendola, Novate 4,pt1	125.01 Nm/s

**Tab. 2.18** Values of load rate, Novate M.se.

The average value is 303.26 Nm/s, and, as can be seen, the values are really similar between them. The divergent one is the fourth test, that is equal to 125.01 Nm/s, number very different from the average one. The reason for this inequality is in the moment-inclination graph. As seen before, this test does not reach high bending moment. Consequently, because of the direct proportion between bending moment and load rate, if moment is low, also speed has to be low, or better, must be lower than the average of the set of tests.

The other results are very close to the average one, this means that they are very similar between them, as can be seen also from the graph. Another time this is remarkable considering the moment-inclination graph. In that case moments were very similar and, if times and duration do not change in a significant way, also load rate must be similar.

Since the plants of the data set are different, the answer to the fact of similar speeds must be search in something else. Again, the terrain can give us the solution, again the thesis of soil-root plate interaction can be valid.

Inclination rate is computed another time. In the following the results are reported in a graph (Fig. 2.19). In this case the numerical values are not inserted, because the conclusion can be similar to the previous ones.

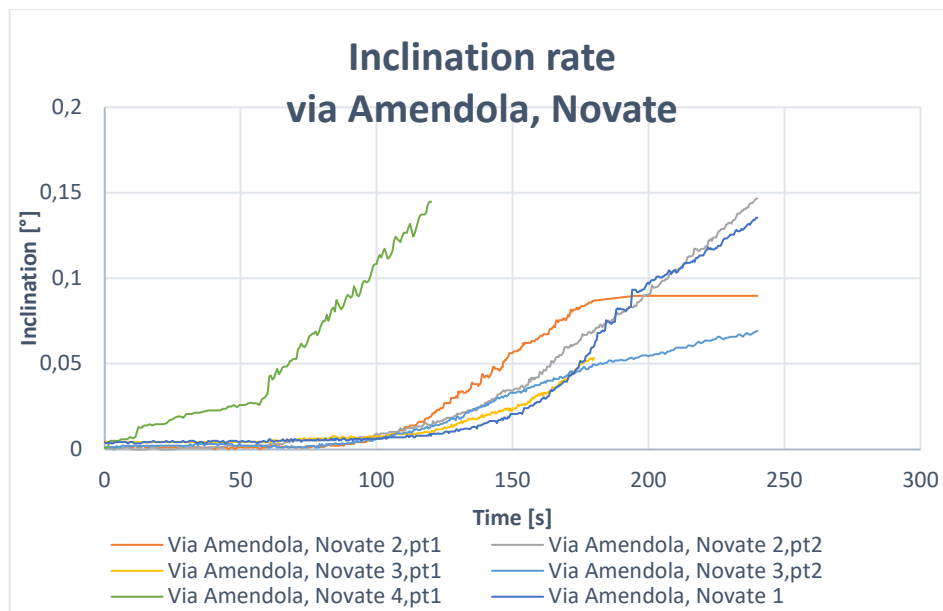


**Fig. 2.19** Inclination rate graph for example of via Amendola, Novate M.se.

## Chapter 2 - Pulling tests results: some considerations

The graph shows the behaviour of inclination rate. The curves are very similar between them, therefore are valid the previous considerations. Also in this case, test number 4 is different from the other. In fact, inclinations of that plant were superior to the other, so also inclination rate, because of direct proportion in the computation, must be bigger than the other ones.

These are the results of the first example reported. Up to now the second one is considered, and other considerations and conclusion can be made.

The set of tests taken into account comes from Tevere square in San Donato M.se. In this first part, another time, are considered the load rate and then inclination rate can confirm or disprove the conclusion, and in this case some deeper analysis will be necessary.

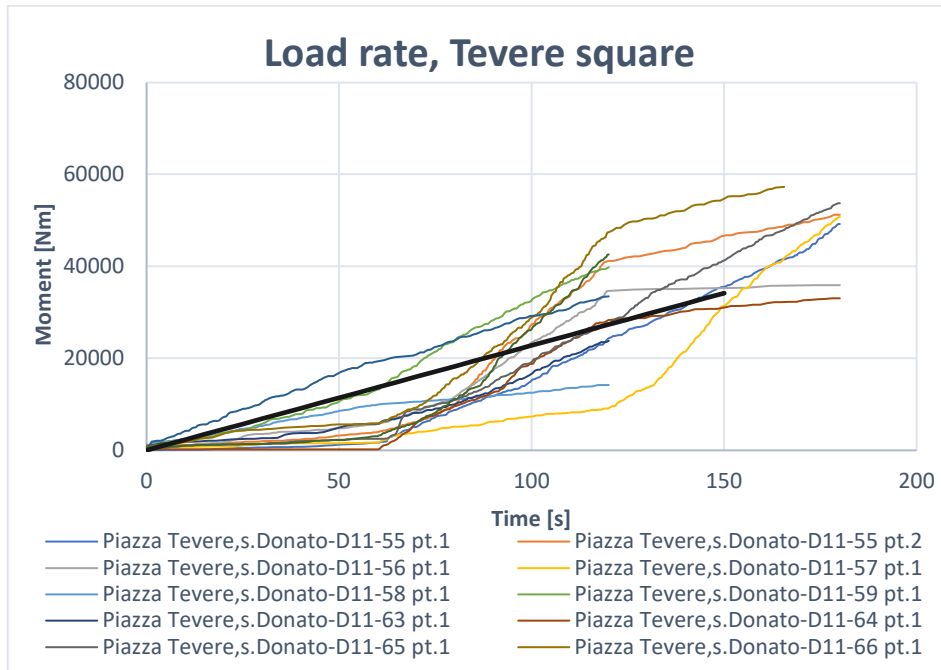


**Fig. 2.20** Load rate graph for example of Tevere square, San Donato M.se

The figure shows the results of load rate for the set of tests done in Tevere square in San Donato M.se (Fig. 2.20). In the following the numerical results and then other considerations can be done (Tab. 2.21).

Test	Load speed	[u.o.m]
Piazza Tevere,s.Donato-D11-55 pt.1	213.2	Nm/s
Piazza Tevere,s.Donato-D11-55 pt.2	252.89	Nm/s
Piazza Tevere,s.Donato-D11-56 pt.1	208.89	Nm/s
Piazza Tevere,s.Donato-D11-57 pt.1	184.94	Nm/s
Piazza Tevere,s.Donato-D11-58 pt.1	147.62	Nm/s
Piazza Tevere,s.Donato-D11-59 pt.1	306.19	Nm/s
Piazza Tevere,s.Donato-D11-63 pt.1	157.87	Nm/s
Piazza Tevere,s.Donato-D11-64 pt.1	181.85	Nm/s
Piazza Tevere,s.Donato-D11-65 pt.1	248.57	Nm/s
Piazza Tevere,s.Donato-D11-66 pt.1	302.11	Nm/s
Piazza Tevere,s.Donato-D11-83 pt.1	301.33	Nm/s
Piazza Tevere,s.Donato-D11-84 pt.1	226.16	Nm/s

**Tab. 2.21 Values of load rate, Novate M.se.**

The values obtained are very similar, but it is better to do an analysis. The mean value is 227.64 Nm/s; considering this value, it is easy to understand that is not far from all the other values. The biggest value is the test D11-59, as it is seen also from the graph, curve in orange. From the graph is possible to see an increasement of this curve up to a certain value around 60 s, that means that after this time the plant increases moments more quickly than at the starting point and this could be dangerous. Once interpolated this curve assumes a linear shape with a higher slope, as seen from the numerical value. More or less the same behaviour of test with code D11-66, violet curve. This test sees a remarkable change of slope.

In the following graph of inclination rate is reported (Fig. 2.22).

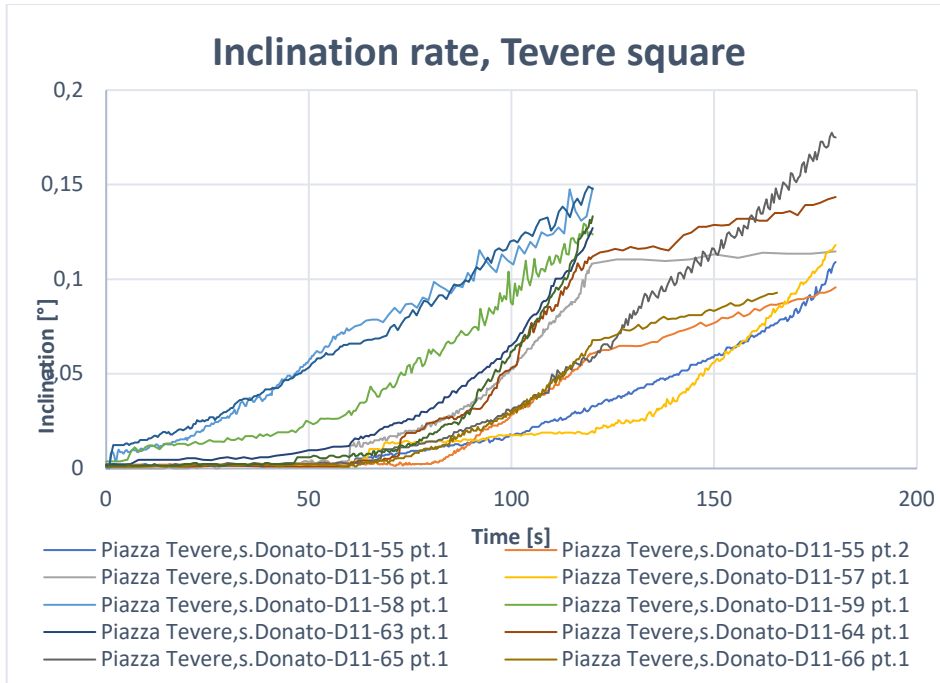


**Fig. 2.22 Load rate graph for example of Tevere square, San Donato M.se.**

The graph above represents the inclination rate for the second set of tests under example. It is easy to understand that, as expected, all of them follow the same behaviour, excluding test D11-55, blue curve, and D11-58, light blue. These tests reach higher inclinations in a little time, this behaviour can be deduced from the bending moment-inclination graph.

In the following, only for a visual reason, are reported the general graphs for what concern load rate and inclination rate (Fig. 2.23; Fig. 2.24). The graphs will be difficult to explain because reported all the tests done and, as seen, they are a lot. For this reason, these typologies of graphs are made only in seek of completeness.



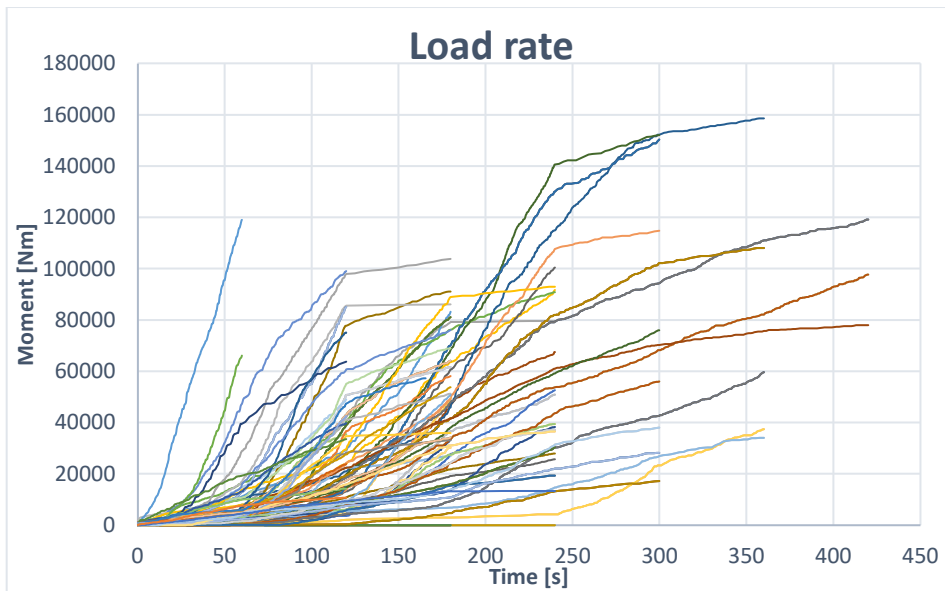


Fig. 2.23 General load rate graph.

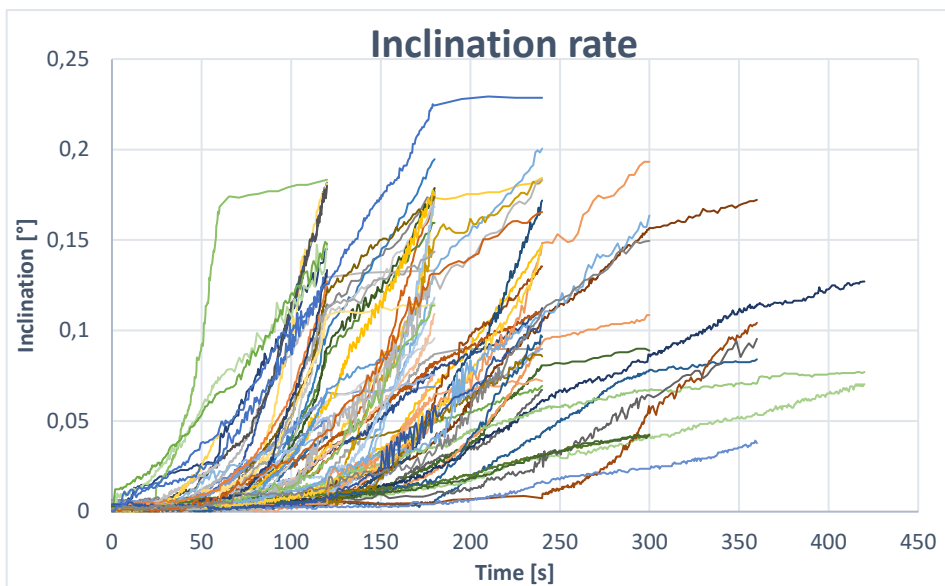


Fig. 2.24 General inclination rate graph.

The choice of omit the legend in the graph is done deliberately. It is very difficult to understand all the colours of the curves from the legend, therefor it has not any sense try to distinguish them from a legend.

Anyway, the two reported graphs want to let know how all the test follow a similar behaviour in the initial part in every case, without distinguish the specie of the tree.

### 2.3.4 Stiffness and maximum bending moment

If moment-inclination curves are considered again (Fig. 2.11), other considerations can be done, without any computations. These observations do not have an important meaning, but they represent a starting point for the next computations.

In the specific it is possible to find an approximation of the initial stiffness of the trees and an approximation of the maximum bending moment that can be reached for each tree with pulling out test. As said, they are found only by a visual way, for this reason they cannot be precise, but a good approximation. It is important to say that in this phase Wessolly's function is not considered.

In the case of initial stiffness of the trees, the idea is to take the initial part of the graph (Fig. 2.8) and take the interpolation of that part of the curve. The interpolation is a linear function, whose slope, angular coefficient, is the approximate initial stiffness. Also in this case, here are reported the results for the example already presented, Amendola way and Tevere square. The results are under the expression:

$$k_0 = \frac{M}{\theta} = \frac{[Nm]}{[^\circ]}$$

In the case of maximum bending moment,  $M_L$ , it is approximated simply reading the maximum value from the graph (Fig. 2.8). The usual two example are considered. The results are in the dimension of  $[Nm]$ .

The results are presented together with the stiffness.

Test	$k_0$ [Nm/°]	Ml [Nm]
Via Amendola, Novate 1	3866440	80000
Via Amendola, Novate 2,pt1	686940	81000
Via Amendola, Novate 2,pt2	1574350	90000
Via Amendola, Novate 3,pt1	2808530	85000
Via Amendola, Novate 3,pt2	536840	95000
Via Amendola, Novate 4,pt1	126820	20000

**Tab. 2.25 Stiffness and limit bending moment for the first example.**

The table shows the results for the first example, via Amendola, for the initial stiffness and limit bending moment (Tab. 2.25).

Studying the table is possible to see how with the same tree, stiffness and maximum bending moment, even if approximations, change; it could be strange, but it is a result that give us some information about tree properties, because stiffness and moment change following the direction of the application of the forces. Consequently, it is possible to understand that they are not constant for a same plant.

The same results can be related with load rate, then shown in a point chart (Fig. 2.26; Fig. 2.27).

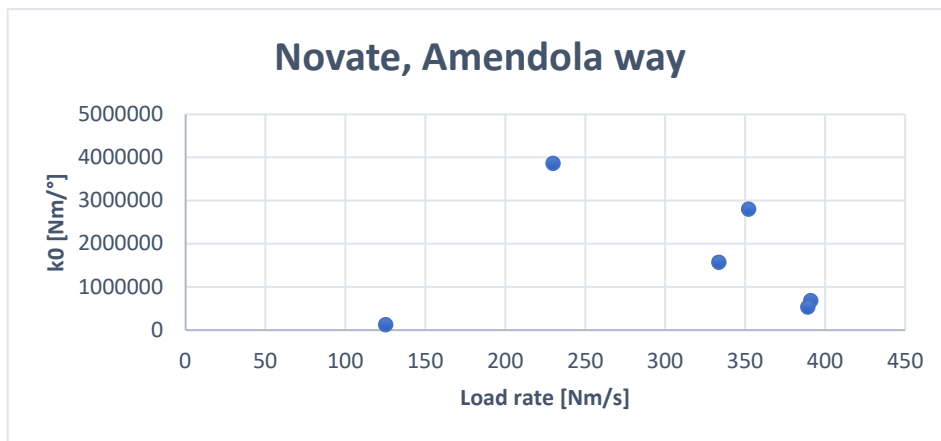


**Fig. 2.26 Velocity-stiffness graph for the first example.**

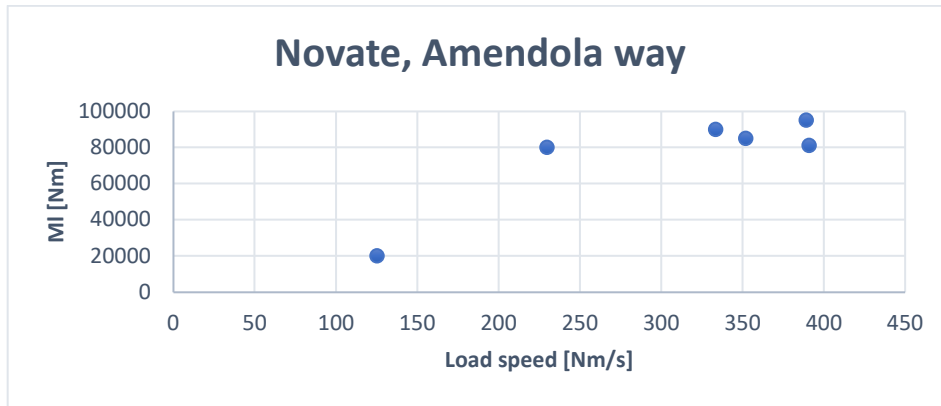


Fig. 2.27 Velocity-limit bending moment graph for the first example.

The two graphs show the distribution of the stiffnesses and limit bending moments for the usual first example related with the load rates; the aim is to find the distribution. However, it is not possible with a little number of tests, as consequence, some other example is necessary.

The results of the second example reported are in the following (Tab. 2.28).

Test	K0 [Nm/°]	MI [Nm]
Piazza Tevere,s.Donato-D11-55 pt.1	794220	52000
Piazza Tevere,s.Donato-D11-55 pt.2	1927730	61000
Piazza Tevere,s.Donato-D11-56 pt.1	537460	50000
Piazza Tevere,s.Donato-D11-57 pt.1	425810	60000
Piazza Tevere,s.Donato-D11-58 pt.1	176060	15000
Piazza Tevere,s.Donato-D11-59 pt.1	366260	49000
Piazza Tevere,s.Donato-D11-63 pt.1	369630	40000
Piazza Tevere,s.Donato-D11-64 pt.1	546390	40000
Piazza Tevere,s.Donato-D11-65 pt.1	1120820	60500
Piazza Tevere,s.Donato-D11-66 pt.1	2452790	63500
Piazza Tevere,s.Donato-D11-83 pt.1	258350	40500
Piazza Tevere,s.Donato-D11-84 pt.1	605780	50000

Tab. 2.28 Stiffness and limit bending moment for the second example.

In this case all the trees are different, there is only a test done on the same plant in two different directions and their values of  $k_0$  are very different. The other tests are done on different plants and their results are similar, with the same magnitude. This fact is observable from the Fig. 2.10. As a matter of fact, it was seen that the initial slope of the curves is similar between them.

Let's see now the visual results with stiffness-velocity graph and limit bending moment-velocity graph (Fig. 2.29; Fig. 2.30).

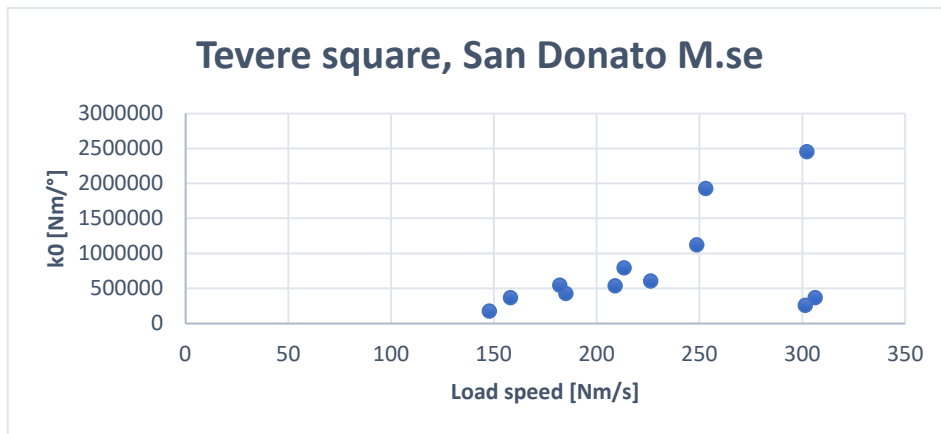


Fig. 2.29 Velocity-stiffness graph for the second example.

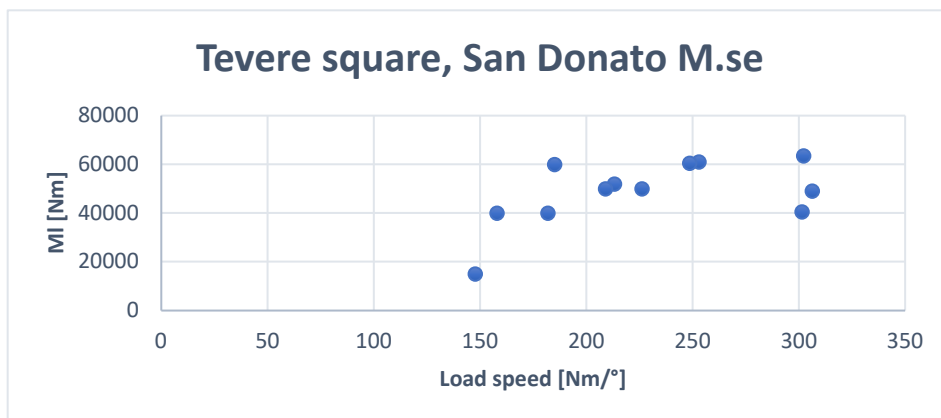
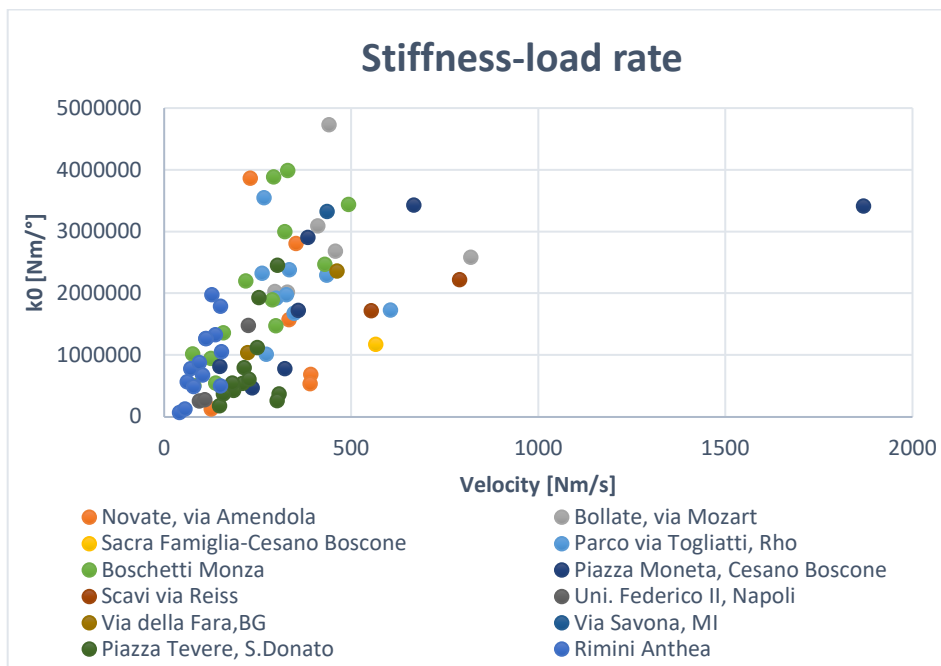


Fig. 2.30 Velocity-limit moment graph for the second example.

## Chapter 2 - Pulling tests results: some considerations

Again, the two graphs show the distribution of initial stiffness and limit bending moment related with the load rate already computed (Fig. 2.31; Fig. 2.32).

These are only approximations, but it can be useful to insert the final results for all the tests for what concerns the two typologies of graphs presented above. This is done only for a visual analysis, in order to see a possible distribution of the two quantities under control.



**Fig. 2.31 Initial stiffness-load rate graph for all the test performed.**

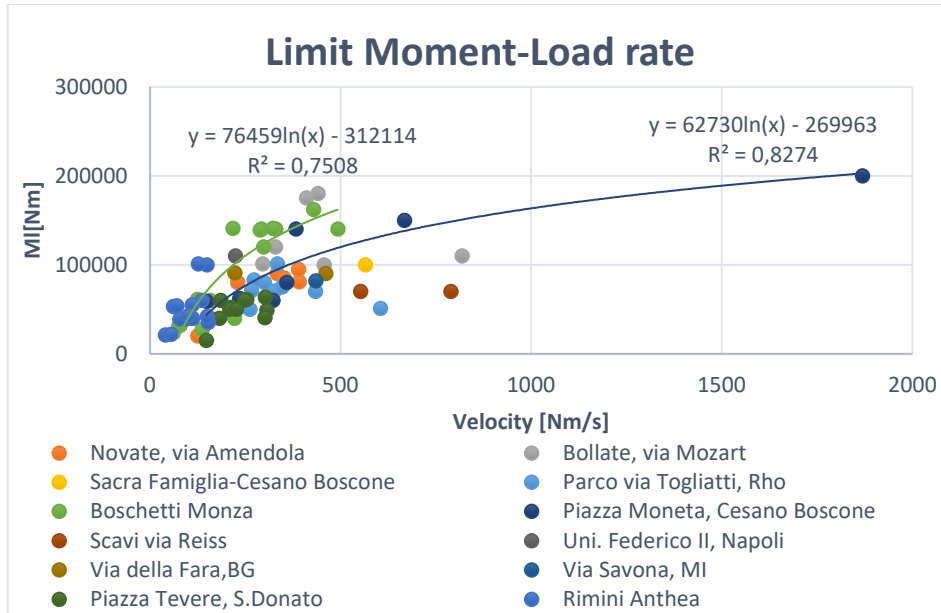


Fig. 2.32 Limit bending moment-load rate graph for all the test performed

Important to say that a logarithmic trend can be seen if all the tests are considered. In fact, two examples of this distribution are reported in the graph above.

To remember is the fact that they are only approximation, but they are a good starting point to try to find a new equation as alternative as Wessolly's one.

## 2.4 Conclusions

After analyzing the results of the pulling test database collected, it was possible to obtain some important information that may be useful for future investigations.

First of all, the results seem depend on numerous different factors, attributable to the type of trees, the environmental and soil conditions and the methods of carrying out the tests. For this last aspect, in particular, the rate of application of the force seems to have a certain importance, which can influence the stiffness of the curves obtained and the limit moment.

## Chapter 2 - Pulling tests results: some considerations

---

In the future it will be necessary, therefore, to investigate the real influence of speed parameter for a correct performance of the pulling tests and for the quality of results obtained.



## Chapter 3

# Geotechnical soil characterization

### 3.1 Introduction

This chapter describes methods and results about the technical characterization of the analysed soils, picked up where some pulling tests are carried out. A total of 23 soil samples were collected in various locations, such as: Monza (MB), La Spezia (SP), Cesano Boscone (MI), San Donato Milanese (MI), Rho (MI), Bergamo (BG), Settimo Milanese (MI), Verderio (LC), Calolziocorte (LC), Gorla Minore (VA) and Oggiono (LC).

### 3.2 Geographical location

Pulling tests are carried out in several location distributed in continental Italy, though most of them are concentrated in town and cities near Milano, Lombardy.

For a large part of all pulling tests has been picked up some soil samples to know their granulometry and try to find some information about terrain could be useful for this study. Trees subject of these study are often grouped in small number for each location, so for each of these places are collected one, two or three soil samples, depending on the size of sites.

The position of each analysed tree located in places where soil samples are picked up has been putted on a software G.I.S. (*Geographic Information System*) with about 1 m of accuracy, using a regional orthophoto as base map.

Some of these maps are shown below (Fig. 3.1; Fig. 3.2; Fig. 3.3), to understand the macroscale geographic features of these places where pulling tests are carried out, instead all the other maps with geo-localized

### Chapter 3 – Geotechnical soil characterization

---

trees are available in the attachment. In effect these trees are located in urban areas, in green spaces like public parks and gardens, rows on streets and private gardens, all characterized by human presence, like people, buildings or vehicles. In these places the risk related to falling trees is relatively high, so a correct assessment of their stability is very important.



**Fig. 3.1** Map with the position of the trees analysed in Boschetti Reali, Monza where soil samples were collected.



**Fig. 3.2** Map with the position of the trees analysed in piazza Tevere, San Donato Milanese where soil samples were collected.



### Chapter 3 – Geotechnical soil characterization

---

were, also, used for sieving, quartering and storage of the material (Fig. 3.4; Fig. 3.5).



**Fig. 3.4 Sieve with soil sample (Crotti bachelor thesis).**



**Fig. 3.5 Vibrating screen with stacked sieves (Crotti bachelor thesis).**

The granulometric test by sieving was developed through several phases: initial weighing with washing, sedimentation, drying by oven, sieving by vibrating screen and weighing of the net weight of the material retained by the sieves. During the first phase, after taking a quantity of sample and weighing it, a washing was carried out in order to separate the finer particles that remained attached to the coarser granules, thus breaking the bonds. Subsequently, the wet soil sample was collected in an aluminum tray and left to settle for a few hours to allow the deposition of the entire amount of material on the bottom of the tray, as shown in Fig. 3.6.



**Fig. 3.6 Sedimentation of the soil inside aluminium trays (Crotti bachelor thesis).**

At the end of the sedimentation phase, the aluminium trays were inserted inside a stove, as shown in Fig. 3.7, to allow the complete drying of the sample, which usually takes several hours.



**Fig. 3.7 Drying of samples inside a stove (Crotti bachelor thesis).**

### Chapter 3 – Geotechnical soil characterization

---

Once the water has evaporated, it was possible to proceed with the sieving phase. Then, after having stacked the sieves with the various diameters of the holes in a decreasing way from top to bottom above the vibrating screen, the contents of the trays were poured into the sieves. The function of the sieves is to retain the fraction of solid whose granules are larger than the diameter of the holes that make up the mesh of the sieve.

Once the vibration phase was completed by vibrating screen, to allow the complete sieving of the material contained within the sieves, the different net weights of material for each sieve were evaluated by a scale and reported in a table.

Finally, the coarse solid fraction (with a diameter greater than 1.18 mm) was collected in a different plastic bag compared to another bag in which the fine fraction was collected (diameter less than 1.18 mm), that will be studied and evaluated later through a laser granulometer, a “Mastersizer 2000” by “Malvern Instruments” as shown in Fig. 3.8 (the choose of the laser granulometer has done to speed up the analysis, while the legislation provides the sedimentation test, called also aerometry).



**Fig. 3.8 Laser granulometer “Mastersizer 2000” by “Malvern Instruments” (Crotti bachelor thesis).**

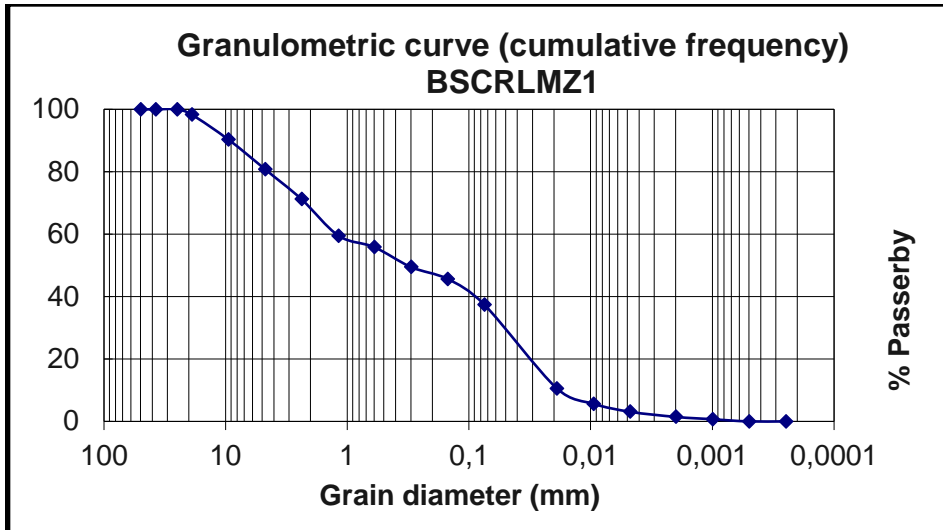
The laser granulometer is an electronic machinery that measures the size of particles or, more specifically, the distribution of different particle sizes within a soil sample by a laser beam, then, as a result, a grain size distribution curve by volume is drawn up.

### 3.3.2 Results of granulometric tests performed

From the combination of the data of the granulometric tests by sieving and the analyses with the laser granulometer, 23 granulometric curves were elaborated which follow on the following pages (from Fig. 3.10 to Fig. 3.33). In addition to the granulometric curve, the relative values of the uniformity and curvature coefficient are also reported, indicated as “Cu” and “Cc” and calculated as follows:  $Cu = D_{60} / D_{10}$  and  $Cc = D_{30}^2 / (D_{60} \times D_{10})$ . Following Tab. 3.9 indicates the location where the soil sampling was performed, the number of samples examined and the relative abbreviations.

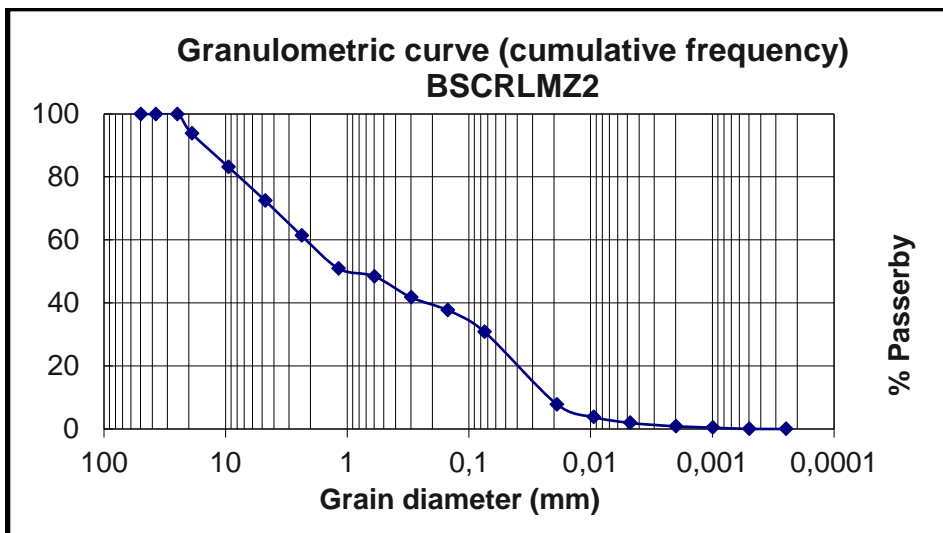
Location	Soil samples	Abbreviation
Boschetti reali, Monza	2	BSCRLMZ1 - BSCRLMZ2
Centro allende, La Spezia	3	CTALLSP1 - CTALLSP2 - CTALLSP3
Piazza Moneta, Cesano Boscone	2	MNTCSNB1 - MNTCSNB2
Piazza Tevere, San Donato Milanese	2	TVRSDNM1 - TVRSDNM2
Piazza Togliatti, Rho	1	TGLTRHO2
Via della Fara, Città Alta, Bergamo	1	DLFARBRG1
Via Pellettier, Monza	1	PLLTMZ1
Via Reiss Romoli, Settimo Milanese	1	RSROMST1
Villa Gallavresi, Verderio	1	VGALVER1
Villa Guagnellini, Calolziocorte	2	VGUACLZ1 - VGUACLZ2
Viale Vittorio Veneto, Monza	2	VTVENMZ1 - VTVENMZ2
Gorla Minore	4	C2 - G1 - G2 - ROBINIA1
Oggiono	1	OGGIONO

**Tab. 3.9 Location where the soil sampling was performed, the number of samples examined and the relative abbreviations.**



ASTM (D422; D653): slightly clayey sand with gravelly silt  
 $C_u = 65$        $C_c = 0,0962$

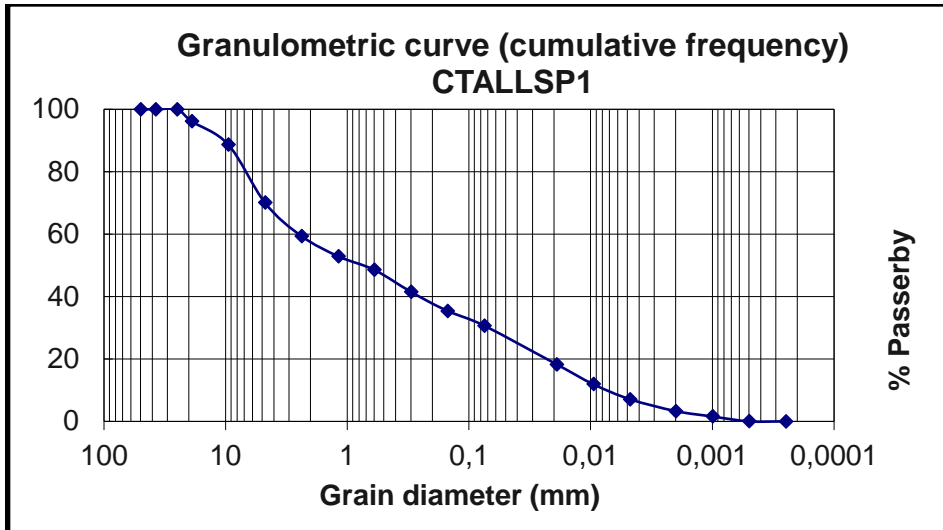
Fig. 3.10 Granulometric curve of BSCRLMZ1 soil sample.



ASTM (D422; D653): slightly clayey sand with gravelly silt  
 $C_u = 125$        $C_c = 0,128$

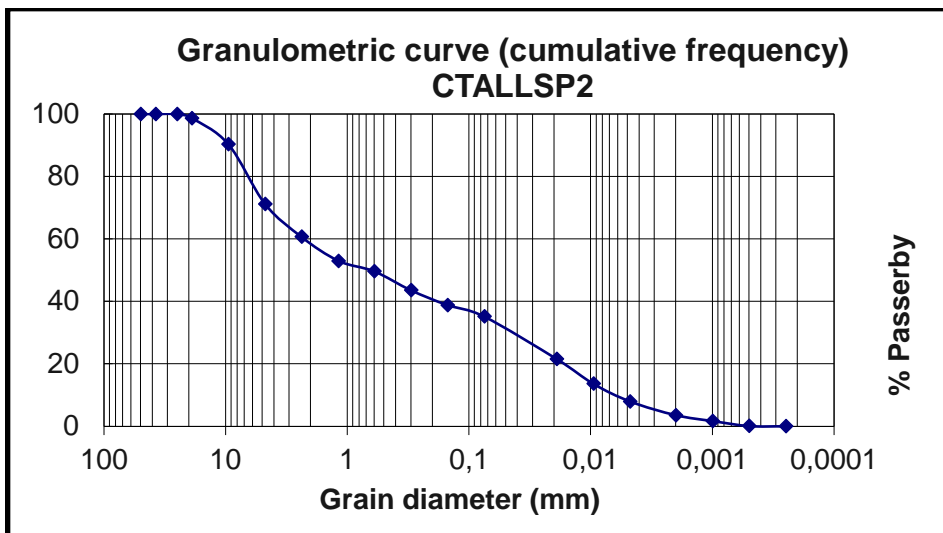
Fig. 3.11 Granulometric curve of BSCRLMZ2 soil sample.





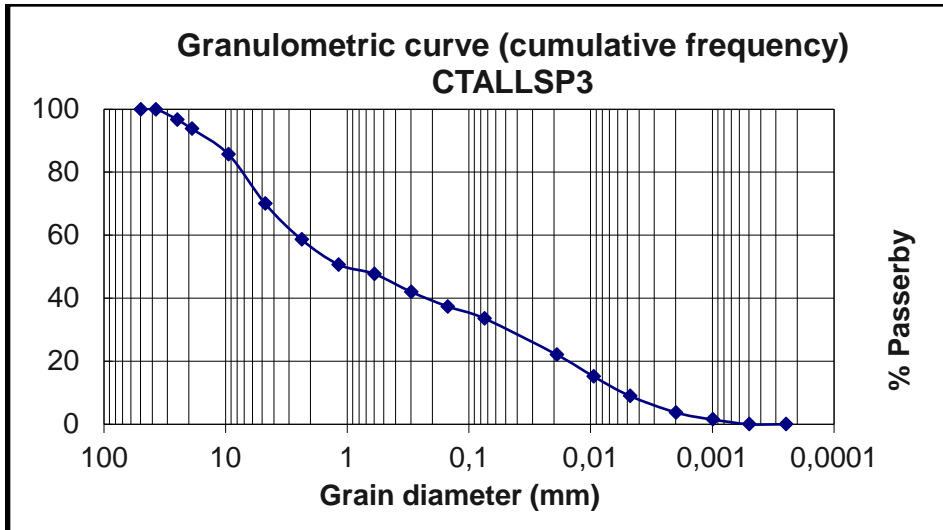
ASTM (D422; D653): slightly clayey sand with gravelly silt  
 $C_u = 312,5$        $C_c = 0,000128$

Fig. 3.12 Granulometric curve of CTALLSP1 soil sample.



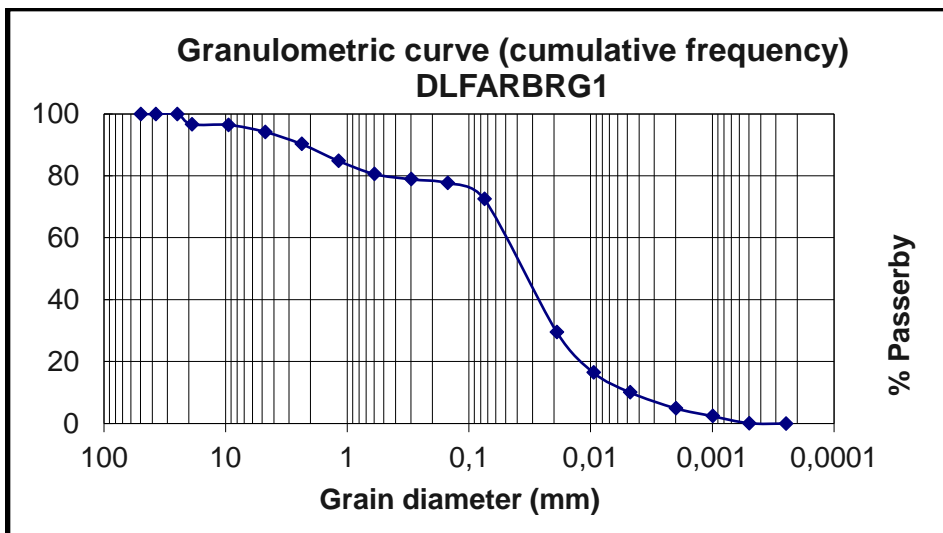
ASTM (D422; D653): slightly clayey sand with gravelly silt  
 $C_u = 357$        $C_c = 0,11$

Fig. 3.13 Granulometric curve of CTALLSP2 soil sample.



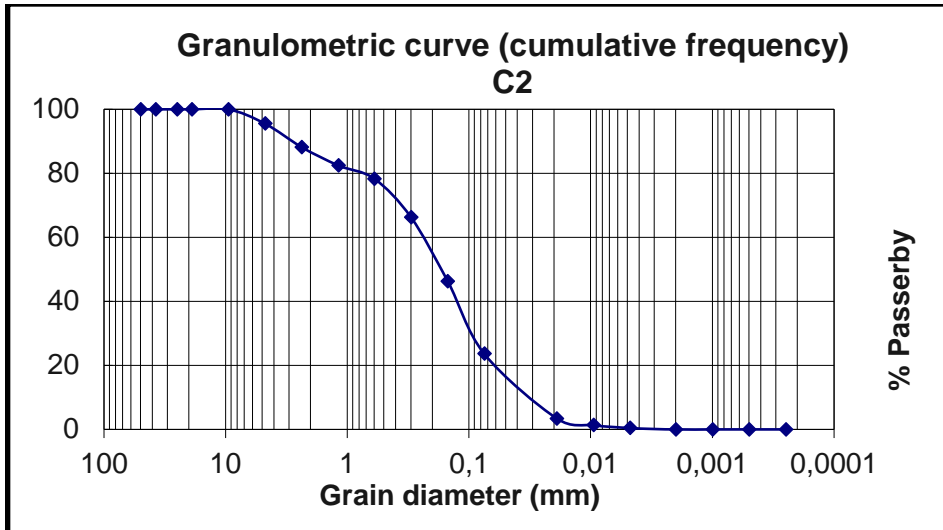
ASTM (D422; D653): slightly clayey sand with gravelly silt  
 $C_u = 500$        $C_c = 0,2$

Fig. 3.14 Granulometric curve of CTALLSP3 soil sample.



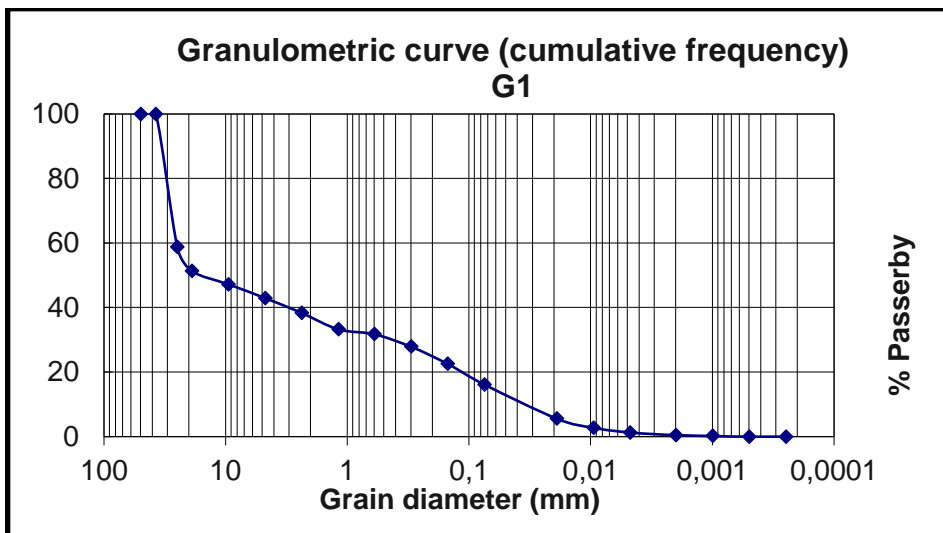
ASTM (D422; D653): silt with slightly gravelly clayey sand  
 $C_u = 10$        $C_c = 1,6$

Fig. 3.15 Granulometric curve of DLFARBRG1 soil sample.



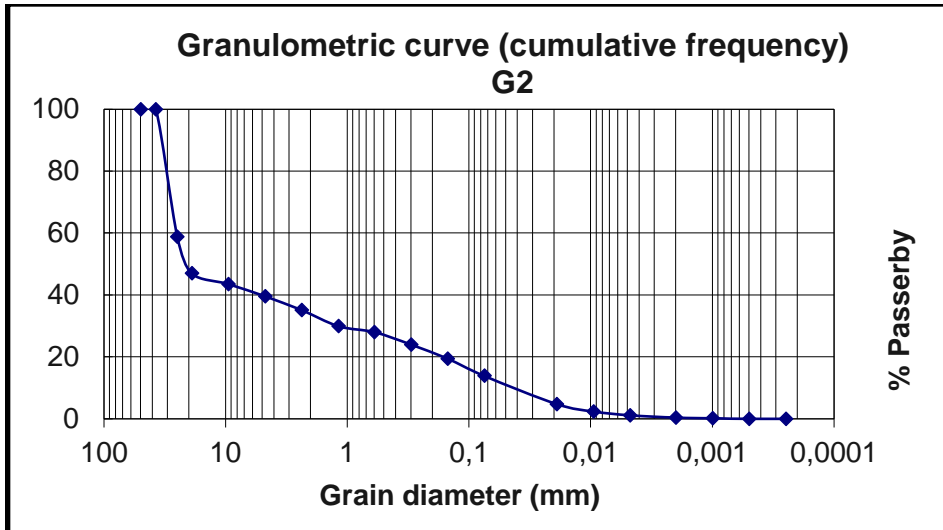
ASTM (D422; D653): sand with slightly clayey gravelly silt  
 $C_u = 8,3$        $C_c = 1,3$

Fig. 3.16 Granulometric curve of C2 soil sample.



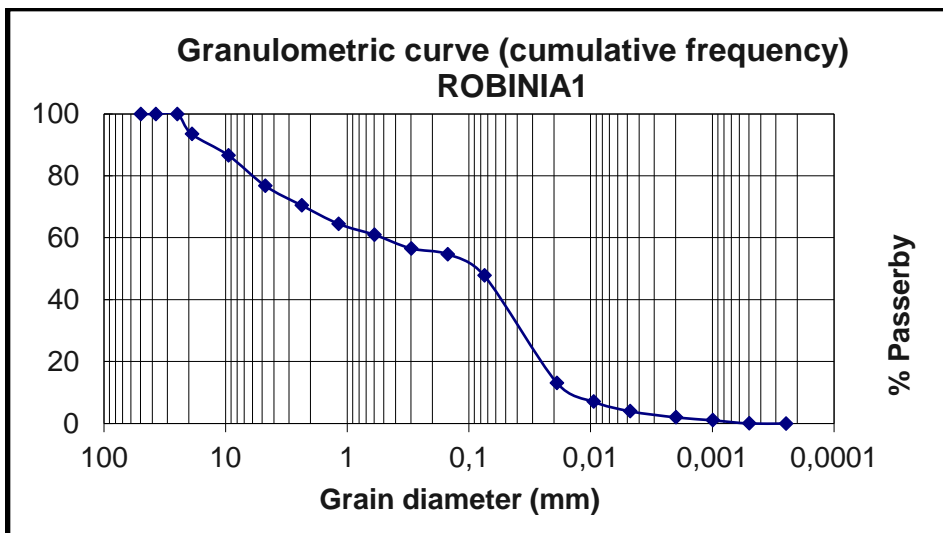
ASTM (D422; D653): gravel with slightly clayey silty sand  
 $C_u = 714$        $C_c = 0,18$

Fig. 3.17 Granulometric curve of G1 soil sample.



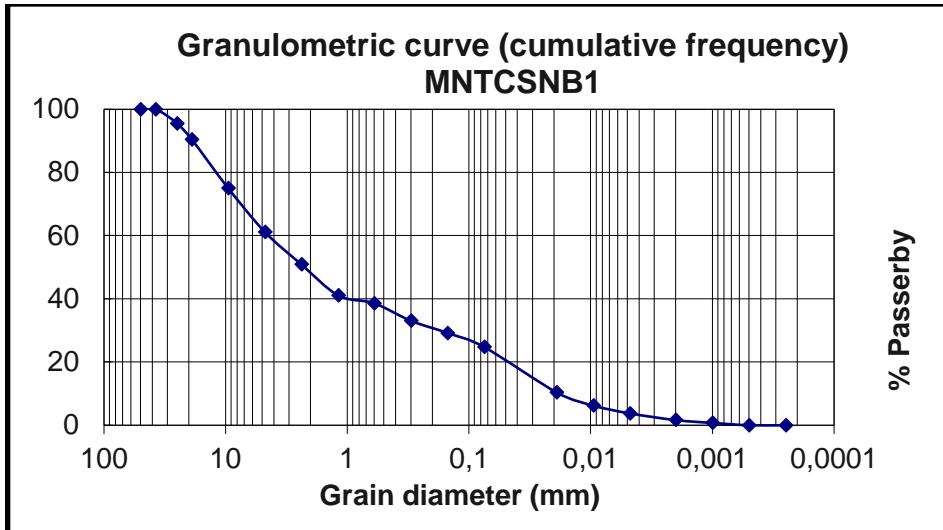
ASTM (D422; D653): gravel with slightly clayey silty sand  
 $C_u = 555$        $C_c = 1,28$

Fig. 3.18 Granulometric curve of G2 soil sample.



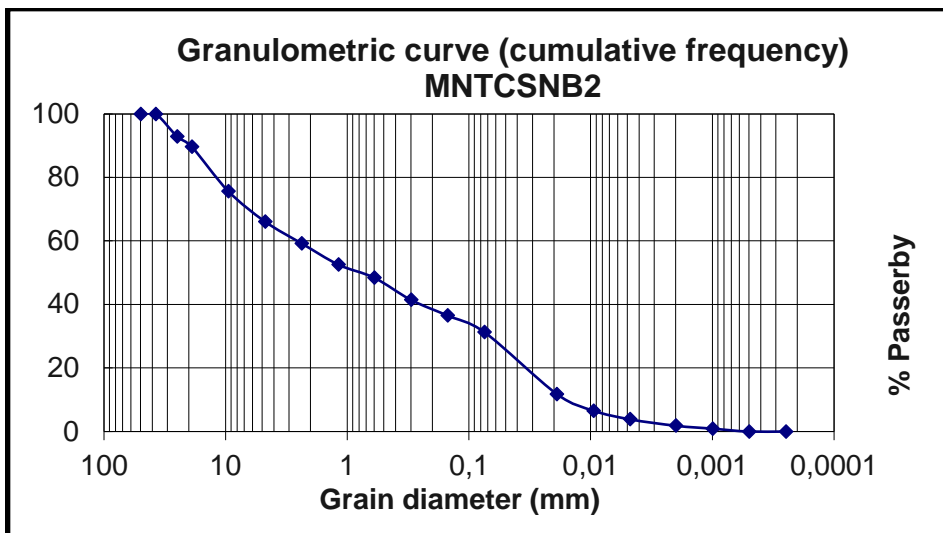
ASTM (D422; D653): silt with slightly clayey gravel sand  
 $C_u = 40$        $C_c = 0,17$

Fig. 3.19 Granulometric curve of ROBINIA1 soil sample.



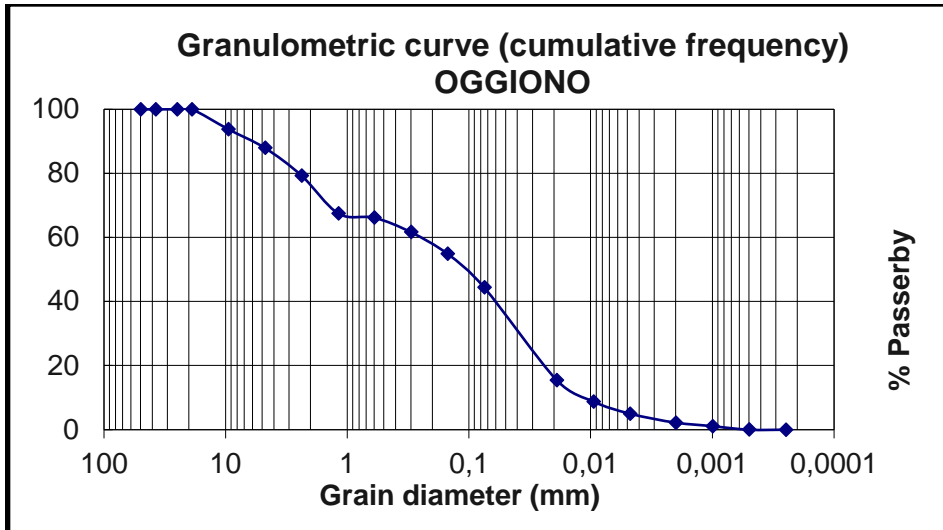
ASTM (D422; D653): silt with slightly clayey gravel sand  
 $C_u = 250$        $C_c = 0,4$

Fig. 3.20 Granulometric curve of MNTCSNB1 soil sample.



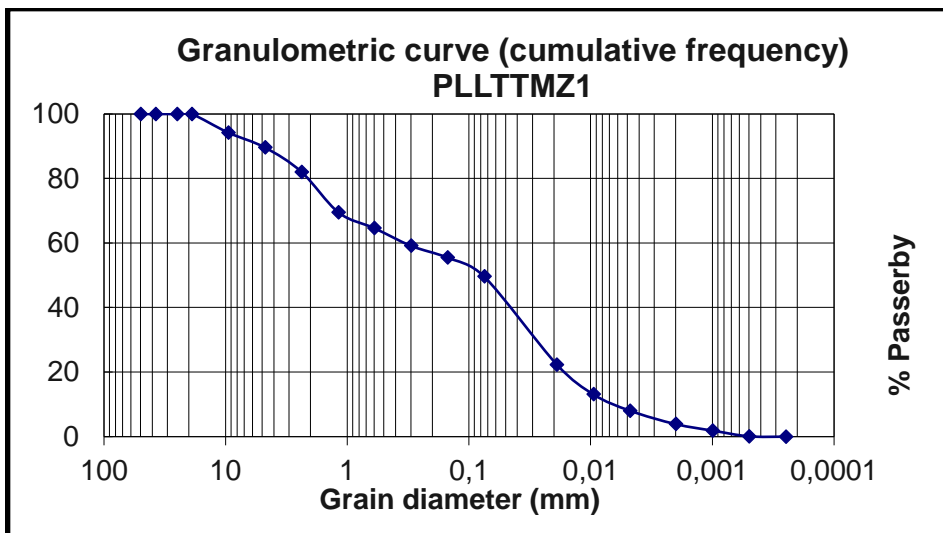
ASTM (D422; D653): silt with slightly clayey gravel sand  
 $C_u = 138$        $C_c = 0,08$

Fig. 3.21 Granulometric curve of MNTCSNB2 soil sample.



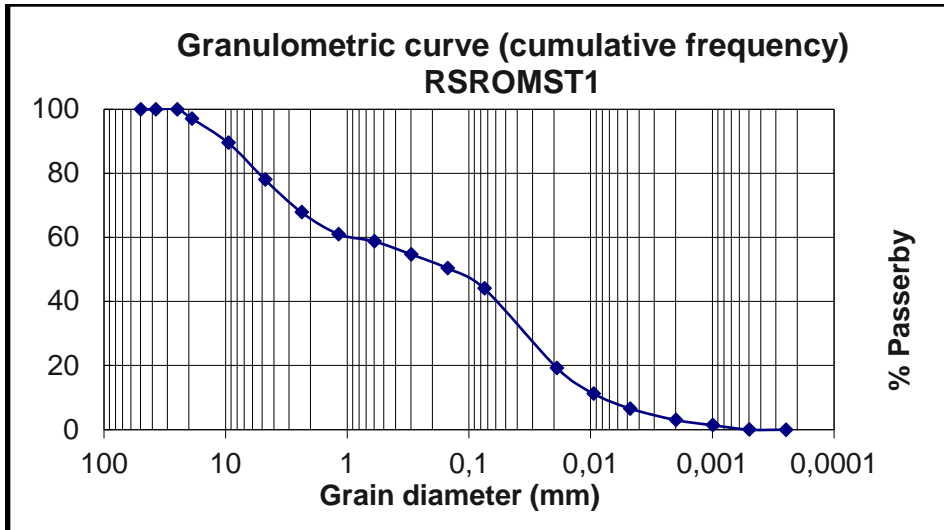
ASTM (D422; D653): sand with slightly clayey gravelly silt  
 $C_u = 25$        $C_c = 0,000065$

Fig. 3.22 Granulometric curve of OGGIONO soil sample.



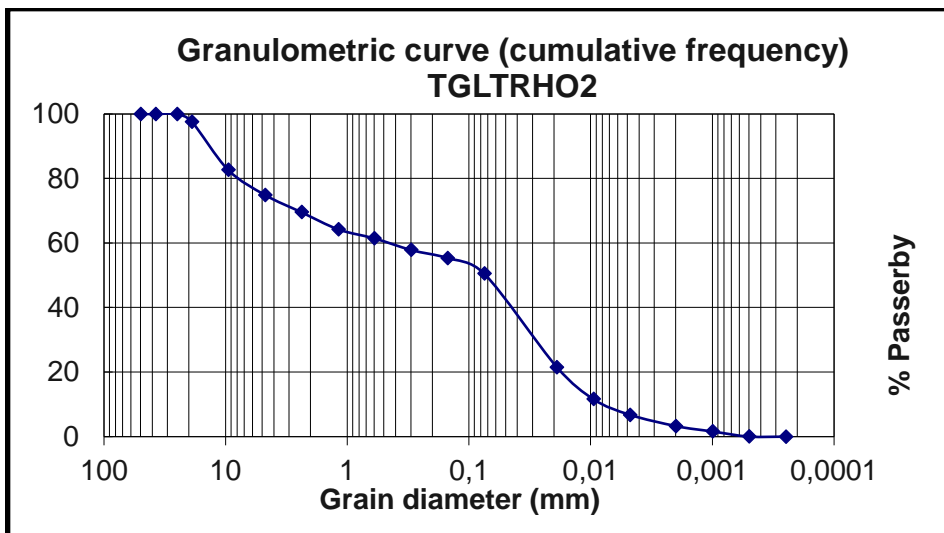
ASTM (D422; D653): sand with slightly gravelly clayey silt  
 $C_u = 46$        $C_c = 0,46$

Fig. 3.23 Granulometric curve of PLLTTMZ1 soil sample.



ASTM (D422; D653): sand with slightly clayey gravelly silt  
 $C_u = 111$        $C_c = 0,13$

Fig. 3.24 Granulometric curve of RSROMST1 soil sample.

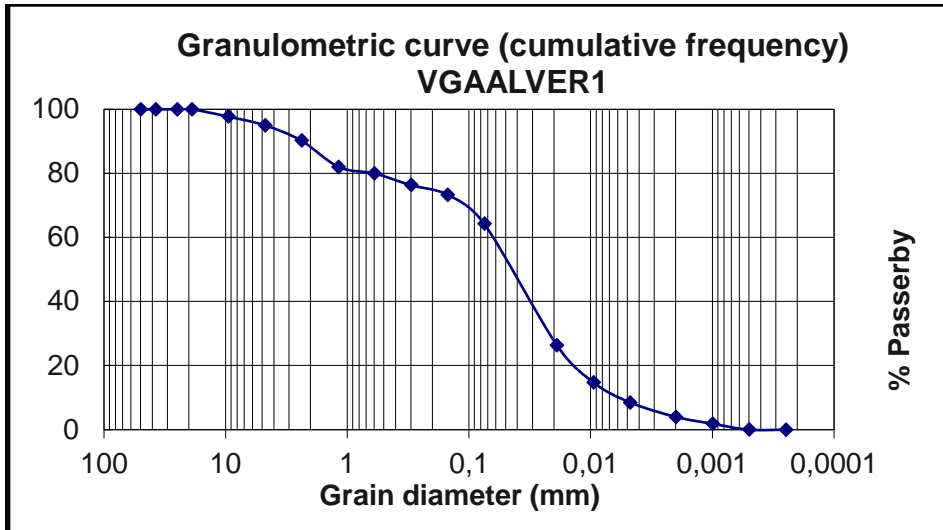


ASTM (D422; D653): silt with slightly clayey gravel sand  
 $C_u = 50$        $C_c = 0,22$

Fig. 3.25 Granulometric curve of TGLTRHO2 soil sample.

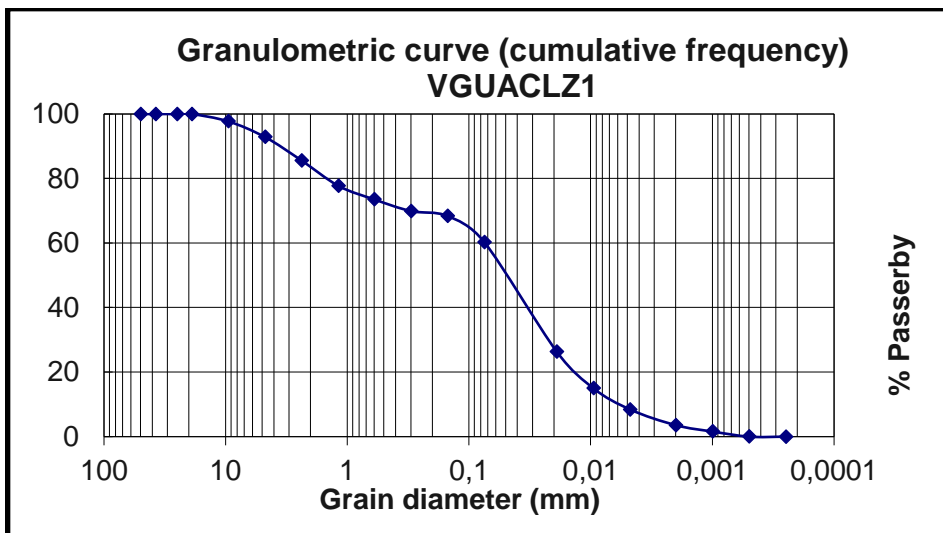






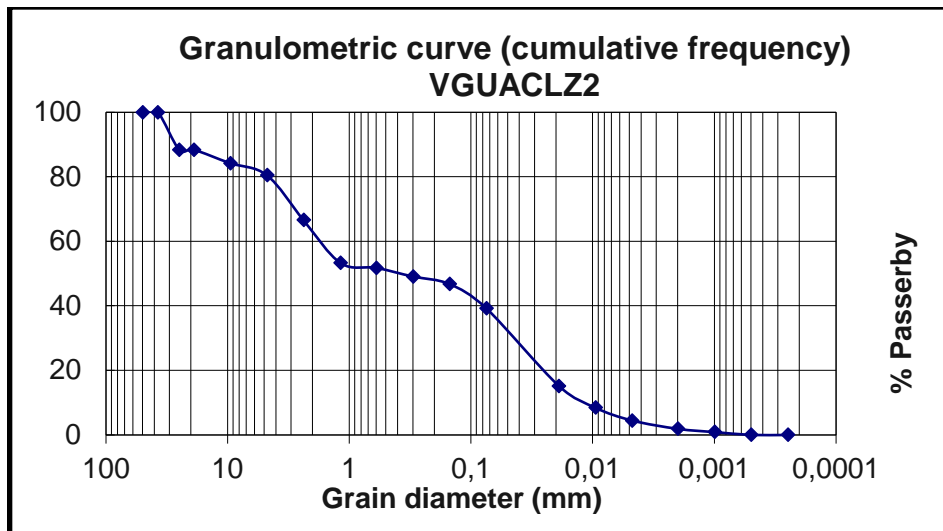
ASTM (D422; D653): silt with slightly gravelly clayey sand  
 $C_u = 10$        $C_c = 1,11$

Fig. 3.28 Granulometric curve of VGAALVER1 soil sample.



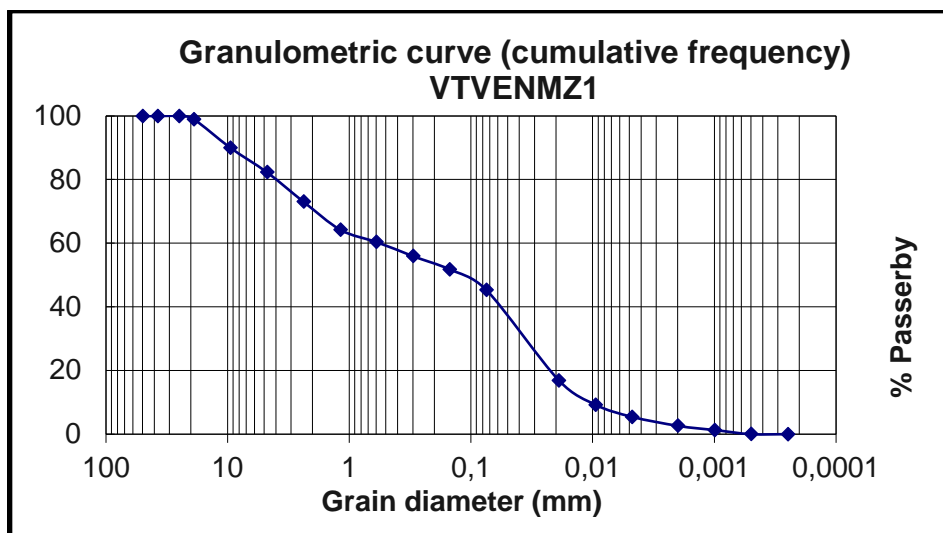
ASTM (D422; D653): silt with slightly clayey gravel sand  
 $C_u = 13,3$        $C_c = 1$

Fig. 3.29 Granulometric curve of VGUACLZ1 soil sample.



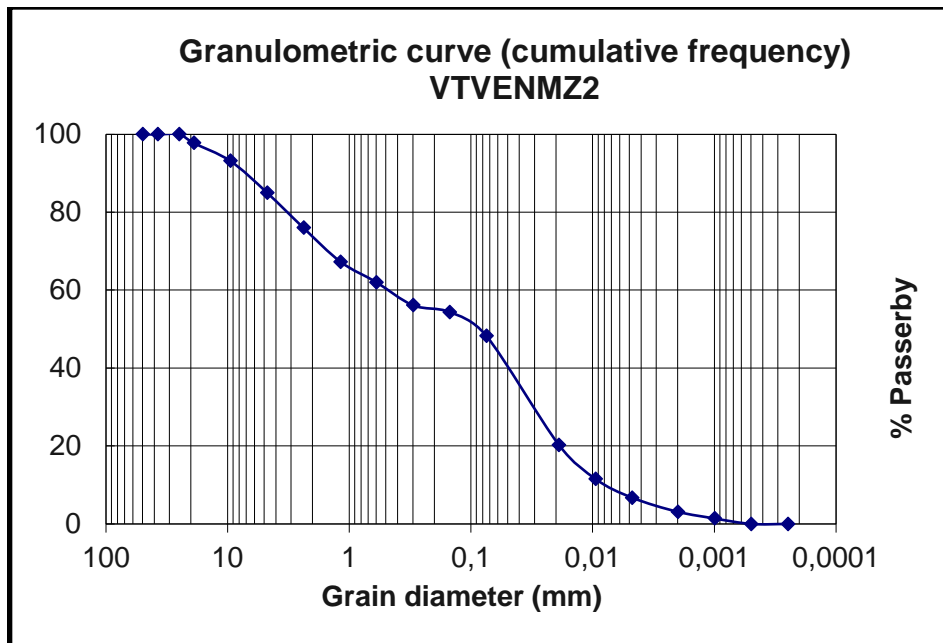
ASTM (D422; D653): sand with slightly clayey gravelly silt  
 $C_u = 150$        $C_c = 0,09$

Fig. 3.30 Granulometric curve of VGUACLZ2 soil sample.



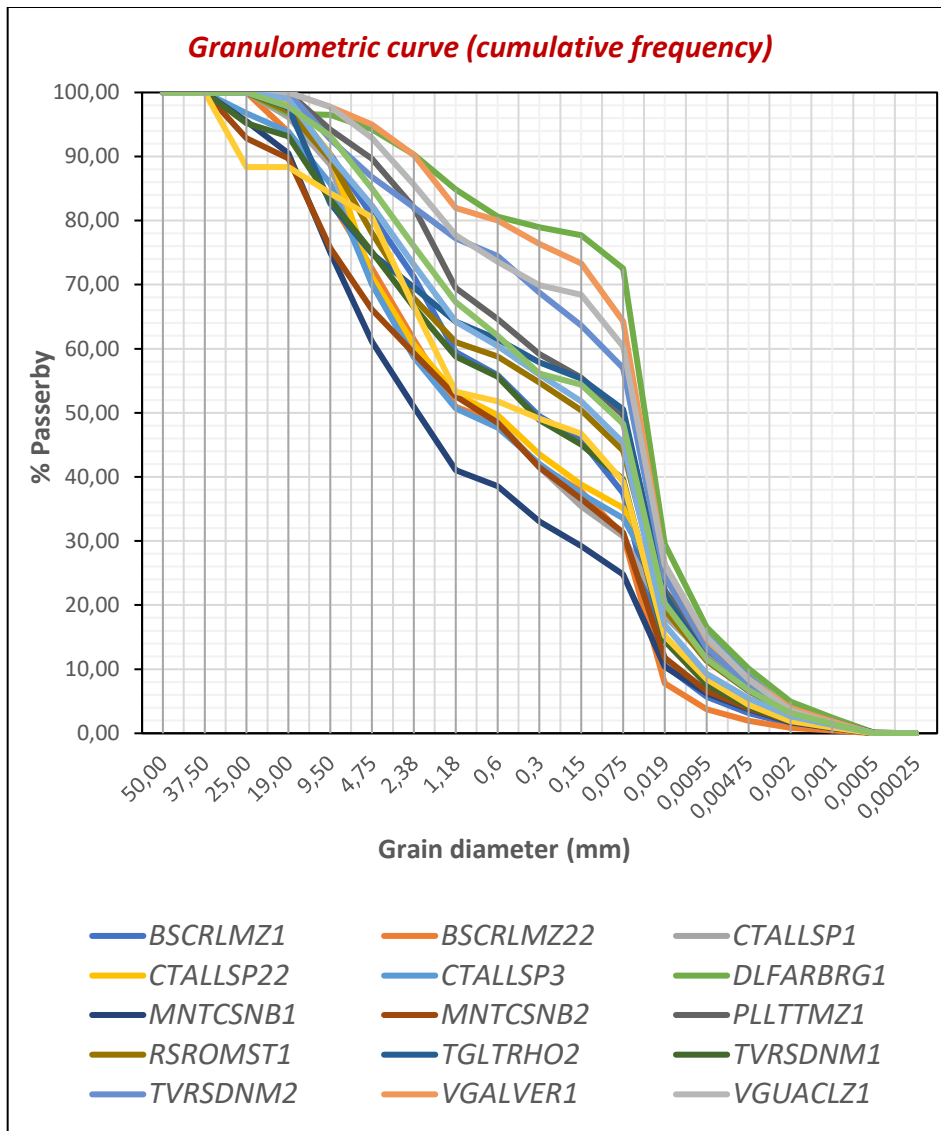
ASTM (D422; D653): sand with slightly clayey gravelly silt  
 $C_u = 60$        $C_c = 0,22$

Fig. 3.31 Granulometric curve of VTVENMZ1 soil sample.



ASTM (D422; D653): silt with slightly clayey gravel sand  
Cu = 62,5      Cc = 0,225

Fig. 3.32 Granulometric curve of VTVENMZ2 soil sample.



**Fig. 3.33** Granulometric curves of all soil samples.

### 3.3.3 Possible correlation between granulometry data and "pulling test"

After having completed the particle size tests, both by sieving and with the laser granulometer, 23 granulometric curves are drawn up and the relative uniformity and curvature coefficients are calculated. For locations where there is more than one grain size curve, an average has been calculated between coefficients  $C_u$  and  $C_c$  values. In addition to this, the % of fine and coarse material has also taken into consideration, in according to the ASTM D422 standard limits.

Subsequently, the different safety factors obtained from the pulling tests carried out in the various locations are taken and an average of safety factors for each location has been calculated and reported in Tab. 3.34 to clearly and immediately visualize the situation in terms of stability and safety of the various trees. In Oggiono and Gorla Minore, data obtained from the tests are not considered because trees has been cutted down.

Location	Av. SF	Av. $C_u$	Av. $C_c$	Av. % fine material	Av. % coarse material
Boschetti Reali, Monza	1,38	95	0,11	37,58	62,41
Centro Allende, La Spezia	2,34	389,83	0,1	33,14	66,86
Parco Togliatti, Rho	2,01	50	0,22	50,54	49,46
P.za Moneta, Cesano B.ne	1,83	194	0,24	28,04	71,95
P.za Tevere, San Donato	1,91	57	0,49	48,28	51,72
Via della Fara, Bergamo	2,58	10	1,6	72,52	27,48
Via Pellettier, Monza	2,82	46	0,46	49,62	50,38
Via Reiss Romoli, Settimo M.se	1,91	111	0,13	44,09	55,91
Via Vittorio Veneto, Monza	4,43	61,25	0,22	46,82	53,17
Villa Gallavresi, Verderio	0,46	10	1,11	64,28	35,72
Villa Guagnellini, Calolziocorte	3,98	81,65	0,54	49,77	50,23

**Tab. 3.34 Pulling tests Safety Factors and relative soil granulometry average data.**

In the following graphs are visually reported the data shown in Tab. 3.34 and the possible correlation between Safety Factor of the pulling tests (SF) and uniformity coefficient ( $C_u$ ), curvature coefficient ( $C_c$ ), % fine material and % coarse material in the soil samples, respectively in Fig. 3.35, Fig. 3.36, Fig. 3.37 and Fig. 3.38.

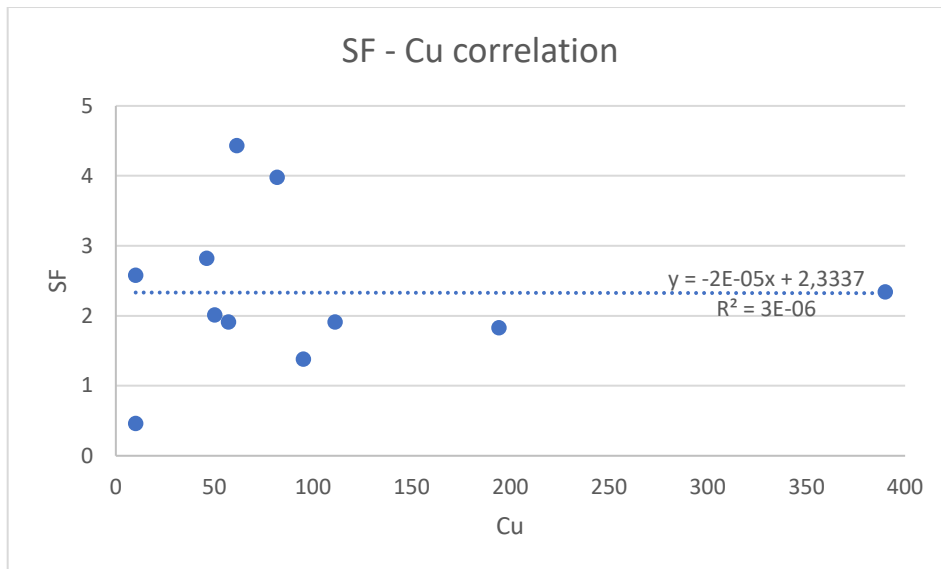


Fig. 3.35 SF – Cu correlation.

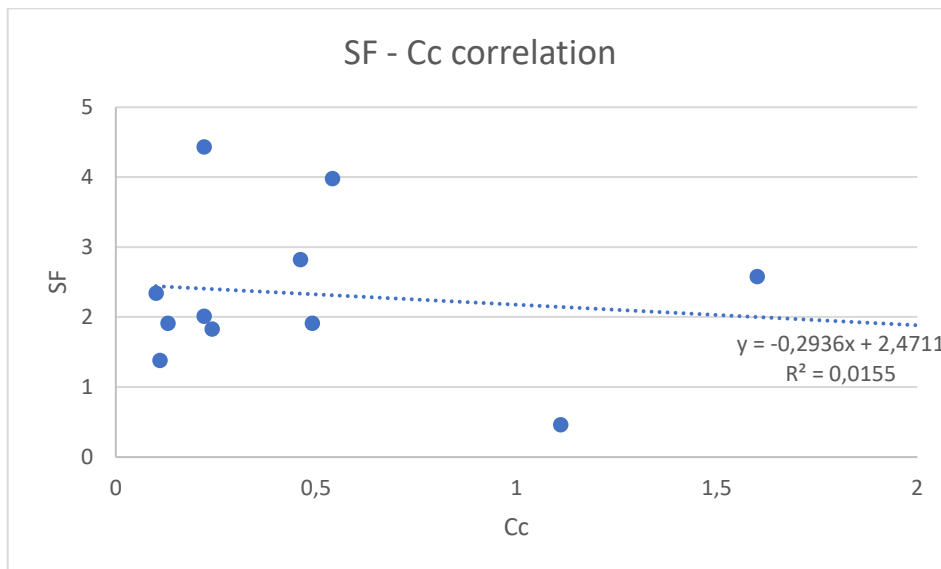
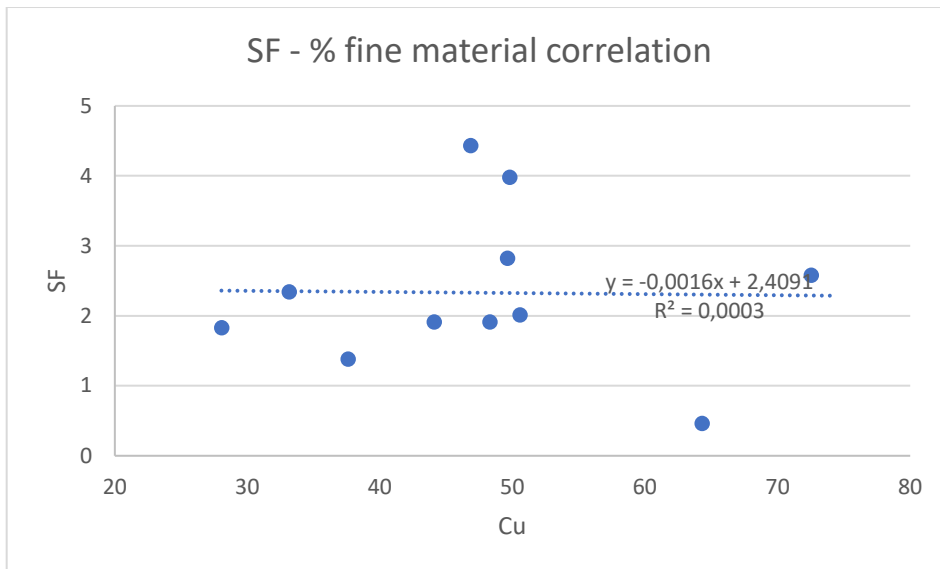
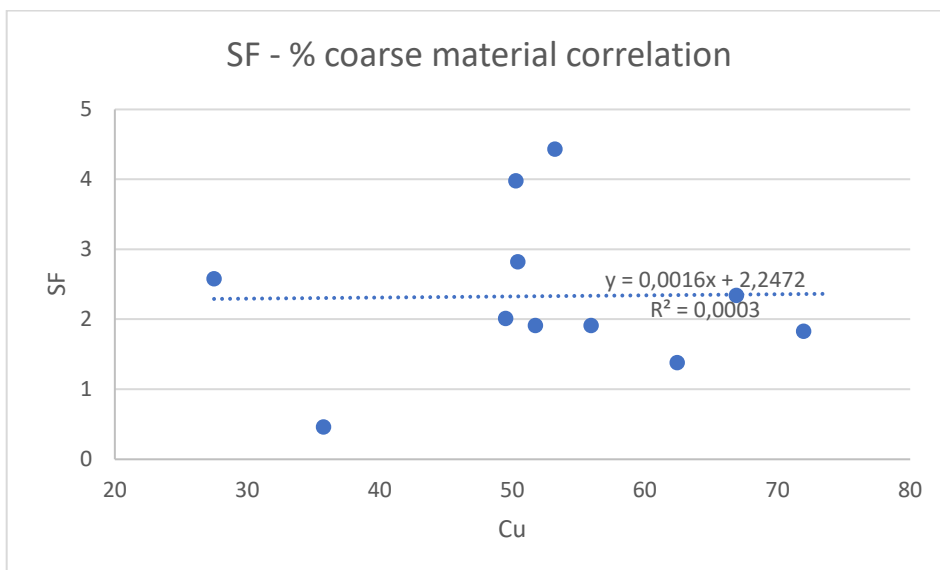


Fig. 3.36 SF – Cc correlation.



**Fig. 3.37 SF – % fine material correlation.**



**Fig. 3.38 SF – % coarse material correlation.**

As easy to predict, these graphs show that there is not a direct correlation between soil granulometry data and pulling test Security Factor. This does not mean that the tree stability does not depend on soil

characteristics, obviously, but several other factors enter into play in addition to them, such as moisture and environmental factors, dimensions and specie of the trees, the architectural structure of their roots and crowns, decay processes by pathogenic fungi, etc.

### **3.4 Direct shear test on urban soil samples**

For completeness, in this paragraph direct share test done on urban soil samples results are reported. This soil samples are picked up near two trees in via Foppa in Milano and, although it is not a location where pulling tests are carried out, the type of soil in this place can be considered similar to those found in that locations, because they are all surface urban soils.

#### **3.4.1 Materials and methods**

For soil samples placed at a depth of 20 cm near plants n. 15431 and n. 15534, direct shear tests were carried out with the Casagrande box and using the equipment shown in the following images (Fig. 3.39; Fig. 3.40).

The test has been carried out according to ASTM D3080-03 on saturated sample. The friction angle in therefore evaluated and it could be applied for low confining stress.

The purpose of the shear tests carried out is to be able to evaluate the value of the friction angle of the soils considered. This evidence, in addition to providing an immediate assessment of the resistance properties of the soil affected by the root system of the plants analysed, is contextualized in a broader process aimed at analysing the stability of tall trees using a deterministic approach. In fact, among the factors contributing to the stability of the tree (such as the extension of the root system, the state and mechanical properties of the woody material constituting the root system and the stem), the angle of friction of the soil plays a important role since it allows to determine the resistance of the soil in dry conditions and through the principle of effective efforts even in saturated or partially saturated conditions.



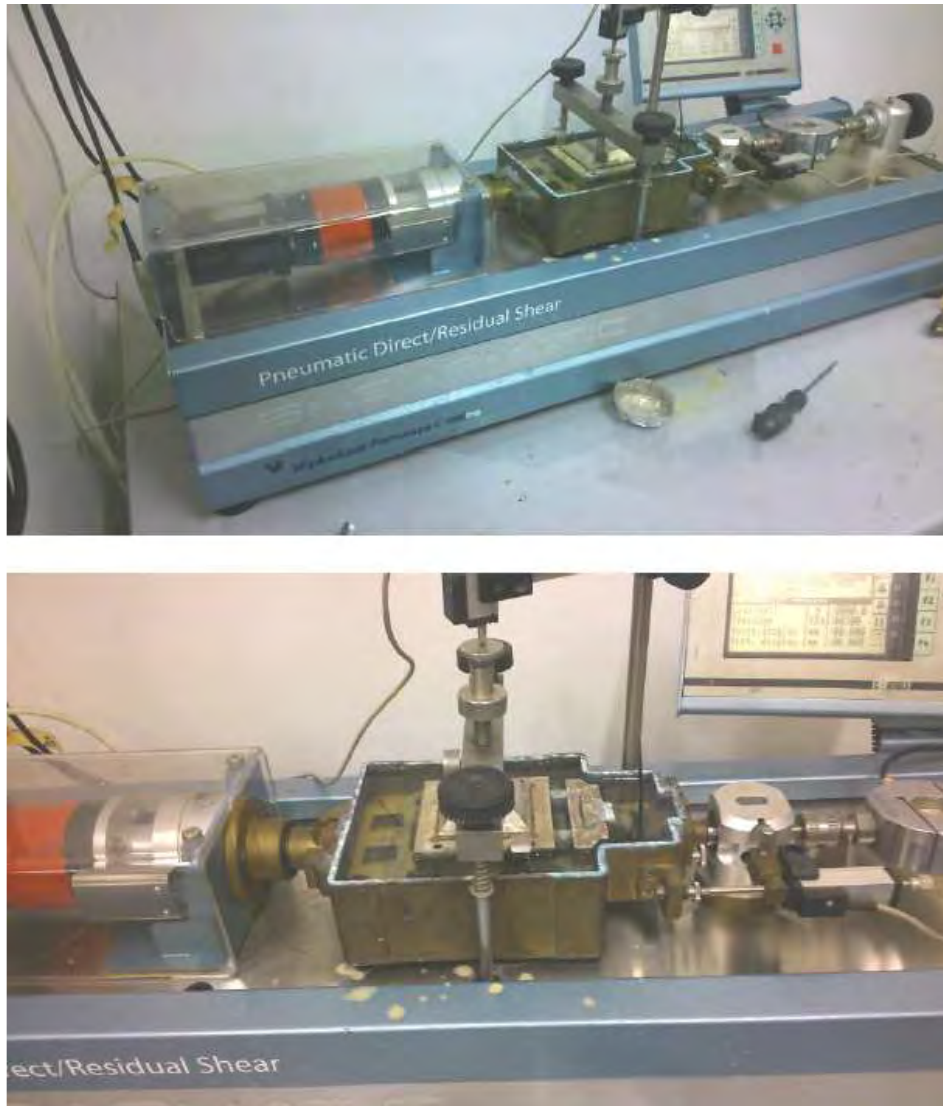


**Fig. 3.39** Equipment used for direct shear tests.

### Chapter 3 – Geotechnical soil characterization

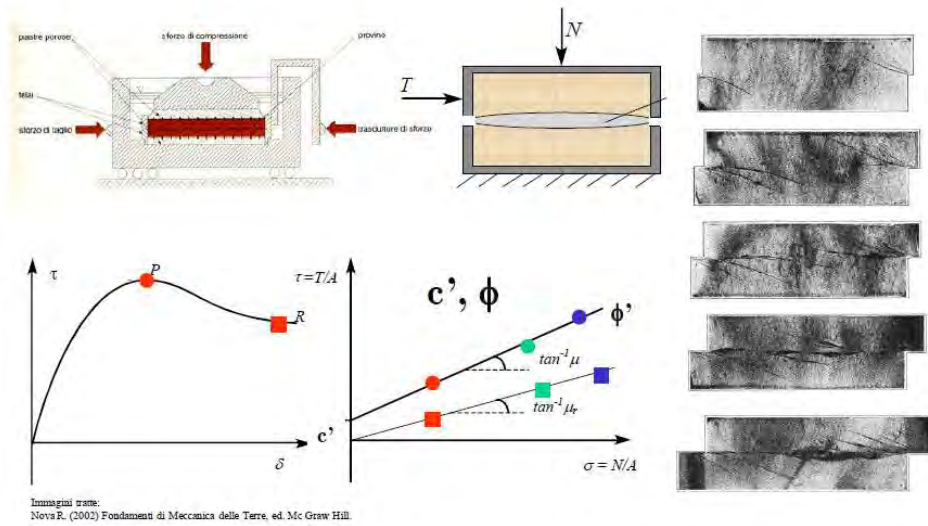


**Fig. 3.40** Test scheme and typical section of the specimen (Castellanza internal report).

### 3.4.2 Results direct shear tests performed

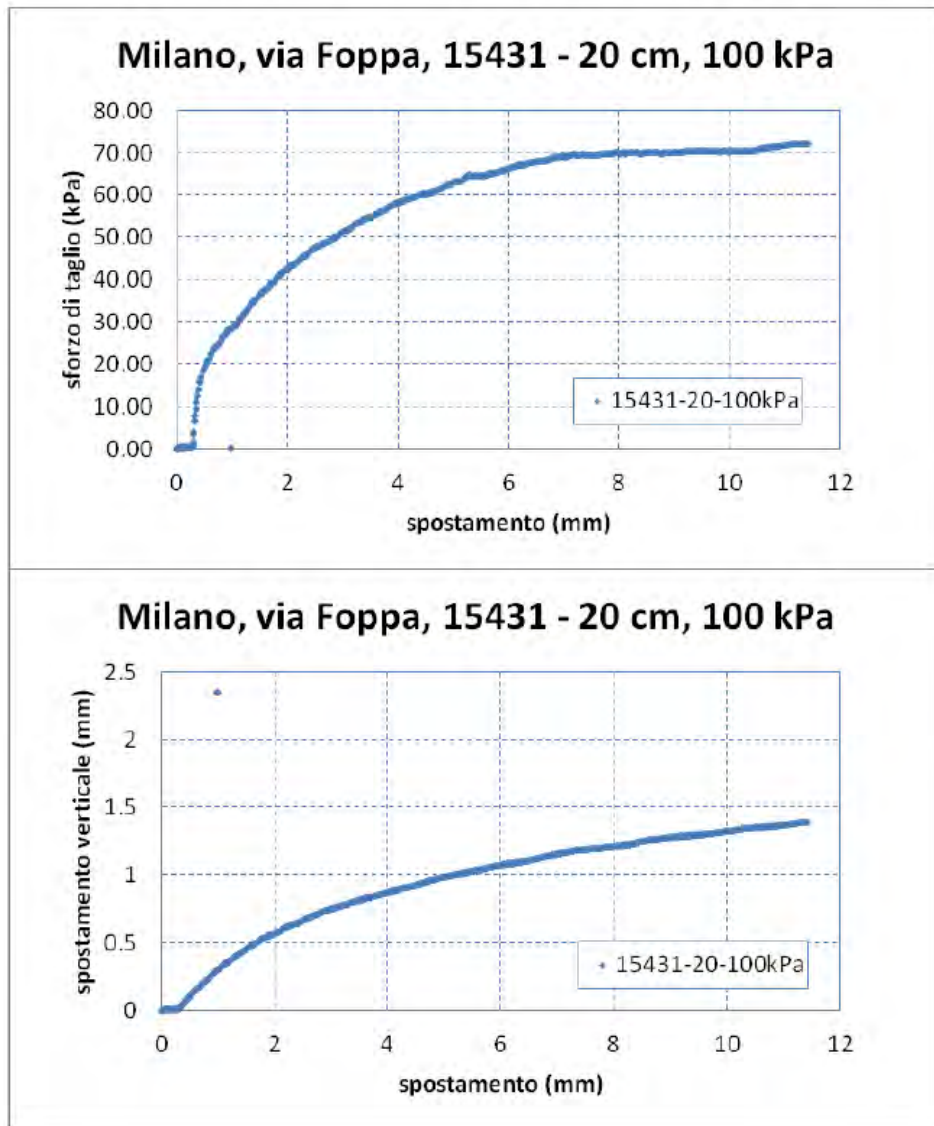


Fig. 3.41 Direct shear tests: specimen 15431-20 step with 100 kPa of vertical stress (Castellanza internal report).

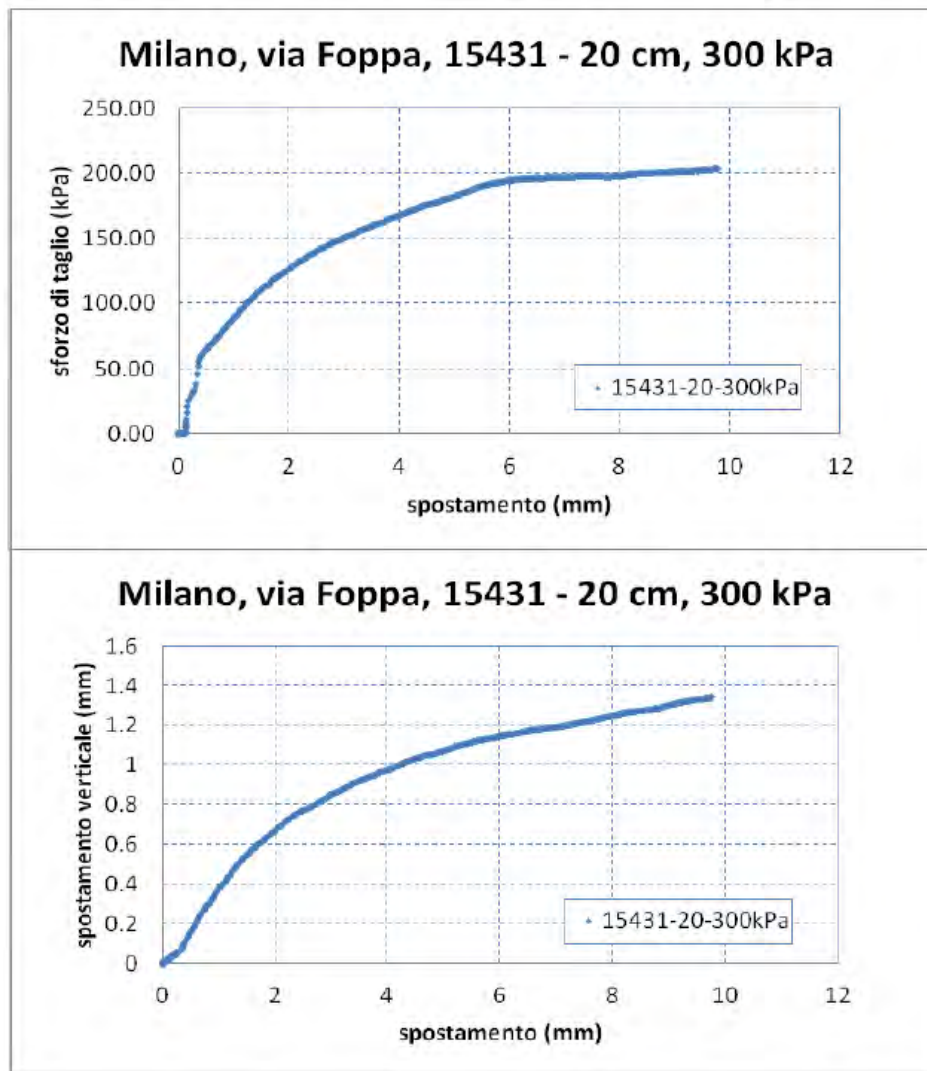


Fig. 3.42 Direct shear tests: specimen 15431-20 step with 300 kPa of vertical stress (Castellanza internal report).

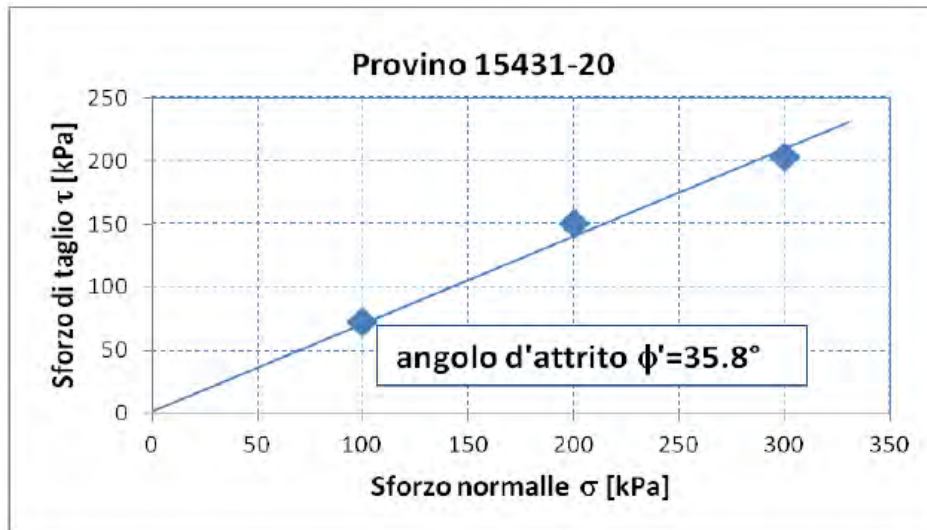


Fig. 3.43 Estimate angle of friction for specimen 15531-20 (Castellanza internal report).

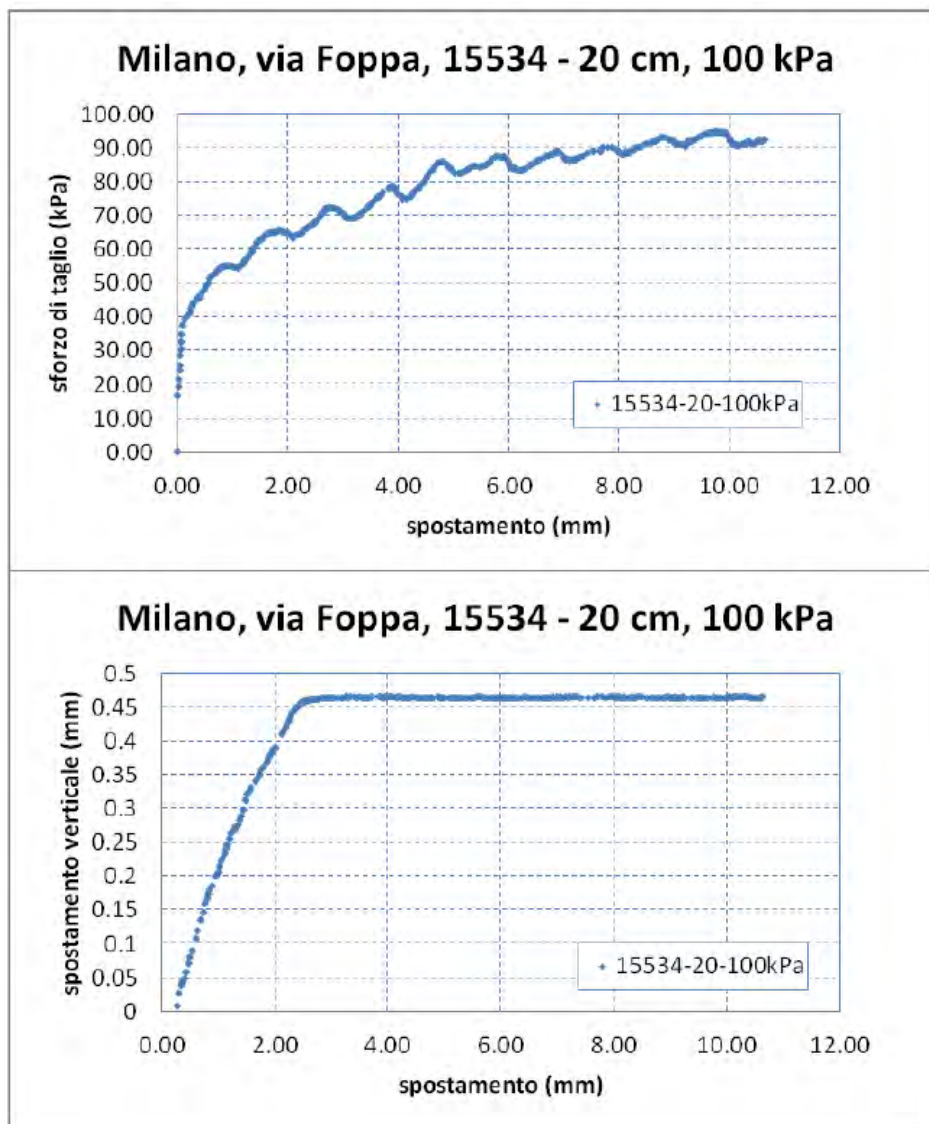


Fig. 3.44 Direct shear tests: specimen 15434-20 step with 100 kPa of vertical stress (Castellanza internal report).

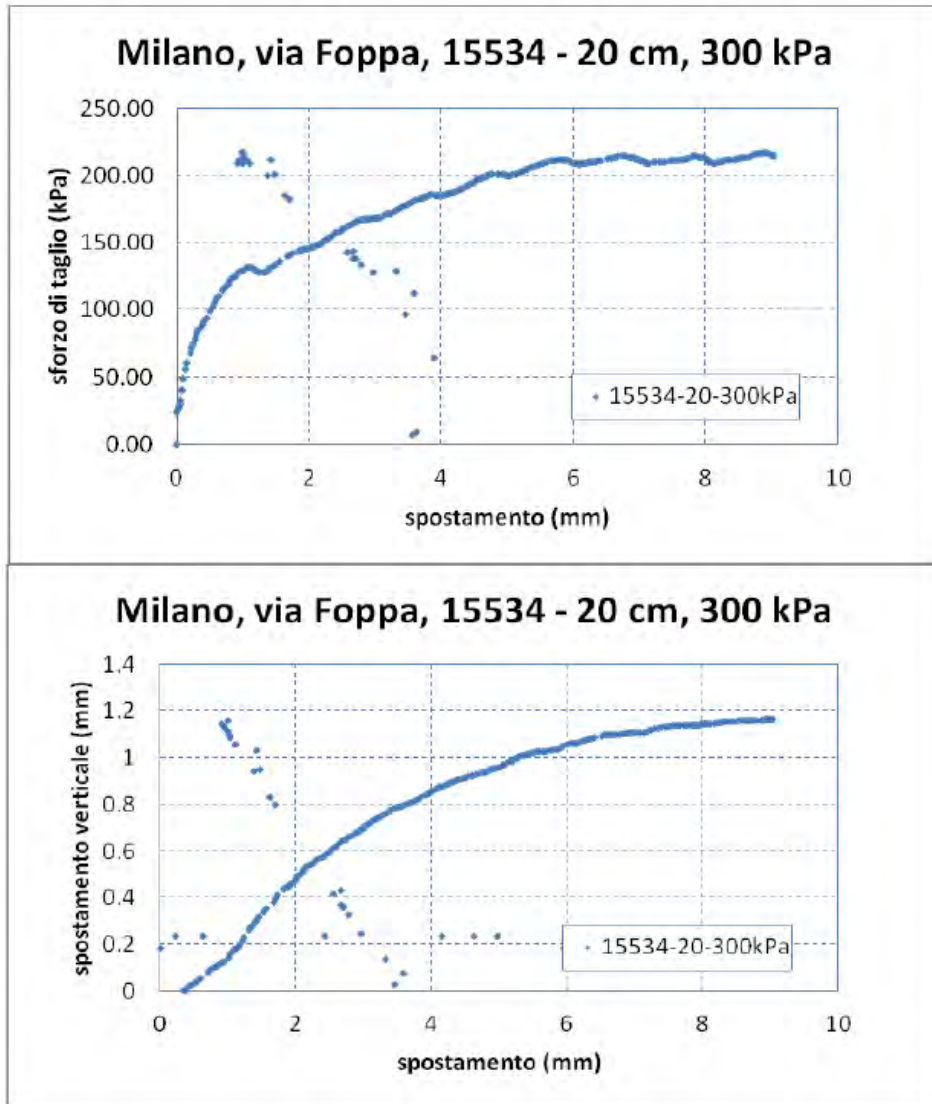


Fig. 3.45 Direct shear tests: specimen 15434-20 step with 300 kPa of vertical stress (Castellanza internal report).

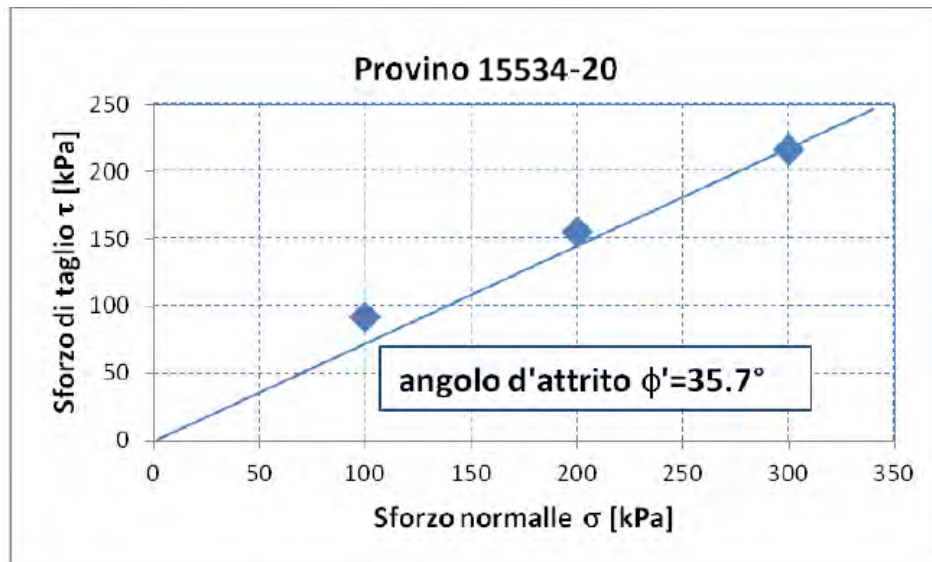


Fig. 3.46 Estimate angle of friction for specimen 15534-20 (Castellanza internal report).

As regards the shear tests shown in previous graphs, it was possible to estimate a value of  $35.8^\circ$  and  $35.7^\circ$  for the two soil samples (from Fig. 3.41 to Fig. 3.46). These values are characteristic of medium / high strength coarse-grained materials even in conditions of complete saturation. The fact remains that when passing from a partially saturated or dry soil to one that is totally saturated with water (for example in the coincidence of significant rainfall) the additional resistance effect provided by the suction decreases until it disappears. The evaluated friction angle value and the grain size curves of the soils can help estimate the residual resistance in saturated conditions.

### 3.5 Conclusions

The geotechnical soils characterization has shown a slight variability between the different rooting sites of the trees analysed, which can however all be defined as urban soils. In the analysed tests, there was no direct correlation between soil granulometries and the safety factors obtained from the pulling tests, but this could be due not to the lack of



### Chapter 3 – Geotechnical soil characterization

---

influence of the soil characteristics on the analyses, but to the fact that on the results of the pulling tests there is the influence of numerous factors, among which the soil granulometry is just one of many.

## Chapter 3 – Geotechnical soil characterization

---

## Chapter 4

### Proposal of a new fitting curve

#### 4.1 Introduction

Since the beginning, pulling tests are executed by applying the Wessolly equation to obtain the overturning curve of a tree starting from the data collected during the test. However, the Wessolly equation seems to have objective limits that could determine a not entirely correct evaluation of the root stability of trees.

For this reason this study tried to hypothesize a new equation that could be used for pulling tests and that does not have the problems of Wessolly's one. This work has been recently described in an article submitted in the international scientific journal *Plant and Soil* (Galli et al. 2021, submitted).

Although in Chapter 2 the importance of the speed of application of force during the execution of the tensile tests emerged, at the moment in this study the speed was not taken into consideration in order not to excessively complicate the calculations.

#### 4.2 Limits of root stability evaluation method

Pulling tests are usually executed by applying a force  $F$  at a height  $H$  and with an inclination  $\alpha$  with respect to the horizontal ground surface, and by recording the corresponding rotation  $\varphi$  of the trunk (Fig. 4.1). The aforementioned Wessolly procedure is based on the numerical fitting of the experimental data by means of the following generalized tipping equation

$$\varphi = \frac{1}{3} \tan \left( \frac{100}{73,85} \frac{F}{F_L} \right) + \frac{1}{2} \left( \frac{F}{F_L} \right)^2 - \frac{1}{10} \frac{F}{F_L},$$

where the fitting parameter  $F_L$  represents the reference limit value of the force  $F$ . Fig. 4.2 shows the analytical trend of equation above and the variability of the database results. In standard practice, in order to prevent possible damage to the roots, the test is usually limited to maximum rotations not exceeding  $0.2^\circ$ , which corresponds to a very limited portion of the curve, and the value of  $F_L$  is then obtained as extrapolation over the measured data.

Over the years, Wessolly equation has been widely employed for professional activities, and got several experimental confirmations (an accuracy ranging from  $\pm 4\%$  to about  $\pm 37\%$  on the evaluation of  $F_L$  was recently reported by Siegert, 2013, on the basis of twelve field tests).

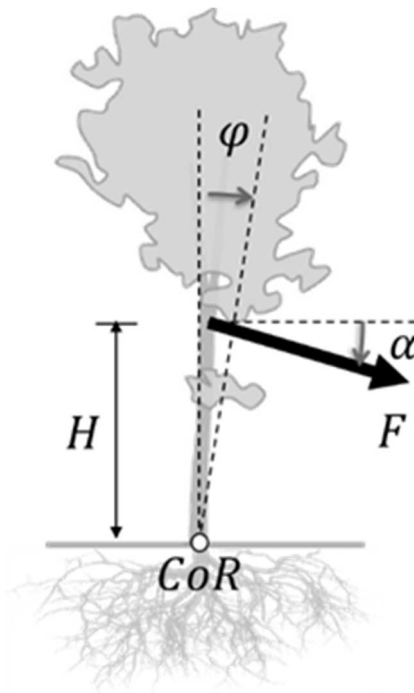


**Fig. 4.1 Schematic view of a pulling test.**

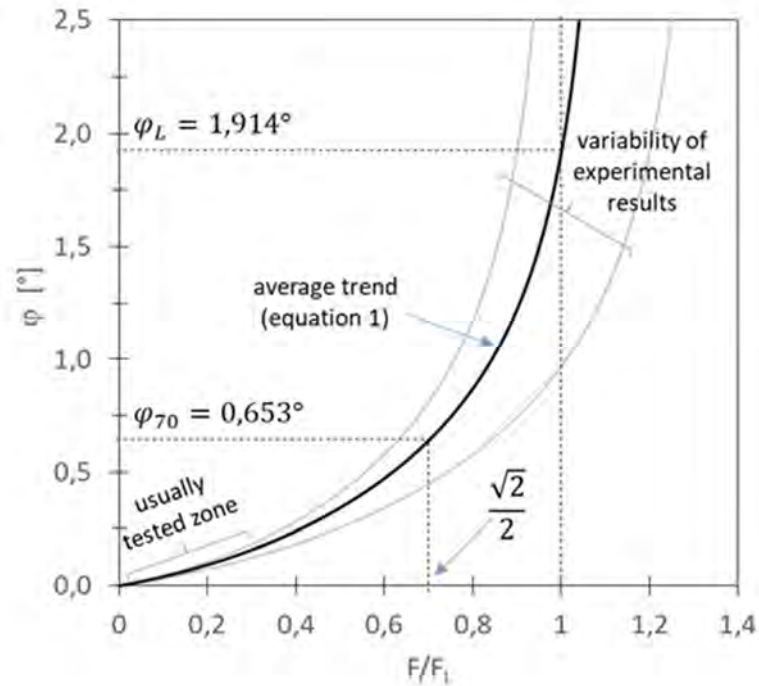


Fig. 4.2 Wessolly curve (solid line)

However in this method there are several points still to be resolved, including errors and difficulties in measurement and evaluation of several data and parameters (see Sani 2017 for a precise review about these kind of practical matters).

Some critical observations can, also, be expressed with reference to the Wessolly equation:

- (a) the limited range of diameters considered in the calibration of Wessolly equation (15-35 cm) makes this latter hardly applicable to larger diameter trees, which represent however a class of trees frequently studied in practical applications, like e.g. in the case of monumental trees;
- (b) the definition of only one fitting parameter ( $F_L$ ) allows to scale the Wessolly curve, during the fitting procedure, only with respect to the load axis (i.e. the axis  $F/F_L$ ), without the possibility to scale the

- curve along the rotation axis too (axis  $\varphi$ ), as it would be useful in order to capture possible scale effects, related to the size of the tree;
- (c) the Wessolly equation does not allow to precisely fit the initial roundness of the experimental curve, thus making potentially largely inaccurate any extrapolation with respect to the measured data;
  - (d) no reference is in general made to the type of soil interacting with the root system.

From a mechanical point of view, moreover, it can be also noted that Wessolly equation:

- (e) does not show any asymptotic trend when  $F$  approaches  $F_L$ , as it should derive from a consistent definition of an ultimate failure condition for a perfect ductile system;
- (f) is expressed in terms of static and kinematic variables ( $F$  and  $\varphi$ , respectively) which are not work-conjugate to each other; as a consequence, it does not represent a meaningful mechanical relationship, and no further interpretations (like e.g. the definition of a representative global rotational stiffness, or the evaluation of the dissipated energy during the test) can be derived;
- (g) does not allow an explicit mathematical inversion, thus making it hard to be applied in displacement-controlled numerical models.

In particular, points (d) and (f) are of fundamental importance in view of possible extensions of the study, like e.g. (i) the search for meaningful correlations with well-defined soil mechanical properties, (ii) the investigation of more complex loading conditions (dynamic effects of wind gusts or repeated loadings, or seismic analyses of monumental trees), (iii) the comparison with advanced numerical modelling approaches (e.g. 3D finite element simulations).

### **4.3 Why is a new curve necessary?**

As described in previous paragraph, Wessolly curve has some problems from a mechanical and accuracy point of view. The realistic application about pulling tests observed in Chapter 2 shows that each force/inclination curve is different each other. The reason of these differences could be

found in different kind of trees and soil, materials, dimensions of the single part of the system (crown, branches, trunk, roots, soil, ...), environmental factors (temperature, moisture, ...), etc.

Considering all these variables, it is therefore logical to think that a single empirical and static equation cannot describe in a realistic way the behavior of all types of trees subjected to pulling test. A new variable curve is then necessary to find for the root stability evaluations, that could adapt itself to the real behavior of each single pulled tree.

#### 4.4 Proposition a new interpolating equation

From a mechanical point of view, the pulling test can be assimilated to a toppling test on a 1 d.o.f. rotational system, described by a rotation  $\varphi$  with respect to its center of rotation (*CoR*, assumed to coincide with the base of the trunk), under a toppling moment  $M$  computed as:

$$M = H \cdot F \cdot \cos \alpha$$

Starting from Wessolly's equation shown below,

$$\varphi = \frac{1}{3} \tan \left( \frac{100}{73,85} \frac{F}{F_L} \right) + \frac{1}{2} \left( \frac{F}{F_L} \right)^2 - \frac{1}{10} \frac{F}{F_L},$$

a new physically-based equation is hereafter proposed. The choice was to neglect the polynomial terms and all the numerical coefficients of this empiric equation, to express the moment  $M$  as a function of the rotation  $\varphi$ , and to enrich the resulting arctangent relationship of an exponent  $b$ .

The resulting equation can then be expressed as:

$$\frac{M}{M_L} = \left[ \frac{2}{\pi} \arctan \left( \alpha \frac{\varphi}{\varphi_{70}} \right) \right]^b$$

with

$$\alpha = \tan \left[ \frac{\pi}{2} \left( \frac{\sqrt{2}}{2} \right)^{1/b} \right]$$

In this case the toppling moment  $M$  (static quantity) takes the place of the applied pulling force  $F$ , and it is directly linked with its work-conjugate kinematic quantity, i.e. the rotation  $\varphi$  measured in the pulling plane (i.e. the plane defined by the direction of applied force  $F$  and by the centre of rotation  $CoR$ ). This new equation represents then a meaningful mechanical relationship, characterized by three parameters, in particular:

- $M_L$  corresponds with the ultimate asymptotic resistance of the root system against toppling;
- $\varphi_{70}$  represents the rotation of the system for an applied toppling moment  $M_{70} = \frac{\sqrt{2}}{2}M_L$  (i.e. about 70% of  $M_L$ );
- $b$  is the exponent that controls the roundness of the curve, in particular for very limited rotation amplitudes.

It is worth noting that the term  $\alpha$  is an internal parameter, uniquely dependent on  $b$  and introduced here only for the sake of clarity of the analytical expression. Its definition derives simply from imposing

$$M/M_L = \sqrt{2}/2 \quad \text{when} \quad \varphi/\varphi_{70} = 1$$

The new equation is then fully non-dimensional, it can be independently scaled along both the  $M$  and  $\varphi$  axes, and its curvature is controlled by parameter  $b$ .

A parametric study of this one is shown in

Fig. 4.3, together with a consistent non-dimensional plot of the Wessolly equation.



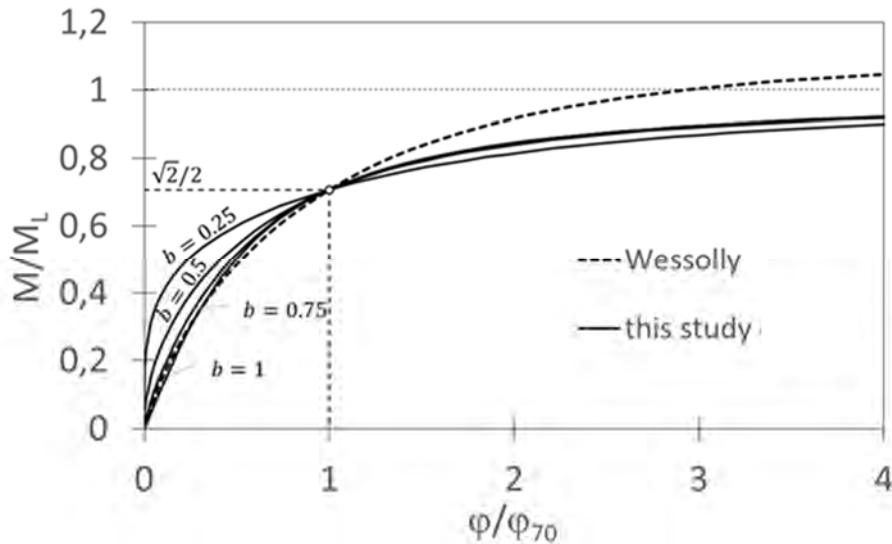


**Fig. 4.3 Parametric study of the new equation and comparison with a dimensionless Wessolly curve.**

This latter was in particular obtained by normalizing the rotation axis  $\varphi$  with respect to the corresponding  $\varphi_{70}$  value of Wessolly equation ( $0.653^\circ$ , as defined in Fig. 4.2), and, owing to the equation  $M = H \cdot F \cdot \cos \alpha$ , by equivalently expressing the ratio  $F/F_L$  as  $M/M_L$ .

Fig. 4.3 highlights in particular the influence of the exponent  $b$  on the roundness of the proposed curve in the field of limited rotations ( $\varphi/\varphi_{70} < 1$ ), where the new equation tends to coincide with Wessolly equation when  $b \cong 1$ . Values of  $b > 1$  would instead induce an upward concavity of the curve and they cannot be accepted. For larger rotations ( $\varphi/\varphi_{70} > 1$ ) a clear asymptotic trend is evident in the new equation, and parameter  $b$  does not significantly affect any longer the curve.

It is worth noting that parameter  $M_L$  both for Wessolly equation and new equation only represents an analytical estimation of the resisting moment when “large” values of the rotation  $\varphi$  are considered. For Wessolly equation, in particular, this conventionally corresponds with a rotation  $\varphi_L = 1.914^\circ$  (see Fig. 4.2); in the new equation  $M_L$  corresponds instead with a theoretical asymptotic condition. In practical cases, however, the global collapse of a tree results from the combination of

several failure mechanisms (partial failure mechanisms in the soil involving the base toppling, local failure of one or more roots, crack opening in the trunk...) which are progressively activated for increasing values of the applied toppling moment. All these aspects are in general associated to larger and larger rotation values, inducing also irreversible local damages to the system (frequently characterized even by fragile responses) and they cannot be explicitly considered in both equations. These are in fact only intended to model the global mechanical response of the root system in the loading phase, and without any possibility to reproduce the post-peak behaviour. Parameter  $M_L$  must then be considered representative only of a “critical” condition for an ideal perfectly ductile toppling failure mechanism, and it may significantly differ from the value of the toppling moment  $M$  inducing the global collapse of the tree in real experimental tests, as it will be discussed in the following.

#### 4.5 Proposition a remark on parameter $\varphi_{70}$

The introduction of parameter  $\varphi_{70}$  is of particular mechanical interest, since it allows to extend the criteria for evaluating the stability of a tree, currently based only on the comparison between the expected working condition (i.e. the applied moment  $M$ ) and the ultimate toppling resistance  $M_L$ , through the definition of a global safety factor  $F_S = M_L/M$ . Such definition, however, follows a so-called capacity-based approach, and completely neglects deformability issues, i.e. the evaluation of the rotation of the tree under the assigned working condition. It is evident in fact that two curves characterized by similar values of  $M_L$  and by remarkably different values of  $\varphi_{70}$ , should be associated to different stability conditions. This concept is schematically sketched in Fig. 4.4, where two ideal curves (a) and (b), subject to the same applied moment  $M_{70}$ , are considered. The two cases are obviously characterized by the same value of the factor of safety  $F_S = M_L/M_{70} = \sqrt{2} \approx 1.4$ , but curve (b) denotes a “less safe” condition. Larger rotations are in fact required for curve (b) to resist the applied moment, thus potentially inducing

- irreversible damages to the root system;

- the loss of the overall stability due to the contribution of the crown weight.

In the assessment procedure, in order to prevent (or, at least, to limit) both these effects to occur, higher values of the factor of safety should then be requested for curve (b) with respect to curve (a). This concept is qualitatively shown in Fig. 4.5, where the acceptability limit for  $F_S$  (i.e. the threshold between the safe and unsafe zone) is a function of parameter  $\varphi_{70}$ , rather to be represented by a constant value as it is commonly assumed in practice (values between 1.3÷1.5 are usually chosen).

Although a quantitative definition of such dependency is beyond the purposes of the present work, but it is a hope that this study can – at least partially – promote the definition of such “performance-based” conceptual framework even for the stability assessment of trees, as it already happens in several field of geotechnical and civil engineering (Priestly et al., 2007; Galli et al., 2017; Galli, 2020; di Prisco et al., 2020).

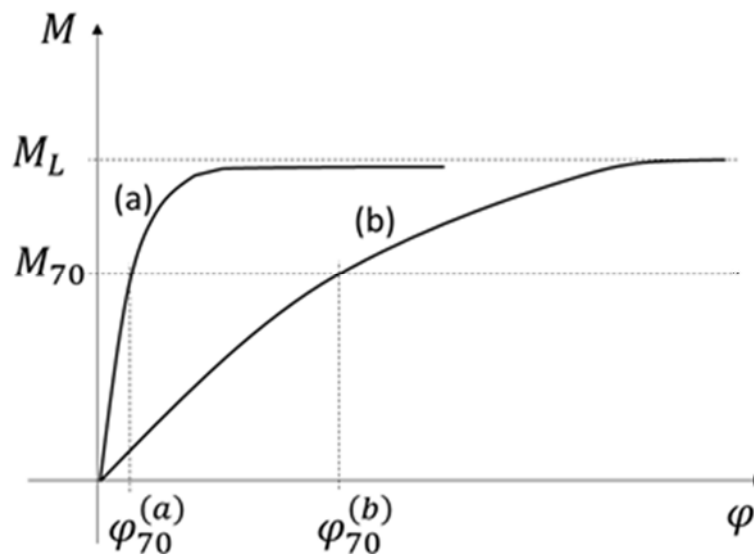


Fig. 4.4 Influence of parameter  $\varphi_{70}$  on the  $M - \varphi$  curve.

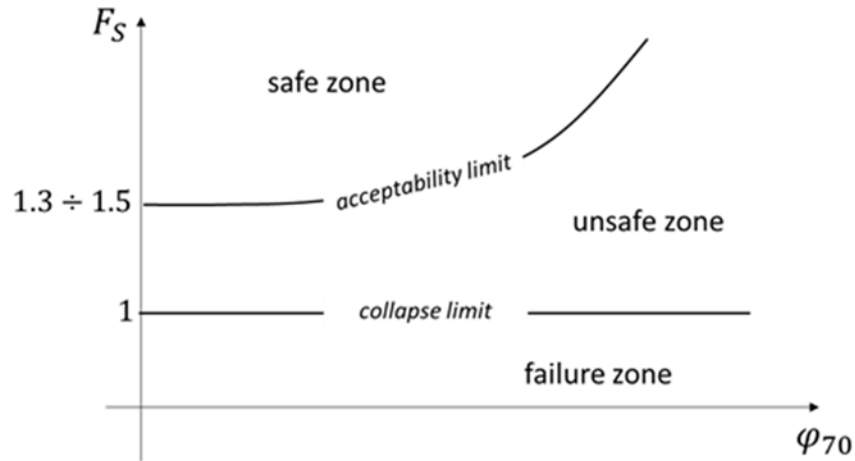


Fig. 4.5 “Performance-based” definition of the acceptability criterion for  $F_S$ .

## 4.6 Conclusions

Starting from the Wessolly equation, a new equation has been created that overcomes some limits that characterize it. This new equation could, therefore, be used for the evaluation of the stability of trees by pulling tests to better describe the overturning curve of trees, as shown in the following chapters. Furthermore, some considerations have been expressed regarding the parameter  $\varphi_{70}$ , which could also be useful during the execution of the pulling tests.

Further tests and investigations are desirable to confirm the preliminary results of this study, possibly supplementing them with further parameters that, at the moment, have not been taken into consideration, i.e. the speed of force application.

## References

- di Prisco, C., Flessati, L., Frigerio, G., Galli, A. (2020). Mathematical modelling of the mechanical response of earth embankments on piled foundations. *Geotechnique*. 70(9), pp755-773.
- Galli A., Maiorano R.M.S., di Prisco C., Aversa S. (2017) – Design of slope-stabilizing piles: From Ultimate Limit State approaches to displacement based methods. *Rivista Italiana di Geotecnica*, 51, n. 3, pp. 77-93.
- Galli A., Sala C., Castellanza R., Marsiglia A., Ciantia M.O. (2021) – An improved interpretation of pulling tests for tree stability assessment. *Plant and Soil*, submitted.
- Galli A. (2020). Macroelement approaches for Geotechnical problems: a promising design frame- work? *Rivista Italiana di Geotecnica* 54(2), 27-49.
- Priestley M.J.N., Calvi G.M., Kowalsky M.J. (2007) – *Direct Displacement-Based Seismic Design*, IUSS Press, Pavia.
- Sani, L. (2017). *Statica delle strutture arboree*. Gifor, ISBN-13: 979-1220016698, 945 p.
- Siegert, B. (2013). Comparative analysis of tools and methods for the evaluation of tree stability: results of a field test in Germany. *Arborist News* 2013 Vol.22 No.2 pp.26-31 ref.1. ISSN: 1542-2399, International Society of Arboriculture.

## Chapter 4 – Proposal of a new fitting curve

---

## Chapter 5

### Experimental pulling tests till overturning

#### 5.1 Introduction

During all this study, several pulling tests were run on real scale trees, following the loading scheme shown in previous chapters. They has been performed in according with a “standard” non-destructive approach, consisting in a single loading phase on relatively large diameter trees, not exceeding a rotation of about  $0.2^\circ$ , before inducing irreversible damages to the trees.

As shown in this Chapter, two other tests (Test 1 and Test 2 in the following) were on the contrary run on smaller diameter trees than all other traditional tests (within the range 15-35 cm, consistently with the calibration of Wessolly equation), followed a non-standard loading path consisting in several loading-unloading cycles at increasing amplitude, until the complete failure. The idea for these two latter tests was to study (although in a quasistatic scheme) the effects of non-monotonic loads on the toppling response of a tree, since this condition, rather than a simple monotonic loading scheme, more accurately reproduces the effect of an intense wind action.

#### 5.2 Description of the experimental work

The tree typologies and the geometrical characteristics of the tests are reported in Tab. 5.1.

test	type of tree	diameter D [cm]	pulling height H [m]	anchoring distance L [m]
1	<i>Prunus avium</i>	22	0.4	16.8
2	<i>Robinia pseudoacacia</i>	30	4.6	39.50

**Tab. 5.1** Tree typologies and geometrical characteristics of experimental Test 1 and Test 2.

The load was applied for all test by means of a manual winch and measured by a commercial load cell (maximum capacity 5 tons), but rotations in Test 1 and Test 2 were measured by means of a 3-axis large scale inclinometer was used (Fig. 5.2; measurement range  $\pm 90^\circ$ ; resolution  $0.05^\circ$ ). This latter was installed with axes  $x$  and  $y$  laying in the pulling plane (along the horizontal and vertical rotation, respectively), while axis  $z$  represents the main axis of rotation of the test (see also Fig. 5.5 and Fig. 5.13). The experimental data were acquired at a frequency of 10 Hz, by using the software provided for the measuring devices.



**Fig. 5.2** Adopted instrumental equipment for pulling test: 3-axis large scale inclinometer (Wit Motion, 2019).

For both test 1 and 2 one soil sample has also been picked up at a depth of about 30 cm. In both cases the soil can be classified as a silty sand, with



important gravelly fractions; the two grain size distributions are reported in Fig. 5.3, whilst the particle size characterization of the two soil samples is summarized in Tab. 5.4. A detailed description of these two non-standard tests is separately reported below in this chapter.

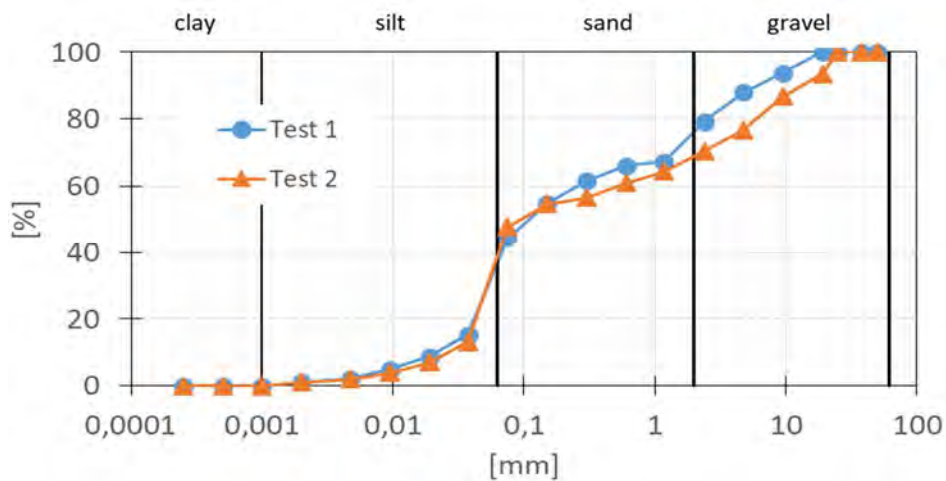


Fig. 5.3 Grain size distributions of the soil samples for Test 1 and Test 2.

	Clay [%]	Silt [%]	Sand [%]	Gravel [%]	$D_{10}$ [mm]	$D_{50}$ [mm]	$D_{60}$ [mm]	$C_U$ [-]	$w_n$ [%]
Test 1	0.02	35.09	40.44	24.45	0.02	0.12	0.26	11.76	27
Test 2	0.06	33.88	34.66	31.40	0.03	0.10	0.53	19.04	13

Tab. 5.4 Particle size characterization of the two soil samples.

### 5.3 Test 1

The test was run on a relatively small *Prunus avium* (diameter of trunk  $D = 22$  cm); this case can be considered as an “ideal” case of a healthy tree (the wood did not present any evidence of structural weakness) perfectly respecting the Wessolly range of diameters (15-35 cm). The trunk was previously completely pruned at a height of about 190 cm from the ground

in order to prevent any second order effects (related e.g. to the weight of the crown) to occur on the  $M - \varphi$  curve, even for large rotation values. The pulling rope was fixed at a height of  $H = 40$  cm from the ground, and it was anchored at the base of another stable tree at a distance of  $L = 16.8$  m (Fig. 5.5). The inclination of the applied pulling force  $F$  was then very limited (angle  $\alpha = 1.36^\circ$ ), so that a negligible vertical load component is transferred to the root system. The load program consisted in three loading-unloading cycles at increasing amplitude (recorded values of moment and rotation histories are plotted in Fig. 5.6; a pause of about 30 minutes between cycles 1 and 2 allowed a preliminary check of the results). The complete toppling of the tree was reached during a following fourth loading phase, whose values have however been here omitted since they are out of scale. The positions of the tree during the different phases of the loading program are schematically represented in Fig. 5.7, whilst Fig. 5.8 and Fig. 5.9 show two final views of the uprooted tree.

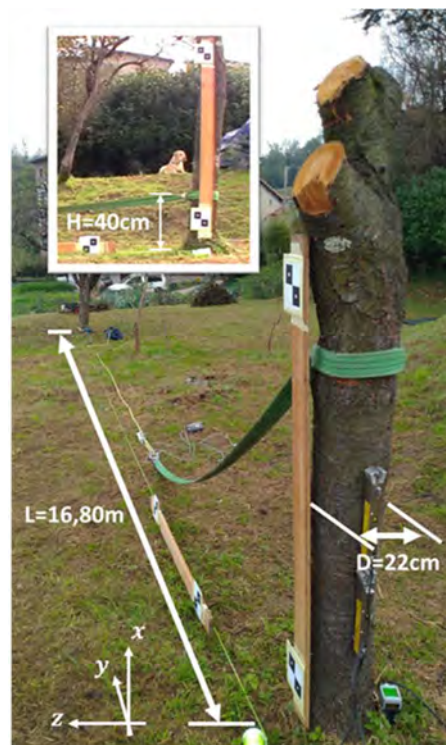


Fig. 5.5 View of the experimental set up of Test 1.

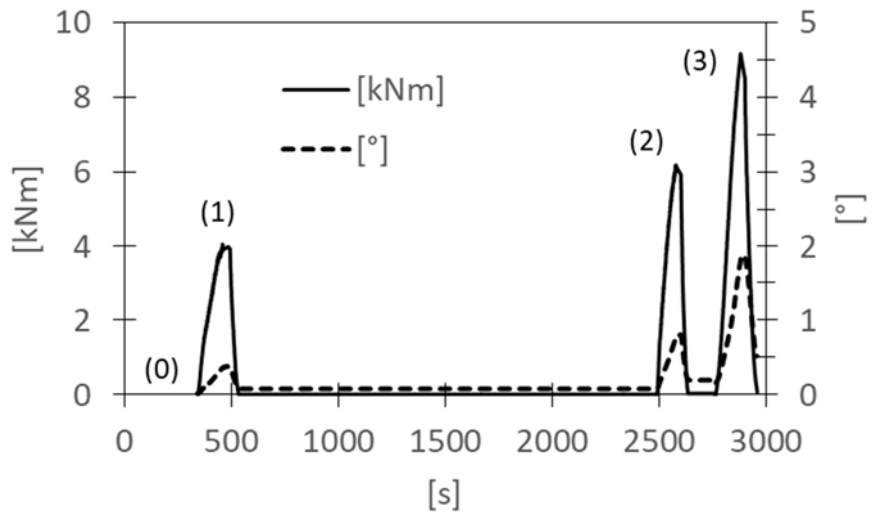


Fig. 5.6 Load (solid line) and rotation (dashed line) records.

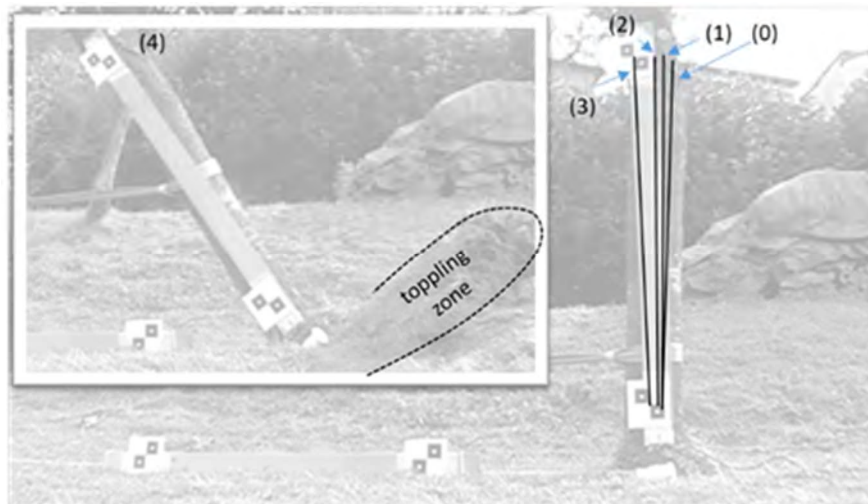


Fig. 5.7 Peak rotation of the tree and observed toppling mechanism.



**Fig. 5.8 View of the uprooted tree (front).**



**Fig. 5.9 View of the uprooted tree (behind).**

The resulting  $M - \varphi$  curve (Fig. 5.10) shows a complex non-linear and irreversible behaviour, with progressive accumulation of permanent rotation at end of each unloading phase. A maximum toppling moment  $M_P = 9.15$  kNm was reached in cycle 3 for a rotation of  $1.78^\circ$  (point P in Fig. 5.10), which can be considered relatively close to the limit condition of Wessolly equation ( $\varphi_L = 1.914^\circ$ ). By considering the different loading-unloading cycles, moreover, it also appears that different partial failure mechanisms are progressively activated during the test. In particular, cycles 1 and 2 appear to be part of the same first partial failure mechanism, as it is witnessed by the negligible rotation accumulation between the first loading phase of cycle 1 and the reloading phase of cycle 2 ( $\Delta\varphi_{12} \approx 0$ , as defined in Fig. 5.10). On the contrary, between cycles 2 and 3 an evident rotation increment is observed ( $\Delta\varphi_{23}$ ), thus possibly suggesting that a secondary partial failure mechanism, characterized by a slightly higher ultimate load and a lower overall stiffness, has been activated. Grey lines in Fig. 5.10 qualitatively represent possible envelopes of such first and second partial failure mechanisms.

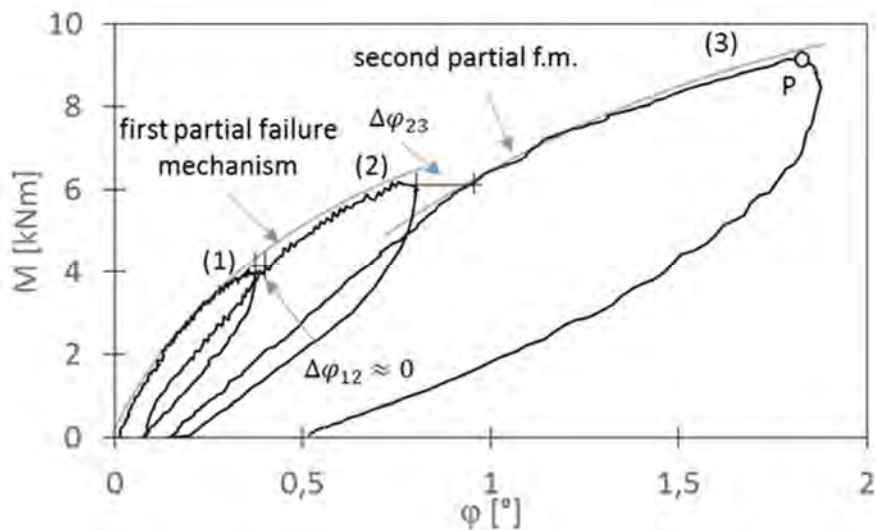


Fig. 5.10  $M - \varphi$  curve for Test 1.

A deep investigation of the progressive activation of such multiple failure mechanisms is beyond the purposes of the present work, since it would require a detailed description of the root geometry and of its local interaction with the soil, which is in general not available for practitioners during standard on site pulling tests. These latter, moreover, usually consist only of a unique monotonic loading phase. In the following, consequently, the fitting procedure will be applied only to the envelope of the overall virgin loading curve, i.e. by disregarding the unloading-reloading cycles, and without a priori considering the presence of multiple partial failure mechanisms. The quantitative analyses of the mechanical response of the system during unloading-reloading cycles is however of great importance for modelling the toppling behaviour of trees, especially in complex loading conditions, and the collected experimental data have been made here available with the aim of promoting, hopefully, further investigations in future papers.

### **5.3.1 3D modeling of the root system in Test 1**

Thanks to the fact that the root system of the tree uprooted during Test 1 in Oggiono (LC) remained almost intact, it has been possible to recover the entire root structure of the plant and realize a 3D photographic relief (Fig. 5.11). So, by a special photographic processing software (Agisoft Metashape), it has been possible to create a 3D digital model of the entire root system of the tree (Fig. 5.12). This is very interesting to visually understand the complexity and variability of the anchoring system of plants to the ground and why their stability evaluation could be very difficult. 3D model is, also, very useful to create realistic models of the root systems in small scale, on which to perform further tests and in-depth studies on tree stability, with obvious advantages in terms of time and costs, as seen in Dattola et al. (2019).



**Fig. 5.11 Root system photographic image .**



**Fig. 5.12 Root system 3D digital model.**

## 5.4 Test 2

The second pulling test was conducted on a *Robinia pseudoacacia* (diameter of trunk  $D=30$  cm), with an estimated height of 14 m. The pulling rope was fixed at an height of  $H=4.6$  m from the ground and anchored at a distance of  $L=39.50$ m (angle  $\alpha=6.64^\circ$ ; Fig. 5.13). The same instrumental equipment described before in this chapter was employed, and the inclinometer was installed consistently with the reference system also shown in Fig. 5.13 and Fig. 5.14. The loading programme consisted again in several loading-unloading cycles at increasing amplitude, whose global  $M - \varphi$  curve is shown in Fig. 5.17. A complex non-linear and irreversible behaviour is again evident, with the possible activation of multiple partial failure mechanisms during cycles 1 and 2 (grey lines in Fig. 5.17), with the mobilization of an evident toppling zone (Fig. 5.17 and Fig. 5.18). During the loading phase of cycle 3, however, a long vertical crack opened on the compressed side of the trunk (Fig. 5.16) which significantly modified the overall mechanical response of the system. The following part of the test (until the failure of the tree, consisted in a sudden trunk breakage, as shown in Fig. 5.19) was then considered not representative of a toppling mechanism. Only the initial part of the test will then be considered for the fitting procedures, up to a rotation  $\varphi$  of about  $1^\circ$  and a maximum toppling moment of 21.48 kNm (point P of

Fig. 5.15). As previously discussed for Test 1, unloading-reloading phases will be disregarded, and the envelope of the virgin loading curve up to point P will only be used.



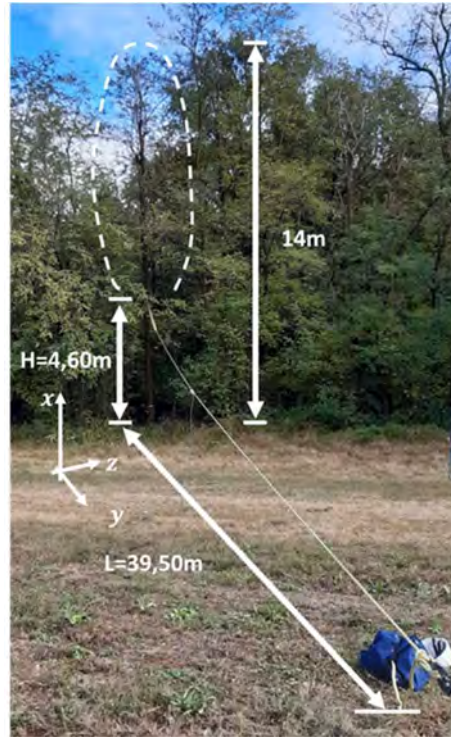


Fig. 5.13 View of the experimental set up of test 2.



Fig. 5.14 Detail of Tests 2.

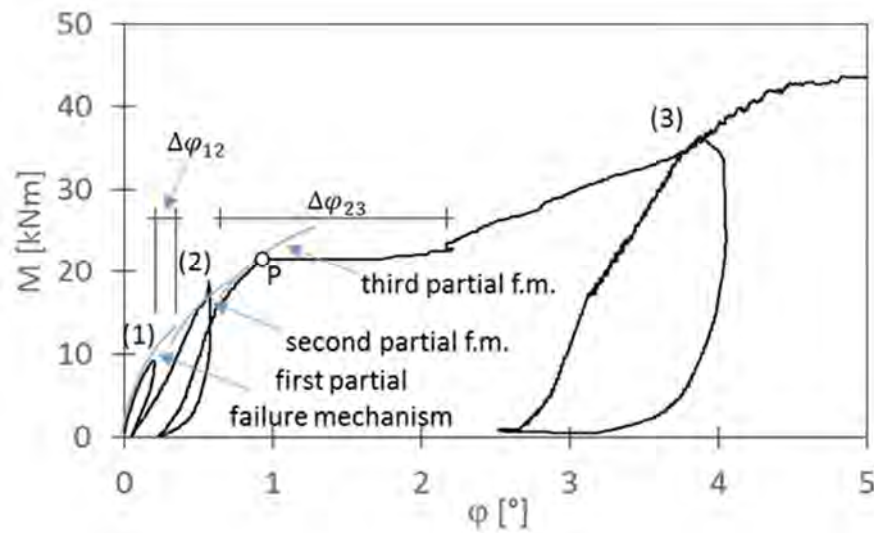


Fig. 5.15  $M - \phi$  curve for Test 2.



**Fig. 5.16 Crack formation during the Test 2.**



**Fig. 5.17 View of the tree at the beginning of the Test 2.**

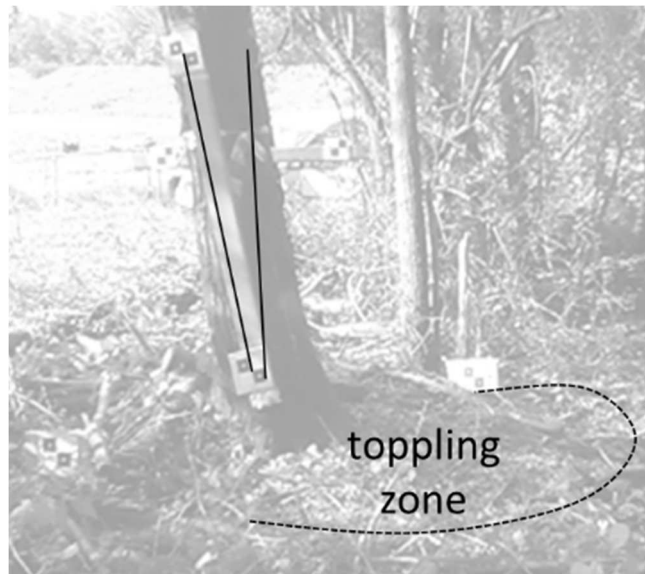


**Fig. 5.18** View of the tree just before the trunk breakage.

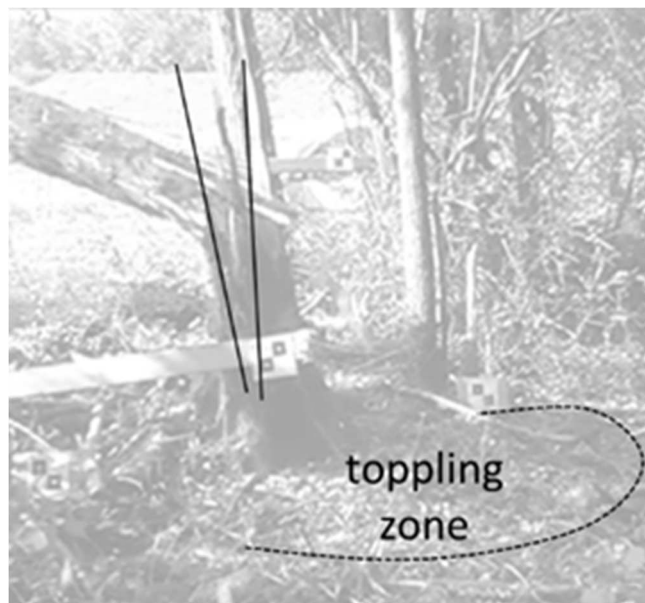


**Fig. 5.19** Views of the tree just after the trunk breakage.

## **5.5 Conclusions**

To better understand the application of the pulling test as a valid method of tree stability evaluation and related mathematical equations, it was necessary to overturn two trees in real scale and investigate their behavior during the entire process.

Through various phases of loading-unloading of the applied force, it was therefore possible to collect important data for the subsequent in-depth analyzes presented in the next chapter.

The exposure of the root system following the overturning also made it possible to carry out a 3D survey of the roots, useful for a small-scale modeling of the tree-roots-soil system.

## **References**

Dattola G., Ciantia M. O., Galli A., Blyth L., Zhang X., Knappet J. A., Castellanza R., Sala C., Leung A.K., (2019) – A macroelement approach for the stability assessment of trees. Lecture Notes in Civil Engineering, 40, pp. 417-426.

## Chapter 6

# Validation on experimental tests

### 6.1 Introduction

In this chapter, the new equation proposed in Chapter 4 to replace the Wessolly equation has been applied in some pulling tests to verify its validity.

In particular, it was initially tested on four "traditional" pulling tests (A-B-C-D) selected from the initial tests database and also on the first "non-destructive" phase of Test 1 and Test 2 previously described. After that, the application of the new equation was extended to the entire overturn curve recorded in Test 1 and Test 2. Finally, we tried to verify the validity of the equation proposed in the overturning tests on a 1:20 small scale performed by a recent study (Dattola et al. 2019)

### 6.2 Standard analysis

The results of the six tests shown in Chapter 4 were firstly analysed from the point of view of a professional user, i.e. with the aim of getting a simple prediction of  $M_L$  values, by considering only "standard" non-destructive pulling tests. To this goal, tests A, B, C and D, together with the very initial part of the experimental curve of tests 1 and 2 (up to a rotation of  $0.2^\circ$ ) were considered by the fitting procedures. The results are graphically summarized in Fig. 6.1 and Fig. 6.2 (grey dots represent the experimental data), and the list of all the fitting parameters is reported in Tab. 6.4.

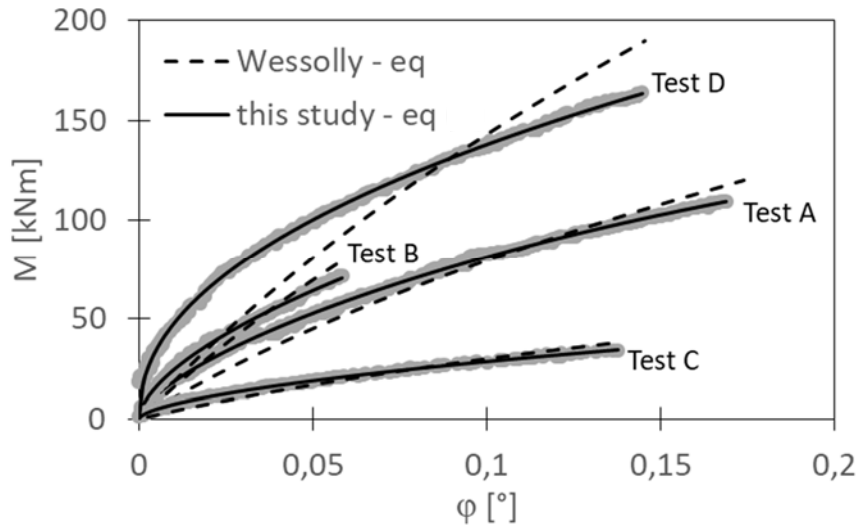


Fig. 6.1 Standard fitting procedure: tests A, B, C and D.

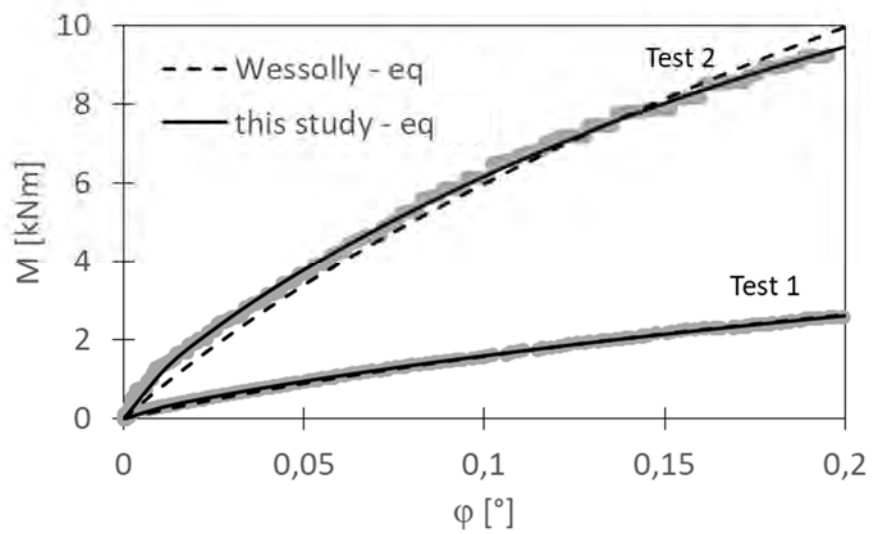


Fig. 6.2 Standard fitting procedure: tests 1 and 2.



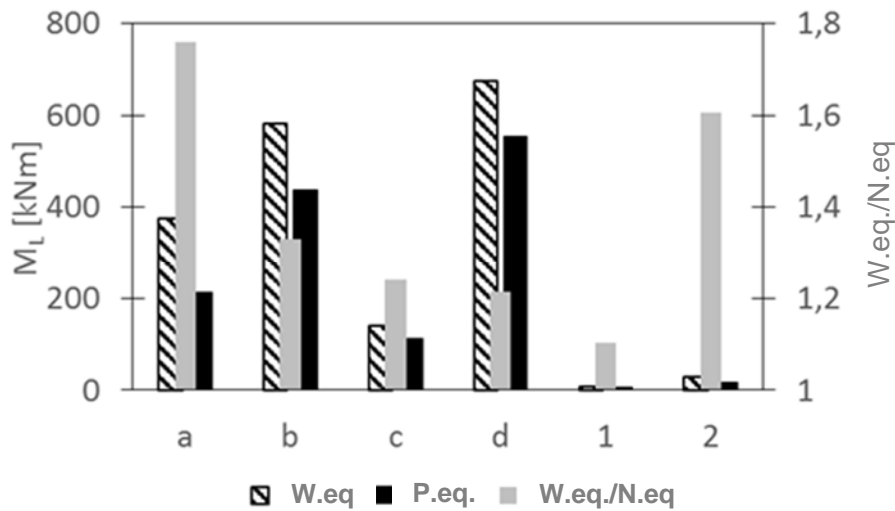


Fig. 6.3 Standard fitting procedure: comparison between the  $M_L$  values fitted from Wessolly equation (W.eq.) and this study new equation (N.eq.).

test	$M_P$ [kNm]	Wessolly – eq	this study – eq		
		$M_L$ [kNm]	$M_L$ [kNm]	$\varphi_{70}$ [°]	$b$ [-]
A	-	374.46	212.83	0.35	0.65
B	-	580.89	436.94	0.94	0.60
C	-	140.81	113.46	0.76	0.60
D	-	673.80	554.77	1.18	0.46
1	9.15	7.44	6.73	0.64	0.77
2	21.48	28.13	17.53	0.37	0.75

Tab. 6.4 List of fitting parameter of experimental tests and of the  $M_P$  values of tests 1 and 2.

The experimental trend is qualitatively well reproduced in all the six cases by both equations, but it is evident how Wessolly model shows a less accurate quantitative agreement with the experimental data, in particular for tests A, B and D (characterized by large diameter values). For tests C, 2 and (although less evident) 1 some inaccuracies also appear. On the contrary, the new equation proposed in this study accurately fits the experimental curves in all the six cases. In general, Wessolly equation

leads to larger estimation of  $M_L$  with respect to the new equation, ranging between +10% and +76% (as shown in Fig. 6.3, where the ratio of the two estimations is also plotted). For Test 1 the obtained values of  $M_L$  are in relatively good agreement with the  $M_P$  value (also reported in Tab. 6.4); whilst for Test 2 it must be reminded that the observed  $M_P$  value is associated to the trunk failure and it has been reported in Tab. 6.4 only for the sake of completeness.

Beyond the discussion on the predicted  $M_L$  values, from a mechanical point of view it is worth noting that the accuracy in reproducing the experimental curvature is fundamental in view of a reliable estimation of the global rotational stiffness of the system. This quantity, in principle, is responsible for the correct modelling of advanced mechanical features (like e.g. second order effects in a large displacement computational scheme, potentially inducing instability collapses due to the self-weight of the tree), or for optimizing the design of mechanical stabilizing interventions for unstable trees (like e.g. the design of ground anchors).

With reference to the short remark reported in previous chapter, a brief comment can moreover be derived by considering the values of the parameter  $\varphi_{70}$  (Tab. 6.4), in particular for tests B and D, where relatively large values are obtained ( $0.94^\circ$  and  $1.18^\circ$ , respectively). For such trees, a hypothetic working condition characterized by  $F_S = 1.4$  is then associated to remarkable rotation values (about  $1^\circ$ ), potentially inducing irreversible damages to the roots. As a consequence,  $F_S = 1.4$  cannot be considered in these cases as a “fully” safe condition, and minimum acceptable values for  $F_S$  should rather be chosen in this case by prescribing a maximum tolerable rotation value. As far as parameter  $b$  is concerned, finally, values between 0.46 and 0.77 are obtained, with a slight decreasing trend for increasing diameter values.

### 6.3 Extended prediction on Test 1 and Test 2

As already observed, the “standard” pulling test procedure usually explores only a very limited portion of the  $M - \varphi$  toppling curve, up to moment values not exceeding 30-40% of the ultimate resistance  $M_L$ . When running the test, however, the user cannot a priori know the value of  $M_L$ , and, hence, he has no idea of the mobilization ratio (i.e. the ratio of the mobilized moment  $M$  to the ultimate resistance  $M_L$ ) currently reached. It is then very important, for assuring the significance of the test, that the

adopted fitting equation “rapidly” tends to stable values of the fitting parameters even at low mobilization ratios. Starting from this idea, the experimental data of tests 1 and 2 have been repeatedly fitted both with Wessolly equation and new equation of this study for increasing mobilization ratios, and for each value the least square fitting procedures were run only on the experimental data falling within that ratio. A mobilization ratio is here expressed as the ratio of the considered toppling moment  $M$  to the  $M_p$  value of the considered test.

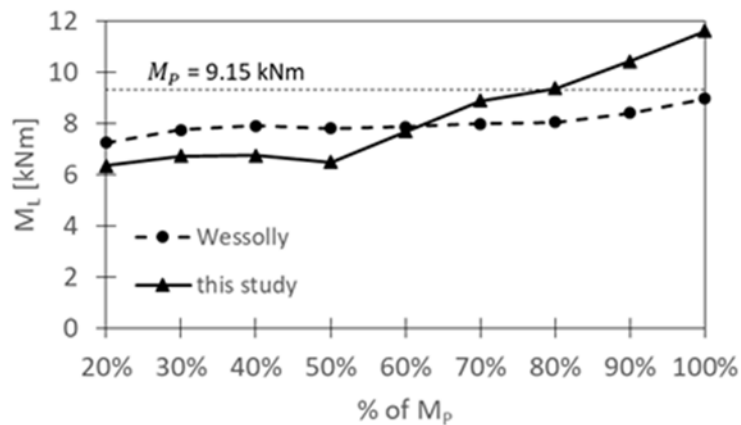


Fig. 6.5 Values of  $M_L$  in fitting of the two equations (Wessolly and this study) over the experimental data from Test 1 for different mobilization ratios.

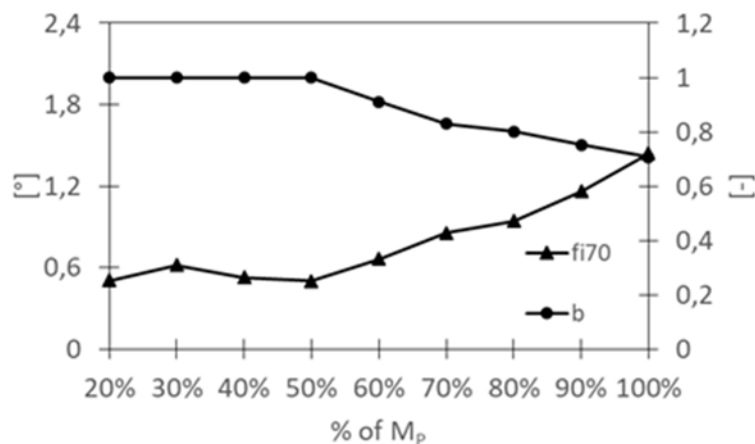


Fig. 6.6 Values of  $\phi_{70}$  and  $b$  in fitting of the two equations (Wessolly and this study) over the experimental data from Test 1 for different mobilization ratios

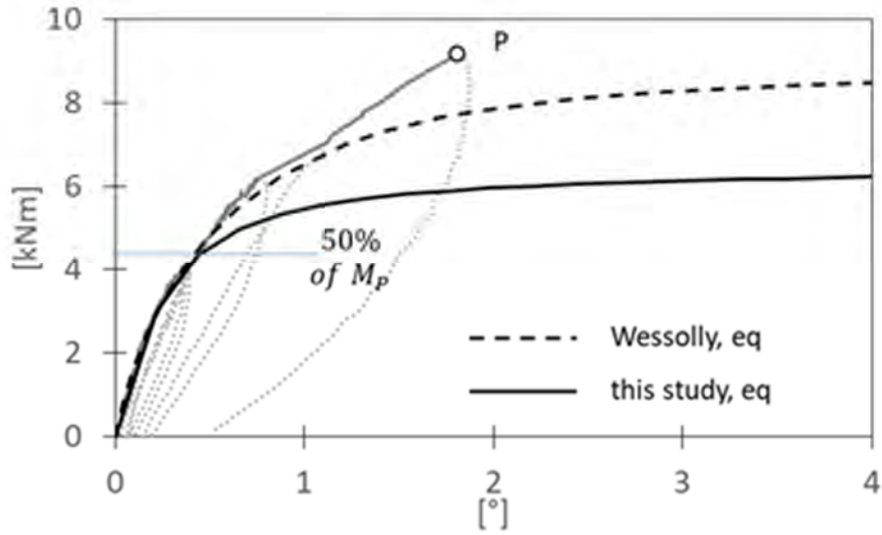


Fig. 6.7 Predictive curves fitted over 50% of  $M_P$  in fitting of the two equations (Wessolly and this study) over the experimental data from Test 1 for different mobilization ratios

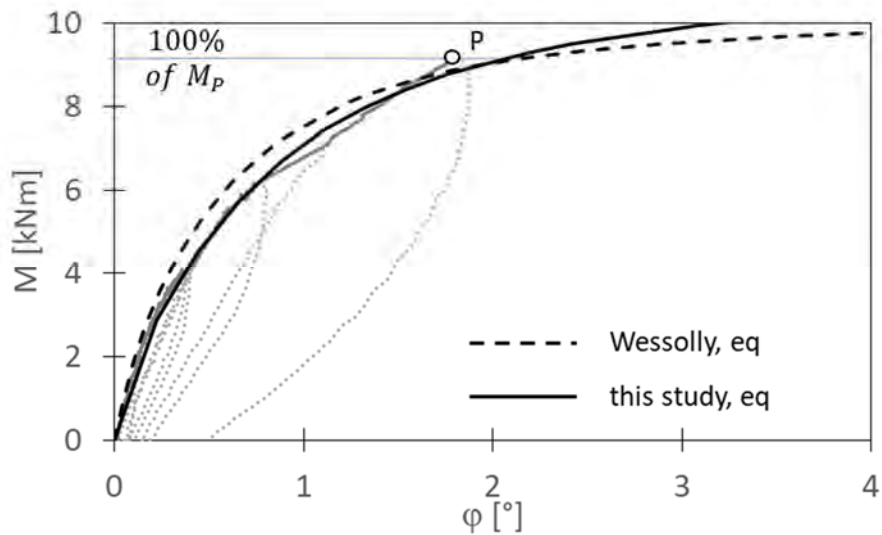


Fig. 6.8 Predictive curves fitted over 100% of  $M_P$  in fitting of the two equations (Wessolly and this study) over the experimental data from Test 1 for different mobilization ratios

With reference to Test 1, Fig. 6.5 shows the obtained values of parameter  $M_L$  both from Wessolly equation and this study equation for mobilization ratios ranging between 20% and 100% of  $M_P$ . It proves how the new equation proposed in this study gives a relatively stable estimation of  $M_L$  (an average value of about 6.6 kNm is obtained) even for low mobilization ratios (between 20% and 50%). This is consistent with the fact that, experimentally, only a first partial failure mechanism is activated in the initial part of the test. For higher mobilization ratios (>50%, in this case) also other partial failure mechanisms (characterized by higher ultimate toppling resistance and lower average rotational stiffness) are activated and, hence, an evident progressive increase in the estimation of  $M_L$  is observed. For 100% of mobilization ratio the estimated value of  $M_L$  (about 11.62 kNm) significantly exceeds the  $M_P$  value. This is however consistent with the definition of  $M_L$  as an ultimate, asymptotic condition, for an indefinitely stable and ductile mechanical response and, as already observed,  $M_P$  must not be considered as an experimental validation for  $M_L$  values.

Three main points can then be derived about the new proposed equation in this study:

- it allows to get stable and safe estimations of  $M_L$  also for relatively low values of the applied toppling load;
- it captures the progressive activation of higher order partial failure mechanisms for increasing toppling loads;
- it correctly gives the estimation of an ultimate condition for the toppling failure mechanism, asymptotically reached for large rotation values.

As far as the  $M_L$  values estimated by means of Wessolly equation are instead concerned, only a slight continuously increasing trend can instead be recognized, without any stable zone for low mobilization ratios and without any evident distinction between the first partial failure mechanism and higher order ones.

Fig. 6.6 plots the trends of parameters  $\varphi_{70}$  and  $b$  of the new equation, showing again relatively stable estimations up to a mobilization ratios of about 50% (average values of  $0.54^\circ$  and 1 are estimated for  $\varphi_{70}$  and  $b$ , respectively), followed by an increase in  $\varphi_{70}$  and a decrease in  $b$ . This is consistent with the fact that higher order failure mechanisms are associated to lower global stiffness (i.e. to larger values of parameter  $\varphi_{70}$ ), and it

could be mechanically interpreted as the effect of possible irreversible damage processes taking place into the root system.

Fig. 6.7 and Fig. 6.8 show instead the fitting curves for 50% and 100% of mobilization ratios, respectively. It is evident how, for 50% mobilization ratio, both the curves accurately reproduce only the first partial failure mechanism, with Wessolly equation slightly overestimating the ultimate resistance with respect to this study equation. For 100% mobilization ratio, Wessolly equation shows an initially stiffer response with respect to the new equation, followed by a flatter trend in the proximity of point P. The new proposed equation appears instead to accurately reproduce the whole experimental trend up to point P.

If Test 1 represents an “ideal” pulling test on a healthy and completely pruned tree, perfectly fitting within the Wessolly calibration database, Test 2 can be on the contrary considered as representative of a “real” case study regarding a complete tree with larger diameter, and characterized by weaker mechanical properties (collapse was in fact reached because of trunk failure rather than because of uprooting). Nevertheless, similar considerations as those derived from last Figures can be also derived for Test 2.

Fig. 6.9, in fact, show the estimated values of  $M_L$  with increasing mobilization ratios (the range 40% - 100 % has been here explored), highlighting again rather stable estimations from this study equation up to a mobilization ratio of about 60%-70% (average  $M_L$  value of 17.76kNm), followed by a pronounced increasing trend. Wessolly equation gives instead a decreasing trend, which could be particularly unsafe for the pulling test interpretation. It in fact implies that higher ultimate toppling resistance values are estimated at low mobilized toppling load, which is exactly the condition explored in practical applications.

Fig. 6.10 shows the evolution of parameters  $\varphi_{70}$  and  $b$ , respectively, witnessing again a rather constant value of  $\varphi_{70}$  until mobilization ratios of about 60%-70% (average value  $0.38^\circ$ ). The following marked increasing trend accounts for a progressive reduction of the overall rotational stiffness, probably due to increasing damaging levels. Parameter  $b$ , instead, is always comprised between 0.6 and 0.8, with a slow decreasing trend, meaning that the experimental curve is always characterized by a major curvature with respect to Wessolly equation. Finally, for the sake of completeness, in Fig. 6.11 and Fig. 6.12 the two fitting curves for 50% and 100% mobilization ratio, respectively, are plotted.

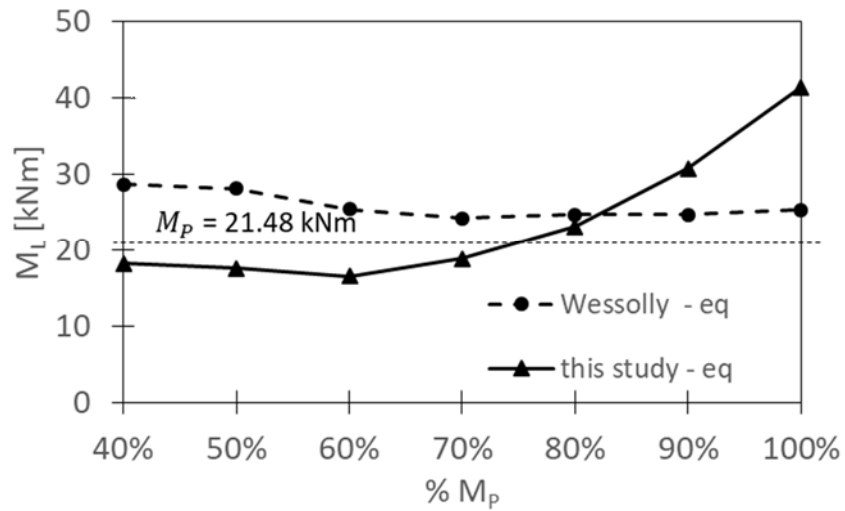


Fig. 6.9 Values of  $M_L$  in fitting of the two equations (Wessolly and this study) over the experimental data from Test 2 for different mobilization ratios.

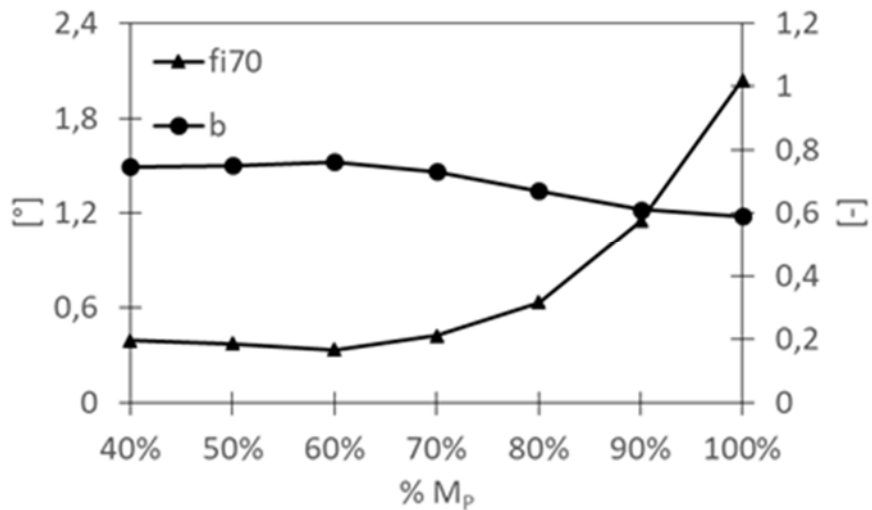


Fig. 6.10 Values of  $\phi_{70}$  and  $b$  in fitting of the two equations (Wessolly and this study) over the experimental data from Test 2 for different mobilization ratios

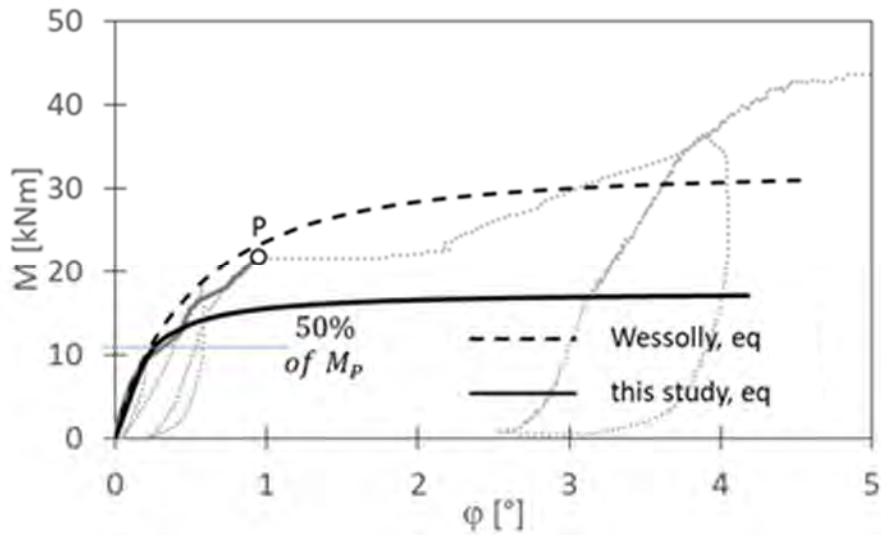


Fig. 6.11 Predictive curves fitted over 50% of  $M_P$  in fitting of the two equations (Wessolly and this study) over the experimental data from Test 2 for different mobilization ratios

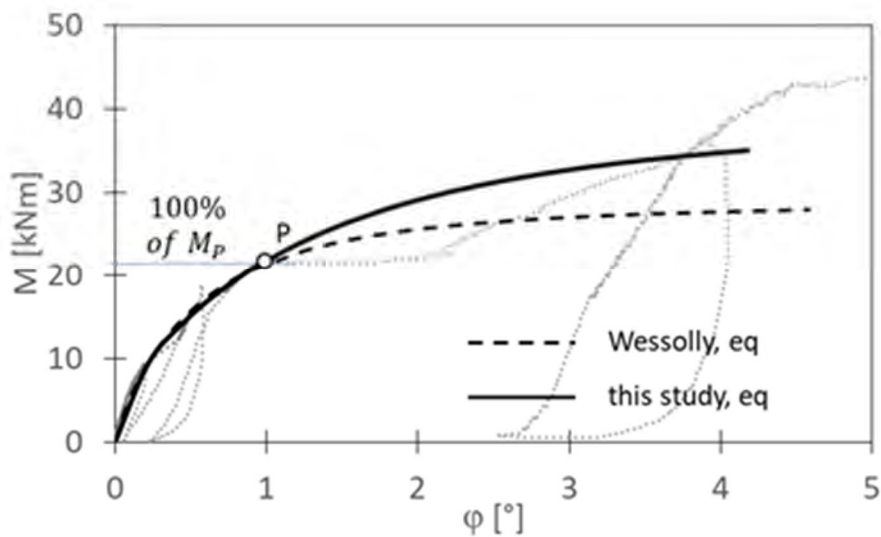


Fig. 6.12 Predictive curves fitted over 100% of  $M_P$  in fitting of the two equations (Wessolly and this study) over the experimental data from Test 2 for different mobilization ratios



## 6.4 Small scale pulling tests

In order to test the capability of the two equations to capture even significantly different scale effects (even beyond the proper range of applicability of Wessolly equation), a seventh experimental pulling test was chosen from literature results, in particular with reference to the aforementioned work of Dattola et al. (2019). A 1:20 small scale displacement controlled laboratory test was considered, run on 3D printed root model, with a global diameter of 220 mm and embedded 6.5 mm below the ground level (Fig. 6.13). The soil was a mixture of 70% dry sand and 30% silt, with a relative density of about 48%. The dry unit weight of the soil was  $16.5\text{kN/m}^3$  and a critical state friction angle, derived from direct shear tests, is  $38^\circ$  (further details can be found in the cited paper). The test (Fig. 6.14) showed a marked non-linear behaviour, with a peak toppling moment of about 1.86 Nm at a rotation of  $13^\circ$  (point P of Fig. 6.14), followed by a strength reduction without any evident plateau, witnessing a global fragile behaviour of the system at large rotation values. A minor local failure phenomenon is observed for a rotation of about  $6.46^\circ$ , beyond which a secondary failure mechanism is apparently activated. It is worth noting that the initial part of the curve (from the origin up to point A, corresponding to a toppling moment of 0.51 Nm) is characterized by a significant stiffening effect, probably due to soil disturbance in model preparation, and it will not be considered in the following fitting procedures.

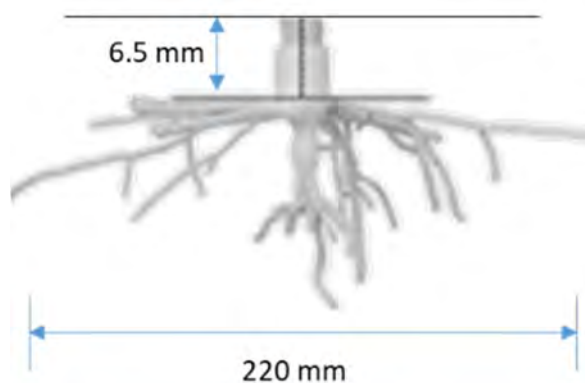


Fig. 6.13 View of the 3D printed root model. Modified from Dattola et al. (2019).

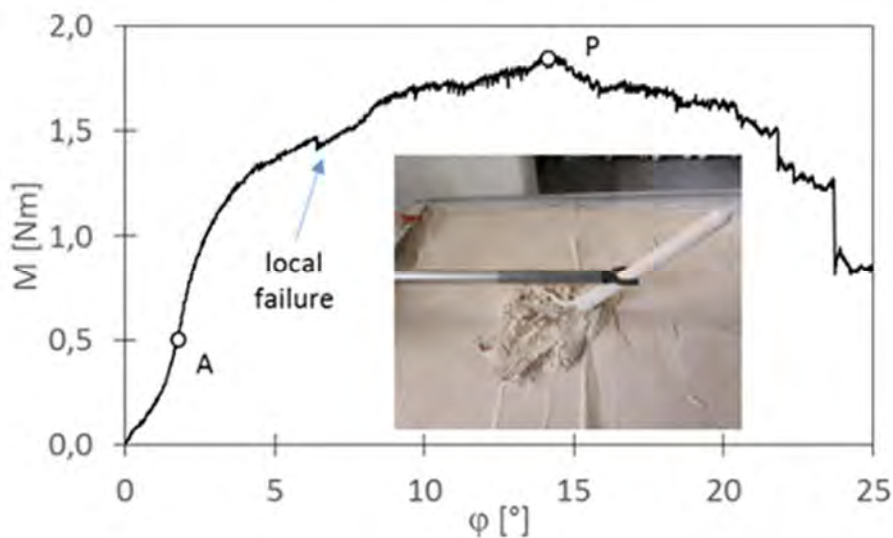


Fig. 6.14 Test results. Modified from Dattola et al. (2019).

The results of the fitting procedures are summarized in following Figures, with the same approach already discussed for tests 1 and 2 (in this case, for the sake of significance with respect to the lower limit represented by point A, only mobilization ratios  $> 50\%$  of  $M_P$  have been considered). The new equation of this study, again, shows stable predictions both in terms of  $M_L$  and  $\varphi_{70}$  for a relatively wide range of mobilization ratios (with average values of about 1.1 Nm and  $2^\circ$ ; see Fig. 6.15 and Fig. 6.16, respectively), followed by a marked increase for higher mobilization ratios ( $> 80\%$ ), due to the activation of a secondary partial failure mechanism. Parameter  $b$  shows instead a marked decrease (from 1 to about 0.2). On the contrary,  $M_L$  values from Wessolly equation show only a minor increasing trend for increasing mobilization ratios, with severe underestimations of about 30 to 50% with respect to the values obtained by means of the new proposed equation. Finally, the two fitting curves are also reported in Fig. 6.17 and Fig. 6.18 for 70% and 100% of mobilization ratios, respectively. It can be noted that Wessolly equation generally shows an initially stiffer mechanical response, very evident even when the complete loading curve (i.e. mobilization ratio of 100%) is considered. This is due to the fact that, as initially pointed out in previous section, a fixed value  $\varphi_{70}=0.653^\circ$  is implicitly assumed in Wessolly equation,

preventing the possibility to scale the curve along the rotation axis too, to best fit the experimental data.

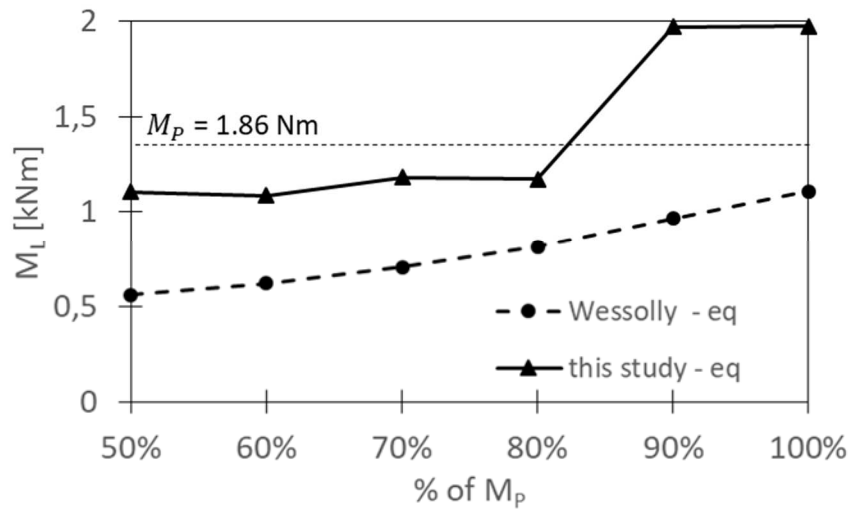


Fig. 6.15 Values of  $M_L$  in fitting of the two equations (Wessolly and this study) over the experimental data from Dattola et al. (2019) for different mobilization ratios.

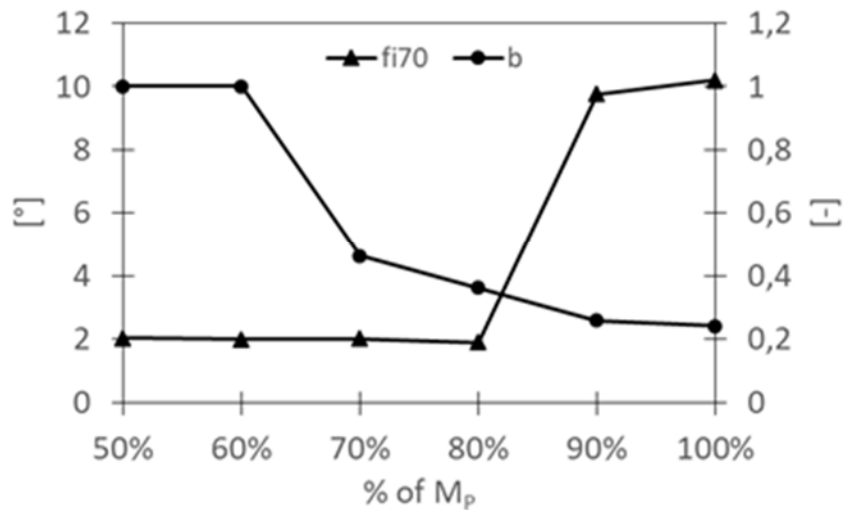


Fig. 6.16 Values of  $\varphi_{70}$  and  $b$  in fitting of the two equations (Wessolly and this study) over the experimental data from Dattola et al. (2019) for different mobilization ratios.

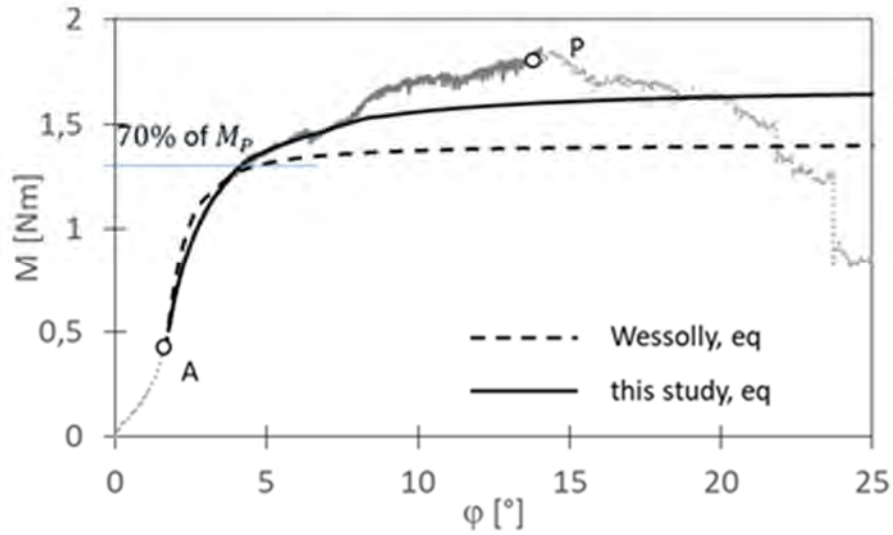


Fig. 6.17 Predictive curves fitted over 70% of  $M_p$  in fitting of the two equations (Wessolly and this study) over the experimental data from Dattola et al. (2019) for different mobilization ratios.

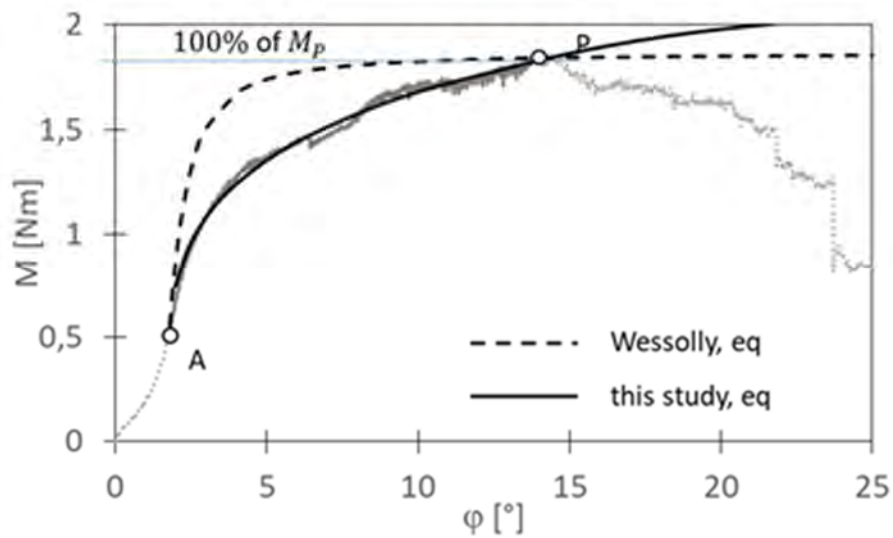


Fig. 6.18 Predictive curves fitted over 100% of  $M_p$  in fitting of the two equations (Wessolly and this study) over the experimental data from Dattola et al. (2019) for different mobilization ratios.

## **6.5 Conclusions**

The new equation, applied to "traditional" pulling tests, to real-scale overturning curves and to small-scale ones, seems to well describe the inclination of a tree subjected to a known force and could, therefore, be used during pulling tests.

Moreover, from the first tests carried out, compared to the Wessolly equation currently used, it seems to better describe the complex behavior of the tree-soil system, identifying when this is modified during the tests and calculating the results with greater accuracy. However, more evidence is needed to confirm these first encouraging results.

## **References**

Dattola G., Ciantia M. O., Galli A., Blyth L., Zhang X., Knappet J. A., Castellanza R., Sala C., Leung A.K., (2019) – A macroelement approach for the stability assessment of trees. *Lecture Notes in Civil Engineering*, 40, pp. 417-426.

## Chapter 7

### Advanced approach in particular cases

#### 7.1 The tree stability in not ordinary cases

The traditional approach seen before in this study (including V.T.A. analysis, S.I.M.-S.I.A. pulling test, etc...) is applied to evaluate the stability of the vast majority of trees. There are, however, some particular situations in which, to obtain an exhaustive assessment of the tree stability and to identify the most appropriate risk mitigation interventions, the ordinary approach is not enough and a more in-depth study is required.

In this chapter, one of these particular cases is exposed: a plane tree in the park of Villa Litta in Milano assessed as dangerous by ordinary methodologies. In this study various types of analysis and evaluation of the tree stability have been applied with an advanced method, accompanied by a consolidation project of the plant to allow an adequate level of security of the surrounding area.

However, the large-scale application of this type of approach to assess in detail the stability of trees in ordinary conditions is currently impractical for reasons of complexity and cost, so it should be limited to exceptional cases (i.e. monumental trees), where the value of the tree justifies the expense.

#### 7.2 Villa Litta study

The activities carried out for increasing the safety with an advanced approach of the plane tree located in Villa Litta (No. 41144 in Fig. 7.1) are set out below. In particular for the plant in question, the specific phases carried out are:

## Chapter 7 – Advanced approach in particular cases

---

- Phase 1: relief with reoradar to estimate the development of the root system in 3D;
- Phase 2: 3D geometry reconstruction of the stem and plant (3D terrestrial laser scanner survey);
- Phase 3: evaluation of soil resistance parameters (laboratory tests);
- Phase 4: Estimation of wind action and predominant direction considering local variables;
- Phase 5 verification of the stability of the plant with and without reinforcements and estimate of the increase in stability adopting FEM 3D analysis;
- Phase 6: installation of anchors (type Flying Fox - FastSystem) to increase the stability of the tree



**Fig. 7.1 Analysed plane tree No. 41144 in Villa Litta, Milano.**

A detailed description of the activities carried out in the various phases is shown below.



### 7.2.1 Phase 1: Relief with Georadar to estimate the development of the root system in 3D

At this stage, we wanted to verify the use of the Georadar as an indirect tool for estimating the root system. In particular, two different frequency ranges were compared. One at more basic frequencies to obtain a maximum volume with less accuracy (Fig. 7.2) and one at higher frequencies to investigate a smaller portion of soil at high resolution with the aim of being able to identify the primary roots of the root system (Fig. 7.3).

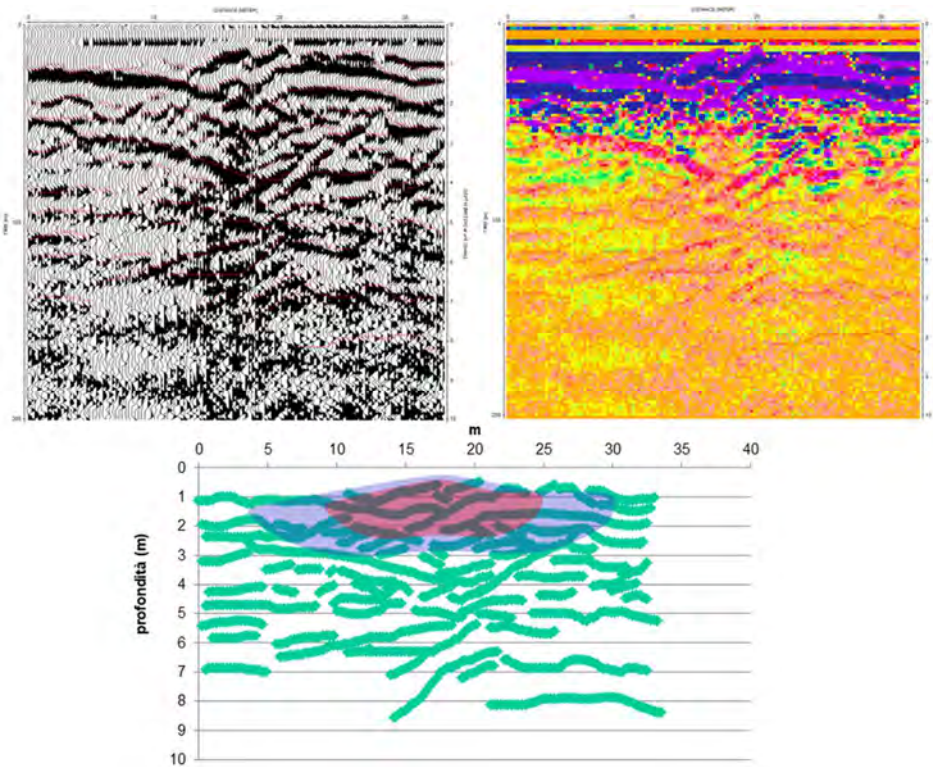


Fig. 7.2 Phase 1 - Estimation of the root system with Georadar at low frequencies

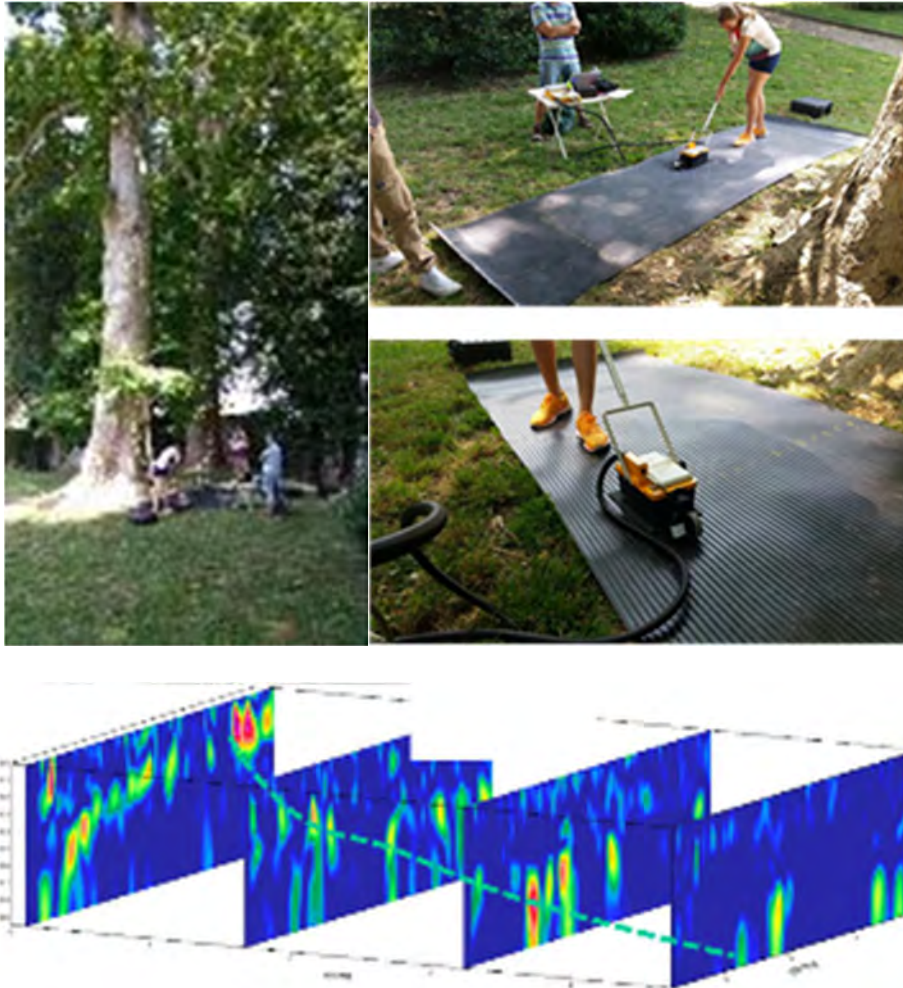
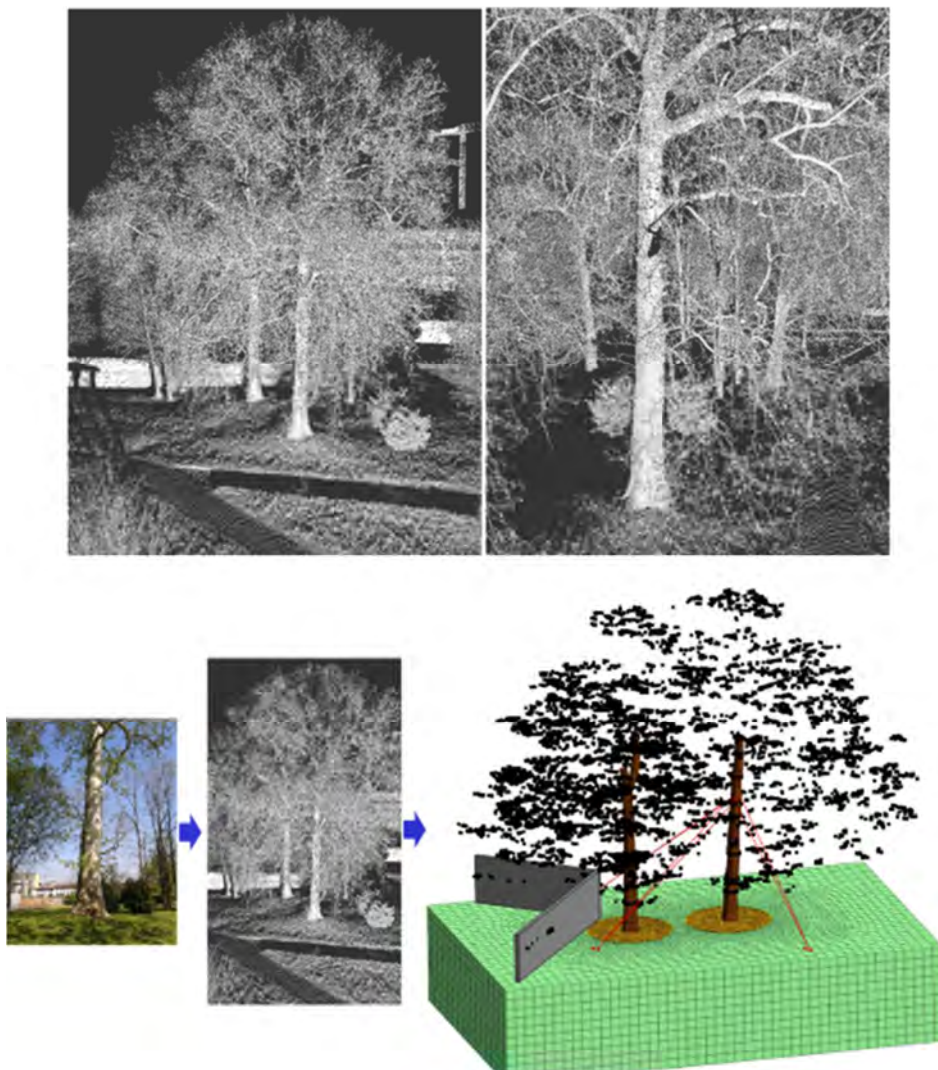


Fig. 7.3 Phase 1 - Estimation of the root system with Georadar

### 7.2.2 Phase 2: 3D geometry reconstruction of the stem and plant (3D terrestrial laser scanner survey)

A detailed three-dimensional reconstruction of the entire tree was created using TLS technology (Laser Scanner). Acquisitions were made aimed at having a 3D model in the absence of leaves (winter) and a 3D

model in the presence of leaves (summer). The two models were used for the next phase aimed at estimating the wind action. In addition, the acquisition included the three-dimensional scan of the context (buildings and other vegetation) in which the plant is inserted, so as to more accurately assess the action of the wind. Fig. 7.4 shows an example of the acquisitions made.



**Fig. 7.4 Phase 2 - Reconstruction of the three-dimensional model .**

### 7.2.3 Phase 3: Evaluation of soil resistance parameters (laboratory tests)

The performed laboratory tests are the study of the granulometry by decanting and sieving and the direct shear tests for each distinct granulometric curve. The processing of the data obtained from the granulometry of the soil of Villa Litta, taken from two different points in the area around the stem (S1 and S2 core), led to the following results:

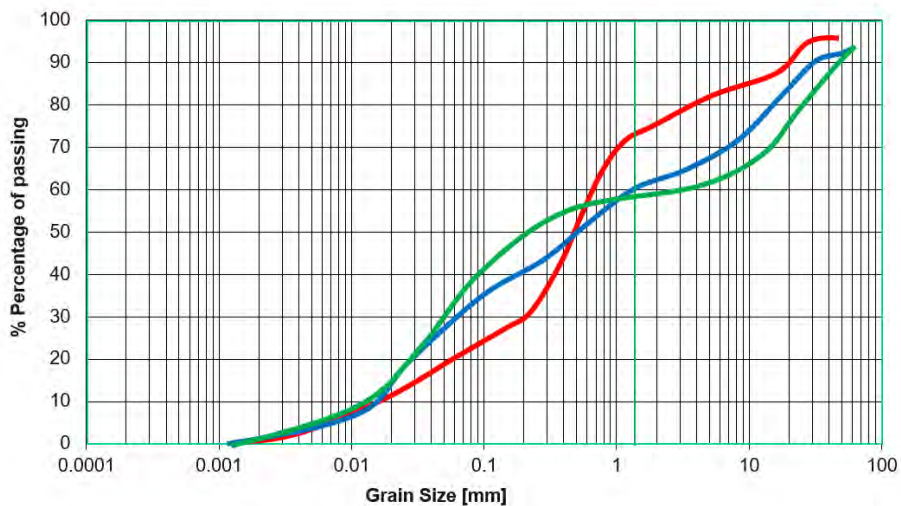


Fig. 7.5 Phase 3 - Definition of grain size curves near Villa Litta.

The cutting test, instead, is performed by preparing the specimen in a Casagrande box (consisting of two overlapping parts, separated along a horizontal plane and made to slide together). The phases in which the test is carried out are divided into consolidation and rupture. From these analyses the peak and residual resistance parameters were obtained.

Furthermore, in the analysed plane tree it was possible to validate the ability to acquire the friction angle values  $\phi$  using a quick tool called BHST (Borehole Shear Test), which was then compared with the direct acquisition carried out by cutting tests in the laboratory (Fig. 7.6 and Fig. 7.7).

The data of the pulling tests carried out on the plant under study were also acquired using laser scanner measurements. These results are useful

in order to refine the estimation of the parameters through a back analysis procedure that also involves the soil. Fig. 7.8 shows the results of the stem displacements measured during a pulling test acquired with the laser scanner (TLS).



**Fig. 7.6 Phase 3 - Definition of strength and deformability parameters - laboratory tests**

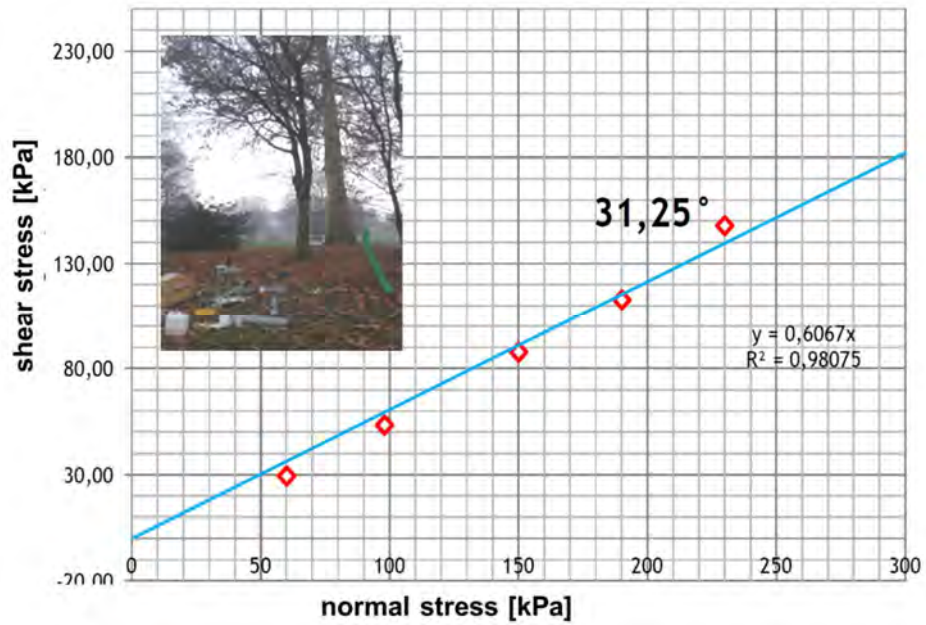


Fig. 7.7 Phase 3 - Definition of strength and deformability parameters - in situ tests with BHST

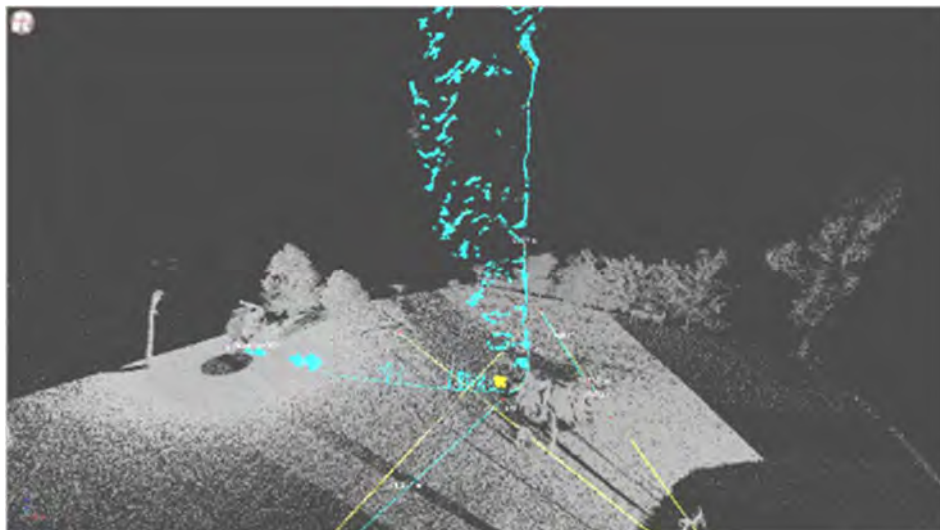
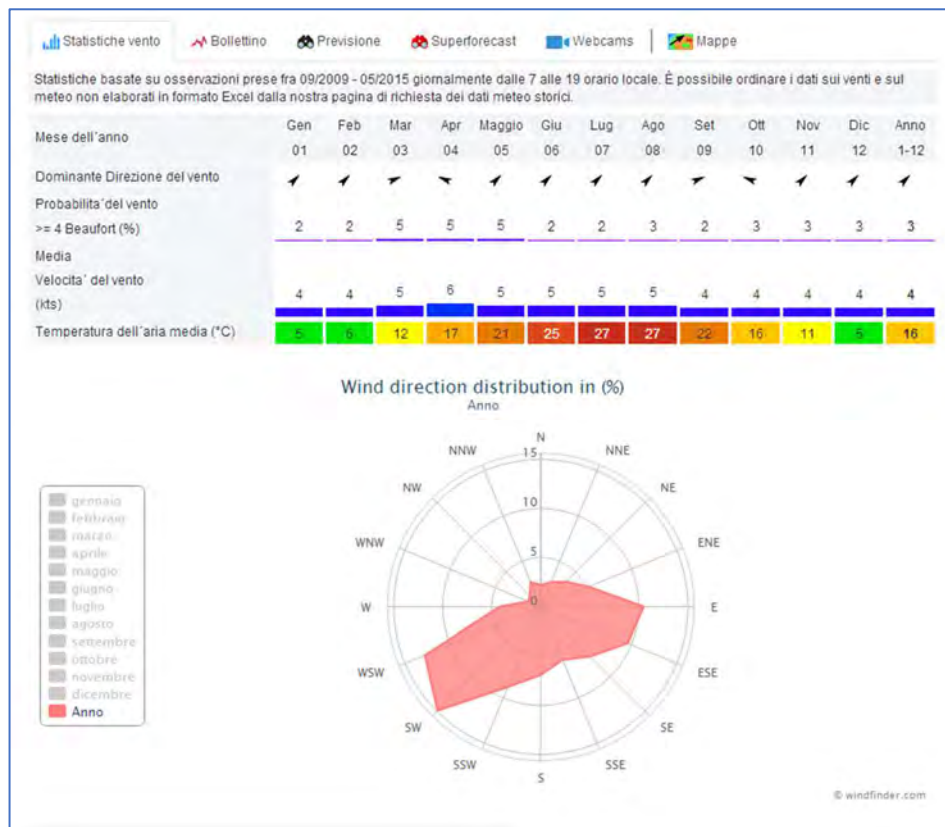
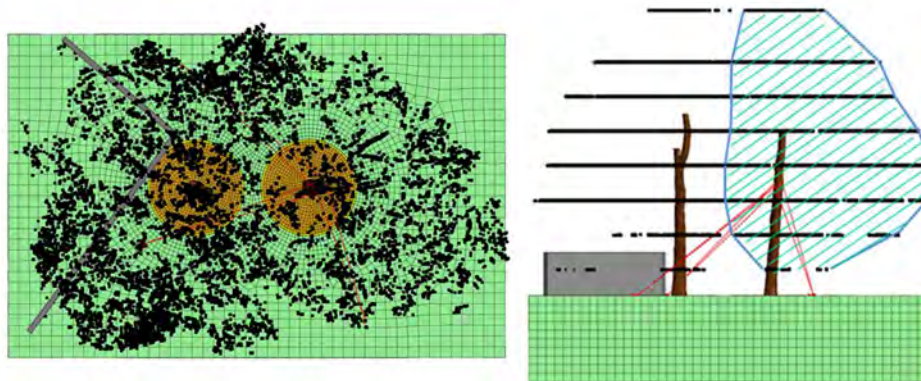


Fig. 7.8 Phase 3 - Definition of strength and deformability parameters - Acquisition of the deformability of the plant by pulling test

### 7.2.4 Phase 4: Estimation of wind action and predominant direction considering local variables

On the basis of all the information collected for both the above ground and the underground parts, the three-dimensional models of the stem, the root system and the soil, the different models for estimating the wind load have been created with the appropriate simplifications. The Fig. 7.9 shows a summary of the analysis carried out and the direction of the predominant winds in the area obtained on the basis of the data acquired from weather stations adjacent to this area.





**3.3.4 PRESSIONE DEL VENTO** **Italian code for wind**

La pressione del vento è data dall'espressione:

$$p = q_b \cdot c_s \cdot c_p \cdot c_d \quad (3.3.2)$$

dove

- $q_b$  è la pressione cinetica di riferimento di cui al § 3.3.6;
- $c_s$  è il coefficiente di esposizione di cui al § 3.3.7;
- $c_p$  è il coefficiente di forma (o coefficiente aerodinamico), funzione della tipologia e della geometria della costruzione e del suo orientamento rispetto alla direzione del vento. Il suo valore può essere ricavato da dati suffragati da opportuna documentazione o da prove sperimentali in galleria del vento;
- $c_d$  è il coefficiente dinamico con cui si tiene conto degli effetti riduttivi associati alla non contemporaneità delle massime pressioni locali e degli effetti amplificativi dovuti alle vibrazioni strutturali. Indicazioni per la sua valutazione sono riportate al § 3.3.8.

**3.3.6 PRESSIONE CINETICA DI RIFERIMENTO.**

La pressione cinetica di riferimento  $q_b$  (in  $N/m^2$ ) è data dall'espressione:

$$q_b = \frac{1}{2} \rho v_b^2$$

dove

- $v_b$  è la velocità di riferimento del vento (in  $m/s$ );
- $\rho$  è la densità dell'aria assunta convenzionalmente costante e pari a  $1.25 \text{ kg/m}^3$ .

$v_b$	25 m/sec
$\rho$	1.25 kg/mc
$\rho$	0.0125 kN/mc
$q_b$	390.63 N/mq
<b><math>q_b</math></b>	<b>0.39 kPa</b>

<b>(p. 3.4)</b>	<b>1.27</b>	<b>kPa</b>
<b>A</b>	<b>608</b>	<b>mq</b>
<b>F max</b>	<b>770</b>	<b>kN</b>
<b>permeab</b>	<b>0.25</b>	
<b>new F</b>	<b>192</b>	<b>kN</b>

<b>a</b>	<b>17.49</b>	<b>mq</b>
<b>q</b>	<b>11.0</b>	<b>kPa</b>

**Fig. 7.9 Phase 4 - 3D model creation and 3D analysis for estimating wind action from Italian wind codes**

### 7.2.5 Phase 5: Verification of the stability of the plant with and without reinforcements and estimate of the increase in stability adopting FEM 3D

Using numerical codes used for geotechnical problems of soil-structure interaction, the response of the tree to operating loads represented for example by severe wind conditions and in extreme conditions (i.e. leading to an incipient collapse condition) was evaluated. By carrying out different



## Chapter 7 – Advanced approach in particular cases

analyses in load directions and with variable stresses, it was possible to estimate the stability with and without reinforcements.

From the analyses carried out, it was possible to obtain a reduction of the moment at the collar of 30% if thought with the installation of 3 anchors in the positions shown in Fig. 7.10).

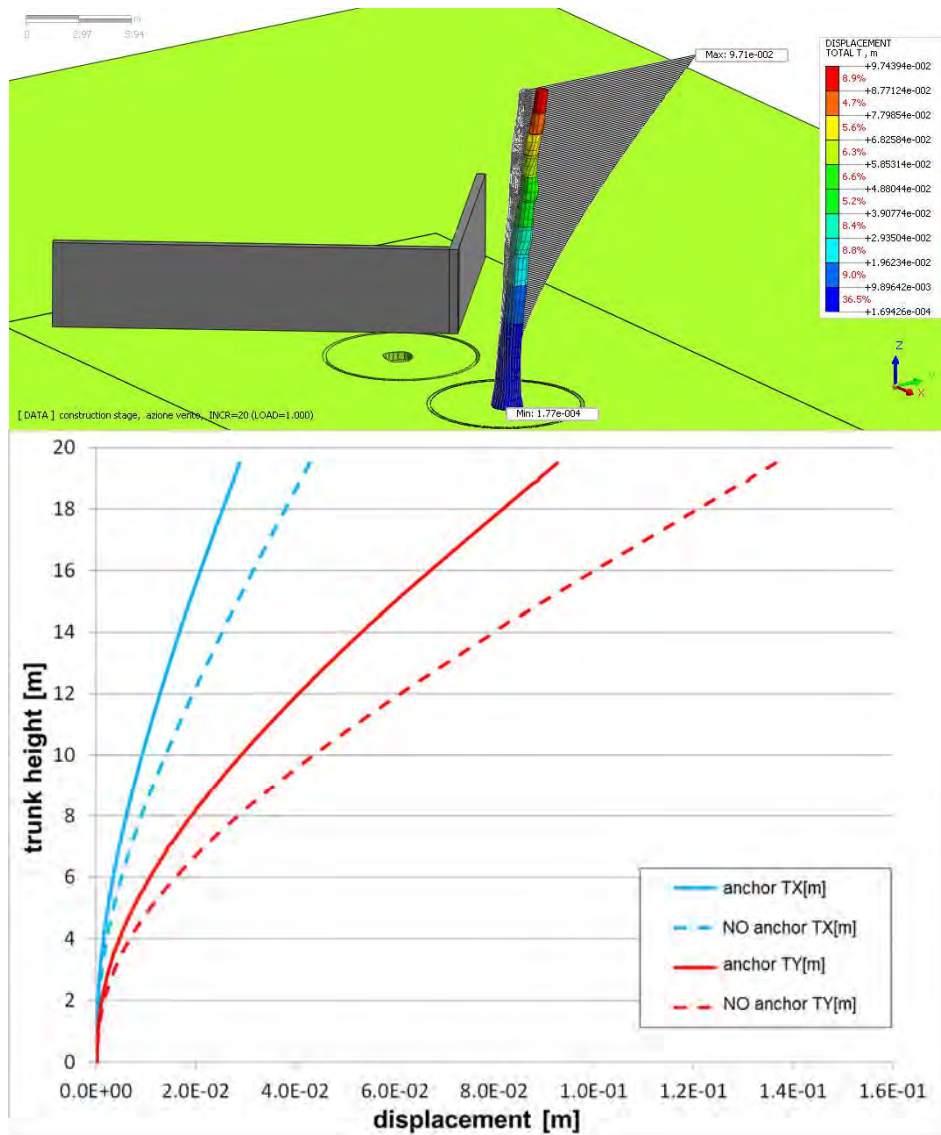


Fig. 7.10 Phase 5 - 3D FEM analysis of soil / plant / wind interaction.

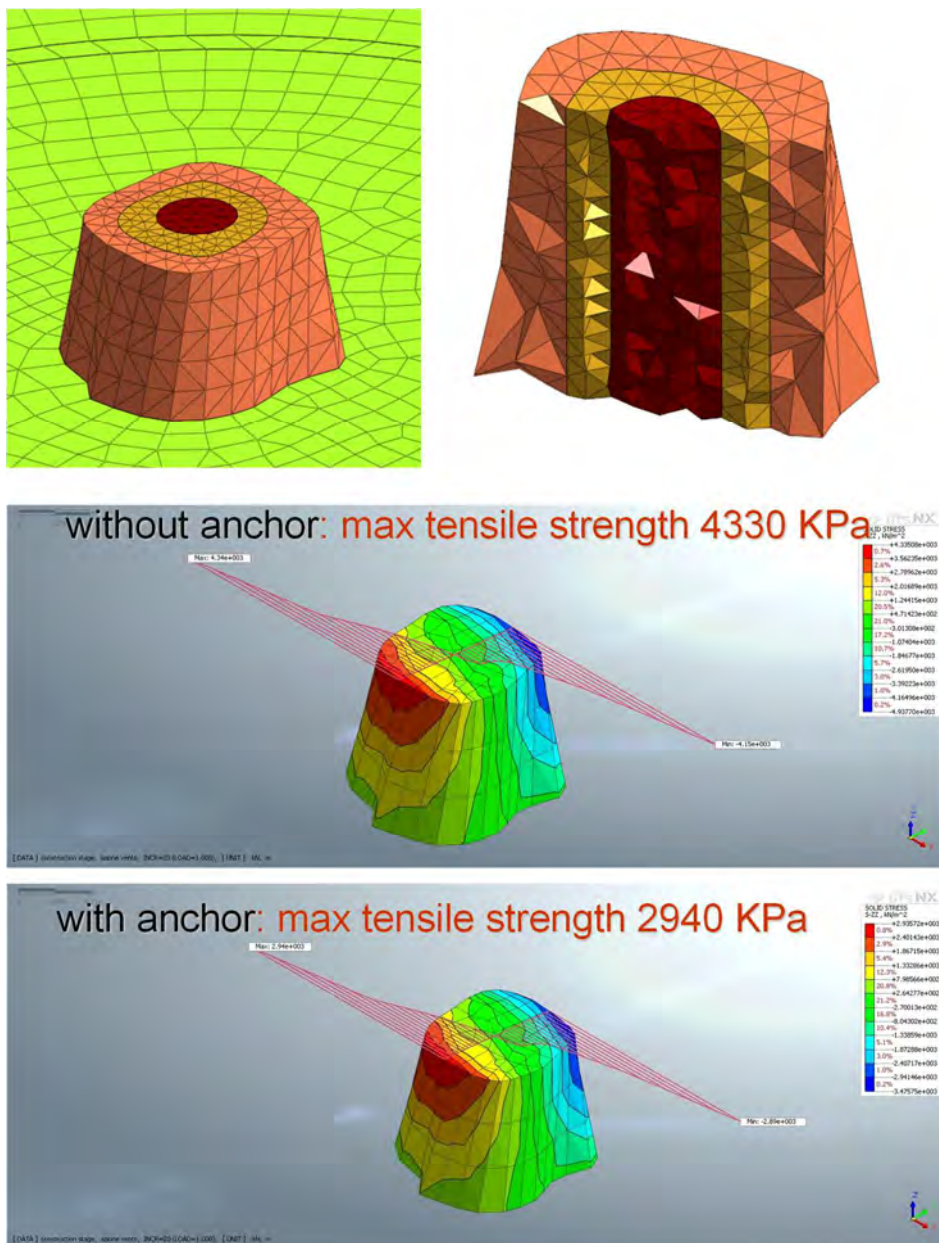


Fig. 7.11 Phase 5 - Effort-reducing effects on the collar.

Once a prediction of the limit resistance of the single tree was obtained, it was possible to make an estimate of the safety factor of the plant by evaluating the action of the wind with a predetermined return time (for example 20 years). In this way it was possible to estimate the risk with an advanced approach.

If the safety factor is less than a critical value, possible interventions aimed at risk mitigation are defined: they can involve both the soil and the root system.

Fig. 7.12 shows the final position of the anchors and in Figure 9 the table with the final calculations made for the evaluation of the increase in plant stability by reducing the actions to the collar by 30%.

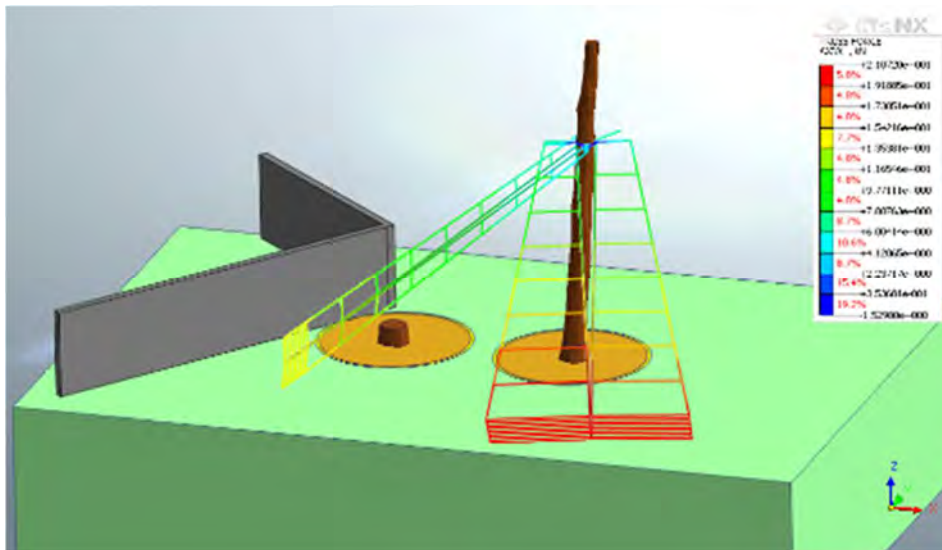


Fig. 7.12 Phase 5 - Example of reinforcement interventions with anchors

Estimate of the increase in the reduction of actions to the collar (increase in stability):

- Elastic modulus of wood: 6000 MPa
- Elastic modulus of soil: 100 MPa
- Elastic modulus of cables: 210000 MPa
- Soil-root interface cohesion: 20 kPa

- Soil-root interface friction angle:	36°
- Tree height:	38 m
- Exposure coefficient:	2,7
- Aerodynamic coefficient:	1
- Reference kinetic pressure:	1,05 kPa
- Crown surface:	608 mq
- Crown permeability:	0,7
- Wind load:	192 kN
→ Max moment induced by wind load: (absence of cables)	<b>1150 kNm</b>
→ Max moment induced by wind load: (absence of cables) (30% reduction of the moment at the base of the trunk after anchoring)	<b>786 kNm</b>
→ Max action in the cables:	<b>21 kN</b>

For the plane tree under study, it was decided to increase the safety level of the tree by creating a passive and deformable ground anchoring system that allows, in the event of strong stress, to discharge part of the horizontal action of the wind to the ground. The specimen, therefore, can benefit from a reduction of the overturning moment at the base of 30% which corresponds to an equally increase in the degree of safety. In addition, in order not to create invasive anchors in concrete, special anchors have been made, tested and put in place to minimize the environmental impact as shown in following phase.

### **7.2.6 Phase 6: Installation of anchors (type Flying Fox - FastSystem) to increase the stability of the tree**

The implementation was anticipated by the assessment in an area adjacent to Villa Litta of the resistance capacity of the single anchor which was assessed to be greater than 5 tons as shown in Fig. 7.13 and Fig. 7.14.

Chapter 7 – Advanced approach in particular cases

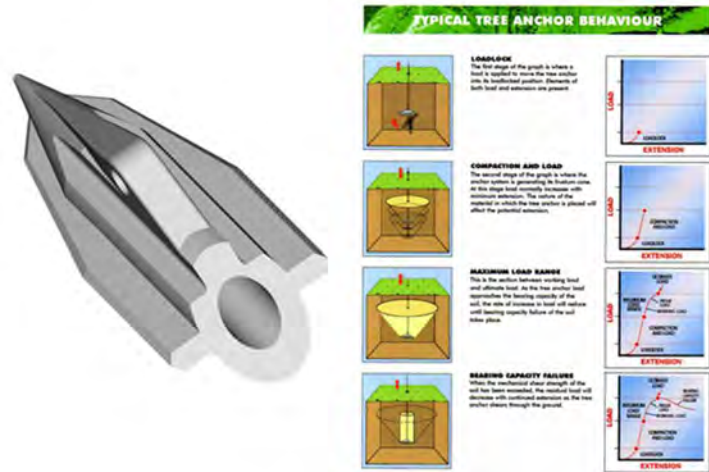
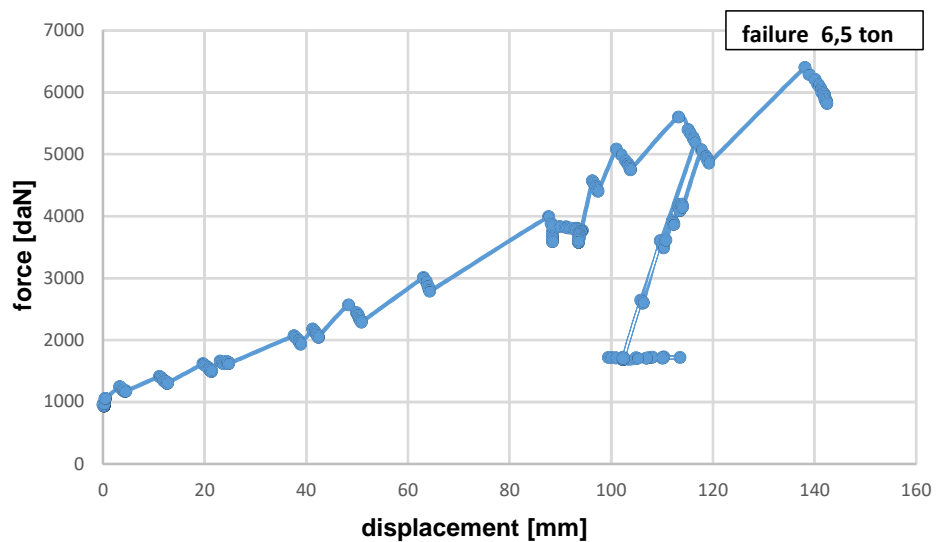


Fig. 7.13 Phase 6 - Check resistance of the anchor.



**Fig. 7.14 Phase 6 - Check resistance of the anchor.**

The final installation phases in Villa Litta are instead shown in the following figures (Fig. 7.15; Fig. 7.16; Fig. 7.17).



**Fig. 7.15 Phase 6 - Final system of tensioners**



Fig. 7.16 Phase 6 - Final system of tensioners

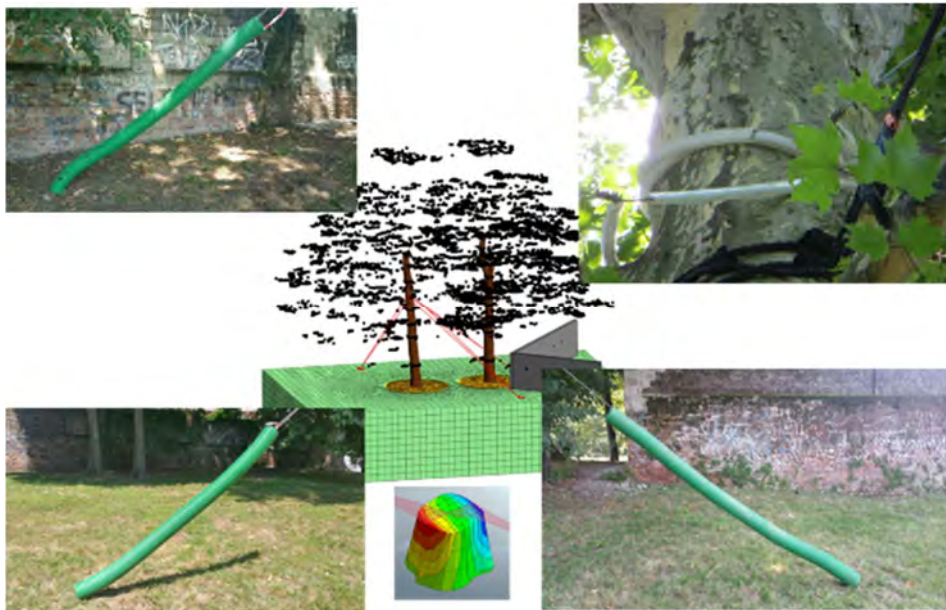


Fig. 7.17 Phase 6 - Final installation plane tree 41144 with stability increase of more than 30%

### **7.2.7 Villa Litta study: conclusions**

The work carried out made it possible to increase the degree of safety of the plane tree in question by 30% through an in-depth study which, following an advanced approach, combined the knowledge of the root system and its extension, the 3D geometric dimensions of the plant, the wind load, the mechanical properties of the soil and the plant. In this way, through a quantitative approach based on 3D numerical analyses, it has made it possible to determine the type of reinforcement intervention to be carried out.

This intervention was thus designed and implemented to allow the plane tree, assessed as dangerous by ordinary methodologies, to increase the degree of safety, preventing felling for the moment. The system and the procedure can be monitored over time and replicable in other similar conditions.



## Chapter 8

### Conclusions

Tree stability assessment is a very complex and difficult matter, not yet well known in its entirety, especially as regards the evaluation of the anchoring to the ground.

There are in-depth methods of instrumental analysis and advanced evaluation of the stability of trees, as seen in Villa Litta plane tree (see in chapter 7), however these ones are very complex and expensive and can only be applied in particular cases for plants of particular value, i.e. monumental trees. So it is necessary to improve the ordinary evaluation methods applicable on a large scale to most trees for a significant increase in the quality of plant management in urban settings.

After analysing the results of several experimental “ordinary” pulling tests, it was possible to obtain some important information that may be useful for future investigations. In fact the results seem depend on numerous different factors, attributable to the type of trees, the environmental and soil conditions and the methods of carrying out the tests, in particular the rate of application of the force, which should be studied and investigated in detail. The topic is very complex and it is not possible to take into consideration only one or a few aspects of the tree-soil system, such as the geotechnical characteristics of the soil which, although useful for better understanding the materials involved, individually do not allow to determine the stability of a tree.

Therefore, approaching the system as a whole, from a mathematical point of view in this study a new interpretative equation is proposed to describe experimental pulling tests on trees. The proposed equation tries to extend and enrich the classical Wessolly model (usually adopted in practice in the last twenty years to describe the toppling behaviour of a tree), and to bypass some of its limitations. In particular, the new equation (controlled by three parameters) represents a meaningful mechanical relationship describing the entire moment-rotation curve of a tree, thought

as a one d.o.f. rotational system. In particular, an innovative “performance-based” approach can be introduced, thus characterizing the system not only in terms of its toppling resistance, but also in terms of the expected rotation for a reference working condition (to this goal, in the study the new parameter  $\varphi_{70}$  is introduced). As a result, standard stability assessments (usually based on the definition of a global factor of safety against the toppling) can be enriched by the evaluation of the expected rotation amplitude, so that the minimum acceptable value of the factor of safety – if needed – could also be chosen with reference to the maximum tolerable rotation for the tree.

The new equation was compared with the classical Wessolly equation and validated on real scale tests (some of them till overturning) and on small scale laboratory tests (last ones taken from Literature data). Both standard (i.e. monotonic) and non-standard (i.e. cyclic) loading schemes have been tested, in order to explore even the response of the systems in complex conditions (like e.g. those represented by repeated and increasing wind gusts). Small (consistently with the original Wessolly database) as well as large diameter trees have been chosen, in order to explore a wider range of cases.

The experimental data revealed that the toppling mechanism is a complex process, consisting in the progressive activation several and subsequent partial failure mechanisms, characterized by increasing strength and decreasing stiffness, in particular when complex non monotonic (or even cyclic) loading schemes are considered.

The new proposed equation satisfactorily fit the experimental data not only qualitatively, but also from a quantitative point of view and it is also able to correctly capture important scale effects. In standard predictions, Wessolly equation showed a general tendency at overestimating the values of the ultimate toppling resistance with respect to the new proposed equation. When considering “extended” predictions (i.e. for progressively increasing values of the mobilization ratios), the new equation proved to rapidly and stably provide safe estimations of the ultimate toppling resistance, even at low value of the mobilized toppling load during the test.

The new equation is also able to adaptively capture the possible progressive activation of higher order failure mechanisms during the tests. This quality is of particular interest, since (with respect to the present standard technique, based on a post-processing fitting procedure of the recorded data) it opens the route to “real-time” fitting approaches, capable to provide practitioners of an immediate estimation of the fitting

parameters already during the execution of a pulling test, thus also limiting possible damages to the root system. It is worth noting that the new equation does not require any significant additional computational cost to the user with respect to standard Wessolly equation (standard least square fitting procedures were in all cases adopted throughout the study).

The importance of developing an innovative, mechanically meaningful interpretative equation as the one presented in this study is twofold:

- provide practitioners and researchers of new physically-based controlling parameters (as  $\varphi_{70}$ ) allowing to introduce more advanced performance-based interpretative frameworks;
- push the scientific research toward the definition of reliable relationships with soil mechanical parameters and root typologies;
- fully model the toppling  $M - \varphi$  curve, with possible positive benefit not only from a scientific point of view (for example, the study of more complex dynamic or seismic loading conditions), but also for practical applications (like e.g. the design of sustainable structural stabilizing interventions for unstable trees).

Then, the final hope of this work is that this study could give a contribution in these directions, promoting the scientific and professional debate on these topics. In fact, despite the fact that so far a large bibliography has been produced on the subject, as has also been shown by this study, the stability of trees is a very complex matter and it is, therefore, necessary to continue scientific research on mechanical aspects, loading rate and further tests in field with different methods and instruments, also to verify the validity of the new proposed equation and much more.

Finally, a specific case study, where advanced experimental and numerical study has been adopted, is presented in the last chapter. The meaning consists in exploring more sophisticated approach to improve the stability of high value monumental tree. This case study shows that advanced approach, even if more expensive, are quite useful in critical cases.

## Chapter 8 – Conclusions

---

## **Appendix 1**

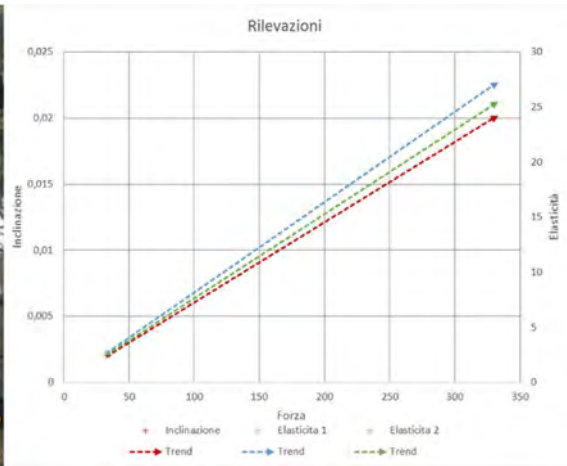
### **Pulling tests**

## Appendix 1 – Pulling tests

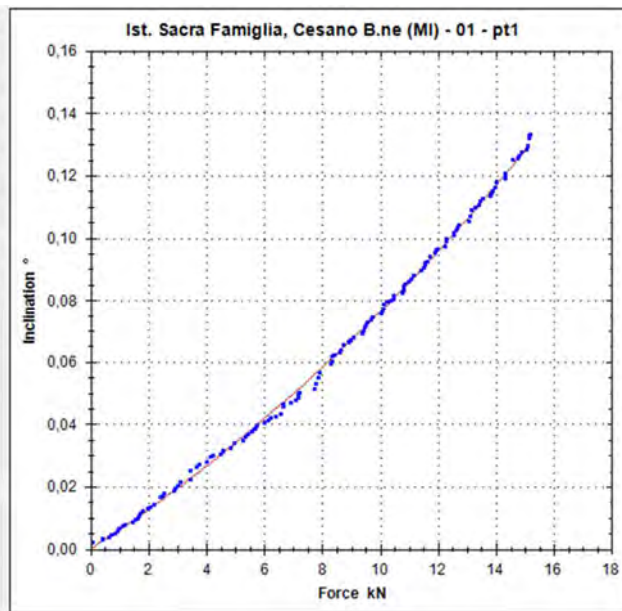
---

Appendix 1 – Pulling tests

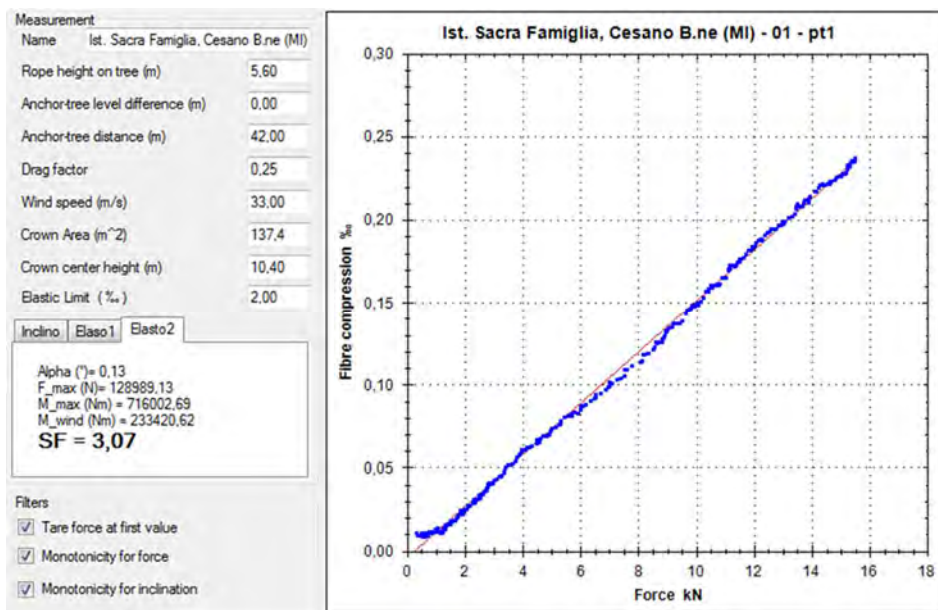
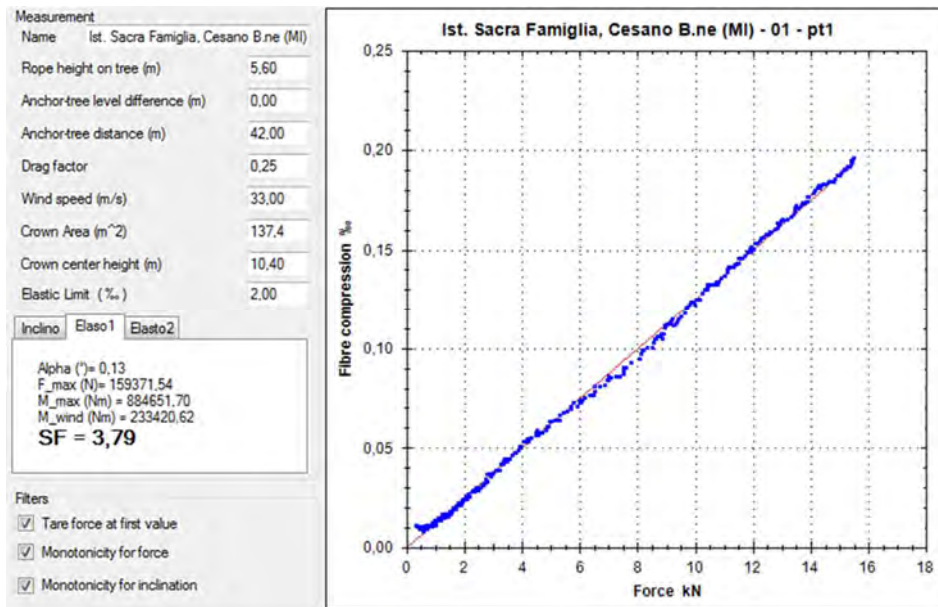
Istituto Sacra Famiglia, Cesano Boscone – 01 – pt1



Measurement	
Name	Ist. Sacra Famiglia, Cesano B.ne (MI)
Rope height on tree (m)	5.60
Anchor-tree level difference (m)	0.00
Anchor-tree distance (m)	42.00
Drag factor	0.25
Wind speed (m/s)	33.00
Crown Area (m <sup>2</sup> )	137.4
Crown center height (m)	10.40
Elastic Limit (%)	2.00
Incino <span style="border: 1px solid black; padding: 2px;">Elasto1</span> <span style="border: 1px solid black; padding: 2px;">Elasto2</span>	
Alpha (°) = 0.13 F <sub>max</sub> (N) = 58617.50 M <sub>max</sub> (Nm) = 325378.47 M <sub>wind</sub> (Nm) = 233420.62 <b>SF = 1,39</b>	
Filters <input checked="" type="checkbox"/> Tare force at first value <input checked="" type="checkbox"/> Monotonicity for force <input checked="" type="checkbox"/> Monotonicity for inclination	

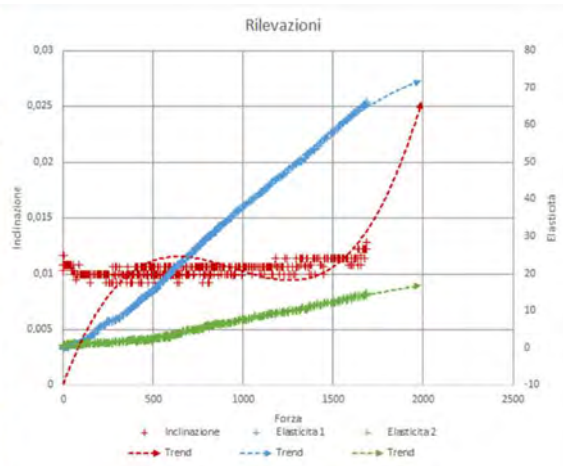


## Appendix 1 – Pulling tests

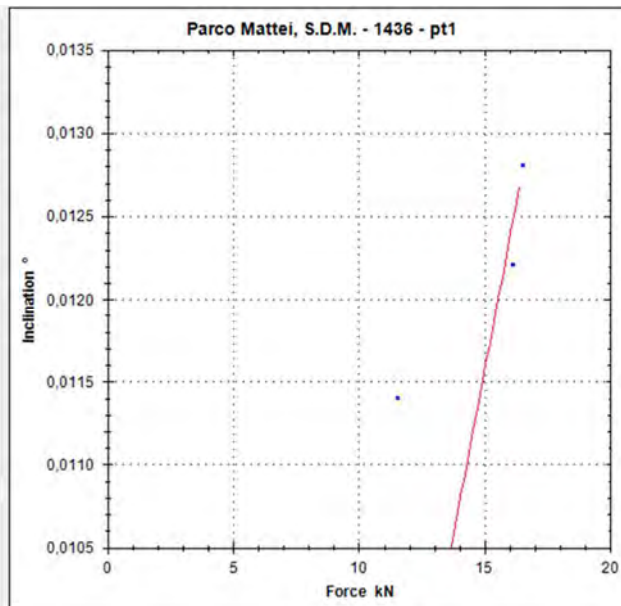




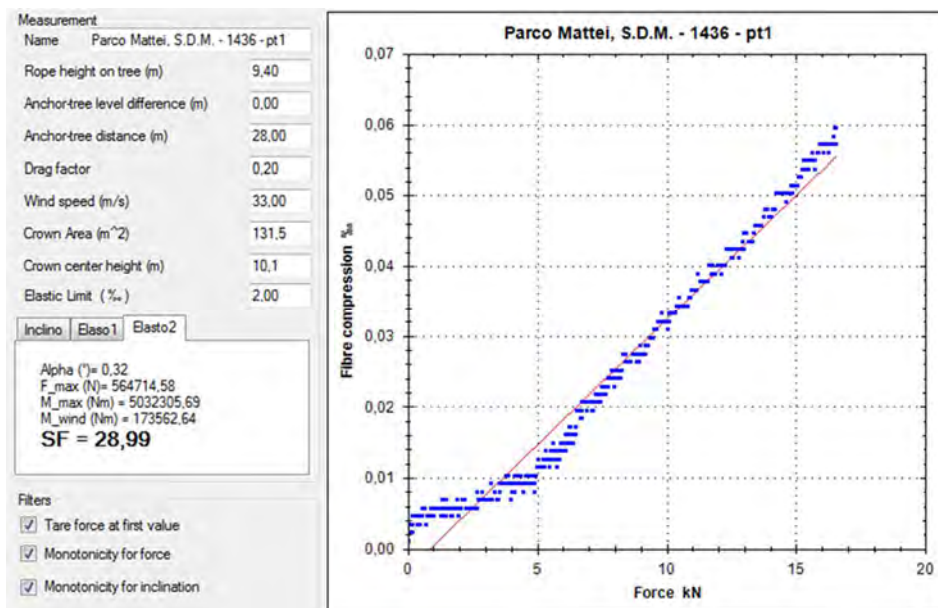
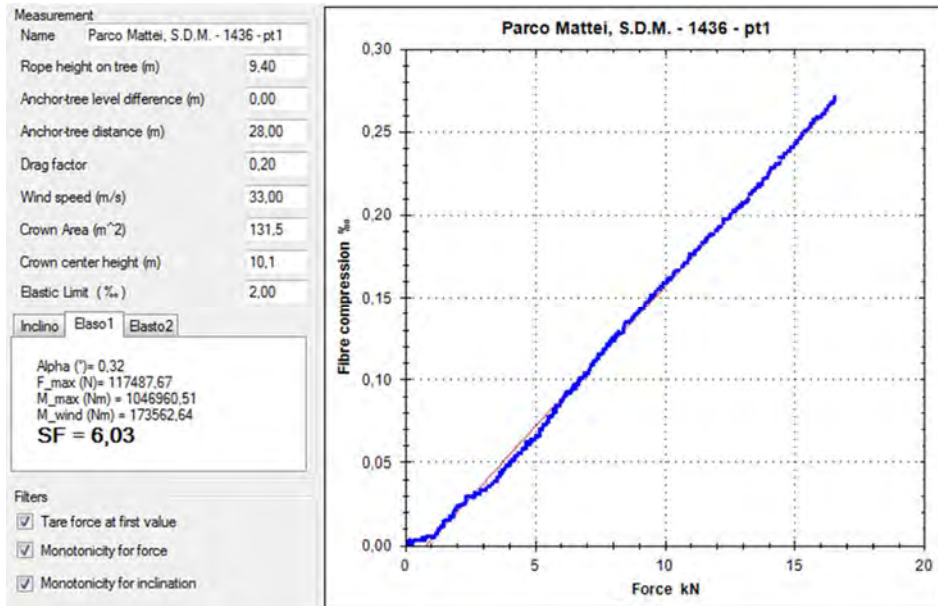
Parco Mattei, San Donato Milanese – 1436 – pt1



Measurement	
Name	Parco Mattei, S.D.M. - 1436 - pt1
Rope height on tree (m)	9,40
Anchor-tree level difference (m)	0,00
Anchor-tree distance (m)	28,00
Drag factor	0,20
Wind speed (m/s)	33,00
Crown Area (m <sup>2</sup> )	131,5
Crown center height (m)	10,1
Elastic Limit (%)	2,00
Inclino <input type="radio"/> Elaso1 <input type="radio"/> Elasto2	
Alpha (°) = 0,32 F_max (N) = 478373,86 M_max (Nm) = 4262903,02 M_wind (Nm) = 173562,64 <b>SF = 24,56</b>	
Filters <input checked="" type="checkbox"/> Tare force at first value <input checked="" type="checkbox"/> Monotonicity for force <input checked="" type="checkbox"/> Monotonicity for inclination	

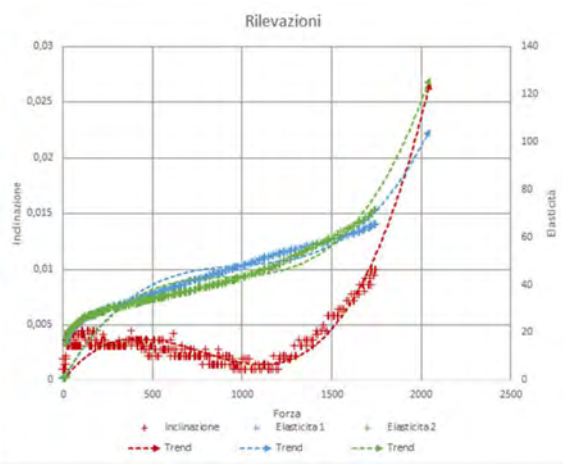


## Appendix 1 – Pulling tests

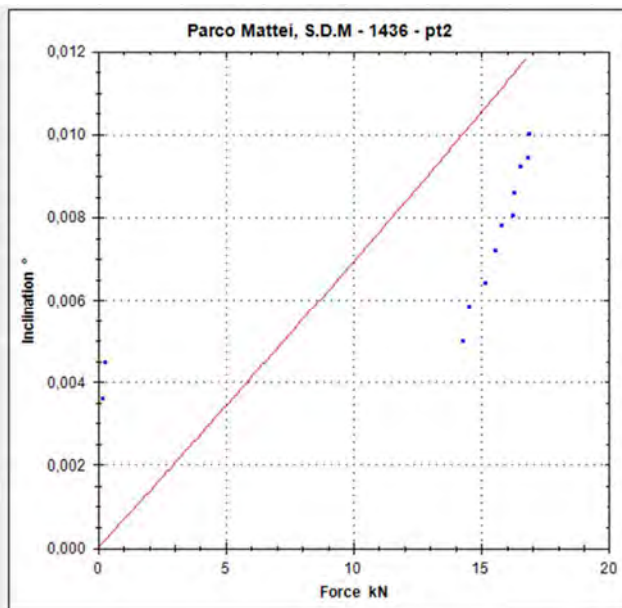


Appendix 1 – Pulling tests

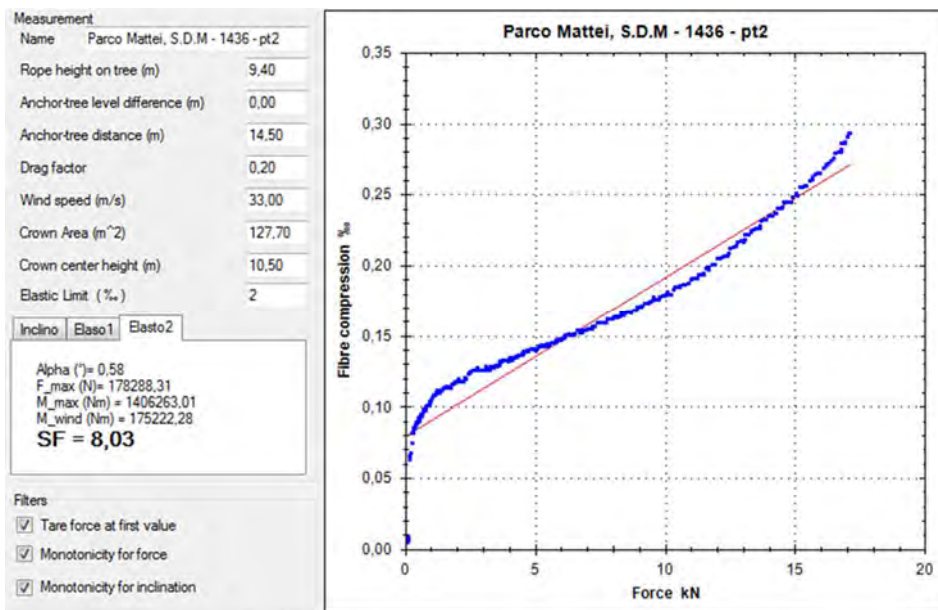
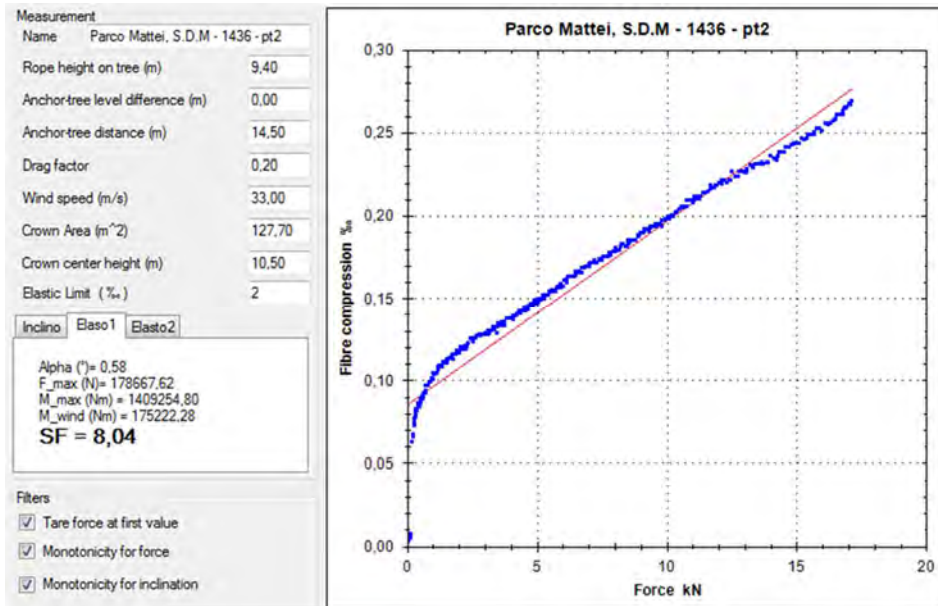
Parco Mattei, San Donato Milanese – 1436 – pt2



Measurement	
Name	Parco Mattei, S.D.M - 1436 - pt2
Rope height on tree (m)	9,40
Anchor-tree level difference (m)	0,00
Anchor-tree distance (m)	14,50
Drag factor	0,20
Wind speed (m/s)	33,00
Crown Area (m <sup>2</sup> )	127,70
Crown center height (m)	10,50
Elastic Limit (%)	2
Inclino <input type="radio"/> Elaso1 <input type="radio"/> Elasto2	
Alpha (°) = 0,58	
F <sub>max</sub> (N) = 523508,49	
M <sub>max</sub> (Nm) = 4129214,21	
M <sub>wind</sub> (Nm) = 175222,28	
<b>SF = 23,57</b>	
Filters	
<input checked="" type="checkbox"/> Tare force at first value	
<input checked="" type="checkbox"/> Monotonicity for force	
<input checked="" type="checkbox"/> Monotonicity for inclination	

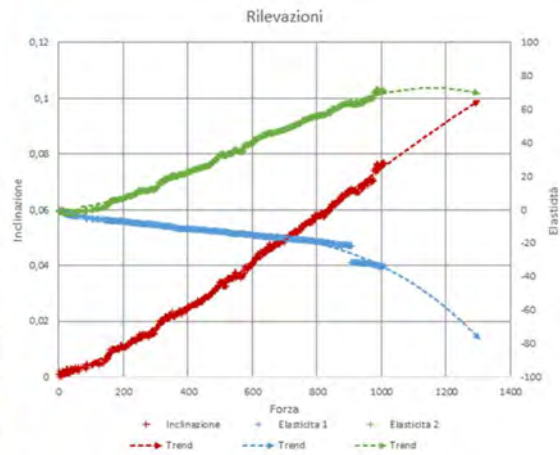


## Appendix 1 – Pulling tests



Appendix 1 – Pulling tests

via Mezzocannone 8, Napoli Università – 01 – pt1



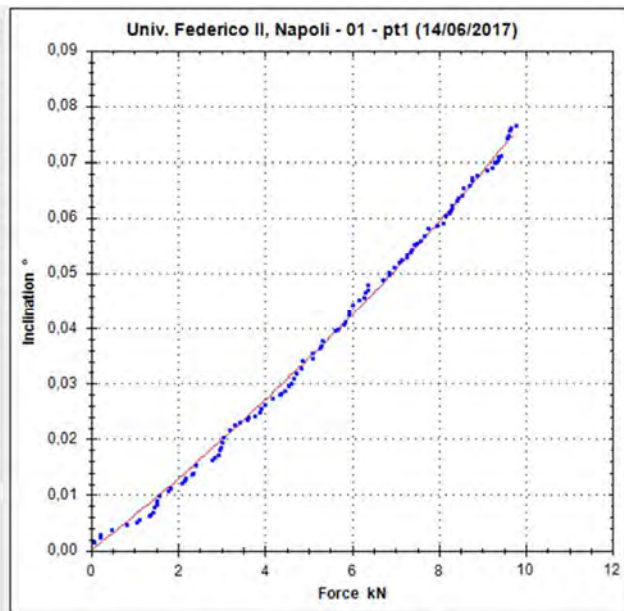
Measurement  
 Name rco II, Napoli - 01 - pt1 (14/06/2017)

Rope height on tree (m) 8.50  
 Anchor-tree level difference (m) 0.30  
 Anchor-tree distance (m) 20.70  
 Drag factor 0,3  
 Wind speed (m/s) 33  
 Crown Area (m<sup>2</sup>) 169  
 Crown center height (m) 13.3  
 Elastic Limit (%) 2

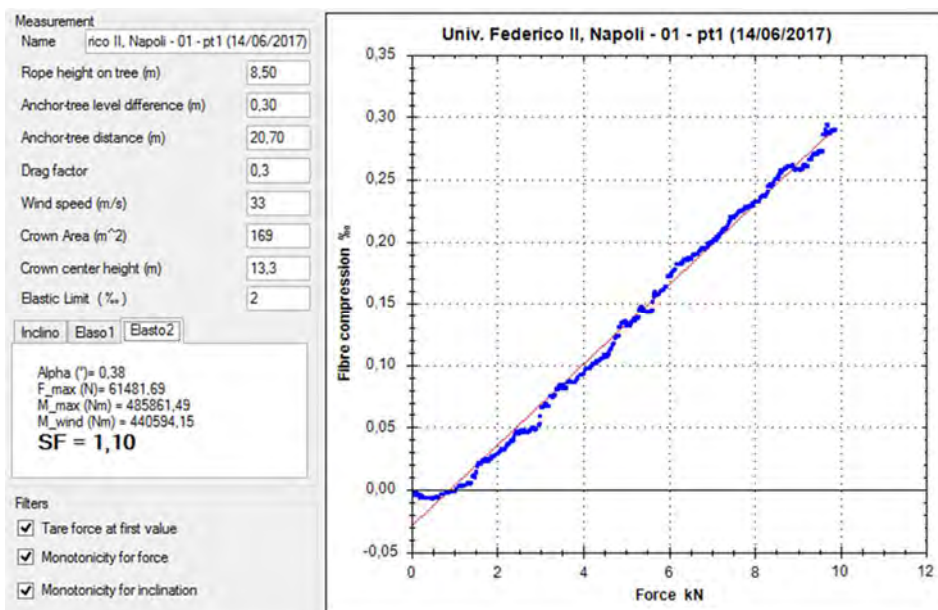
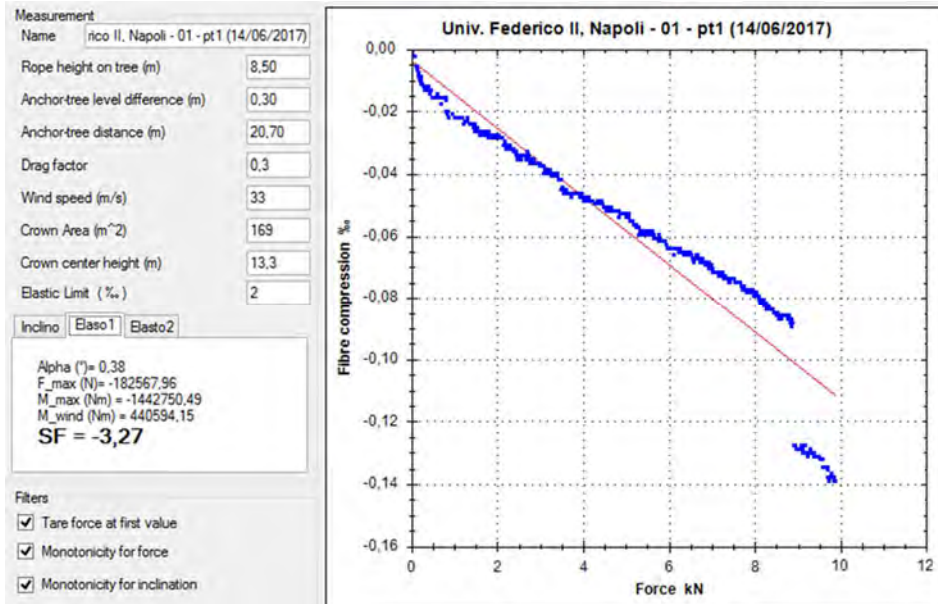
Inclino Elaso1 Elasto2

Alpha (°) = 0,38  
 F<sub>max</sub> (N) = 57705,36  
 M<sub>max</sub> (Nm) = 456018,91  
 M<sub>wind</sub> (Nm) = 440594,15  
**SF = 1,04**

Filters  
 Tare force at first value  
 Monotonicity for force  
 Monotonicity for inclination

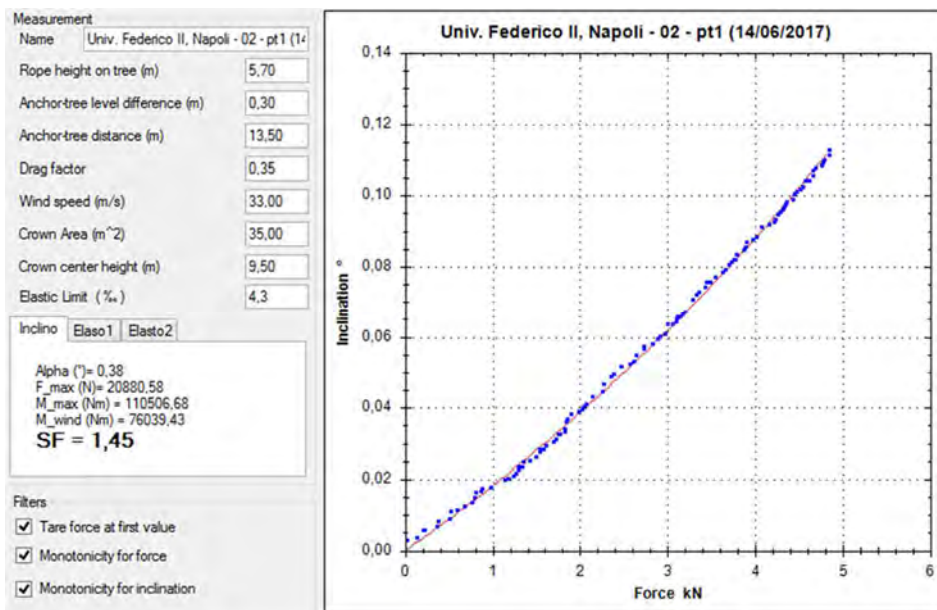
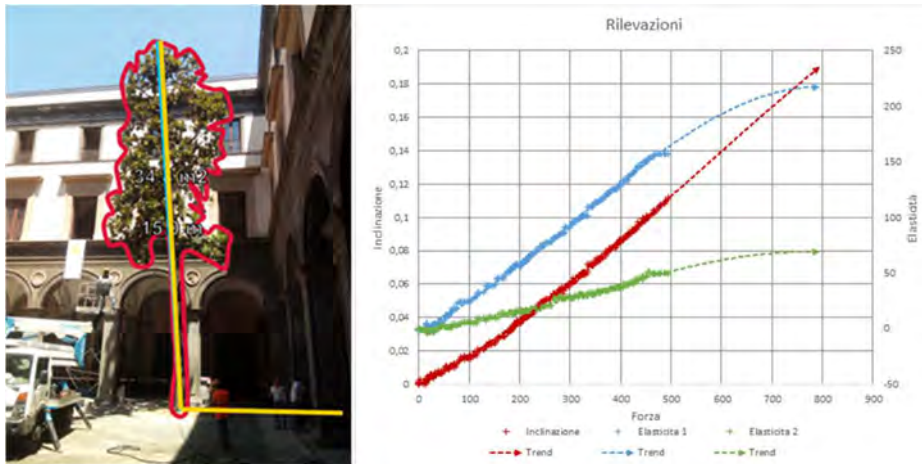


## Appendix 1 – Pulling tests



## Appendix 1 – Pulling tests

via Monteoliveto 3, Napoli Università – 02 – pt1



## Appendix 1 – Pulling tests

Measurement

Name Univ. Federico II, Napoli - 02 - pt1 (14/06/2017)

Rope height on tree (m) 5,70

Anchor-tree level difference (m) 0,30

Anchor-tree distance (m) 13,50

Drag factor 0,35

Wind speed (m/s) 33,00

Crown Area (m<sup>2</sup>) 35,00

Crown center height (m) 9,50

Elastic Limit (%) 4,3

Inclino Elaso1 Elasto2

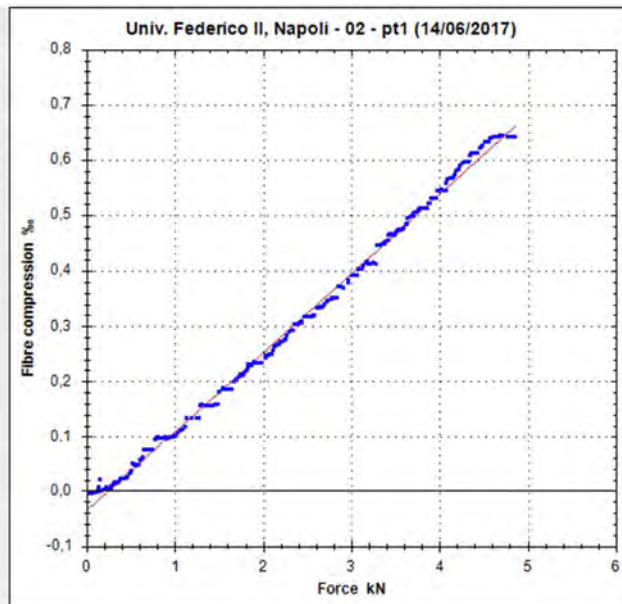
Alpha (°)= 0,38  
 F\_max (N)= 29989,13  
 M\_max (Nm) = 158711,99  
 M\_wind (Nm) = 76039,43  
**SF = 2,09**

Filters

Tare force at first value

Monotonicity for force

Monotonicity for inclination



Measurement

Name Univ. Federico II, Napoli - 02 - pt1 (14/06/2017)

Rope height on tree (m) 5,70

Anchor-tree level difference (m) 0,30

Anchor-tree distance (m) 13,50

Drag factor 0,35

Wind speed (m/s) 33,00

Crown Area (m<sup>2</sup>) 35,00

Crown center height (m) 9,50

Elastic Limit (%) 4,3

Inclino Elaso1 Elasto2

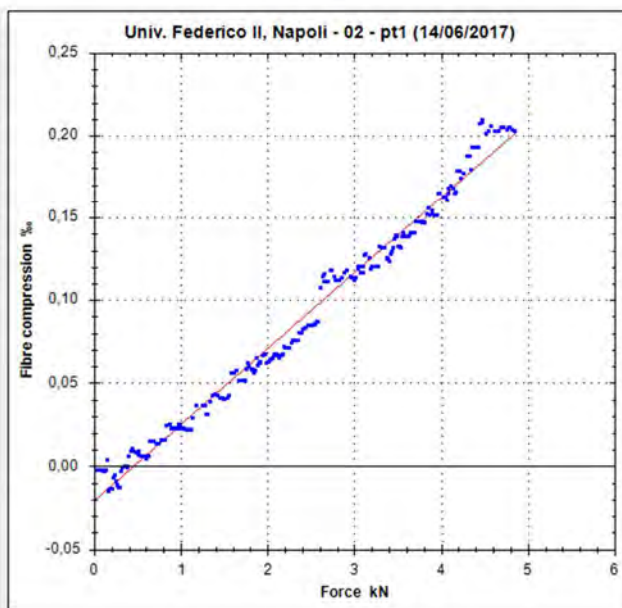
Alpha (°)= 0,38  
 F\_max (N)= 93776,37  
 M\_max (Nm) = 496294,28  
 M\_wind (Nm) = 76039,43  
**SF = 6,53**

Filters

Tare force at first value

Monotonicity for force

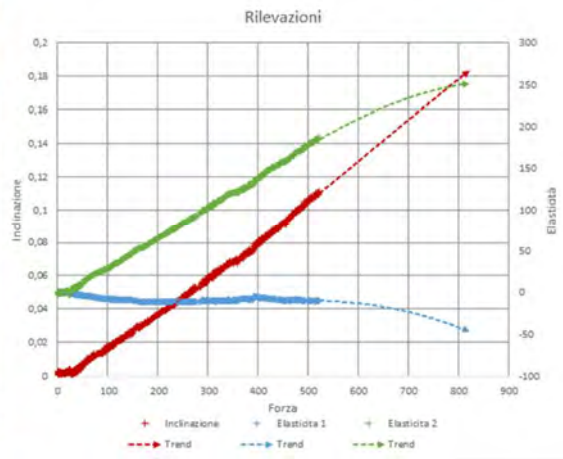
Monotonicity for inclination



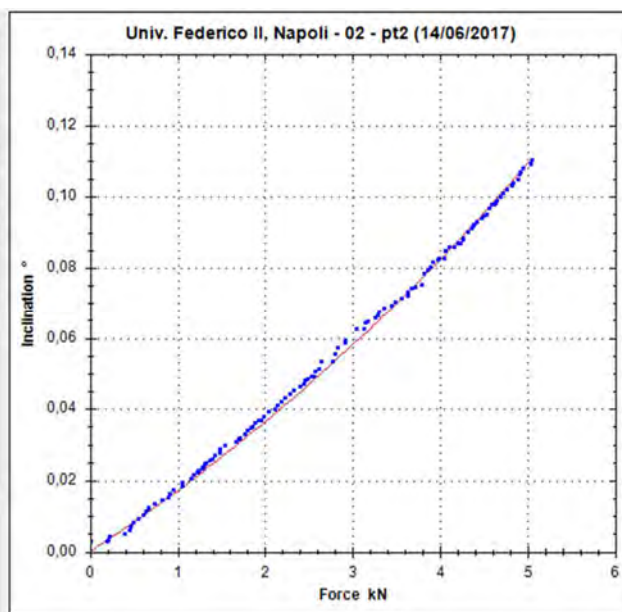


Appendix 1 – Pulling tests

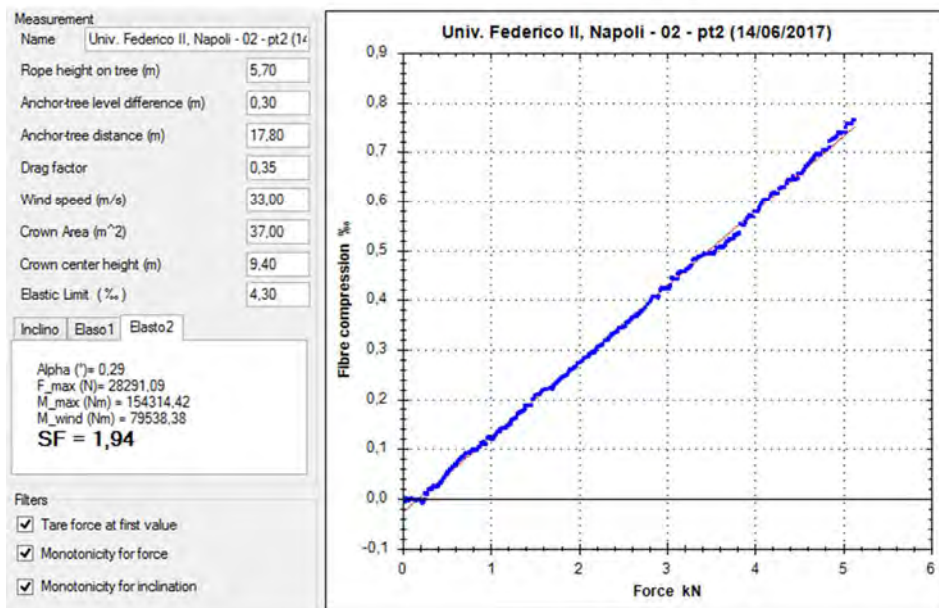
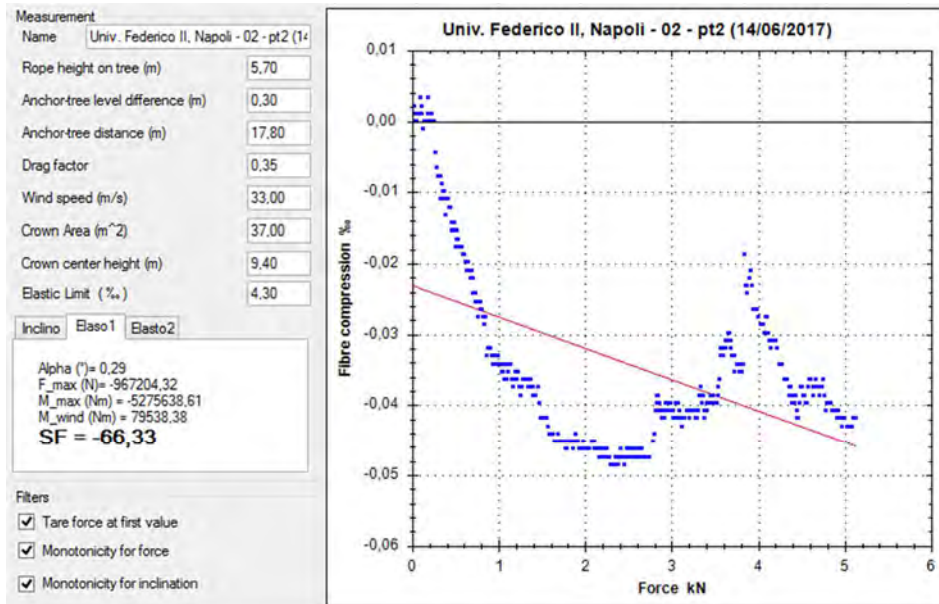
via Monteoliveto 3, Napoli Università – 02 – pt2



Measurement	
Name	Univ. Federico II, Napoli - 02 - pt2 (14/06/2017)
Rope height on tree (m)	5.70
Anchor-tree level difference (m)	0.30
Anchor-tree distance (m)	17.80
Drag factor	0.35
Wind speed (m/s)	33.00
Crown Area (m <sup>2</sup> )	37.00
Crown center height (m)	9.40
Elastic Limit (%)	4.30
Inclino <input type="radio"/> Elaso1 <input type="radio"/> Elasto2	
Alpha (°) = 0.29 F_max (N) = 22027.37 M_max (Nm) = 120148.83 M_wind (Nm) = 79538.38 <b>SF = 1,51</b>	
Filters	
<input checked="" type="checkbox"/> Tare force at first value	
<input checked="" type="checkbox"/> Monotonicity for force	
<input checked="" type="checkbox"/> Monotonicity for inclination	

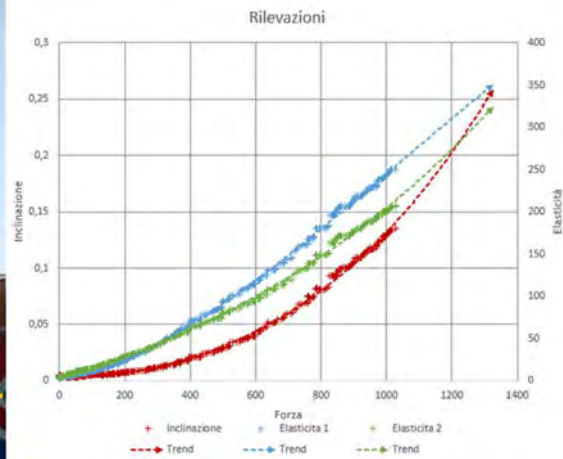


## Appendix 1 – Pulling tests



Appendix 1 – Pulling tests

via Amendola 42, Novate Milanese – 01 – pt1



Measurement

Name: via Amendola 42, Novate M.se-01-pt

Rope height on tree (m): 7,00

Anchor-tree level difference (m): 0,90

Anchor-tree distance (m): 19,92

Drag factor: 0,25

Wind speed (m/s): 33,00

Crown Area (m<sup>2</sup>): 57,60

Crown center height (m): 9,00

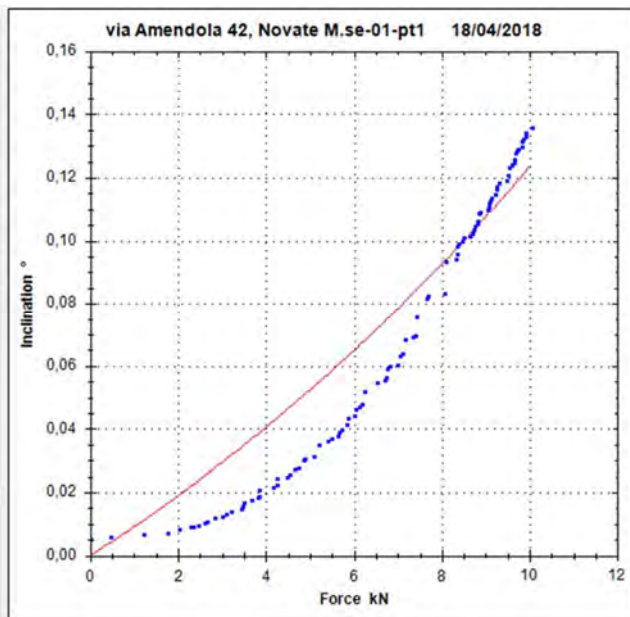
Elastic Limit (%): 3,20

Inclino Elaso1 Elasto2

Alpha (°) = 0,30  
 F<sub>max</sub> (N) = 40097,98  
 M<sub>max</sub> (Nm) = 268384,13  
 M<sub>wind</sub> (Nm) = 84680,64  
**SF = 3,17**

Filters

- Tare force at first value
- Monotonicity for force
- Monotonicity for inclination



## Appendix 1 – Pulling tests

Measurement

Name: via Amendola 42, Novate M.se-01-pt

Rope height on tree (m): 7,00

Anchor-tree level difference (m): 0,90

Anchor-tree distance (m): 19,92

Drag factor: 0,25

Wind speed (m/s): 33,00

Crown Area (m<sup>2</sup>): 57,60

Crown center height (m): 9,00

Elastic Limit (%): 3,20

Inclino: Elaso1 Elasto2

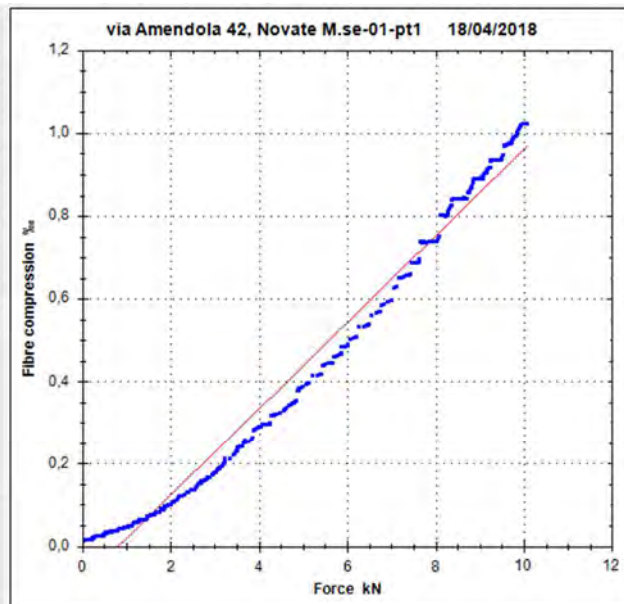
Alpha (°) = 0,30  
 F\_max (N) = 30499,18  
 M\_max (Nm) = 204137,35  
 M\_wind (Nm) = 84680,64  
**SF = 2,41**

Filters

Tare force at first value

Monotonicity for force

Monotonicity for inclination



Measurement

Name: via Amendola 42, Novate M.se-01-pt

Rope height on tree (m): 7,00

Anchor-tree level difference (m): 0,90

Anchor-tree distance (m): 19,92

Drag factor: 0,25

Wind speed (m/s): 33,00

Crown Area (m<sup>2</sup>): 57,60

Crown center height (m): 9,00

Elastic Limit (%): 3,20

Inclino: Elaso1 Elasto2

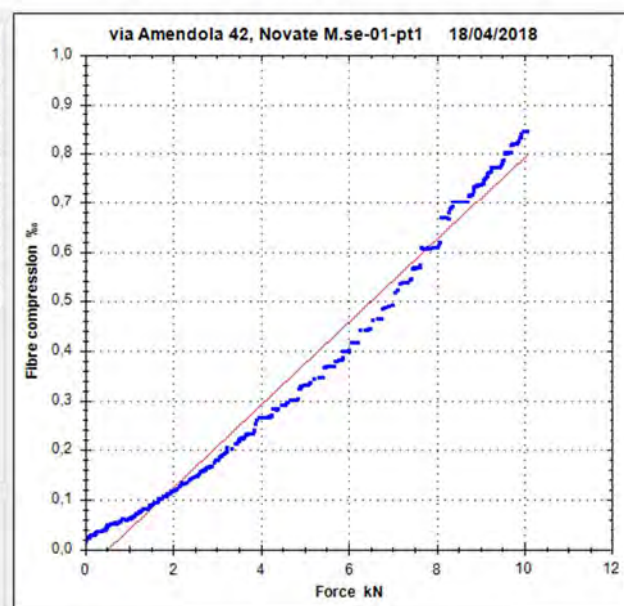
Alpha (°) = 0,30  
 F\_max (N) = 38331,53  
 M\_max (Nm) = 256560,92  
 M\_wind (Nm) = 84680,64  
**SF = 3,03**

Filters

Tare force at first value

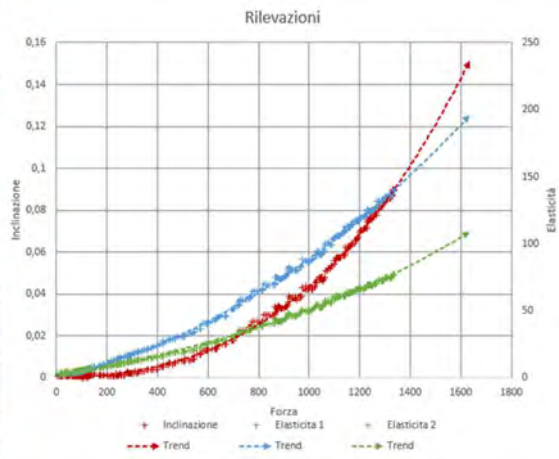
Monotonicity for force

Monotonicity for inclination



Appendix 1 – Pulling tests

via Amendola 42, Novate Milanese – 02 – pt1



Measurement

Name: via Amendola 42, Novate M.se-02-pt

Rope height on tree (m): 6.50

Anchor-tree level difference (m): 1.10

Anchor-tree distance (m): 14.23

Drag factor: 0.25

Wind speed (m/s): 33.00

Crown Area (m<sup>2</sup>): 68

Crown center height (m): 9.5

Elastic Limit (%): 1.50

Inclino Elasto1 Elasto2

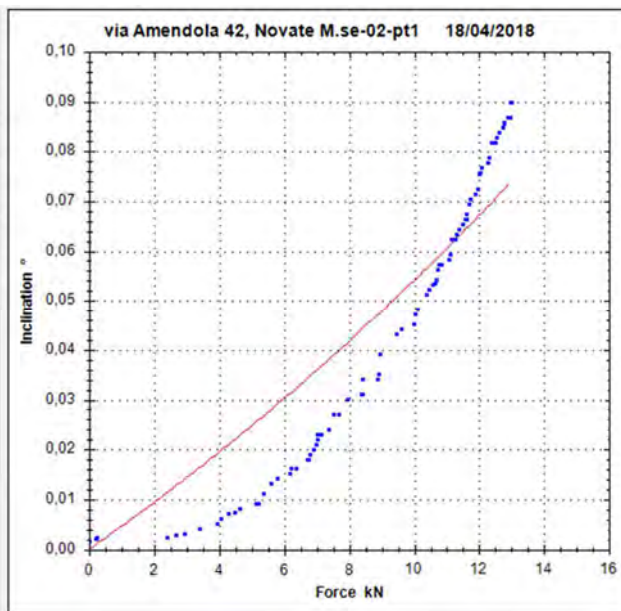
Alpha (°) = 0.36  
 F<sub>max</sub> (N) = 77977.04  
 M<sub>max</sub> (Nm) = 473877.55  
 M<sub>wind</sub> (Nm) = 105524.10  
**SF = 4.49**

Filters

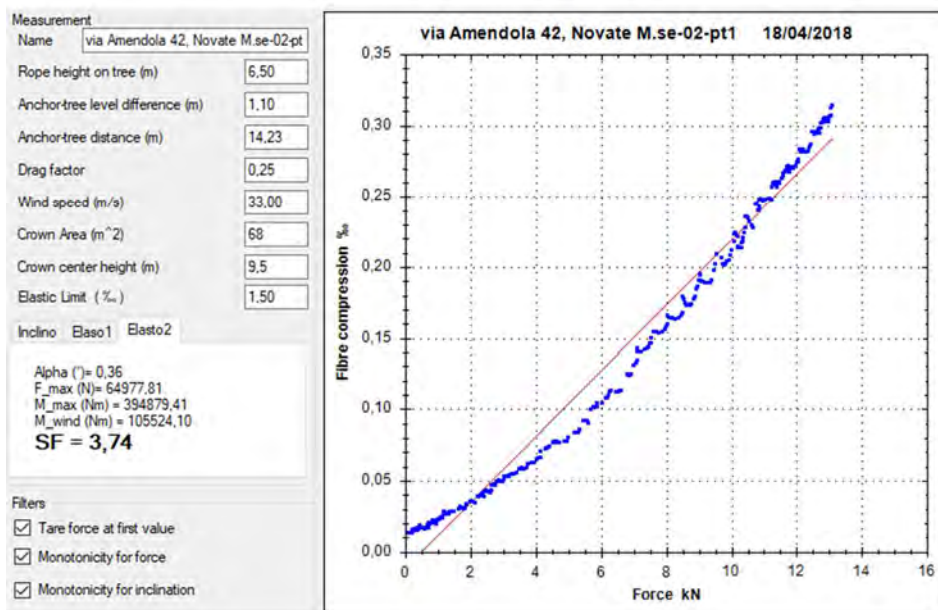
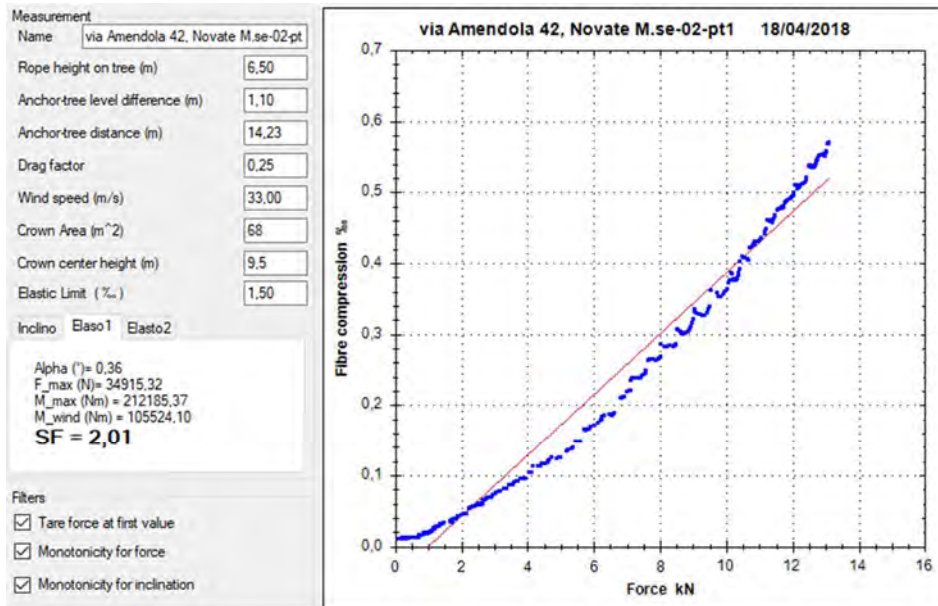
Tare force at first value

Monotonicity for force

Monotonicity for inclination

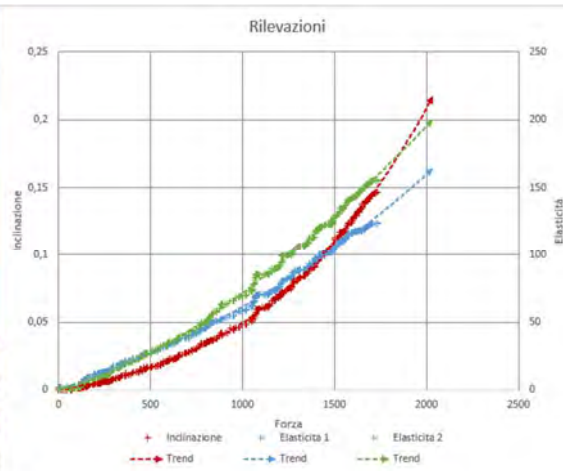


## Appendix 1 – Pulling tests



## Appendix 1 – Pulling tests

via Amendola 42, Novate Milanese – 02 – pt2



Measurement

Name endola 42, Novate M.se-02-pt2 18

Rope height on tree (m) 6.5

Anchor-tree level difference (m) 0.10

Anchor-tree distance (m) 9.48

Drag factor 0.25

Wind speed (m/s) 33

Crown Area (m<sup>2</sup>) 95.9

Crown center height (m) 10.1

Elastic Limit (%) 1.5

Inclino Elaso1 Elasto2

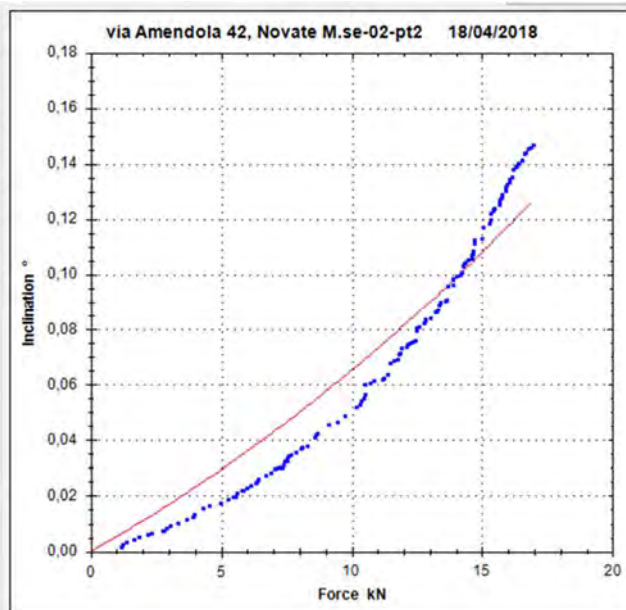
Alpha (°) = 0.59  
 F<sub>max</sub> (N) = 66565.95  
 M<sub>max</sub> (Nm) = 358607.61  
 M<sub>wind</sub> (Nm) = 158219.18  
**SF = 2,27**

Filters

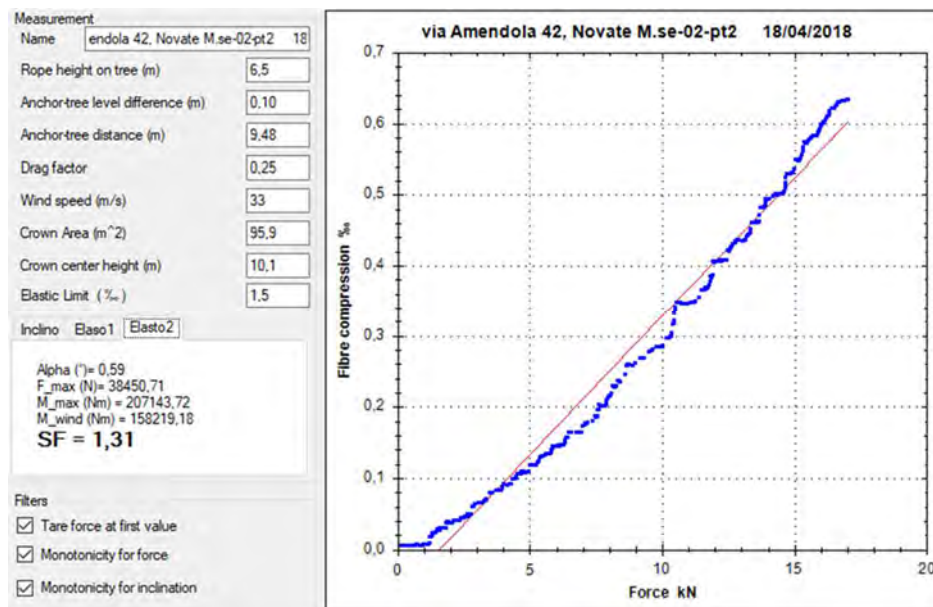
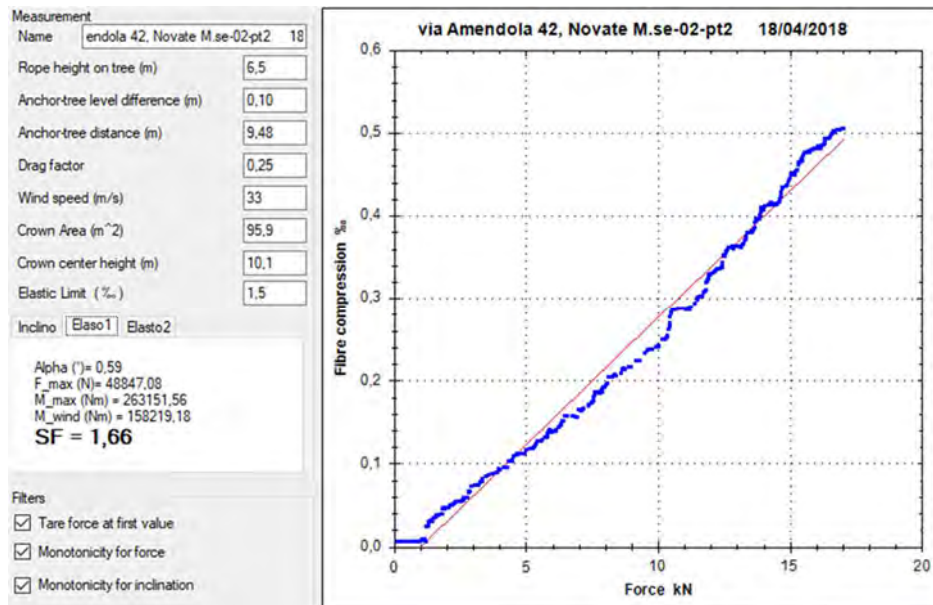
Tare force at first value

Monotonicity for force

Monotonicity for inclination



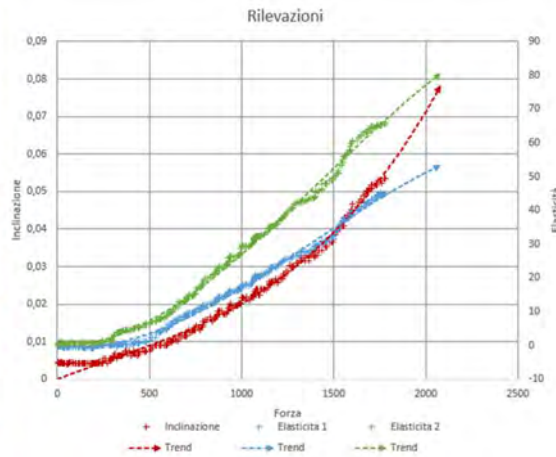
## Appendix 1 – Pulling tests





Appendix 1 – Pulling tests

via Amendola 42, Novate Milanese – 03 – pt1



Measurement

Name: Novate M.se-03-pt1 18/04/2018

Rope height on tree (m): 5.5

Anchor-tree level difference (m): 0

Anchor-tree distance (m): 9.48

Drag factor: 0.25

Wind speed (m/s): 33

Crown Area (m<sup>2</sup>): 95.6

Crown center height (m): 10.1

Elastic Limit (%): 1.5

Inclino Elaso1 Elasto2

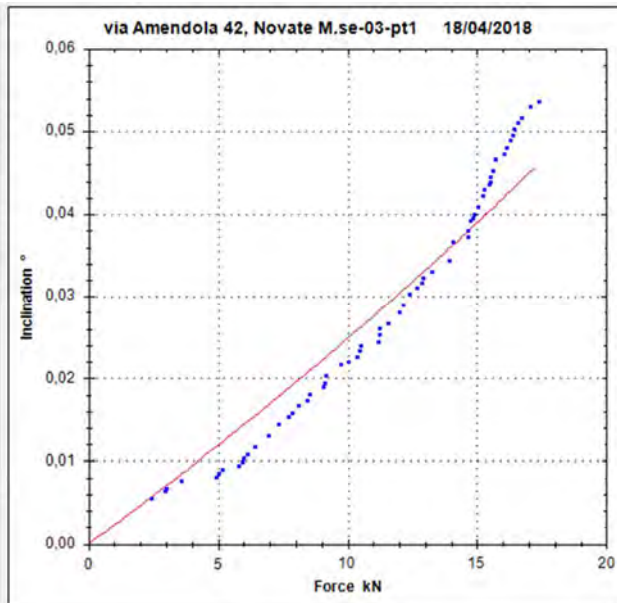
Alpha (°) = 0.53  
 F\_max (N) = 155494.58  
 M\_max (Nm) = 739737.96  
 M\_wind (Nm) = 157724.23  
**SF = 4,69**

Filters

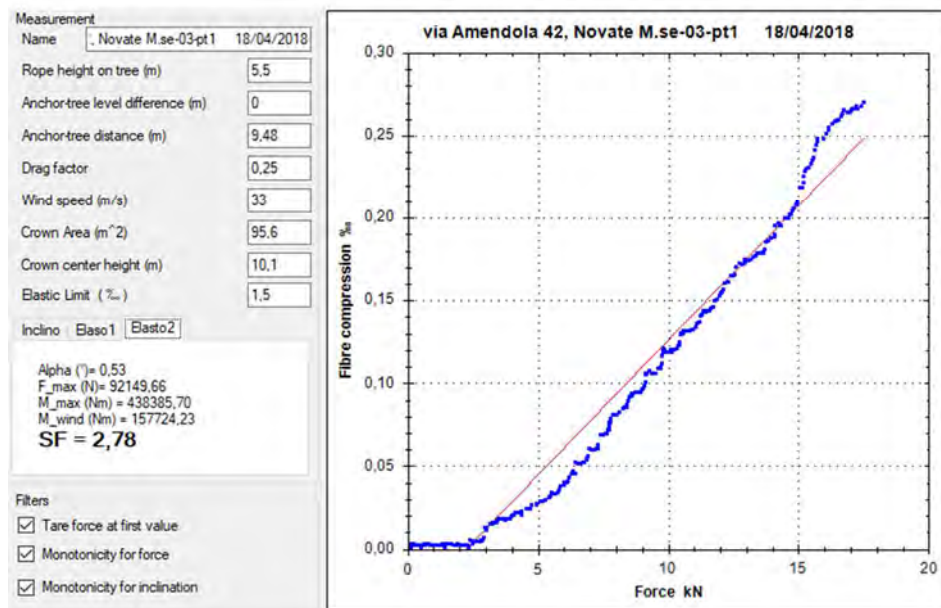
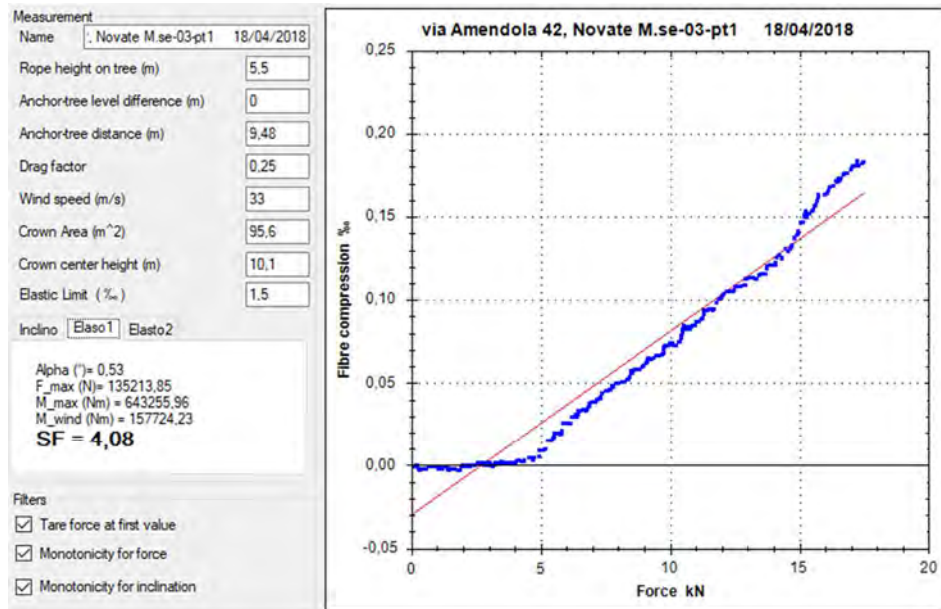
Tare force at first value

Monotonicity for force

Monotonicity for inclination

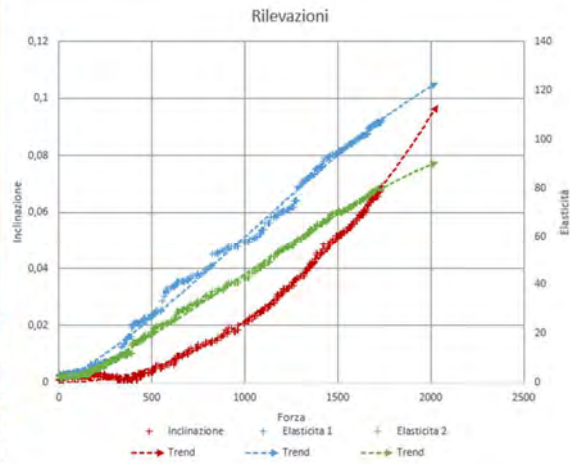


## Appendix 1 – Pulling tests



## Appendix 1 – Pulling tests

via Amendola 42, Novate Milanese – 03 – pt2



Measurement

Name: Novate M.se-03-pt2 18/04/2018

Rope height on tree (m): 5,5

Anchor-tree level difference (m): 0,60

Anchor-tree distance (m): 19,07

Drag factor: 0,25

Wind speed (m/s): 33

Crown Area (m<sup>2</sup>): 148,7

Crown center height (m): 10,8

Elastic Limit (%): 1,5

Inclino Elaso1 Elaso2

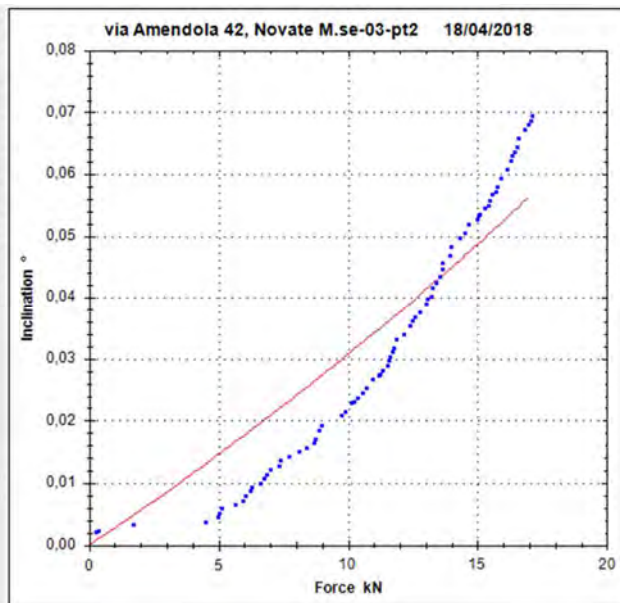
Alpha (°) = 0,25  
 F\_max (N) = 128070,24  
 M\_max (Nm) = 682225,19  
 M\_wind (Nm) = 262333,57  
**SF = 2,60**

Filters

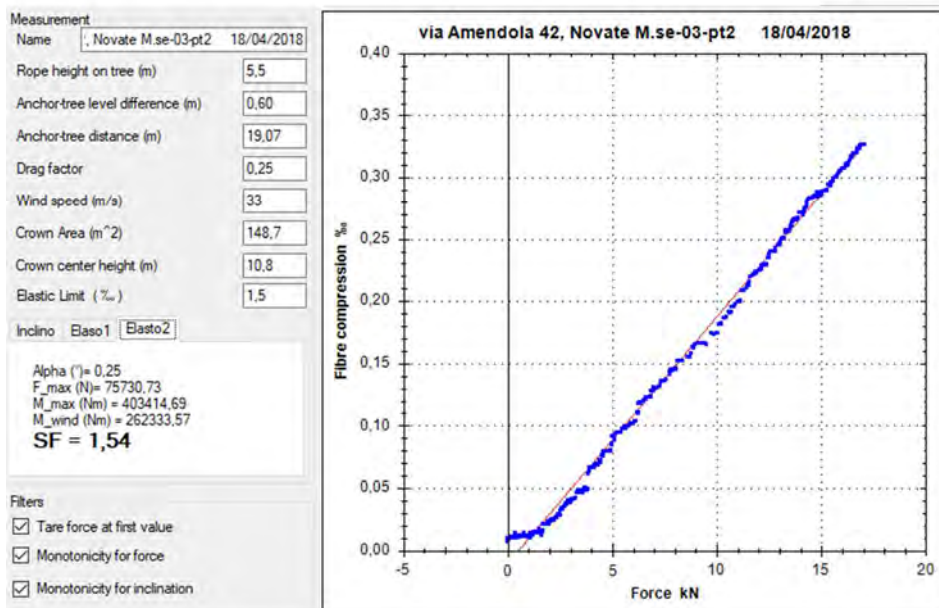
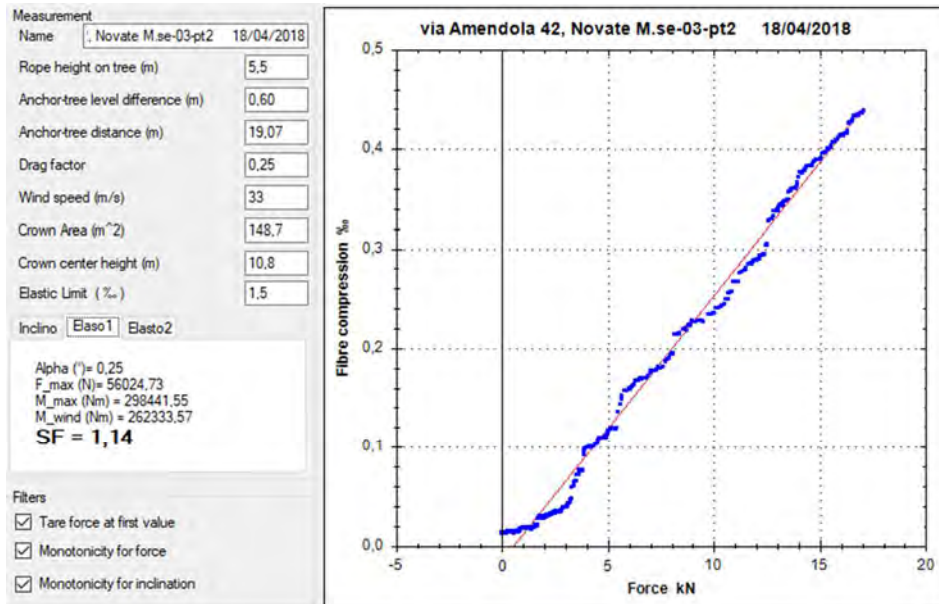
Tare force at first value

Monotonicity for force

Monotonicity for inclination

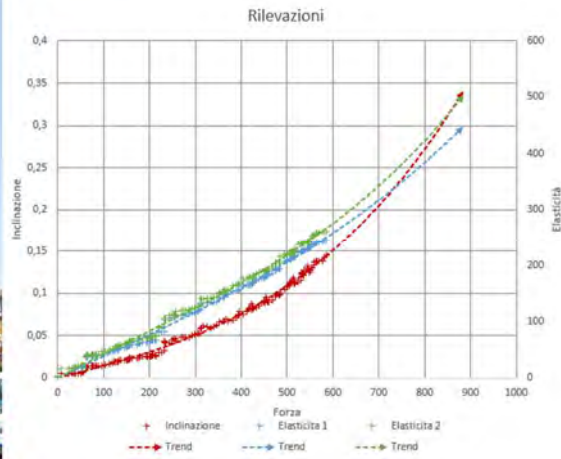


## Appendix 1 – Pulling tests



Appendix 1 – Pulling tests

via Amendola 42, Novate Milanese – 04 – pt1



Measurement

Name: Novate M.se-04-pt1 18/04/2018

Rope height on tree (m): 2.7

Anchor-tree level difference (m): 0.20

Anchor-tree distance (m): 16.67

Drag factor: 0.25

Wind speed (m/s): 33

Crown Area (m<sup>2</sup>): 13.8

Crown center height (m): 4.1

Elastic Limit (%): 3.2

Inclino Elaso1 Elasto2

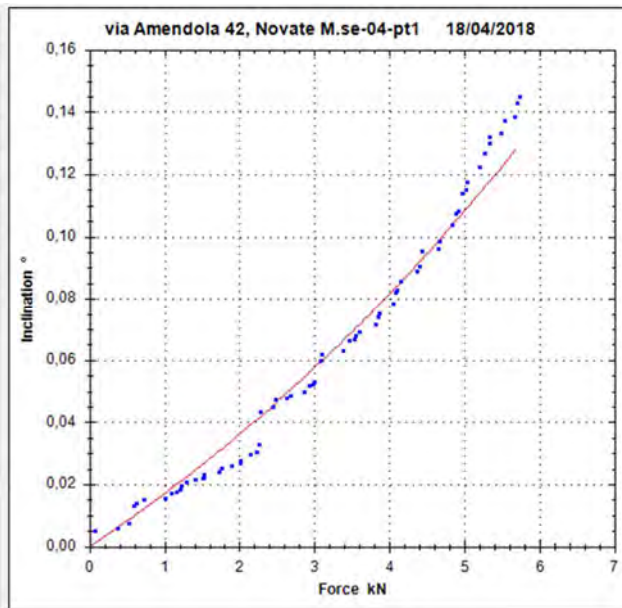
Alpha (°) = 0.15  
 F\_max (N) = 22209.35  
 M\_max (Nm) = 59302.07  
 M\_wind (Nm) = 9242.34  
**SF = 6,42**

Filters

Tare force at first value

Monotonicity for force

Monotonicity for inclination



## Appendix 1 – Pulling tests

Measurement

Name: Novate M.se-04-pt1 18/04/2018

Rope height on tree (m): 2,7

Anchor-tree level difference (m): 0,20

Anchor-tree distance (m): 16,67

Drag factor: 0,25

Wind speed (m/s): 33

Crown Area (m<sup>2</sup>): 13,8

Crown center height (m): 4,1

Elastic Limit (%): 3,2

Inclino:  Elaso1  Elasto2

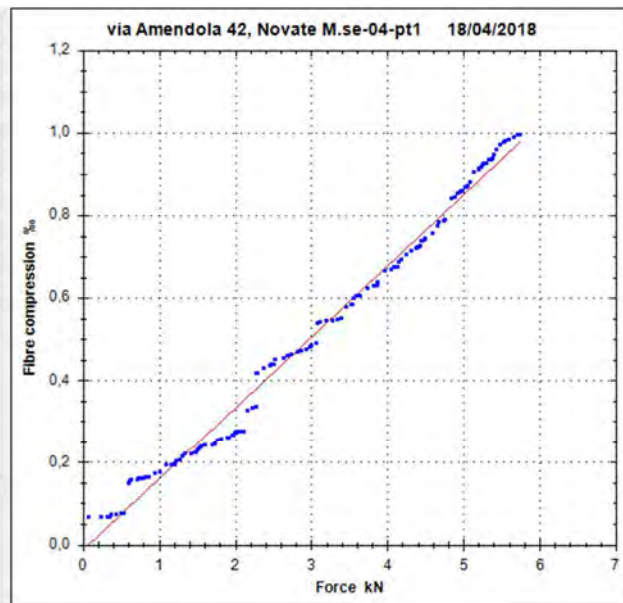
Alpha (°) = 0,15  
 F<sub>max</sub> (N) = 18468,68  
 M<sub>max</sub> (Nm) = 49313,96  
 M<sub>wind</sub> (Nm) = 9242,34  
**SF = 5,34**

Filters

Tare force at first value

Monotonicity for force

Monotonicity for inclination



Measurement

Name: Novate M.se-04-pt1 18/04/2018

Rope height on tree (m): 2,7

Anchor-tree level difference (m): 0,20

Anchor-tree distance (m): 16,67

Drag factor: 0,25

Wind speed (m/s): 33

Crown Area (m<sup>2</sup>): 13,8

Crown center height (m): 4,1

Elastic Limit (%): 3,2

Inclino:  Elaso1  Elasto2

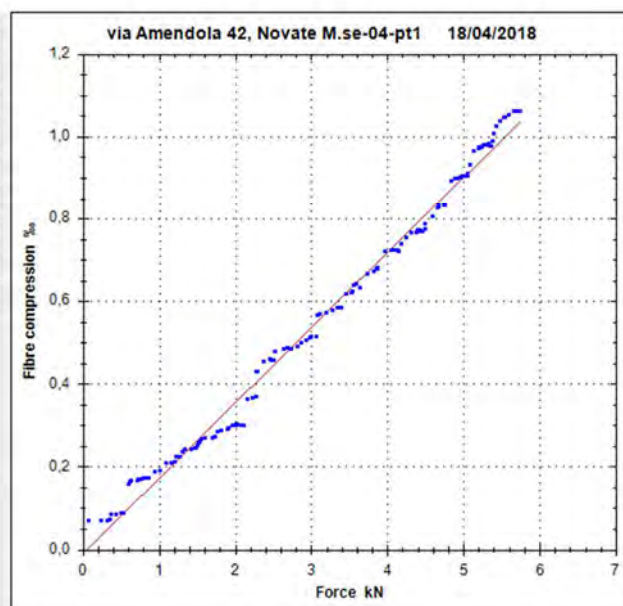
Alpha (°) = 0,15  
 F<sub>max</sub> (N) = 17547,46  
 M<sub>max</sub> (Nm) = 46954,19  
 M<sub>wind</sub> (Nm) = 9242,34  
**SF = 5,07**

Filters

Tare force at first value

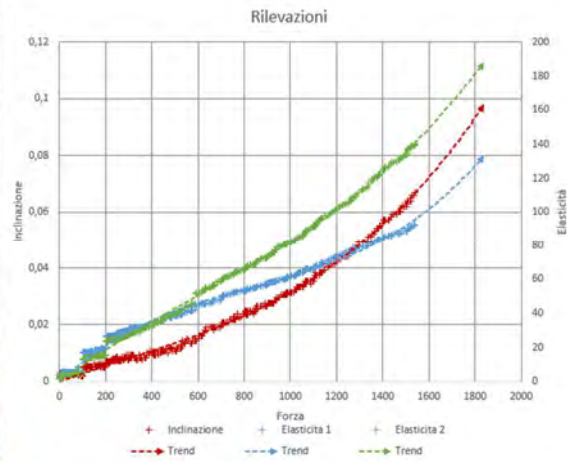
Monotonicity for force

Monotonicity for inclination



Appendix 1 – Pulling tests

Via Mozart 11, Bollate – 01 – pt1



Measurement

Name: via Mozart 11, Bollate (MI) - 01 - pt1

Rope height on tree (m): 7

Anchor-tree level difference (m): 0,5

Anchor-tree distance (m): 19,60

Drag factor: 0,30

Wind speed (m/s): 33

Crown Area (m<sup>2</sup>): 124

Crown center height (m): 7,5

Elastic Limit (%): 2

Inclino: Elaso1 Elaso2

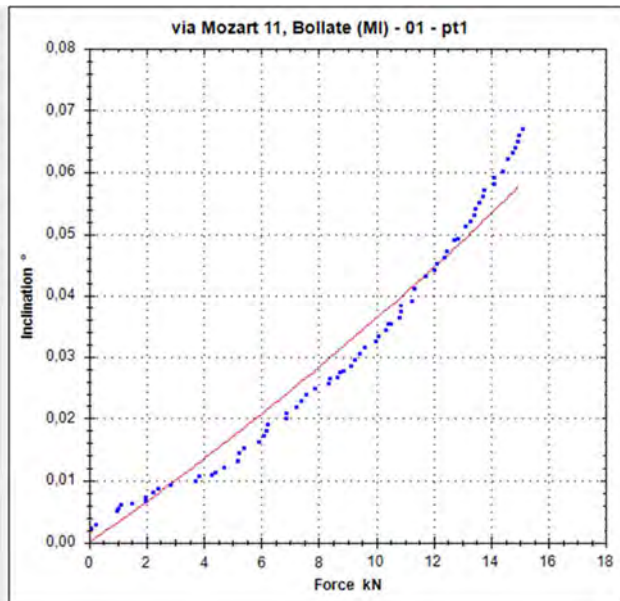
Alpha (°) = 0,32  
 F\_max (N) = 110514,36  
 M\_max (Nm) = 734275,65  
 M\_wind (Nm) = 182298,60  
**SF = 4,03**

Filters

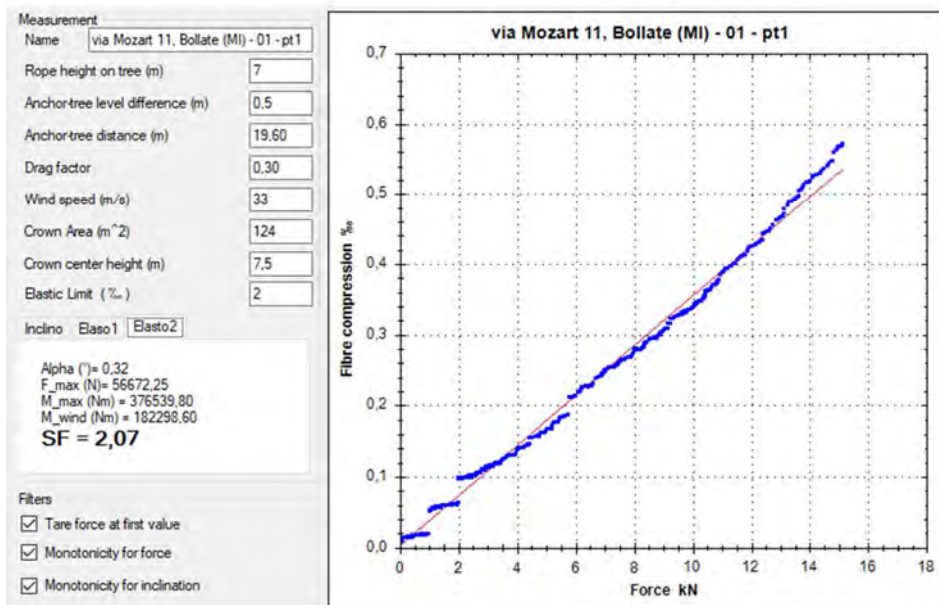
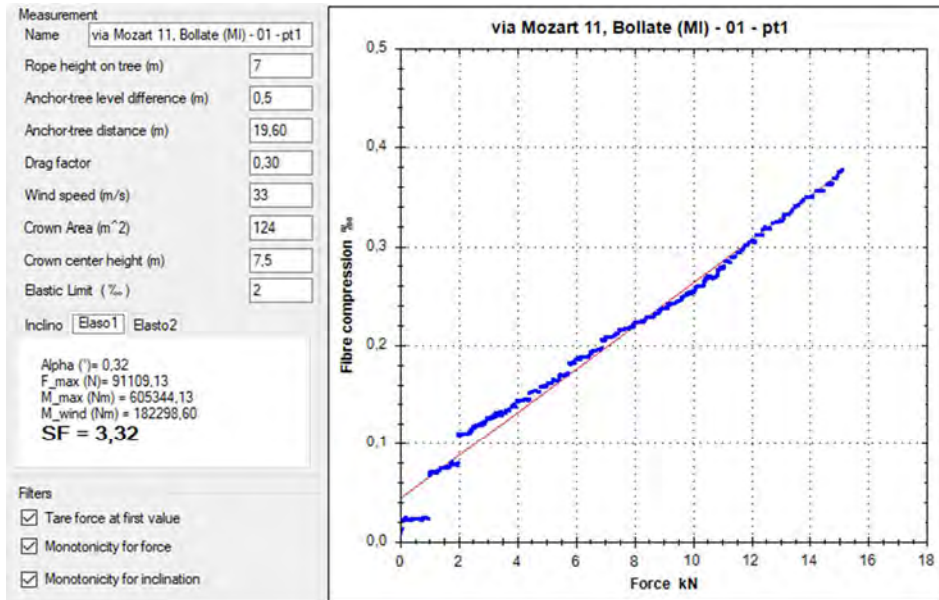
Tare force at first value

Monotonicity for force

Monotonicity for inclination



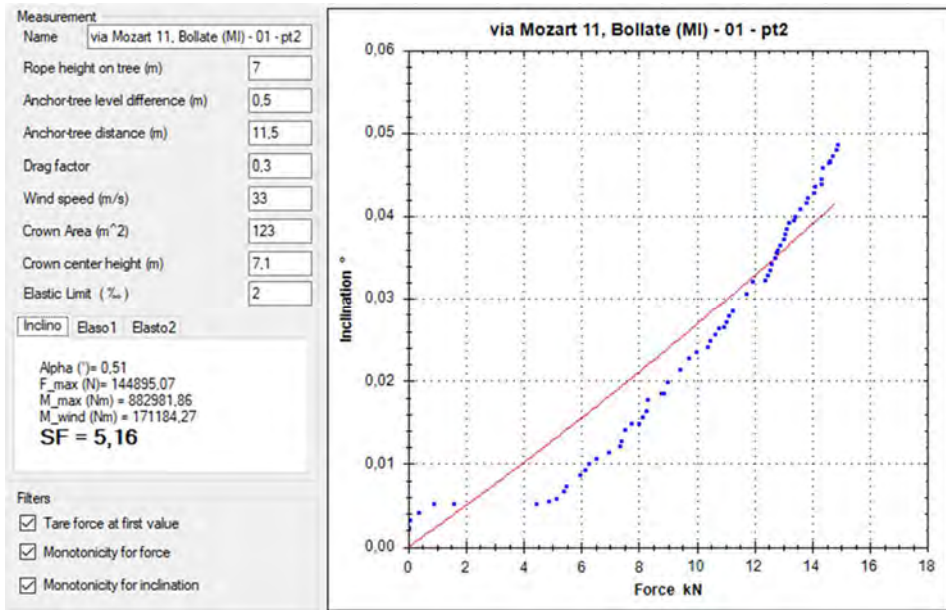
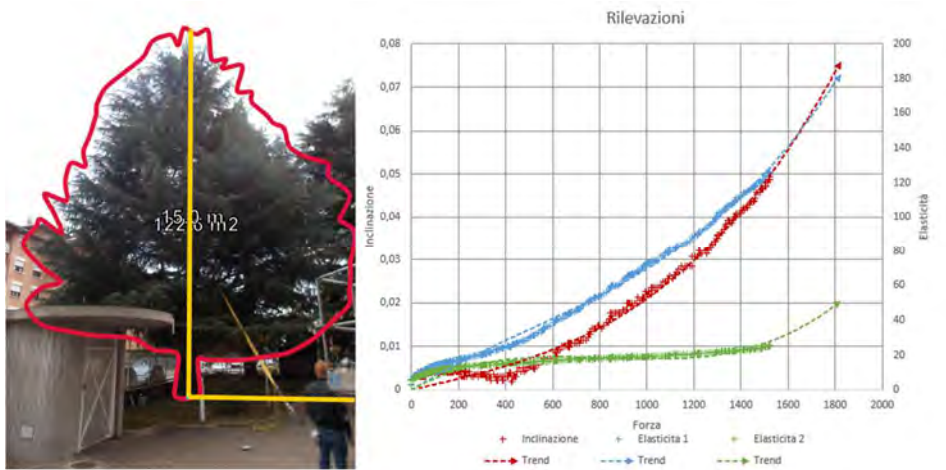
## Appendix 1 – Pulling tests



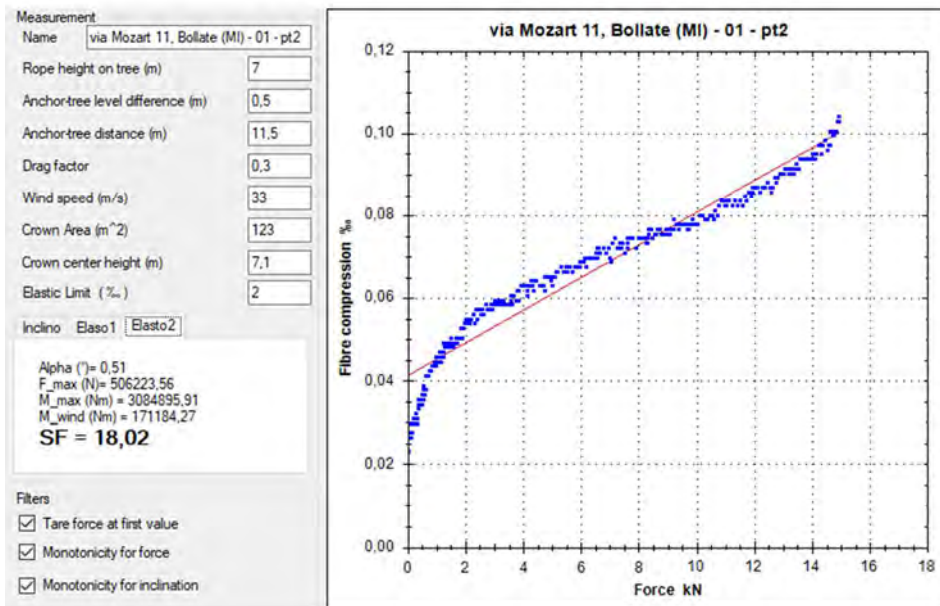
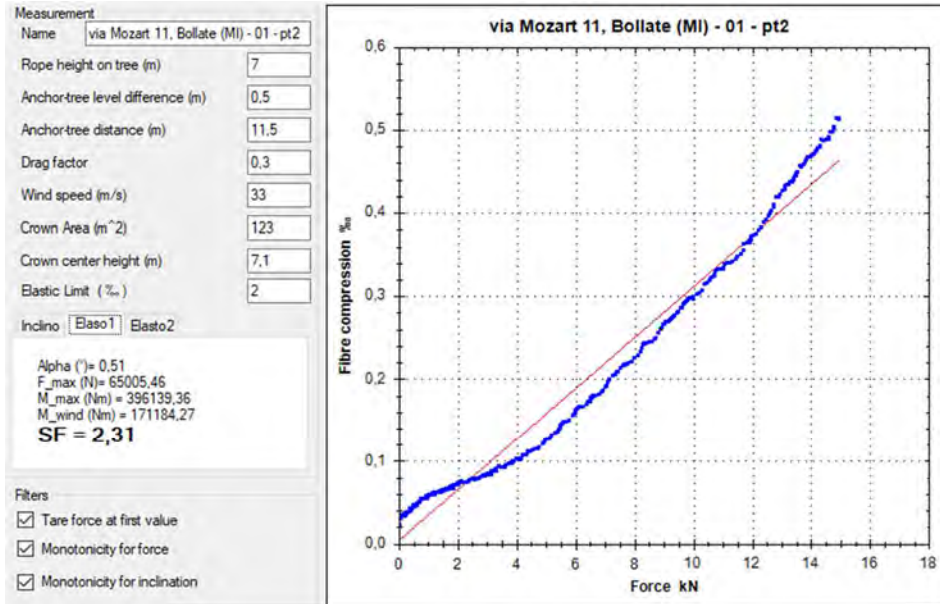


Appendix 1 – Pulling tests

Via Mozart 11, Bollate – 01 – pt2

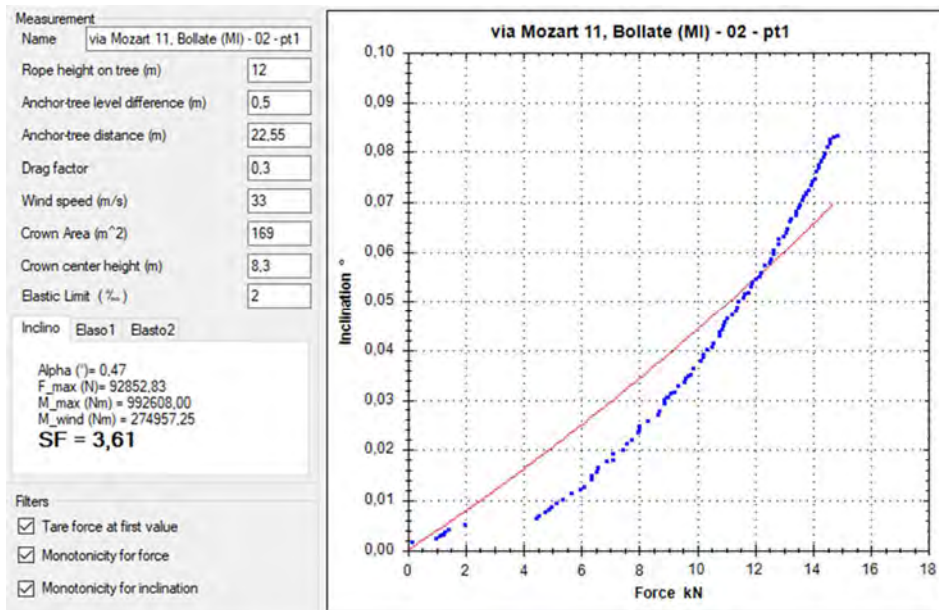
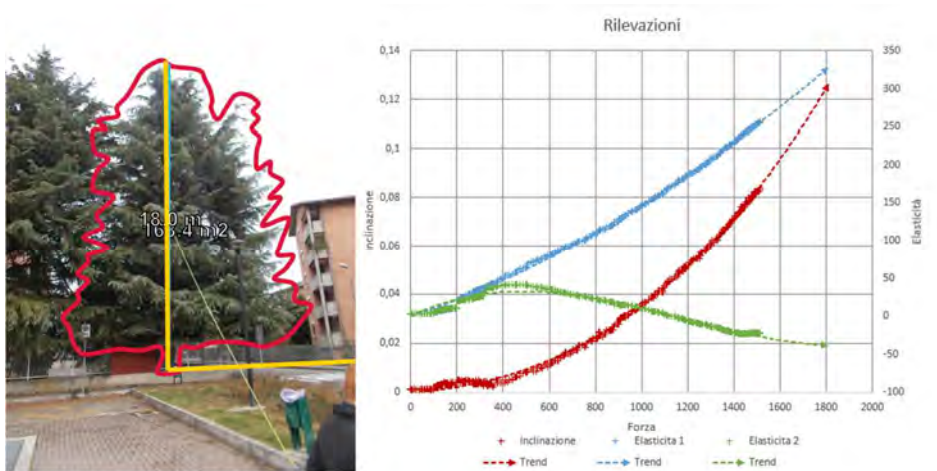


## Appendix 1 – Pulling tests

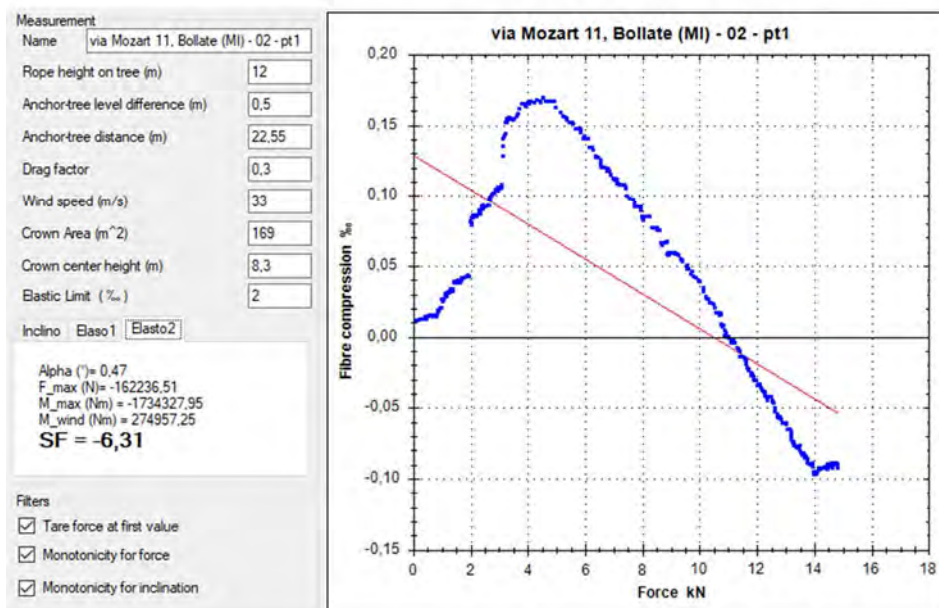
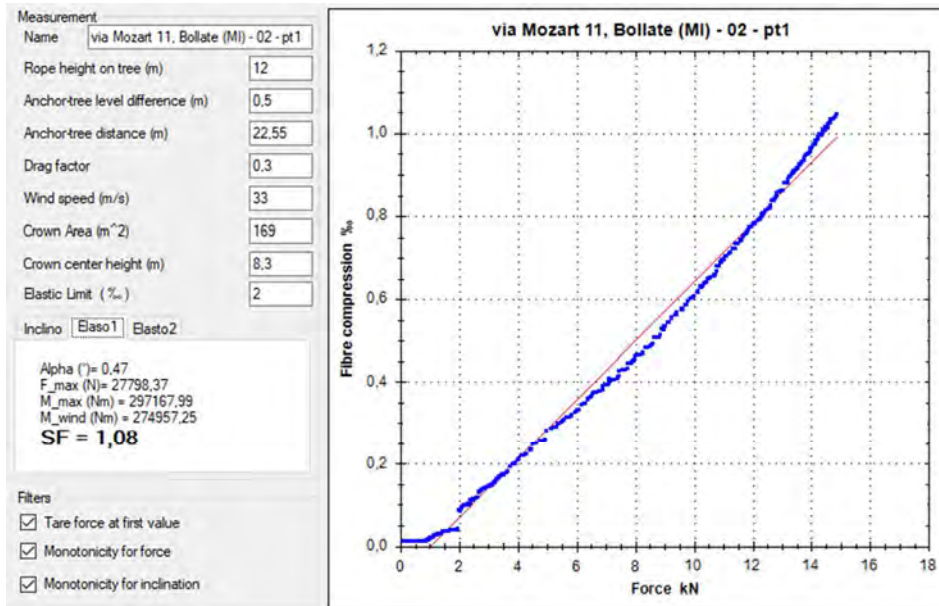


## Appendix 1 – Pulling tests

Via Mozart 11, Bollate – 02 – pt1

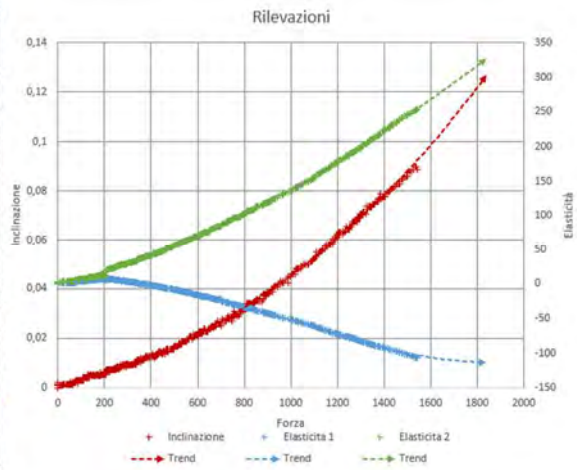


## Appendix 1 – Pulling tests



Appendix 1 – Pulling tests

Via Mozart 11, Bollate – 02 – pt2



Measurement

Name: via Mozart 11, Bollate (MI) - 02 - pt2

Rope height on tree (m): 12

Anchor-tree level difference (m): 0.5

Anchor-tree distance (m): 17.7

Drag factor: 0.3

Wind speed (m/s): 33

Crown Area (m<sup>2</sup>): 171

Crown center height (m): 8.2

Elastic Limit (%): 2

Inclino: Elaso1 Elasto2

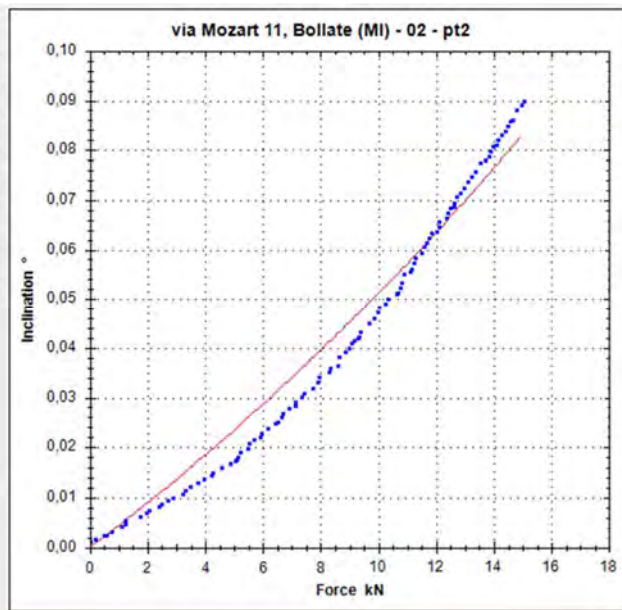
Alpha (°) = 0.58  
 F<sub>max</sub> (N) = 81810.69  
 M<sub>max</sub> (Nm) = 823230.07  
 M<sub>wind</sub> (Nm) = 274859.24  
**SF = 3,00**

Filters

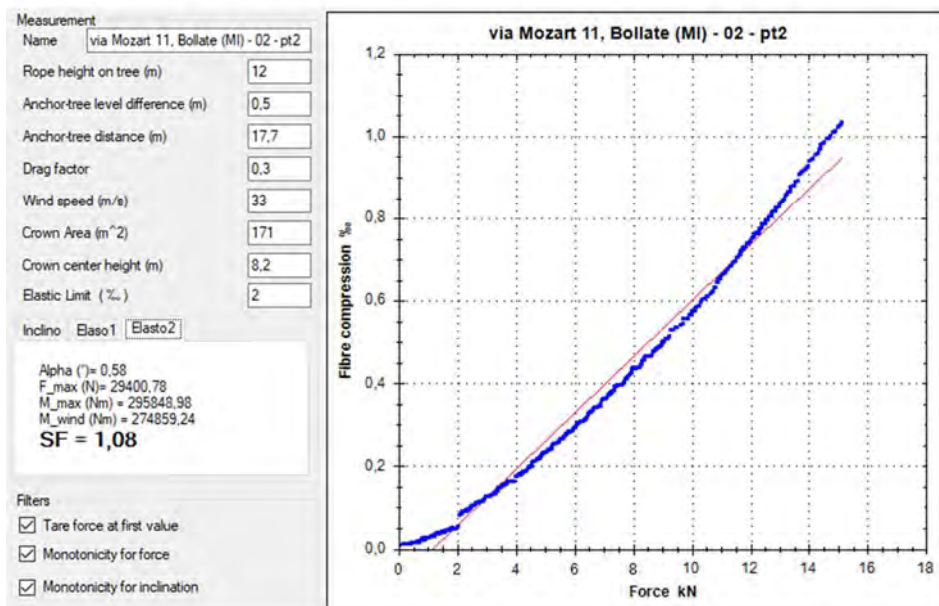
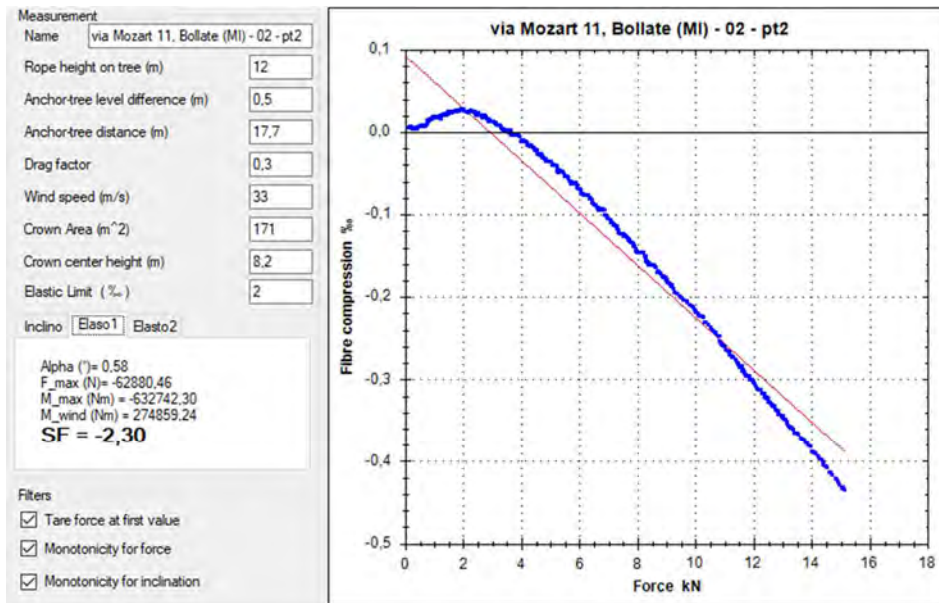
Tare force at first value

Monotonicity for force

Monotonicity for inclination

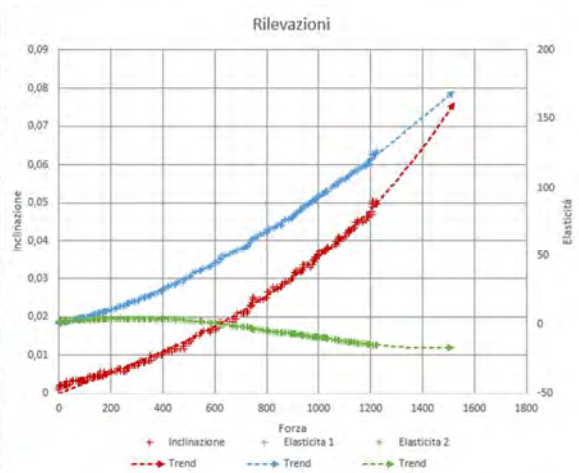


## Appendix 1 – Pulling tests



Appendix 1 – Pulling tests

Via Mozart 11, Bollate – 03 – pt1



Measurement

Name

Rope height on tree (m)

Anchor-tree level difference (m)

Anchor-tree distance (m)

Drag factor

Wind speed (m/s)

Crown Area (m<sup>2</sup>)

Crown center height (m)

Elastic Limit (%)

Inclino Elaso1 Elasto2

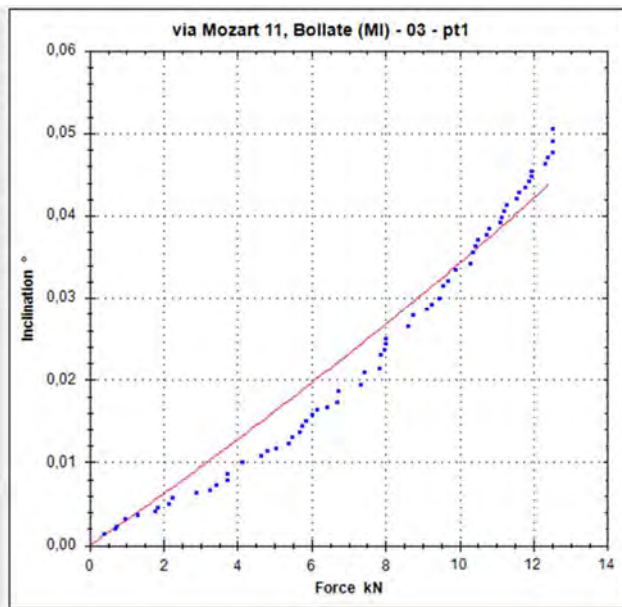
Alpha (°) = 0,41  
F<sub>max</sub> (N) = 116253,99  
M<sub>max</sub> (Nm) = 958453,07  
M<sub>wind</sub> (Nm) = 229343,40  
**SF = 4,18**

Filters

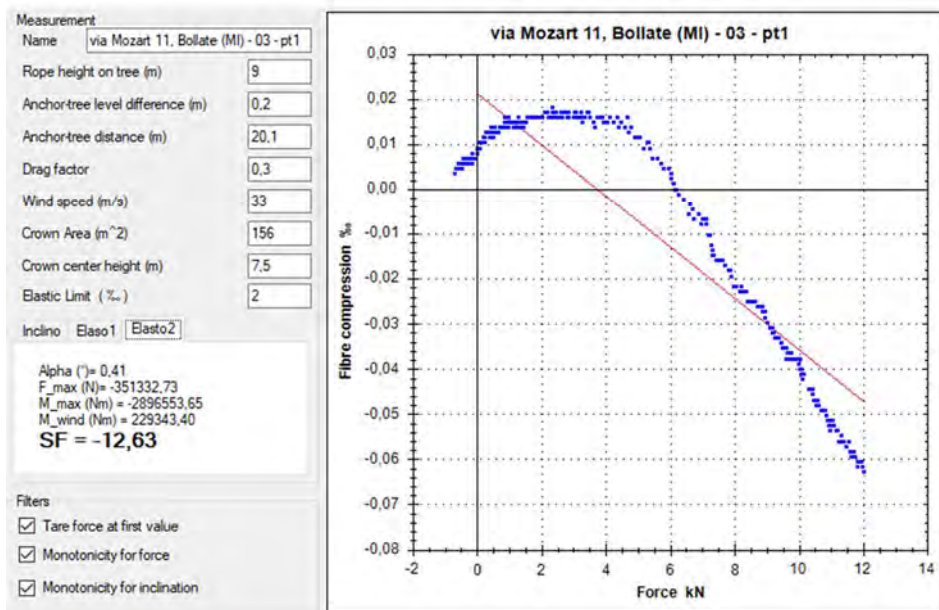
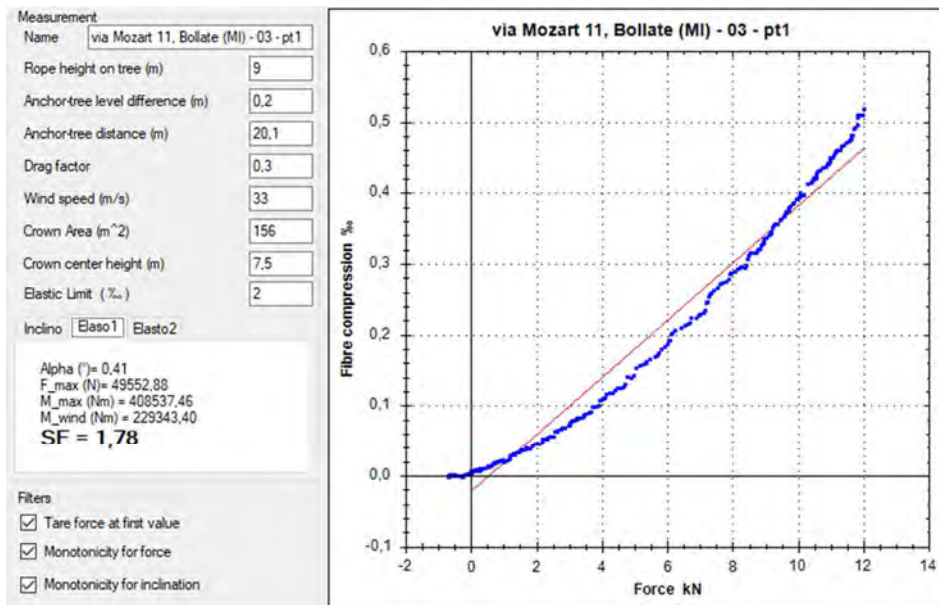
Tare force at first value

Monotonicity for force

Monotonicity for inclination



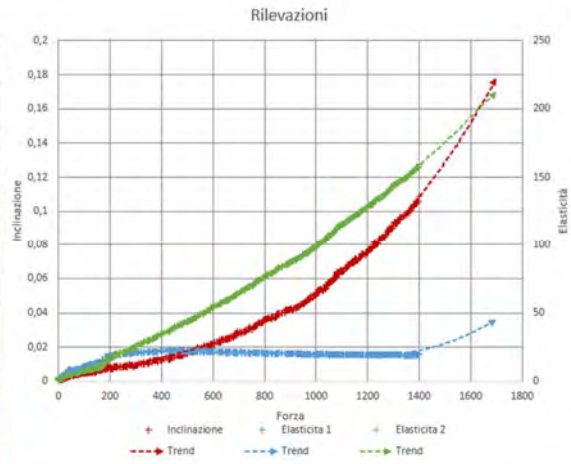
## Appendix 1 – Pulling tests





Appendix 1 – Pulling tests

Via Mozart 11, Bollate – 03 – pt2



Measurement

Name: via Mozart 11, Bollate (MI) - 03 - pt2

Rope height on tree (m): 9

Anchor tree level difference (m): 0,4

Anchor tree distance (m): 21,44

Drag factor: 0,3

Wind speed (m/s): 33

Crown Area (m<sup>2</sup>): 122

Crown center height (m): 8,7

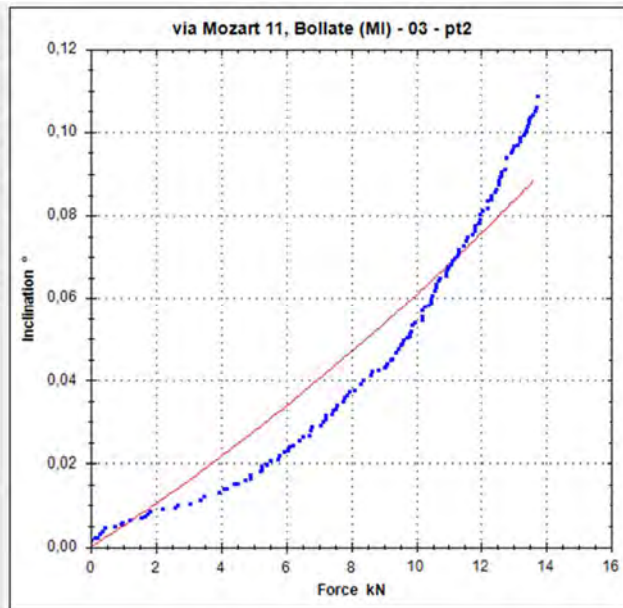
Elastic Limit (%): 2

Inclino Elaso1 Elasto2

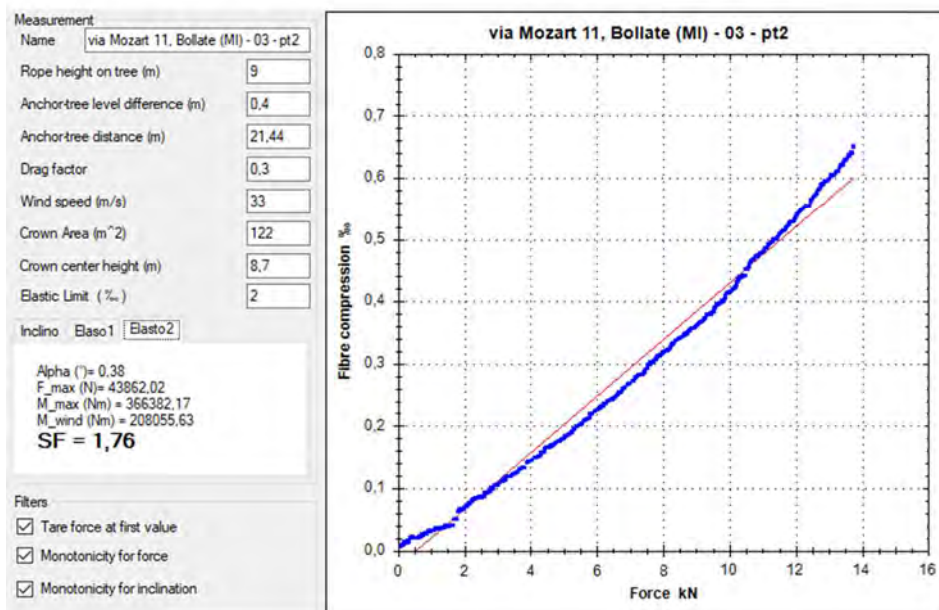
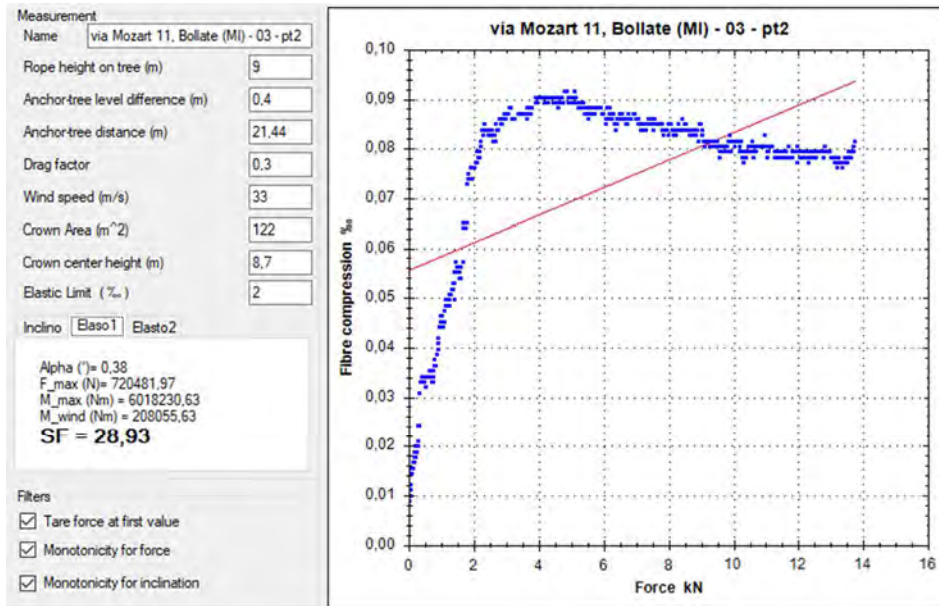
Alpha (°) = 0,38  
 F<sub>max</sub> (N) = 70679,58  
 M<sub>max</sub> (Nm) = 590390,90  
 M<sub>wind</sub> (Nm) = 208055,63  
**SF = 2,84**

Filters

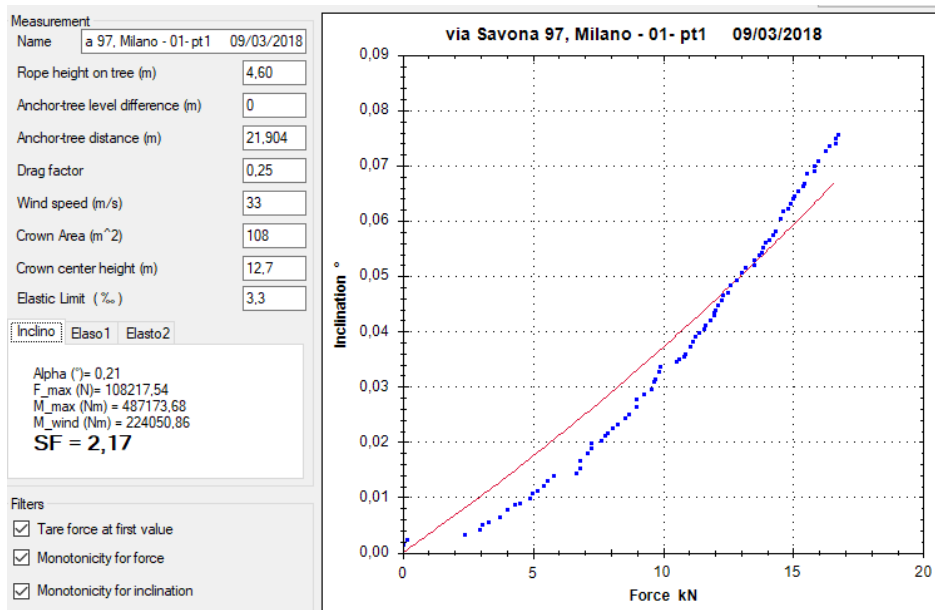
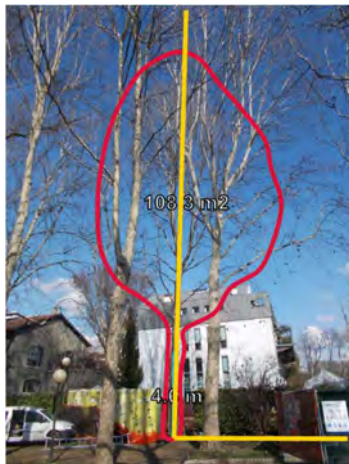
- Tare force at first value
- Monotonicity for force
- Monotonicity for inclination



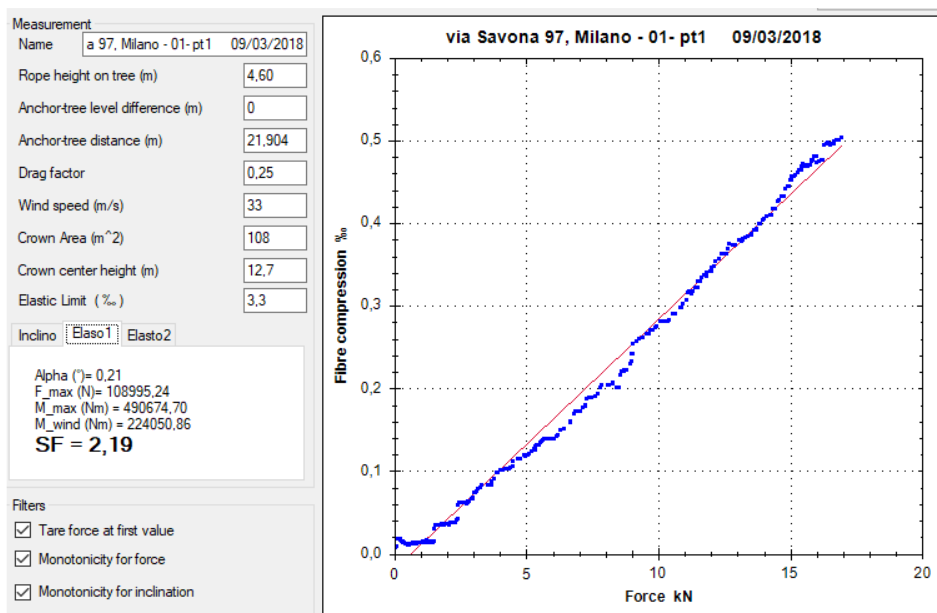
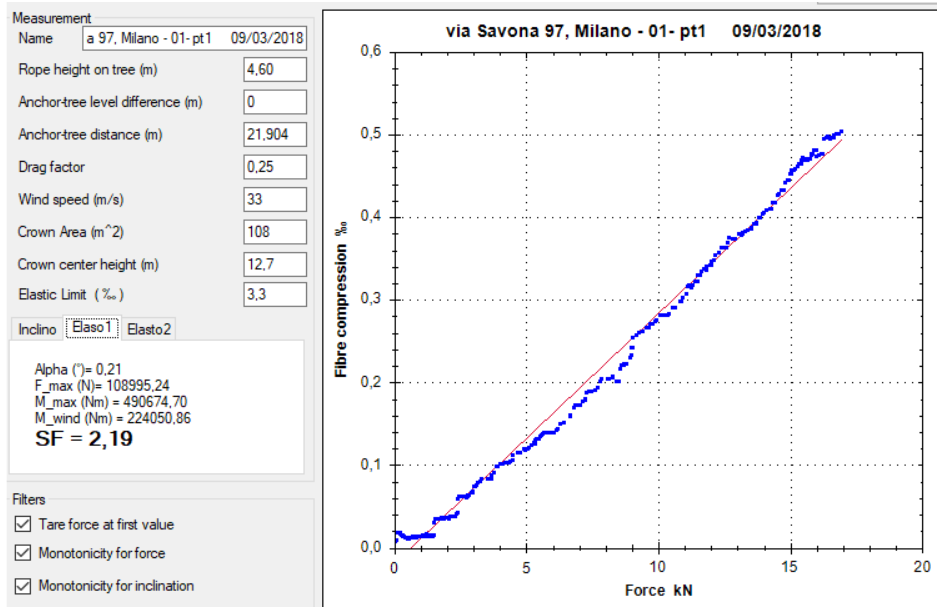
## Appendix 1 – Pulling tests



Via Savona 97, Milano – 01 – pt1

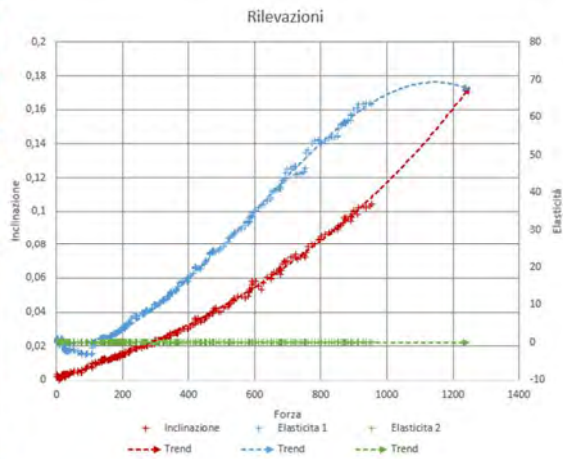


## Appendix 1 – Pulling tests



Appendix 1 – Pulling tests

Via Dante, Rimini – 165 – 31755 – pt1



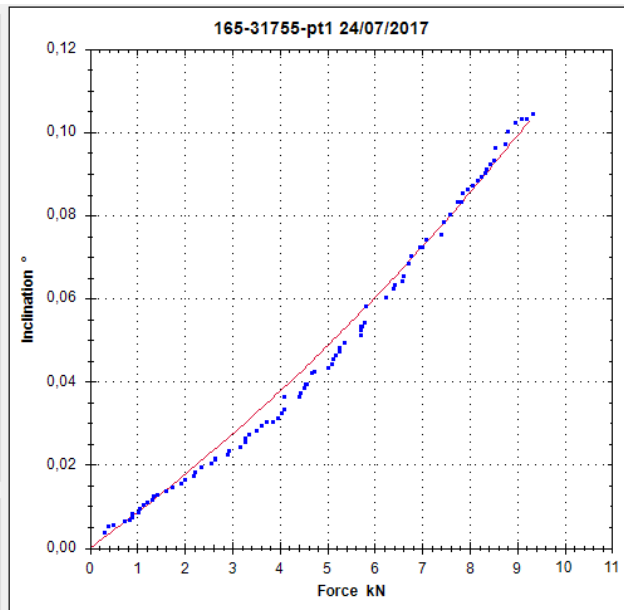
Measurement  
 Name 165-31755-pt1 24/07/2017

Rope height on tree (m) 4,50  
 Anchor-tree level difference (m) 0,40  
 Anchor-tree distance (m) 8,00  
 Drag factor 0,20  
 Wind speed (m/s) 33,00  
 Crown Area (m<sup>2</sup>) 44,00  
 Crown center height (m) 8,70  
 Elastic Limit (%) 2

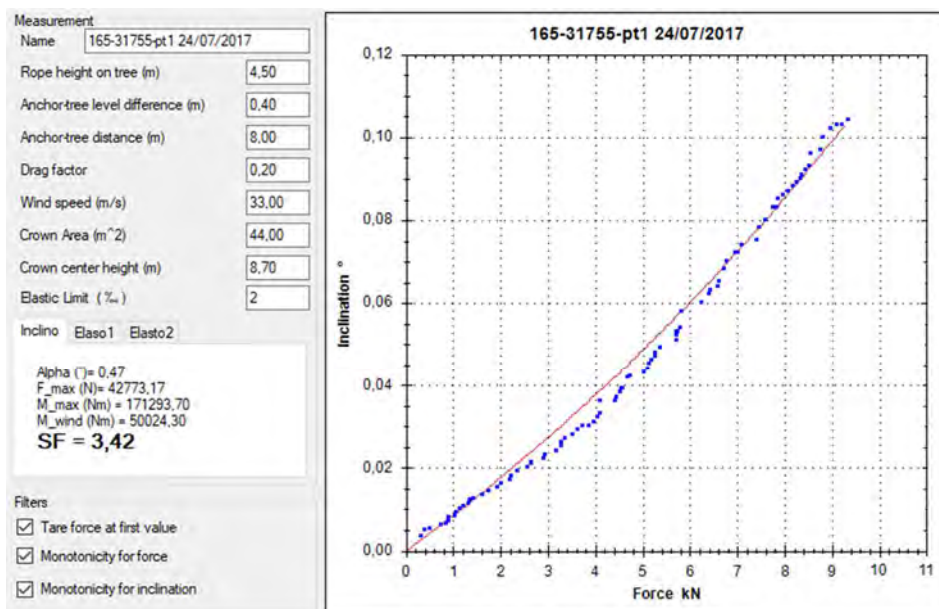
Inclino Elaso1 Elasto2

Alpha (°)= 0,47  
 F\_max (N)= 42773,17  
 M\_max (Nm) = 171293,70  
 M\_wind (Nm) = 50024,30  
**SF = 3,42**

Filters  
 Tare force at first value  
 Monotonicity for force  
 Monotonicity for inclination



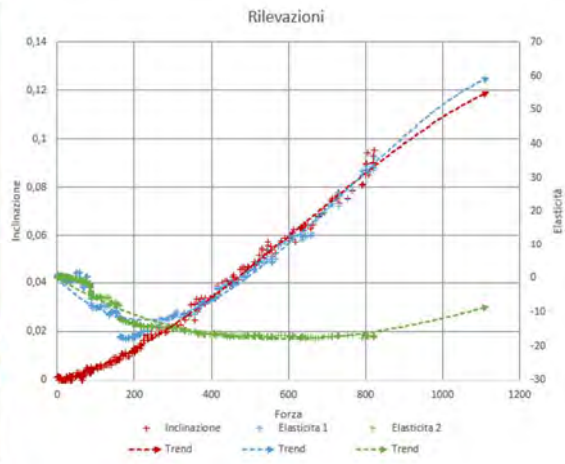
## Appendix 1 – Pulling tests



- Elastometer n. 2 N.D. -

Appendix 1 – Pulling tests

Via Dante, Rimini – 165 – 31755 – pt2



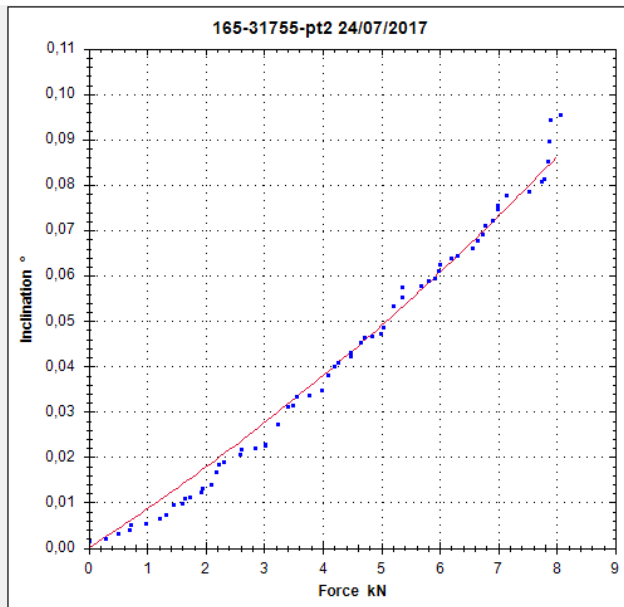
Measurement  
 Name 165-31755-pt2 24/07/2017

Rope height on tree (m) 4,5  
 Anchor-tree level difference (m) 0,35  
 Anchor-tree distance (m) 11,20  
 Drag factor 0,2  
 Wind speed (m/s) 33  
 Crown Area (m<sup>2</sup>) 40  
 Crown center height (m) 8,4  
 Elastic Limit (%) 2

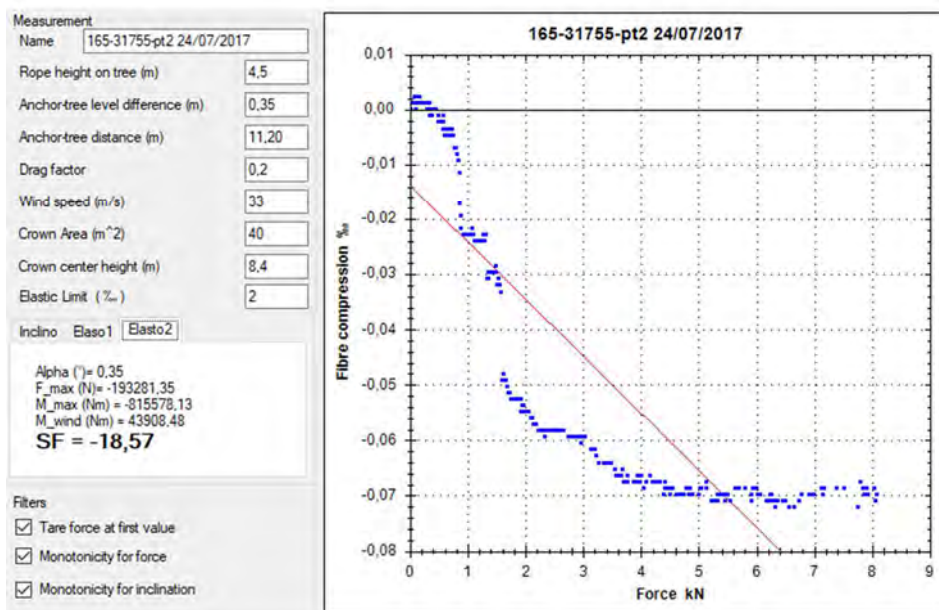
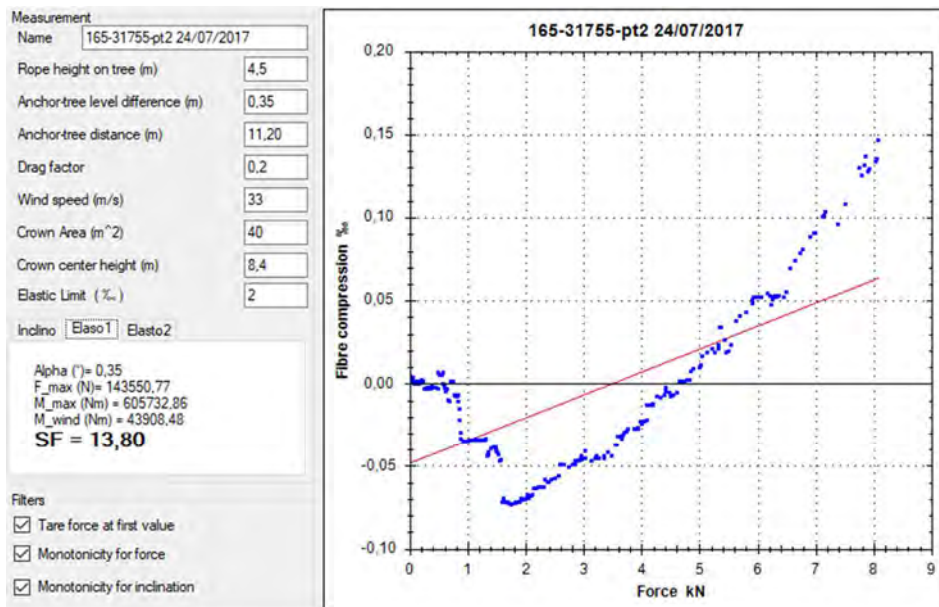
Inclino Elaso1 Elasto2

Alpha (°)= 0,35  
 F<sub>max</sub> (N)= 42467,29  
 M<sub>max</sub> (Nm) = 179196,78  
 M<sub>wind</sub> (Nm) = 43908,48  
**SF = 4,08**

Filters  
 Tare force at first value  
 Monotonicity for force  
 Monotonicity for inclination



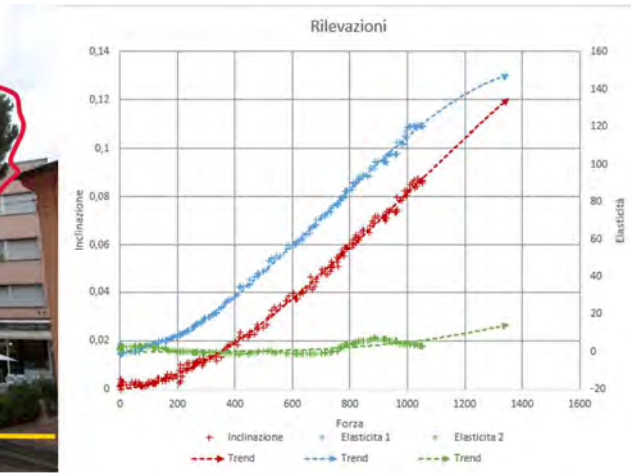
## Appendix 1 – Pulling tests





## Appendix 1 – Pulling tests

Via Dante, Rimini – 165 – 31756 – pt1



Measurement  
Name 165-31756-pt1 24/07/2017

Rope height on tree (m) 4,00

Anchor-tree level difference (m) 0,60

Anchor-tree distance (m) 10,70

Drag factor 0,20

Wind speed (m/s) 33,00

Crown Area (m<sup>2</sup>) 43,00

Crown center height (m) 8,30

Elastic Limit (%) 2

Inclino Elaso1 Elasto2

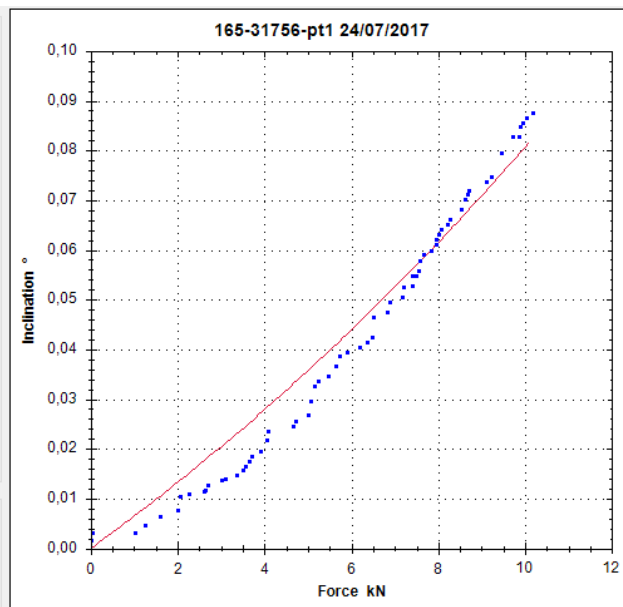
Alpha (°) = 0,31  
F\_max (N) = 55951,34  
M\_max (Nm) = 213296,04  
M\_wind (Nm) = 46639,69  
**SF = 4,57**

Filters

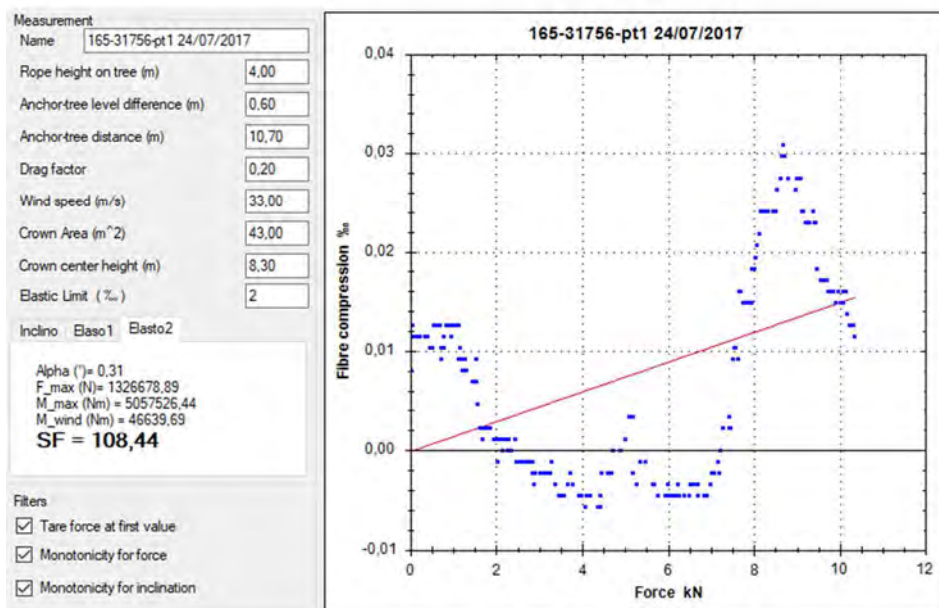
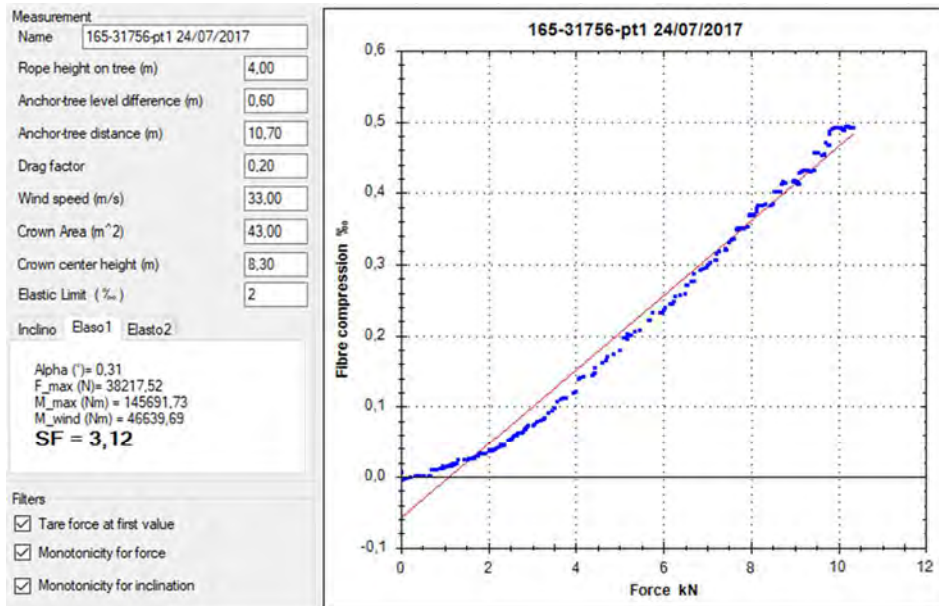
Tare force at first value

Monotonicity for force

Monotonicity for inclination

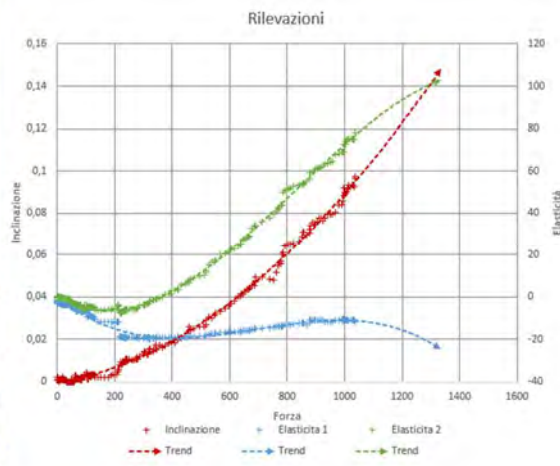


## Appendix 1 – Pulling tests



## Appendix 1 – Pulling tests

Via Dante, Rimini – 165 – 31756 – pt2



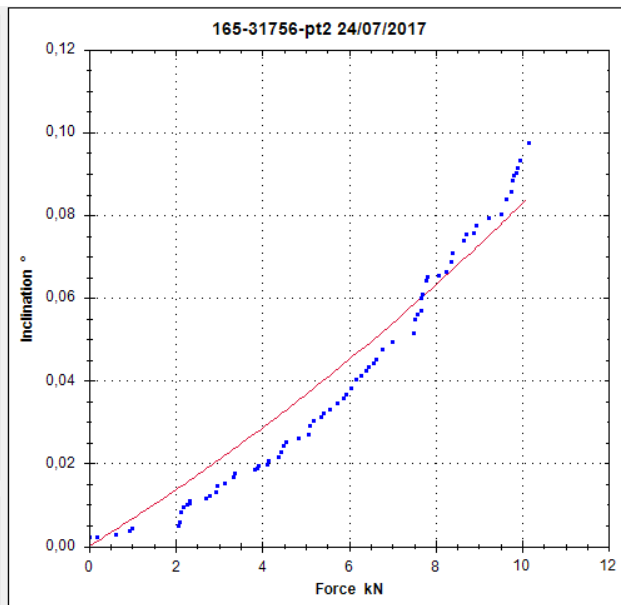
Measurement  
 Name: 165-31756-pt2 24/07/2017

Rope height on tree (m): 4  
 Anchor-tree level difference (m): 0,4  
 Anchor-tree distance (m): 10  
 Drag factor: 0,2  
 Wind speed (m/s): 33  
 Crown Area (m<sup>2</sup>): 38  
 Crown center height (m): 8,3  
 Elastic Limit (%): 2

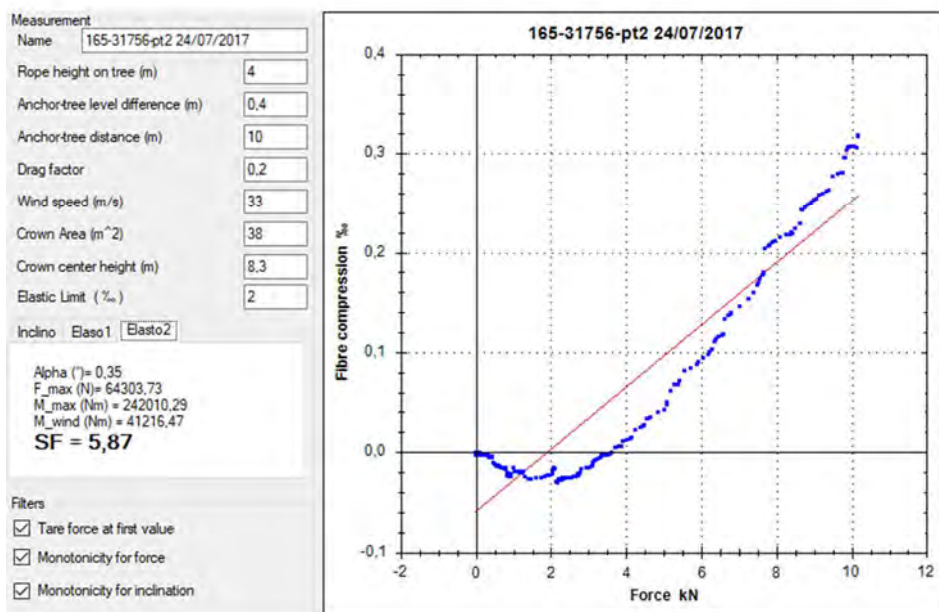
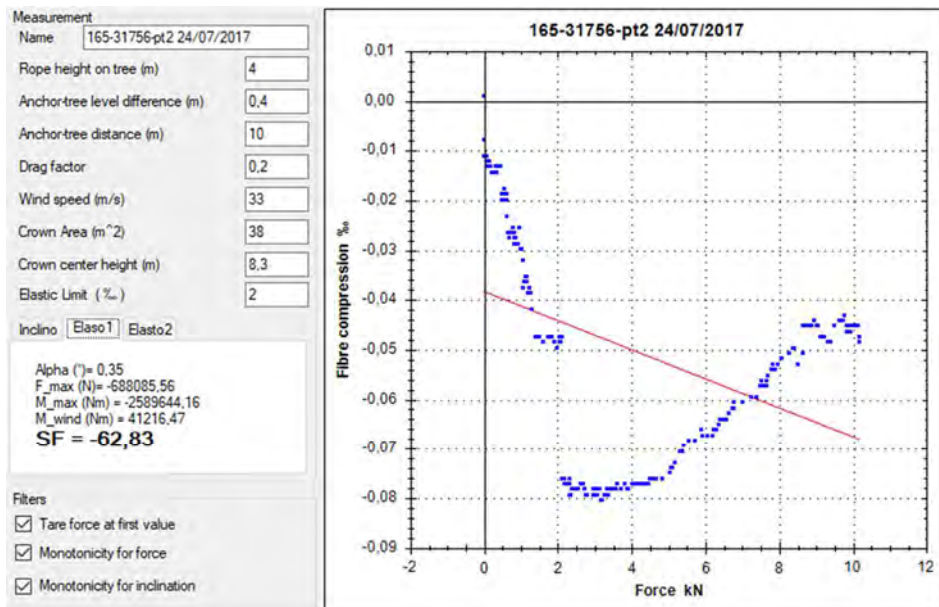
Inclino | Elaso1 | Elasto2

Alpha (°) = 0,35  
 F\_max (N) = 54779,43  
 M\_max (Nm) = 206165,11  
 M\_wind (Nm) = 41216,47  
**SF = 5,00**

Filters  
 Tare force at first value  
 Monotonicity for force  
 Monotonicity for inclination

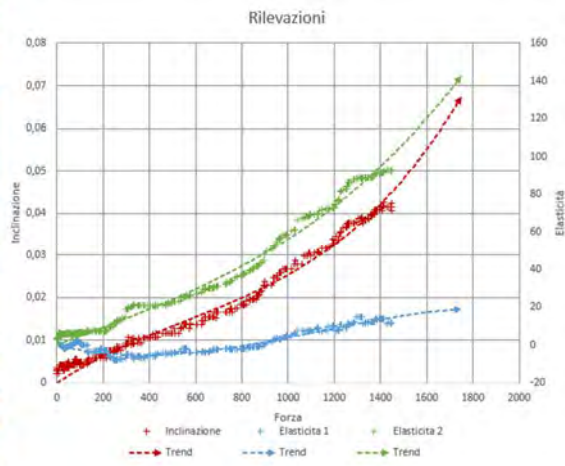


## Appendix 1 – Pulling tests



## Appendix 1 – Pulling tests

Via Roma, Rimini – 17223 - 38790 – pt1



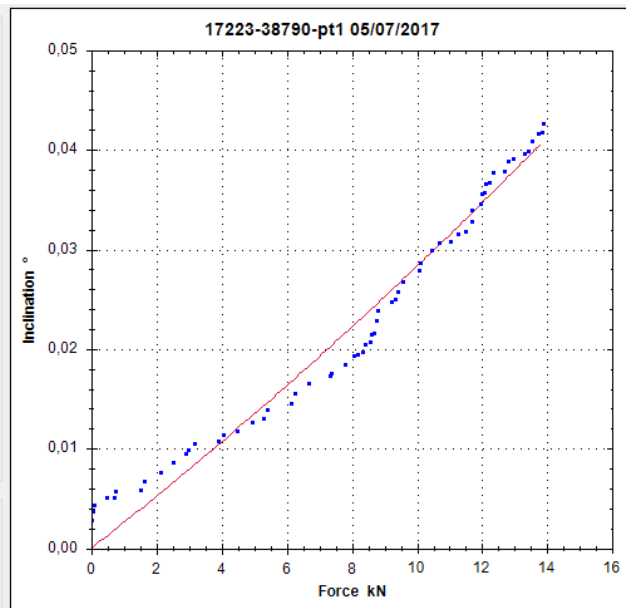
Measurement  
Name 17223-38790-pt1 05/07/2017

Rope height on tree (m) 4,00  
Anchor-tree level difference (m) 0,50  
Anchor-tree distance (m) 19,00  
Drag factor 0,30  
Wind speed (m/s) 33,00  
Crown Area (m<sup>2</sup>) 72,00  
Crown center height (m) 9,90  
Elastic Limit (%) 2,40

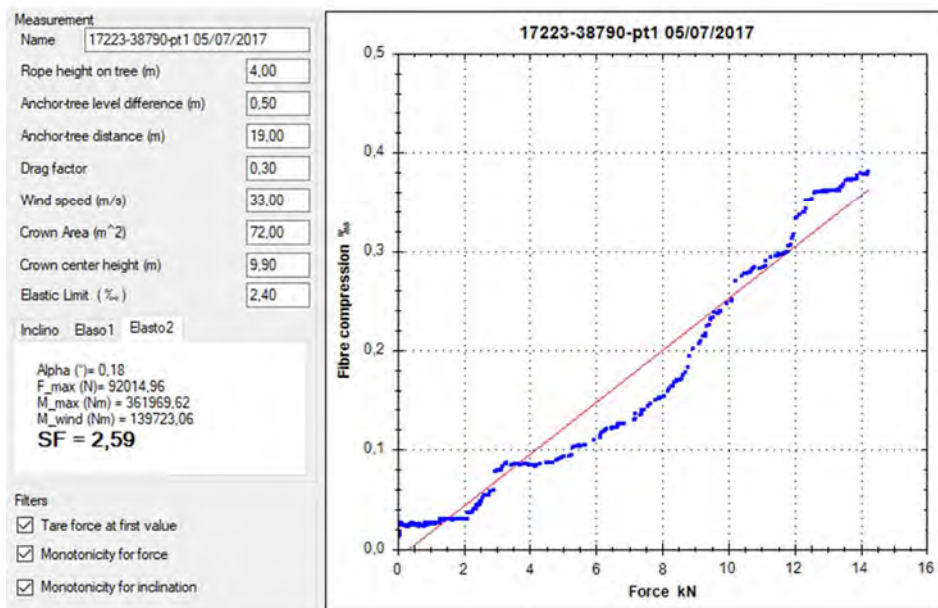
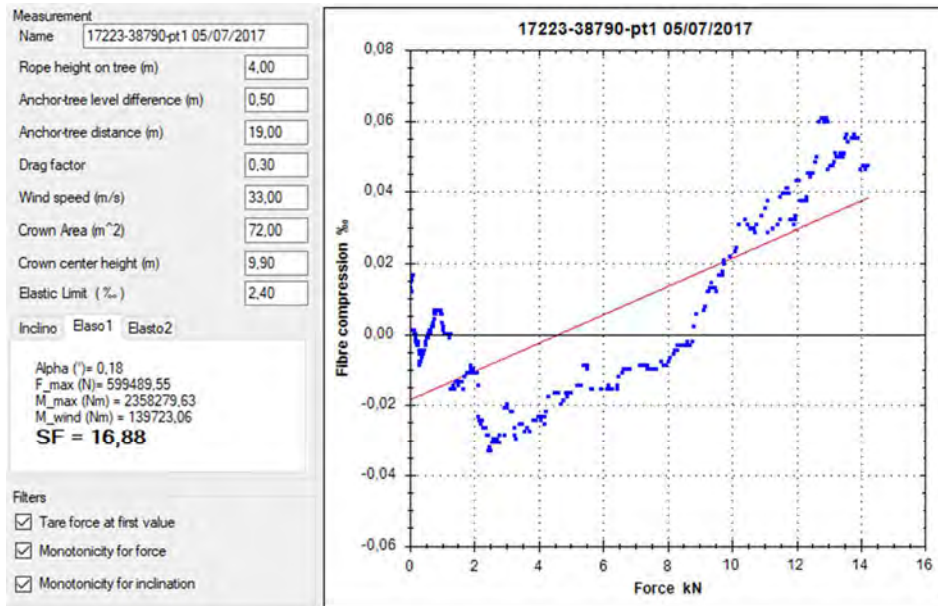
Inclino Elaso1 Elasto2

Alpha (°) = 0,18  
F<sub>max</sub> (N) = 137895,64  
M<sub>max</sub> (Nm) = 542455,62  
M<sub>wind</sub> (Nm) = 139723,06  
**SF = 3,88**

Filters  
 Tare force at first value  
 Monotonicity for force  
 Monotonicity for inclination

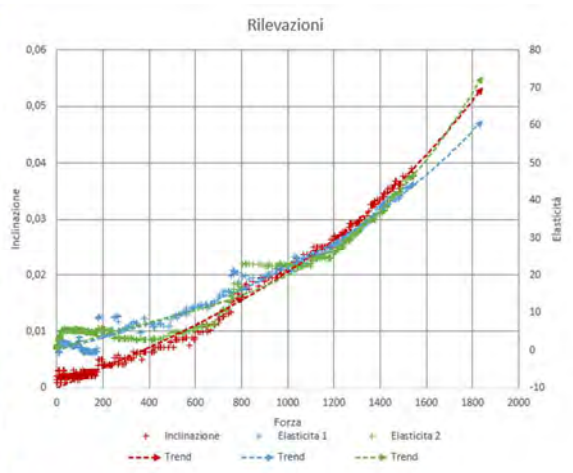


## Appendix 1 – Pulling tests



Appendix 1 – Pulling tests

Via Roma, Rimini – 17223 - 38790 – pt2



Measurement

Name: 17223-38790-pt2 05/07/2017

Rope height on tree (m): 4,00

Anchor-tree level difference (m): 0,50

Anchor-tree distance (m): 19,00

Drag factor: 0,30

Wind speed (m/s): 33,00

Crown Area (m<sup>2</sup>): 75,00

Crown center height (m): 10,00

Elastic Limit (%): 2,40

Inclino: Elaso1 Elaso2

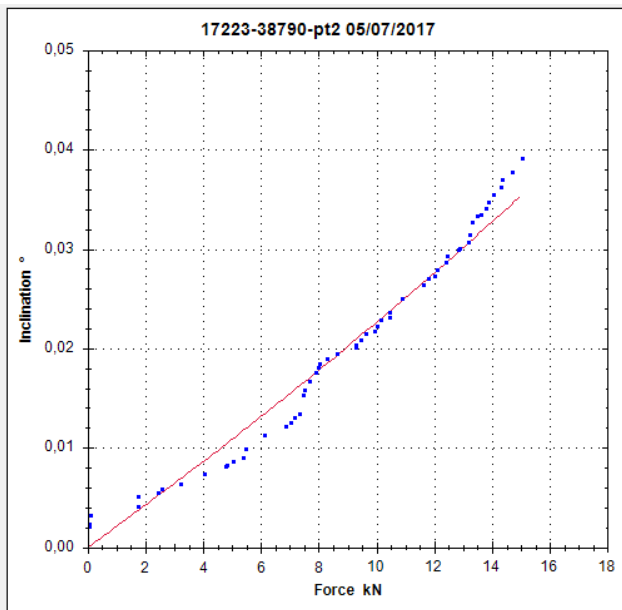
Alpha (°) = 0,18  
 F\_max (N) = 169516,80  
 M\_max (Nm) = 666847,35  
 M\_wind (Nm) = 147015,00  
**SF = 4,54**

Filters

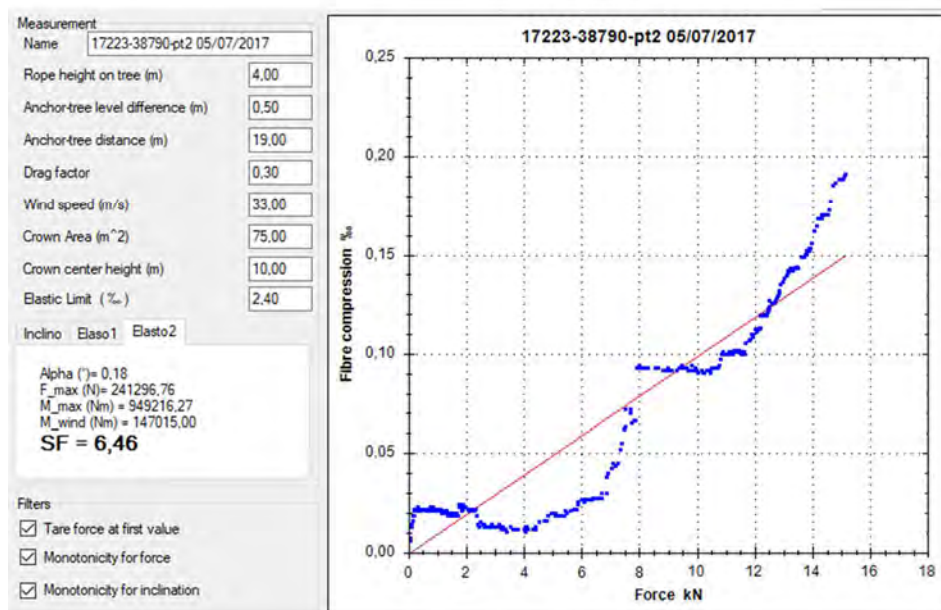
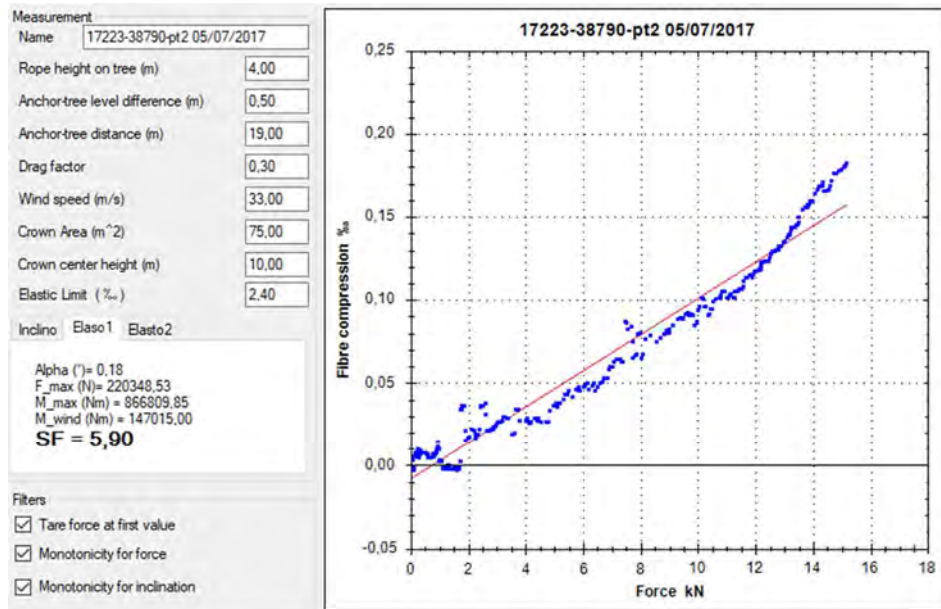
Tare force at first value

Monotonicity for force

Monotonicity for inclination



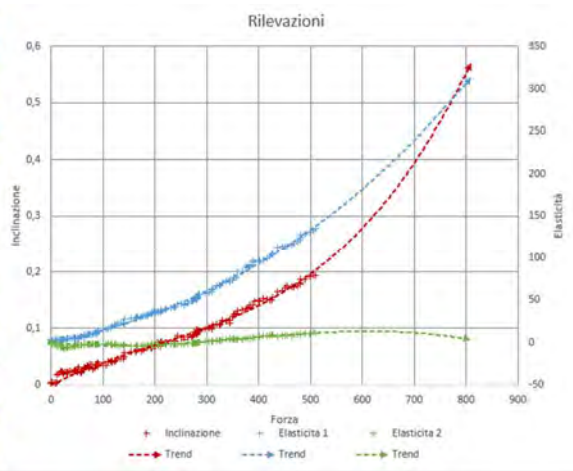
## Appendix 1 – Pulling tests





## Appendix 1 – Pulling tests

Via Roma, Rimini – 17223 - 38792 – pt1



Measurement

Name 17223-38792-pt1 05/07/2017

Rope height on tree (m) 3.50

Anchor-tree level difference (m) 0.50

Anchor-tree distance (m) 16.50

Drag factor 0.30

Wind speed (m/s) 33.00

Crown Area (m<sup>2</sup>) 38.00

Crown center height (m) 7.10

Elastic Limit (%) 2.40

Inclino Elaso1 Elasto2

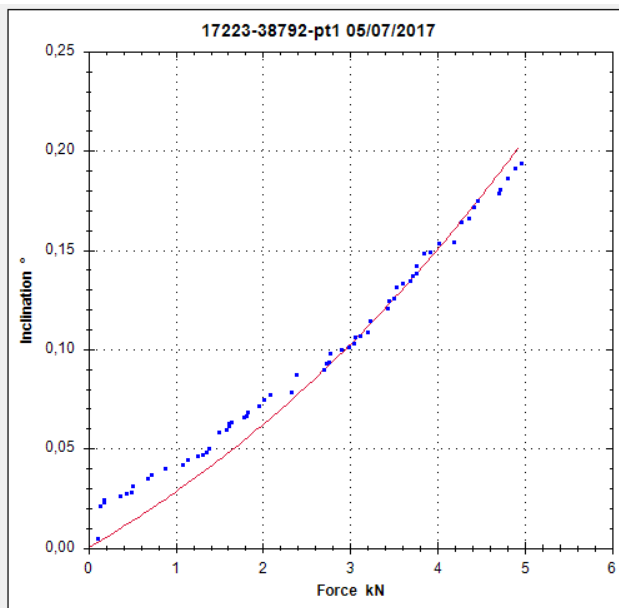
Alpha (°) = 0.18  
 F\_max (N) = 13898.81  
 M\_max (Nm) = 47861.17  
 M\_wind (Nm) = 52886.20  
**SF = 0,90**

Filters

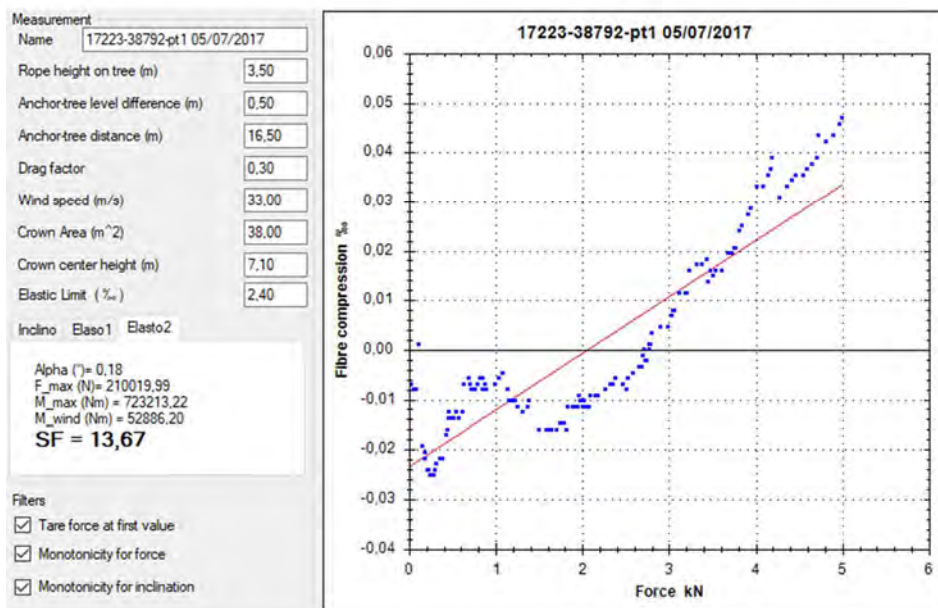
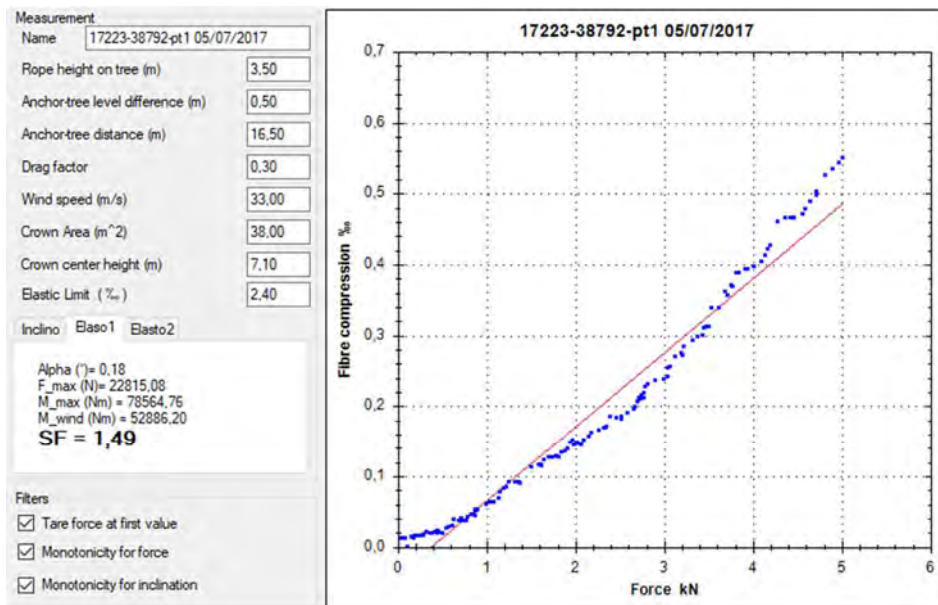
Tare force at first value

Monotonicity for force

Monotonicity for inclination

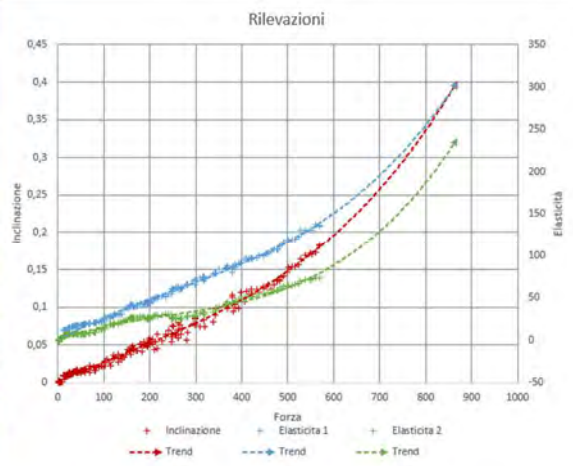


## Appendix 1 – Pulling tests



## Appendix 1 – Pulling tests

Via Roma, Rimini – 17223 - 38792 – pt2



Measurement

Name: 17223-38792-pt2 05/07/2017

Rope height on tree (m): 3.50

Anchor tree level difference (m): 0.50

Anchor tree distance (m): 17.50

Drag factor: 0.30

Wind speed (m/s): 33.00

Crown Area (m<sup>2</sup>): 34.00

Crown center height (m): 7.20

Elastic Limit (%): 2.40

Inclino: Elaso1 Elasto2

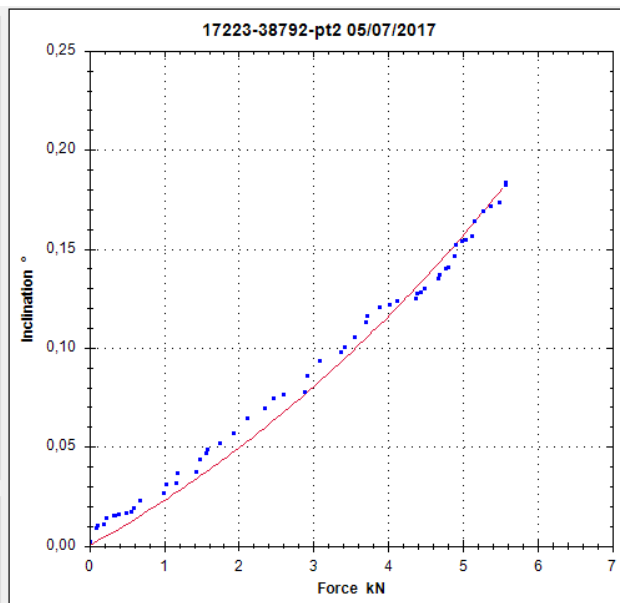
Alpha (°) = 0.17  
 F\_max (N) = 16857.31  
 M\_max (Nm) = 58152.28  
 M\_wind (Nm) = 47985.70  
**SF = 1,21**

Filters

Tare force at first value

Monotonicity for force

Monotonicity for inclination



## Appendix 1 – Pulling tests

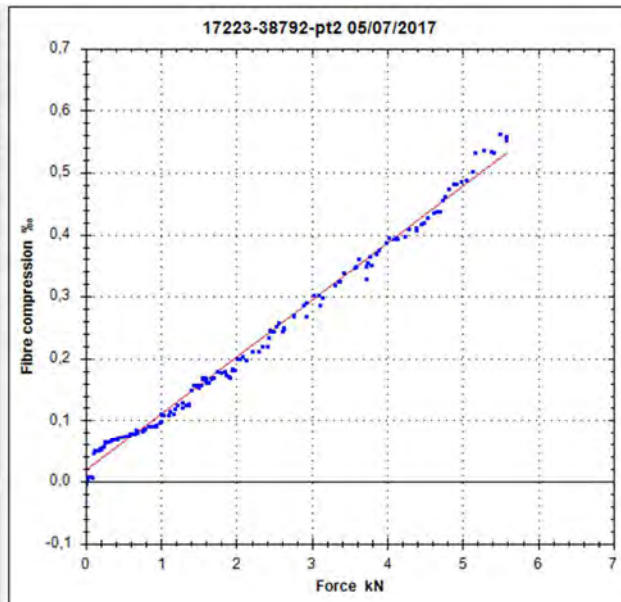
Measurement  
 Name 17223-38792-pt2 05/07/2017

Rope height on tree (m) 3,50  
 Anchor-tree level difference (m) 0,50  
 Anchor-tree distance (m) 17,50  
 Drag factor 0,30  
 Wind speed (m/s) 33,00  
 Crown Area (m<sup>2</sup>) 34,00  
 Crown center height (m) 7,20  
 Elastic Limit (%) 2,40

Inclino Elaso1 Elasto2

Alpha (°)= 0,17  
 F\_max (N)= 26067,30  
 M\_max (Nm) = 89923,80  
 M\_wind (Nm) = 47985,70  
**SF = 1,87**

Filters  
 Tare force at first value  
 Monotonicity for force  
 Monotonicity for inclination



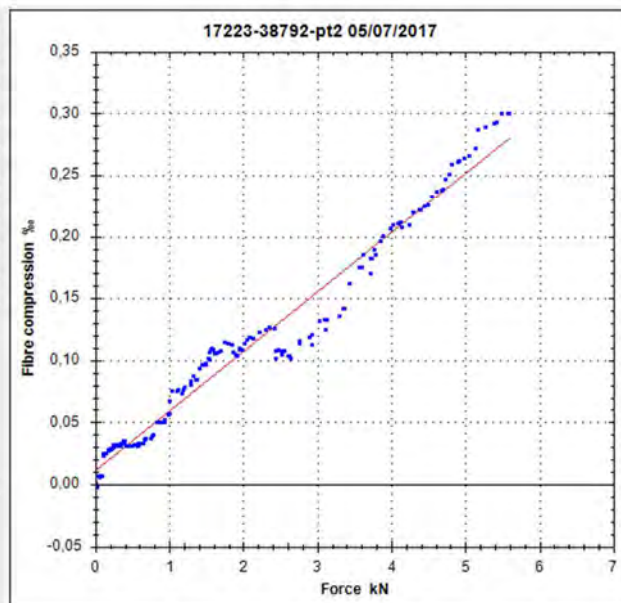
Measurement  
 Name 17223-38792-pt2 05/07/2017

Rope height on tree (m) 3,50  
 Anchor-tree level difference (m) 0,50  
 Anchor-tree distance (m) 17,50  
 Drag factor 0,30  
 Wind speed (m/s) 33,00  
 Crown Area (m<sup>2</sup>) 34,00  
 Crown center height (m) 7,20  
 Elastic Limit (%) 2,40

Inclino Elaso1 Elasto2

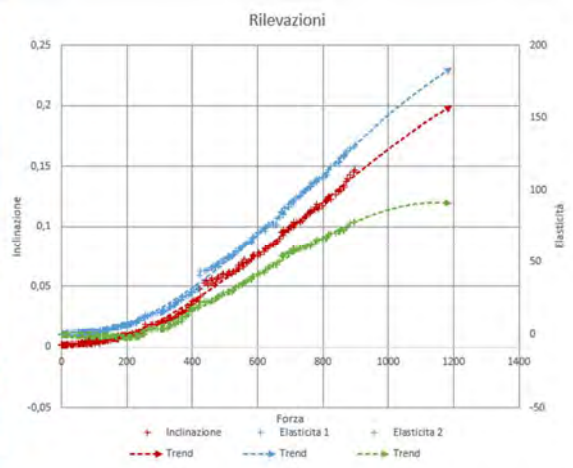
Alpha (°)= 0,17  
 F\_max (N)= 49865,33  
 M\_max (Nm) = 172019,32  
 M\_wind (Nm) = 47985,70  
**SF = 3,58**

Filters  
 Tare force at first value  
 Monotonicity for force  
 Monotonicity for inclination



## Appendix 1 – Pulling tests

Via Roma, Rimini – 17223 - 38793 – pt1



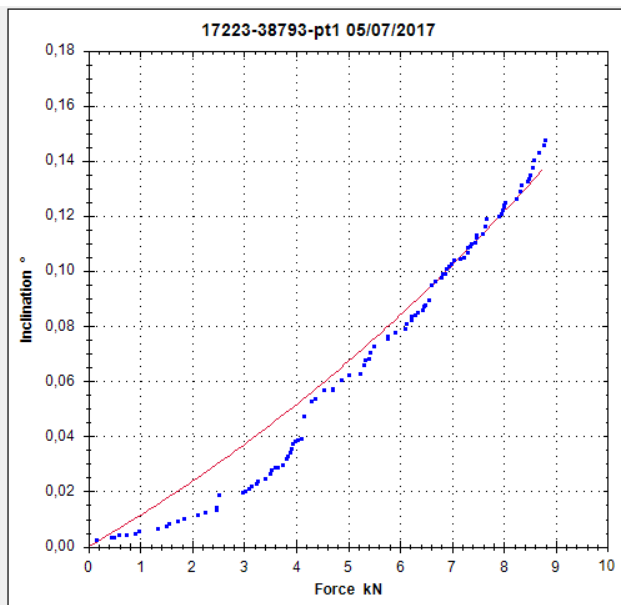
Measurement  
 Name 17223-38793-pt1 05/07/2017

Rope height on tree (m) 3.50  
 Anchor-tree level difference (m) 0.50  
 Anchor-tree distance (m) 17.00  
 Drag factor 0.30  
 Wind speed (m/s) 33.00  
 Crown Area (m<sup>2</sup>) 37.00  
 Crown center height (m) 7.20  
 Elastic Limit (%) 2.40

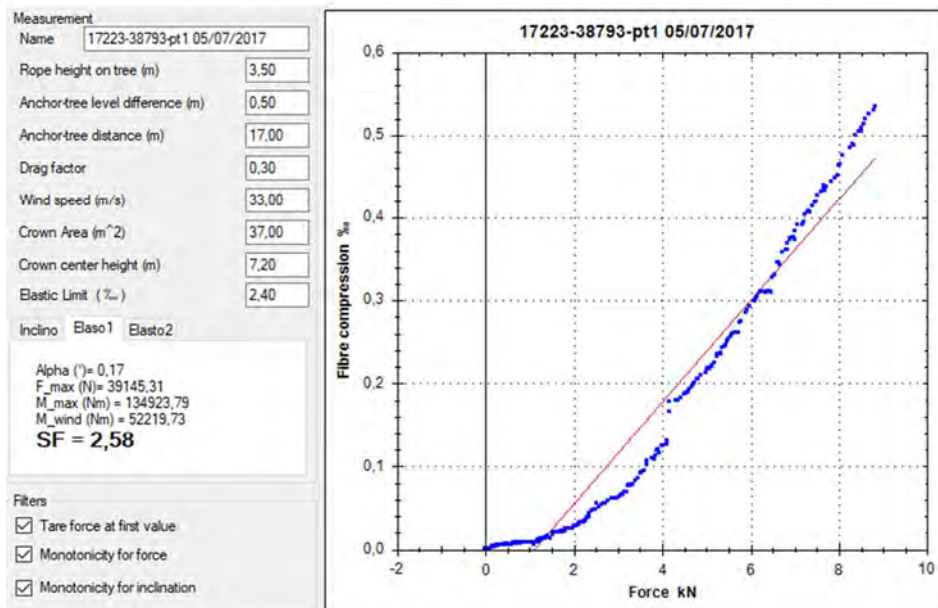
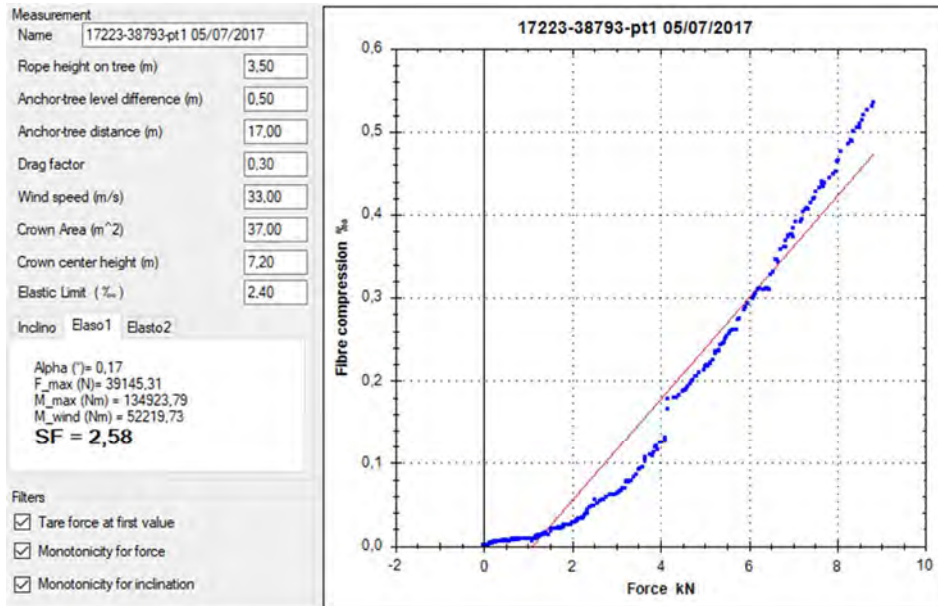
Inclino Elaso1 Elasto2

Alpha (°) = 0,17  
 F\_max (N) = 32506,61  
 M\_max (Nm) = 112041,92  
 M\_wind (Nm) = 52219,73  
**SF = 2,15**

Filters  
 Tare force at first value  
 Monotonicity for force  
 Monotonicity for inclination

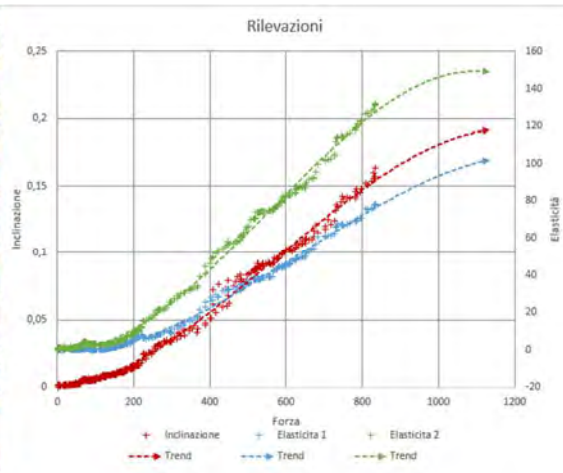


## Appendix 1 – Pulling tests



Appendix 1 – Pulling tests

Via Roma, Rimini – 17223 - 38793 – pt2



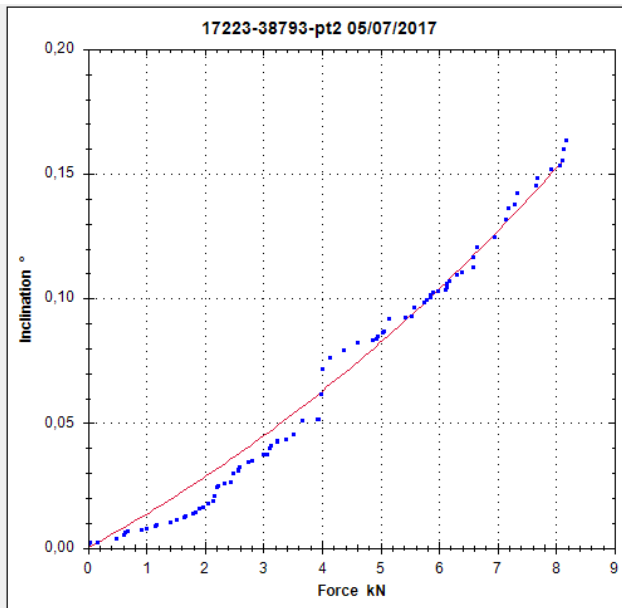
Measurement  
 Name: 17223-38793-pt2 05/07/2017

Rope height on tree (m): 3,5  
 Anchor-tree level difference (m): 0,50  
 Anchor-tree distance (m): 17  
 Drag factor: 0,30  
 Wind speed (m/s): 33  
 Crown Area (m<sup>2</sup>): 40  
 Crown center height (m): 7,4  
 Elastic Limit (‰): 2,4

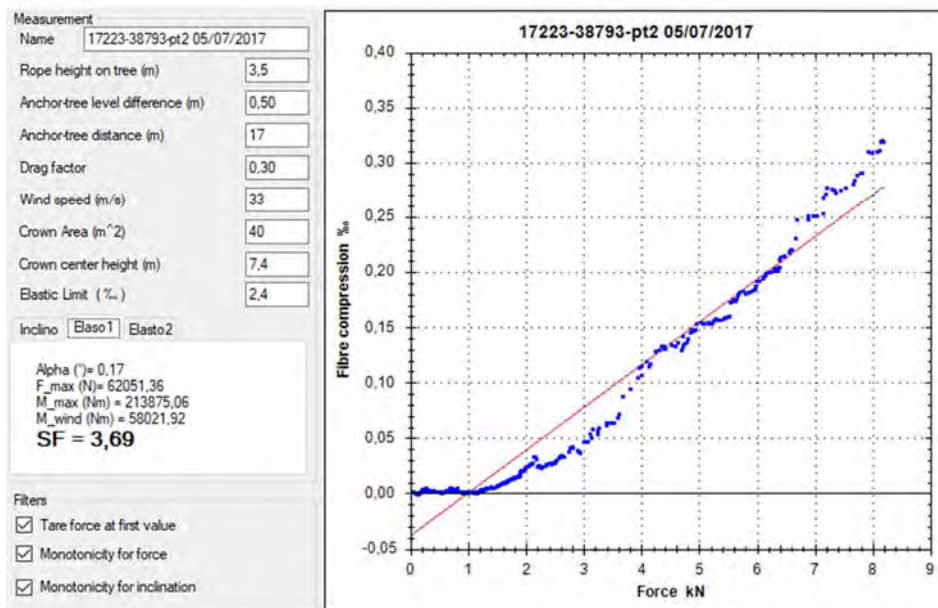
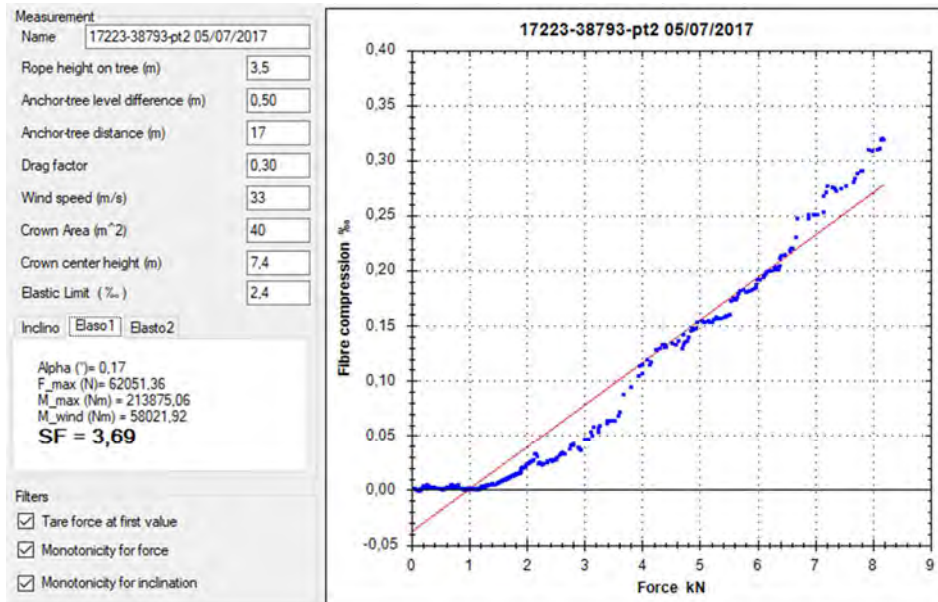
Inclino: Elaso1 Elasto2

Alpha (°) = 0,17  
 F\_max (N) = 27538,73  
 M\_max (Nm) = 94918,91  
 M\_wind (Nm) = 58021,92  
**SF = 1,64**

Filters  
 Tare force at first value  
 Monotonicity for force  
 Monotonicity for inclination



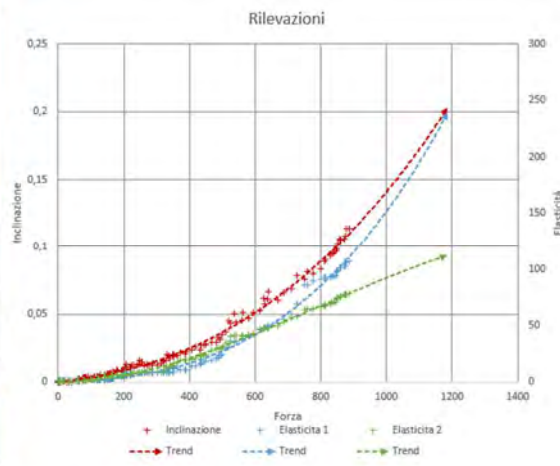
## Appendix 1 – Pulling tests





## Appendix 1 – Pulling tests

Via Roma, Rimini – 17223 - 38797 – pt1



Measurement

Name: 17223-38797-pt1 05/07/2017

Rope height on tree (m): 4,00

Anchor-tree level difference (m): 0,50

Anchor-tree distance (m): 18,20

Drag factor: 0,30

Wind speed (m/s): 33,00

Crown Area (m<sup>2</sup>): 50,00

Crown center height (m): 8,70

Elastic Limit (%): 2,40

Inclino: Elaso1 Elaso2

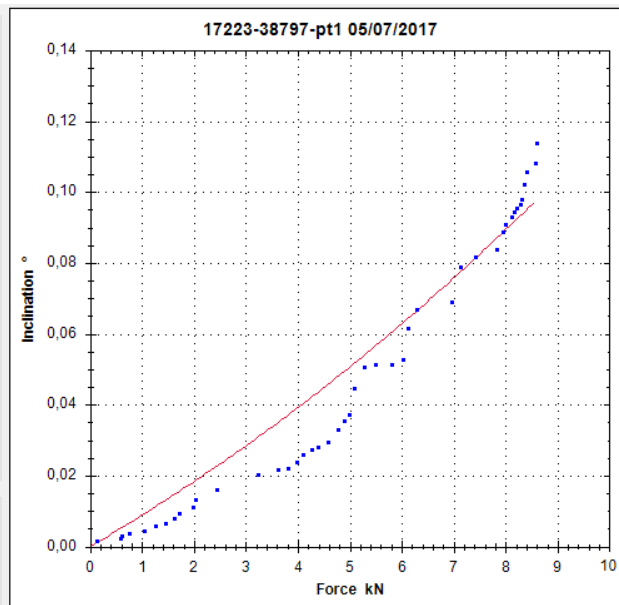
Alpha (°) = 0,19  
 F<sub>max</sub> (N) = 41257,13  
 M<sub>max</sub> (Nm) = 162059,08  
 M<sub>wind</sub> (Nm) = 85268,70  
**SF = 1,90**

Filters

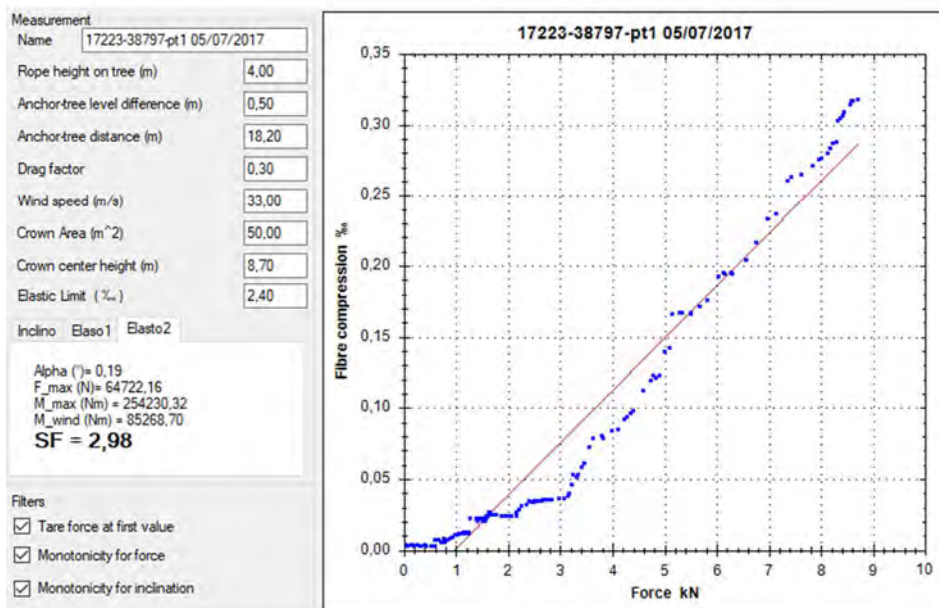
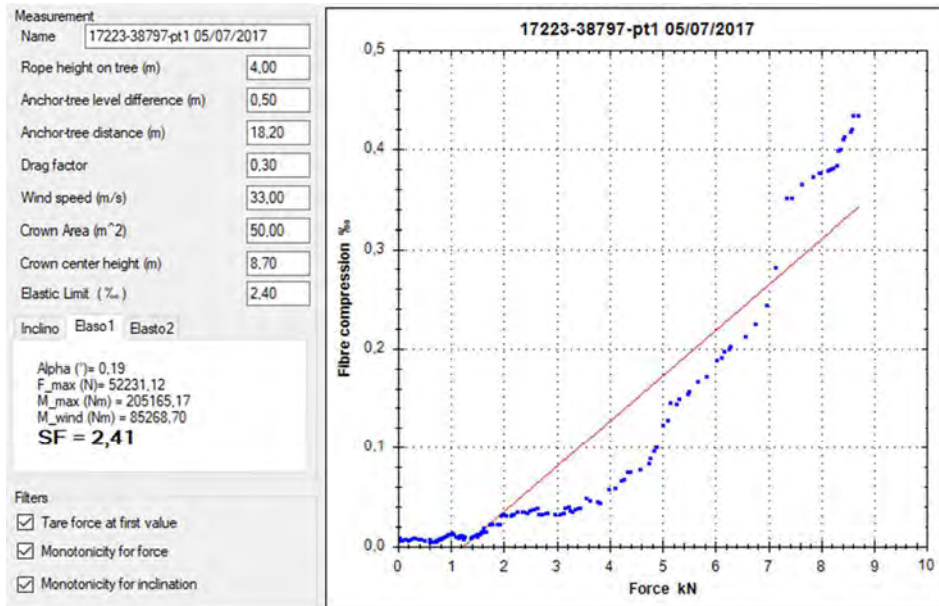
Tare force at first value

Monotonicity for force

Monotonicity for inclination

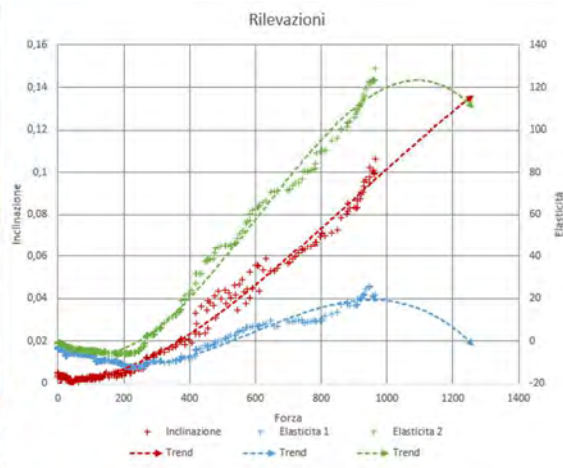


## Appendix 1 – Pulling tests



## Appendix 1 – Pulling tests

Via Roma, Rimini – 17223 - 38797 – pt2



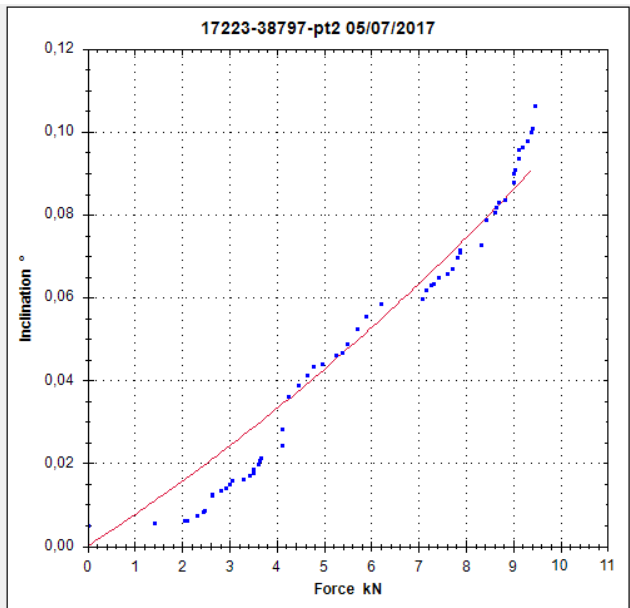
Measurement  
 Name: 17223-38797-pt2 05/07/2017

Rope height on tree (m): 4,00  
 Anchor-tree level difference (m): 0,50  
 Anchor-tree distance (m): 18,20  
 Drag factor: 0,30  
 Wind speed (m/s): 33,00  
 Crown Area (m<sup>2</sup>): 66,00  
 Crown center height (m): 9,10  
 Elastic Limit (%): 2,40

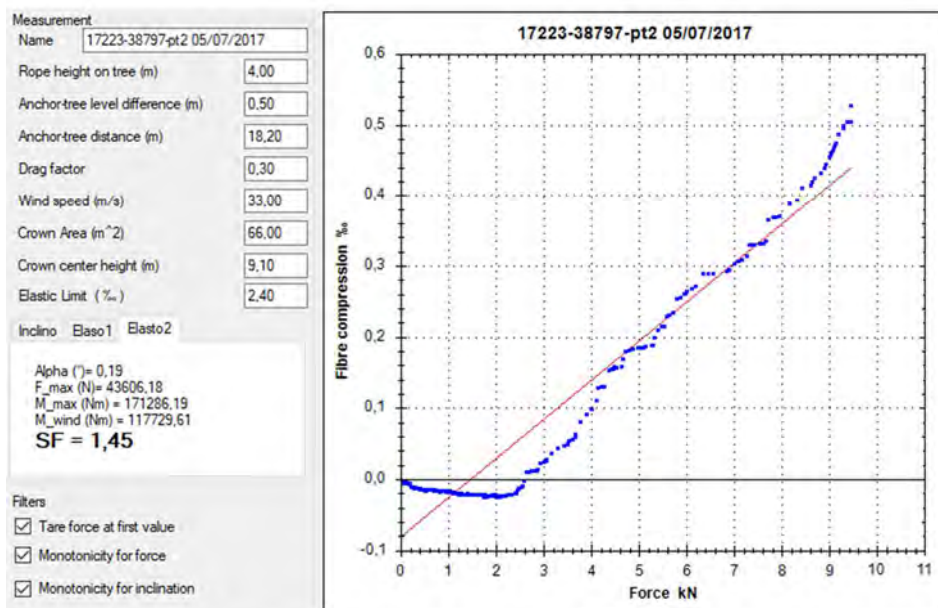
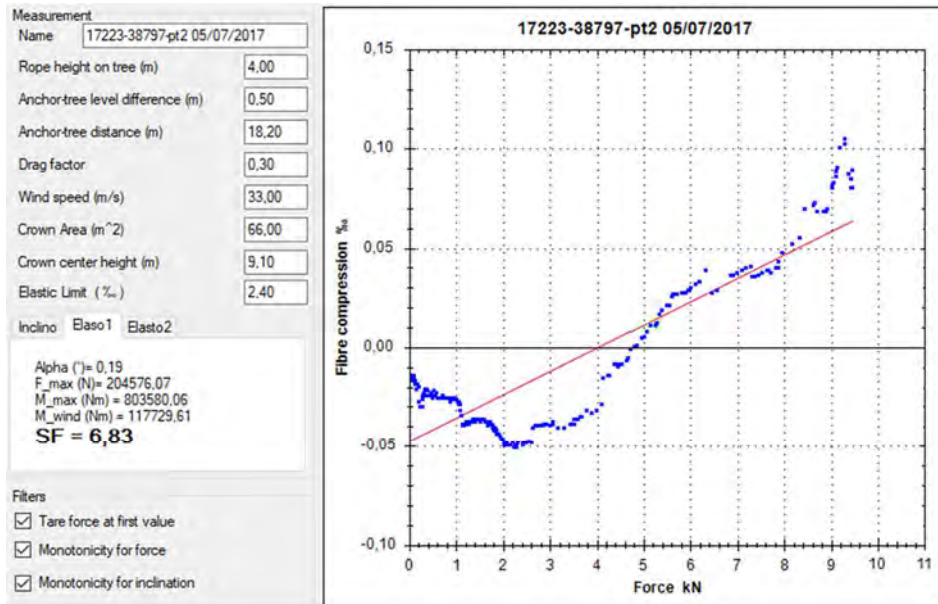
Inclino Elaso1 Elasto2

Alpha (°) = 0,19  
 F\_max (N) = 47851,61  
 M\_max (Nm) = 187962,36  
 M\_wind (Nm) = 117729,61  
**SF = 1,60**

Filters  
 Tare force at first value  
 Monotonicity for force  
 Monotonicity for inclination

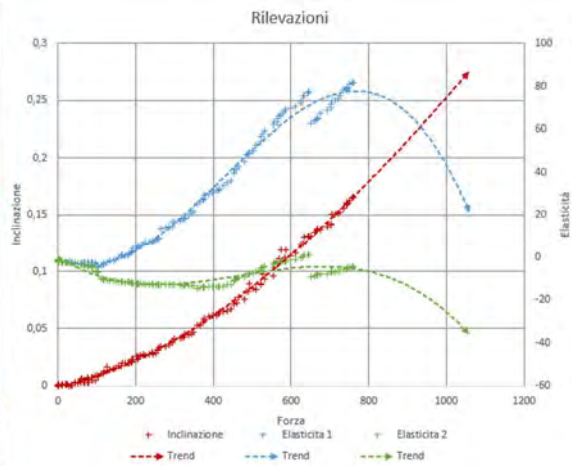


## Appendix 1 – Pulling tests



Appendix 1 – Pulling tests

Via Roma, Rimini – 17223 - 38798 – pt1



Measurement

Name 17223-38798-pt1 05/07/2017

Rope height on tree (m) 5,00

Anchor-tree level difference (m) 0,50

Anchor-tree distance (m) 23,50

Drag factor 0,30

Wind speed (m/s) 33,00

Crown Area (m<sup>2</sup>) 69,00

Crown center height (m) 8,80

Elastic Limit (%) 2,40

Inclino Elaso1 Elasto2

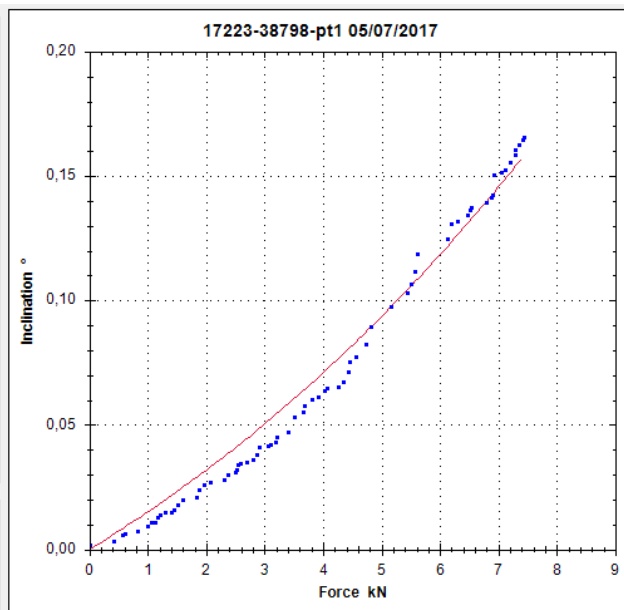
Alpha (°) = 0,19  
 F<sub>max</sub> (N) = 24868,94  
 M<sub>max</sub> (Nm) = 122125,79  
 M<sub>wind</sub> (Nm) = 119023,34  
**SF = 1,03**

Filters

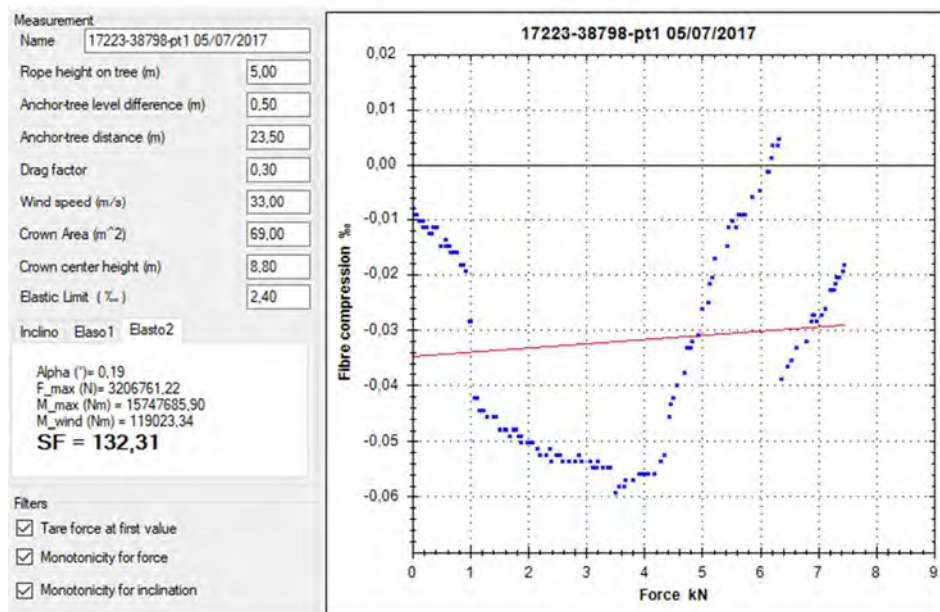
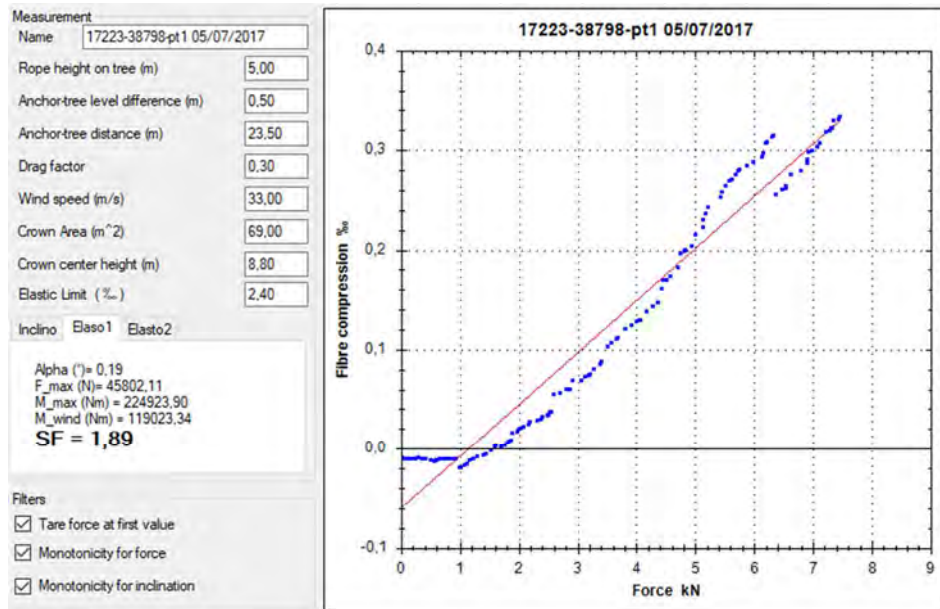
Tare force at first value

Monotonicity for force

Monotonicity for inclination

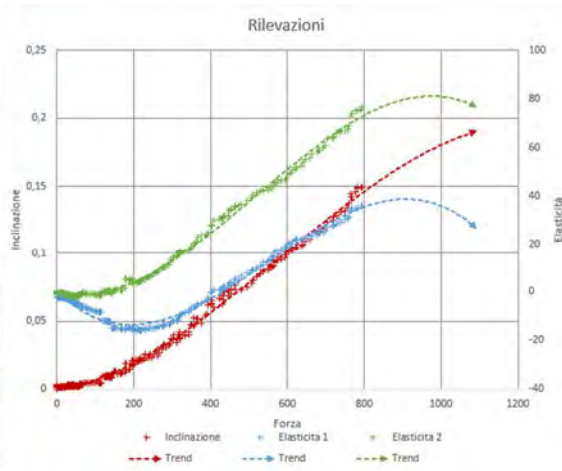


## Appendix 1 – Pulling tests



Appendix 1 – Pulling tests

Via Roma, Rimini – 17223 - 38798 – pt2



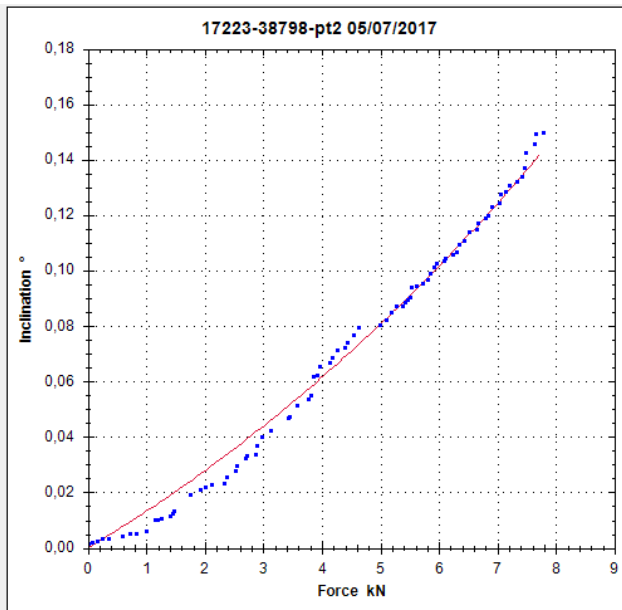
Measurement  
 Name 17223-38798-pt2 05/07/2017

Rope height on tree (m) 5,00  
 Anchor-tree level difference (m) 0,50  
 Anchor-tree distance (m) 19,85  
 Drag factor 0,30  
 Wind speed (m/s) 33,00  
 Crown Area (m<sup>2</sup>) 68,00  
 Crown center height (m) 8,80  
 Elastic Limit (%) 2,40

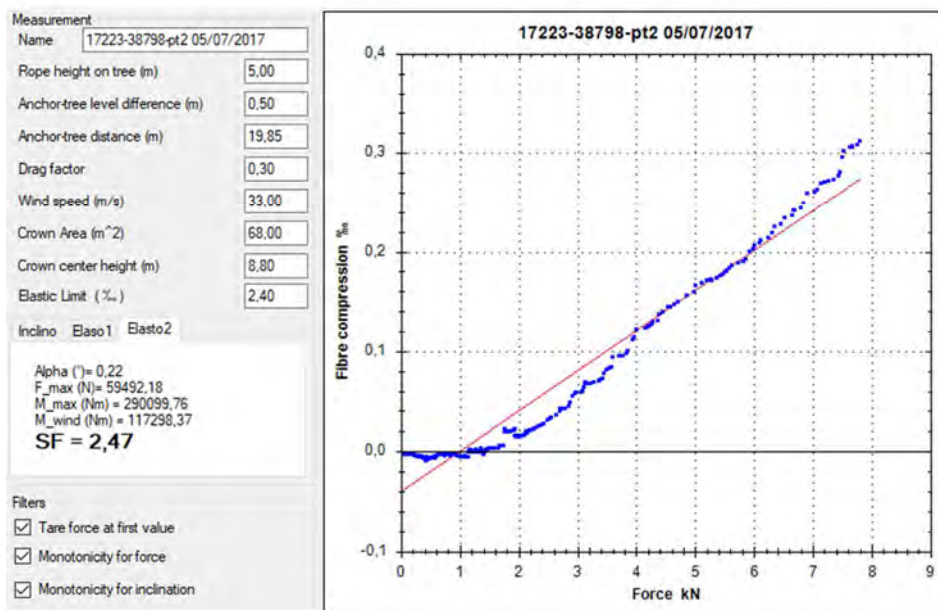
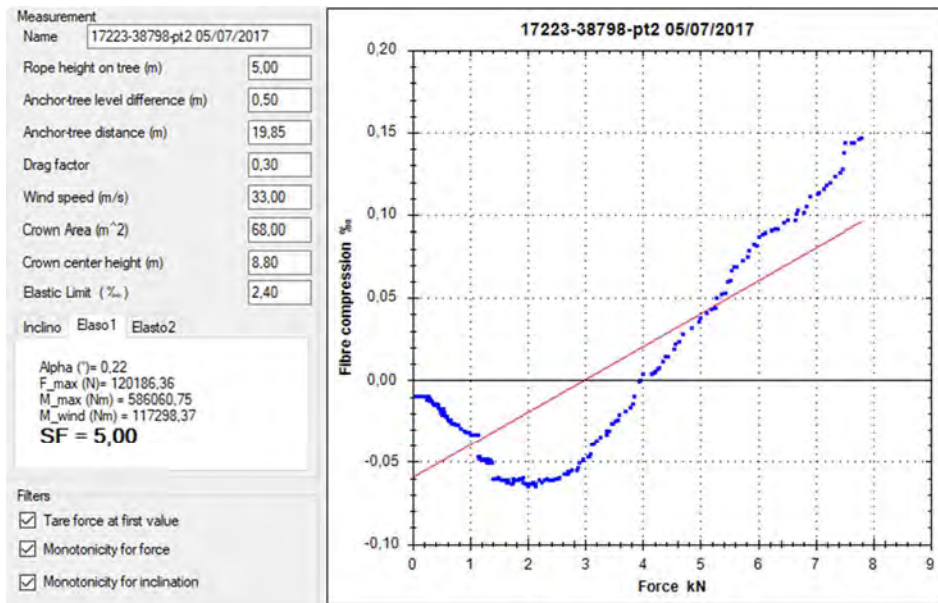
Inclino Elaso1 Elasto2

Alpha (°) = 0,22  
 F\_max (N) = 27963,01  
 M\_max (Nm) = 136355,11  
 M\_wind (Nm) = 117298,37  
**SF = 1,16**

Filters  
 Tare force at first value  
 Monotonicity for force  
 Monotonicity for inclination



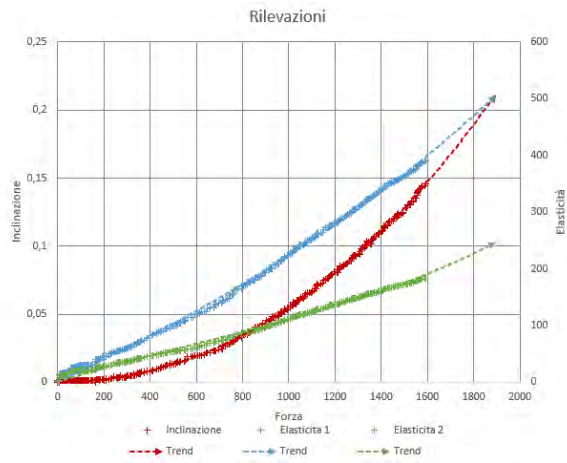
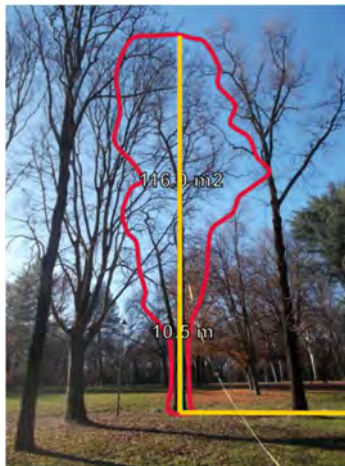
## Appendix 1 – Pulling tests





## Appendix 1 – Pulling tests

Boschetti Reali, Monza – 400 – 11869 – pt1



Measurement  
Name 400-11869-pt1 06/12/2017

Rope height on tree (m) 10,5

Anchor-tree level difference (m) 0,45

Anchor-tree distance (m) 22,95

Drag factor 0,3

Wind speed (m/s) 33

Crown Area (m<sup>2</sup>) 117

Crown center height (m) 14,9

Elastic Limit (%) 3,4

Inclino Elaso1 Elaso2

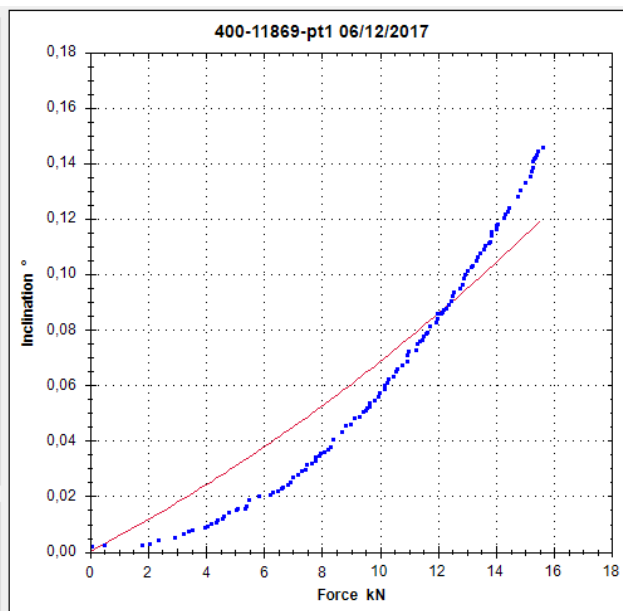
Alpha (°) = 0,41  
F<sub>max</sub> (N) = 63955,90  
M<sub>max</sub> (Nm) = 615141,22  
M<sub>wind</sub> (Nm) = 341721,67  
**SF = 1,80**

Filters

Tare force at first value

Monotonicity for force

Monotonicity for inclination



## Appendix 1 – Pulling tests

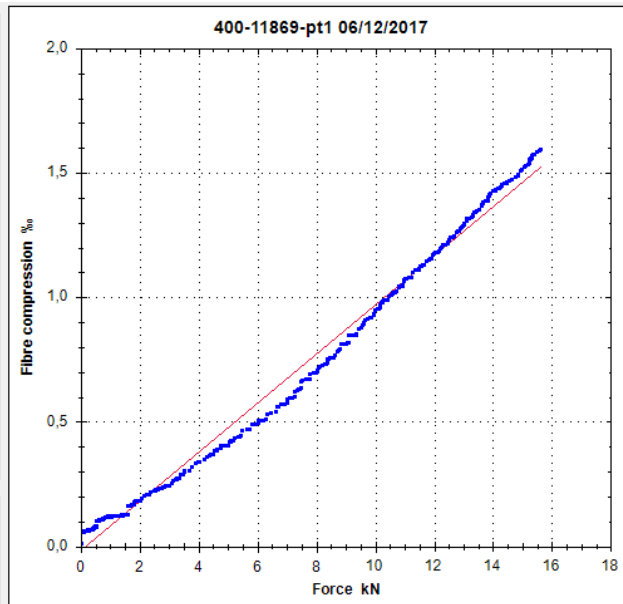
Measurement  
 Name: 400-11869-pt1 06/12/2017

Rope height on tree (m): 10,5  
 Anchor-tree level difference (m): 0,45  
 Anchor-tree distance (m): 22,95  
 Drag factor: 0,3  
 Wind speed (m/s): 33  
 Crown Area (m<sup>2</sup>): 117  
 Crown center height (m): 14,9  
 Elastic Limit (%): 3,4

Inclino:  Elaso1  Elasto2

Alpha (°) = 0,41  
 F<sub>max</sub> (N) = 34413,01  
 M<sub>max</sub> (Nm) = 330991,47  
 M<sub>wind</sub> (Nm) = 341721,67  
**SF = 0,97**

Filters  
 Tare force at first value  
 Monotonicity for force  
 Monotonicity for inclination



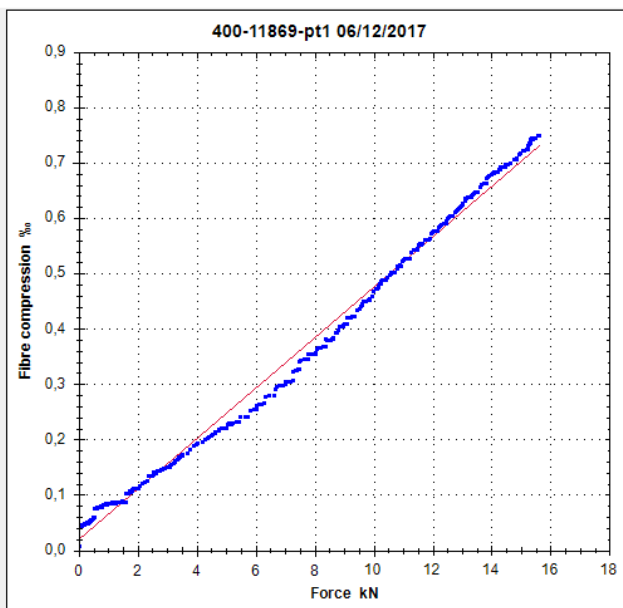
Measurement  
 Name: 400-11869-pt1 06/12/2017

Rope height on tree (m): 10,5  
 Anchor-tree level difference (m): 0,45  
 Anchor-tree distance (m): 22,95  
 Drag factor: 0,3  
 Wind speed (m/s): 33  
 Crown Area (m<sup>2</sup>): 117  
 Crown center height (m): 14,9  
 Elastic Limit (%): 3,4

Inclino:  Elaso1  Elasto2

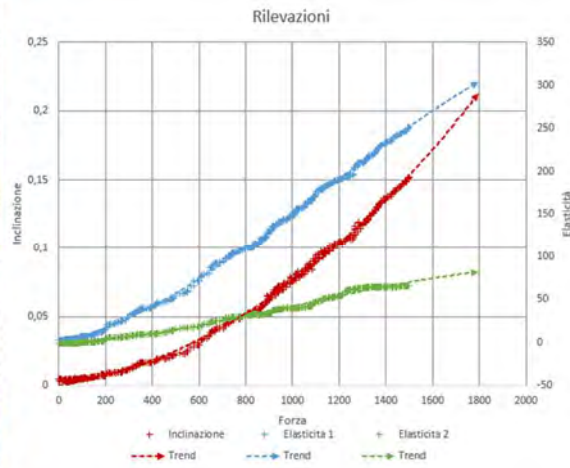
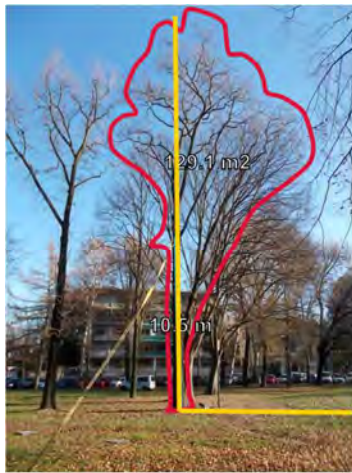
Alpha (°) = 0,41  
 F<sub>max</sub> (N) = 74684,64  
 M<sub>max</sub> (Nm) = 718332,46  
 M<sub>wind</sub> (Nm) = 341721,67  
**SF = 2,10**

Filters  
 Tare force at first value  
 Monotonicity for force  
 Monotonicity for inclination



Appendix 1 – Pulling tests

Boschetti Reali, Monza – 400 – 11869 – pt2



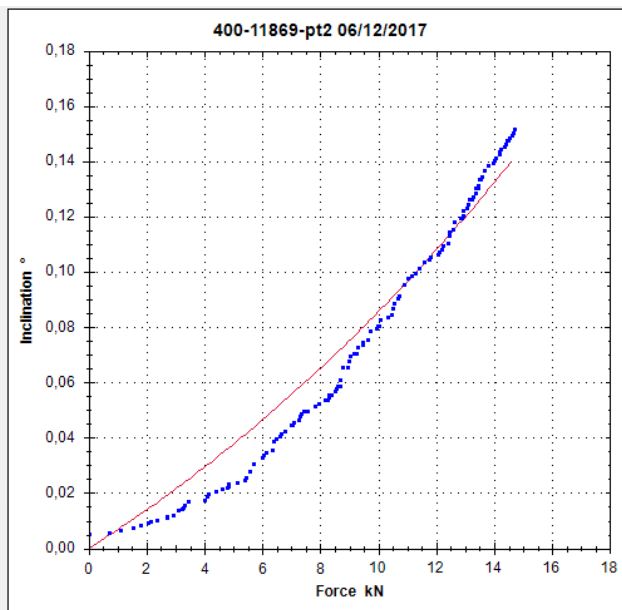
Measurement  
 Name: 400-11869-pt2 06/12/2017

Rope height on tree (m): 10.5  
 Anchor-tree level difference (m): 0.7  
 Anchor-tree distance (m): 24.85  
 Drag factor: 0.3  
 Wind speed (m/s): 33  
 Crown Area (m<sup>2</sup>): 130  
 Crown center height (m): 15.3  
 Elastic Limit (%): 3.4

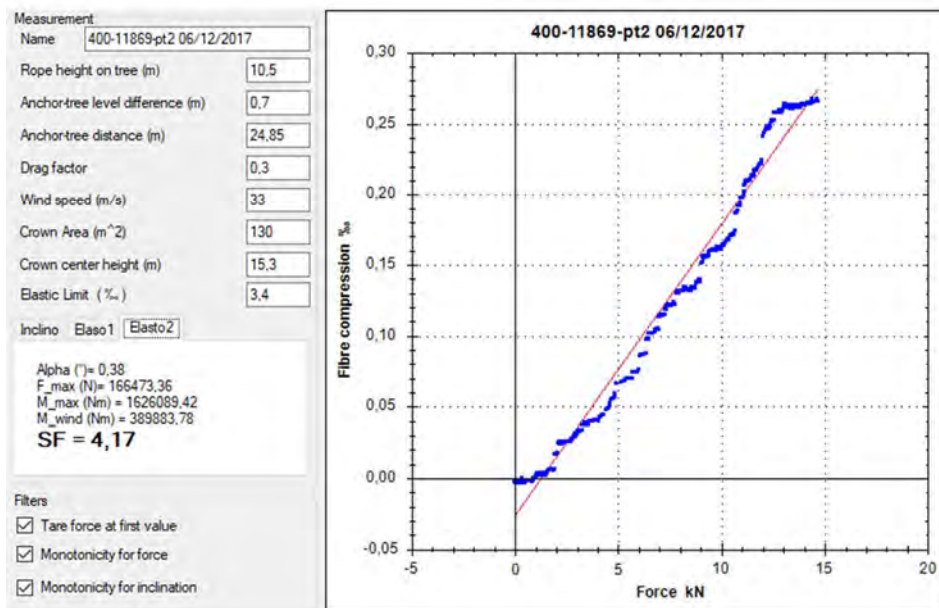
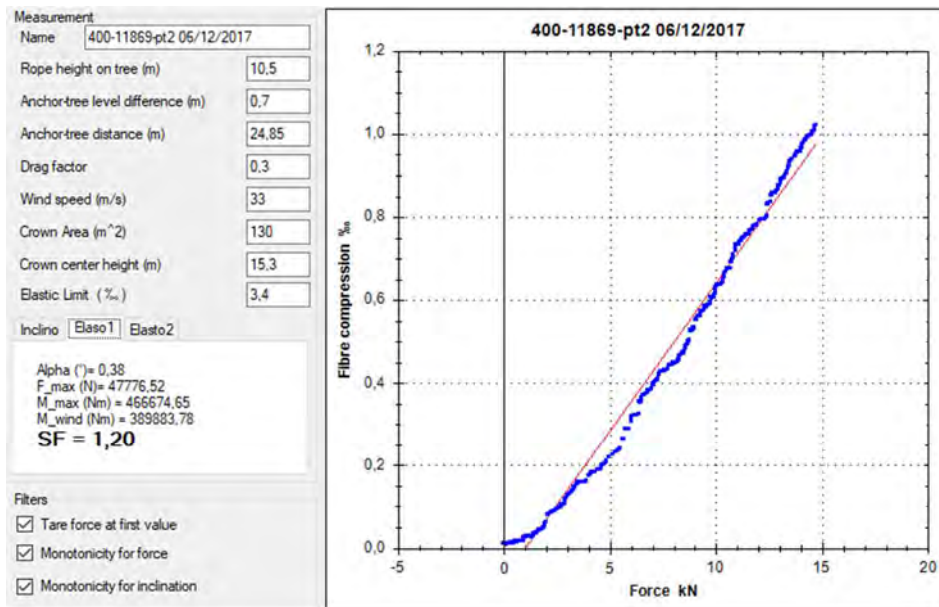
Inclino | Elaso1 | Elasto2

Alpha (°) = 0.38  
 F\_max (N) = 53344.23  
 M\_max (Nm) = 521059.27  
 M\_wind (Nm) = 389883.78  
**SF = 1,34**

Filters  
 Tare force at first value  
 Monotonicity for force  
 Monotonicity for inclination

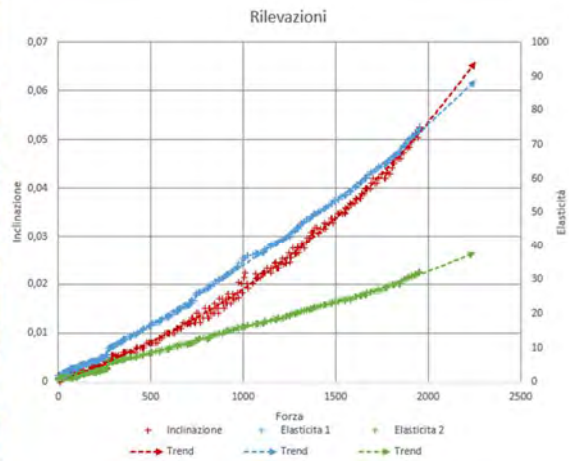


## Appendix 1 – Pulling tests



Appendix 1 – Pulling tests

Boschetti Reali, Monza – 400 – 11874 – pt1



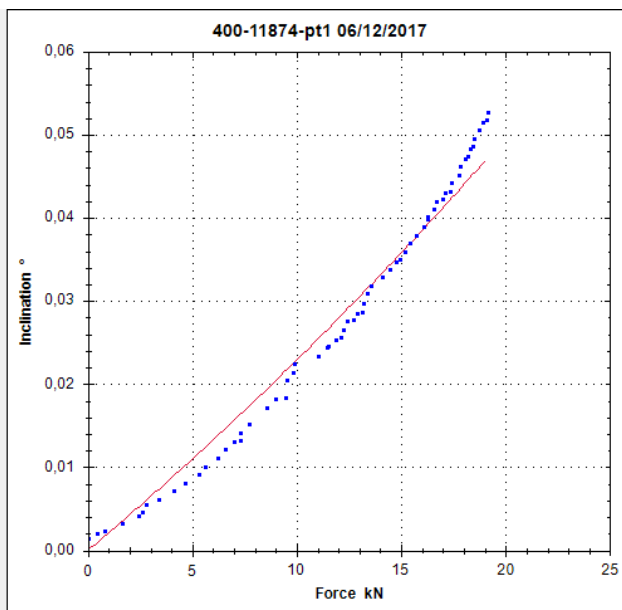
Measurement  
 Name 400-11874-pt1 06/12/2017

Rope height on tree (m) 4,3  
 Anchor-tree level difference (m) 0,7  
 Anchor-tree distance (m) 18,8  
 Drag factor 0,3  
 Wind speed (m/s) 33  
 Crown Area (m<sup>2</sup>) 248  
 Crown center height (m) 13,1  
 Elastic Limit (‰) 2,6

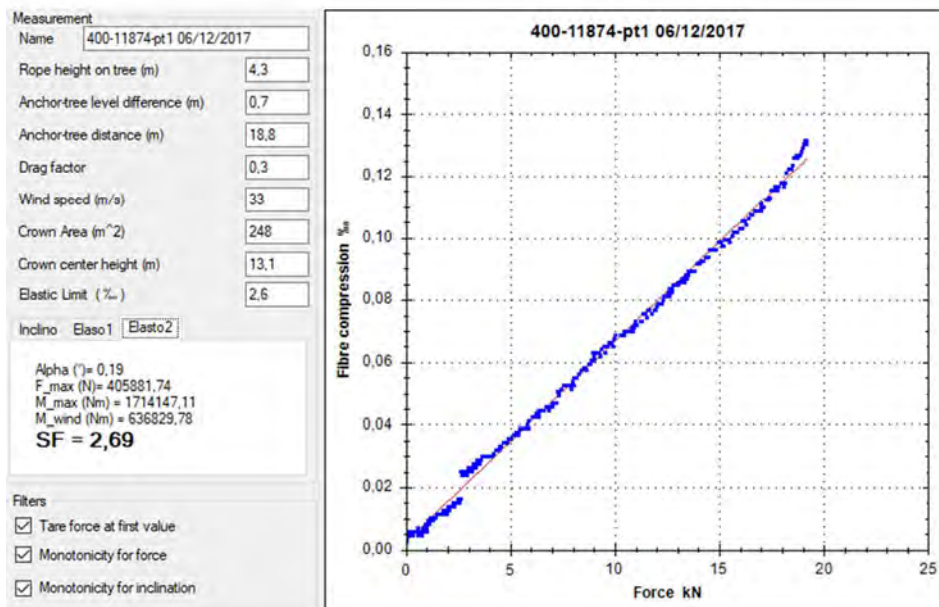
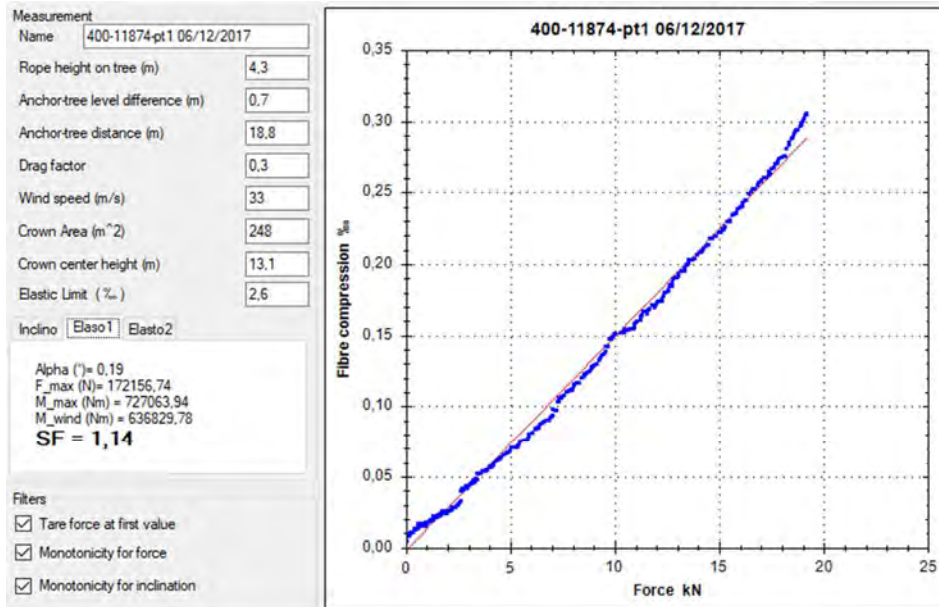
Inclino: Elaso1 Elasto2

Alpha (°) = 0,19  
 F\_max (N) = 167620,53  
 M\_max (Nm) = 707906,29  
 M\_wind (Nm) = 636829,78  
**SF = 1,11**

Filters  
 Tare force at first value  
 Monotonicity for force  
 Monotonicity for inclination

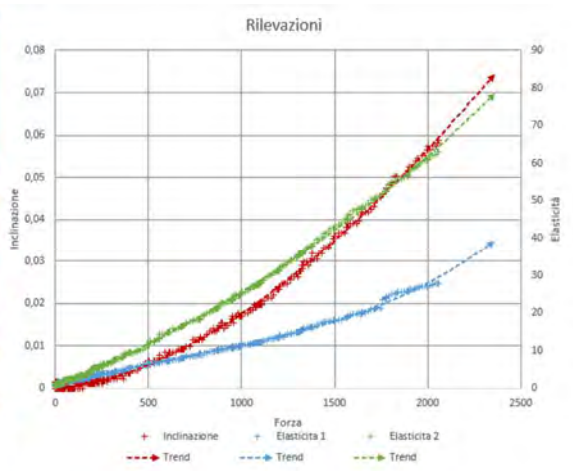


## Appendix 1 – Pulling tests



Appendix 1 – Pulling tests

Boschetti Reali, Monza – 400 – 11874 – pt2



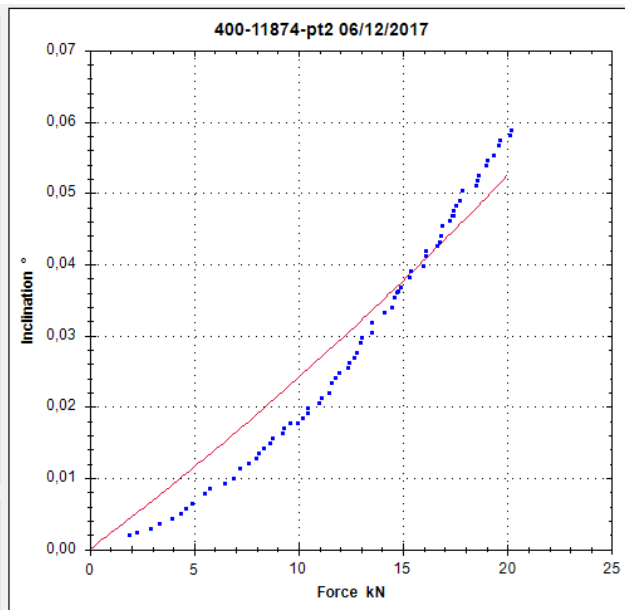
Measurement  
 Name 400-11874-pt2 06/12/2017

Rope height on tree (m) 4,3  
 Anchor-tree level difference (m) 0,5  
 Anchor-tree distance (m) 18,45  
 Drag factor 0,3  
 Wind speed (m/s) 33  
 Crown Area (m<sup>2</sup>) 295  
 Crown center height (m) 13,7  
 Elastic Limit (%) 0,26

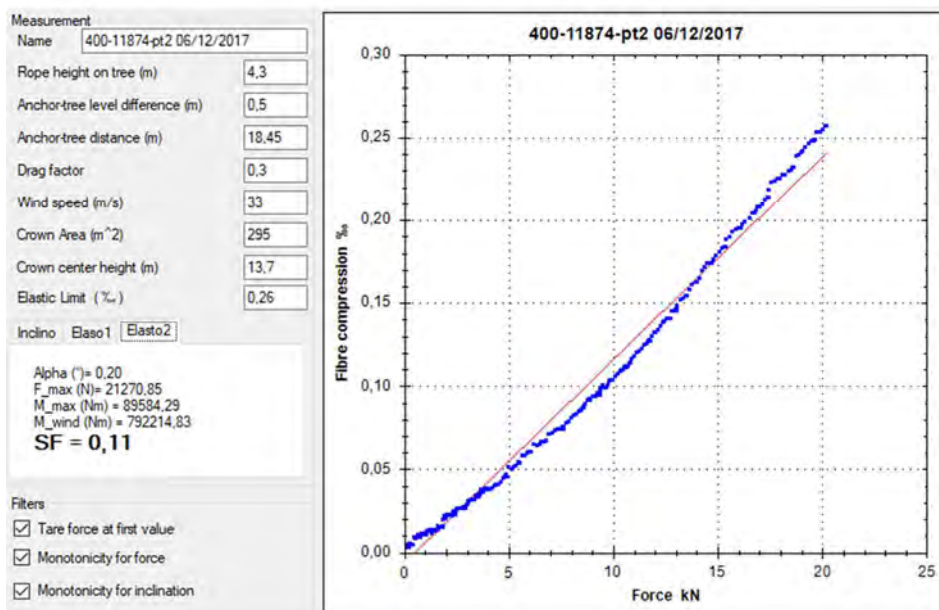
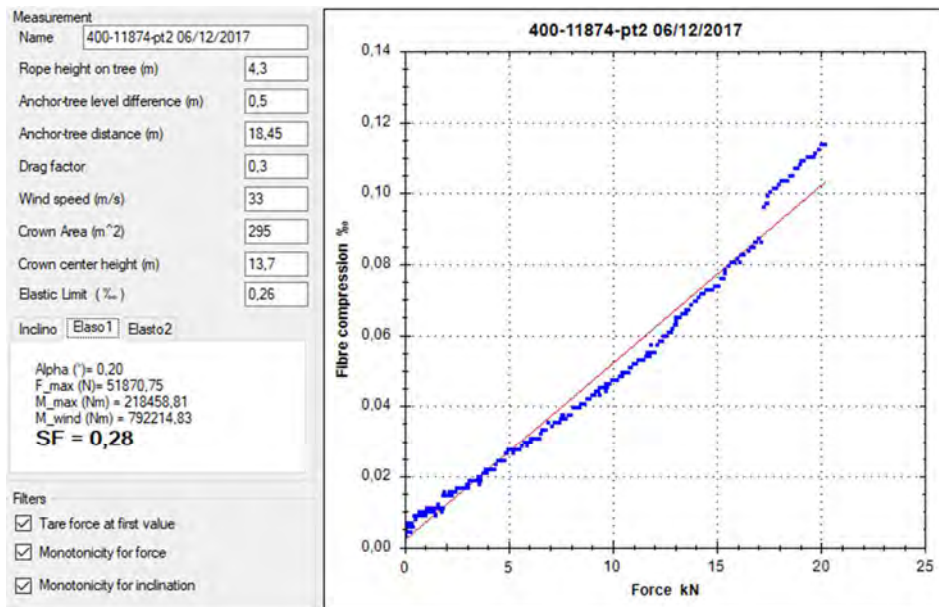
Inclino Elaso1 Elasto2

Alpha (°)= 0,20  
 F\_max (N)= 160222,61  
 M\_max (Nm) = 674793,38  
 M\_wind (Nm) = 792214,83  
**SF = 0,85**

Filters  
 Tare force at first value  
 Monotonicity for force  
 Monotonicity for inclination



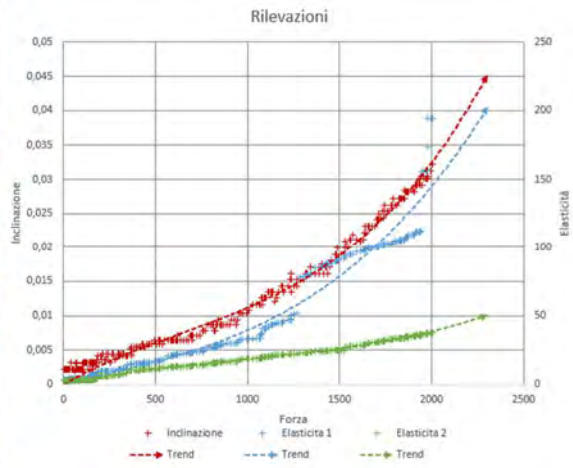
## Appendix 1 – Pulling tests





Appendix 1 – Pulling tests

Boschetti Reali, Monza – 400 – 11878 – pt1



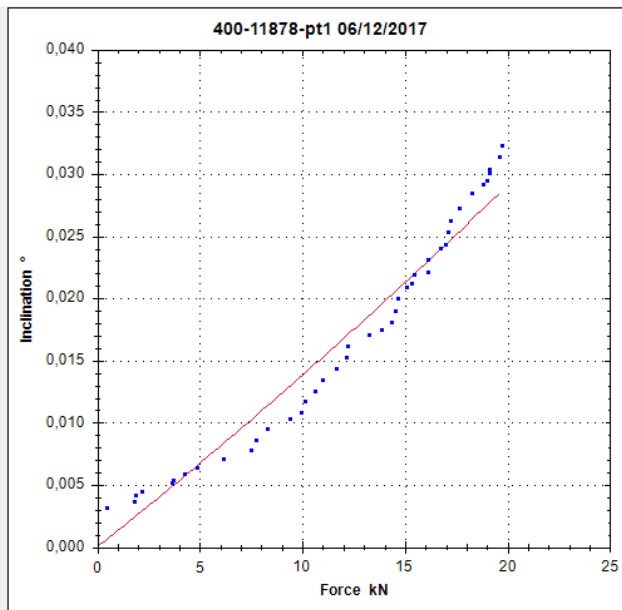
Measurement  
 Name: 400-11878-pt1 06/12/2017

Rope height on tree (m): 3,3  
 Anchor-tree level difference (m): 0,7  
 Anchor-tree distance (m): 15,65  
 Drag factor: 0,3  
 Wind speed (m/s): 33  
 Crown Area (m<sup>2</sup>): 146  
 Crown center height (m): 13,1  
 Elastic Limit (%): 3,5

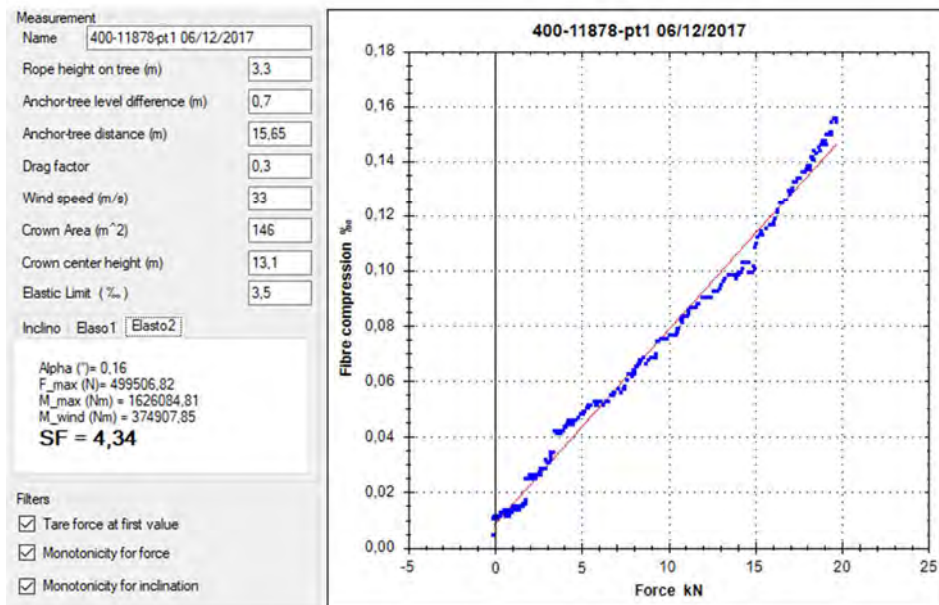
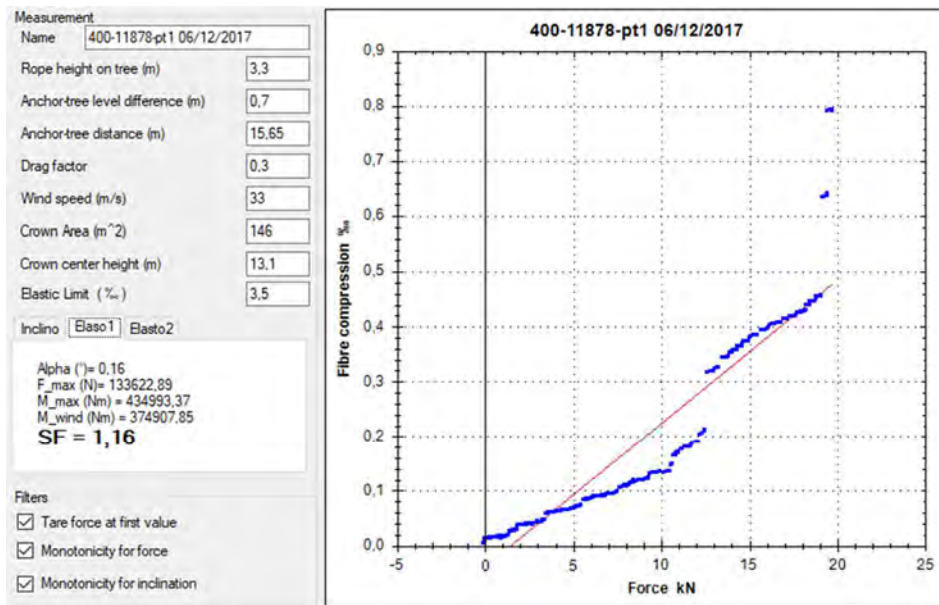
Inclino | Elaso1 | Elaso2

Alpha (°) = 0,16  
 F\_max (N) = 269222,50  
 M\_max (Nm) = 876421,71  
 M\_wind (Nm) = 374907,85  
**SF = 2,34**

Filters  
 Tare force at first value  
 Monotonicity for force  
 Monotonicity for inclination

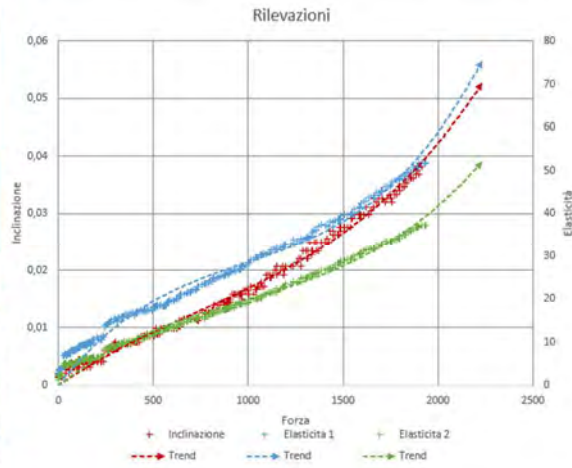


## Appendix 1 – Pulling tests



Appendix 1 – Pulling tests

Boschetti Reali, Monza – 400 – 11878 – pt2



Measurement

Name: 400-11878-pt2

Rope height on tree (m): 3.3

Anchor-tree level difference (m): 0.5

Anchor-tree distance (m): 15.6

Drag factor: 0.3

Wind speed (m/s): 33

Crown Area (m<sup>2</sup>): 279

Crown center height (m): 14.7

Elastic Limit (%): 3.5

Inclino | Elaso1 | Elaso2

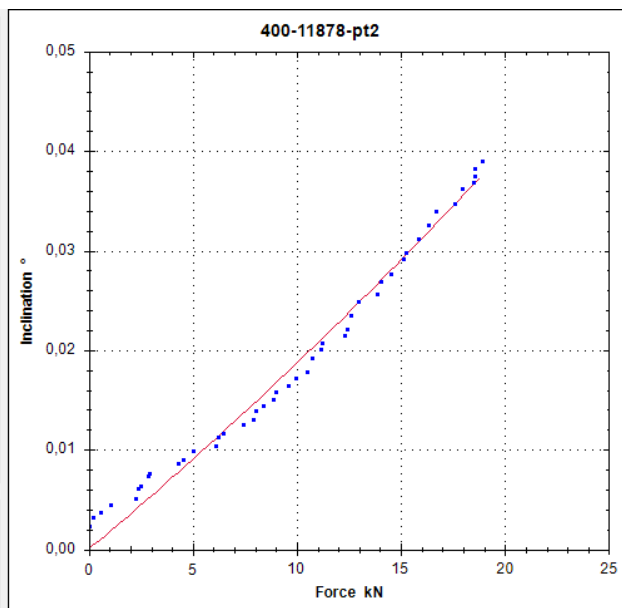
Alpha (°) = 0.18  
 F\_max (N) = 202292.11  
 M\_max (Nm) = 657063.98  
 M\_wind (Nm) = 803936.83  
**SF = 0,82**

Filters

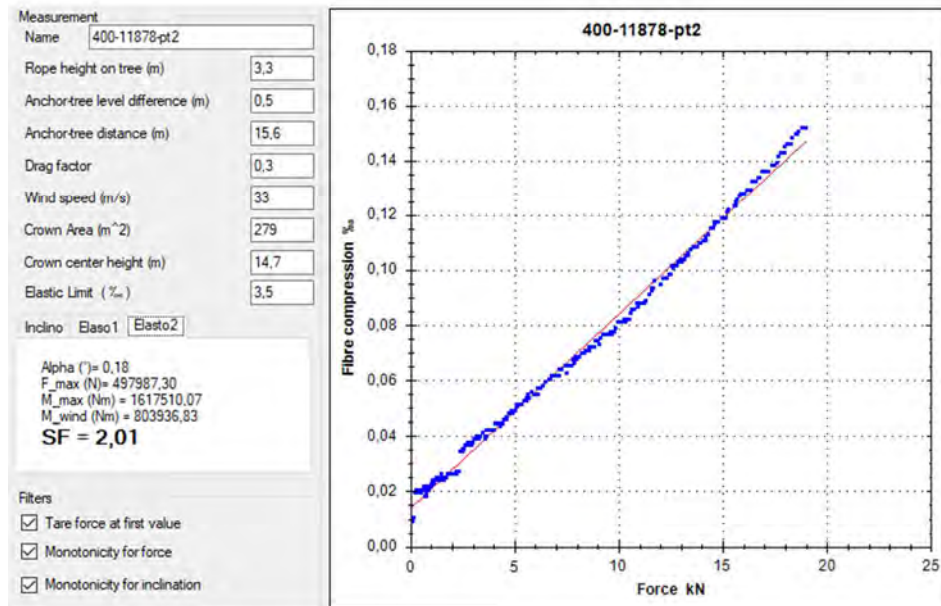
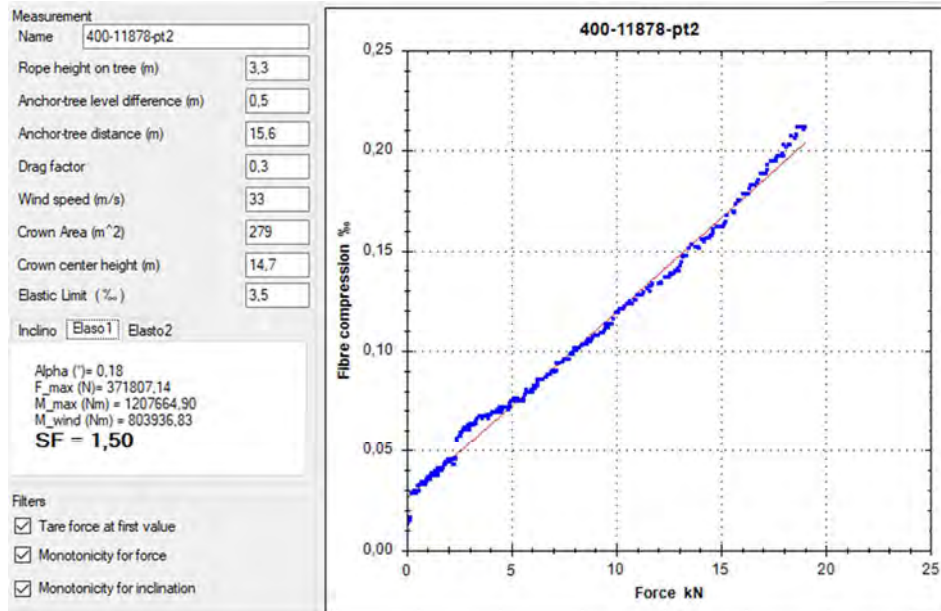
Tare force at first value

Monotonicity for force

Monotonicity for inclination

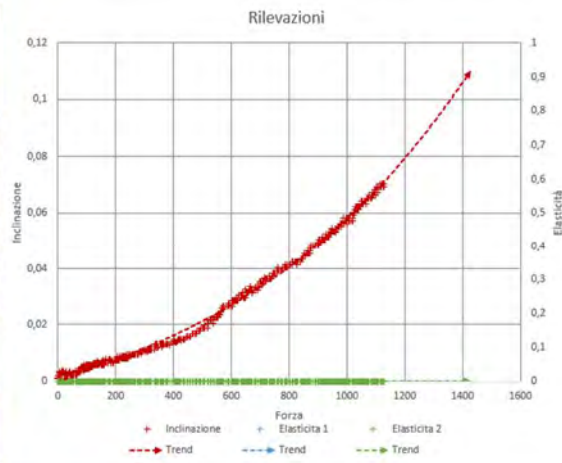


## Appendix 1 – Pulling tests



## Appendix 1 – Pulling tests

Via Pellettier, Monza – 393 – 11150 – pt1



Measurement  
 Name 393-11150-pt1 05/12/2017

Rope height on tree (m) 9

Anchor-tree level difference (m) 0,3

Anchor-tree distance (m) 43,1

Drag factor 0,25

Wind speed (m/s) 33

Crown Area (m<sup>2</sup>) 138

Crown center height (m) 9,1

Elastic Limit (%) 2,9

Inclino Elaso1 Elasto2

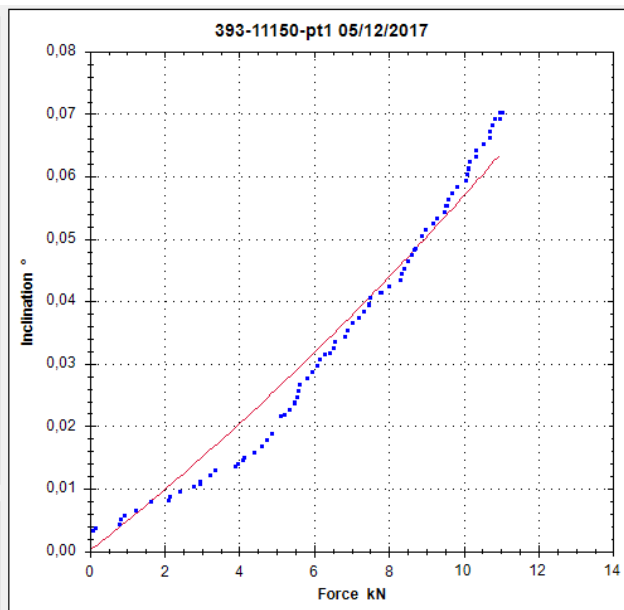
Alpha (°) = 0,20  
 F\_max (N) = 74715,41  
 M\_max (Nm) = 659144,08  
 M\_wind (Nm) = 205134,93  
**SF = 3,21**

Filters

Tare force at first value

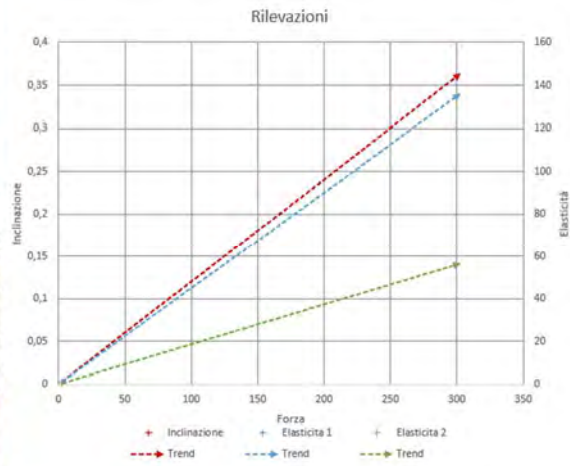
Monotonicity for force

Monotonicity for inclination



## Appendix 1 – Pulling tests

Via Pellettier, Monza – 393 – 11151 – pt1



Measurement

Name 393-11151-pt1 05/12/2017

Rope height on tree (m) 8,00

Anchor-tree level difference (m) 0,3

Anchor-tree distance (m) 46,75

Drag factor 0,25

Wind speed (m/s) 33

Crown Area (m<sup>2</sup>) 111,00

Crown center height (m) 8,40

Elastic Limit (%) 2,9

Inclino | Elaso1 | Elaso2

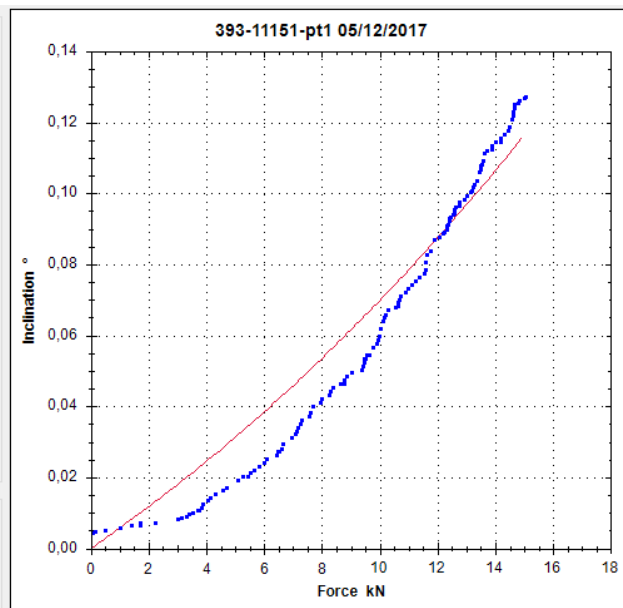
Alpha (°) = 0,16  
 F<sub>max</sub> (N) = 62943,90  
 M<sub>max</sub> (Nm) = 496856,95  
 M<sub>wind</sub> (Nm) = 152307,54  
**SF = 3,26**

Filters

Tare force at first value

Monotonicity for force

Monotonicity for inclination



## Appendix 1 – Pulling tests

Measurement  
Name: 393-11151-pt1 05/12/2017

Rope height on tree (m): 8,00

Anchor-tree level difference (m): 0,3

Anchor-tree distance (m): 46,75

Drag factor: 0,25

Wind speed (m/s): 33

Crown Area (m<sup>2</sup>): 111,00

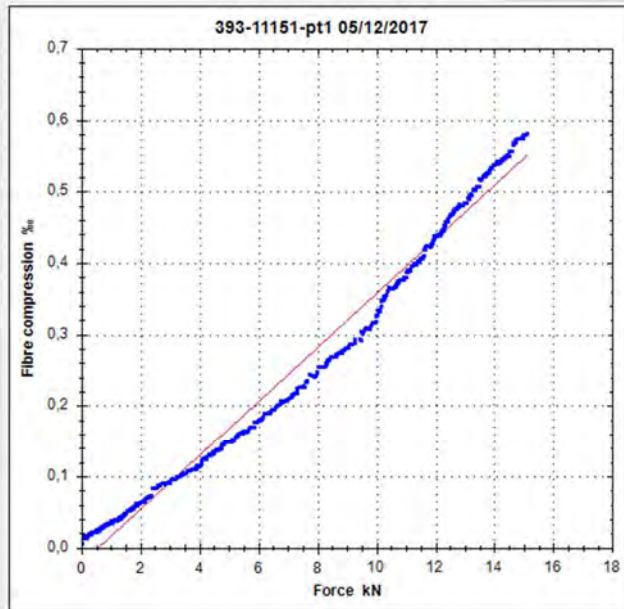
Crown center height (m): 8,40

Elastic Limit (%): 2,9

Inclino:  Elaso1  Elasto2

Alpha (°) = 0,16  
 F<sub>max</sub> (N) = 76324,57  
 M<sub>max</sub> (Nm) = 602479,18  
 M<sub>wind</sub> (Nm) = 152307,54  
**SF = 3,96**

Filters  
 Tare force at first value  
 Monotonicity for force  
 Monotonicity for inclination



Measurement  
Name: 393-11151-pt1 05/12/2017

Rope height on tree (m): 8,00

Anchor-tree level difference (m): 0,3

Anchor-tree distance (m): 46,75

Drag factor: 0,25

Wind speed (m/s): 33

Crown Area (m<sup>2</sup>): 111,00

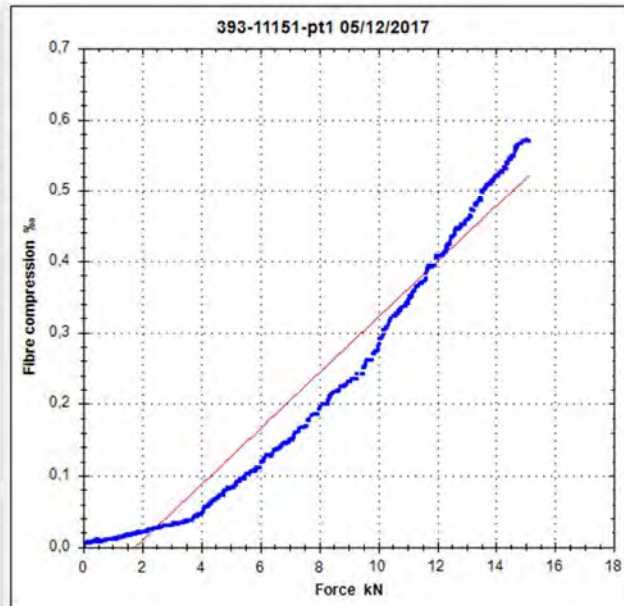
Crown center height (m): 8,40

Elastic Limit (%): 2,9

Inclino:  Elaso1  Elasto2

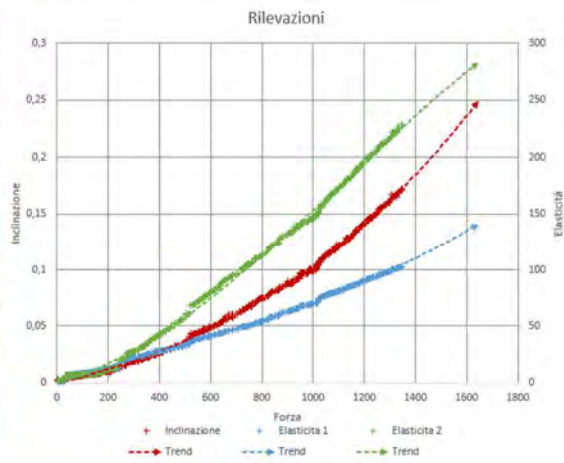
Alpha (°) = 0,16  
 F<sub>max</sub> (N) = 74064,98  
 M<sub>max</sub> (Nm) = 584642,83  
 M<sub>wind</sub> (Nm) = 152307,54  
**SF = 3,84**

Filters  
 Tare force at first value  
 Monotonicity for force  
 Monotonicity for inclination



## Appendix 1 – Pulling tests

Via Pellettier, Monza – 393 – 11152 – pt1



Measurement

Name 393-11152-pt1 05/12/2017

Rope height on tree (m) 8,3

Anchor-tree level difference (m) 0,3

Anchor-tree distance (m) 47,35

Drag factor 0,25

Wind speed (m/s) 33

Crown Area (m<sup>2</sup>) 140

Crown center height (m) 7,9

Elastic Limit (%) 2,9

Inclino Elaso1 Elasto2

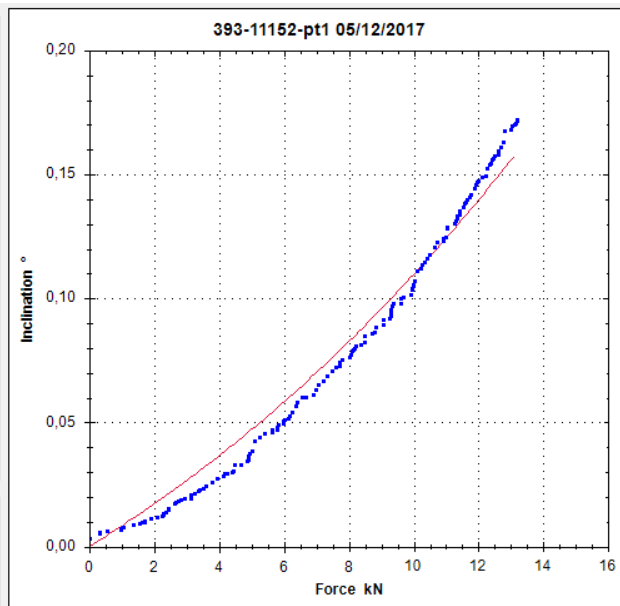
Alpha (°) = 0,17  
 F<sub>max</sub> (N) = 43937,52  
 M<sub>max</sub> (Nm) = 359585,22  
 M<sub>wind</sub> (Nm) = 180665,10  
**SF = 1,99**

Filters

Tare force at first value

Monotonicity for force

Monotonicity for inclination





## Appendix 1 – Pulling tests

Measurement  
Name 393-11152-pt1 05/12/2017

Rope height on tree (m) 8,3

Anchor-tree level difference (m) 0,3

Anchor-tree distance (m) 47,35

Drag factor 0,25

Wind speed (m/s) 33

Crown Area (m<sup>2</sup>) 140

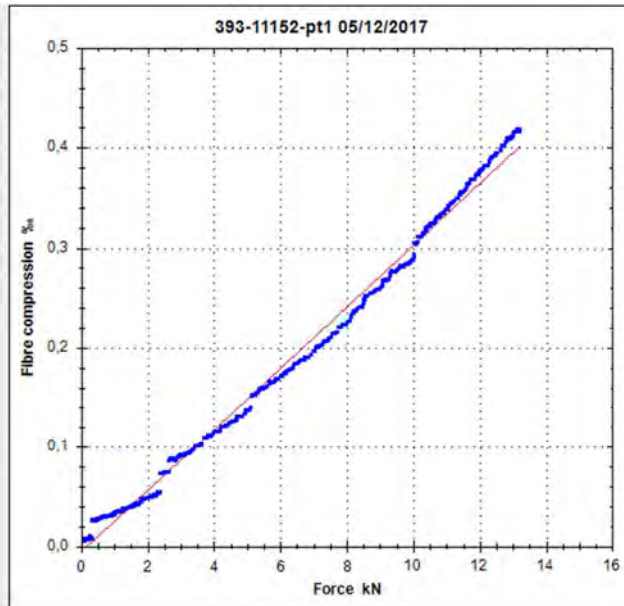
Crown center height (m) 7,9

Elastic Limit (%) 2,9

Inclino  Elaso1  Elasto2

Alpha (°)= 0,17  
F<sub>max</sub> (N)= 94097,53  
M<sub>max</sub> (Nm) = 770095,43  
M<sub>wind</sub> (Nm) = 180665,10  
**SF = 4,26**

Filters  
 Tare force at first value  
 Monotonicity for force  
 Monotonicity for inclination



Measurement  
Name 393-11152-pt1 05/12/2017

Rope height on tree (m) 8,3

Anchor-tree level difference (m) 0,3

Anchor-tree distance (m) 47,35

Drag factor 0,25

Wind speed (m/s) 33

Crown Area (m<sup>2</sup>) 140

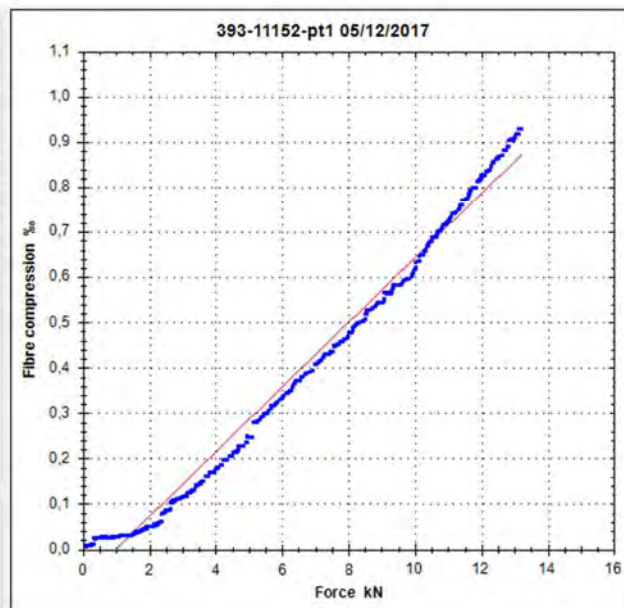
Crown center height (m) 7,9

Elastic Limit (%) 2,9

Inclino  Elaso1  Elasto2

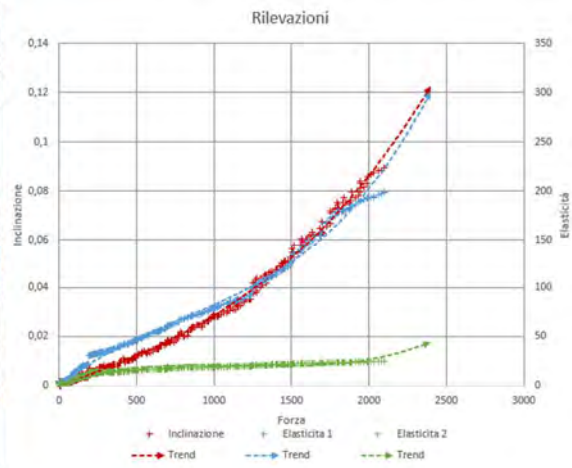
Alpha (°)= 0,17  
F<sub>max</sub> (N)= 40633,19  
M<sub>max</sub> (Nm) = 332542,55  
M<sub>wind</sub> (Nm) = 180665,10  
**SF = 1,84**

Filters  
 Tare force at first value  
 Monotonicity for force  
 Monotonicity for inclination



## Appendix 1 – Pulling tests

Via Vittorio Veneto, Monza – 339 – 9531 – pt1



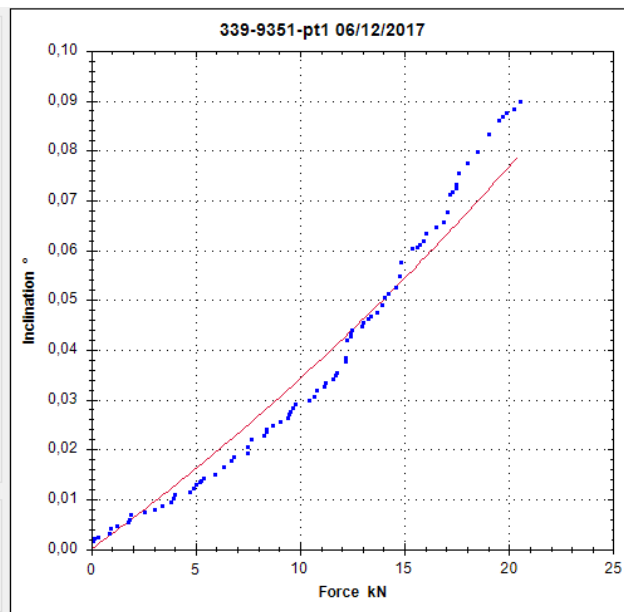
Measurement  
 Name 339-9351-pt1 06/12/2017

Rope height on tree (m) 2,55  
 Anchor-tree level difference (m) 0,3  
 Anchor-tree distance (m) 8,6  
 Drag factor 0,2  
 Wind speed (m/s) 33  
 Crown Area (m<sup>2</sup>) 58  
 Crown center height (m) 8,2  
 Elastic Limit (%) 4,2

Inclino Elasto1 Elasto2

Alpha (°) = 0,26  
 F\_max (N) = 116529,56  
 M\_max (Nm) = 287474,51  
 M\_wind (Nm) = 62151,41  
**SF = 4,63**

Filters  
 Tare force at first value  
 Monotonicity for force  
 Monotonicity for inclination



## Appendix 1 – Pulling tests

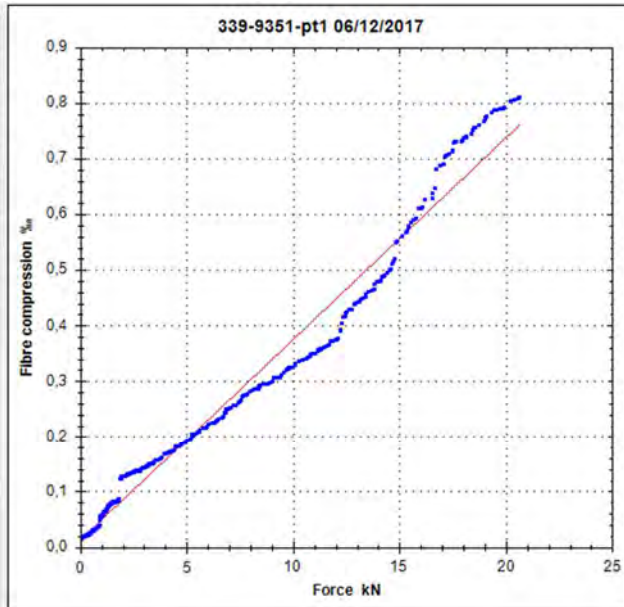
Measurement  
 Name: 339-9351-pt1 06/12/2017

Rope height on tree (m): 2,55  
 Anchor-tree level difference (m): 0,3  
 Anchor-tree distance (m): 8,6  
 Drag factor: 0,2  
 Wind speed (m/s): 33  
 Crown Area (m<sup>2</sup>): 58  
 Crown center height (m): 8,2  
 Elastic Limit (%): 4,2

Inclino:  Elaso1  Elasto2

Alpha (°)= 0,26  
 F<sub>max</sub> (N)= 115479,62  
 M<sub>max</sub> (Nm) = 284884,35  
 M<sub>wind</sub> (Nm) = 62151,41  
**SF = 4,58**

Filters  
 Tare force at first value  
 Monotonicity for force  
 Monotonicity for inclination



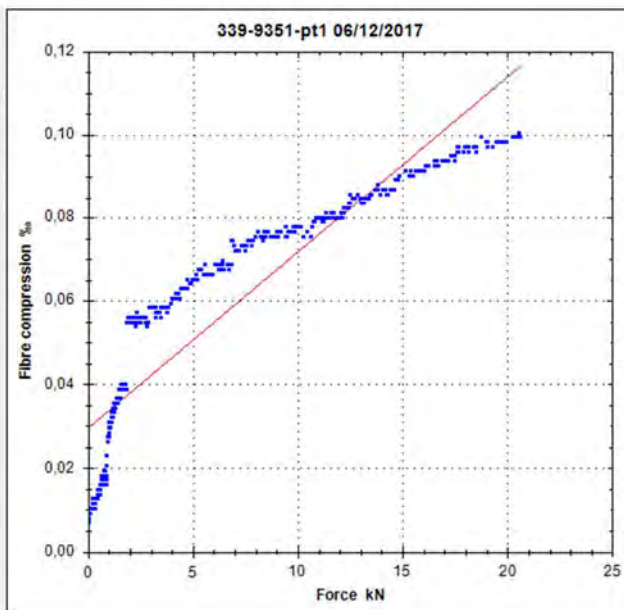
Measurement  
 Name: 339-9351-pt1 06/12/2017

Rope height on tree (m): 2,55  
 Anchor-tree level difference (m): 0,3  
 Anchor-tree distance (m): 8,6  
 Drag factor: 0,2  
 Wind speed (m/s): 33  
 Crown Area (m<sup>2</sup>): 58  
 Crown center height (m): 8,2  
 Elastic Limit (%): 4,2

Inclino:  Elaso1  Elasto2

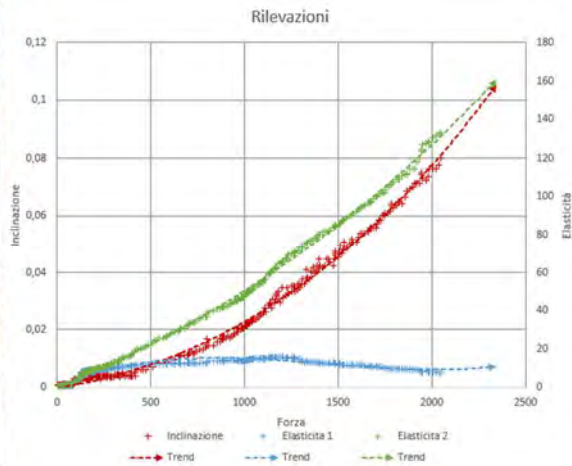
Alpha (°)= 0,26  
 F<sub>max</sub> (N)= 994843,30  
 M<sub>max</sub> (Nm) = 2454245,08  
 M<sub>wind</sub> (Nm) = 62151,41  
**SF = 39,49**

Filters  
 Tare force at first value  
 Monotonicity for force  
 Monotonicity for inclination



## Appendix 1 – Pulling tests

Via Vittorio Veneto, Monza – 339 – 9531 – pt2



Measurement  
Name 339-9351-pt2 06/12/2017

Rope height on tree (m) 2,55

Anchor-tree level difference (m) 0,3

Anchor-tree distance (m) 8,2

Drag factor 0,2

Wind speed (m/s) 33

Crown Area (m<sup>2</sup>) 53

Crown center height (m) 8,5

Elastic Limit (%) 4,2

Inclino Elaso1 Elasto2

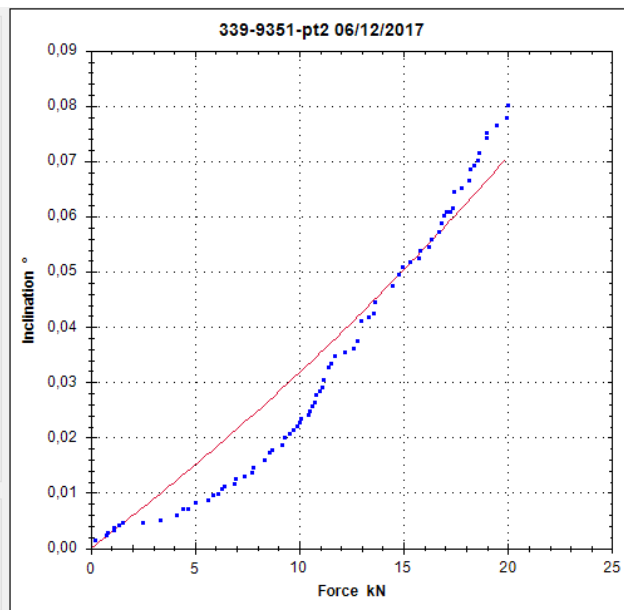
Alpha (°) = 0,27  
F\_max (N) = 124477,13  
M\_max (Nm) = 306102,54  
M\_wind (Nm) = 58871,34  
**SF = 5,20**

Filters

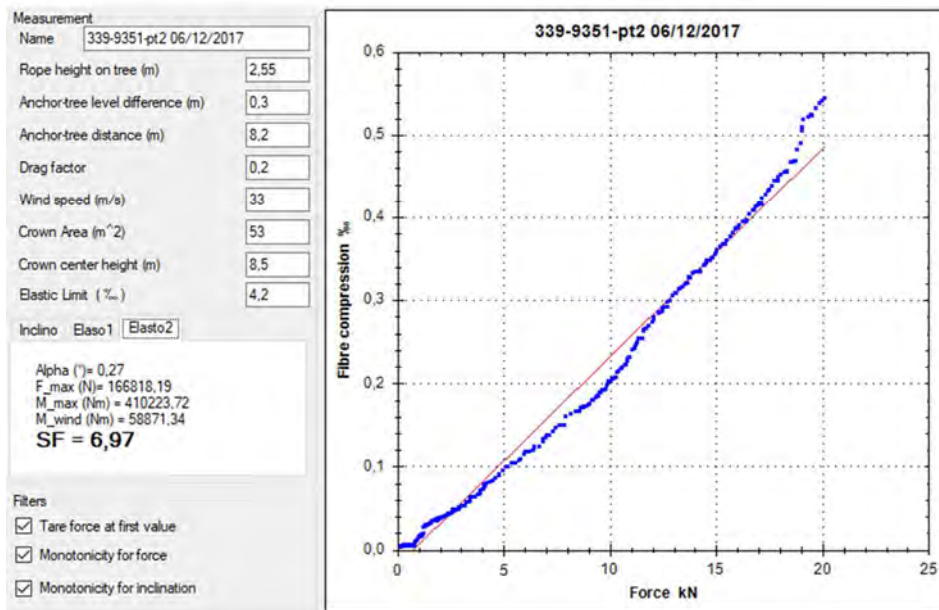
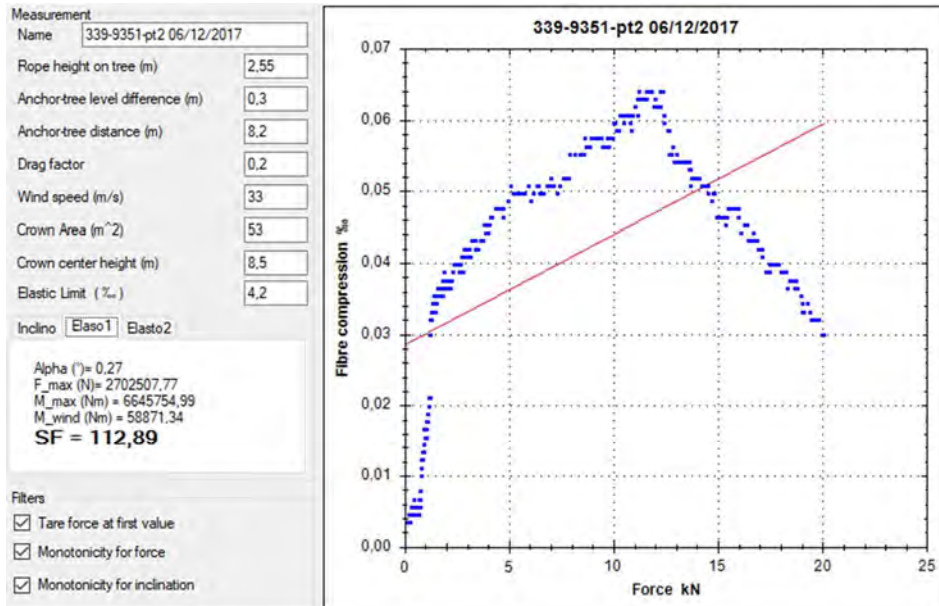
Tare force at first value

Monotonicity for force

Monotonicity for inclination

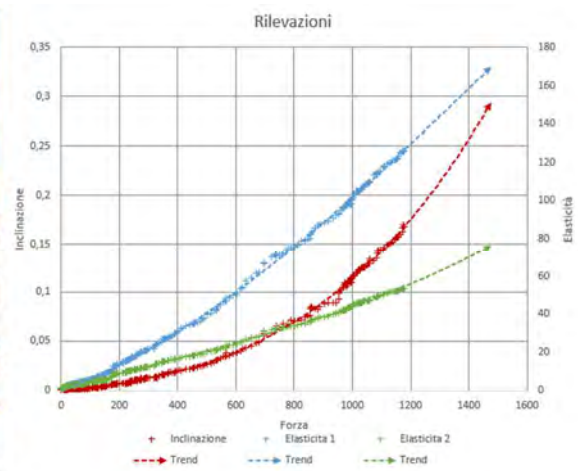


## Appendix 1 – Pulling tests



## Appendix 1 – Pulling tests

Via Vittorio Veneto, Monza – 339 – 9368 – pt1



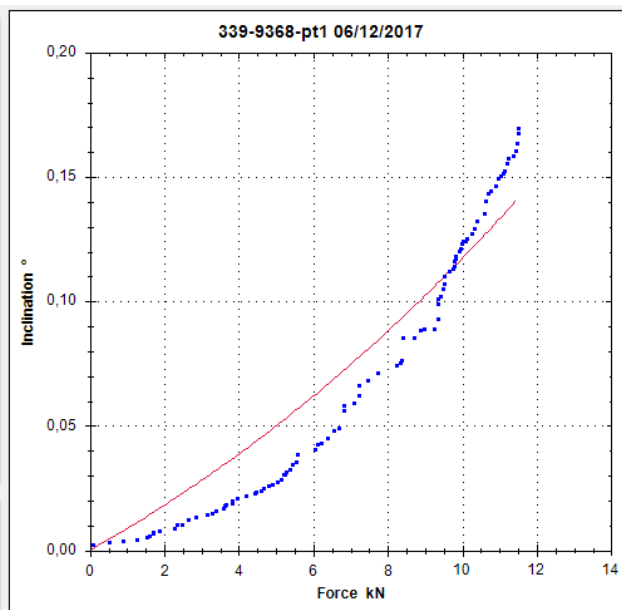
Measurement  
Name 339-9368-pt1 06/12/2017

Rope height on tree (m) 2,4  
Anchor-tree level difference (m) 0,4  
Anchor-tree distance (m) 8  
Drag factor 0,2  
Wind speed (m/s) 33  
Crown Area (m<sup>2</sup>) 26  
Crown center height (m) 5,4  
Elastic Limit (%) 3,3

Inclino Elaso1 Elasto2

Alpha (°) = 0,24  
F<sub>max</sub> (N) = 41726,84  
M<sub>max</sub> (Nm) = 97154,34  
M<sub>wind</sub> (Nm) = 18347,47  
**SF = 5,30**

Filters  
 Tare force at first value  
 Monotonicity for force  
 Monotonicity for inclination



## Appendix 1 – Pulling tests

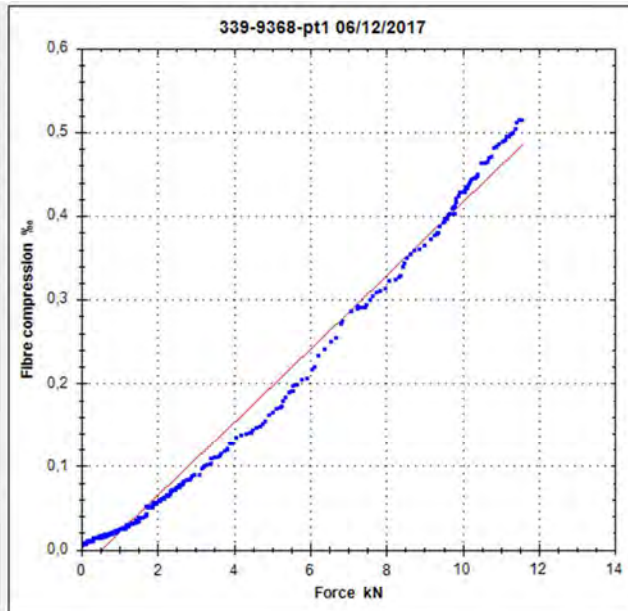
Measurement  
 Name: 339-9368-pt1 06/12/2017

Rope height on tree (m): 2,4  
 Anchor-tree level difference (m): 0,4  
 Anchor-tree distance (m): 8  
 Drag factor: 0,2  
 Wind speed (m/s): 33  
 Crown Area (m<sup>2</sup>): 26  
 Crown center height (m): 5,4  
 Elastic Limit (%): 3,3

Inclino:  Elaso1  Elasto2

Alpha (°) = 0,24  
 F<sub>max</sub> (N) = 75042,99  
 M<sub>max</sub> (Nm) = 174725,76  
 M<sub>wind</sub> (Nm) = 18347,47  
**SF = 9,52**

Filters  
 Tare force at first value  
 Monotonicity for force  
 Monotonicity for inclination



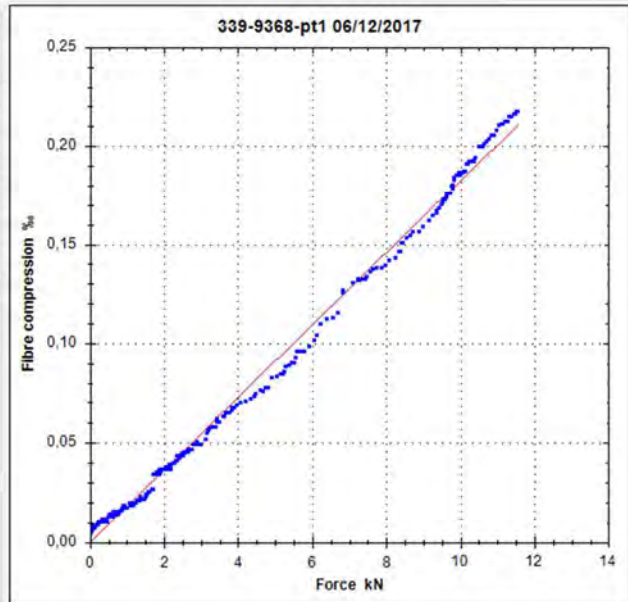
Measurement  
 Name: 339-9368-pt1 06/12/2017

Rope height on tree (m): 2,4  
 Anchor-tree level difference (m): 0,4  
 Anchor-tree distance (m): 8  
 Drag factor: 0,2  
 Wind speed (m/s): 33  
 Crown Area (m<sup>2</sup>): 26  
 Crown center height (m): 5,4  
 Elastic Limit (%): 3,3

Inclino:  Elaso1  Elasto2

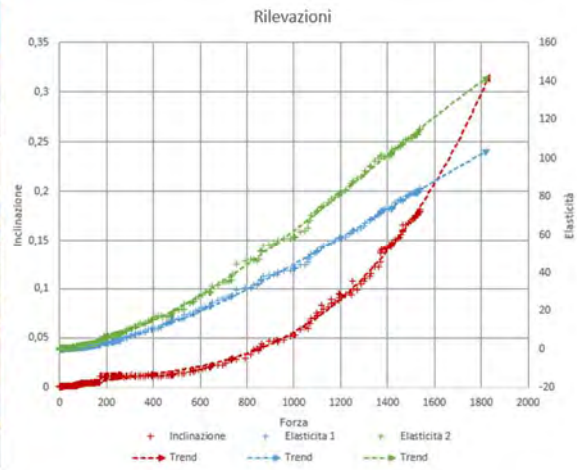
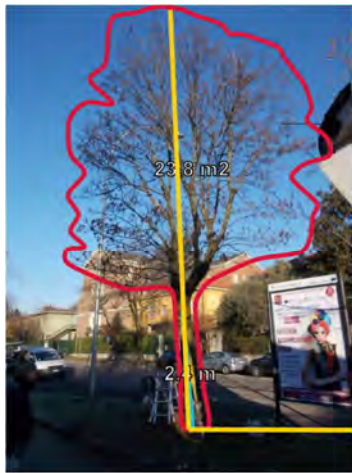
Alpha (°) = 0,24  
 F<sub>max</sub> (N) = 180566,32  
 M<sub>max</sub> (Nm) = 420420,15  
 M<sub>wind</sub> (Nm) = 18347,47  
**SF = 22,91**

Filters  
 Tare force at first value  
 Monotonicity for force  
 Monotonicity for inclination



## Appendix 1 – Pulling tests

Via Vittorio Veneto, Monza – 339 – 9368 – pt2



Measurement

Name: 339-9368-pt2 06/12/2017

Rope height on tree (m): 2,4

Anchor-tree level difference (m): 0,45

Anchor-tree distance (m): 9,2

Drag factor: 0,2

Wind speed (m/s): 33

Crown Area (m<sup>2</sup>): 24

Crown center height (m): 5,3

Elastic Limit (%): 4,2

Inclino: Elaso1 Elasto2

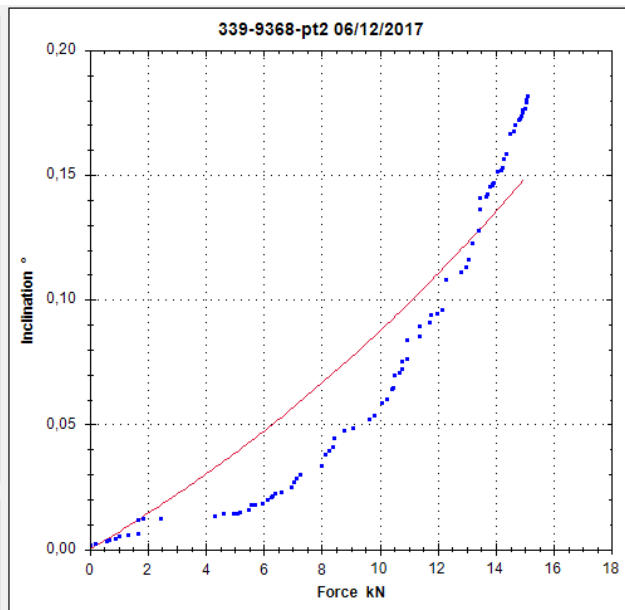
Alpha (°) = 0,21  
 F\_max (N) = 52505,47  
 M\_max (Nm) = 123274,47  
 M\_wind (Nm) = 16622,50  
**SF = 7,42**

Filters

Tare force at first value

Monotonicity for force

Monotonicity for inclination





## Appendix 1 – Pulling tests

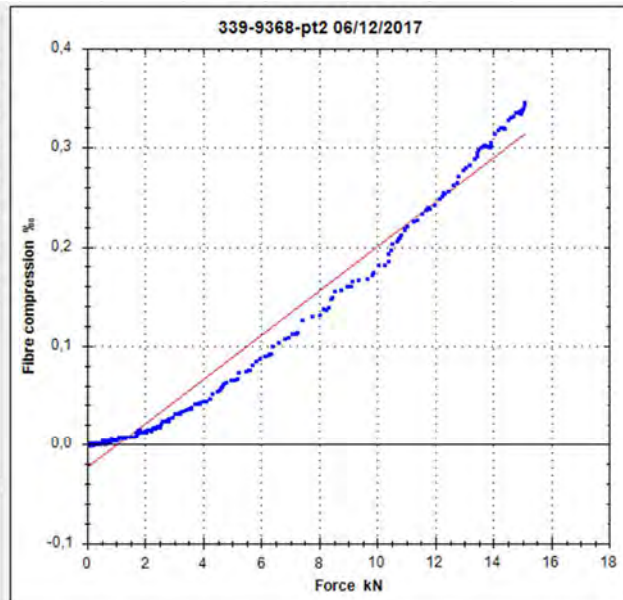
Measurement  
Name: 339-9368-pt2 06/12/2017

Rope height on tree (m): 2,4  
Anchor-tree level difference (m): 0,45  
Anchor-tree distance (m): 9,2  
Drag factor: 0,2  
Wind speed (m/s): 33  
Crown Area (m<sup>2</sup>): 24  
Crown center height (m): 5,3  
Elastic Limit (%): 4,2

Inclino:  Elaso1  Elasto2

Alpha (°) = 0,21  
F\_max (N) = 187159,95  
M\_max (Nm) = 439421,69  
M\_wind (Nm) = 16622,50  
**SF = 26,44**

Filters  
 Tare force at first value  
 Monotonicity for force  
 Monotonicity for inclination



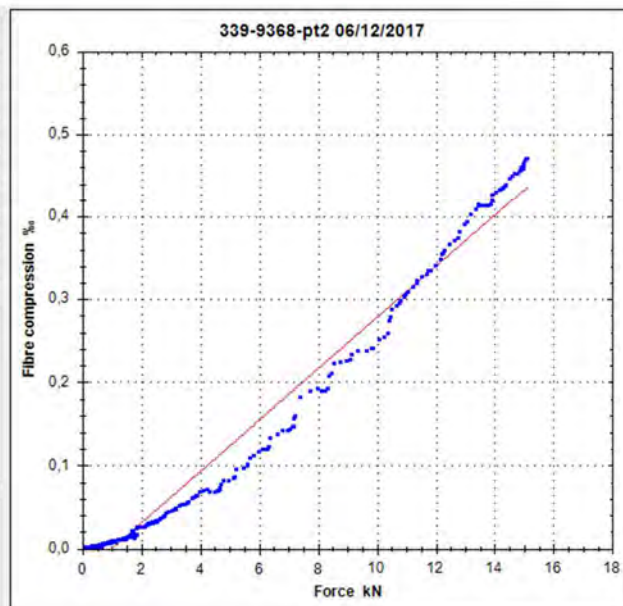
Measurement  
Name: 339-9368-pt2 06/12/2017

Rope height on tree (m): 2,4  
Anchor-tree level difference (m): 0,45  
Anchor-tree distance (m): 9,2  
Drag factor: 0,2  
Wind speed (m/s): 33  
Crown Area (m<sup>2</sup>): 24  
Crown center height (m): 5,3  
Elastic Limit (%): 4,2

Inclino:  Elaso1  Elasto2

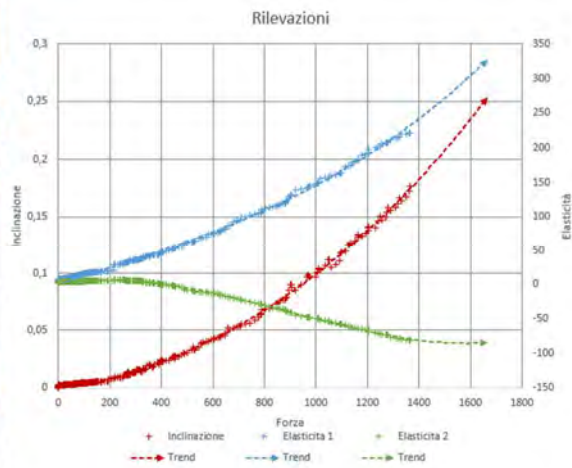
Alpha (°) = 0,21  
F\_max (N) = 135803,35  
M\_max (Nm) = 318844,58  
M\_wind (Nm) = 16622,50  
**SF = 19,18**

Filters  
 Tare force at first value  
 Monotonicity for force  
 Monotonicity for inclination



## Appendix 1 – Pulling tests

Via Vittorio Veneto, Monza – 339 – 9400 – pt1



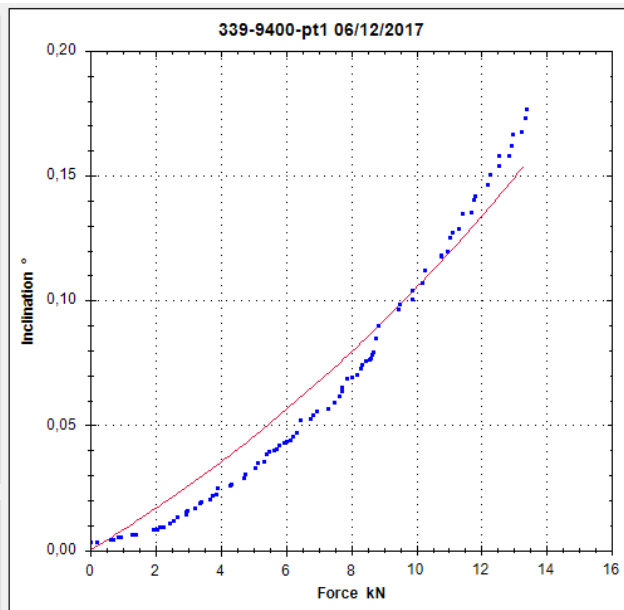
Measurement  
Name 339-9400-pt1 06/12/2017

Rope height on tree (m) 2,55  
Anchor-tree level difference (m) 0,4  
Anchor-tree distance (m) 9,3  
Drag factor 0,2  
Wind speed (m/s) 33  
Crown Area (m<sup>2</sup>) 59  
Crown center height (m) 6,9  
Elastic Limit (%) 4,2

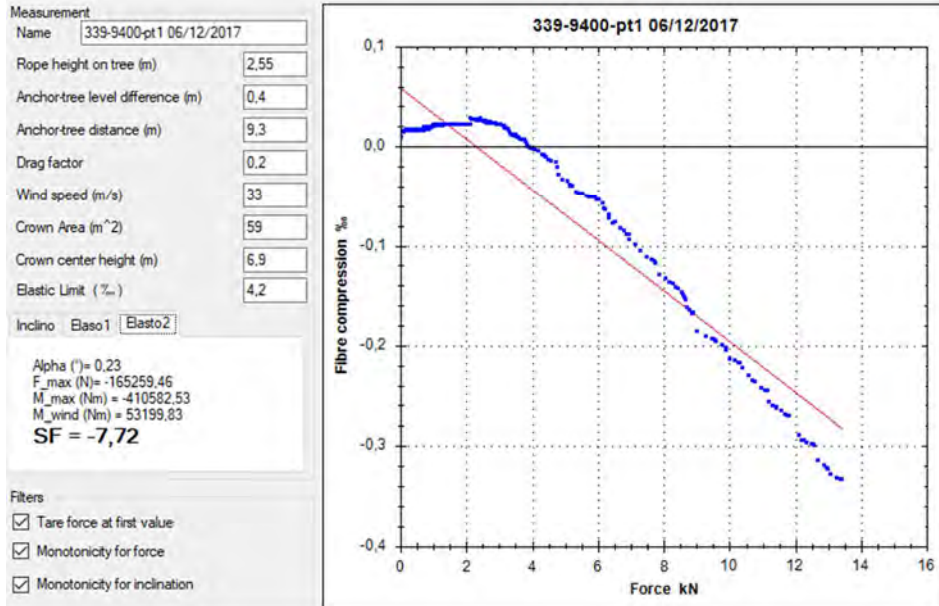
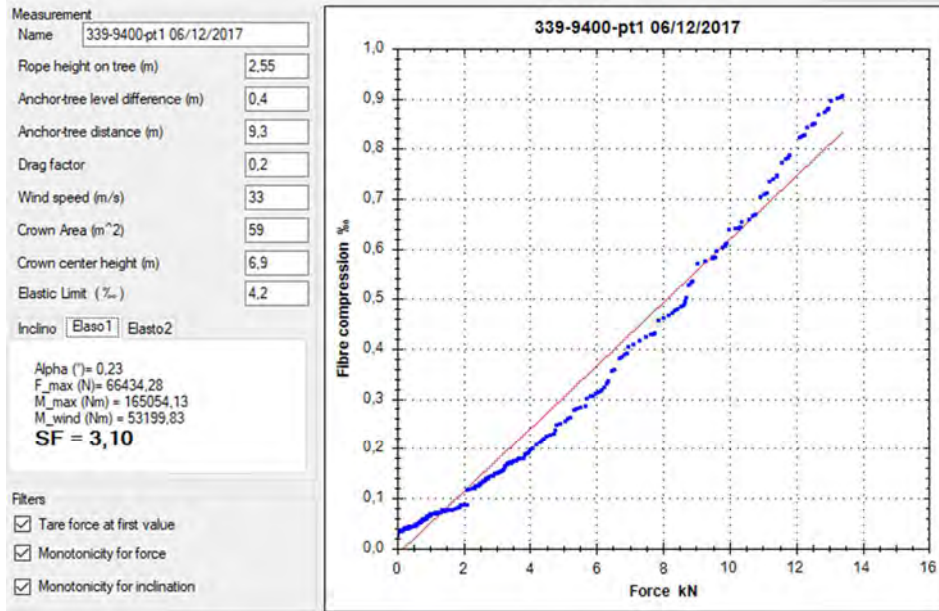
Inclino Elaso1 Elasto2

Alpha (°) = 0,23  
F\_max (N) = 45427,56  
M\_max (Nm) = 112863,51  
M\_wind (Nm) = 53199,83  
**SF = 2,12**

Filters  
 Tare force at first value  
 Monotonicity for force  
 Monotonicity for inclination

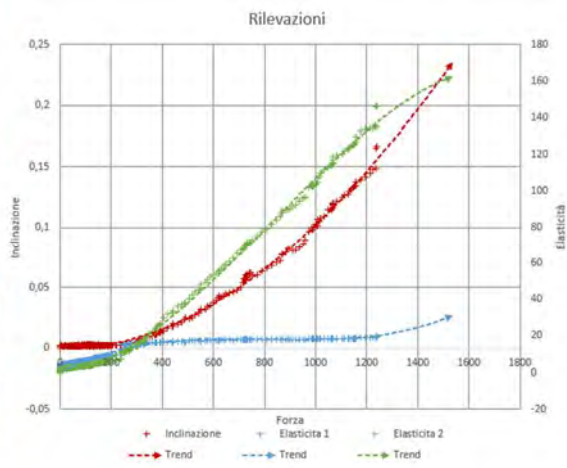


## Appendix 1 – Pulling tests



## Appendix 1 – Pulling tests

Via Vittorio Veneto, Monza – 339 – 9400 – pt2



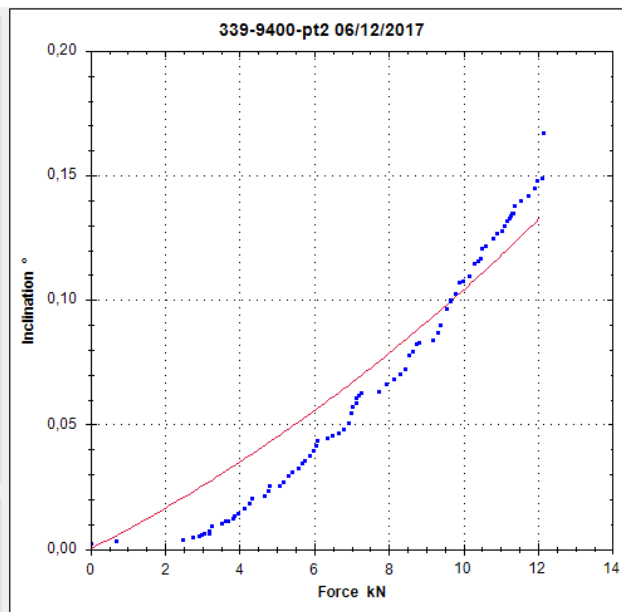
Measurement  
Name: 339-9400-pt2 06/12/2017

Rope height on tree (m): 2.55  
Anchor-tree level difference (m): 0.4  
Anchor-tree distance (m): 9.3  
Drag factor: 0.2  
Wind speed (m/s): 33  
Crown Area (m<sup>2</sup>): 64  
Crown center height (m): 7.1  
Elastic Limit (%): 4.2

Inclino | Elaso1 | Elasto2

Alpha (°) = 0.23  
F\_max (N) = 45785.82  
M\_max (Nm) = 113753.60  
M\_wind (Nm) = 59380.99  
**SF = 1,92**

Filters  
 Tare force at first value  
 Monotonicity for force  
 Monotonicity for inclination



## Appendix 1 – Pulling tests

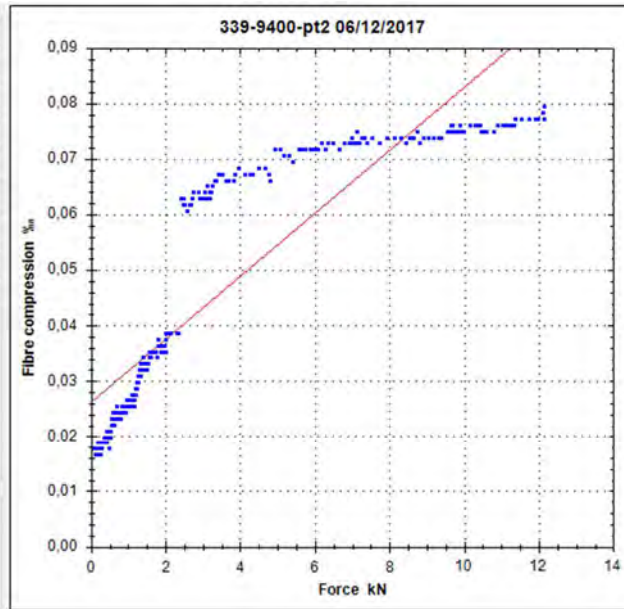
Measurement  
Name: 339-9400-pt2 06/12/2017

Rope height on tree (m): 2,55  
Anchor-tree level difference (m): 0,4  
Anchor-tree distance (m): 9,3  
Drag factor: 0,2  
Wind speed (m/s): 33  
Crown Area (m<sup>2</sup>): 64  
Crown center height (m): 7,1  
Elastic Limit (%): 4,2

Inclino:  Elaso1  Elasto2

Alpha (°) = 0,23  
F\_max (N) = 741409,87  
M\_max (Nm) = 1842012,24  
M\_wind (Nm) = 59380,99  
**SF = 31,02**

Filters  
 Tare force at first value  
 Monotonicity for force  
 Monotonicity for inclination



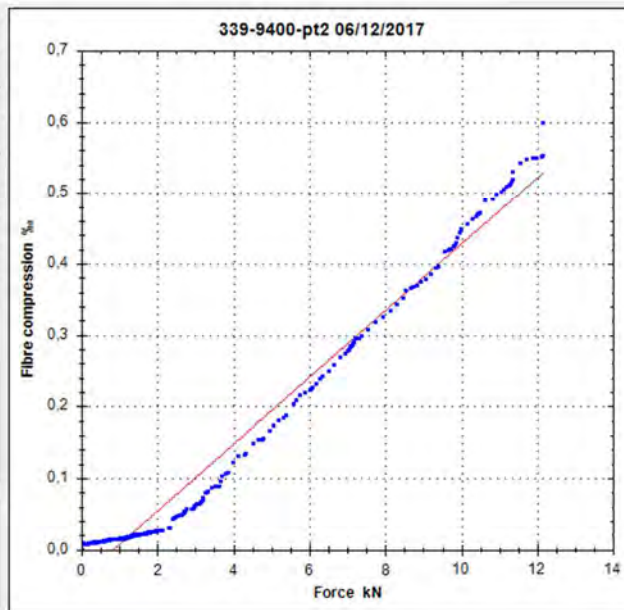
Measurement  
Name: 339-9400-pt2 06/12/2017

Rope height on tree (m): 2,55  
Anchor-tree level difference (m): 0,4  
Anchor-tree distance (m): 9,3  
Drag factor: 0,2  
Wind speed (m/s): 33  
Crown Area (m<sup>2</sup>): 64  
Crown center height (m): 7,1  
Elastic Limit (%): 4,2

Inclino:  Elaso1  Elasto2

Alpha (°) = 0,23  
F\_max (N) = 89939,08  
M\_max (Nm) = 223451,16  
M\_wind (Nm) = 59380,99  
**SF = 3,76**

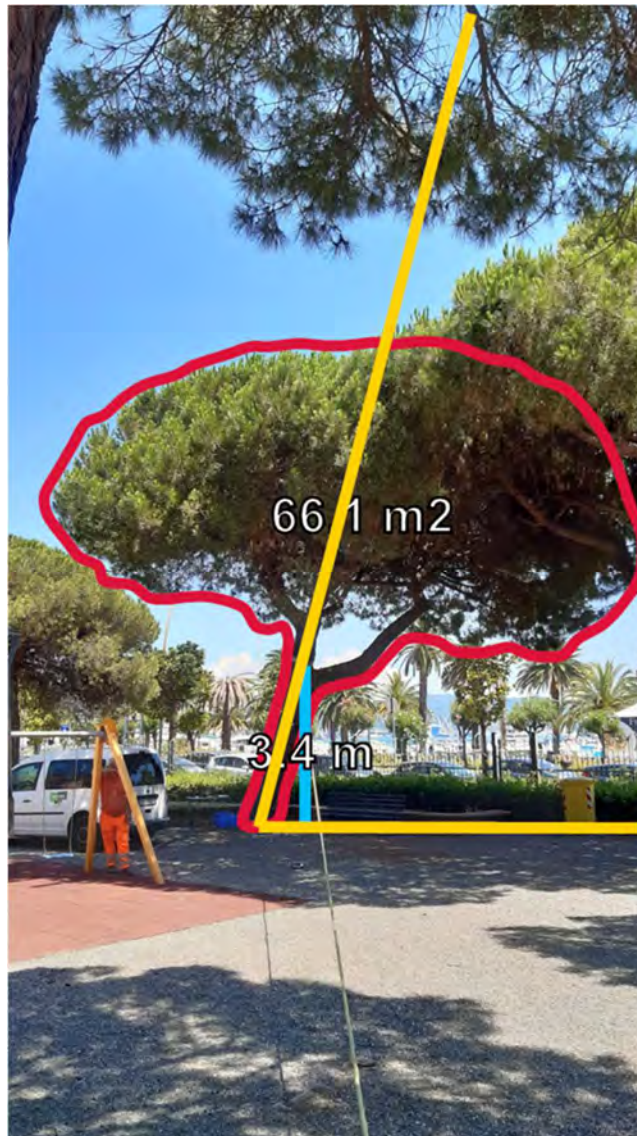
Filters  
 Tare force at first value  
 Monotonicity for force  
 Monotonicity for inclination



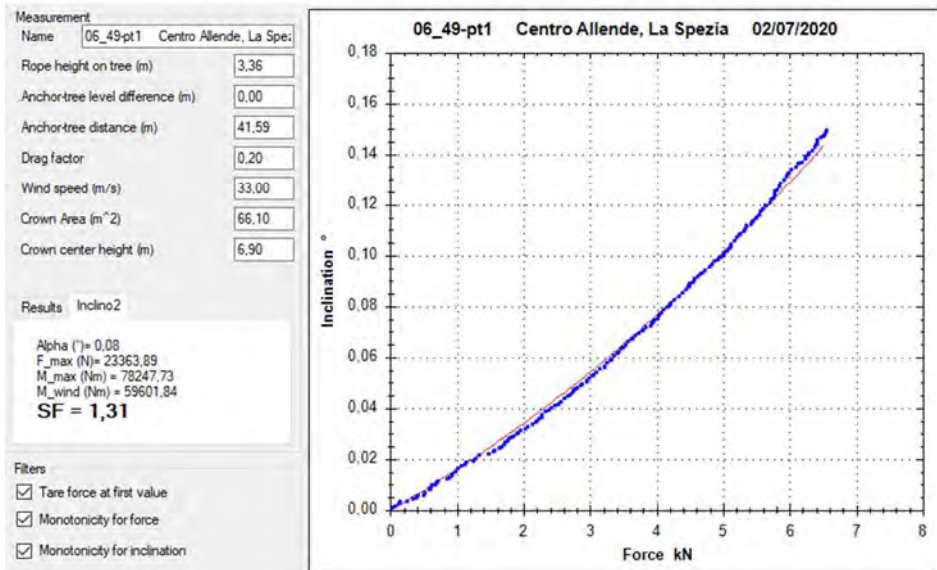
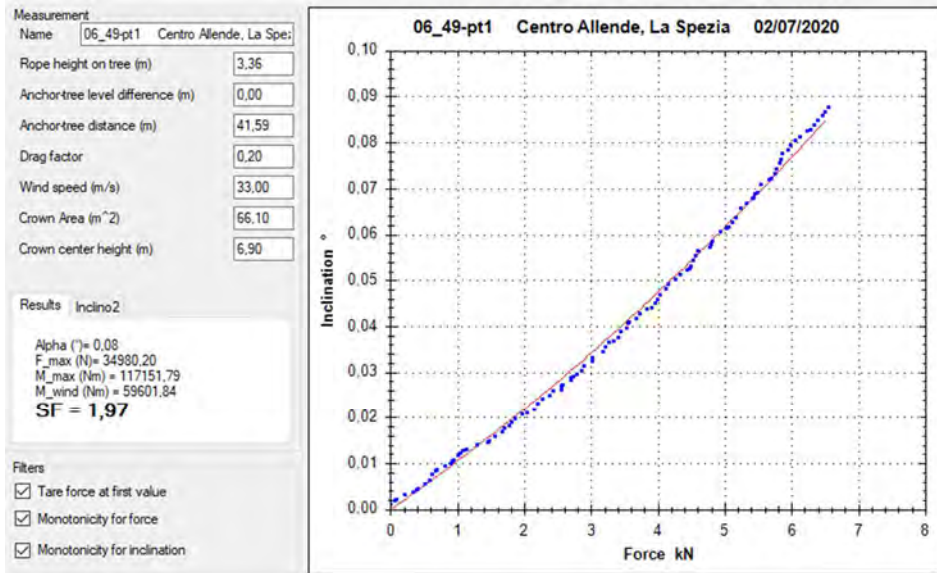
Appendix 1 – Pulling tests

---

Centro Allende, La Spezia – 06\_49 – pt1



## Appendix 1 – Pulling tests



Appendix 1 – Pulling tests

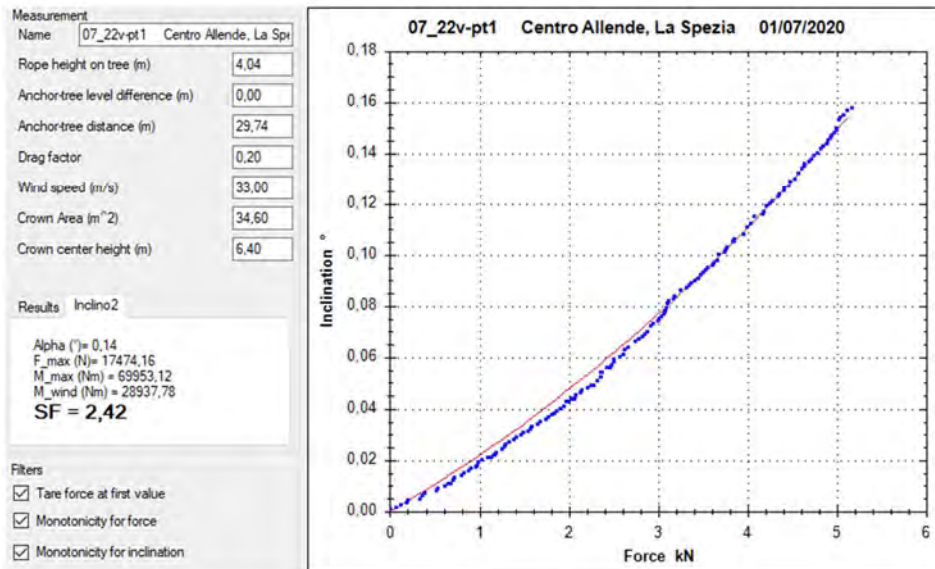
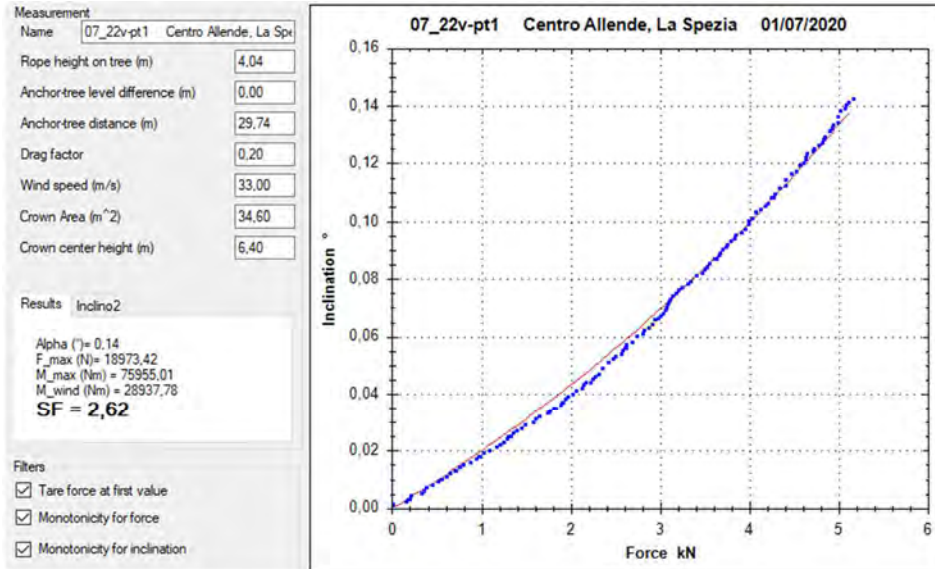
---

Centro Allende, La Spezia – 07\_22v – pt1





## Appendix 1 – Pulling tests



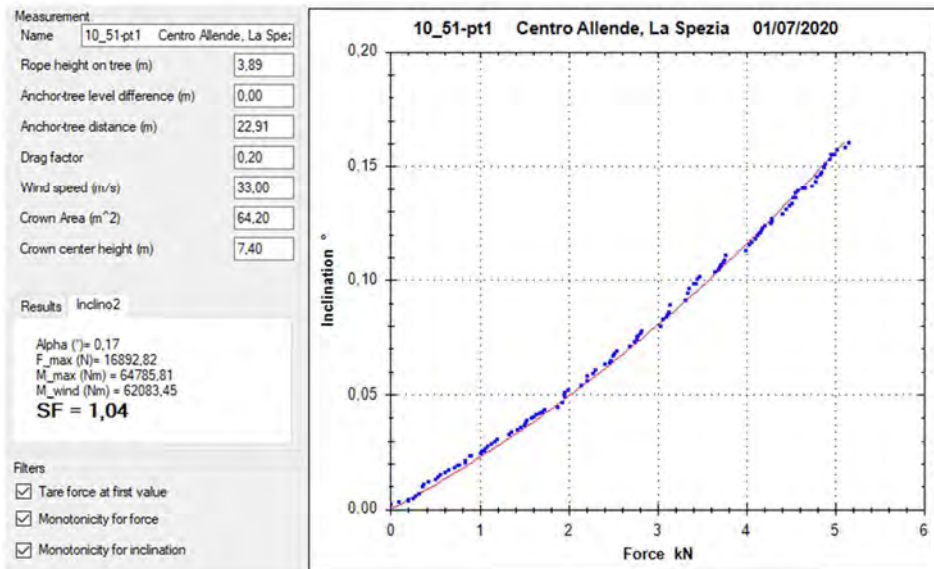
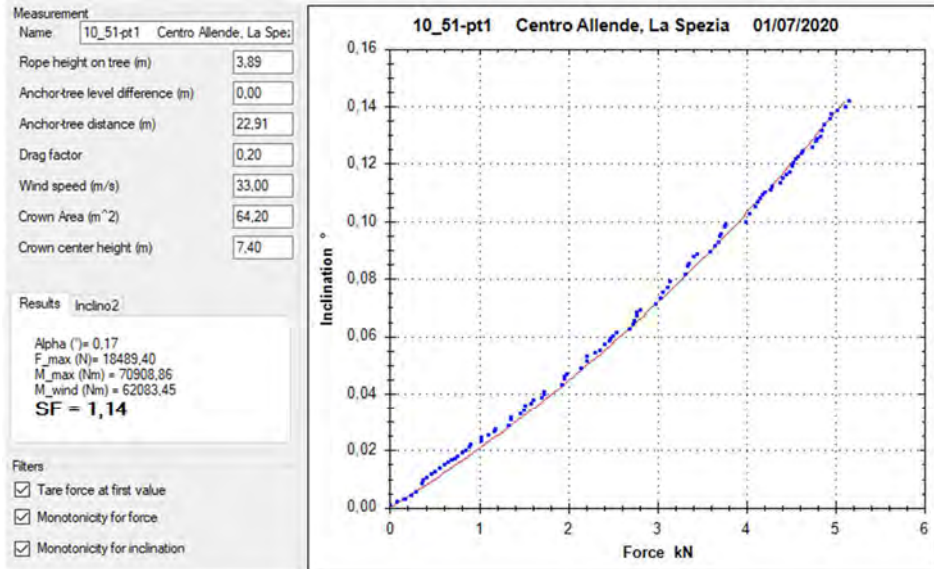
Appendix 1 – Pulling tests

---

Centro Allende, La Spezia – 10\_51 – pt1



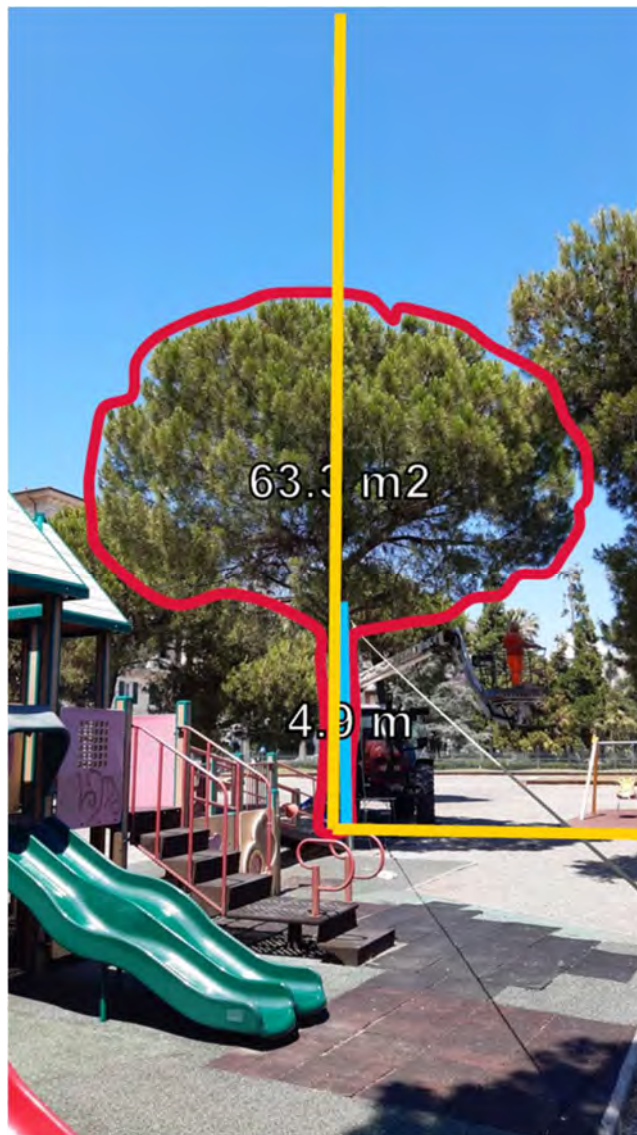
## Appendix 1 – Pulling tests



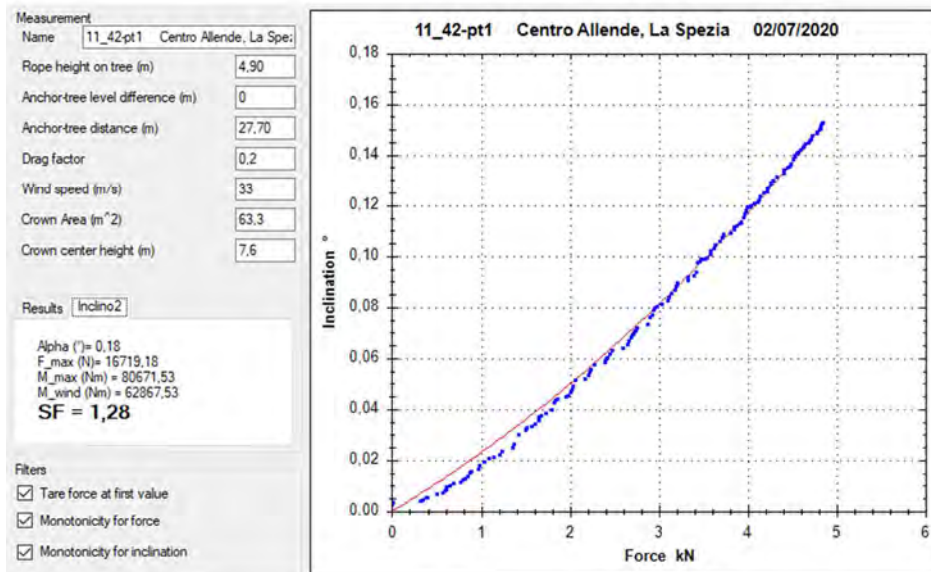
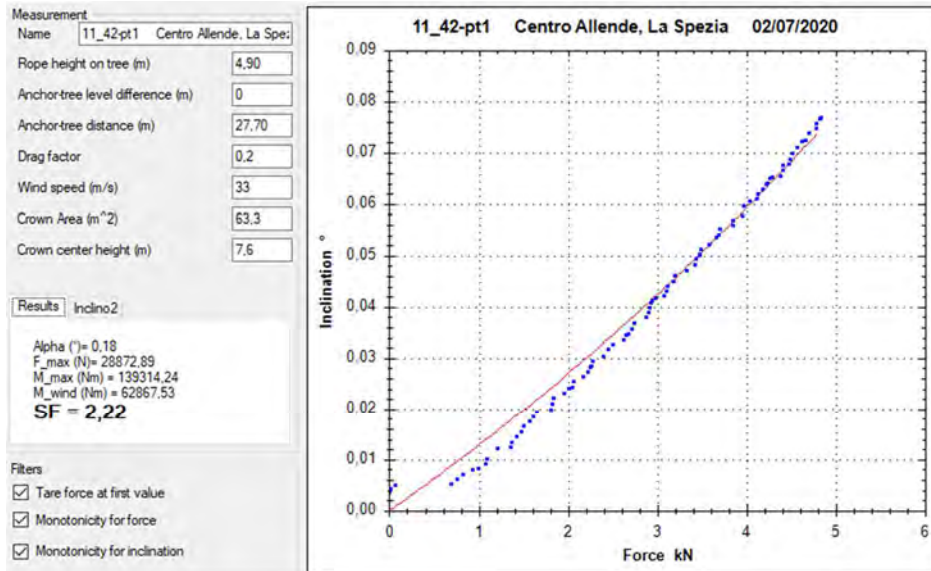
Appendix 1 – Pulling tests

---

Centro Allende, La Spezia – 11\_42 – pt1



## Appendix 1 – Pulling tests



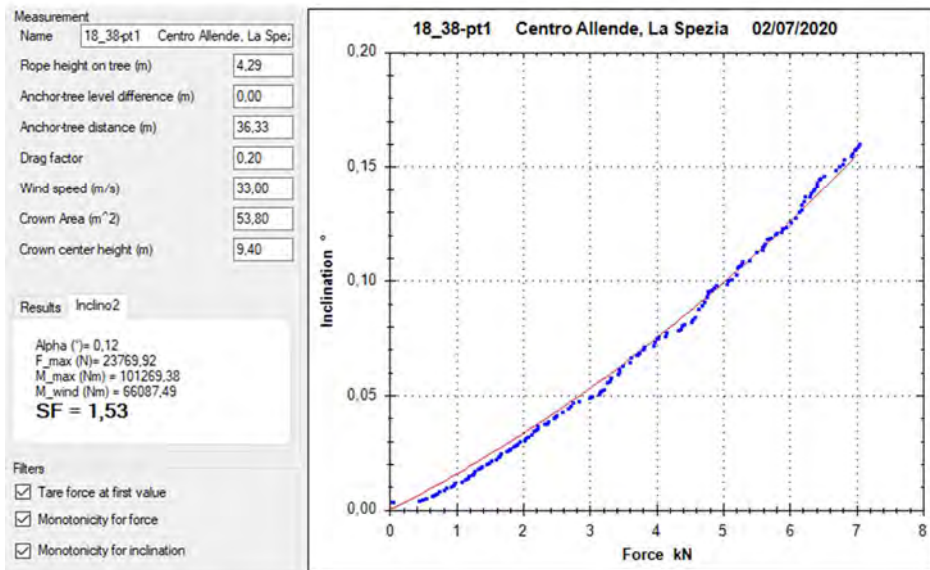
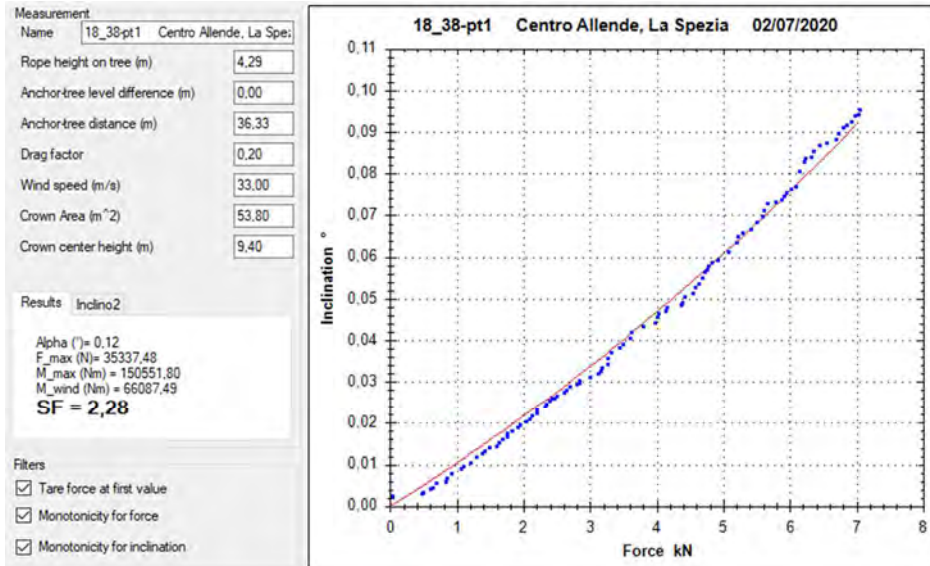
Appendix 1 – Pulling tests

---

Centro Allende, La Spezia – 18\_38 – pt1



## Appendix 1 – Pulling tests



Appendix 1 – Pulling tests

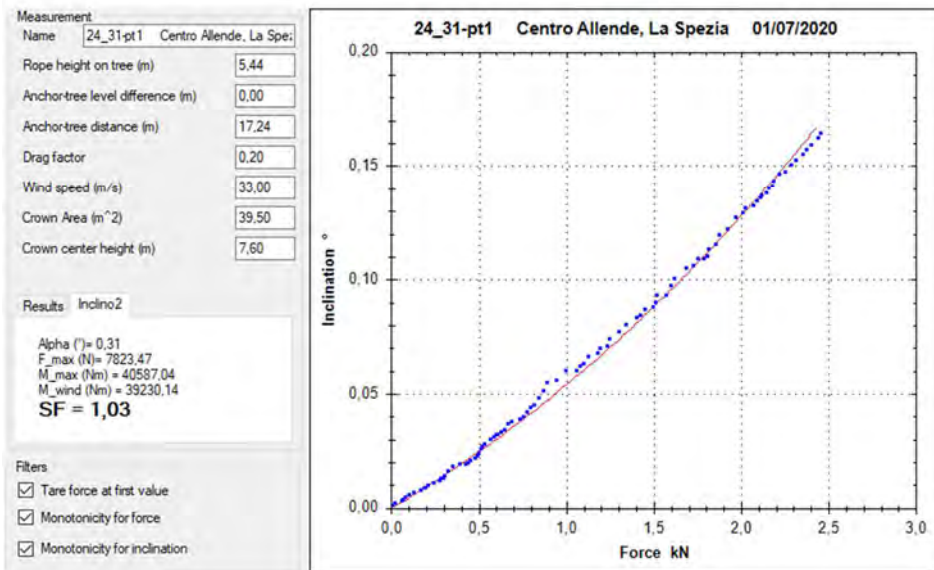
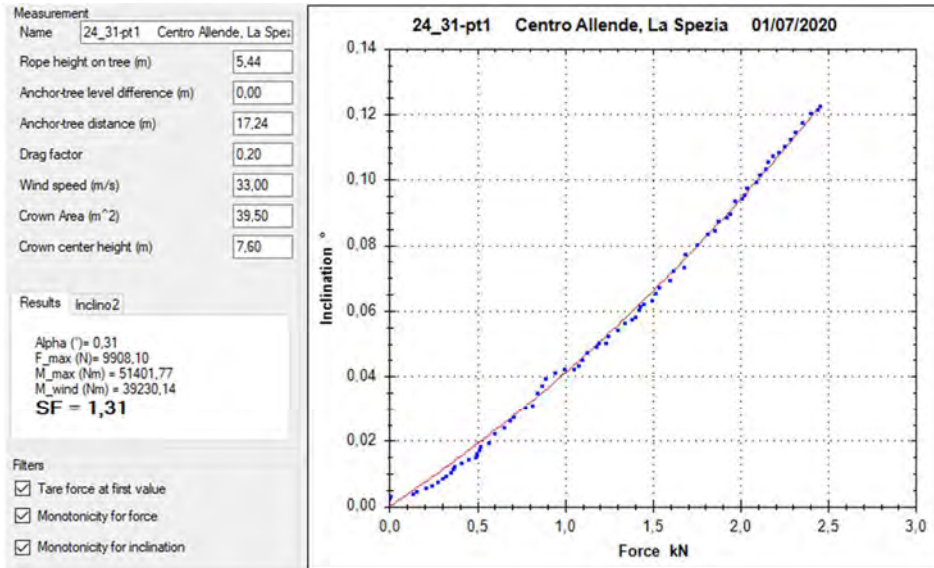
---

Centro Allende, La Spezia – 24\_31 – pt1





## Appendix 1 – Pulling tests



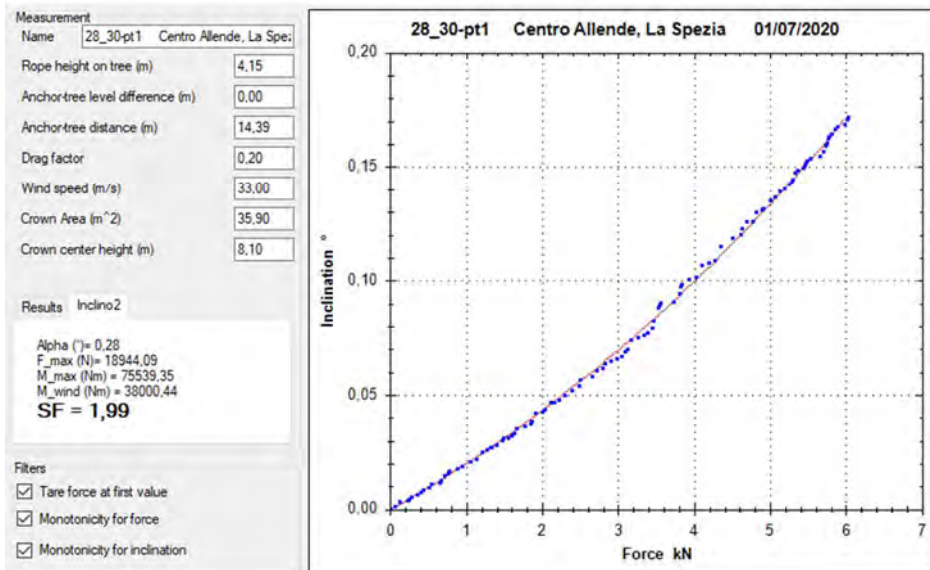
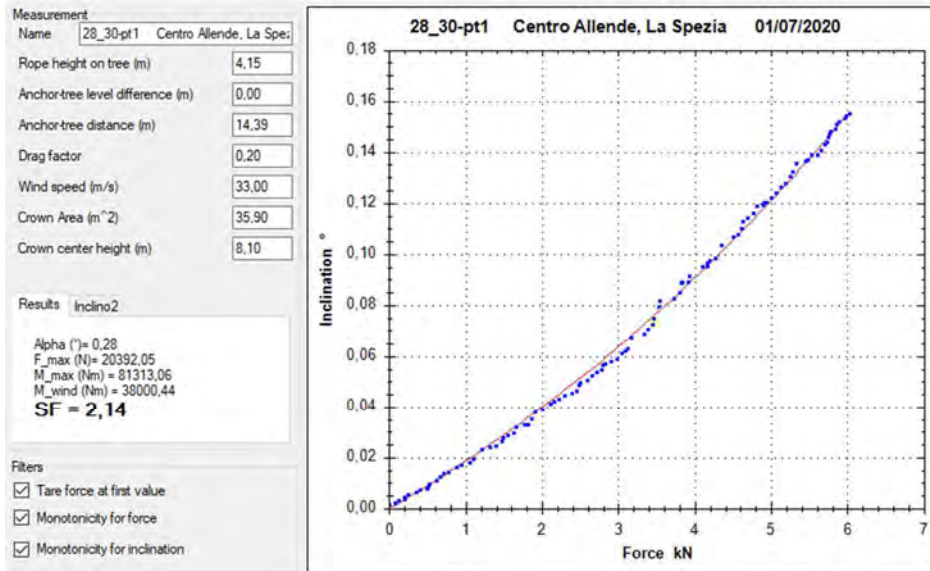
Appendix 1 – Pulling tests

---

Centro Allende, La Spezia – 28\_30 – pt1



## Appendix 1 – Pulling tests



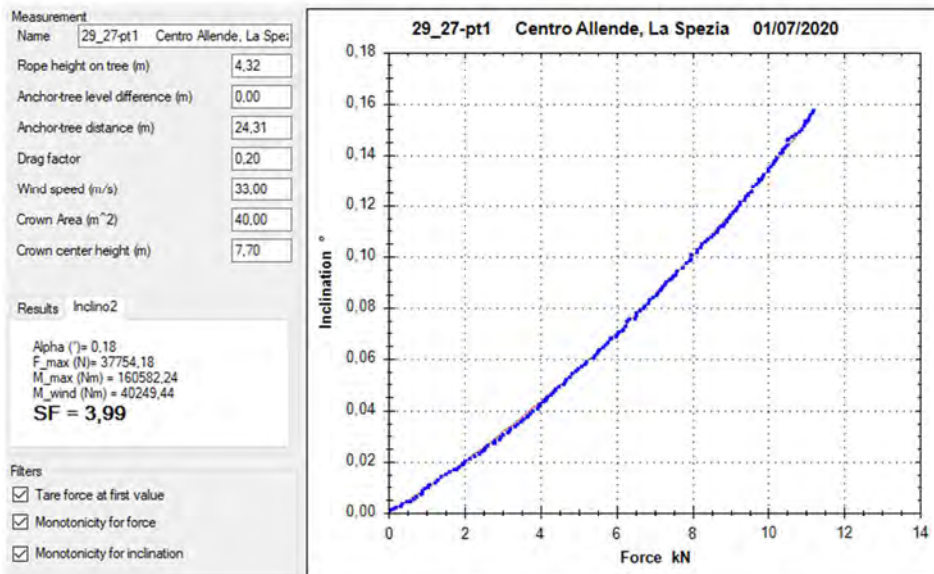
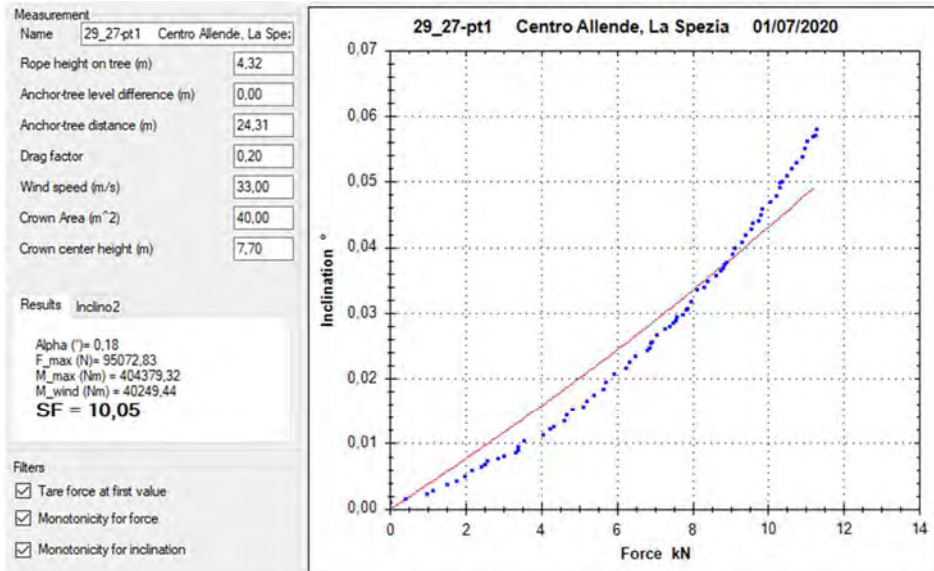
Appendix 1 – Pulling tests

---

Centro Allende, La Spezia – 29\_27 – pt1



## Appendix 1 – Pulling tests



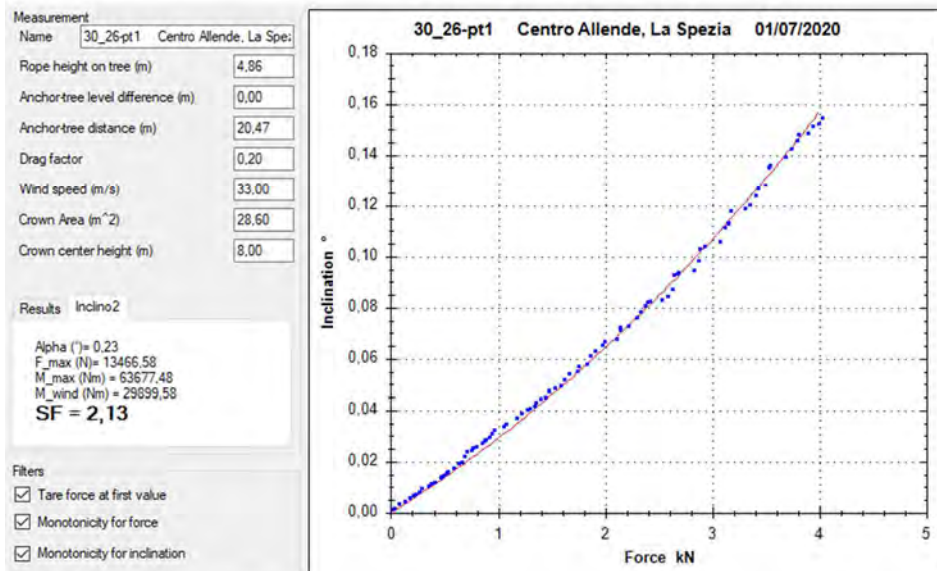
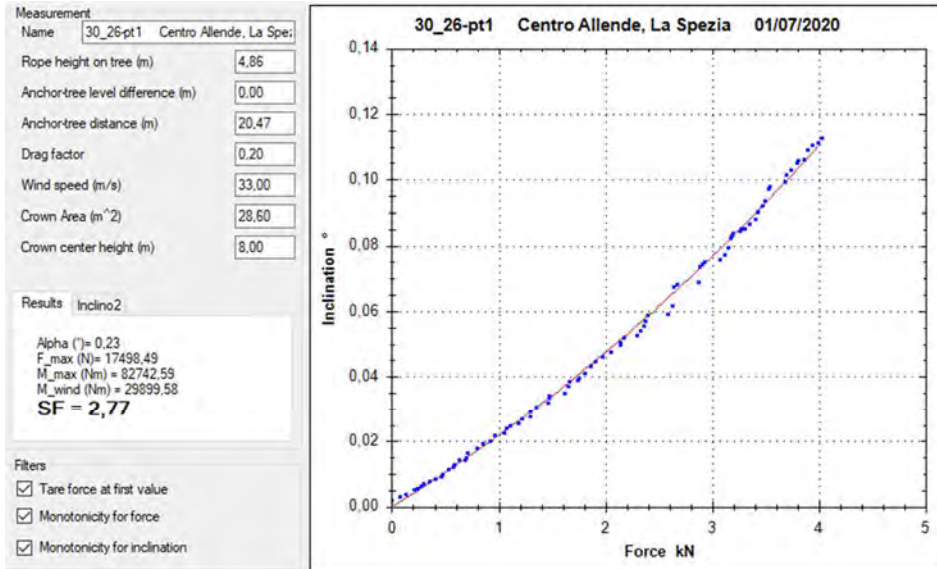
Appendix 1 – Pulling tests

---

Centro Allende, La Spezia – 30\_26 – pt1



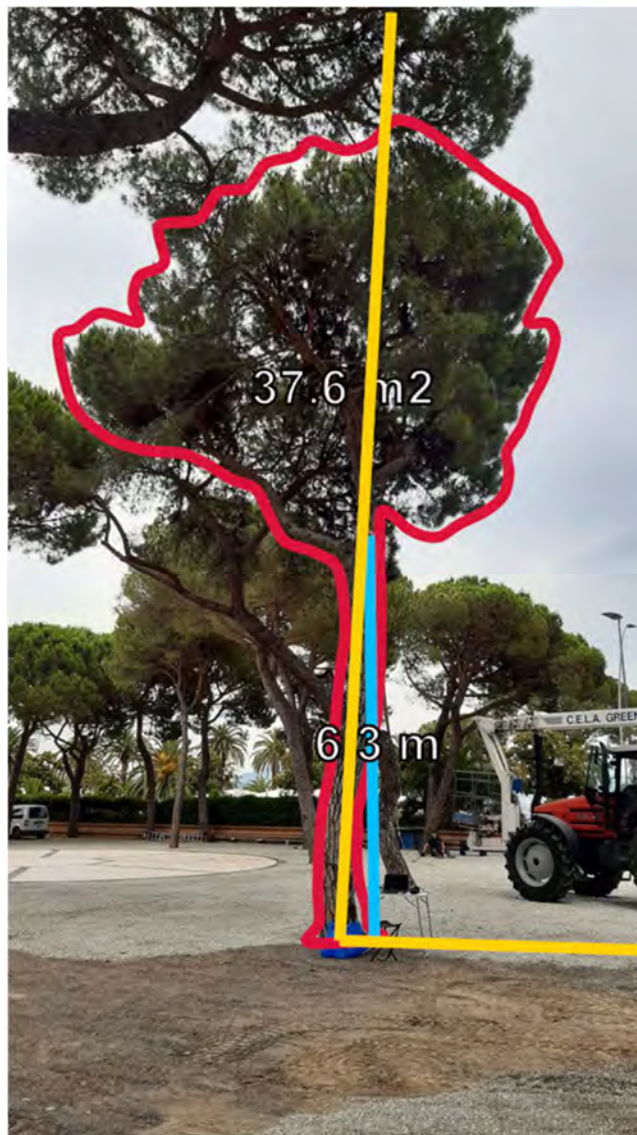
## Appendix 1 – Pulling tests



Appendix 1 – Pulling tests

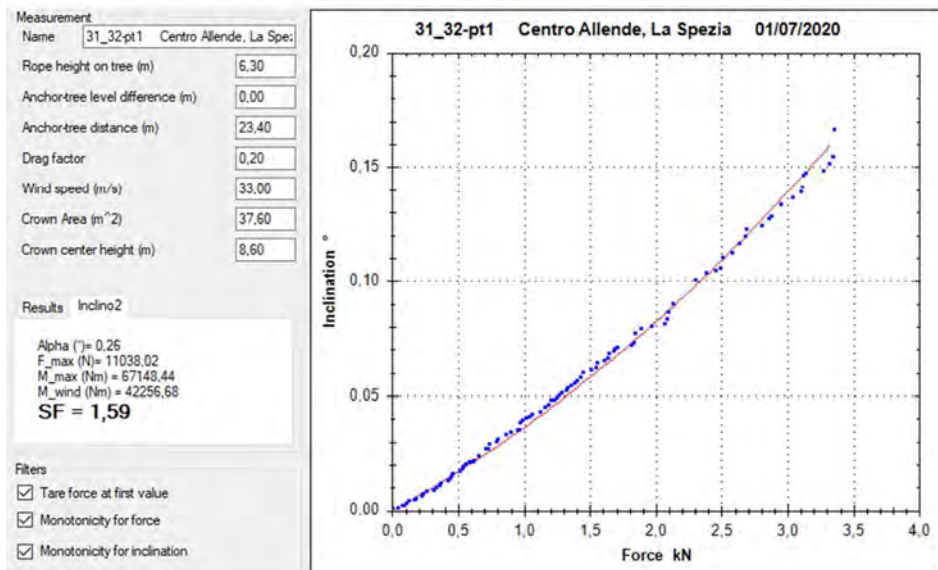
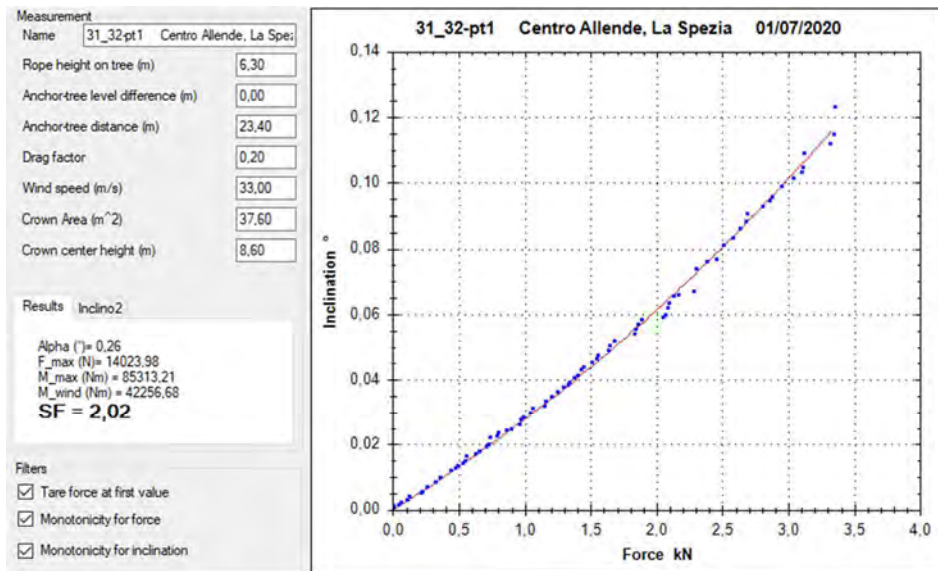
---

Centro Allende, La Spezia – 31\_32 – pt1





## Appendix 1 – Pulling tests



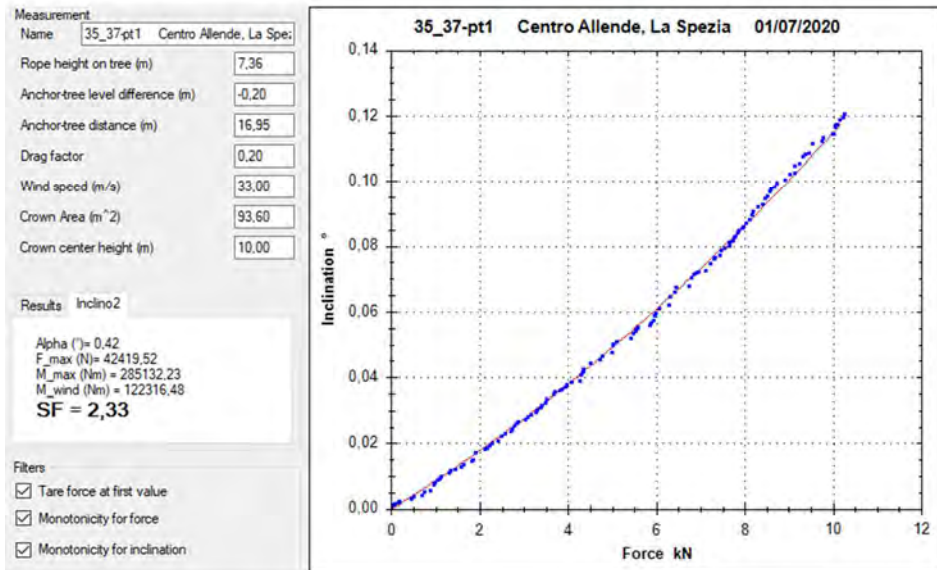
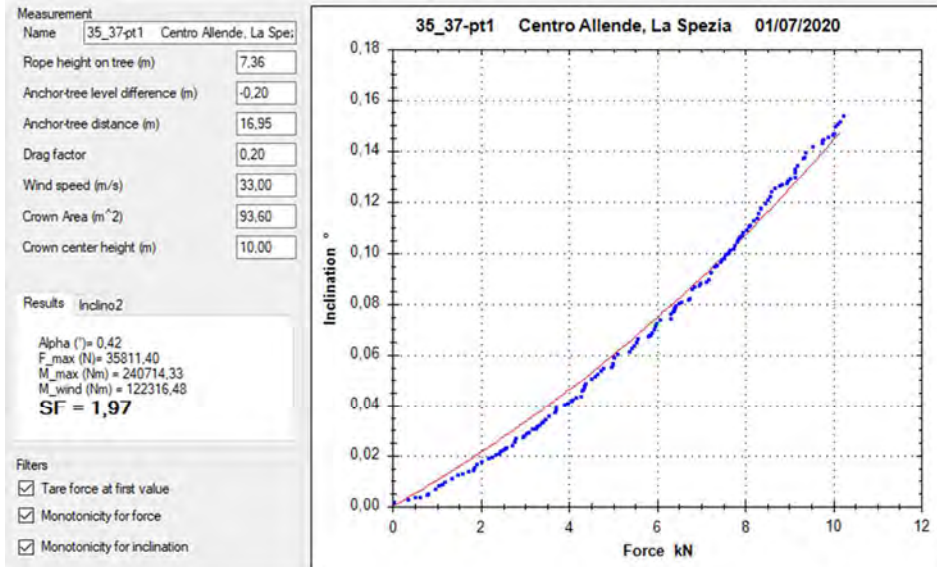
Appendix 1 – Pulling tests

---

Centro Allende, La Spezia – 35\_37 – pt1



## Appendix 1 – Pulling tests



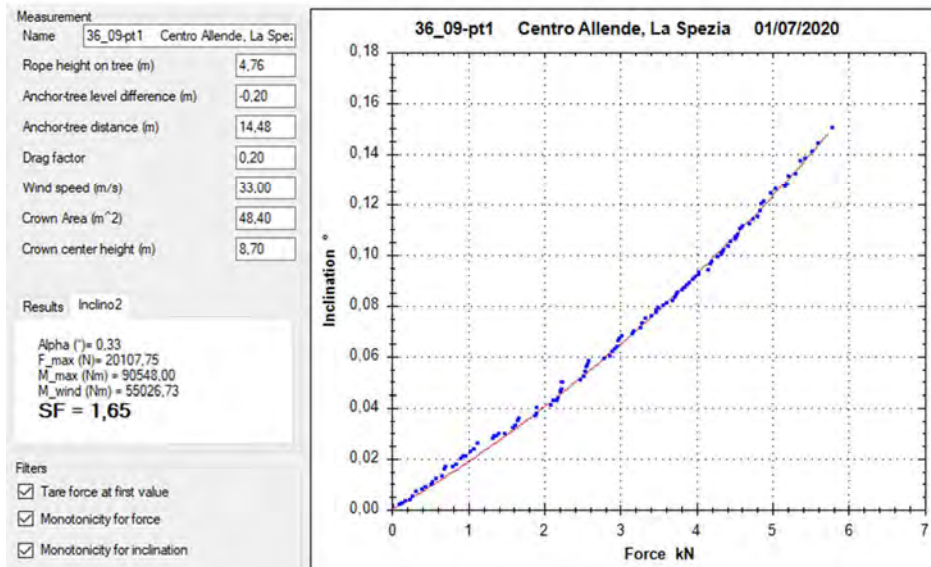
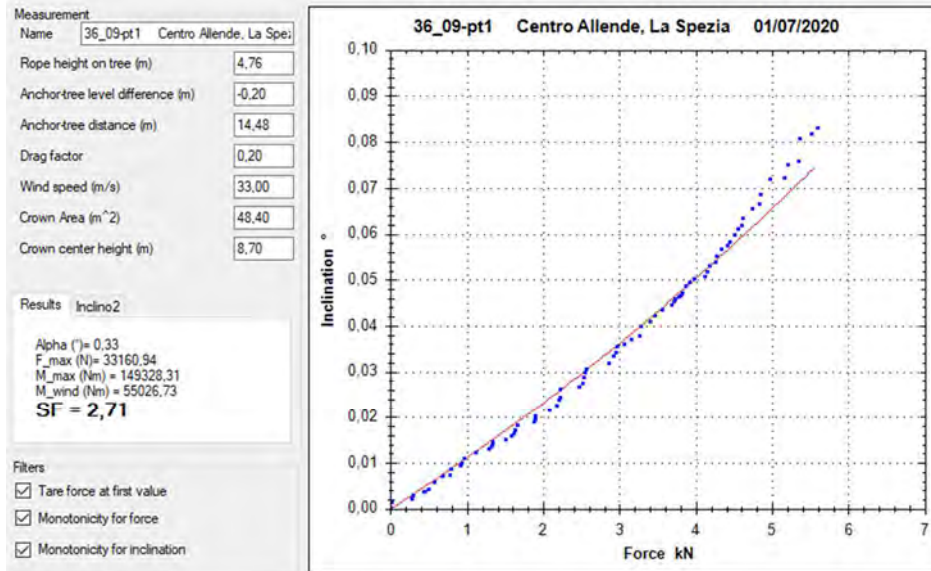
Appendix 1 – Pulling tests

---

Centro Allende, La Spezia – 36\_09 – pt1



## Appendix 1 – Pulling tests



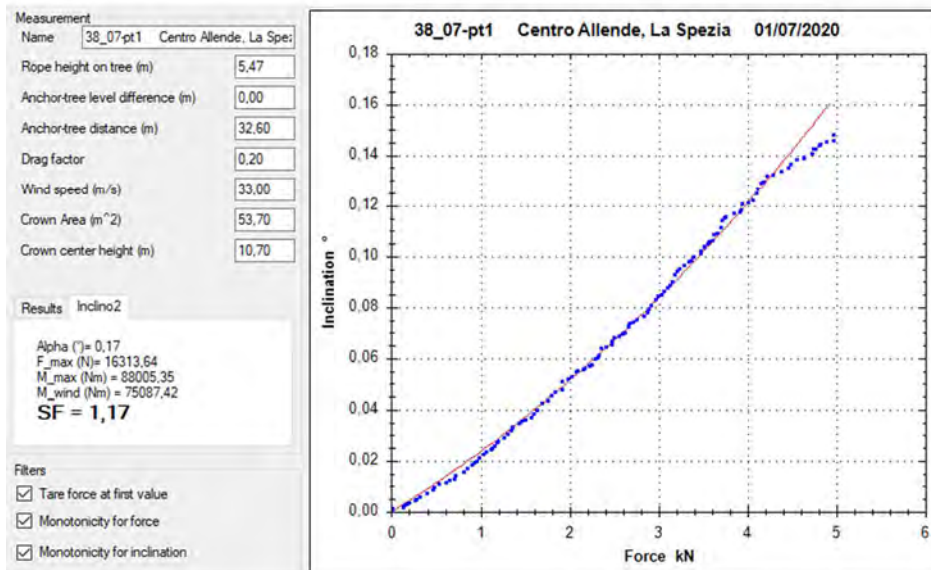
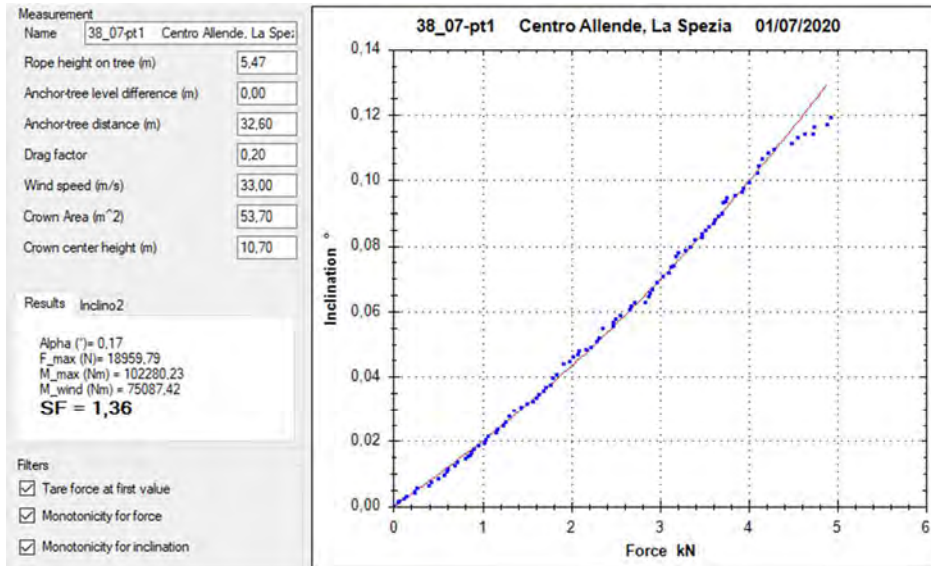
Appendix 1 – Pulling tests

---

Centro Allende, La Spezia – 38\_07 – pt1



## Appendix 1 – Pulling tests



Appendix 1 – Pulling tests

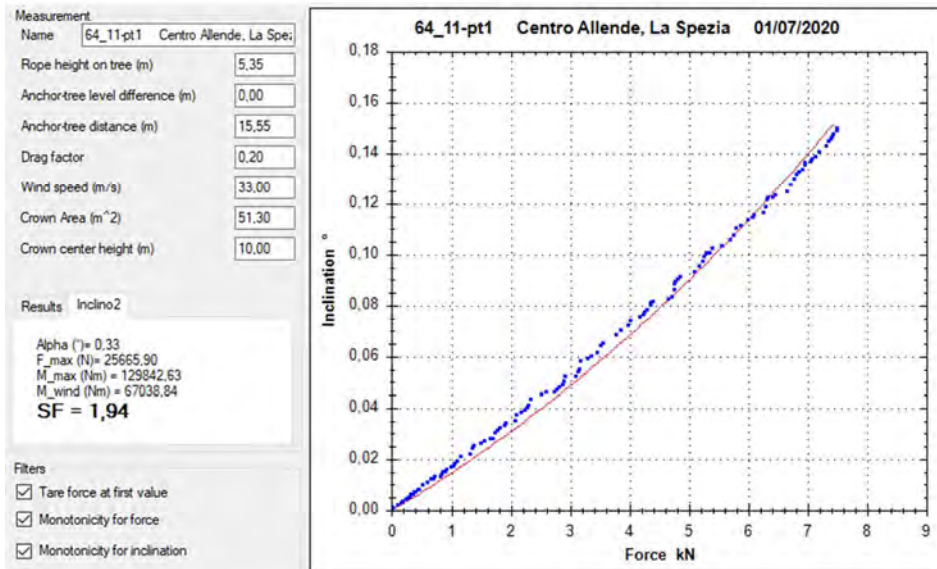
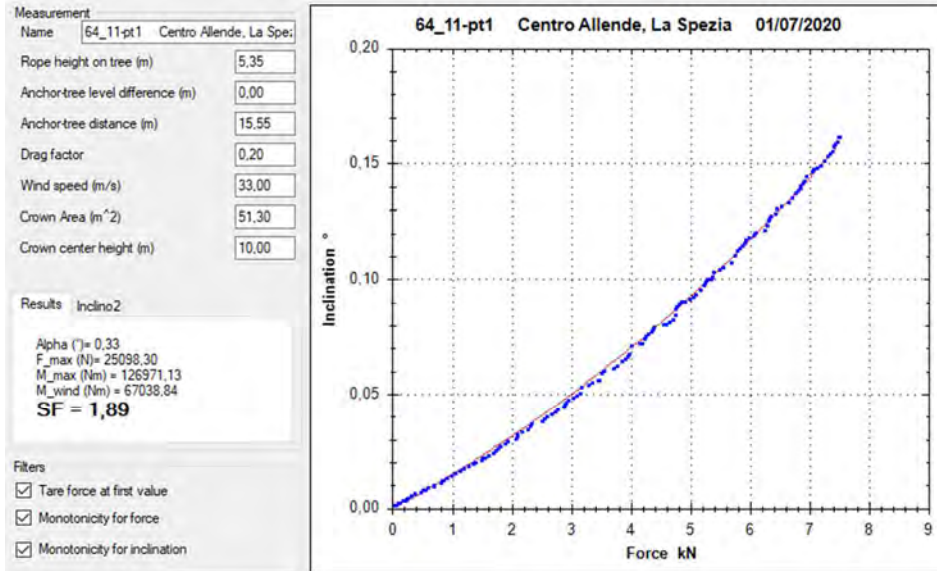
---

Centro Allende, La Spezia – 64\_11 – pt1





## Appendix 1 – Pulling tests



Appendix 1 – Pulling tests

---

Centro Allende, La Spezia – 65\_38v – pt1



## Appendix 1 – Pulling tests

Measurement

Name  Centro Allende, La Spezia

Rope height on tree (m)

Anchor-tree level difference (m)

Anchor-tree distance (m)

Drag factor

Wind speed (m/s)

Crown Area (m<sup>2</sup>)

Crown center height (m)

Results Incino2

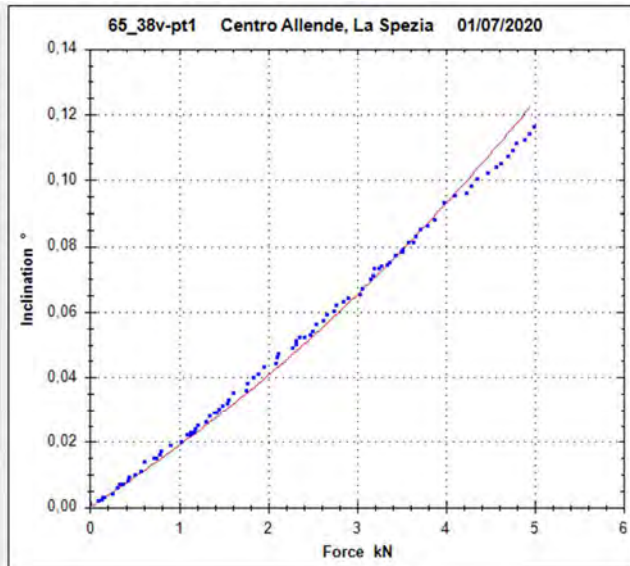
Alpha (°)= 0,28  
 F<sub>max</sub> (N)= 20023,09  
 M<sub>max</sub> (Nm) = 99739,10  
 M<sub>wind</sub> (Nm) = 84670,19  
**SF = 1,18**

Filters

Tare force at first value

Monotonicity for force

Monotonicity for inclination



Measurement

Name  Centro Allende, La Spezia

Rope height on tree (m)

Anchor-tree level difference (m)

Anchor-tree distance (m)

Drag factor

Wind speed (m/s)

Crown Area (m<sup>2</sup>)

Crown center height (m)

Results Incino2

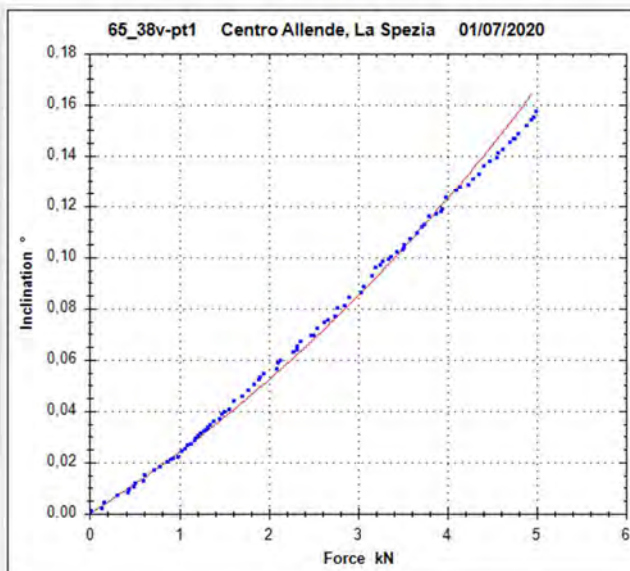
Alpha (°)= 0,28  
 F<sub>max</sub> (N)= 16128,33  
 M<sub>max</sub> (Nm) = 80338,47  
 M<sub>wind</sub> (Nm) = 84670,19  
**SF = 0,95**

Filters

Tare force at first value

Monotonicity for force

Monotonicity for inclination



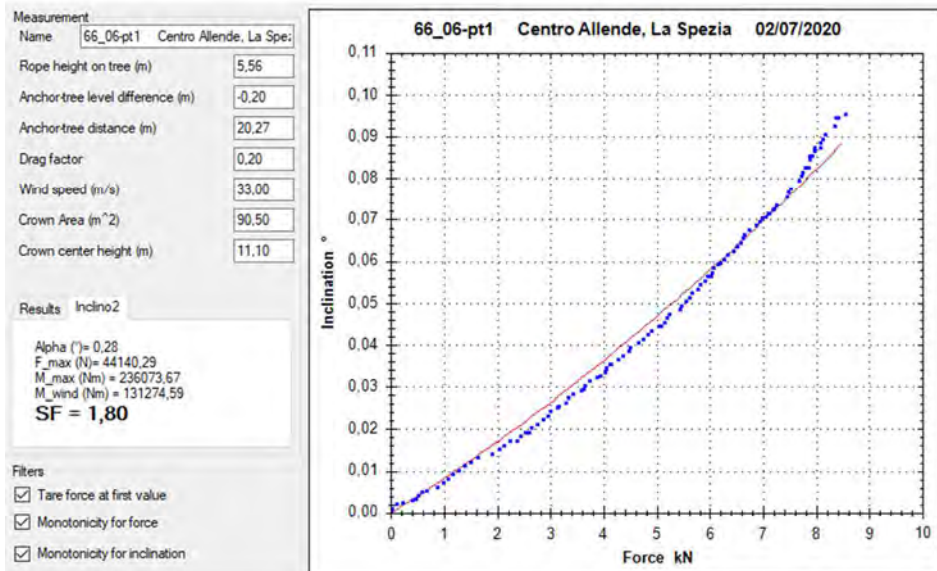
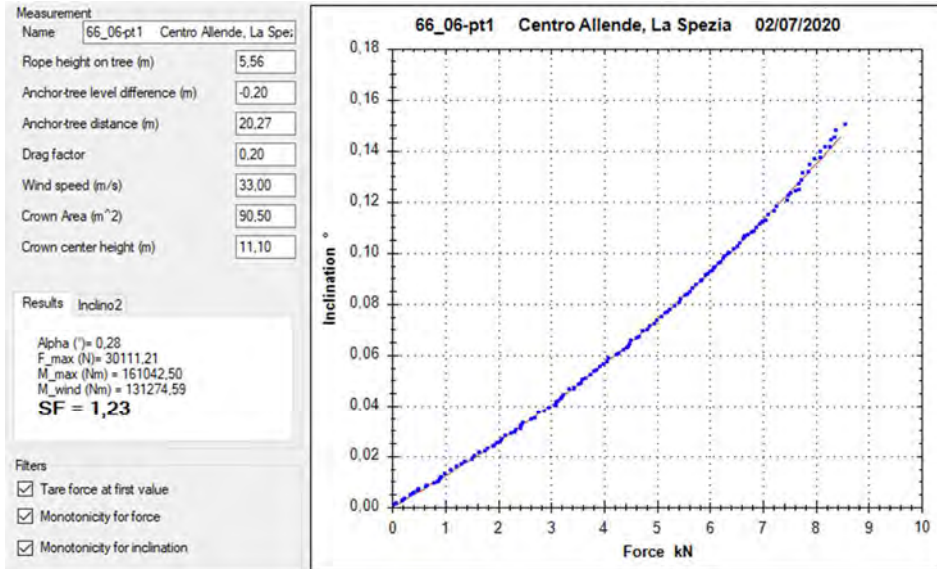
Appendix 1 – Pulling tests

---

Centro Allende, La Spezia – 66\_06 – pt1



## Appendix 1 – Pulling tests



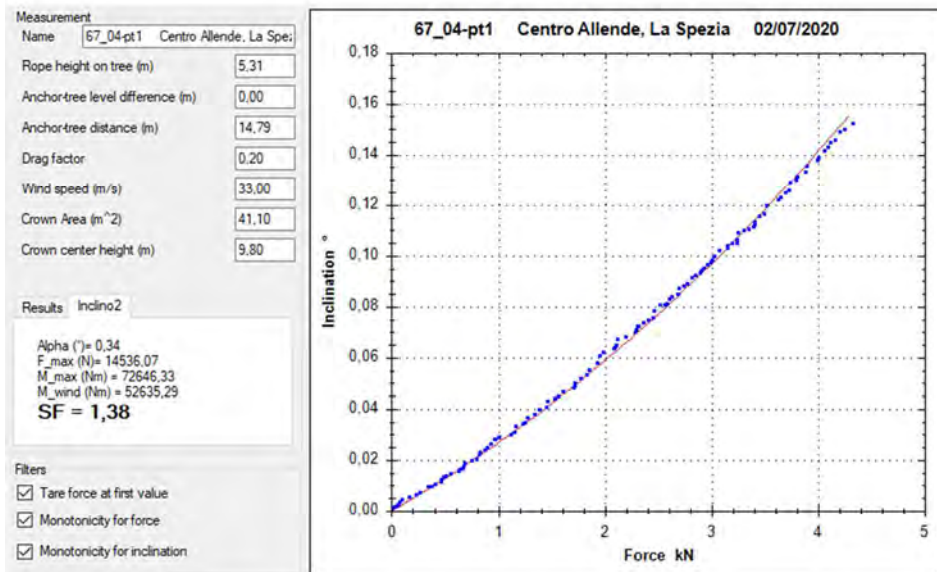
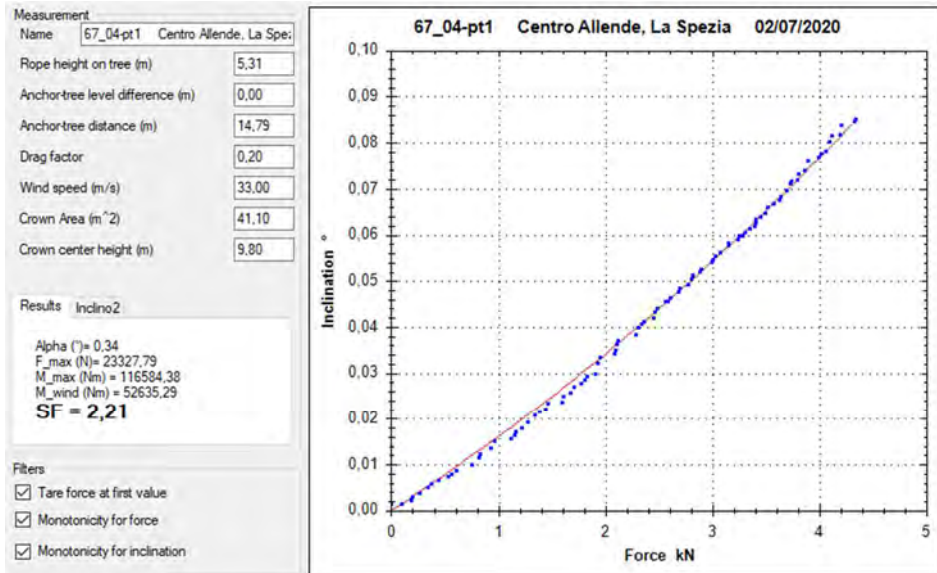
Appendix 1 – Pulling tests

---

Centro Allende, La Spezia – 67\_04 – pt1



## Appendix 1 – Pulling tests



Appendix 1 – Pulling tests

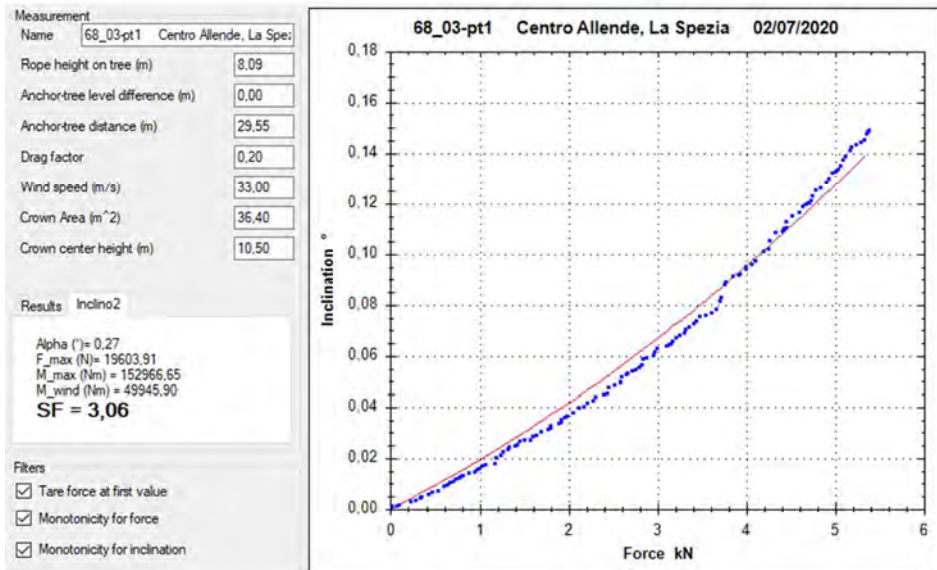
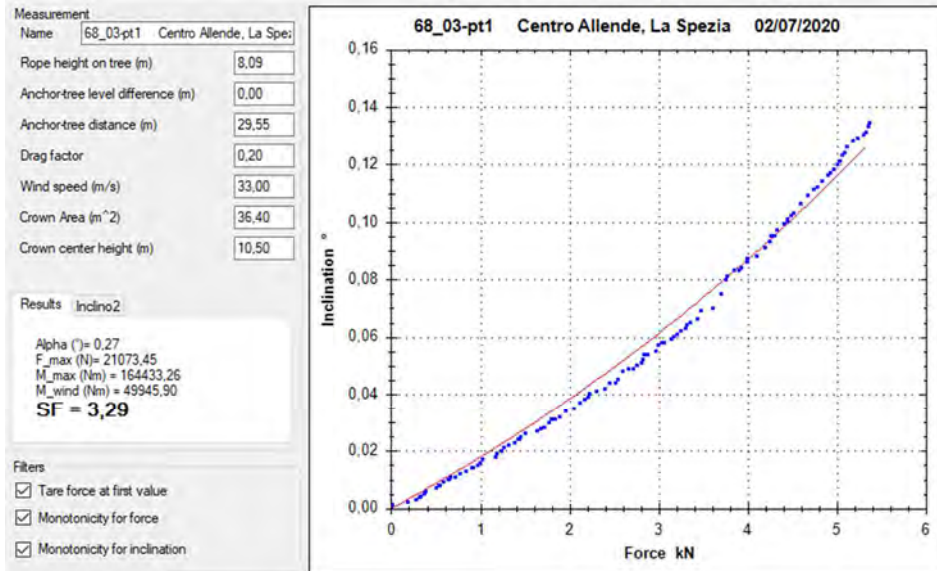
---

Centro Allende, La Spezia – 68\_03 – pt1





## Appendix 1 – Pulling tests



Appendix 1 – Pulling tests

---

Centro Allende, La Spezia – 69\_02 – pt1



## Appendix 1 – Pulling tests

Measurement

Name 69\_02-pt1 Centro Allende, La Spezia

Rope height on tree (m) 6,78

Anchor-tree level difference (m) 0,00

Anchor-tree distance (m) 27,37

Drag factor 0,20

Wind speed (m/s) 33,00

Crown Area (m<sup>2</sup>) 62,70

Crown center height (m) 11,40

Results Inclino2

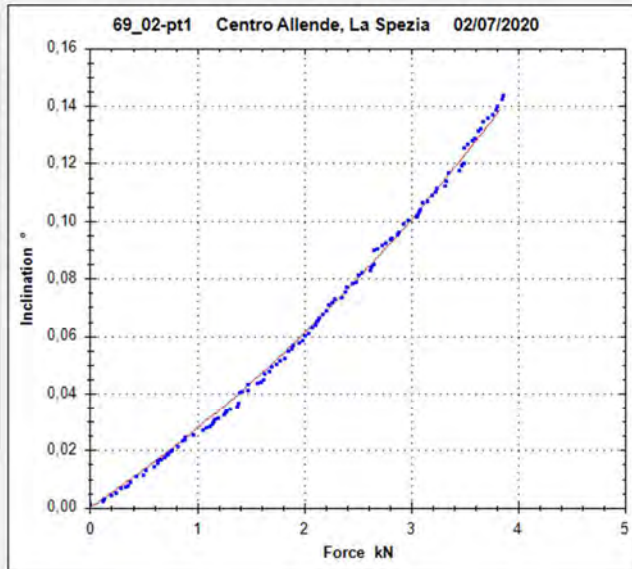
Alpha (°)= 0,24  
 F\_max (N)= 14107,76  
 M\_max (Nm) = 92844,40  
 M\_wind (Nm) = 93407,45  
**SF = 0,99**

Filters

Tare force at first value

Monotonicity for force

Monotonicity for inclination



Measurement

Name 69\_02-pt1 Centro Allende, La Spezia

Rope height on tree (m) 6,78

Anchor-tree level difference (m) 0,00

Anchor-tree distance (m) 27,37

Drag factor 0,20

Wind speed (m/s) 33,00

Crown Area (m<sup>2</sup>) 62,70

Crown center height (m) 11,40

Results Inclino2

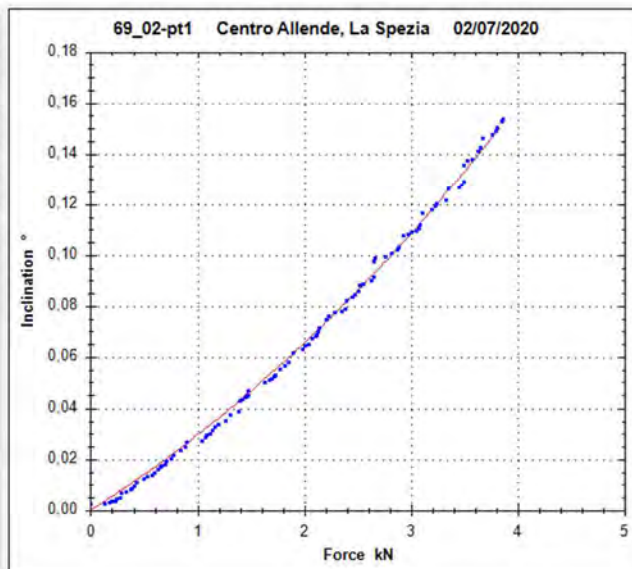
Alpha (°)= 0,24  
 F\_max (N)= 13296,08  
 M\_max (Nm) = 87502,67  
 M\_wind (Nm) = 93407,45  
**SF = 0,94**

Filters

Tare force at first value

Monotonicity for force

Monotonicity for inclination



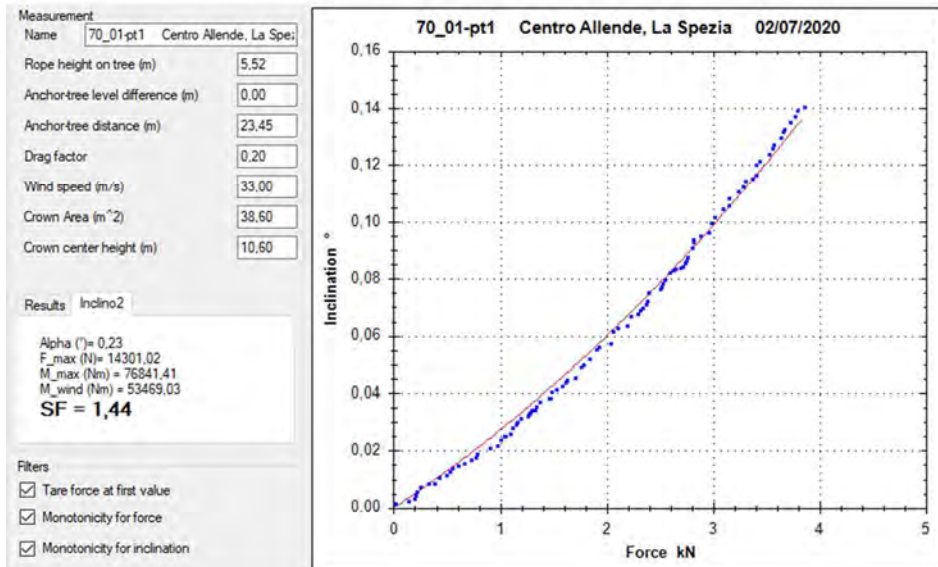
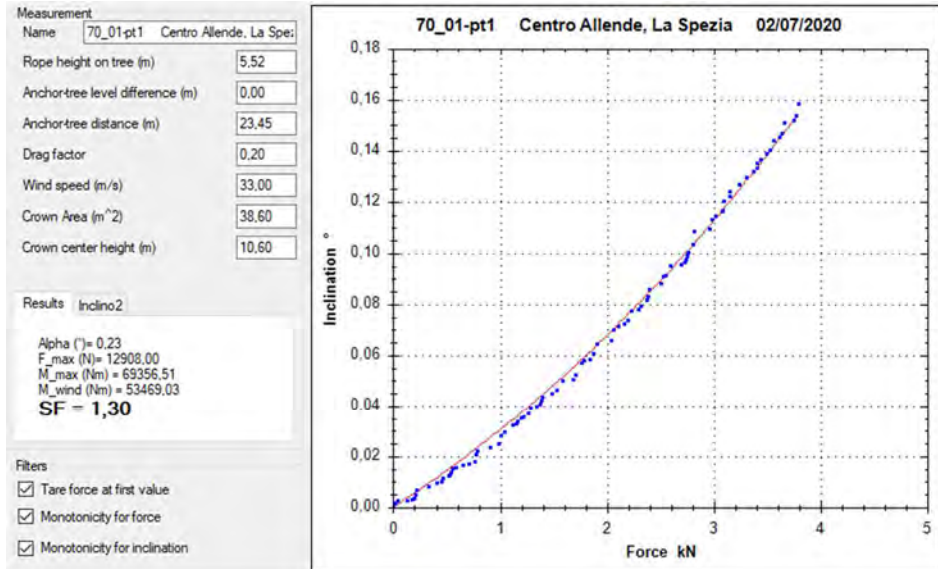
Appendix 1 – Pulling tests

---

Centro Allende, La Spezia – 70\_01 – pt1



## Appendix 1 – Pulling tests



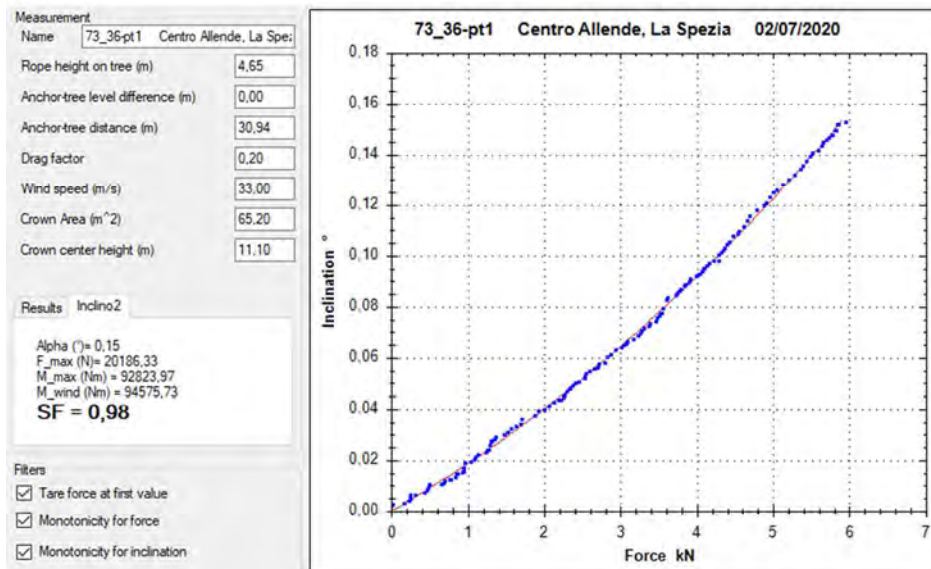
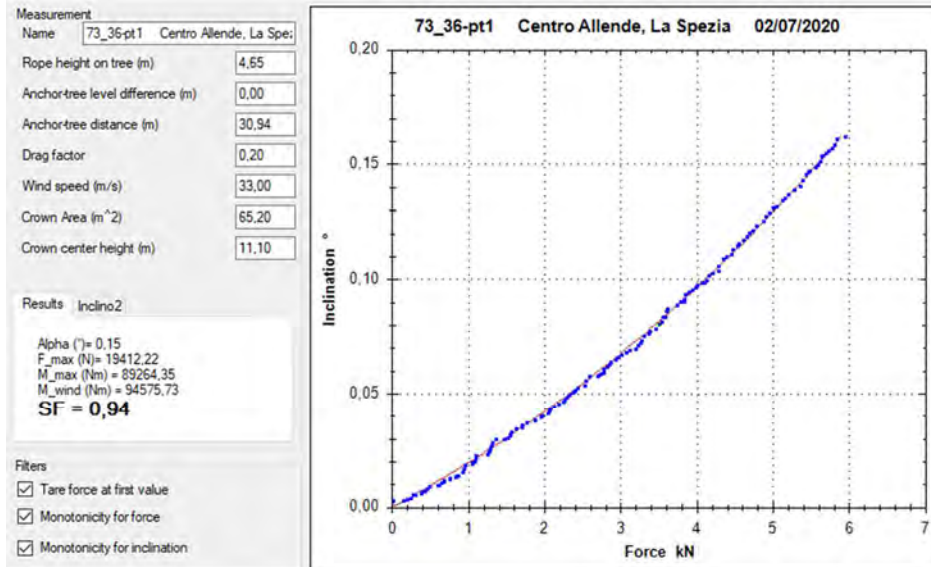
Appendix 1 – Pulling tests

---

Centro Allende, La Spezia – 73\_36 – pt1



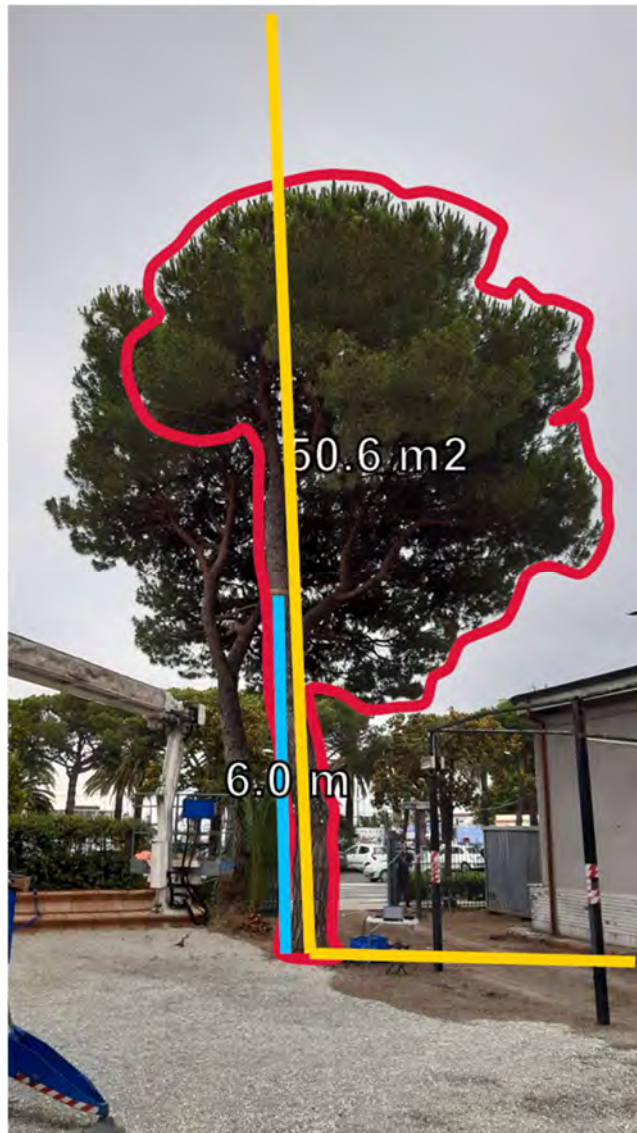
## Appendix 1 – Pulling tests



Appendix 1 – Pulling tests

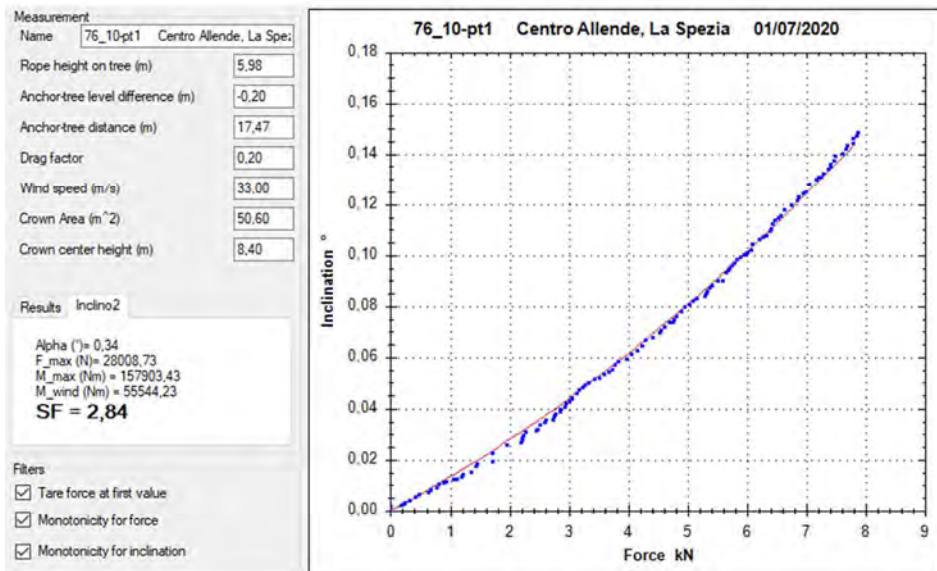
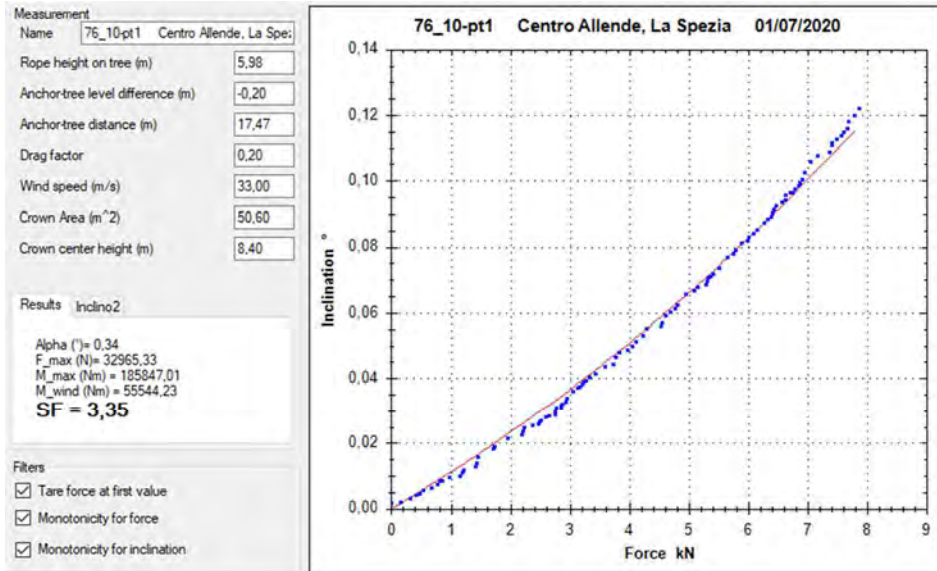
---

Centro Allende, La Spezia – 76\_10 – pt1





## Appendix 1 – Pulling tests



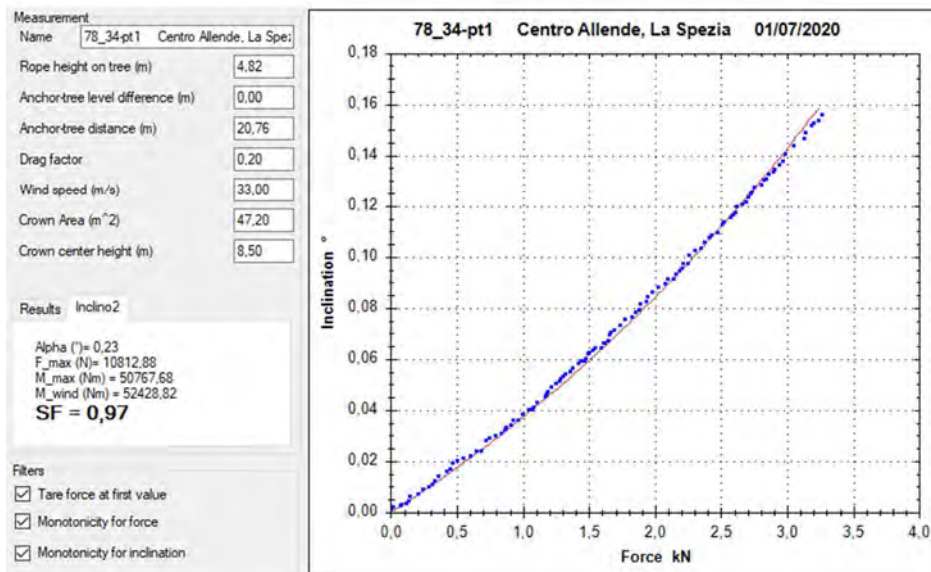
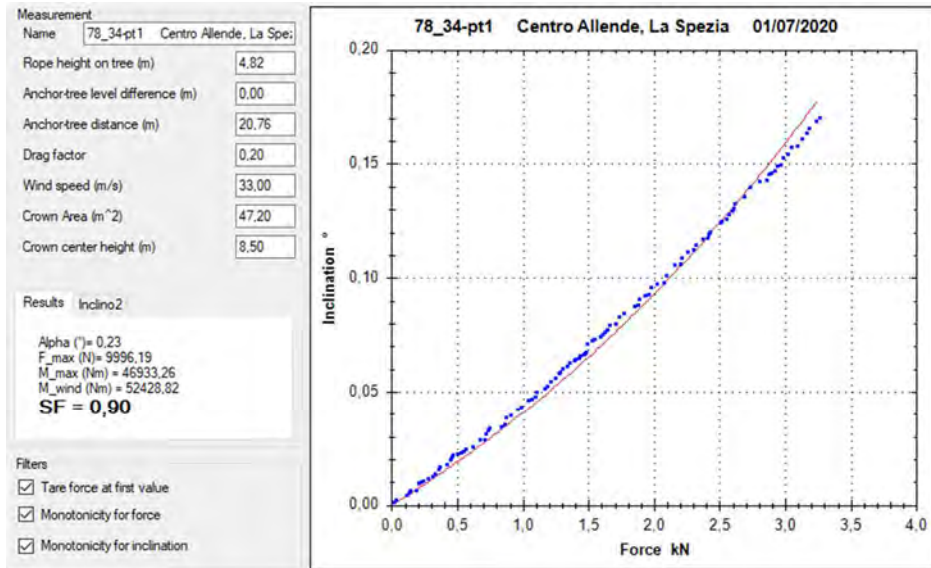
Appendix 1 – Pulling tests

---

Centro Allende, La Spezia – 78\_34 – pt1



## Appendix 1 – Pulling tests



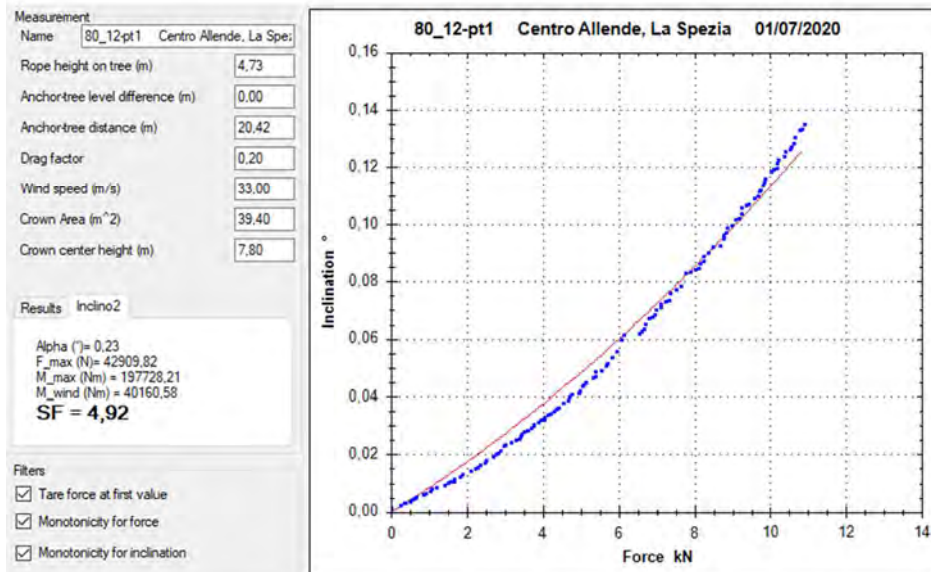
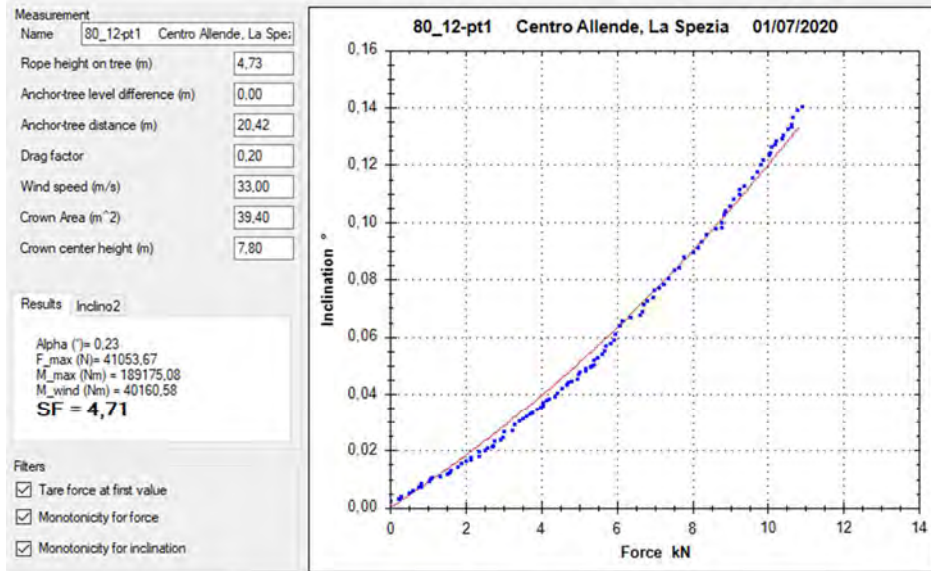
Appendix 1 – Pulling tests

---

Centro Allende, La Spezia – 80\_12 – pt1



## Appendix 1 – Pulling tests



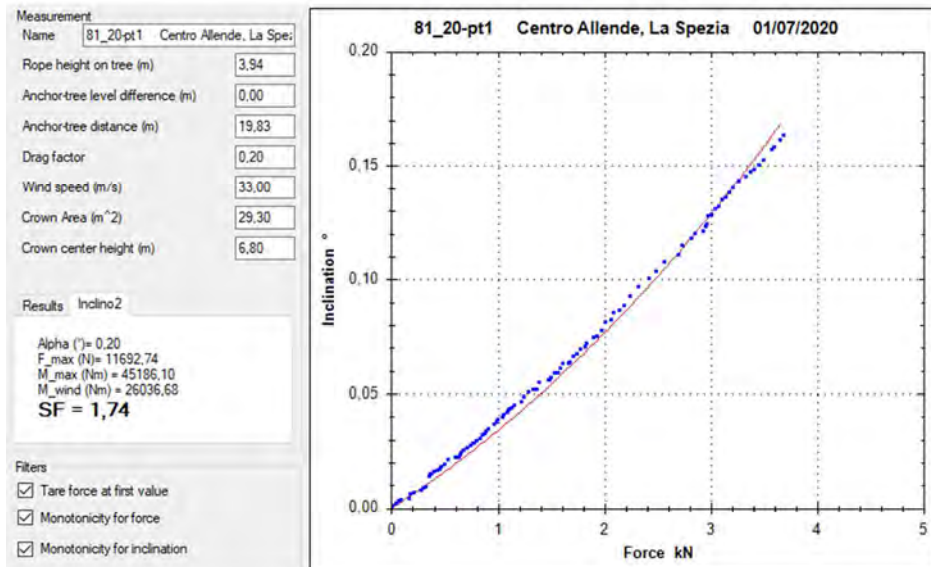
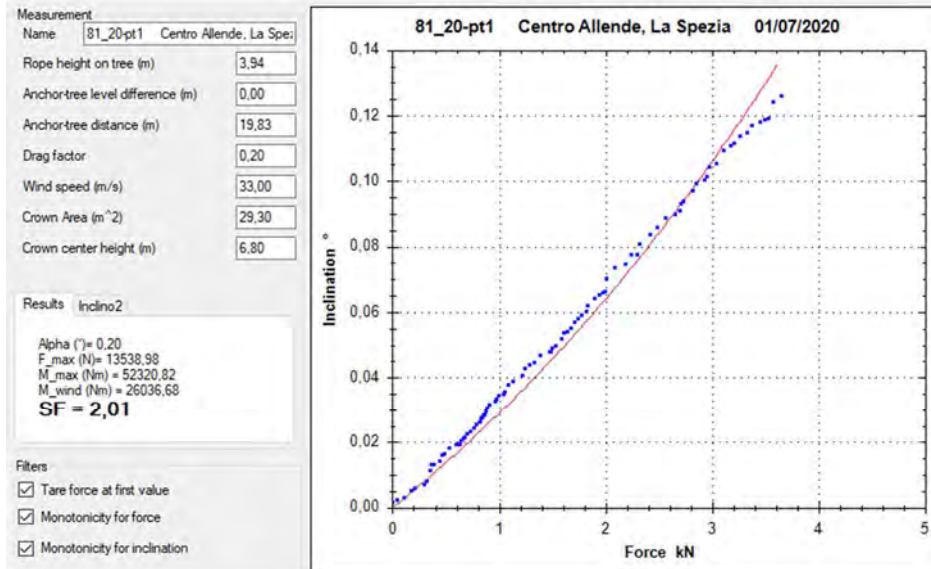
Appendix 1 – Pulling tests

---

Centro Allende, La Spezia – 81\_20 – pt1

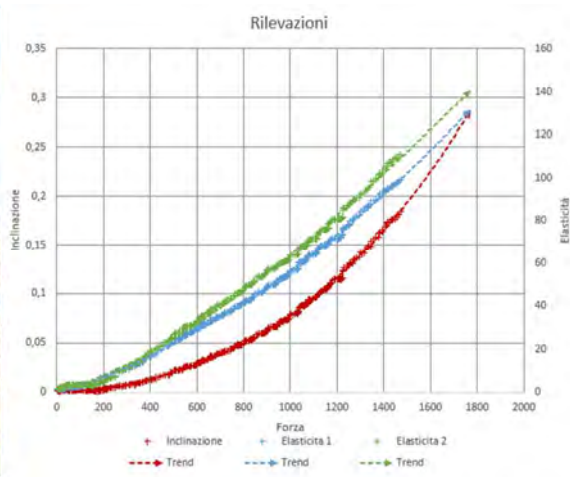


## Appendix 1 – Pulling tests



## Appendix 1 – Pulling tests

### Parco Togliatti, Rho – E19a – 10523 – pt1



Measurement

Name: E19a Parco via Togliatti, Rho-10523

Rope height on tree (m): 5,10

Anchor-tree level difference (m): -0,70

Anchor-tree distance (m): 21,39

Drag factor: 0,25

Wind speed (m/s): 33,00

Crown Area (m<sup>2</sup>): 86,80

Crown center height (m): 7,80

Elastic Limit (%): 2,00

Inclino Elaso1 Elasto2

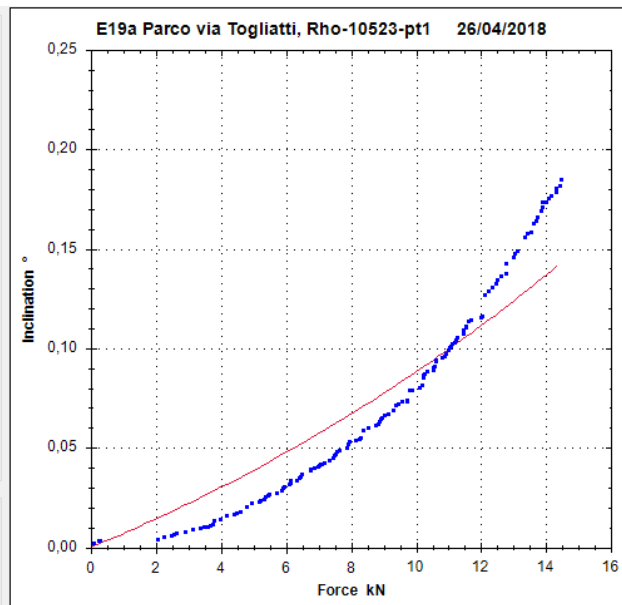
Alpha (°) = 0,26  
 F\_max (N) = 52091,10  
 M\_max (Nm) = 256405,68  
 M\_wind (Nm) = 110594,48  
**SF = 2,32**

Filters

Tare force at first value

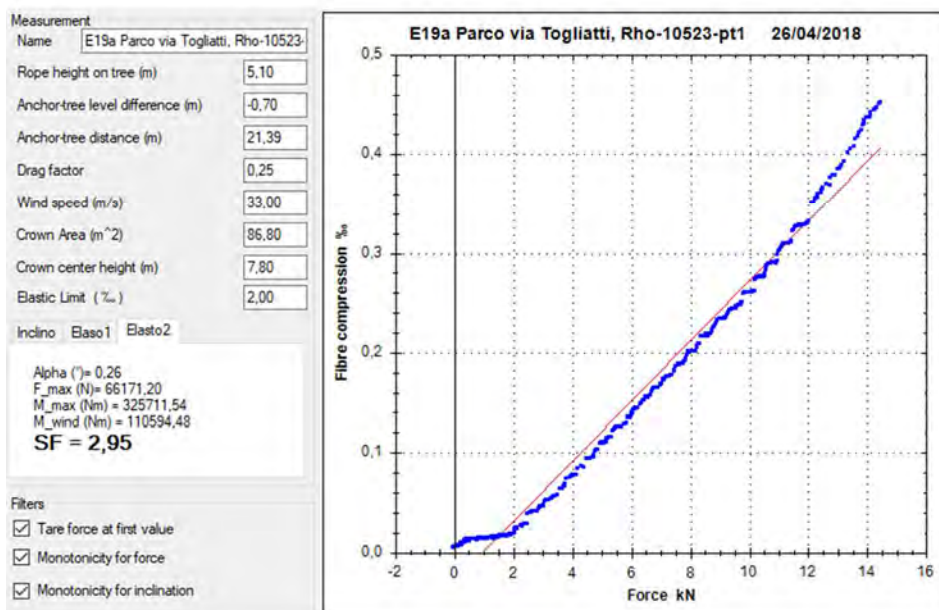
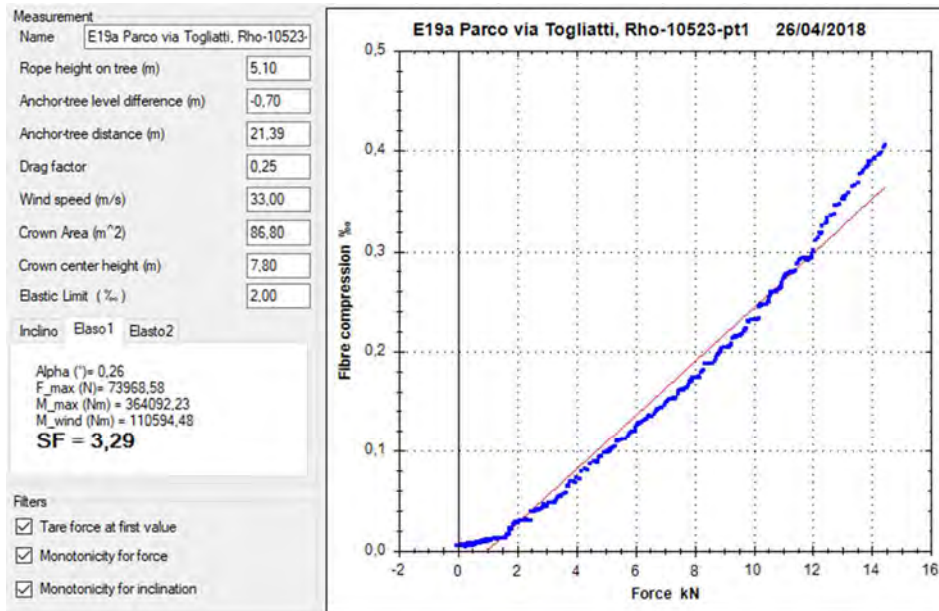
Monotonicity for force

Monotonicity for inclination



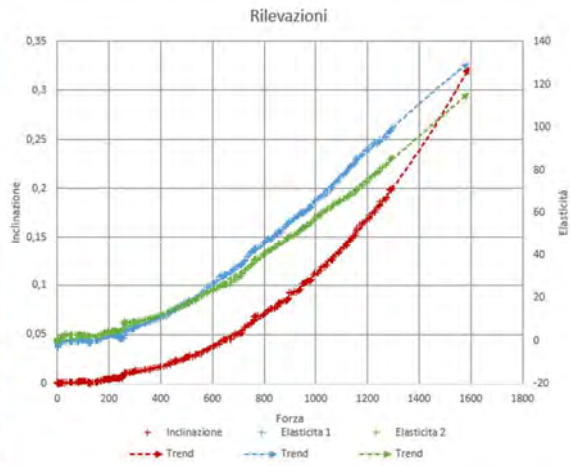


## Appendix 1 – Pulling tests



## Appendix 1 – Pulling tests

### Parco Togliatti, Rho – E19a – 10524 – pt1



Measurement

Name gliatti, Rho-10524-pt1 26/04/2018

Rope height on tree (m) 6,7

Anchor-tree level difference (m) 1

Anchor-tree distance (m) 14,86

Drag factor 0,25

Wind speed (m/s) 33

Crown Area (m<sup>2</sup>) 109,3

Crown center height (m) 8,8

Elastic Limit (%) 2

Inclino Elaso1 Elasto2

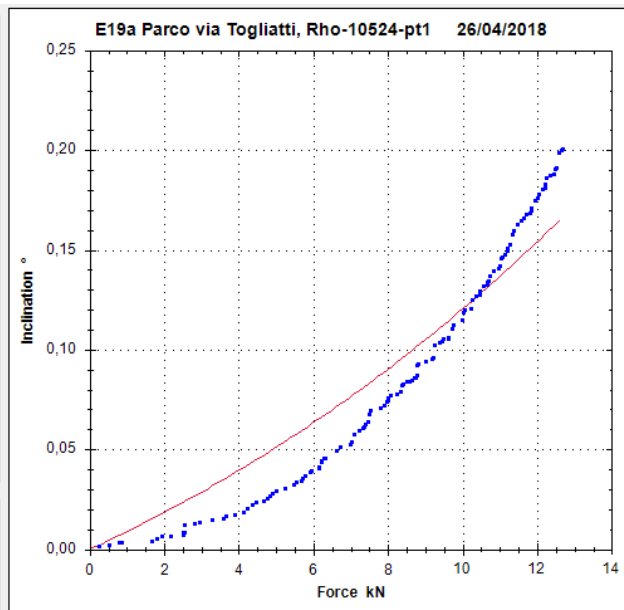
Alpha (°)= 0,37  
 F\_max (N)= 40906,72  
 M\_max (Nm) = 255895,37  
 M\_wind (Nm) = 157116,56  
**SF = 1,63**

Filters

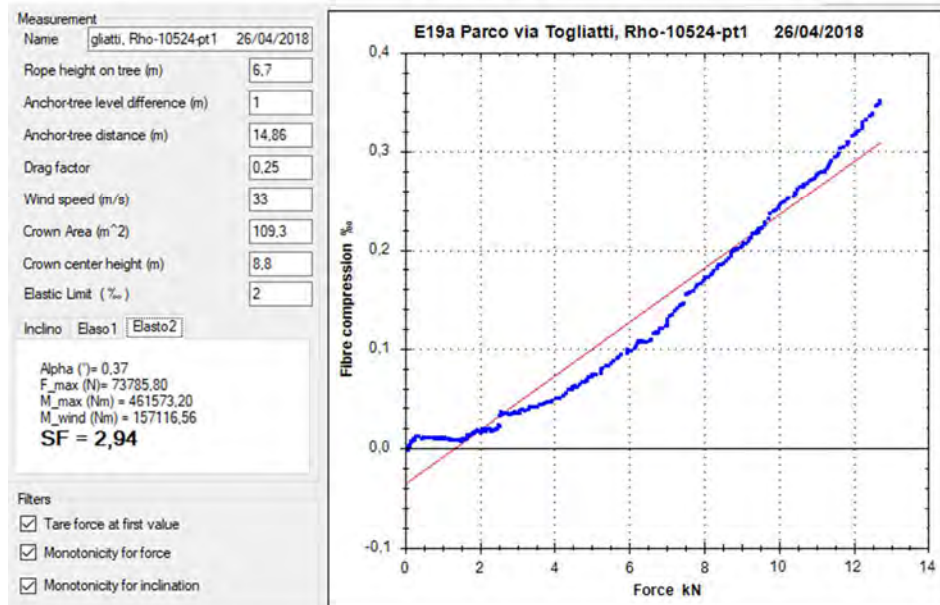
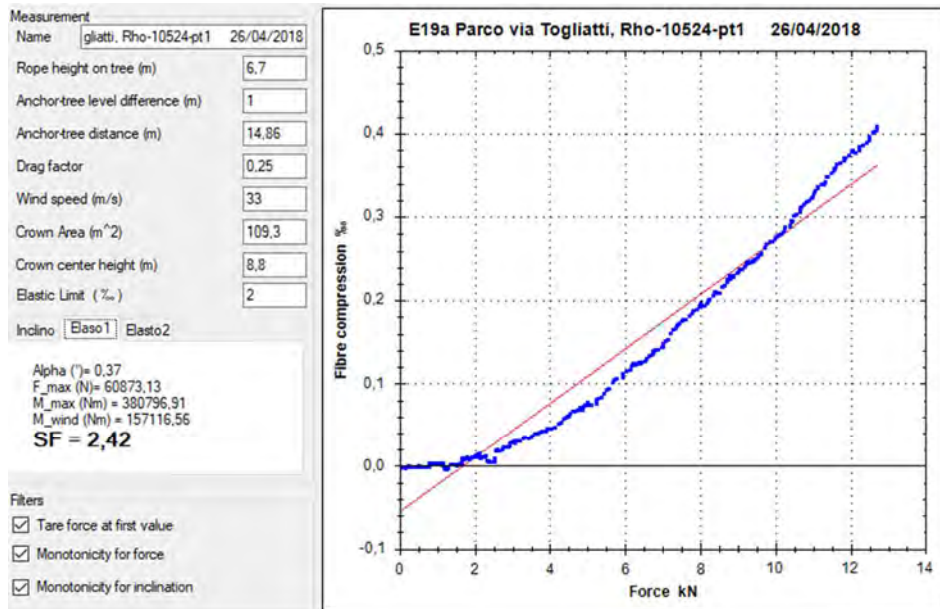
Tare force at first value

Monotonicity for force

Monotonicity for inclination

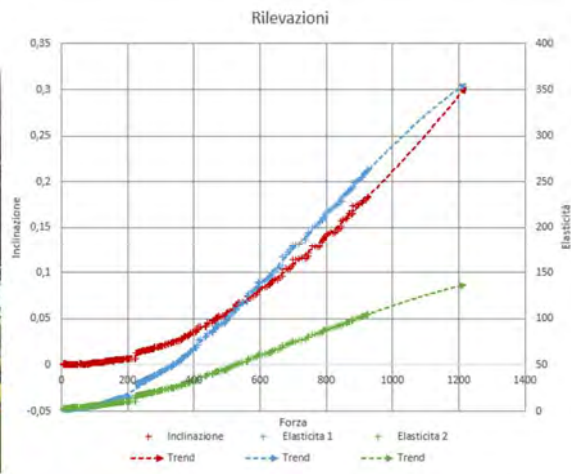


## Appendix 1 – Pulling tests



## Appendix 1 – Pulling tests

### Parco Togliatti, Rho – E19a – 10529 – pt1



Measurement

Name: E19a Parco via Togliatti, Rho-10529-

Rope height on tree (m): 5,40

Anchor-tree level difference (m): 0,70

Anchor-tree distance (m): 21,30

Drag factor: 0,20

Wind speed (m/s): 33,00

Crown Area (m<sup>2</sup>): 70,50

Crown center height (m): 9,40

Elastic Limit (%): 1,80

Inclino: Elaso1 Elasto2

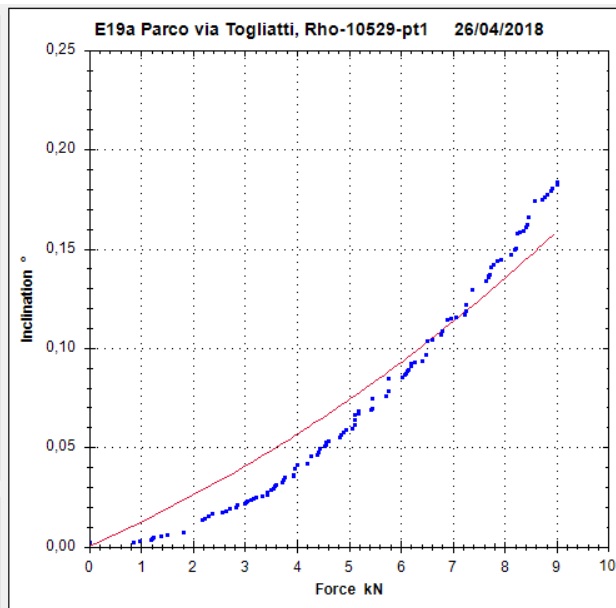
Alpha (°) = 0,22  
 F\_max (N) = 30053,92  
 M\_max (Nm) = 158478,86  
 M\_wind (Nm) = 86601,64  
**SF = 1,83**

Filters

Tare force at first value

Monotonicity for force

Monotonicity for inclination



## Appendix 1 – Pulling tests

Measurement  
 Name

Rope height on tree (m)

Anchor-tree level difference (m)

Anchor-tree distance (m)

Drag factor

Wind speed (m/s)

Crown Area (m<sup>2</sup>)

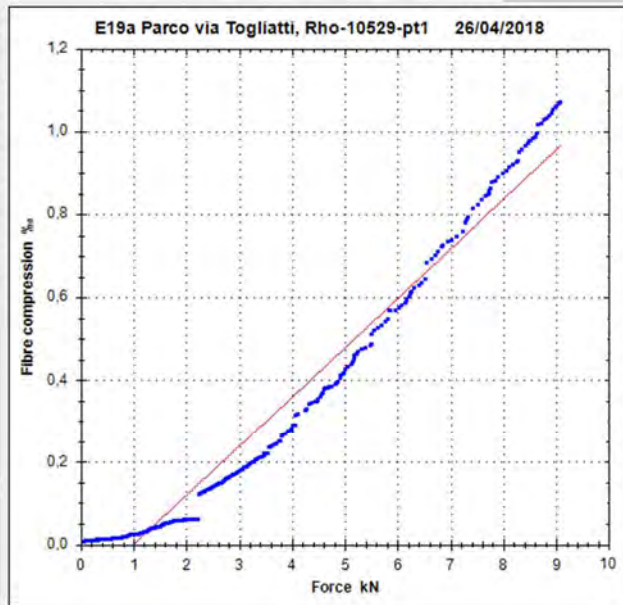
Crown center height (m)

Elastic Limit (%)

Inclino  Elaso1  Elaso2

Alpha (°)= 0.22  
 F\_max (N)= 15025.06  
 M\_max (Nm) = 79229.43  
 M\_wind (Nm) = 86601.64  
**SF = 0,91**

Filters  
 Tare force at first value  
 Monotonicity for force  
 Monotonicity for inclination



Measurement  
 Name

Rope height on tree (m)

Anchor-tree level difference (m)

Anchor-tree distance (m)

Drag factor

Wind speed (m/s)

Crown Area (m<sup>2</sup>)

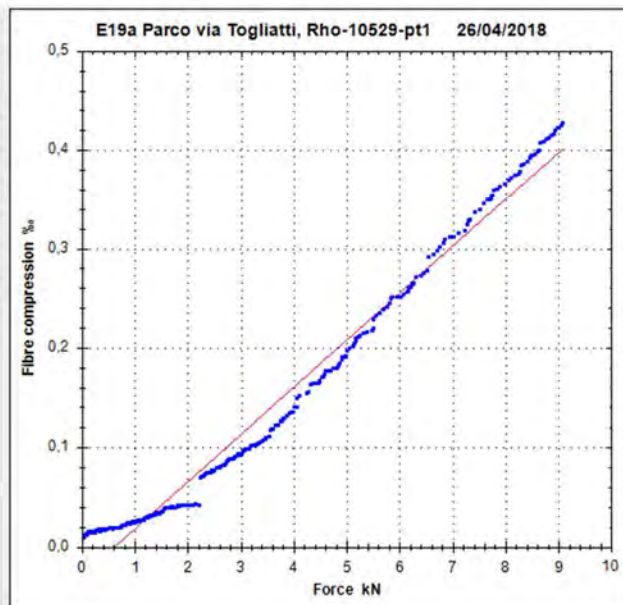
Crown center height (m)

Elastic Limit (%)

Inclino  Elaso1  Elaso2

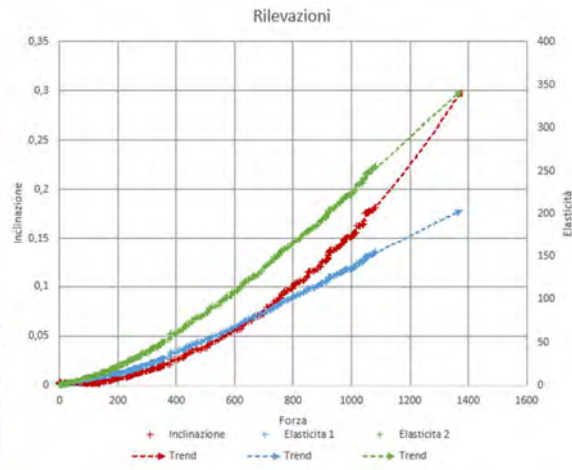
Alpha (°)= 0.22  
 F\_max (N)= 37977.43  
 M\_max (Nm) = 200260.74  
 M\_wind (Nm) = 86601.64  
**SF = 2,31**

Filters  
 Tare force at first value  
 Monotonicity for force  
 Monotonicity for inclination



## Appendix 1 – Pulling tests

### Parco Togliatti, Rho – E19a – 10530 – pt1



Measurement

Name: E19a Parco via Togliatti, Rho-10530

Rope height on tree (m): 6,15

Anchor-tree level difference (m): 0,90

Anchor-tree distance (m): 24,60

Drag factor: 0,20

Wind speed (m/s): 33,00

Crown Area (m<sup>2</sup>): 67,70

Crown center height (m): 9,40

Elastic Limit (%): 1,80

Inclino: Elaso1 Elasto2

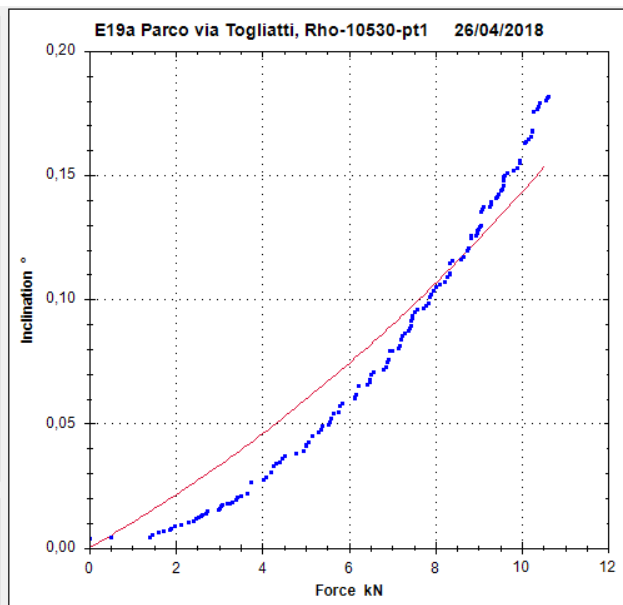
Alpha (°) = 0,21  
 F<sub>max</sub> (N) = 35982,88  
 M<sub>max</sub> (Nm) = 216421,08  
 M<sub>wind</sub> (Nm) = 83162,14  
**SF = 2,60**

Filters

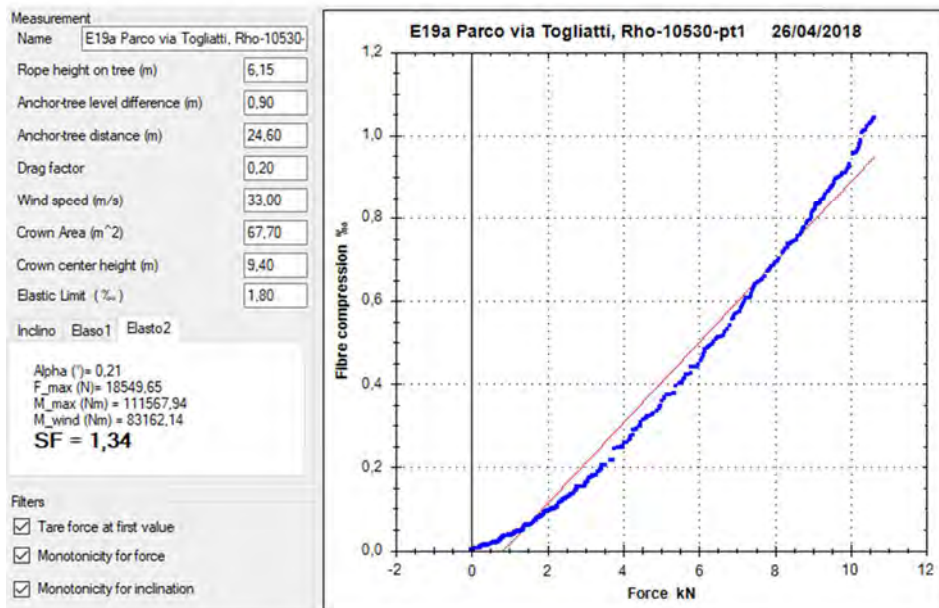
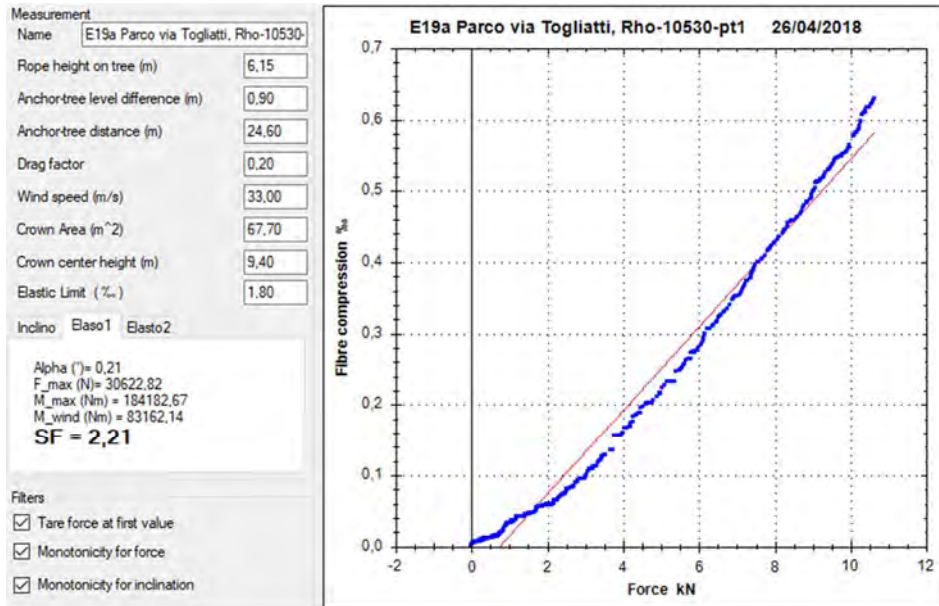
Tare force at first value

Monotonicity for force

Monotonicity for inclination

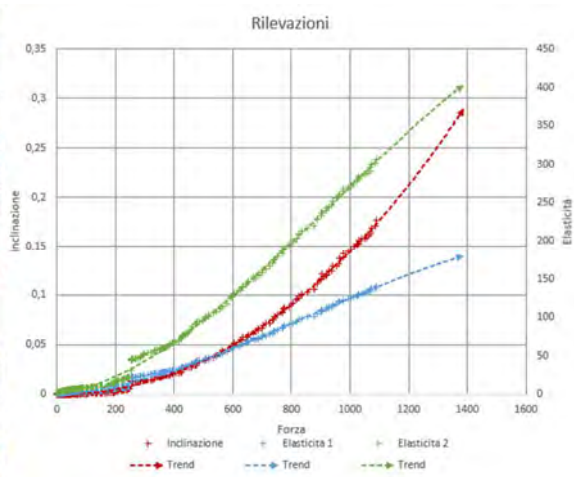


## Appendix 1 – Pulling tests



## Appendix 1 – Pulling tests

### Parco Togliatti, Rho – E19a – 10531 – pt1



Measurement

Name: E19a Parco via Togliatti, Rho-10531-

Rope height on tree (m): 6,80

Anchor-tree level difference (m): 0,20

Anchor-tree distance (m): 15,46

Drag factor: 0,20

Wind speed (m/s): 33,00

Crown Area (m<sup>2</sup>): 88,60

Crown center height (m): 8,90

Elastic Limit (%): 1,80

Inclino: Elaso1 Elasto2

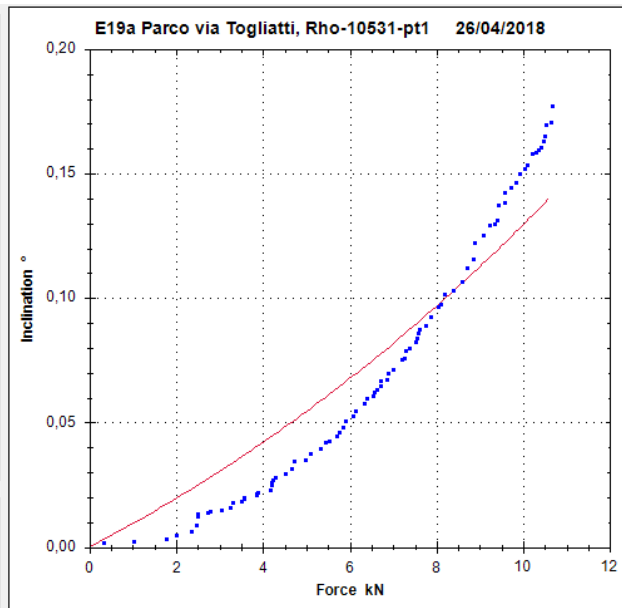
Alpha (°) = 0,40  
 F\_max (N) = 38744,01  
 M\_max (Nm) = 242302,93  
 M\_wind (Nm) = 103046,41  
**SF = 2,35**

Filters

Tare force at first value

Monotonicity for force

Monotonicity for inclination





## Appendix 1 – Pulling tests

Measurement

Name: E19a Parco via Togliatti, Rho-10531-

Rope height on tree (m): 6,80

Anchor-tree level difference (m): 0,20

Anchor-tree distance (m): 15,46

Drag factor: 0,20

Wind speed (m/s): 33,00

Crown Area (m<sup>2</sup>): 88,60

Crown center height (m): 8,90

Elastic Limit (%): 1,80

Inclino: Elaso1 Elasto2

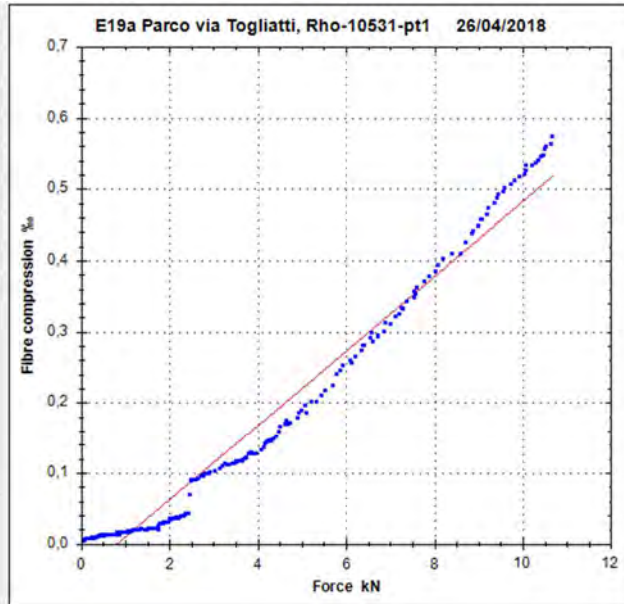
Alpha (°) = 0,40  
 F<sub>max</sub> (N) = 34244,35  
 M<sub>max</sub> (Nm) = 214162,31  
 M<sub>wind</sub> (Nm) = 103046,41  
**SF = 2,08**

Filters

Tare force at first value

Monotonicity for force

Monotonicity for inclination



Measurement

Name: E19a Parco via Togliatti, Rho-10531-

Rope height on tree (m): 6,80

Anchor-tree level difference (m): 0,20

Anchor-tree distance (m): 15,46

Drag factor: 0,20

Wind speed (m/s): 33,00

Crown Area (m<sup>2</sup>): 88,60

Crown center height (m): 8,90

Elastic Limit (%): 1,80

Inclino: Elaso1 Elasto2

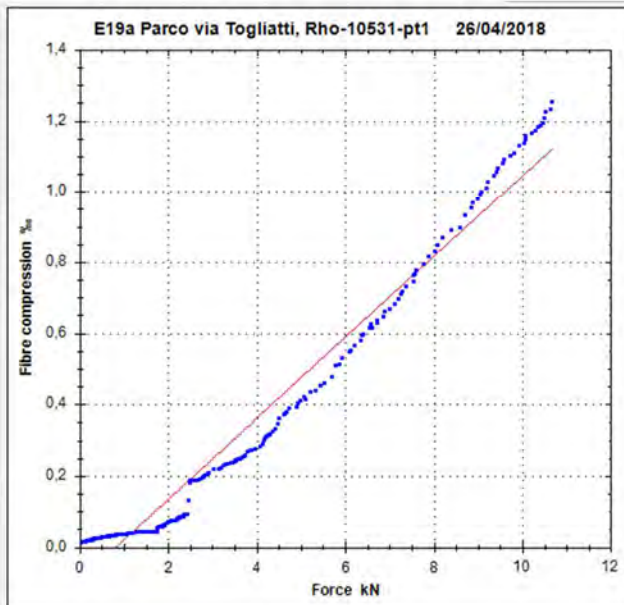
Alpha (°) = 0,40  
 F<sub>max</sub> (N) = 15799,98  
 M<sub>max</sub> (Nm) = 98812,25  
 M<sub>wind</sub> (Nm) = 103046,41  
**SF = 0,96**

Filters

Tare force at first value

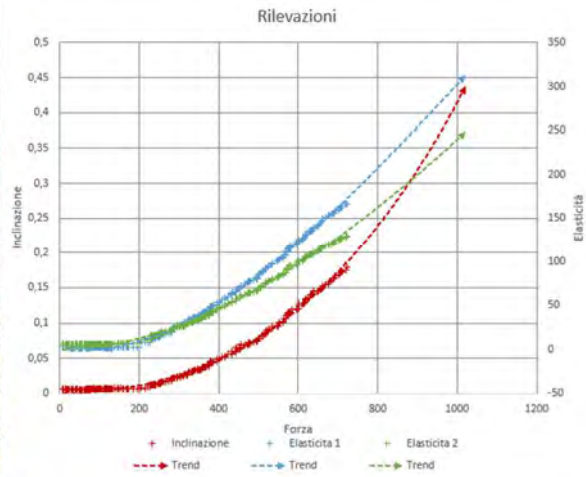
Monotonicity for force

Monotonicity for inclination



## Appendix 1 – Pulling tests

### Parco Togliatti, Rho – E19a – 10532 – pt1



Measurement

Name: E19a Parco via Togliatti, Rho-10532

Rope height on tree (m): 6.80

Anchor-tree level difference (m): 0.40

Anchor-tree distance (m): 17.74

Drag factor: 0.20

Wind speed (m/s): 33.00

Crown Area (m<sup>2</sup>): 93.10

Crown center height (m): 10.30

Elastic Limit (%): 1.80

Inclino: Elaso1 Elasto2

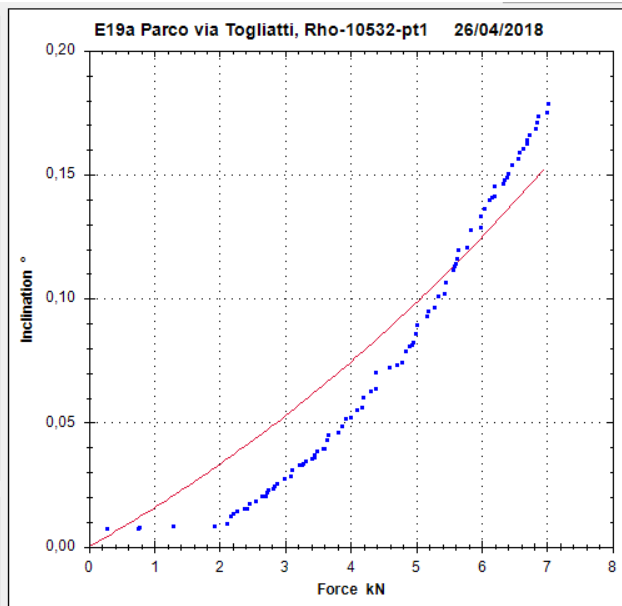
Alpha (°) = 0.35  
 F<sub>max</sub> (N) = 23918.25  
 M<sub>max</sub> (Nm) = 152992.38  
 M<sub>wind</sub> (Nm) = 125312.97  
**SF = 1,22**

Filters

Tare force at first value

Monotonicity for force

Monotonicity for inclination



## Appendix 1 – Pulling tests

Measurement  
 Name

Rope height on tree (m)

Anchor-tree level difference (m)

Anchor-tree distance (m)

Drag factor

Wind speed (m/s)

Crown Area (m<sup>2</sup>)

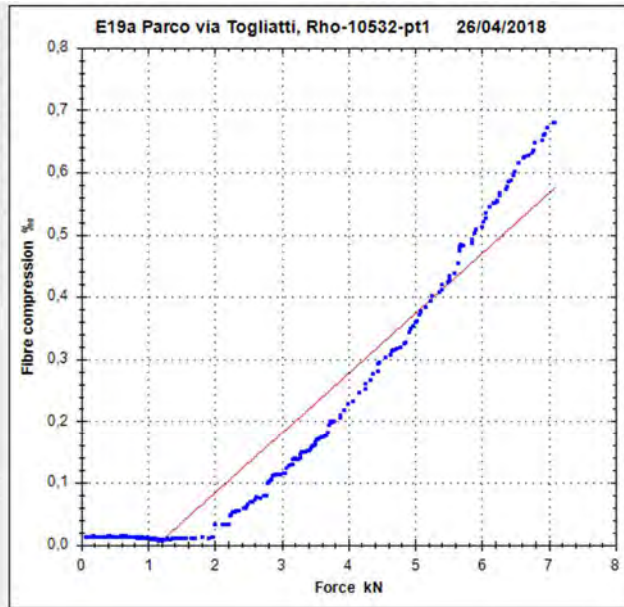
Crown center height (m)

Elastic Limit (%)

Inclino  Elaso1  Elasto2

Alpha (°) = 0,35  
 F<sub>max</sub> (N) = 18598,34  
 M<sub>max</sub> (Nm) = 118963,72  
 M<sub>wind</sub> (Nm) = 125312,97  
**SF = 0,95**

Filters  
 Tare force at first value  
 Monotonicity for force  
 Monotonicity for inclination



Measurement  
 Name

Rope height on tree (m)

Anchor-tree level difference (m)

Anchor-tree distance (m)

Drag factor

Wind speed (m/s)

Crown Area (m<sup>2</sup>)

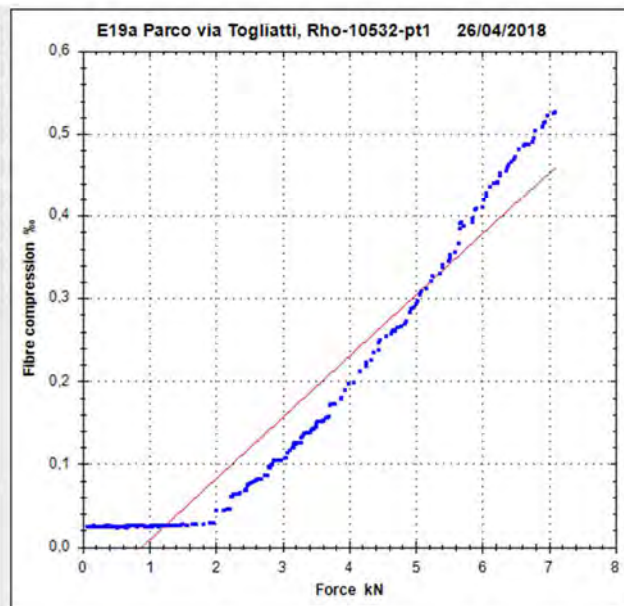
Crown center height (m)

Elastic Limit (%)

Inclino  Elaso1  Elasto2

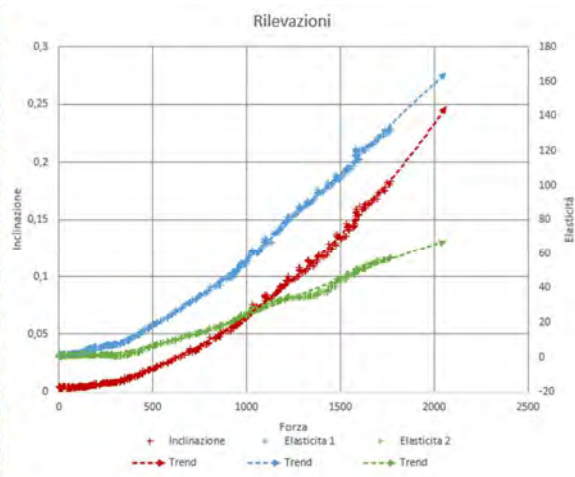
Alpha (°) = 0,35  
 F<sub>max</sub> (N) = 24270,95  
 M<sub>max</sub> (Nm) = 155248,39  
 M<sub>wind</sub> (Nm) = 125312,97  
**SF = 1,24**

Filters  
 Tare force at first value  
 Monotonicity for force  
 Monotonicity for inclination



## Appendix 1 – Pulling tests

### Parco Togliatti, Rho – E19a – 10536 – pt1



Measurement

Name: E19a Parco via Togliatti, Rho-10536-

Rope height on tree (m): 5.60

Anchor-tree level difference (m): -0.40

Anchor-tree distance (m): 14.66

Drag factor: 0.25

Wind speed (m/s): 33.00

Crown Area (m<sup>2</sup>): 99.00

Crown center height (m): 10.00

Elastic Limit (%): 1.50

Inclino: Elaso1 Elasto2

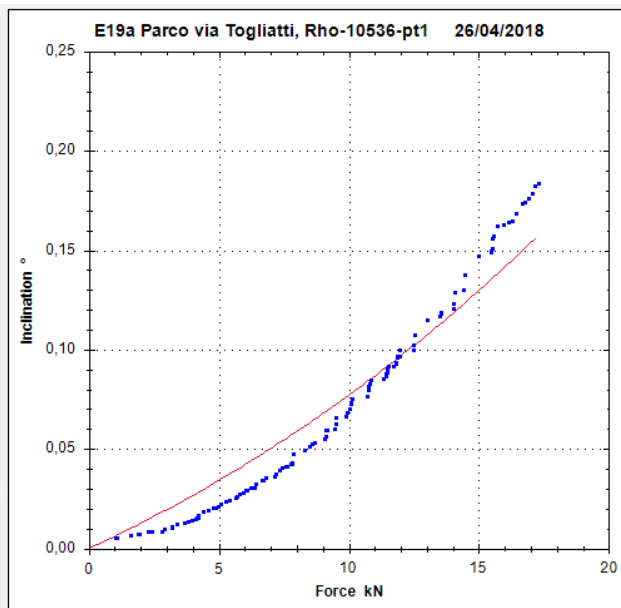
Alpha (°) = 0.39  
 F<sub>max</sub> (N) = 58036.94  
 M<sub>max</sub> (Nm) = 300789.51  
 M<sub>wind</sub> (Nm) = 161716.50  
**SF = 1,86**

Filters

Tare force at first value

Monotonicity for force

Monotonicity for inclination



## Appendix 1 – Pulling tests

Measurement  
 Name

Rope height on tree (m)

Anchor-tree level difference (m)

Anchor-tree distance (m)

Drag factor

Wind speed (m/s)

Crown Area (m<sup>2</sup>)

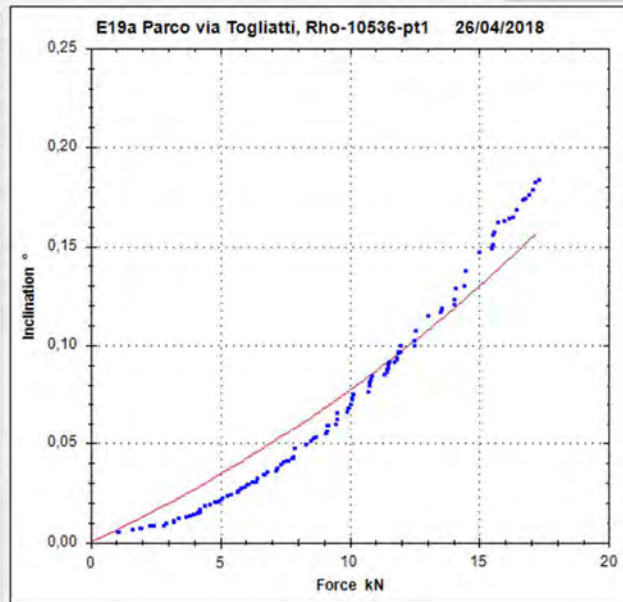
Crown center height (m)

Elastic Limit (%)

Inclino  Elaso1  Elasto2

Alpha (°) = 0.39  
 F<sub>max</sub> (N) = 58036.94  
 M<sub>max</sub> (Nm) = 300789.51  
 M<sub>wind</sub> (Nm) = 161716.50  
**SF = 1,86**

Filters  
 Tare force at first value  
 Monotonicity for force  
 Monotonicity for inclination



Measurement  
 Name

Rope height on tree (m)

Anchor-tree level difference (m)

Anchor-tree distance (m)

Drag factor

Wind speed (m/s)

Crown Area (m<sup>2</sup>)

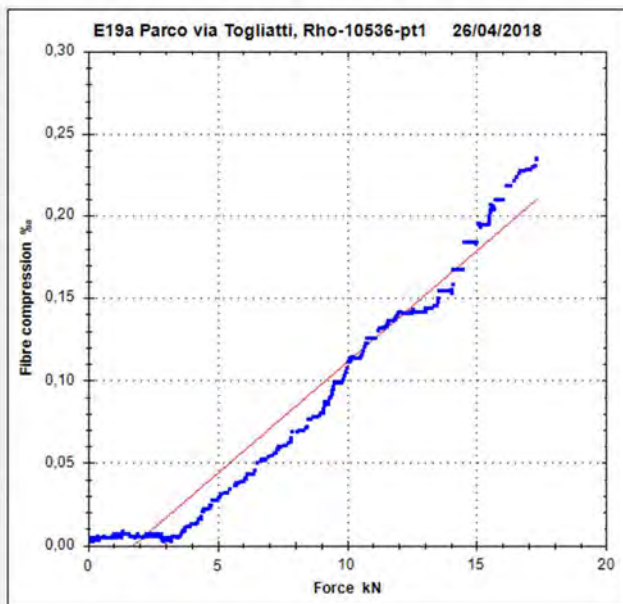
Crown center height (m)

Elastic Limit (%)

Inclino  Elaso1  Elasto2

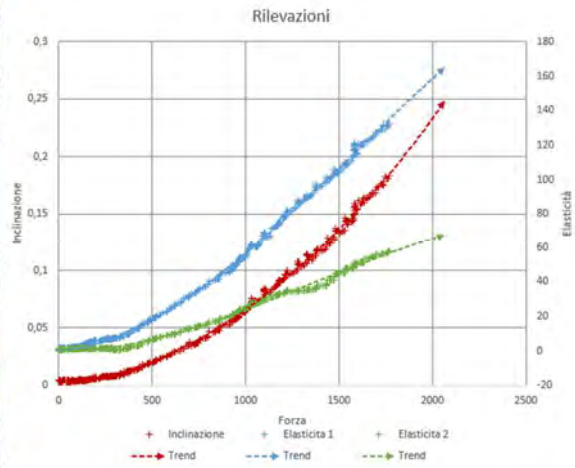
Alpha (°) = 0.39  
 F<sub>max</sub> (N) = 111487.50  
 M<sub>max</sub> (Nm) = 577809.04  
 M<sub>wind</sub> (Nm) = 161716.50  
**SF = 3,57**

Filters  
 Tare force at first value  
 Monotonicity for force  
 Monotonicity for inclination



## Appendix 1 – Pulling tests

### Parco Togliatti, Rho – E19a – 10537 – pt1



Measurement

Name: E19a Parco via Togliatti, Rho-10537-

Rope height on tree (m): 6,70

Anchor-tree level difference (m): 0,00

Anchor-tree distance (m): 18,06

Drag factor: 0,25

Wind speed (m/s): 33,00

Crown Area (m<sup>2</sup>): 103,50

Crown center height (m): 10,80

Elastic Limit (%): 1,50

Inclino: Elaso1 | Elasto2

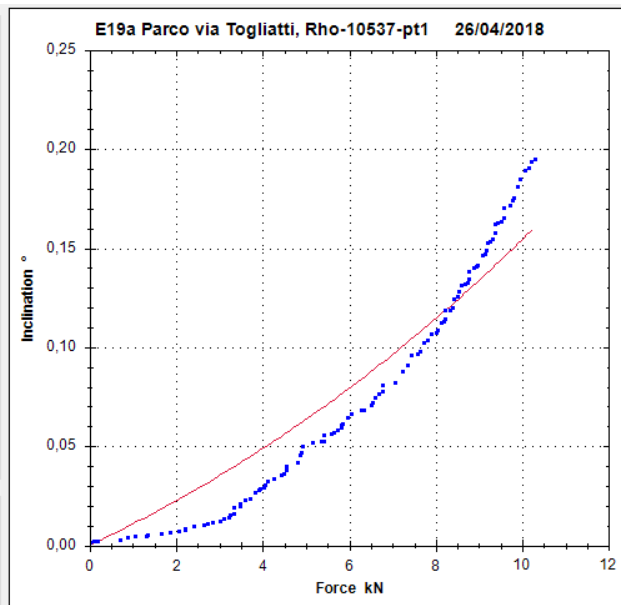
Alpha (°) = 0,36  
 F<sub>max</sub> (N) = 34024,02  
 M<sub>max</sub> (Nm) = 213727,24  
 M<sub>wind</sub> (Nm) = 182592,63  
**SF = 1,17**

Filters

Tare force at first value

Monotonicity for force

Monotonicity for inclination



## Appendix 1 – Pulling tests

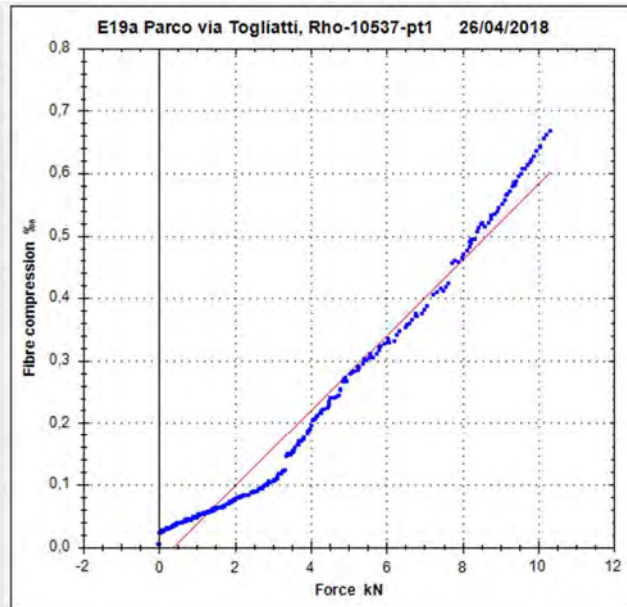
Measurement  
 Name: E19a Parco via Togliatti, Rho-10537-

Rope height on tree (m): 6.70  
 Anchor-tree level difference (m): 0.00  
 Anchor-tree distance (m): 18.06  
 Drag factor: 0.25  
 Wind speed (m/s): 33.00  
 Crown Area (m<sup>2</sup>): 103.50  
 Crown center height (m): 10.80  
 Elastic Limit (%): 1.50

Inclino: Elaso1 Elasto2

Alpha (°) = 0.36  
 F\_max (N) = 24668.74  
 M\_max (Nm) = 154960.55  
 M\_wind (Nm) = 182592.63  
**SF = 0,85**

Filters  
 Tare force at first value  
 Monotonicity for force  
 Monotonicity for inclination



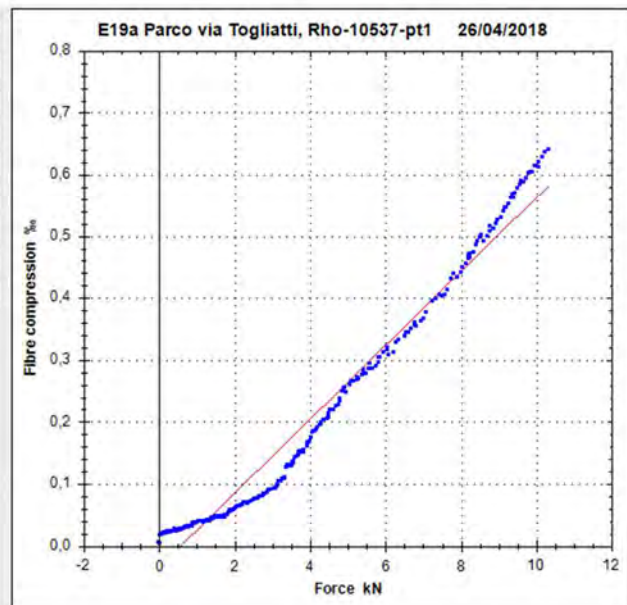
Measurement  
 Name: E19a Parco via Togliatti, Rho-10537-

Rope height on tree (m): 6.70  
 Anchor-tree level difference (m): 0.00  
 Anchor-tree distance (m): 18.06  
 Drag factor: 0.25  
 Wind speed (m/s): 33.00  
 Crown Area (m<sup>2</sup>): 103.50  
 Crown center height (m): 10.80  
 Elastic Limit (%): 1.50

Inclino: Elaso1 Elasto2

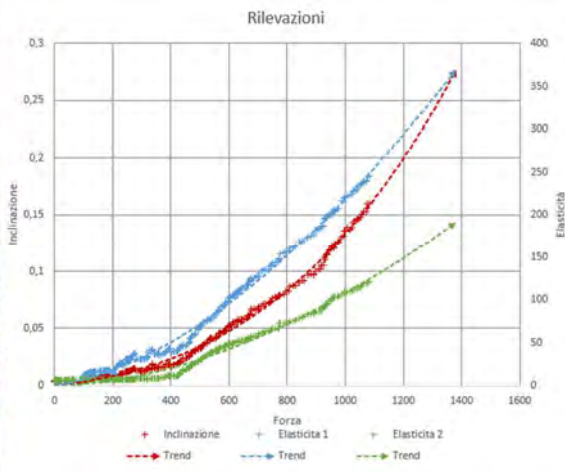
Alpha (°) = 0.36  
 F\_max (N) = 25129.07  
 M\_max (Nm) = 157852.17  
 M\_wind (Nm) = 182592.63  
**SF = 0,86**

Filters  
 Tare force at first value  
 Monotonicity for force  
 Monotonicity for inclination



## Appendix 1 – Pulling tests

### Parco Togliatti, Rho – E19a – 10574 – pt1



Measurement

Name: E19a Parco via Togliatti, Rho-10578-

Rope height on tree (m): 6,70

Anchor-tree level difference (m): 1,20

Anchor-tree distance (m): 21,83

Drag factor: 0,25

Wind speed (m/s): 33,00

Crown Area (m<sup>2</sup>): 82,40

Crown center height (m): 6,70

Elastic Limit (%): 1,80

Inclino: Elaso1 | Elasto2

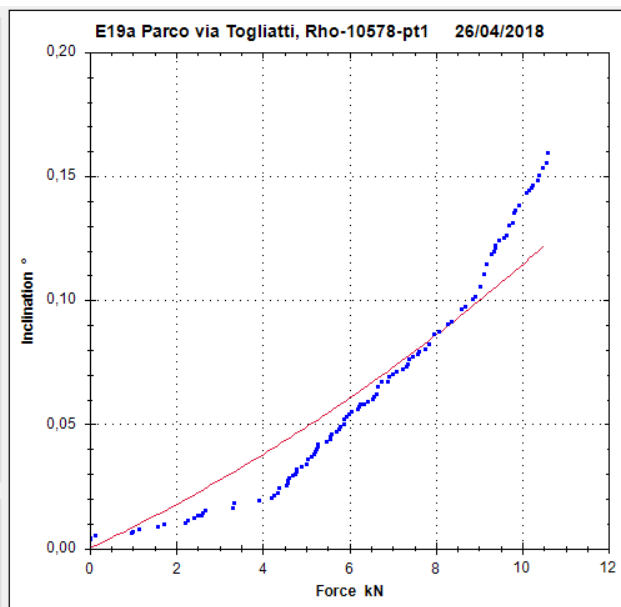
Alpha (°) = 0,25  
 F\_max (N) = 42551,66  
 M\_max (Nm) = 276456,76  
 M\_wind (Nm) = 90182,27  
**SF = 3,07**

Filters

Tare force at first value

Monotonicity for force

Monotonicity for inclination





## Appendix 1 – Pulling tests

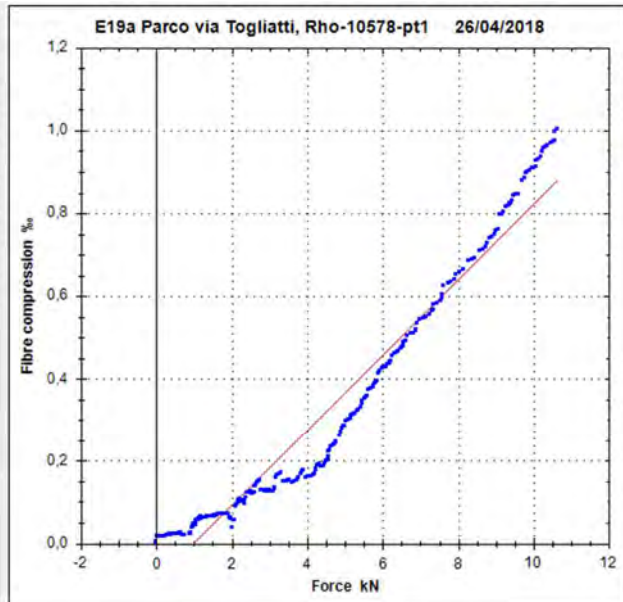
Measurement  
Name: E19a Parco via Togliatti, Rho-10578

Rope height on tree (m): 6.70  
Anchor-tree level difference (m): 1.20  
Anchor-tree distance (m): 21.83  
Drag factor: 0.25  
Wind speed (m/s): 33.00  
Crown Area (m<sup>2</sup>): 82.40  
Crown center height (m): 6.70  
Elastic Limit (%): 1.80

Inclino: Elaso1 Elasto2

Alpha (°) = 0.25  
F\_max (N) = 19756.41  
M\_max (Nm) = 128356.75  
M\_wind (Nm) = 90182.27  
**SF = 1,42**

Filters  
 Tare force at first value  
 Monotonicity for force  
 Monotonicity for inclination



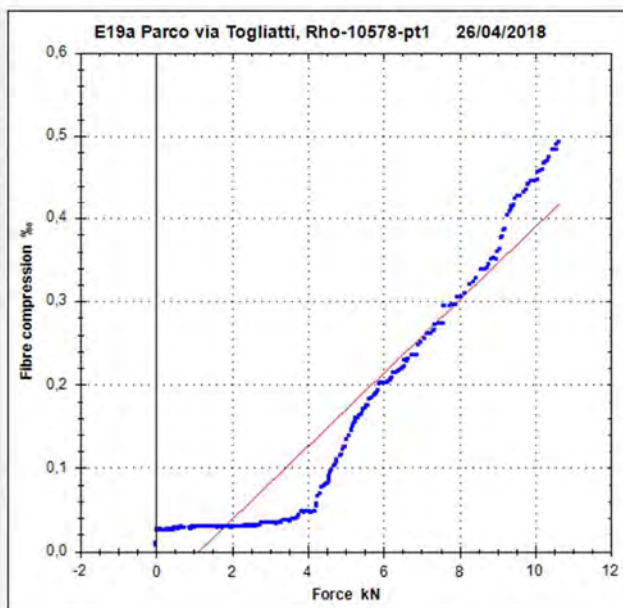
Measurement  
Name: E19a Parco via Togliatti, Rho-10578

Rope height on tree (m): 6.70  
Anchor-tree level difference (m): 1.20  
Anchor-tree distance (m): 21.83  
Drag factor: 0.25  
Wind speed (m/s): 33.00  
Crown Area (m<sup>2</sup>): 82.40  
Crown center height (m): 6.70  
Elastic Limit (%): 1.80

Inclino: Elaso1 Elasto2

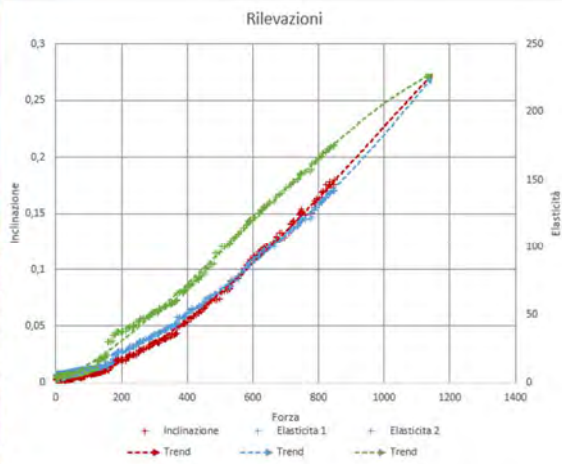
Alpha (°) = 0.25  
F\_max (N) = 40952.00  
M\_max (Nm) = 266063.81  
M\_wind (Nm) = 90182.27  
**SF = 2,95**

Filters  
 Tare force at first value  
 Monotonicity for force  
 Monotonicity for inclination



## Appendix 1 – Pulling tests

### Piazza Moneta, Cesano Boscone – 02 – pt1



Measurement

Name: Cesano B.ne-02-pt1 09/03/2018

Rope height on tree (m): 6

Anchor-tree level difference (m): 0

Anchor-tree distance (m): 30,60

Drag factor: 0,25

Wind speed (m/s): 33

Crown Area (m<sup>2</sup>): 98

Crown center height (m): 9,8

Elastic Limit (%): 1,5

Inclino | Elaso1 | Elasto2

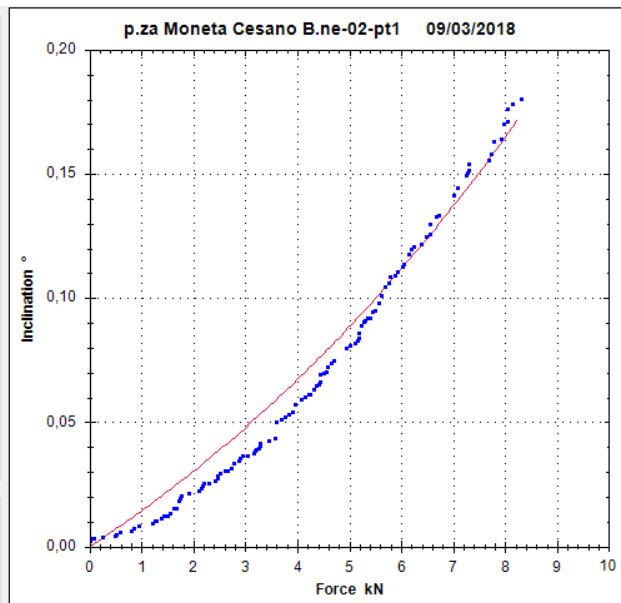
Alpha (°) = 0,19  
 F\_max (N) = 26007,39  
 M\_max (Nm) = 153128,45  
 M\_wind (Nm) = 156881,34  
**SF = 0,98**

Filters

Tare force at first value

Monotonicity for force

Monotonicity for inclination



## Appendix 1 – Pulling tests

Measurement

Name  09/03/2018

Rope height on tree (m)

Anchor-tree level difference (m)

Anchor-tree distance (m)

Drag factor

Wind speed (m/s)

Crown Area (m<sup>2</sup>)

Crown center height (m)

Elastic Limit (%)

Inclino  Elaso1  Elasto2

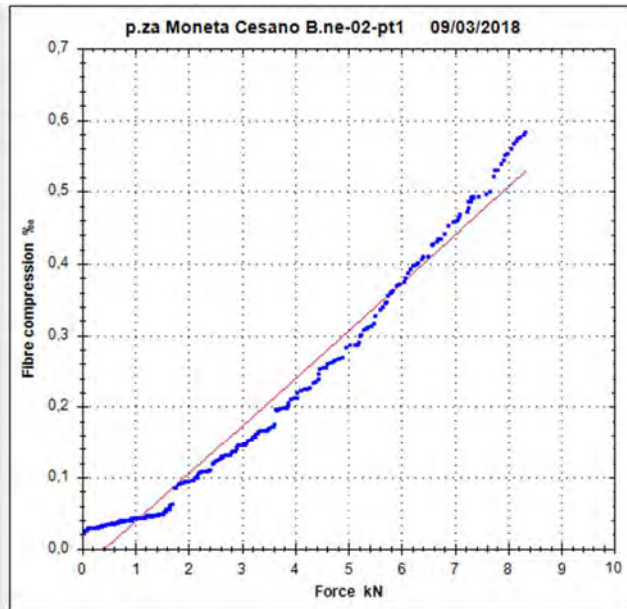
Alpha (°) = 0.19  
 F\_max (N) = 22383.49  
 M\_max (Nm) = 131791.34  
 M\_wind (Nm) = 156881.34  
**SF = 0,84**

Filters

Tare force at first value

Monotonicity for force

Monotonicity for inclination



Measurement

Name  09/03/2018

Rope height on tree (m)

Anchor-tree level difference (m)

Anchor-tree distance (m)

Drag factor

Wind speed (m/s)

Crown Area (m<sup>2</sup>)

Crown center height (m)

Elastic Limit (%)

Inclino  Elaso1  Elasto2

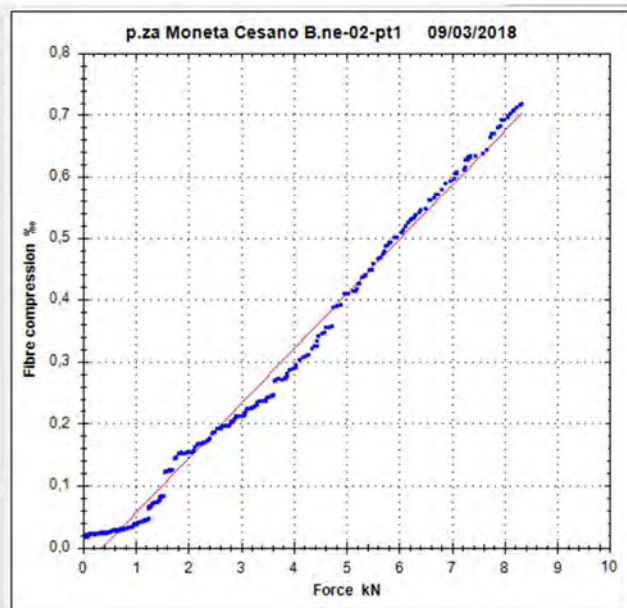
Alpha (°) = 0.19  
 F\_max (N) = 16981.66  
 M\_max (Nm) = 99986.03  
 M\_wind (Nm) = 156881.34  
**SF = 0,64**

Filters

Tare force at first value

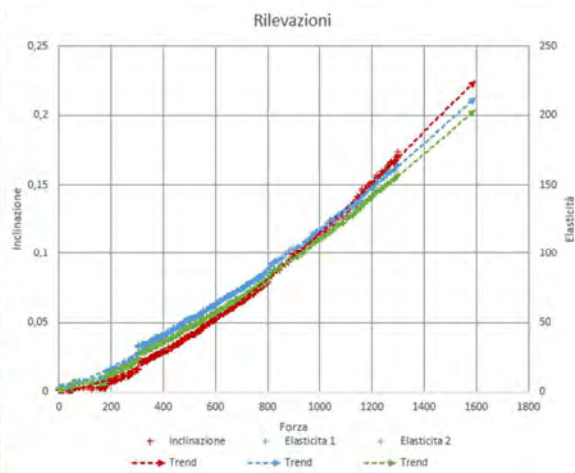
Monotonicity for force

Monotonicity for inclination



## Appendix 1 – Pulling tests

### Piazza Moneta, Cesano Boscone – 03 – pt1



Measurement

Name p.za Moneta Cesano B.ne-03-pt1 (

Rope height on tree (m) 5,50

Anchor-tree level difference (m) 0,00

Anchor-tree distance (m) 28,00

Drag factor 0,25

Wind speed (m/s) 33,00

Crown Area (m<sup>2</sup>) 151,00

Crown center height (m) 11,80

Elastic Limit (%) 1,5

Inclino Elaso1 Elasto2

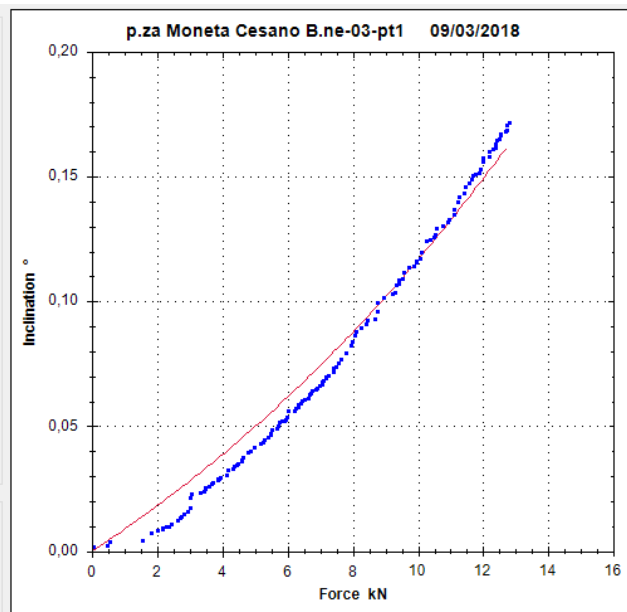
Alpha (°)= 0,19  
 F\_max (N)= 41894,78  
 M\_max (Nm) = 226100,63  
 M\_wind (Nm) = 291057,03  
**SF = 0,78**

Filters

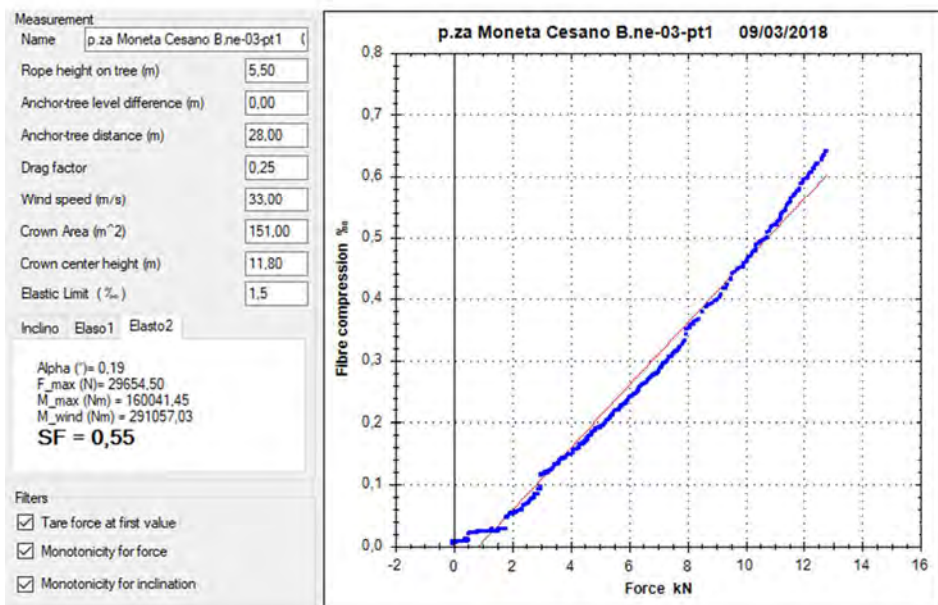
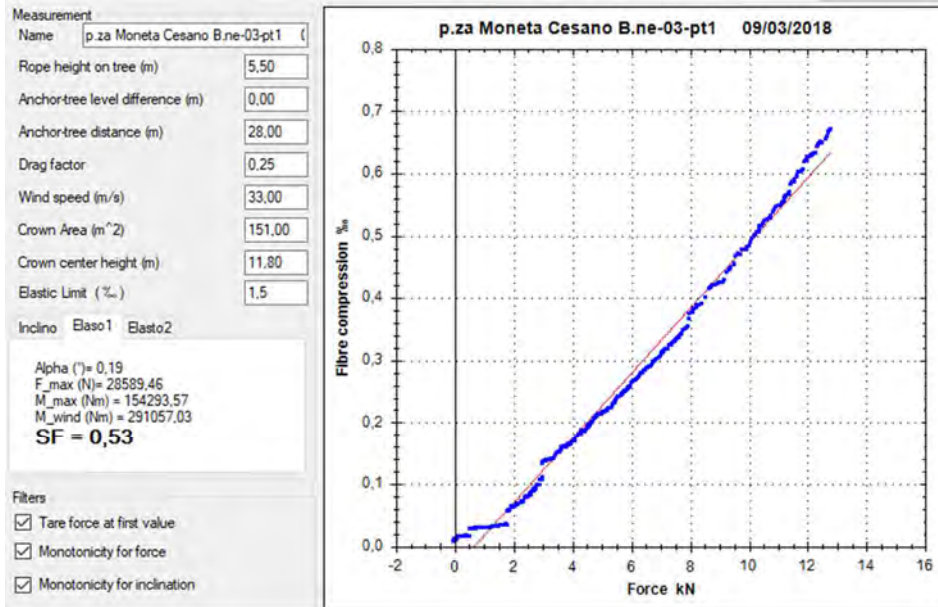
Tare force at first value

Monotonicity for force

Monotonicity for inclination

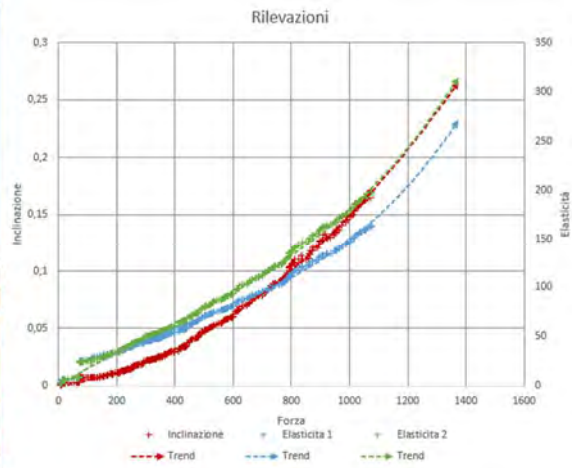


## Appendix 1 – Pulling tests



## Appendix 1 – Pulling tests

### Piazza Moneta, Cesano Boscone – 04 – pt1



Measurement

Name: Cesano B.ne-04-pt1 09/03/2018

Rope height on tree (m): 5,10

Anchor-tree level difference (m): 0

Anchor-tree distance (m): 24,2

Drag factor: 0,25

Wind speed (m/s): 33

Crown Area (m<sup>2</sup>): 130

Crown center height (m): 9,8

Elastic Limit (%): 1,5

Inclino | Elaso1 | Elasto2

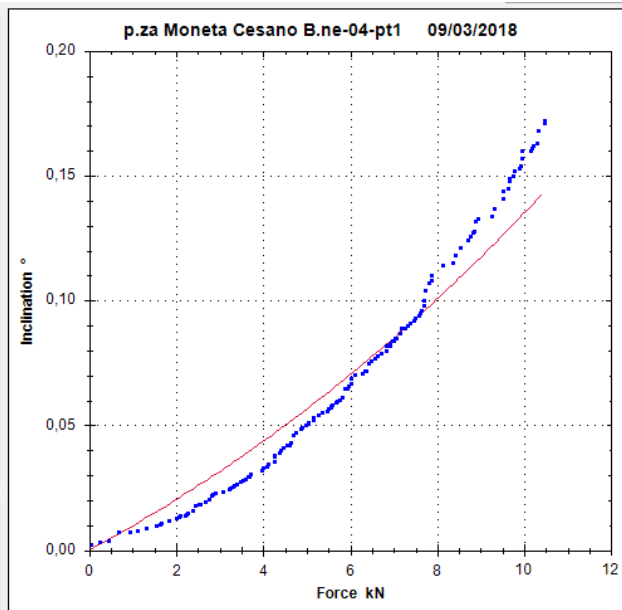
Alpha (°) = 0,21  
 F\_max (N) = 37543,07  
 M\_max (Nm) = 187354,35  
 M\_wind (Nm) = 208107,90  
**SF = 0,90**

Filters

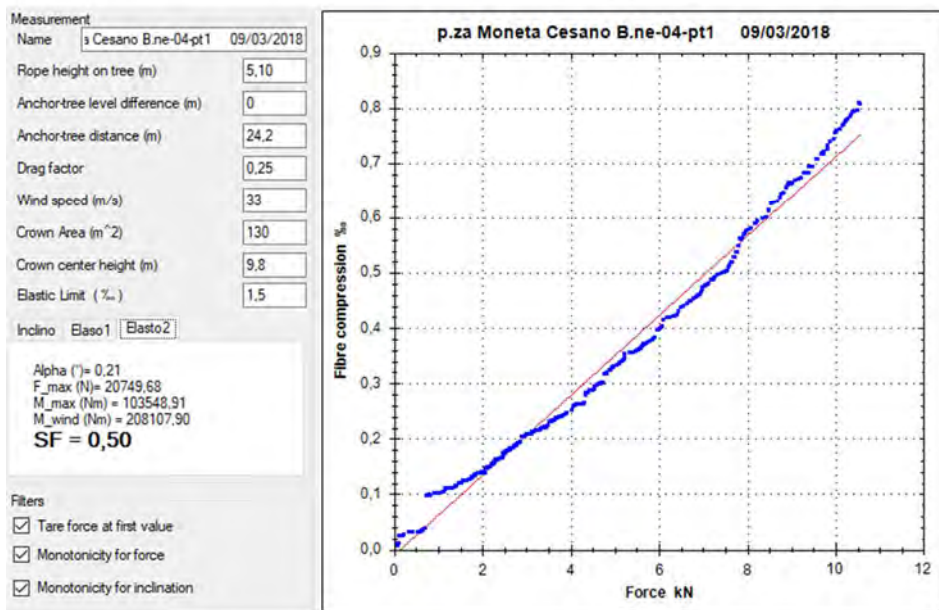
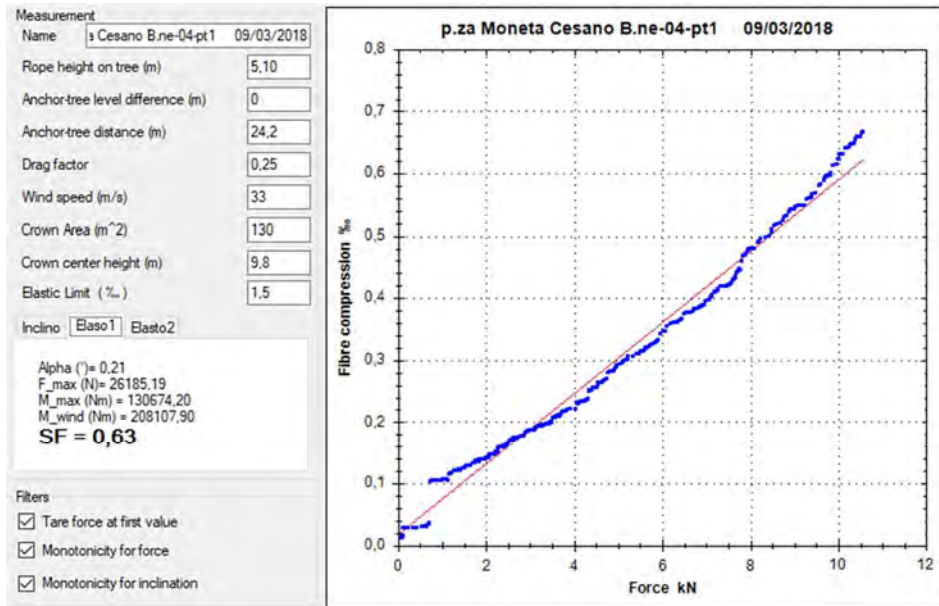
Tare force at first value

Monotonicity for force

Monotonicity for inclination

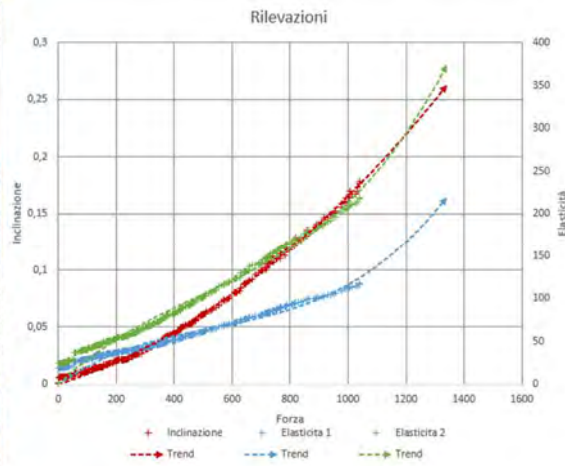


## Appendix 1 – Pulling tests



## Appendix 1 – Pulling tests

### Piazza Moneta, Cesano Boscone – 05 – pt1



Measurement

Name: Cesano B.ne-05-pt1    09/03/2018

Rope height on tree (m): 6

Anchor-tree level difference (m): 0

Anchor-tree distance (m): 17.8

Drag factor: 0,25

Wind speed (m/s): 33

Crown Area (m<sup>2</sup>): 107

Crown center height (m): 9,9

Elastic Limit (%): 1,5

Inclino | Elaso1 | Elasto2

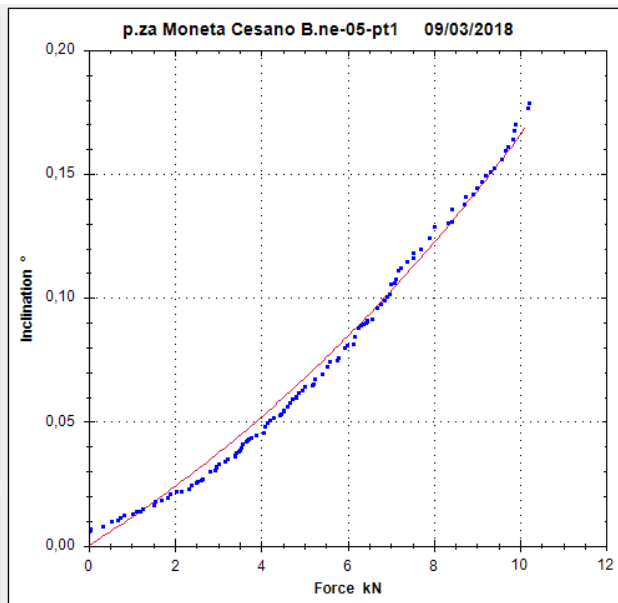
Alpha (°) = 0.33  
 F<sub>max</sub> (N) = 32372.71  
 M<sub>max</sub> (Nm) = 184060.82  
 M<sub>wind</sub> (Nm) = 173036.66  
**SF = 1,06**

Filters

Tare force at first value

Monotonicity for force

Monotonicity for inclination





## Appendix 1 – Pulling tests

Measurement  
 Name: s Cesano B.ne-05-pt1 09/03/2018

Rope height on tree (m): 6

Anchor-tree level difference (m): 0

Anchor-tree distance (m): 17,8

Drag factor: 0,25

Wind speed (m/s): 33

Crown Area (m<sup>2</sup>): 107

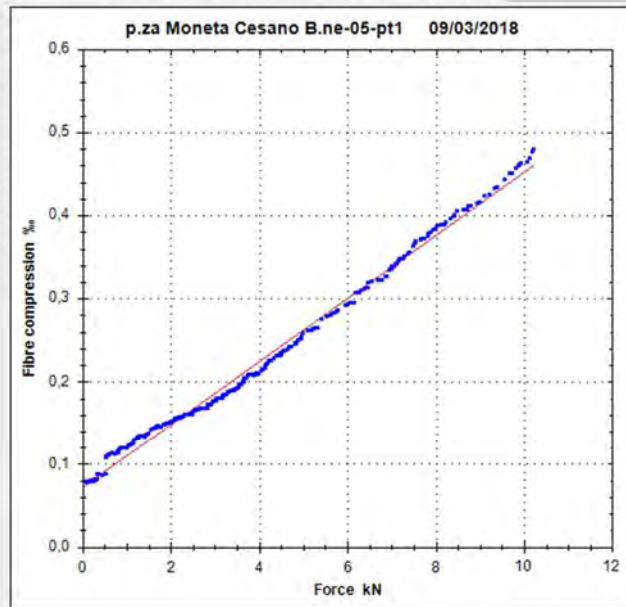
Crown center height (m): 9,9

Elastic Limit (%): 1,5

Inclino:  Elaso1  Elasto2

Alpha (°) = 0,33  
 F\_max (N) = 39484,52  
 M\_max (Nm) = 224496,31  
 M\_wind (Nm) = 173036,66  
**SF = 1,30**

Filters  
 Tare force at first value  
 Monotonicity for force  
 Monotonicity for inclination



Measurement  
 Name: s Cesano B.ne-05-pt1 09/03/2018

Rope height on tree (m): 6

Anchor-tree level difference (m): 0

Anchor-tree distance (m): 17,8

Drag factor: 0,25

Wind speed (m/s): 33

Crown Area (m<sup>2</sup>): 107

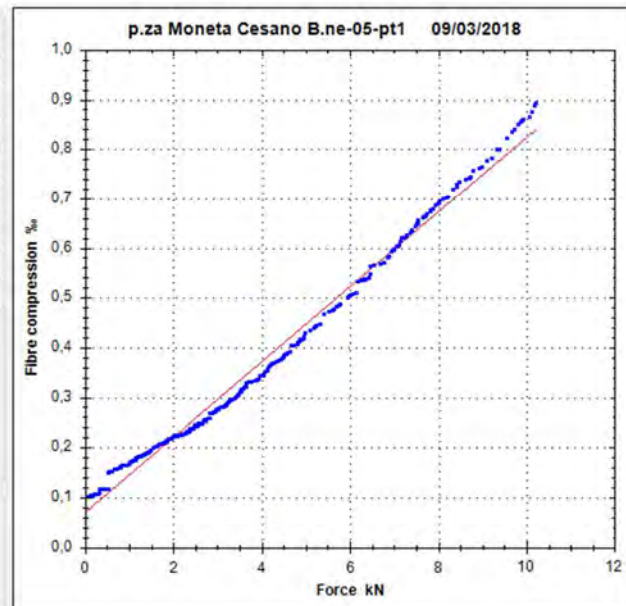
Crown center height (m): 9,9

Elastic Limit (%): 1,5

Inclino:  Elaso1  Elasto2

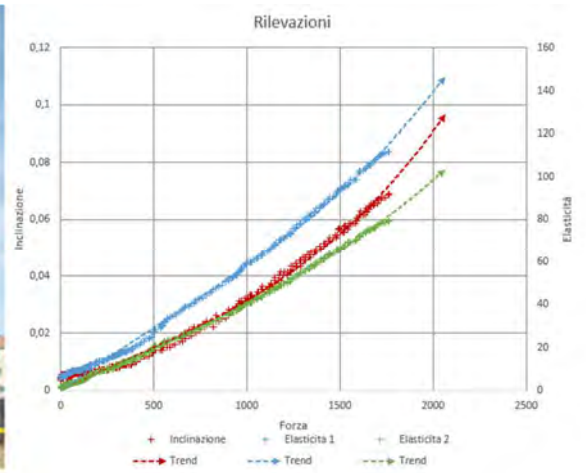
Alpha (°) = 0,33  
 F\_max (N) = 19841,31  
 M\_max (Nm) = 112811,33  
 M\_wind (Nm) = 173036,66  
**SF = 0,65**

Filters  
 Tare force at first value  
 Monotonicity for force  
 Monotonicity for inclination



## Appendix 1 – Pulling tests

### Piazza Moneta, Cesano Boscone – 16 – pt1



Measurement

Name: Cesano B.ne-16-pt1 09/03/2018

Rope height on tree (m): 6.9

Anchor-tree level difference (m): 0

Anchor-tree distance (m): 12.15

Drag factor: 0.25

Wind speed (m/s): 33

Crown Area (m<sup>2</sup>): 157

Crown center height (m): 11

Elastic Limit (%): 1.5

Inclino: Elaso1 Elasto2

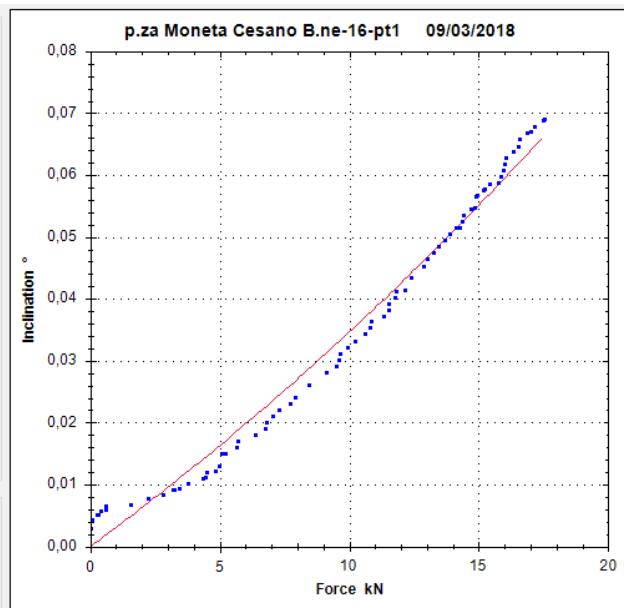
Alpha (°) = 0.52  
 F\_max (N) = 115081.60  
 M\_max (Nm) = 690486.52  
 M\_wind (Nm) = 282105.45  
**SF = 2,45**

Filters

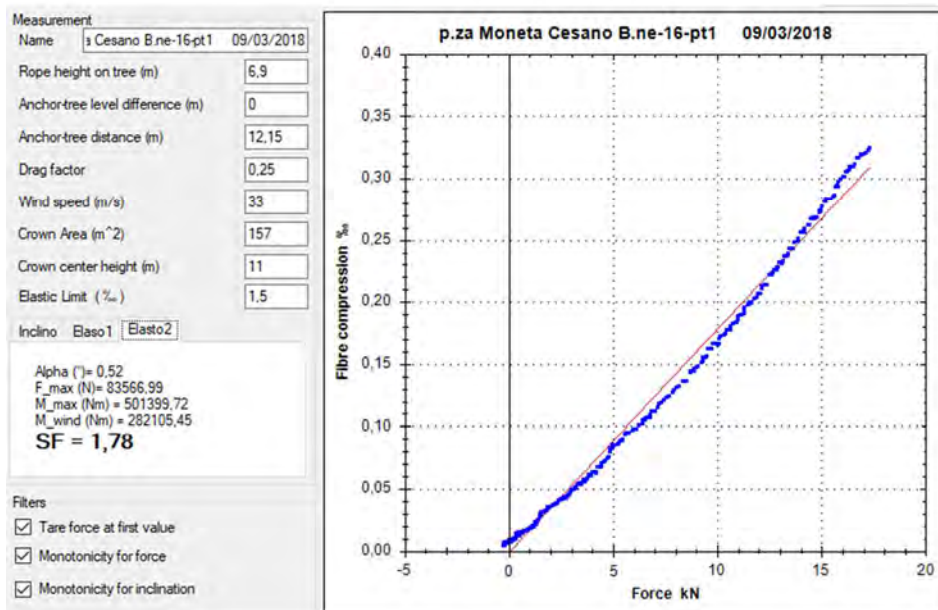
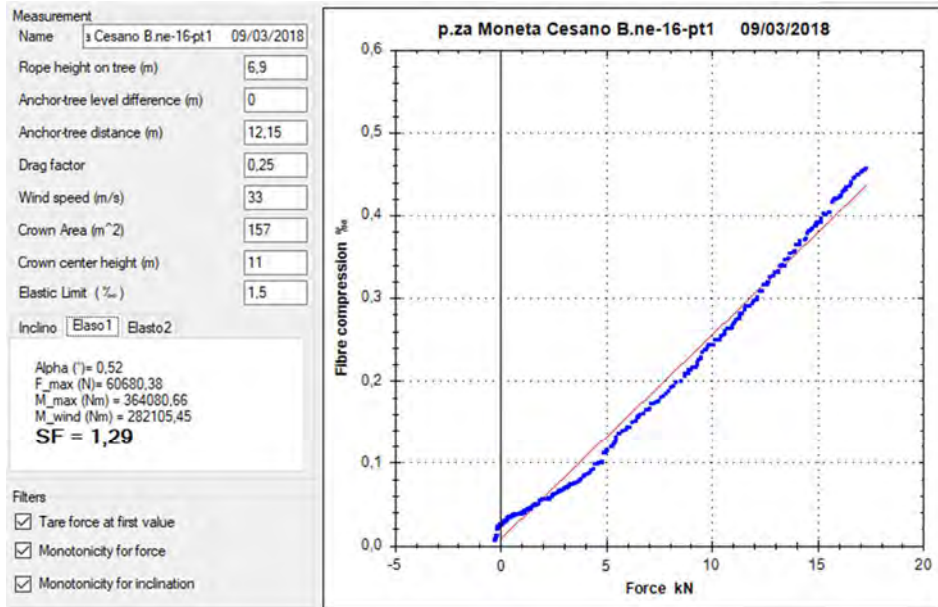
Tare force at first value

Monotonicity for force

Monotonicity for inclination

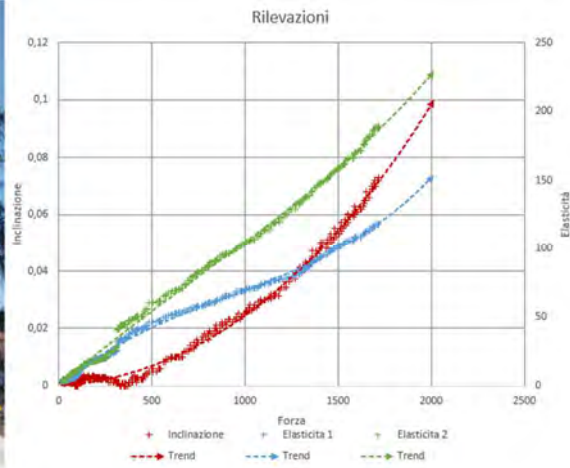


## Appendix 1 – Pulling tests



## Appendix 1 – Pulling tests

### Piazza Moneta, Cesano Boscone – 17 – pt1



Measurement

Name: p.za Moneta Cesano B.ne-17-pt1

Rope height on tree (m): 6

Anchor-tree level difference (m): 0

Anchor-tree distance (m): 14,1

Drag factor: 0,25

Wind speed (m/s): 33

Crown Area (m<sup>2</sup>): 140

Crown center height (m): 9,6

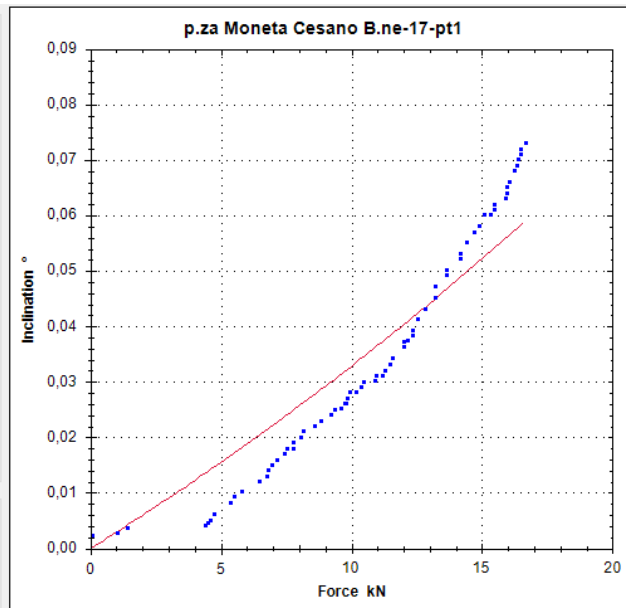
Elastic Limit (%): 1,5

Inclino: Elaso1 Elasto2

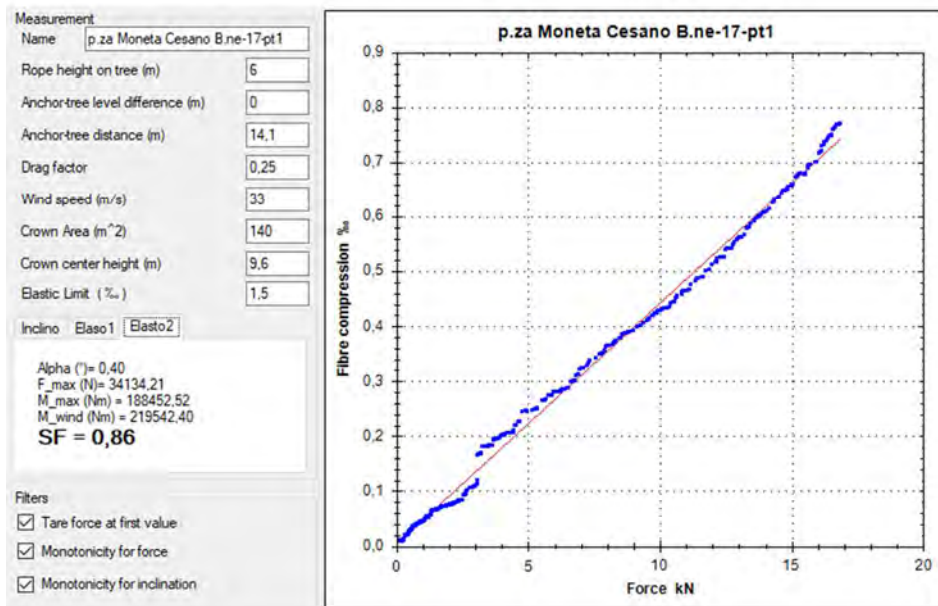
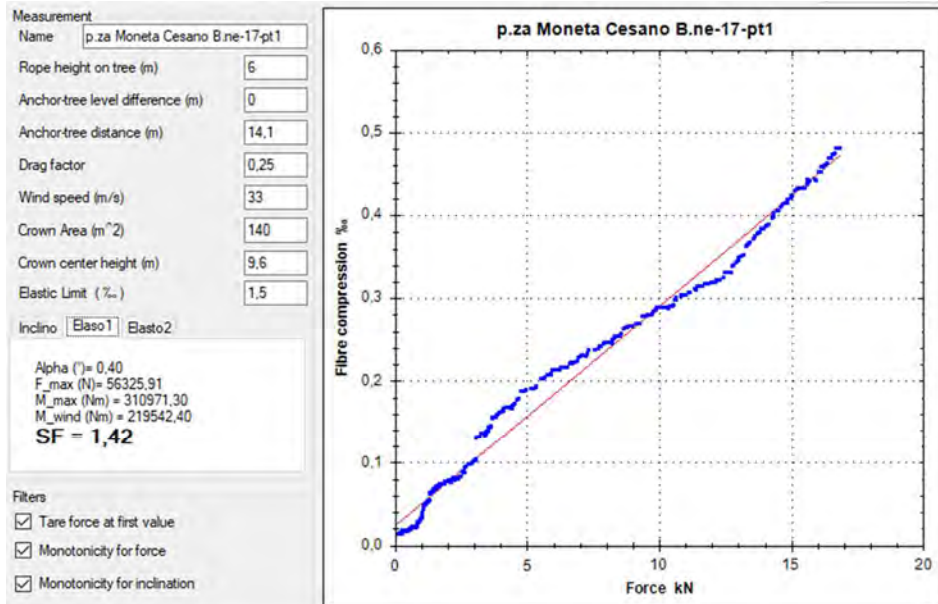
Alpha (°) = 0.40  
 F\_max (N) = 120620.42  
 M\_max (Nm) = 665936.66  
 M\_wind (Nm) = 219542.40  
**SF = 3,03**

Filters

- Tare force at first value
- Monotonicity for force
- Monotonicity for inclination

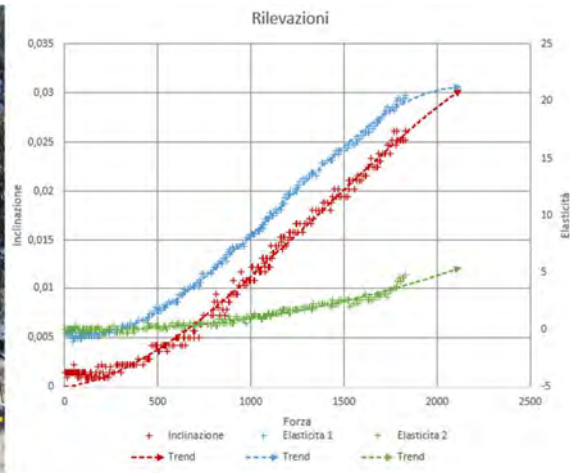


## Appendix 1 – Pulling tests



## Appendix 1 – Pulling tests

### Piazza Moneta, Cesano Boscone – 18 – pt1



Measurement

Name Cesano B.ne-18-pt1 09/03/2018

Rope height on tree (m) 7,5

Anchor-tree level difference (m) 0

Anchor-tree distance (m) 14,1

Drag factor 0,25

Wind speed (m/s) 33

Crown Area (m<sup>2</sup>) 263

Crown center height (m) 12,5

Elastic Limit (%) 2

Inclino Elaso1 Elasto2

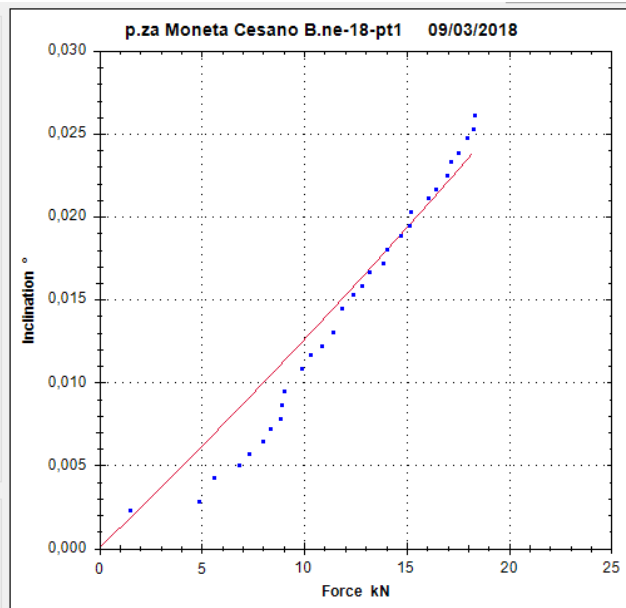
Alpha (°) = 0,49  
 F<sub>max</sub> (N) = 295114,62  
 M<sub>max</sub> (Nm) = 1954114,14  
 M<sub>wind</sub> (Nm) = 537013,13  
**SF = 3,64**

Filters

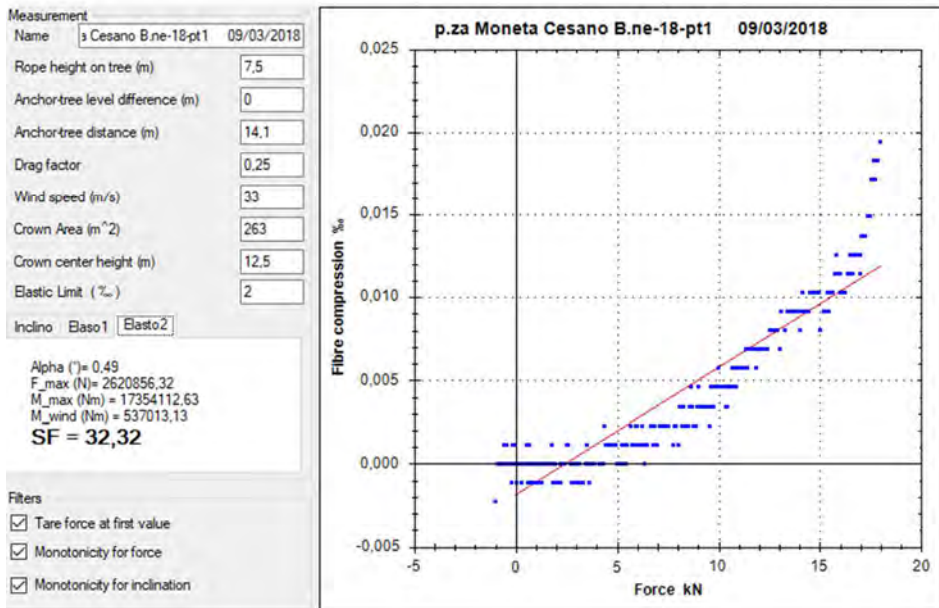
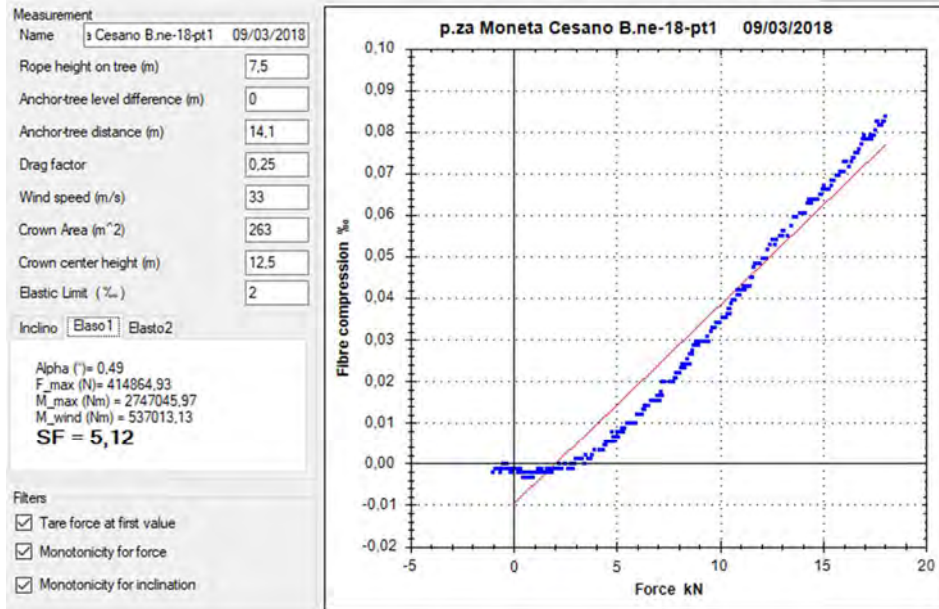
Tare force at first value

Monotonicity for force

Monotonicity for inclination

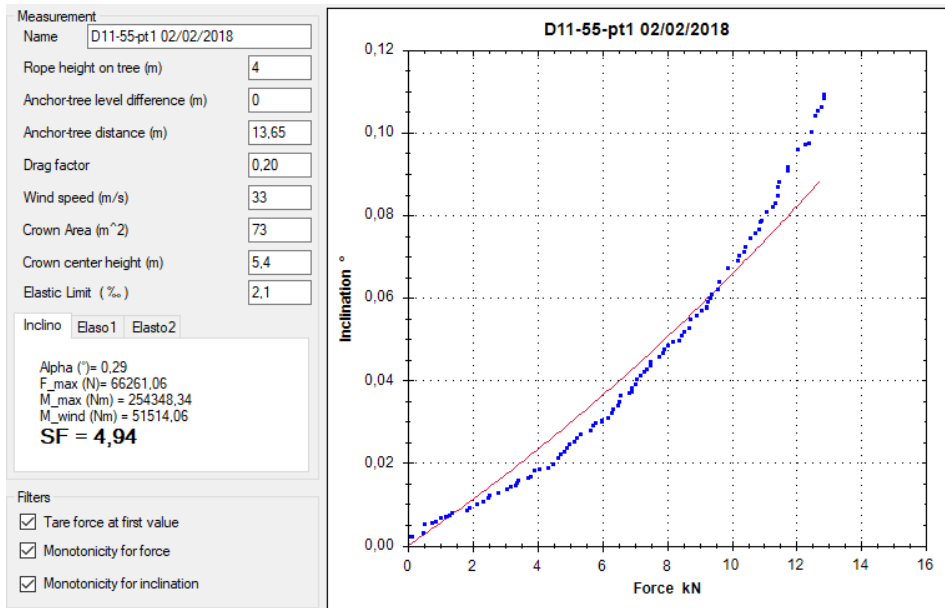
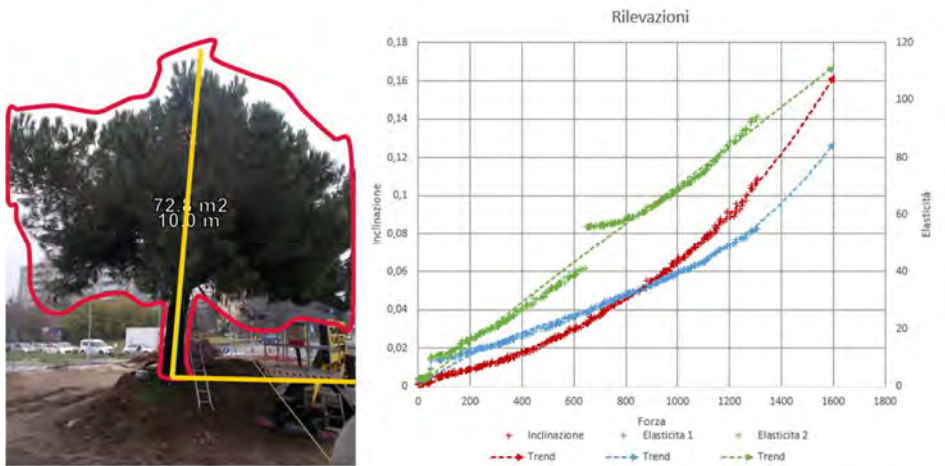


## Appendix 1 – Pulling tests



## Appendix 1 – Pulling tests

Piazza Tevere, San Donato Milanese – D11 – 55 – pt1





## Appendix 1 – Pulling tests

Measurement  
 Name

Rope height on tree (m)

Anchor-tree level difference (m)

Anchor-tree distance (m)

Drag factor

Wind speed (m/s)

Crown Area (m<sup>2</sup>)

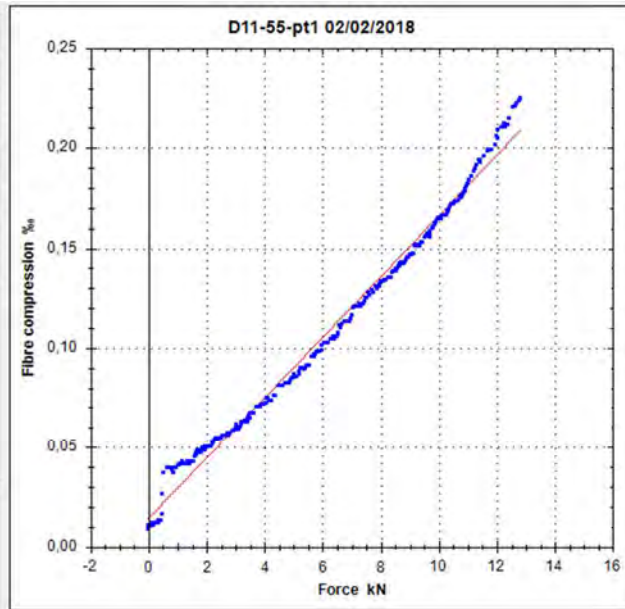
Crown center height (m)

Elastic Limit (%<sub>w</sub>)

Inclino

Alpha (°) = 0,29  
 F<sub>max</sub> (N) = 138509,45  
 M<sub>max</sub> (Nm) = 531679,55  
 M<sub>wind</sub> (Nm) = 51514,06  
**SF = 10,32**

Filters  
 Tare force at first value  
 Monotonicity for force  
 Monotonicity for inclination



Measurement  
 Name

Rope height on tree (m)

Anchor-tree level difference (m)

Anchor-tree distance (m)

Drag factor

Wind speed (m/s)

Crown Area (m<sup>2</sup>)

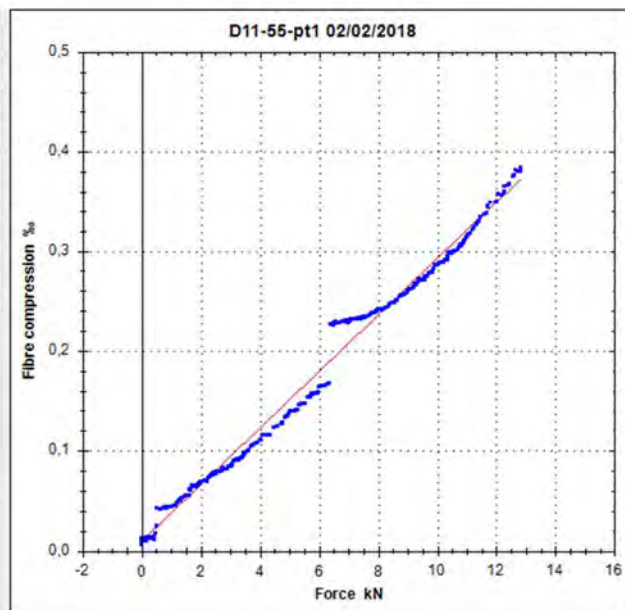
Crown center height (m)

Elastic Limit (%<sub>w</sub>)

Inclino

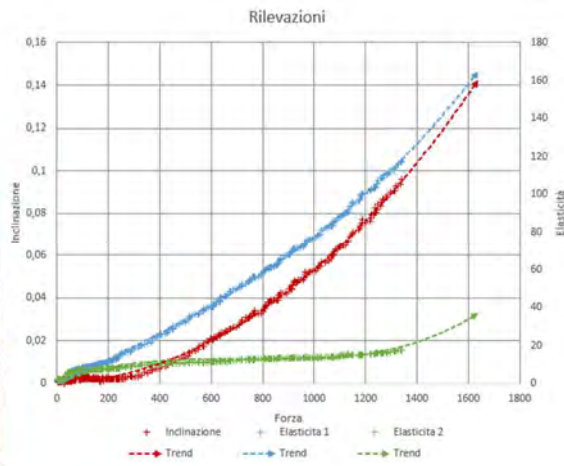
Alpha (°) = 0,29  
 F<sub>max</sub> (N) = 73925,31  
 M<sub>max</sub> (Nm) = 283768,20  
 M<sub>wind</sub> (Nm) = 51514,06  
**SF = 5,51**

Filters  
 Tare force at first value  
 Monotonicity for force  
 Monotonicity for inclination



## Appendix 1 – Pulling tests

Piazza Tevere, San Donato Milanese – D11 – 55 – pt2



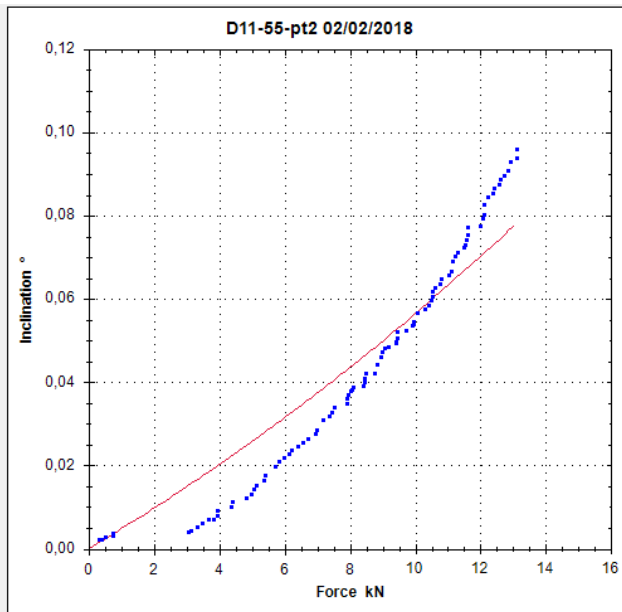
Measurement  
 Name: D11-55-pt2 02/02/2018

Rope height on tree (m): 4  
 Anchor-tree level difference (m): 0  
 Anchor-tree distance (m): 17,36  
 Drag factor: 0,20  
 Wind speed (m/s): 33  
 Crown Area (m<sup>2</sup>): 77  
 Crown center height (m): 5,4  
 Elastic Limit (%): 2,1

Inclino | Elaso1 | Elasto2

Alpha (°) = 0,23  
 F<sub>max</sub> (N) = 75210,72  
 M<sub>max</sub> (Nm) = 293161,40  
 M<sub>wind</sub> (Nm) = 54336,74  
**SF = 5,40**

Filters  
 Tare force at first value  
 Monotonicity for force  
 Monotonicity for inclination



## Appendix 1 – Pulling tests

Measurement  
 Name: D11-55-pt2 02/02/2018

Rope height on tree (m): 4

Anchor-tree level difference (m): 0

Anchor-tree distance (m): 17.36

Drag factor: 0.20

Wind speed (m/s): 33

Crown Area (m<sup>2</sup>): 77

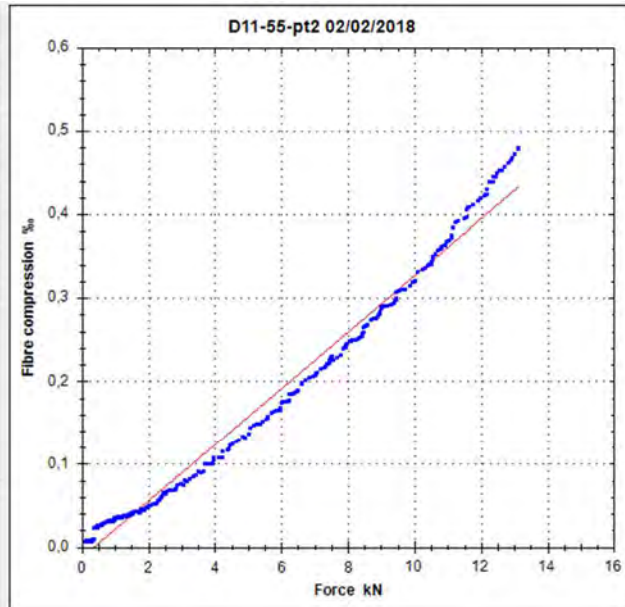
Crown center height (m): 5.4

Elastic Limit (%): 2.1

Inclino:  Elaso1  Elasto2

Alpha (°) = 0.23  
 F\_max (N) = 61843.29  
 M\_max (Nm) = 241056.93  
 M\_wind (Nm) = 54336.74  
**SF = 4,44**

Filters  
 Tare force at first value  
 Monotonicity for force  
 Monotonicity for inclination



Measurement  
 Name: D11-55-pt2 02/02/2018

Rope height on tree (m): 4

Anchor-tree level difference (m): 0

Anchor-tree distance (m): 17.36

Drag factor: 0.20

Wind speed (m/s): 33

Crown Area (m<sup>2</sup>): 77

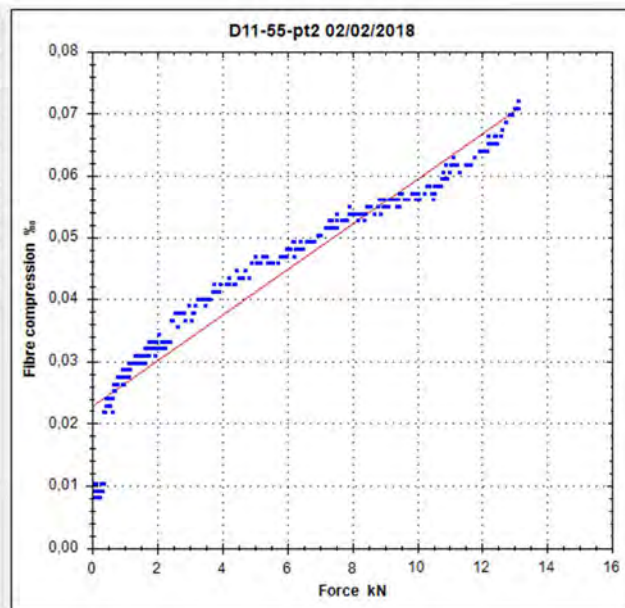
Crown center height (m): 5.4

Elastic Limit (%): 2.1

Inclino:  Elaso1  Elasto2

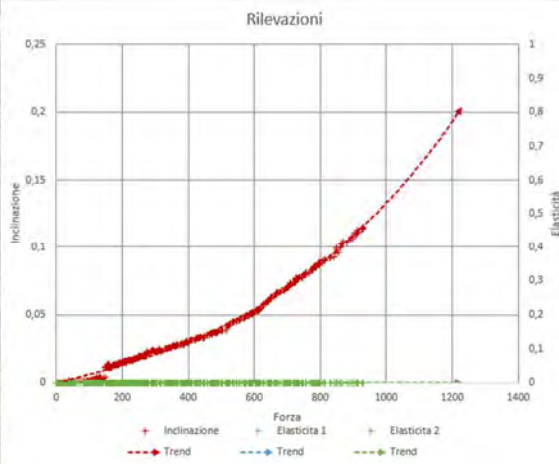
Alpha (°) = 0.23  
 F\_max (N) = 571722.28  
 M\_max (Nm) = 2228497.56  
 M\_wind (Nm) = 54336.74  
**SF = 41,01**

Filters  
 Tare force at first value  
 Monotonicity for force  
 Monotonicity for inclination



## Appendix 1 – Pulling tests

### Piazza Tevere, San Donato Milanese – D11 – 56 – pt1



Measurement

Name: D11-56-pt1 02/02/2018

Rope height on tree (m): 4,00

Anchor-tree level difference (m): 0,00

Anchor-tree distance (m): 21,56

Drag factor: 0,30

Wind speed (m/s): 33,00

Crown Area (m<sup>2</sup>): 69,00

Crown center height (m): 6,60

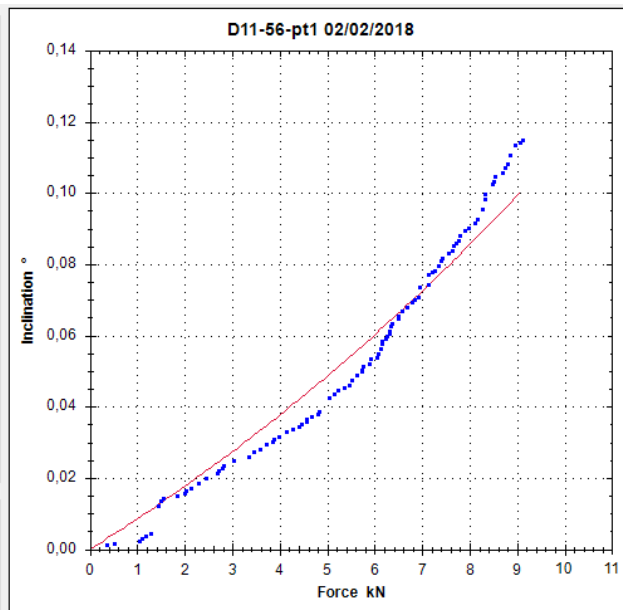
Elastic Limit (%): 2,5

Inclino: Elaso1 Elasto2

Alpha (°) = 0,18  
 F<sub>max</sub> (N) = 42742,95  
 M<sub>max</sub> (Nm) = 168103,16  
 M<sub>wind</sub> (Nm) = 89267,51  
**SF = 1,88**

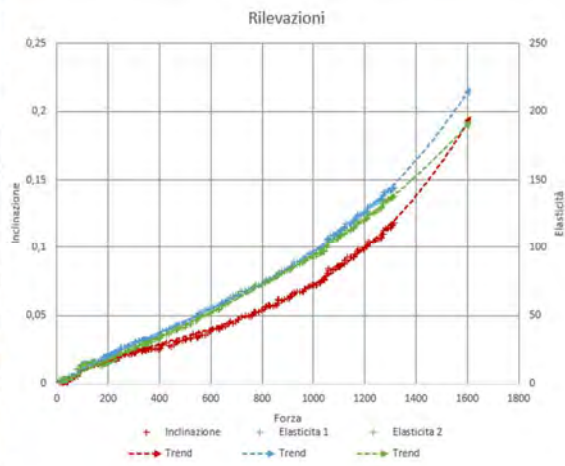
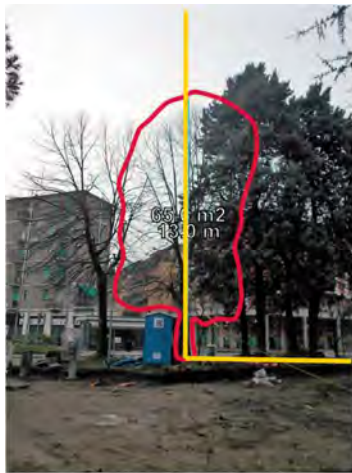
Filters

- Tare force at first value
- Monotonicity for force
- Monotonicity for inclination



Appendix 1 – Pulling tests

Piazza Tevere, San Donato Milanese – D11 – 57 – pt1



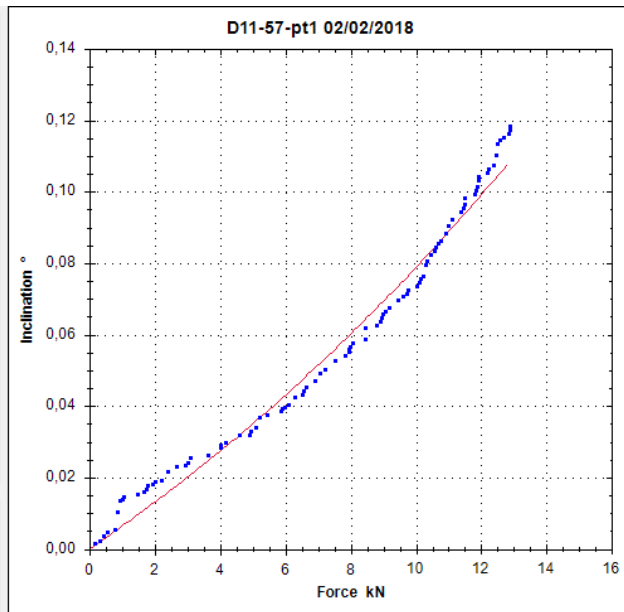
Measurement  
 Name D11-57-pt1 02/02/2018

Rope height on tree (m) 4,00  
 Anchor-tree level difference (m) 0,00  
 Anchor-tree distance (m) 21,77  
 Drag factor 0,30  
 Wind speed (m/s) 33,00  
 Crown Area (m<sup>2</sup>) 66,00  
 Crown center height (m) 7,30  
 Elastic Limit (%) 2,5

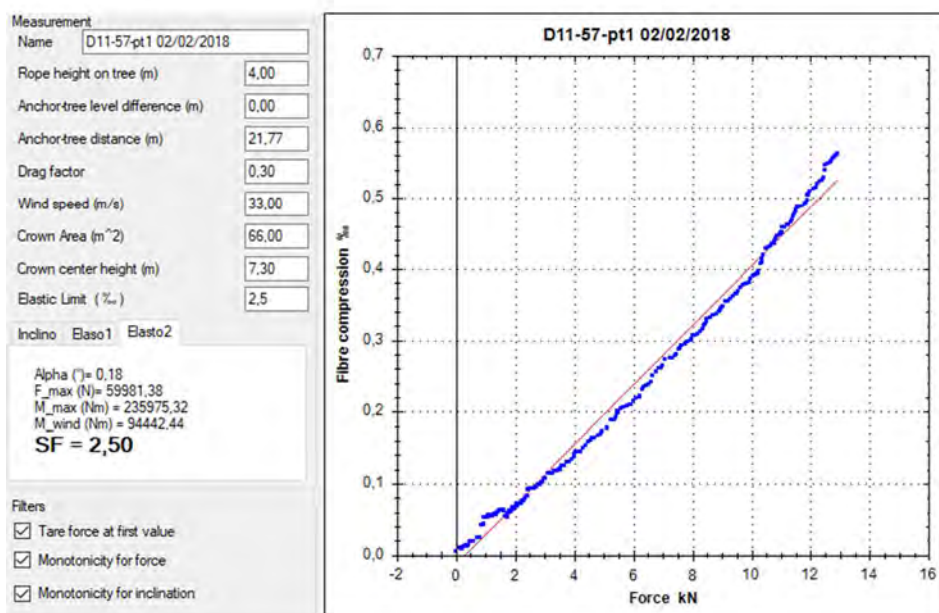
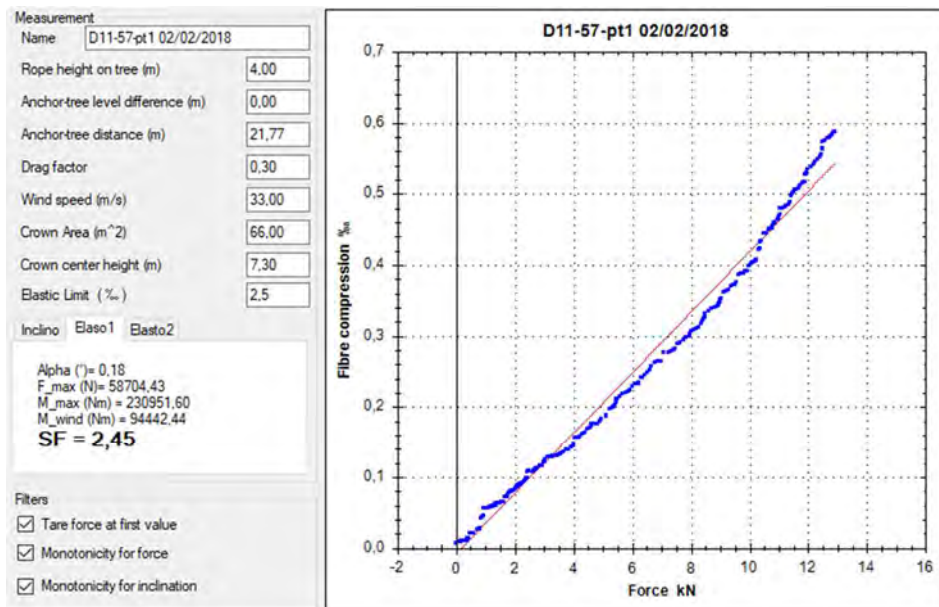
Inclino Elaso1 Elasto2

Alpha (°)= 0,18  
 F\_max (N)= 57018,66  
 M\_max (Nm) = 224319,56  
 M\_wind (Nm) = 94442,44  
**SF = 2,38**

Filters  
 Tare force at first value  
 Monotonicity for force  
 Monotonicity for inclination

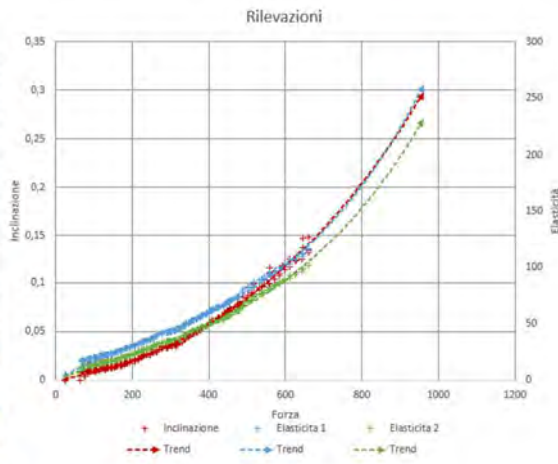


## Appendix 1 – Pulling tests



Appendix 1 – Pulling tests

Piazza Tevere, San Donato Milanese – D11 – 58 – pt1



Measurement

Name: D11-58-pt1 02/02/2018

Rope height on tree (m): 2,2

Anchor-tree level difference (m): 0

Anchor-tree distance (m): 20,50

Drag factor: 0,30

Wind speed (m/s): 33

Crown Area (m<sup>2</sup>): 83

Crown center height (m): 9

Elastic Limit (%): 2,5

Inclino | Elaso1 | Elasto2

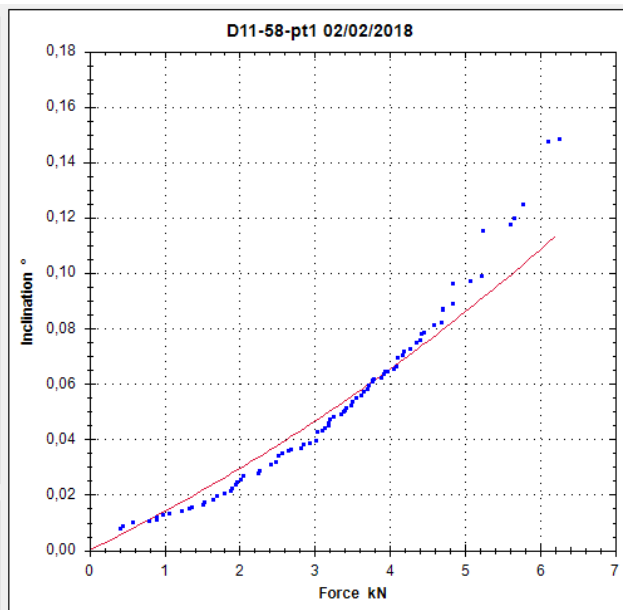
Alpha (°) = 0,11  
 F\_max (N) = 26599,82  
 M\_max (Nm) = 58185,49  
 M\_wind (Nm) = 146426,94  
**SF = 0,40**

Filters

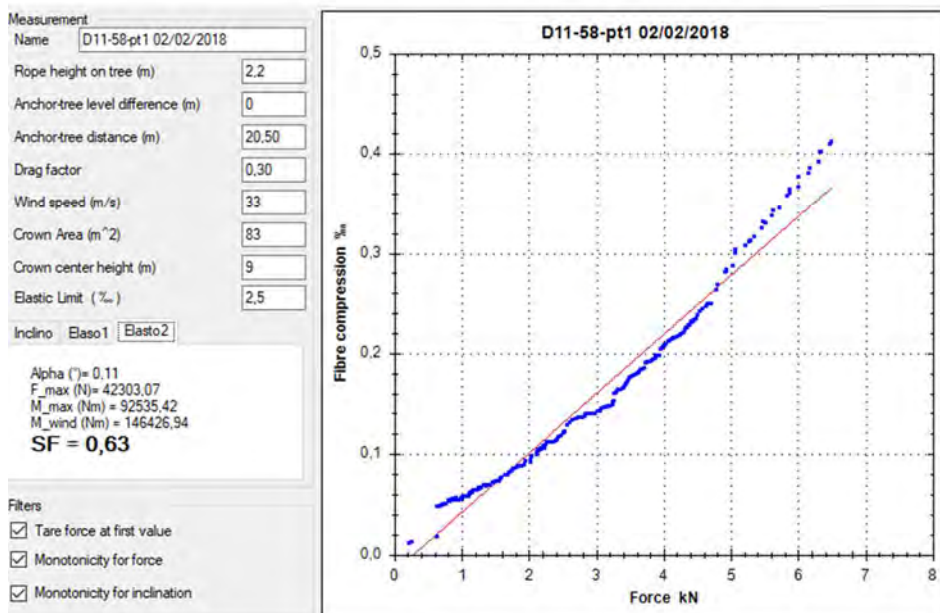
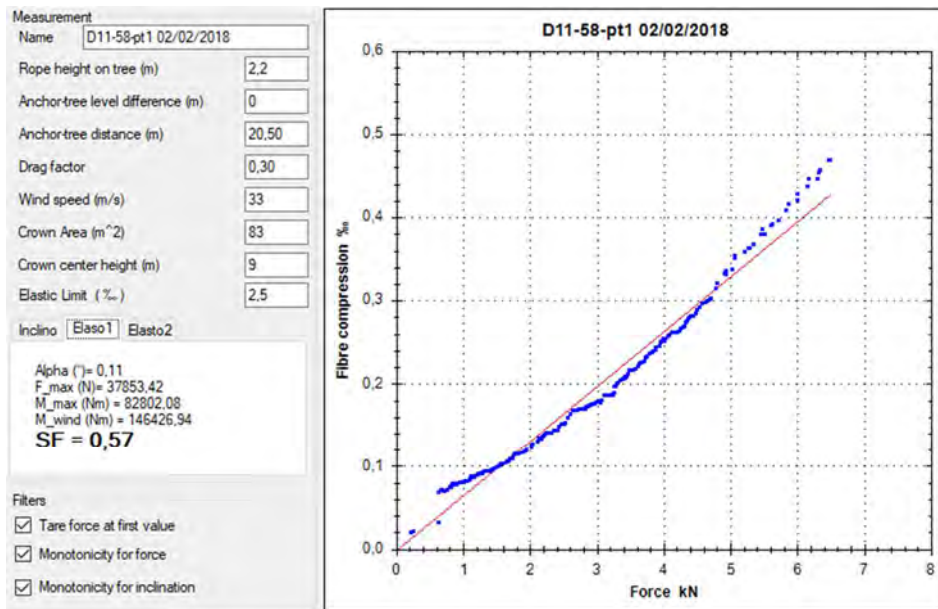
Tare force at first value

Monotonicity for force

Monotonicity for inclination



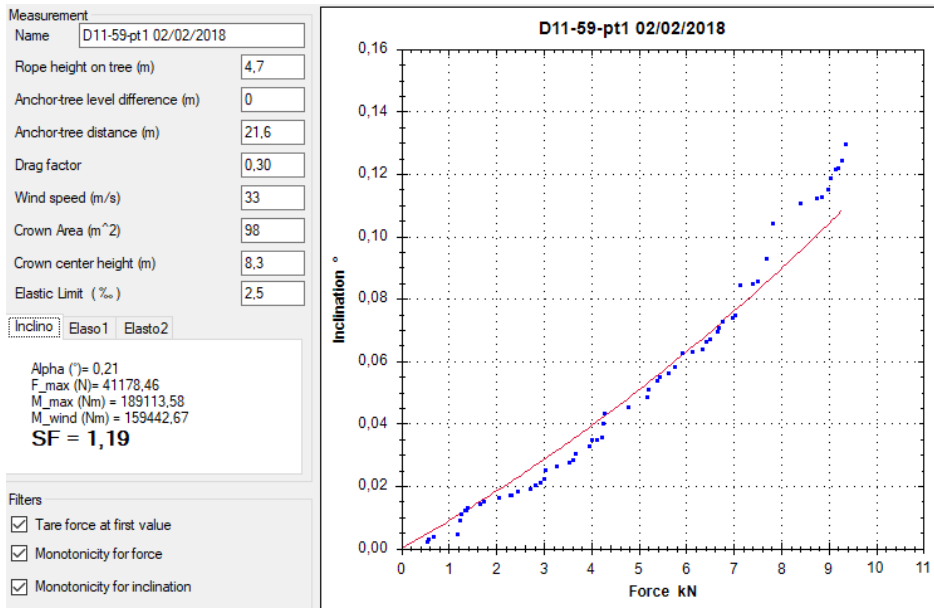
## Appendix 1 – Pulling tests





## Appendix 1 – Pulling tests

Piazza Tevere, San Donato Milanese – D11 – 59 – pt1



## Appendix 1 – Pulling tests

Measurement  
Name: D11-59-pt1 02/02/2018

Rope height on tree (m): 4,7

Anchor-tree level difference (m): 0

Anchor-tree distance (m): 21,6

Drag factor: 0,30

Wind speed (m/s): 33

Crown Area (m<sup>2</sup>): 98

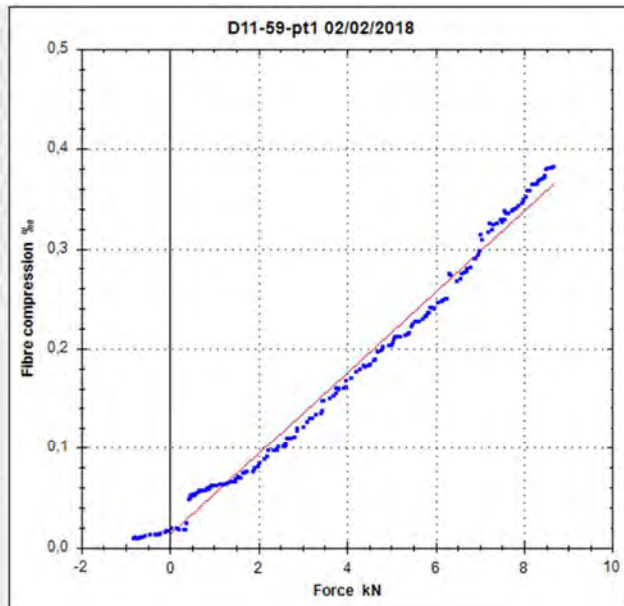
Crown center height (m): 8,3

Elastic Limit (%): 2,5

Inclino:  Elaso1  Elasto2

Alpha (°) = 0,21  
F<sub>max</sub> (N) = 61744,71  
M<sub>max</sub> (Nm) = 283564,84  
M<sub>wind</sub> (Nm) = 159442,67  
**SF = 1,78**

Filters  
 Tare force at first value  
 Monotonicity for force  
 Monotonicity for inclination



Measurement  
Name: D11-59-pt1 02/02/2018

Rope height on tree (m): 4,7

Anchor-tree level difference (m): 0

Anchor-tree distance (m): 21,6

Drag factor: 0,30

Wind speed (m/s): 33

Crown Area (m<sup>2</sup>): 98

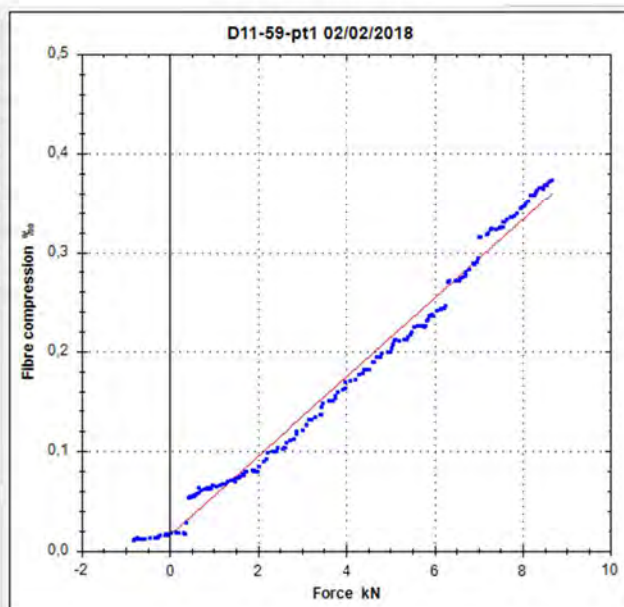
Crown center height (m): 8,3

Elastic Limit (%): 2,5

Inclino:  Elaso1  Elasto2

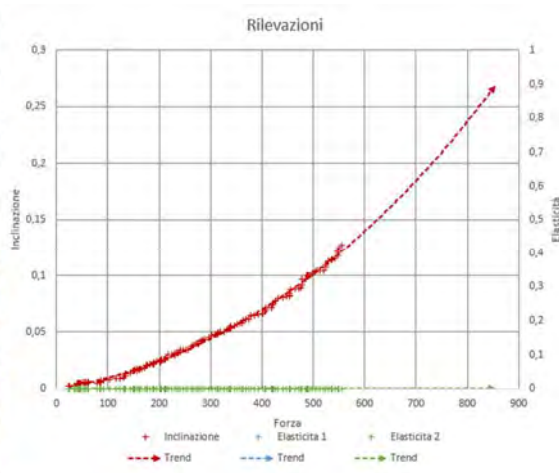
Alpha (°) = 0,21  
F<sub>max</sub> (N) = 63128,98  
M<sub>max</sub> (Nm) = 289922,18  
M<sub>wind</sub> (Nm) = 159442,67  
**SF = 1,82**

Filters  
 Tare force at first value  
 Monotonicity for force  
 Monotonicity for inclination



## Appendix 1 – Pulling tests

Piazza Tevere, San Donato Milanese – D11 – 63 – pt1



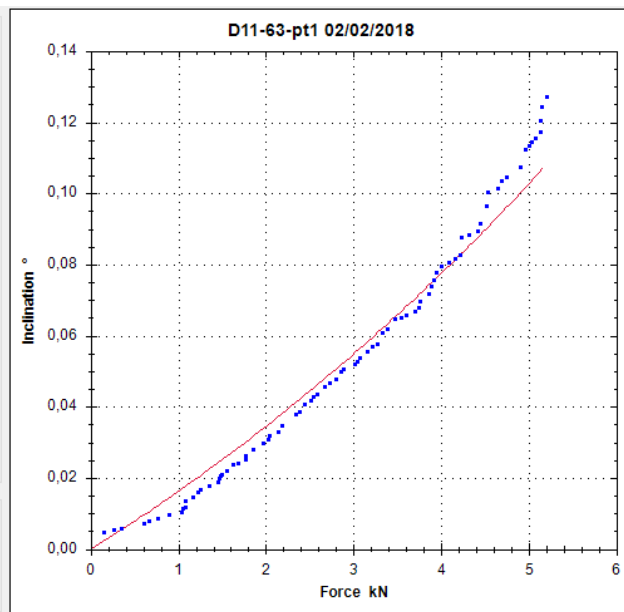
Measurement  
 Name: D11-63-pt1 02/02/2018

Rope height on tree (m): 4,5  
 Anchor-tree level difference (m): 0  
 Anchor-tree distance (m): 18,5  
 Drag factor: 0,25  
 Wind speed (m/s): 33  
 Crown Area (m<sup>2</sup>): 100  
 Crown center height (m): 7  
 Elastic Limit (%): 2

Inclino | Elaso1 | Elaso2

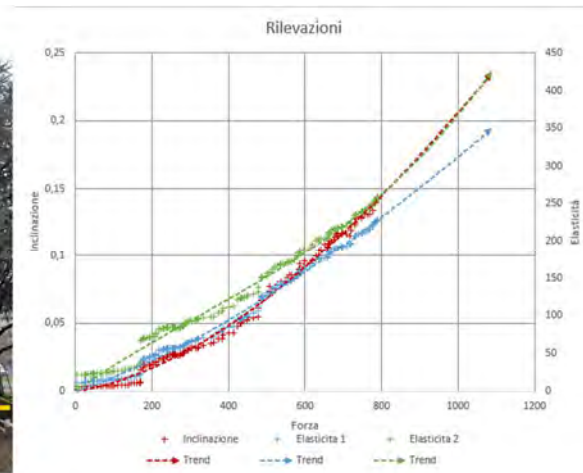
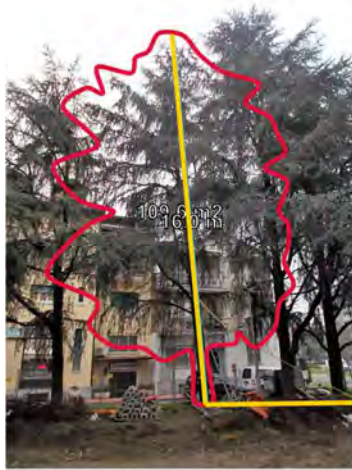
Alpha (°) = 0,24  
 F\_max (N) = 23128,45  
 M\_max (Nm) = 101129,24  
 M\_wind (Nm) = 114345,00  
**SF = 0,88**

Filters  
 Tare force at first value  
 Monotonicity for force  
 Monotonicity for inclination



## Appendix 1 – Pulling tests

Piazza Tevere, San Donato Milanese – D11 – 64 – pt1



Measurement  
Name D11-64-pt1 02/02/2018

Rope height on tree (m) 4.40

Anchor-tree level difference (m) 0

Anchor-tree distance (m) 18.03

Drag factor 0.25

Wind speed (m/s) 33

Crown Area (m<sup>2</sup>) 110

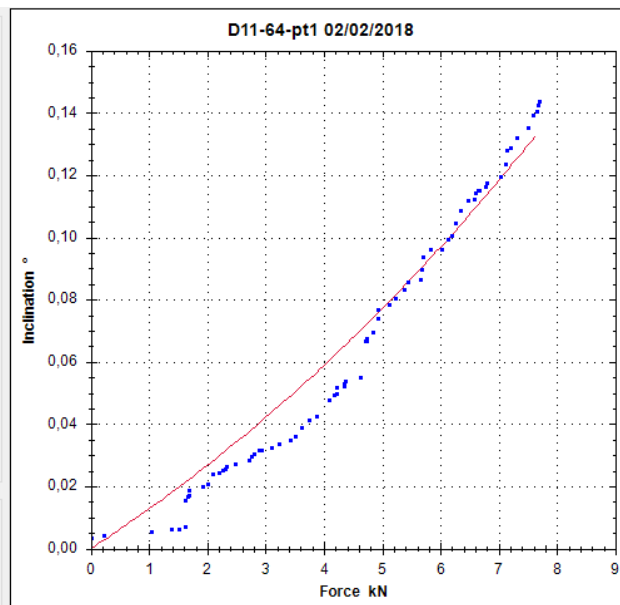
Crown center height (m) 8.5

Elastic Limit (%) 2

Inclino | Elaso1 | Elasto2

Alpha (°) = 0.24  
F\_max (N) = 29032.20  
M\_max (Nm) = 124099.79  
M\_wind (Nm) = 152732.25  
**SF = 0,81**

Filters  
 Tare force at first value  
 Monotonicity for force  
 Monotonicity for inclination



## Appendix 1 – Pulling tests

Measurement  
 Name

Rope height on tree (m)

Anchor-tree level difference (m)

Anchor-tree distance (m)

Drag factor

Wind speed (m/s)

Crown Area (m<sup>2</sup>)

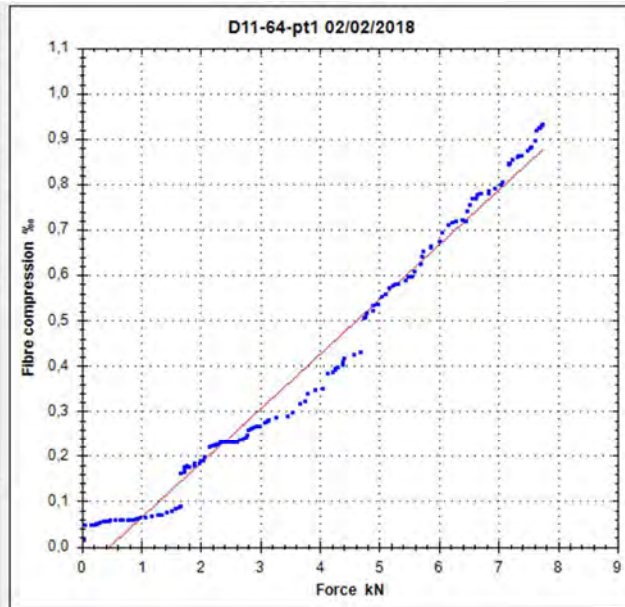
Crown center height (m)

Elastic Limit (%)

Inclino

Alpha (°) = 0,24  
 F<sub>max</sub> (N) = 16533,01  
 M<sub>max</sub> (Nm) = 70671,26  
 M<sub>wind</sub> (Nm) = 152732,25  
**SF = 0,46**

Filters  
 Tare force at first value  
 Monotonicity for force  
 Monotonicity for inclination



Measurement  
 Name

Rope height on tree (m)

Anchor-tree level difference (m)

Anchor-tree distance (m)

Drag factor

Wind speed (m/s)

Crown Area (m<sup>2</sup>)

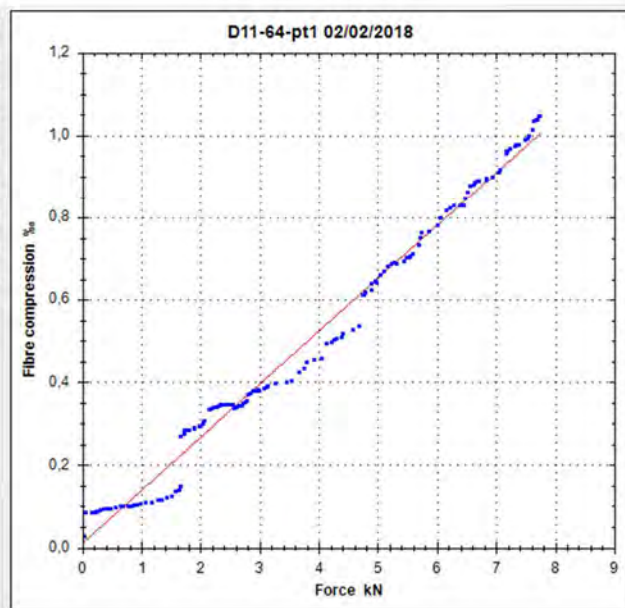
Crown center height (m)

Elastic Limit (%)

Inclino

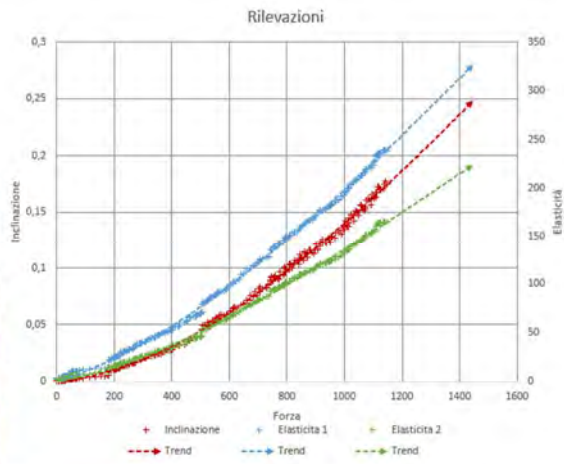
Alpha (°) = 0,24  
 F<sub>max</sub> (N) = 15526,47  
 M<sub>max</sub> (Nm) = 66368,76  
 M<sub>wind</sub> (Nm) = 152732,25  
**SF = 0,43**

Filters  
 Tare force at first value  
 Monotonicity for force  
 Monotonicity for inclination



## Appendix 1 – Pulling tests

### Piazza Tevere, San Donato Milanese – D11 – 65 – pt1



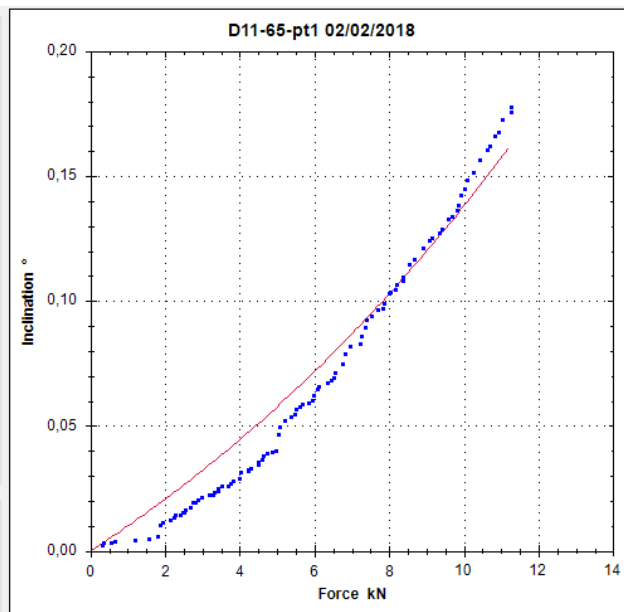
Measurement  
Name: D11-65-pt1 02/02/2018

Rope height on tree (m): 5  
Anchor-tree level difference (m): 0  
Anchor-tree distance (m): 15,88  
Drag factor: 0,25  
Wind speed (m/s): 33  
Crown Area (m<sup>2</sup>): 140  
Crown center height (m): 9,3  
Elastic Limit (%): 2

Inclino: Elaso1 Elasto2

Alpha (°) = 0,31  
F<sub>max</sub> (N) = 36922,58  
M<sub>max</sub> (Nm) = 176090,54  
M<sub>wind</sub> (Nm) = 212681,70  
**SF = 0,83**

Filters  
 Tare force at first value  
 Monotonicity for force  
 Monotonicity for inclination



## Appendix 1 – Pulling tests

Measurement  
 Name

Rope height on tree (m)

Anchor-tree level difference (m)

Anchor-tree distance (m)

Drag factor

Wind speed (m/s)

Crown Area (m<sup>2</sup>)

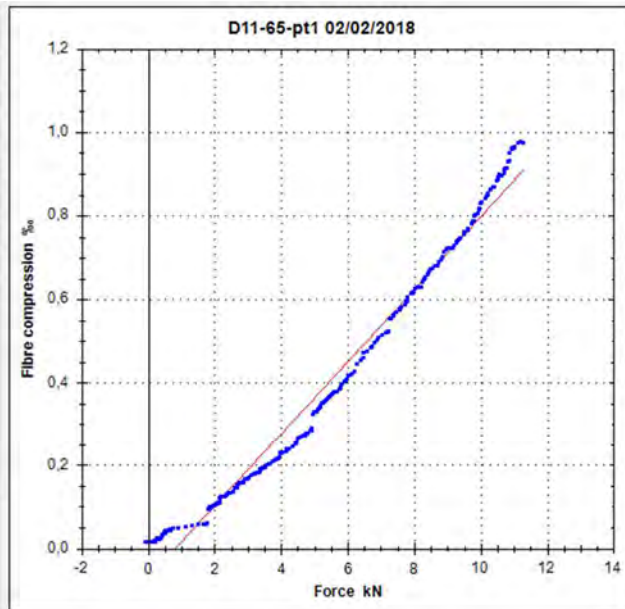
Crown center height (m)

Elastic Limit (%)

Inclino

Alpha (°) = 0,31  
 F<sub>max</sub> (N) = 23004,38  
 M<sub>max</sub> (Nm) = 109712,07  
 M<sub>wind</sub> (Nm) = 212681,70  
**SF = 0,52**

Filters  
 Tare force at first value  
 Monotonicity for force  
 Monotonicity for inclination



Measurement  
 Name

Rope height on tree (m)

Anchor-tree level difference (m)

Anchor-tree distance (m)

Drag factor

Wind speed (m/s)

Crown Area (m<sup>2</sup>)

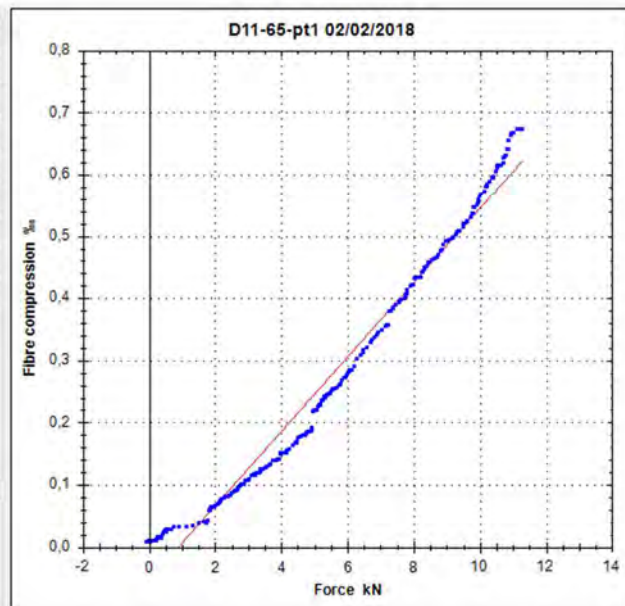
Crown center height (m)

Elastic Limit (%)

Inclino

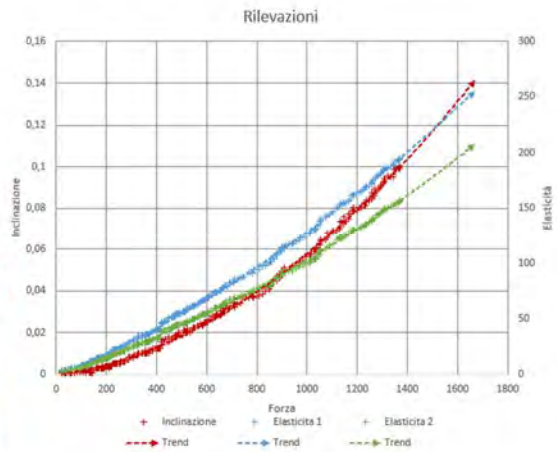
Alpha (°) = 0,31  
 F<sub>max</sub> (N) = 33299,80  
 M<sub>max</sub> (Nm) = 158812,81  
 M<sub>wind</sub> (Nm) = 212681,70  
**SF = 0,75**

Filters  
 Tare force at first value  
 Monotonicity for force  
 Monotonicity for inclination



## Appendix 1 – Pulling tests

### Piazza Tevere, San Donato Milanese – D11 – 66 – pt1



Measurement

Name: D11-66-pt1 02/02/2018

Rope height on tree (m): 4,6

Anchor-tree level difference (m): 0

Anchor-tree distance (m): 18,82

Drag factor: 0,25

Wind speed (m/s): 33

Crown Area (m<sup>2</sup>): 136

Crown center height (m): 7,8

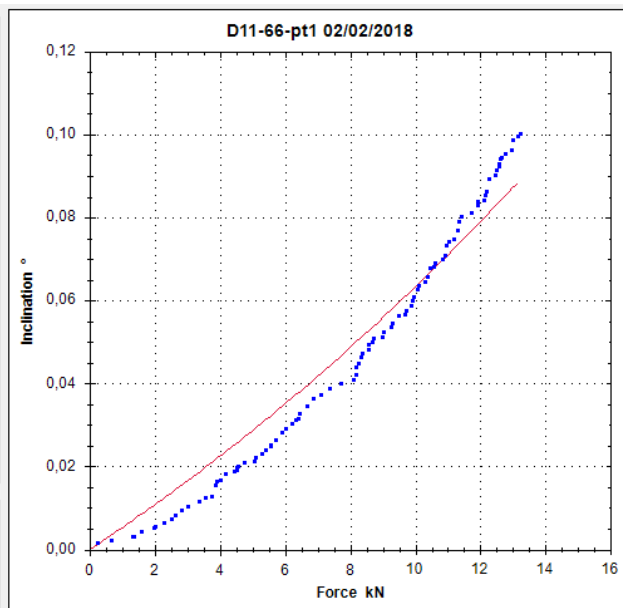
Elastic Limit (%): 2

Inclino Elaso1 Elasto2

Alpha (°) = 0,24  
 F<sub>max</sub> (N) = 68285,84  
 M<sub>max</sub> (Nm) = 305132,53  
 M<sub>wind</sub> (Nm) = 173281,68  
**SF = 1,76**

Filters

- Tare force at first value
- Monotonicity for force
- Monotonicity for inclination





## Appendix 1 – Pulling tests

Measurement  
Name: D11-66-pt1 02/02/2018

Rope height on tree (m): 4,6

Anchor-tree level difference (m): 0

Anchor-tree distance (m): 18,82

Drag factor: 0,25

Wind speed (m/s): 33

Crown Area (m<sup>2</sup>): 136

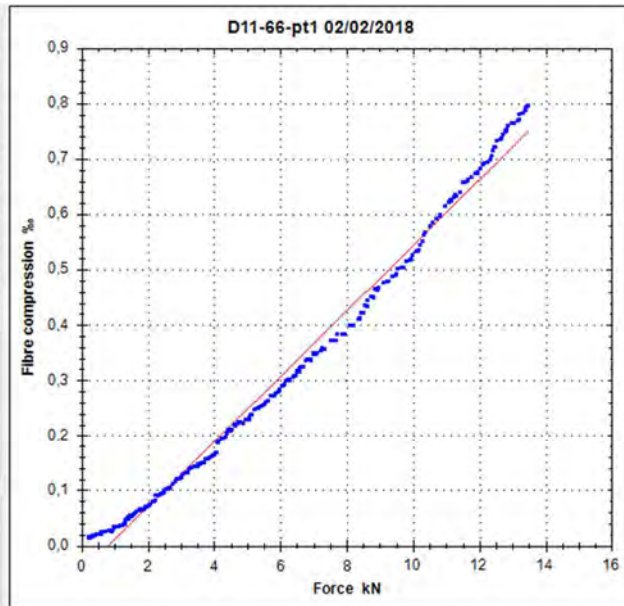
Crown center height (m): 7,8

Elastic Limit (%): 2

Inclino:  Elaso1  Elasto2

Alpha (°) = 0,24  
F<sub>max</sub> (N) = 33692,58  
M<sub>max</sub> (Nm) = 150553,93  
M<sub>wind</sub> (Nm) = 173281,68  
**SF = 0,87**

Filters  
 Tare force at first value  
 Monotonicity for force  
 Monotonicity for inclination



Measurement  
Name: D11-66-pt1 02/02/2018

Rope height on tree (m): 4,6

Anchor-tree level difference (m): 0

Anchor-tree distance (m): 18,82

Drag factor: 0,25

Wind speed (m/s): 33

Crown Area (m<sup>2</sup>): 136

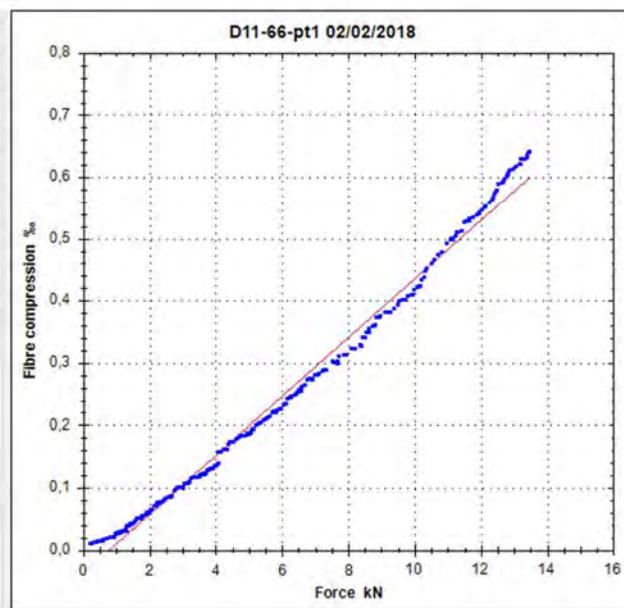
Crown center height (m): 7,8

Elastic Limit (%): 2

Inclino:  Elaso1  Elasto2

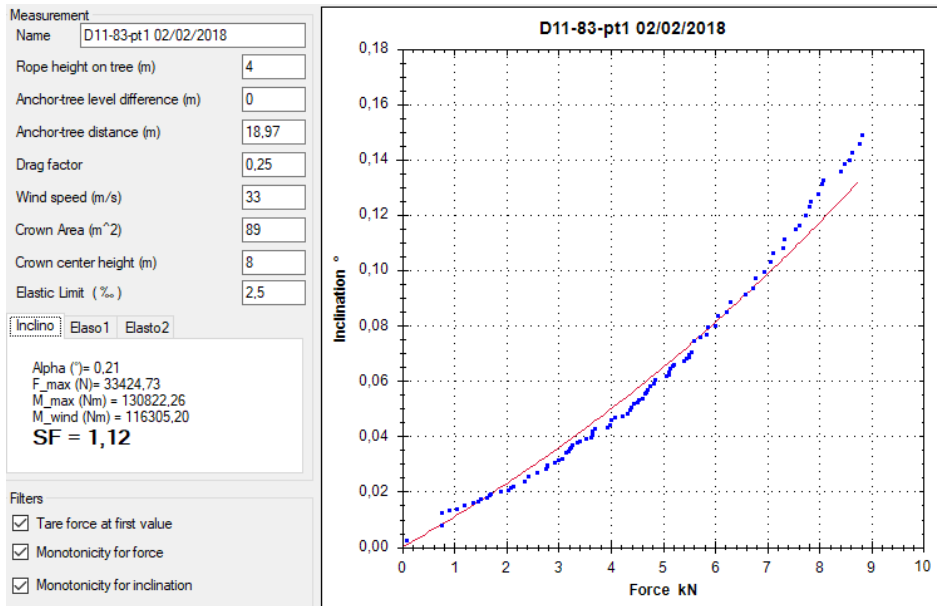
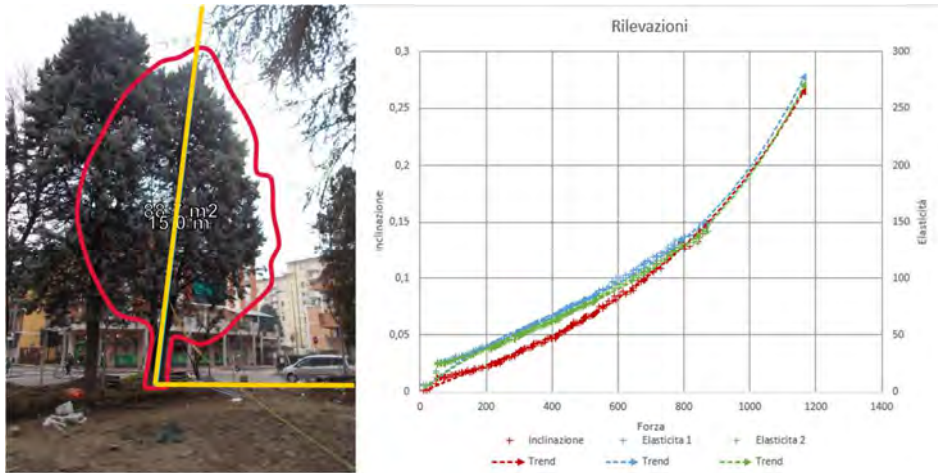
Alpha (°) = 0,24  
F<sub>max</sub> (N) = 42184,84  
M<sub>max</sub> (Nm) = 188501,24  
M<sub>wind</sub> (Nm) = 173281,68  
**SF = 1,09**

Filters  
 Tare force at first value  
 Monotonicity for force  
 Monotonicity for inclination



## Appendix 1 – Pulling tests

Piazza Tevere, San Donato Milanese – D11 – 83 – pt1



## Appendix 1 – Pulling tests

Measurement  
 Name

Rope height on tree (m)

Anchor-tree level difference (m)

Anchor-tree distance (m)

Drag factor

Wind speed (m/s)

Crown Area (m<sup>2</sup>)

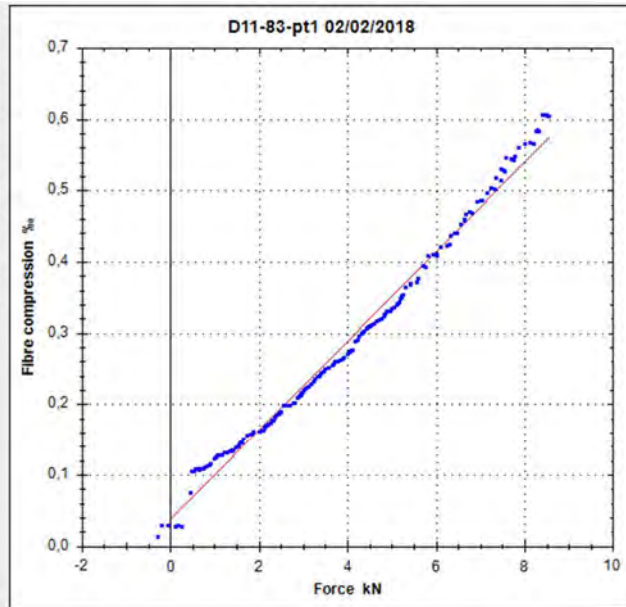
Crown center height (m)

Elastic Limit (%<sub>o</sub>)

Inclino

Alpha (°)= 0,21  
 F<sub>max</sub> (N)= 39816,00  
 M<sub>max</sub> (Nm) = 155837,28  
 M<sub>wind</sub> (Nm) = 116305,20  
**SF = 1,34**

Filters  
 Tare force at first value  
 Monotonicity for force  
 Monotonicity for inclination



Measurement  
 Name

Rope height on tree (m)

Anchor-tree level difference (m)

Anchor-tree distance (m)

Drag factor

Wind speed (m/s)

Crown Area (m<sup>2</sup>)

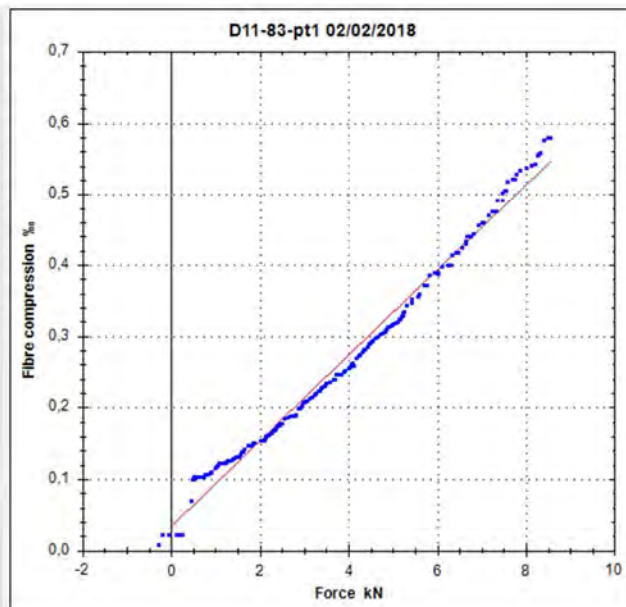
Crown center height (m)

Elastic Limit (%<sub>o</sub>)

Inclino

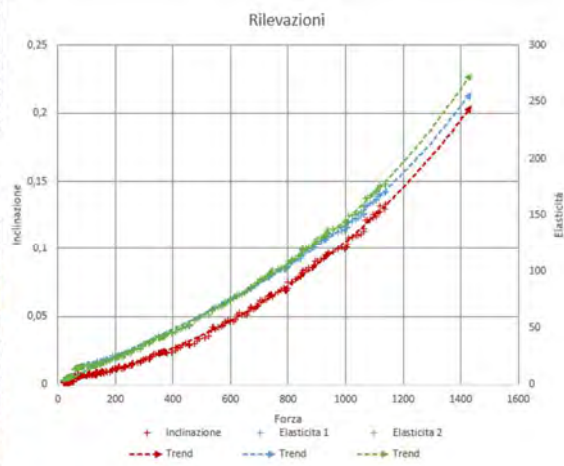
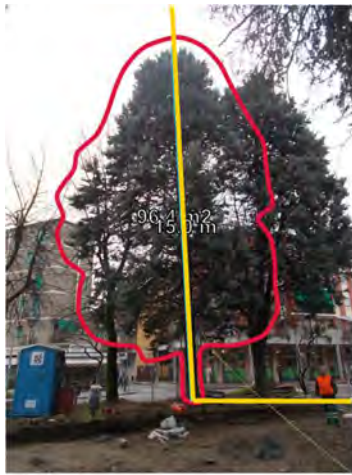
Alpha (°)= 0,21  
 F<sub>max</sub> (N)= 41785,79  
 M<sub>max</sub> (Nm) = 163546,93  
 M<sub>wind</sub> (Nm) = 116305,20  
**SF = 1,41**

Filters  
 Tare force at first value  
 Monotonicity for force  
 Monotonicity for inclination



## Appendix 1 – Pulling tests

Piazza Tevere, San Donato Milanese – D11 – 84 – pt1



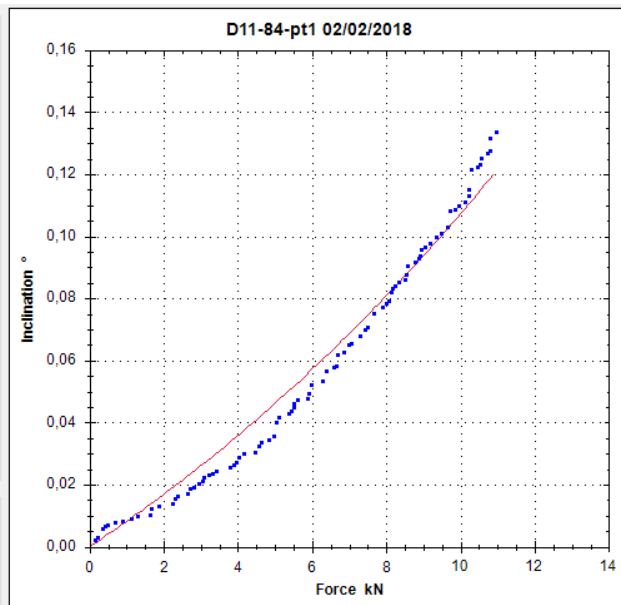
Measurement  
Name: D11-84-pt1 02/02/2018

Rope height on tree (m): 3,9  
Anchor-tree level difference (m): 0  
Anchor-tree distance (m): 18,25  
Drag factor: 0,25  
Wind speed (m/s): 33  
Crown Area (m<sup>2</sup>): 97  
Crown center height (m): 7,9  
Elastic Limit (%): 2,5

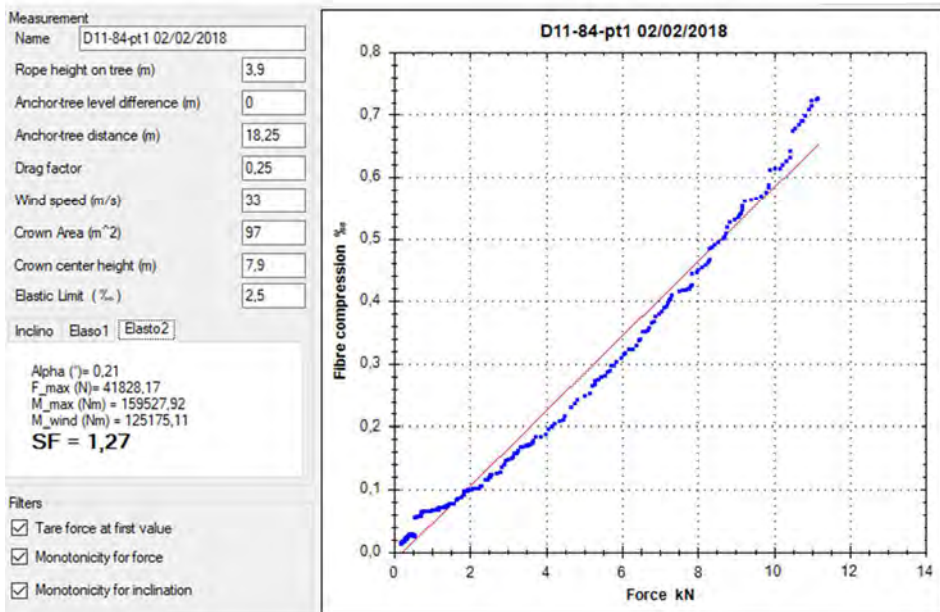
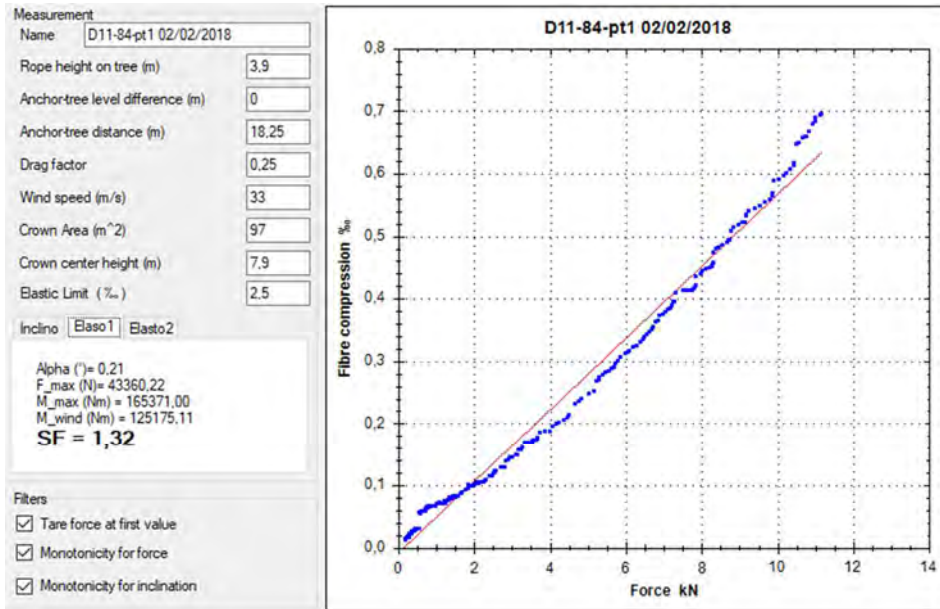
Inclino Elaso1 Elasto2

Alpha (°) = 0,21  
F<sub>max</sub> (N) = 44677,98  
M<sub>max</sub> (Nm) = 170396,78  
M<sub>wind</sub> (Nm) = 125175,11  
**SF = 1,36**

Filters  
 Tare force at first value  
 Monotonicity for force  
 Monotonicity for inclination

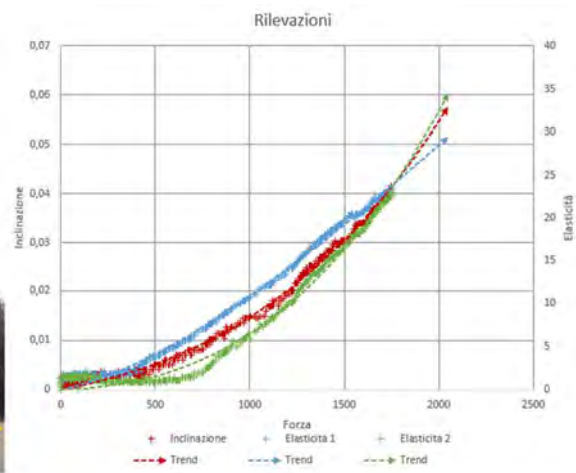


## Appendix 1 – Pulling tests



## Appendix 1 – Pulling tests

### Via della Fara, Bergamo – 331 – 1386 – pt1



Measurement

Name

Rope height on tree (m)

Anchor-tree level difference (m)

Anchor-tree distance (m)

Drag factor

Wind speed (m/s)

Crown Area (m<sup>2</sup>)

Crown center height (m)

Elastic Limit (%)

Inclino  Elaso1  Elasto2

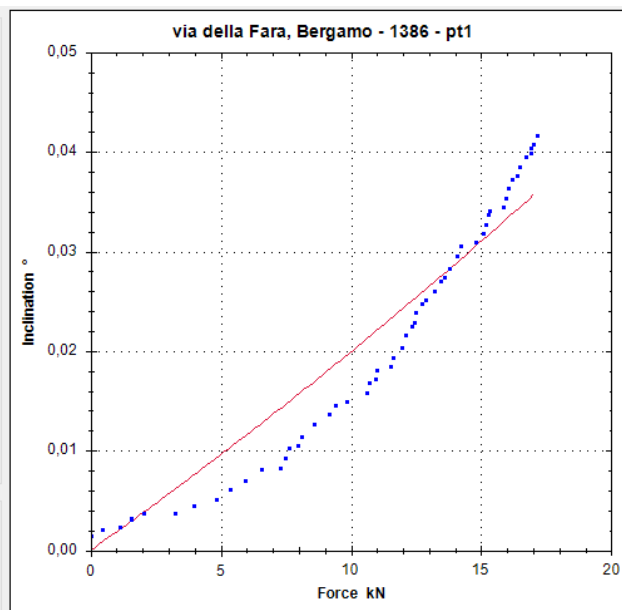
Alpha (°) = 0.44  
 F<sub>max</sub> (N) = 190621.94  
 M<sub>max</sub> (Nm) = 794946.37  
 M<sub>wind</sub> (Nm) = 302801.90  
**SF = 2,63**

Filters

Tare force at first value

Monotonicity for force

Monotonicity for inclination



## Appendix 1 – Pulling tests

Measurement

Name

Rope height on tree (m)

Anchor-tree level difference (m)

Anchor-tree distance (m)

Drag factor

Wind speed (m/s)

Crown Area (m<sup>2</sup>)

Crown center height (m)

Elastic Limit (%)

Inclino  Elaso1  Elasto2

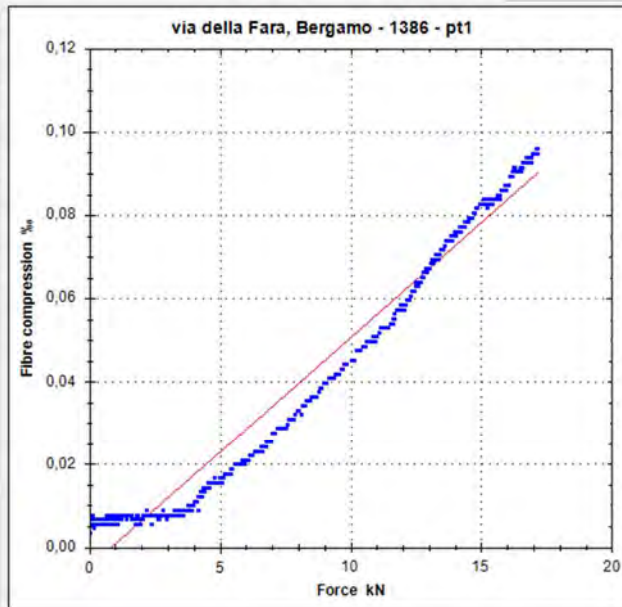
Alpha (°) = 0,44  
 F\_max (N) = 778658,57  
 M\_max (Nm) = 3247222,30  
 M\_wind (Nm) = 302801,90  
**SF = 10,72**

Filters

Tare force at first value

Monotonicity for force

Monotonicity for inclination



Measurement

Name

Rope height on tree (m)

Anchor-tree level difference (m)

Anchor-tree distance (m)

Drag factor

Wind speed (m/s)

Crown Area (m<sup>2</sup>)

Crown center height (m)

Elastic Limit (%)

Inclino  Elaso1  Elasto2

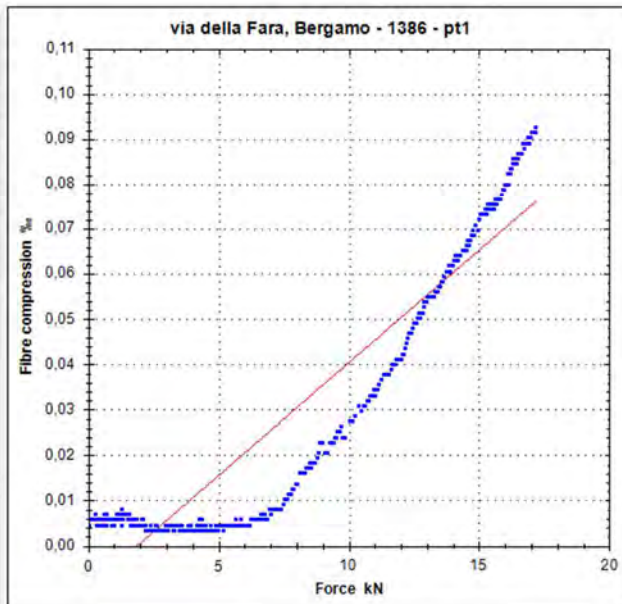
Alpha (°) = 0,44  
 F\_max (N) = 863154,96  
 M\_max (Nm) = 3599595,69  
 M\_wind (Nm) = 302801,90  
**SF = 11,89**

Filters

Tare force at first value

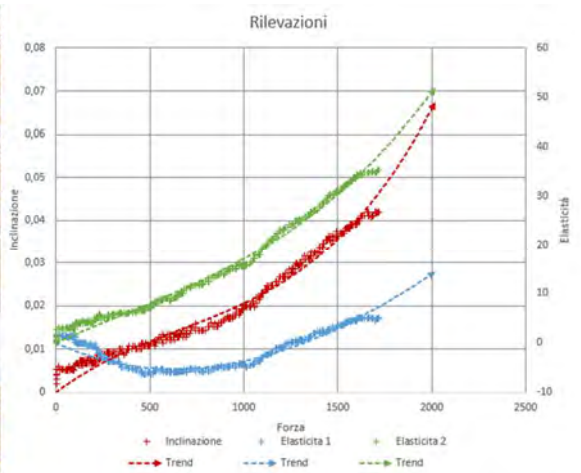
Monotonicity for force

Monotonicity for inclination



## Appendix 1 – Pulling tests

### Via della Fara, Bergamo – 331 – 1386 – pt2



Measurement

Name

Rope height on tree (m)

Anchor-tree level difference (m)

Anchor-tree distance (m)

Drag factor

Wind speed (m/s)

Crown Area (m<sup>2</sup>)

Crown center height (m)

Elastic Limit (%)

Incino     Elaso1     Elasto2

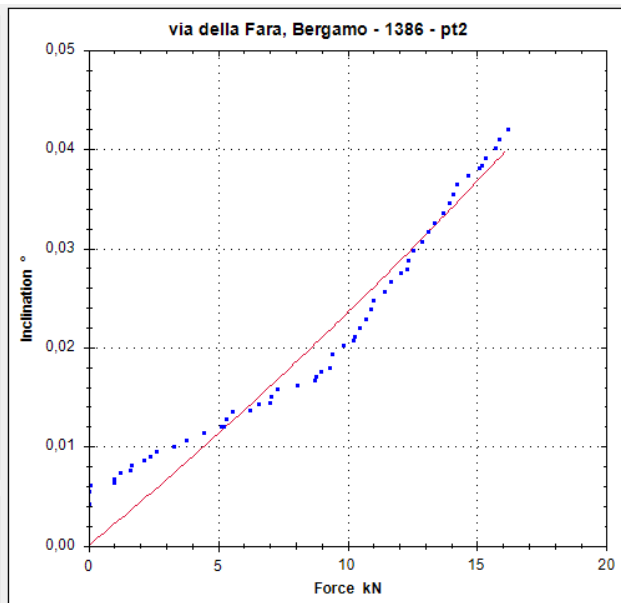
Alpha (°) = 0.20  
 F<sub>max</sub> (N) = 163717.72  
 M<sub>max</sub> (Nm) = 738621.36  
 M<sub>wind</sub> (Nm) = 291089.70  
**SF = 2,54**

Filters

Tare force at first value

Monotonicity for force

Monotonicity for inclination





## Appendix 1 – Pulling tests

Measurement

Name:

Rope height on tree (m):

Anchor-tree level difference (m):

Anchor-tree distance (m):

Drag factor:

Wind speed (m/s):

Crown Area (m<sup>2</sup>):

Crown center height (m):

Elastic Limit (%):

Inclino:

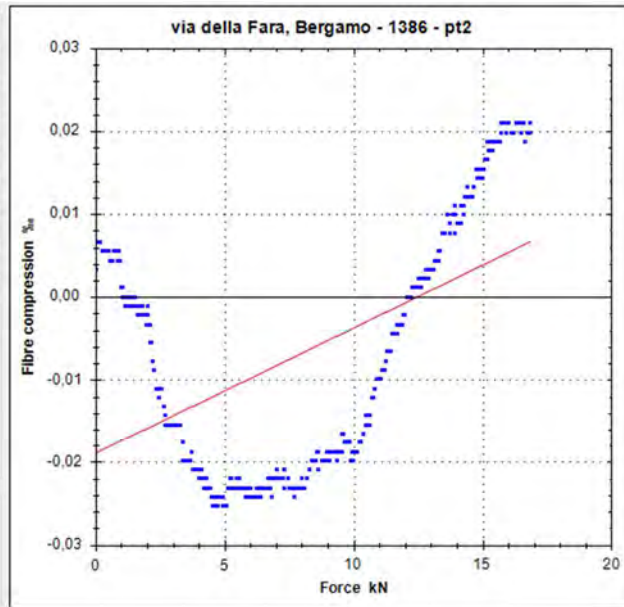
Alpha (°) = 0,20  
 F<sub>max</sub> (N) = 2840201,21  
 M<sub>max</sub> (Nm) = 12813721,85  
 M<sub>wind</sub> (Nm) = 291089,70  
**SF = 44,02**

Filters

Tare force at first value

Monotonicity for force

Monotonicity for inclination



Measurement

Name:

Rope height on tree (m):

Anchor-tree level difference (m):

Anchor-tree distance (m):

Drag factor:

Wind speed (m/s):

Crown Area (m<sup>2</sup>):

Crown center height (m):

Elastic Limit (%):

Inclino:

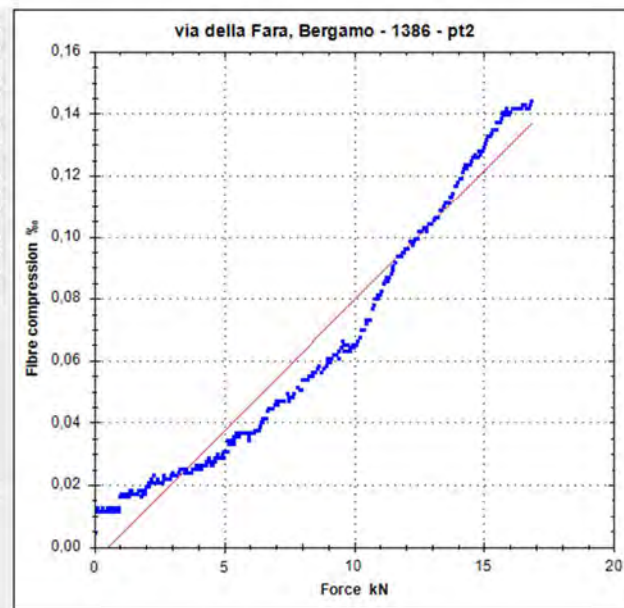
Alpha (°) = 0,20  
 F<sub>max</sub> (N) = 511866,59  
 M<sub>max</sub> (Nm) = 2309313,89  
 M<sub>wind</sub> (Nm) = 291089,70  
**SF = 7,93**

Filters

Tare force at first value

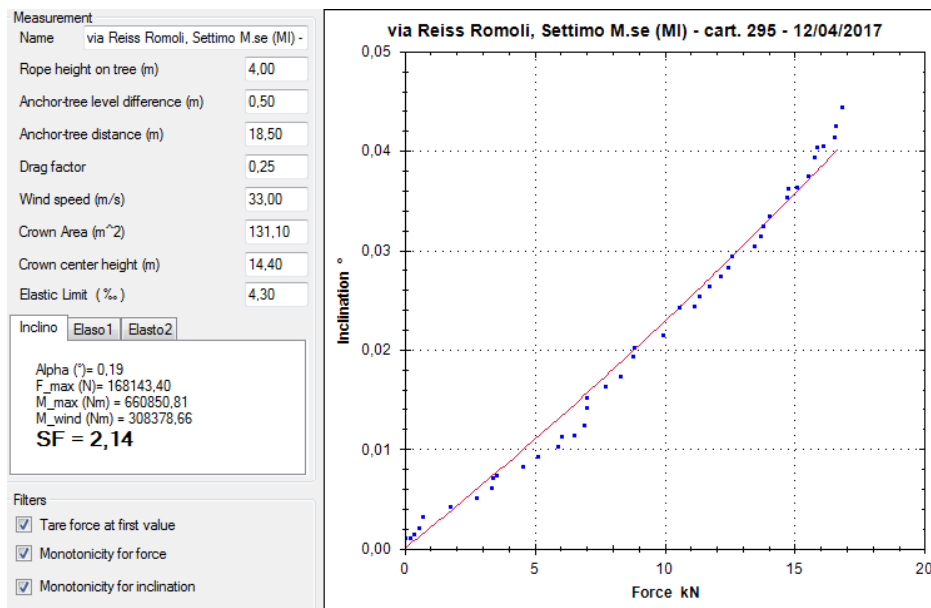
Monotonicity for force

Monotonicity for inclination



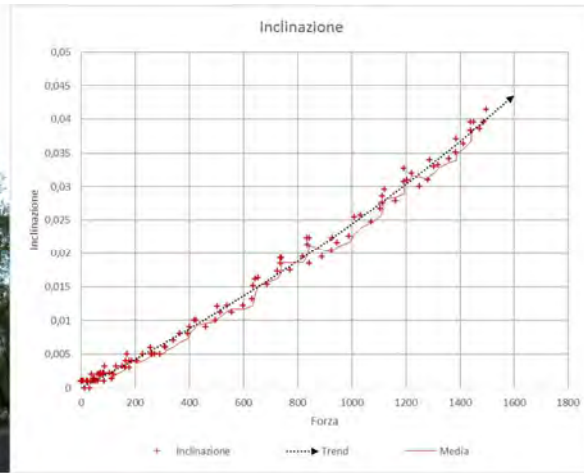
## Appendix 1 – Pulling tests

Via Reiss Romoli, Settimo Milanese – 295 – pt1

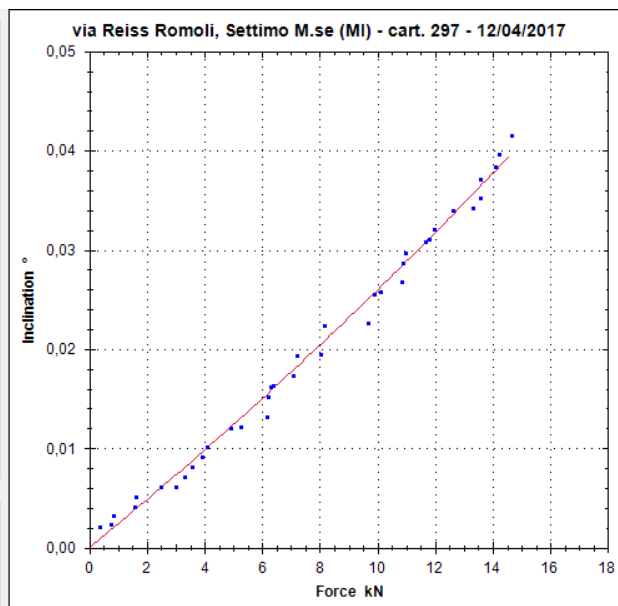


## Appendix 1 – Pulling tests

Via Reiss Romoli, Settimo Milanese – 297 – pt1



Measurement	
Name	io M.se (MI) - cart. 297 - 12/04/2017
Rope height on tree (m)	4,5
Anchor-tree level difference (m)	0,5
Anchor-tree distance (m)	14,4
Drag factor	0,25
Wind speed (m/s)	33,00
Crown Area (m <sup>2</sup> )	156,6
Crown center height (m)	15
Elastic Limit (%)	4,3
Inclino <input type="radio"/> Elaso1 <input type="radio"/> Elaso2	
Alpha (°) = 0,27 F_max (N) = 149399,24 M_max (Nm) = 647769,78 M_wind (Nm) = 383709,15 <b>SF = 1,69</b>	
Filters <input checked="" type="checkbox"/> Tare force at first value <input checked="" type="checkbox"/> Monotonicity for force <input checked="" type="checkbox"/> Monotonicity for inclination	



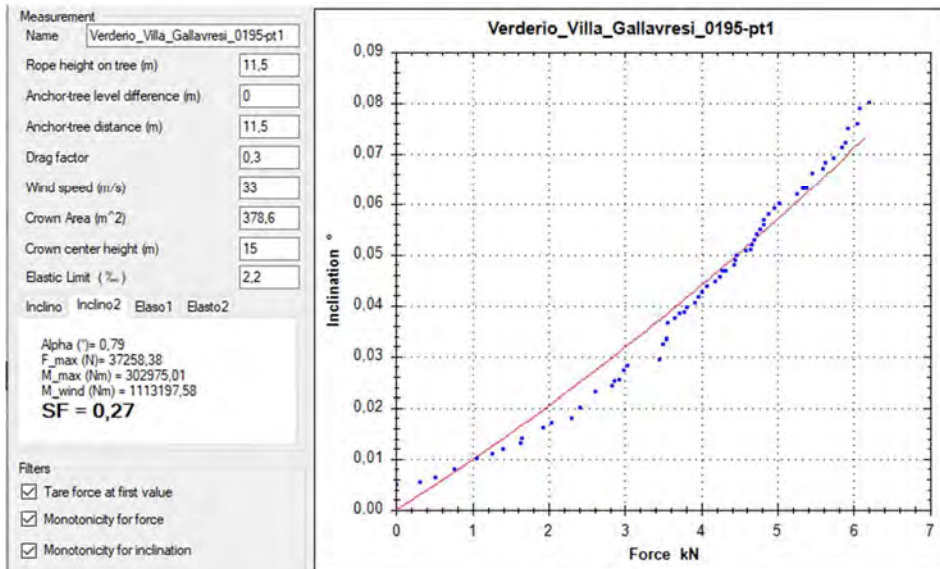
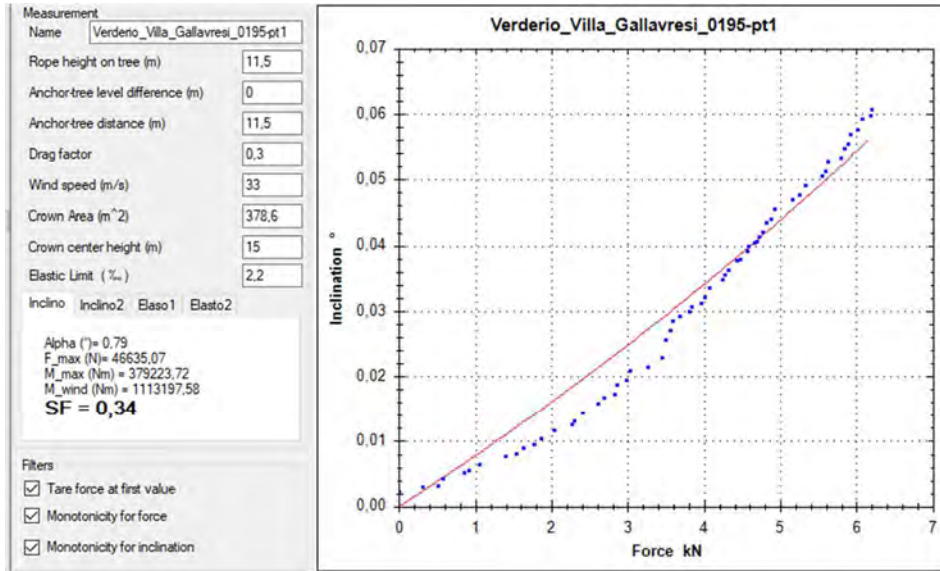
Appendix 1 – Pulling tests

---

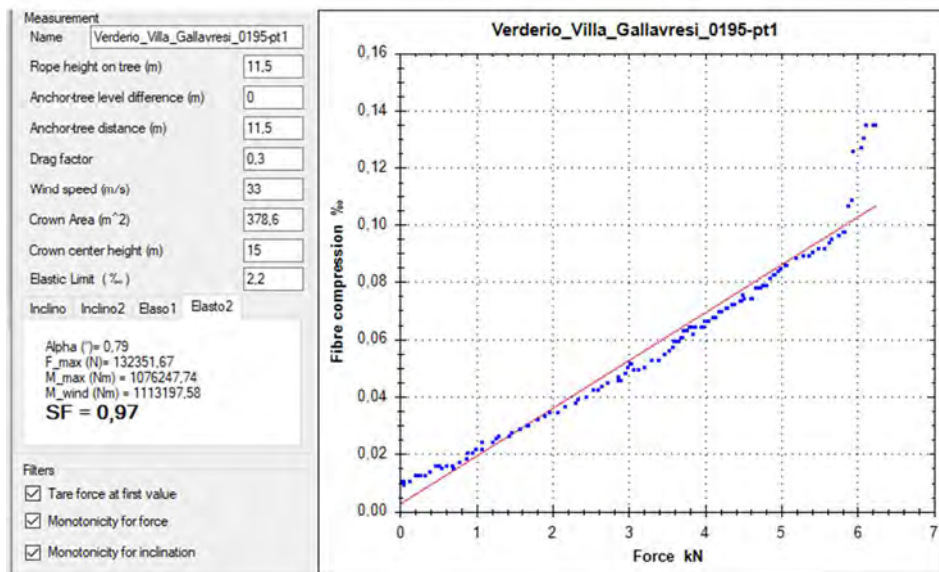
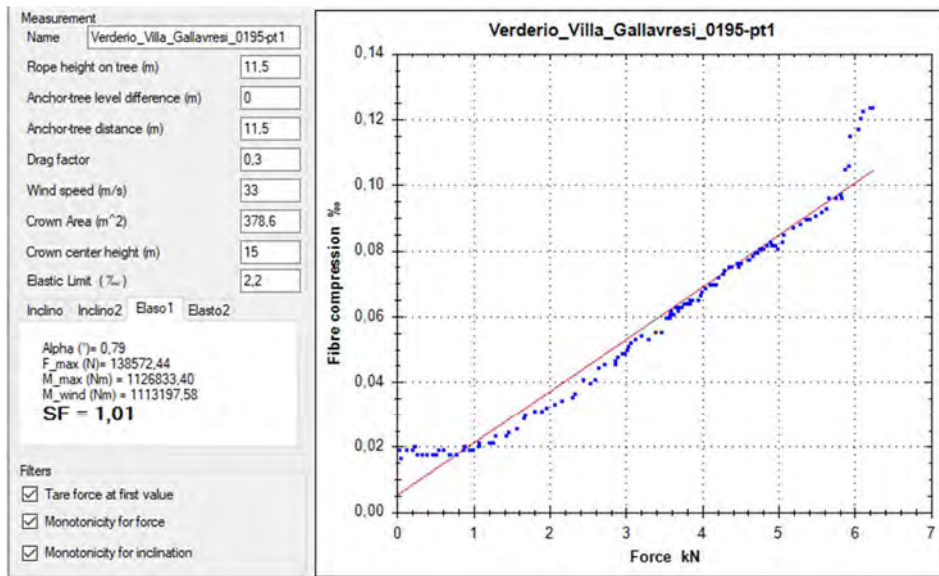
Villa Gallavresi, Verderio – 0195 – pt1



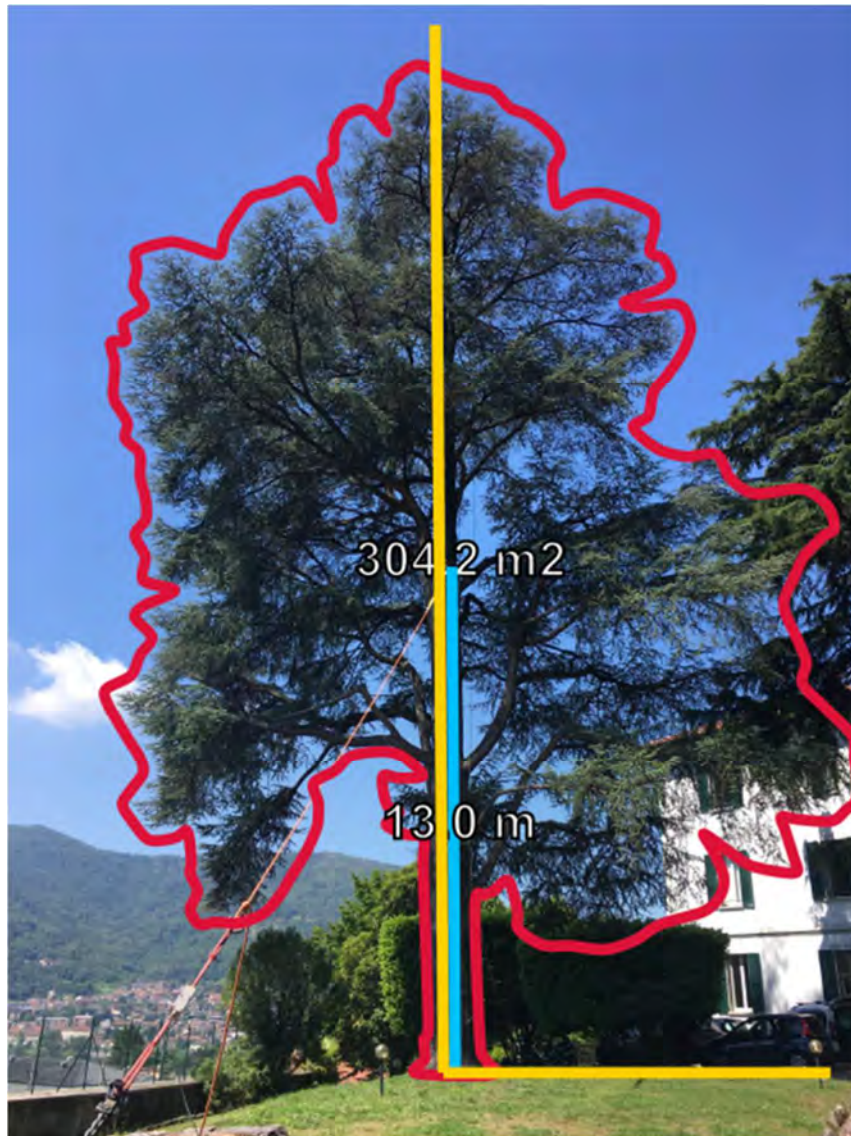
## Appendix 1 – Pulling tests



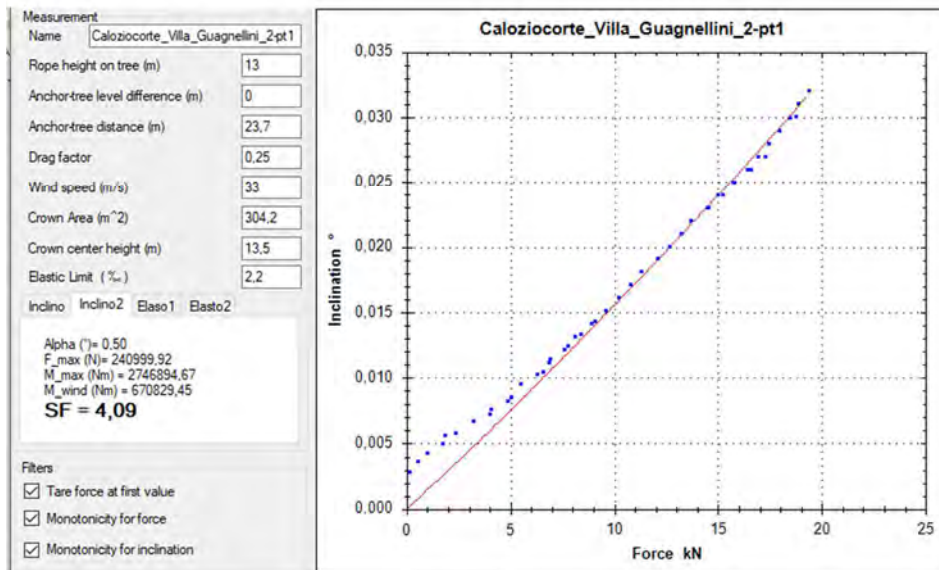
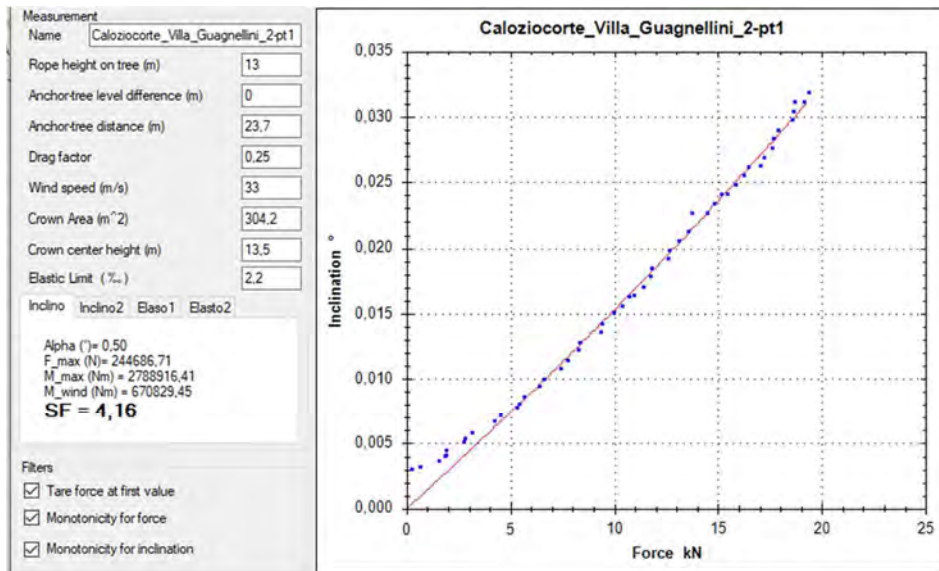
## Appendix 1 – Pulling tests



Villa Guagnellini, Calolziocorte – 2 – pt1

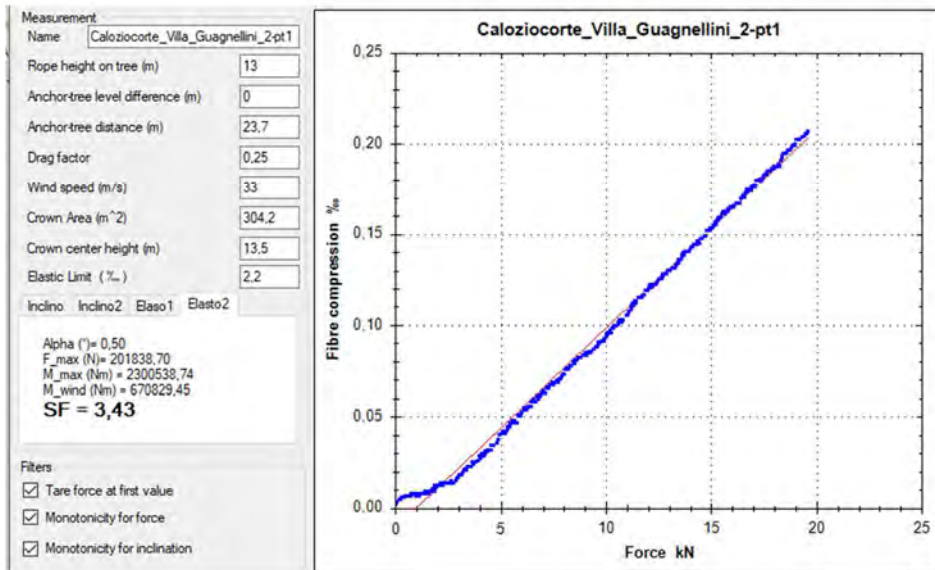
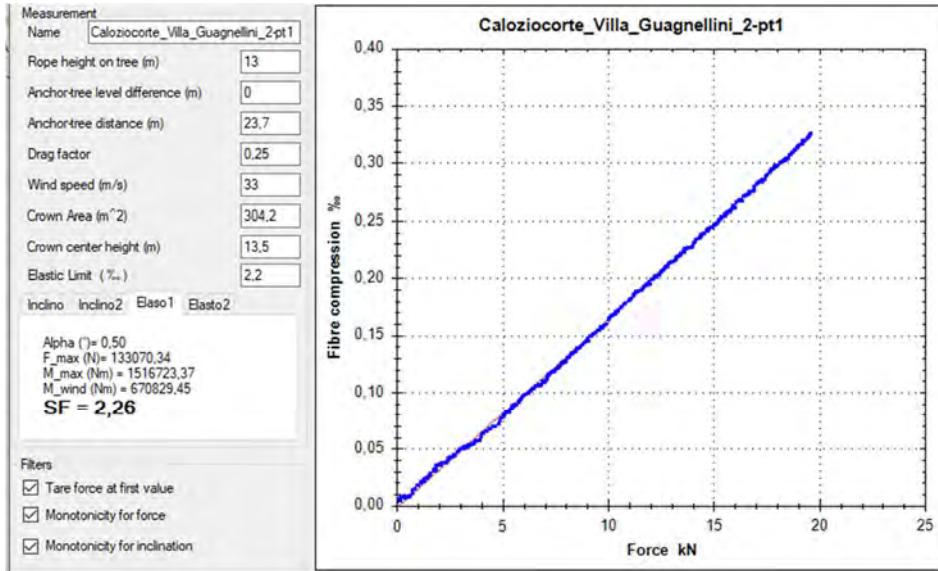


## Appendix 1 – Pulling tests





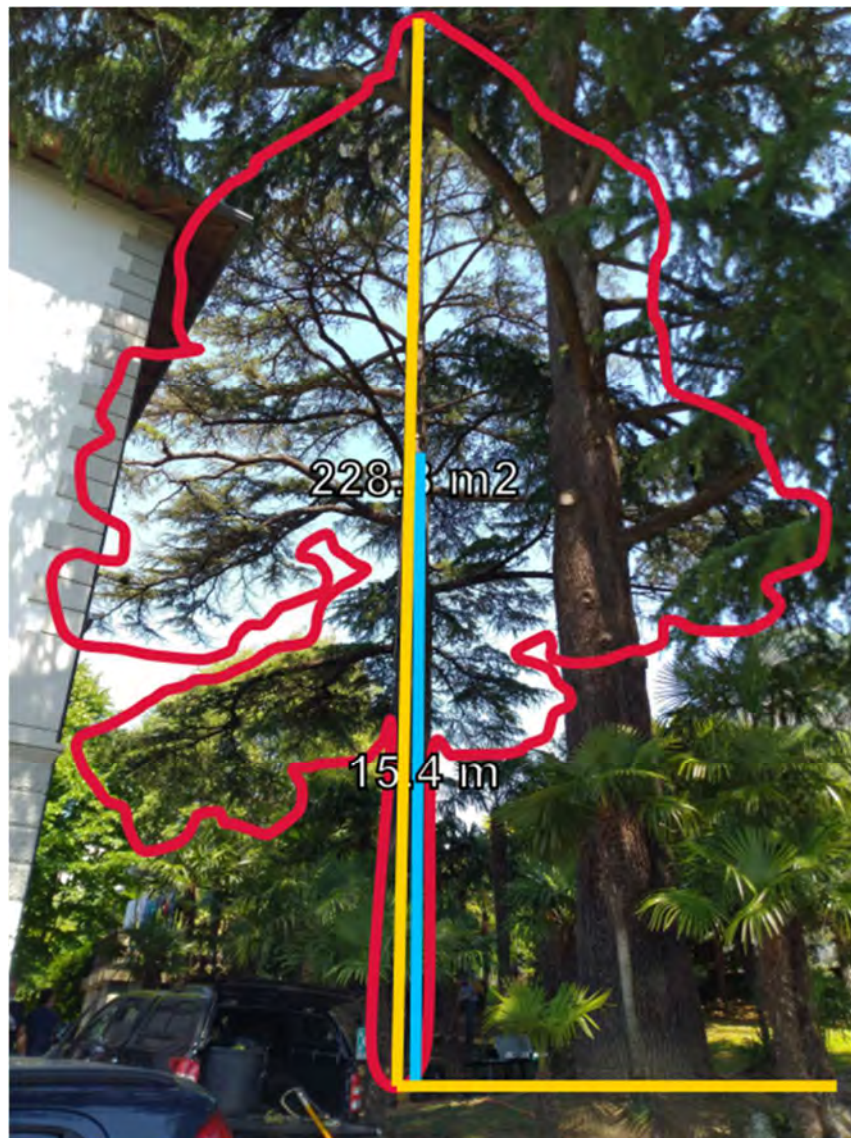
## Appendix 1 – Pulling tests



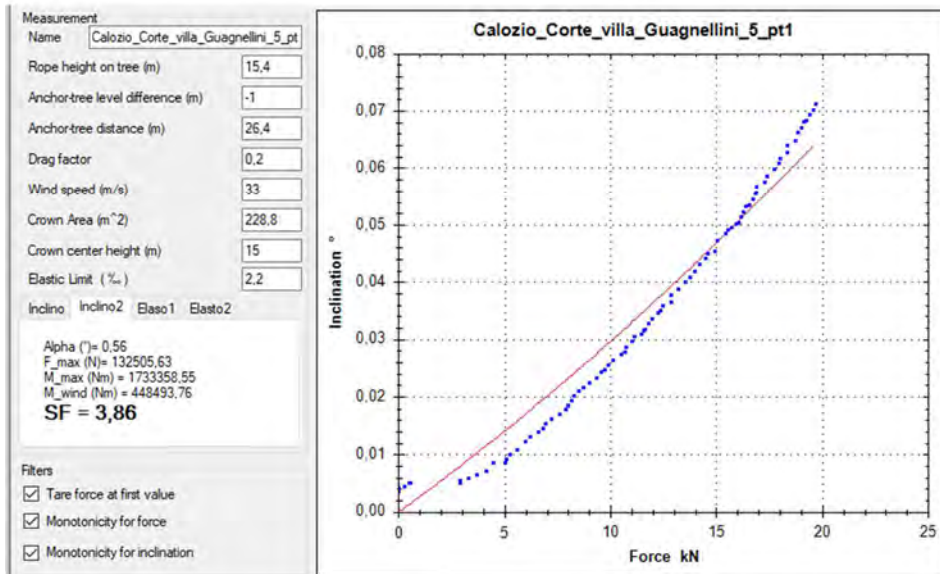
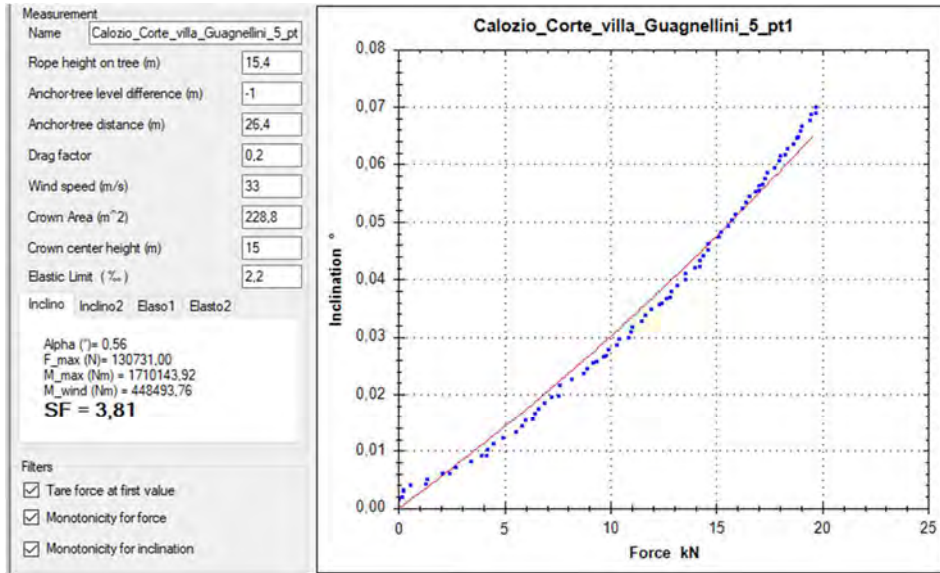
Appendix 1 – Pulling tests

---

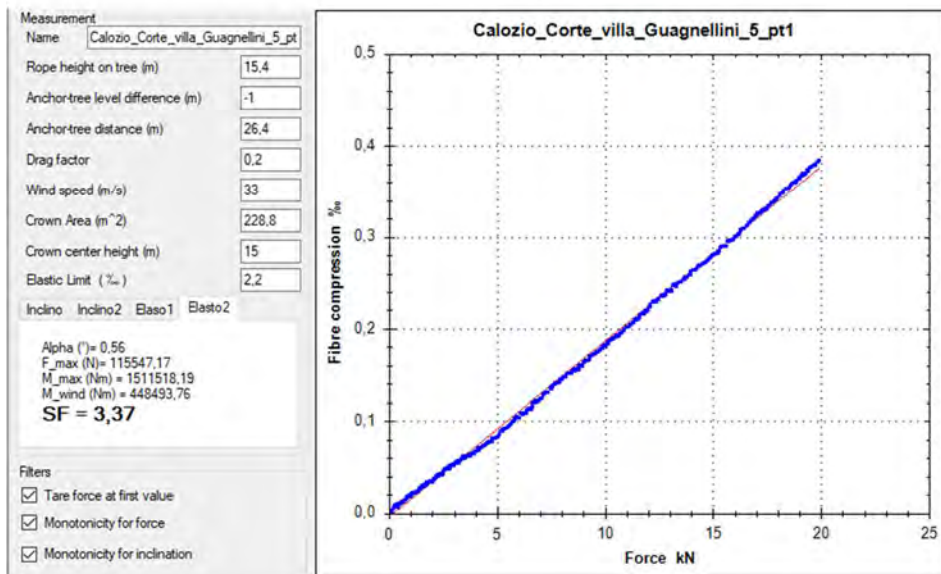
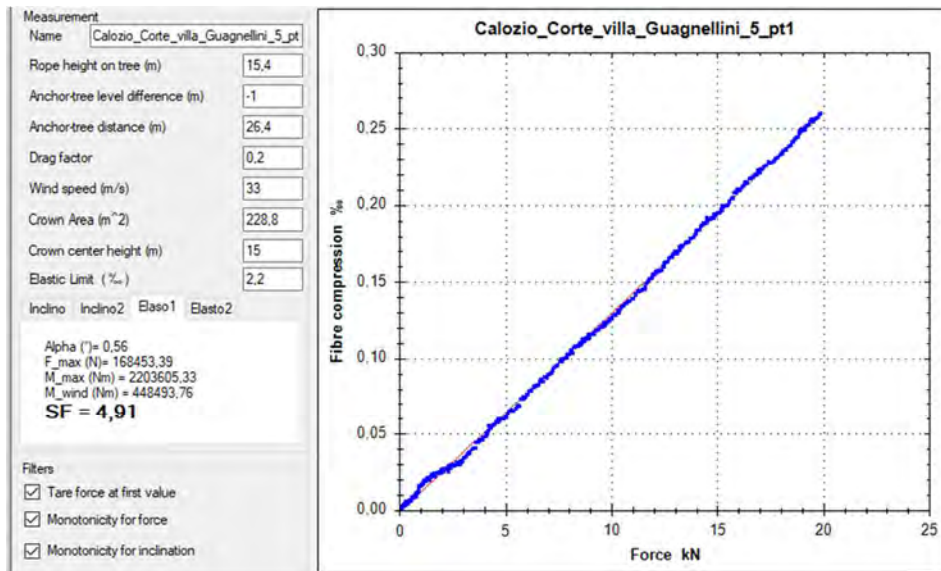
Villa Guagnellini, Calolziocorte – 5 – pt1



## Appendix 1 – Pulling tests



## Appendix 1 – Pulling tests



## **Appendix 2**

### **Geographical location**

## Appendix 2 – Geographical location

---

Appendix 2 – Geographical location

---

Boschetti Reali, Monza



Viale Vittorio Veneto, Monza



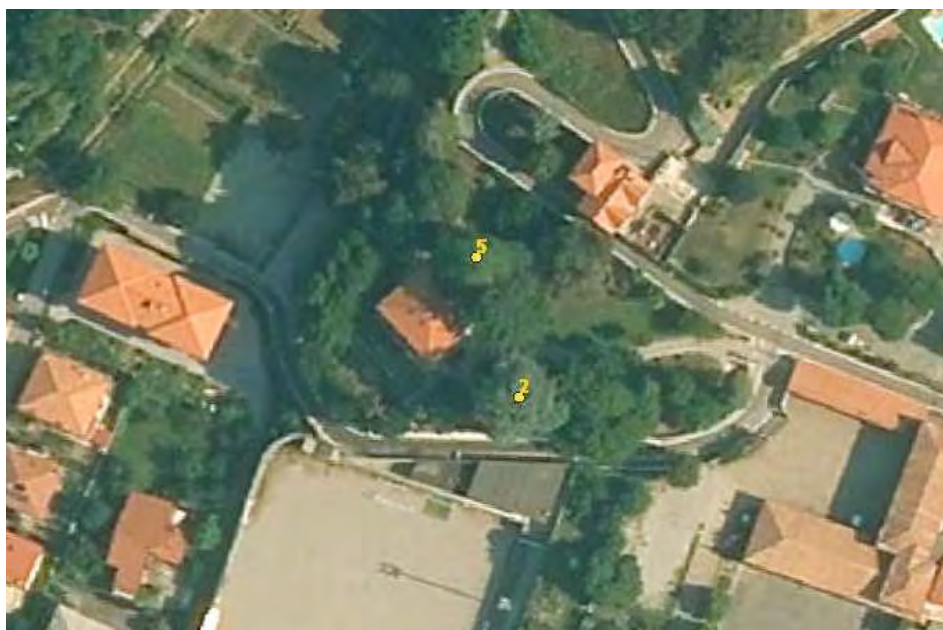
Appendix 2 – Geographical location

---

Via Pellettier, Monza



Villa Guagnellini, Calolziocorte





Appendix 2 – Geographical location

---

Villa Gallavresi, Verderio



Via Reiss Romoli, Settimo Milanese



## Appendix 2 – Geographical location

---

### Via della Fara, Bergamo



### Piazza Togliatti, Rho



Appendix 2 – Geographical location

---

Piazza Tevere, San Donato Milanese



Piazza Moneta, Cesano Boscone



Appendix 2 – Geographical location

---

Centro Allende, La Spezia

